XV International Conference
on Chemical Reactors
Helsinki, Finland, June 5-8, 2001

CHEMREACTOR-15

ABSTRACTS

CITY OF HELSINKI

Helsinki-2001

Boreskov Institute of Catalysis of the Siberian Branch of the Russian Academy of Sciences

Finnish Catalytic Society

Russian Center of International Scientific and Cultural Cooperation under RF Government

Ministry of Industry, Science and Technologies of the Russian Federation

Scientific Council on Catalysis of the Russian Academy of Sciences

European Federation on Chemical Technologies

Russian Scientific and Cultural Center in Helsinki

XV International Conference on Chemical Reactors CHEMREACTOR-15

Helsinki, Finland
June 5-8, 2001

ABSTRACTS

Novosibirsk, 2001

INTERNATIONAL SCIENTIFIC ADVISORY COMMITTEE

Mikhail G. Slinko, Honour Chairman	State Research Center "Karpov NIPCI", Moscow, Russia
Valentin N. Parmon, Chairman	Boreskov Institute of Catalysis, Novosibirsk, Russia
Anatolii G. Bazanov	RSC «Applied Chemistry», St. Petersburg, Russia
Alexis T. Bell	University of California, Berkeley, USA
Boris N. Chetverushkin	Institute for Mathematical Modelling RAS, Moscow, Russia
M.P. Duduković	Washington University, St. Louis, USA
Robert J. Farrauto	Engelhard Corporation, Iselin, USA
Pio Forzatti	Technical University of Milan, Milan, Italy
Gilbert F. Froment	Texas A&M University, USA
Sergei S. Ivanchev	St. Petersburg Department of the Boreskov Institute of Catalysis, St. Petersburg, Russia
Valerii A. Kirillov	Boreskov Institute of Catalysis, Novosibirsk, Russia
Alexander I. Lugovskoi	JSC "Ryazan Oil Refinery Plant", Ryazan, Russia
Miloš Marek	Prague Institute of Chemical Technology, Prague, Czech Republic
Hariz V. Mustafin	JSC «Nizhnekamskneftehim», Nizhnekamsk, Russia
Vladimir S. Novitskii	State Committee of Ukraine in Industrial Politics, Kiev, Ukraine
Alexander V. Putilov	Ministry of Industry, Science and Technologies RF, Moscow, Russia
Albert Renken	Swiss Federal Institute of Technology, Lausanne, Switzerland
Tapio Salmi	Finnish Catalytic Society, Turku, Finland
Karl R. Westerterp	University of Twente, Twente, The Netherlands

ORGANIZING COMMITTEE

Alexander S. Noskov, Chairman	Boreskov Institute of Catalysis, Novosibirsk, Russia
Victor A. Chumachenko	JSC «Katalizator», Novosibirsk, Russia
Dmitrii V. Gorokhov	Russian Scientific and Cultural Centre, Helsinki, Finland
Vladimir Mikhailov	RSC «Applied Chemistry», St. Petersburg, Russia
Alexander P. Mitronov	State Design and Research Institute for Chemical Engineering "Khimtekhnologiya", Severodonetsk, Ukraine
Dmitrii Yu. Murzin	Laboratory of Industrial Chemistry, Åbo Akademi University, Turku, Finland
Svetlana A. Pokrovskaya	Boreskov Institute of Catalysis, Novosibirsk, Russia
Sergei I. Reshetnikov	Boreskov Institute of Catalysis, Novosibirsk, Russia
Yurii I. Ryazanov	JSC «Nizhnekamskneftehim», Nizhnekamsk, Russia
Andrei N. Zagoruiko	Boreskov Institute of Catalysis, Novosibirsk, Russia
Tatiana V. Zamulina, Secretary	Boreskov Institute of Catalysis, Novosibirsk, Russia

The organizers express their gratitude to

Ministry of Industry, Science and Technologies of the Russian Federation, Moscow, Russia

SIBACADEMBANK, Novosibirsk, Russia

JSC «Nizhnekamskneftehim», Nizhnekamsk, Russia

for the financial support.

PLENARY LECTURES

CATALYTIC COMBUSTION IN SOLVING THE ENVIRONMENTAL AND ENERGY PROBLEMS

V.N. Parmon, Z.R. Ismagilov, V.A. Kirillov, A.D. Simonov

Boreskov Institute of Catalysis, Novosibirsk 630090, Russia
e-mail: parmon@catalysis.nsk.su

The presentation is devoted to the recent developments of the Boreskov Institute of Catalysis in the field of small and medium autonomous energetics. Under discussion are commercial boilers and heat producing installations which are operating on the basis of environmentally benign catalytic combustion of various gaseous, liquid and solid fuels.

An important advantage of these systems is their environmental purity, small geometric size as well as high energy converting efficiency. In addition, the heat generating installations which are based on the reactors with the fluidized catalyst bed have appeared to be able to utilize practically any kinds of available fuels, like natural gas, diesel fuel, crude oil, low quality coals and even wet sludges and sewages as well as biomass (wood chips, peat, rice husk, etc.).

PL-2

CATALYTIC MICROREACTORS

Albert Renken

Laboratory of Chemical Reaction Engineering (LGRC)
Swiss Federal Institute of Technology (EPFL), CH-1015, Lausanne, Switzerland
Phone: +41-21-693 31 81; Fax:+41-21-693 31 81; e-mail: albert.renken@epfl.ch

New process routes must consider a high efficient use of materials and energy. Chemicals have to be produced with high selectivity thus minimizing the formation of by-products. Furthermore, the reactor volumes should be small and the whole process should be inherently safe. Such processes require new types of chemical reactors. The solution to some of the mentioned challenges might lie in the use of microreactors [1]. The majority of today's microreactor/heat exchanger consists of many parallel channels with typical width of 50 to 500 μm. The wall-thickness of the microchannels can be kept very thin and lies in the range of 20 to 200 μm depending on the material used. As a result of the small dimensions heat transfer coefficient in the order of 25 kW/(m^2·K) can be obtained [2], exceeding those of conventional devices by more than one order of magnitude. As a consequence of the small channel dimensions extremely high surface to volume ratios in the order of 10'000 to 50'000 m^2/m^3 can be realized. The high exchange capacity guarantees isothermal reactor operation even for fast exothermic or endothermic reactions.

A further advantage of the microchannels concerns the short radial diffusion time leading to high radial mass transfer. Although the flow in the channels is laminar, a uniform radial concentration profile and consequently a narrow residence time distribution is obtained [3]. This allows to optimise the contact time in the reactor and to avoid consecutive reactions. Narrow residence time distribution and low inventory allow to operate microreactors under forced periodic concentration variations at high frequencies of up to 1 Hz [3], thus adding another possibility for process optimisation [4, 5].

The fast heating and cooling capacity of microreactors and the isothermal behaviour present further advantages for process optimisation [6, 7]. This was demonstrated for the catalytic dehydration of methanol to formaldehyde, where temperature gradients of up to 6'400 K/s could be realized, leading to an efficient freezing of consecutive decomposition reactions [8].

Microsystems for the use in chemical reaction engineering was mainly developed within the last 5-6 years. In consequence, the potential benefits of this new technology is by far not known. It is evident that catalytic microreactor are a powerful tool for studying the kinetics of

fast complex reactions. In addition, the microreactor concept allows to extend significantly the temperature and concentration range compared to conventional reactors. Therefore, micro-reactors are beneficial for an efficient process intensification and should be considered for the design of flexible, inherently safe small-scale reaction units.

References:

1. Lerou, J.J., M.P. Harold, J. Ryley, J. Ashmead, T.C. O'Brien, M. Johnson, J. Perrotto, C.T. Blaisdell, T.A. Rensi, and J. Nyquist, *Microfabricated minichemical systems: Technical feasibility*, in *Microsystem Technology for Chemical and Biological Microreactors*. 1995, DECHEMA. DECHEMA Monographs, **132**, 51-69.
2. Schubert, K., W. Bier, J. Brandner, M. Fichtner, C. Franz, and G. Lindner, *Realization and testing of microstructure reactors, micro heat exchanger and micro mixers for industrial applications in chemical engineering*, in *Process Miniurization: 2nd International Conference on Microreaction Technology*, I.H.R. W. Ehrfeld, R.S. Wegeng, Editor. 1998, AIChE: New York 88-95.
3. Rouge, A., B. Spoetzl, K. Gebauer, R. Schenk, and A. Renken, *Microchannel reactors for fast periodic operation: the catalytic dehydrogenation of isopropanol.* Chem. Eng. Sci., 2000. **accepted**: .
4. Silveston, P.L., R.R. Hudgins, and A. Renken, *Periodic Operation of Catalytic Reactors.* Catalysis Today (Special Issue), 1995. **25**: 89-195.
5. Silveston, P.L., R.R. Hudgins, and A. Renken, *Periodic operation of catalytic reactors - Overview;*. Catalysis Today, 1995. **25**: 91 - 112.
6. Alépée, C., L. Paratte, P. Renaud, R. Maurer, and A. Renken. *Fast heating and cooling for high temperature chemical microreactors.* in *3th International Conference on Microreaction Technology*.2000. Frankfurt am Main 514-525.
7. Alépée, C., L. Vulpescu, P. Cousseau, P. Renaud, R. Maurer, and A.Renken. *Microsystem for high temperature gas phase reactions.* in *4th International Conference on Microreaction Technology*. 2000. Atlanta: AIChE, 71-77.
8. Maurer, R., M. Fichtner, K. Schubert, and A.Renken. *A microstructured reactor system for the methanol dehydrogenation to water-free formaldehyde.* in *4th International Conference on Microreaction Technology*. 2000. Atlanta 100-105.

PL-3

FLOW MAPING AND MODELING OF LIQUID-SOLID RISERS

M.P. Duduković, Shantanu Roy* and M.H. Al-Dahhan

Chemical Reaction Engineering Laboratory Washington University St. Louis, MO 63130, USA
**Current Address: Process Engineering and Modeling, Corning Incorporated, SP TD 01 2, Corning, NY 14831, USA.*

Multiphase reactors are prevalent in the chemical, petroleum and associated process industries. Proper reactor selection determines the features and costs of the whole plant. Environmental considerations play an ever increasing role in selection of process chemistry which in turn must be matched by an appropriate reactor type. The old fashioned approach of conducting the reaction on a multitude of reactor scales is increasingly replaced by a more systematic systems approach. In it one attempts to develop reactor models that isolate the key features of the multiphase flow pattern, measure the relevant physical quantities, and model them with suitable accuracy. Only with well-understood flow field information can an accurate kinetic model describing the reaction chemistry produce meaningful predictions of reactor performance. (Villermaux, 1993; Krishna and Sie, 1994; Lerou and Ng, 1996; Duduković et al., 1999).

It should be noted that it is the desire to establish clean and safe, environmentally acceptable process that leads us to novel chemistries and reactors. For example, the push for replacement of liquid catalysts like HF and sulfuric acid in alkylation processes has resulted in the development of solid acid catalysts which in turn require novel multiphase reactors. In this contribution, we present the case of the riser in a liquid-solid circulating fluidized bed system. These systems are rapidly gaining popularity as reactors of choice in a variety of industrial processes like alkylation reactions, synthesis of fine chemicals, petrochemicals and in petroleum refining (Gibilaro et al., 1988; Liang et al., 1995). The process requirements that motivate the use of such reactors is the presence of a liquid phase reactant, which is typically a hydrocarbon under high pressure and low temperature (Thomas, 1970), and a solid phase catalyst which gets deactivated rapidly (Corma and Martinez, 1993). The principal reaction is accomplished in a vertical riser column of high L/D ratio (in which the solids are fluidized and transported by the liquid phase). Regeneration of the deactivated catalyst is done in a separate vessel, which is coupled to the principal reaction in the riser by circulating the solids continuously in a closed loop. Very little is known about the flow patterns in the riser, which are highly turbulent, chaotic and contain a high volume fraction of solids. A detailed experi-

mental and theoretical study of their behavior, as well as an assessment of their performance as reactors, is clearly of prime importance.

This contribution describes three areas of importance in reaction engineering of liquid-solid risers. First, the principal results from a extensive experimental program dedicated to studies of the flow pattern in a laboratory scale cold-flow unit are presented. The unit was a 6-inch diameter, 7 feet tall cylindrical liquid-solid riser. The solid phase inventory was around 100 lbs. of 2.5-mm glass particles, and liquid flow rates from 44 gpm to 67 gpm were studied under varying solids-to-liquid flow ratios (variable inventory operation). All experiments were performed using non-invasive gamma radiation based techniques, since it is impossible to use other means to noninvasively probe into these dense systems.

As part of the experimental program, a method was developed for accurate in situ measurement of the solids flow rates, which enabled accurate experimental investigation at variable solids and liquid flow rates. Gamma radiation based transmission computed tomography (CT) was used to measure the time-averaged cross-sectional solids volume fraction distribution at various riser elevations as a function of operating conditions. The solids velocity field was studied using the Computer Automated Radioactive Particle Tracking (CARPT) technique, by labeling a single solid particle with radioactive Sc-46 and monitoring its motion in the riser over a long time. Ensemble averaging of the collected Lagrangian data provided information on mean velocity fields, RMS velocities and ìturbulenceî in the particle assembly, as a function of operating conditions. Lagrangian analysis of the data provided information about the eddy diffusivities, the residence time distribution of the solids in the riser section, trajectory length distributions, mixing indices, the degree of randomness in the solids motion (Hurst exponents) and information on internal circulation patterns (return length and circulation time distributions).

In parallel with the experimental effort, numerical simulation of the flow pattern in the laboratory riser was attempted using computational fluid dynamics (CFD) techniques. A "twofluid" approach (Sinclair and Jackson, 1989; Ding and Gidaspow, 1990) was adopted, and both solid and liquid phases were modeled as interpenetrating continua. The coupling between the mean velocity fields of the solid and liquid phases is affected through a drag coefficient, modified for presence of finite volume fractions. Momentum transfer through solid-solid collisions is modeled by writing a balance equation for the pseudo-thermal granular temperature of the solid phase, accounting for presence of the continuous liquid phase.

The boundary condition for the solids at the wall is obtained via a modified Johnson-Jackson (1987) approach. Continuum liquid phase turbulence is modeled using a

k-(formulation, modified for presence of the dispersed solid phase (Elgobashi and Abou-Arab, 1983). The simulations are performed in two-dimensional axisymmetric and three-dimensional geometries, using the FLUENT library of codes. The predictions were compared against the results from the experiments on the laboratory scale riser. The flow pattern simulations were utilized to predict residence time distributions of the phases by simulating the transport of an inert tracer tagging the phases.

Finally, the key findings from the detailed experimental and numerical fluid dynamics efforts were used as inputs in phenomenological reaction engineering models, of varying levels of sophistication, for reactor performance prediction. It is shown that these models are computationally less involved as compared to transient CFD methods, but when provided with accurate parameters they can be used for making optimal choices of feed ratios, location of feed points, and other variables of interest to the practicing engineer.

References:

1. Corma, A. and A. Martinez (1993) "Chemistry, Catalysts and Processes for Isoparaffin Alkylation: Actual Situation and Future Trends", Catal. Rev., - Sci. & Engng. 35(4), 483.
2. Ding, J. and D. Gidaqspow (1990) "A Bubbling Fluidization Model Using Kinetic Theory of Granular Flow", AIChE J. 36, 523.
3. Elgobashi, S. E. and T. W. Abou-Arab (1983) "A Two-Equation Turbulence Model for Two-Phase Flows", Phys. Fluids 26(4), 931.
4. Johnson, P. C. and R. Jackson (1987) "Frictional-Collisional Constitutive Relations for Granular Materials with Application to Plane Shearing, Sheared in an Annular Cell", J. Fluid Mech. 176, 67.
5. Krishna, R. and S. T. Sie (1994) "Strategies for Multiphase Reactor Selection", Chem. Engng. Sci. 49(24A), 4029.
6. Dudukovic, M. P., P. L. Mills, F. Larachi (1999) "Multiphase Reactors - Revisited", Chem. Engng. Sci. 54(13-14), 1975.
7. Gibilaro, L. G. and R. di Felice and P. U. Foscolo, "A Circulating Liquid Fluidized Bed", Chem. Engng. Sci. 43(10), 2901 (1988).
8. Lerou, J. J. and K. M. Ng (1996) "Chemical Reaction Engineering: A Multiscale Approach to a Multiobjective Task", Chem. Engng. Sci. 51, 1595.
9. Liang, W., Z. Yu, Y. Jin, Z. Wang, Y. Wang (1995) "Synthesis of Linear Alkylbenzene in a Liquid-Solid Circulating Fluidized Bed Reactor", J. Chem. Techol. Biotechnol. 62(1), 98.
10. Sinclair, J. L. and R. Jackson (1989) "Gas-Particle Flow in a Vertical Pipe with Particle-Particle Interactions", AIChE J. 35, 1473.
11. Thomas, C. L. (1970) Catalytic Processes and Proven Catalysts, Academic Press, New York.
12. Villermaux, J. (1993) "Future Challenges for Basic Research in Chemical Engineering", Chem. Engng. Sci. 48, 2525.

RENEWABLE FUELS AND CHEMICALS BY THERMAL PROCESSING OF BIOMASS

A.V. Bridgwater

Bio-Energy Research Group, Aston University, Birmingham B4 7ET, UK

Biomass and wastes offer significant potential for greenhouse gas mitigation through conversion to electricity, heat and chemicals and avoiding use of fossil fuels. Conversion can be achieved by thermal and biological routes to give a range of gaseous, liquid and solid products. This paper reviews the processes and products, and focuses on thermal processes as cost effective and energetically efficient routes to meeting the increasing demands for more environmentally acceptable products.

Gasification, pyrolysis and liquefaction are thermochemical processes that can convert solid biomass and wastes into gaseous or liquid products. Biomass gasification is the more established technology. Commercial reactors are now available and development effort is concentrated on integration into systems that can generate electricity from wood. Several substantial projects are underway to demonstrate electricity generation in Europe and the USA. High temperature pyrolysis has been extensively developed for waste processing but there are currently few commercial applications.

Fast pyrolysis for production of liquids from biomass is a lower temperature process that has been in development since 1980. Liquid yields of 75% are typically achieved from wood. This process has the unique advantage of delivering liquid product that can be stored and transported. One process has now achieved commercialisation for speciality chemicals and several more are at pilot and demonstration stage. Commercial operation is anticipated in several years time.

Although liquefaction wasone of the earliest processes to be demonstrated in the early 1980s, technical and economic problems inhibited further development. There is now a re-newed interest in this process as a means of utilising wet material and delivering a liquid product.

PL-5

REGENERATIVE & REACTIVE MANIPULATION OF TEMPERATURE & CONCENTRATION PROFILES IN CHEMICAL REACTORS

Department of Chemical Engineering, University of Dortmund
Emil-Figge-Str. 66, 44227 Dortmund, Germany
Tel.: +49 231 755 2697, Fax: +49 231 755 2698, E-mail: agar@ct.uni-dortmund.de

The performance of chemical reactors dictated by the cumulative impact of the local conditions of concentration, temperature and catalytic activity under which the reaction takes place. In the simplest case of an adiabatic fixed-bed reactor one is dealing with a uniform activity profile and rigidly coupled temperature and concentrations. Reactor output can thus only be adjusted using the residence time. Appropriate structuring of the catalytic activity along the reactor is a powerful but inflexible means of controlling the course of the reaction process. Manipulation of temperature and concentration profiles by the introduction / removal of heat / components of the reaction system is thus usually the of technique of choice. The processes employed can be classified as being either:

1. convective (direct addition or withdrawal via sidestream(s))
2. recuperative (spatial segregation of reactor volume from material/heat sink/source)
3. regenerative (chronological segregation of reaction volume from material/heat sink/source)
4. reactive (supplementary reaction system serves as material/heat source/sink)

The first two alternatives are much more commonly encountered in industrial practice, for example in the imposition of an expedient temperature profile by means of 'cold-shot' or multitubular reactors, than are the regenerative or reactive options. It is illuminating both to consider why this is the case and to examine the particular merits of the neglected variants.

The consideration of three endothermic, heterogeneously catalysed, high temperature reaction systems - the dehydrogenation of ethylbenzene at around 600°C, steam reforming of hydrocarbons at 800°C and the synthesis of hydrogen cyanide from methane and ammonia at 1200°C – suggest that the decision as to which of the four processes be used to supply the heat required is by no means straightforward. For example, most hydrogen cyanide is manufactured using the reactive alternative in the Andrussow process, but a recuperative process – the BMA technology – is also still industrially relevant.

An analysis of the HCN synthesis suggests that the regenerative option deserves further attention, since it incorporates the benefits of the alternatives without their major drawbacks [1]. The direct reactive combination of the actual endothermic synthesis reaction ($CH_4 + NH_3 \rightarrow HCN + 3\ H_2$ $\Delta H_R = +256$ kJ) with the exothermic combustion of the hydrogen by-product ($3\ H_2 + 1.5\ O_2 \rightarrow 3\ H_2O$ $\Delta H_R = -726$ kJ) as practised in the Andrussow process leads to a simple reactor with high thermal efficiencies, but suffers from poor yields owing to the loss of feedstocks in unwanted oxidative side-reactions. The high temperature recuperative heat change of the BMA process utilises only about half of the energy in the heating medium and necessitates a fragile ceramic reactor construction with special catalytic surfaces. A regenerative coupling of the two reactions, in which a catalyst bed is periodically heated with combustion gases to store the heat required in a subsequent synthesis phase permits one, in principle, to achieve the high yields and hydrogen cyanide concentrations of the BMA process in a much simpler and more robust reactor.

Numerical simulation of the regenerative reactor for hydrogen cyanide synthesis demonstrated that it would be necessary to use monolithic catalysts to deal with the high heating gas throughputs needed for reasonable cycle times. so, the limited heat storage capacity of the catalyst together with the inefficient utilisation of the heat stored due to formation of a pronounced 'cold spot', mean that the cycle times of around 4 minutes are at the lower end of what would be considered industrially feasible.

The exploitation of regenerative heat exchange in chemical reactors is, of course, hardly new. The pioneering work of Matros and coworkers on the use of reverse flow reactors exothermic reactions with 'cold' lean feeds together with the industrial application of such reactors for catalytic waste gas treatment illustrate the potential available. The extension to endothermic reactions has proved illusive however [2] with the temperature profile needed for efficient heat recovery often resulting in undesirable side-reactions, such as polymerisation, coke formation or the reverse reaction in equilibrium systems.

The enhancement of the heat storage capacity to extend cycle duration would greatly expand the horizons of regenerative processes. The use of fusion latent heat effects has already been proposed for this purpose. A further possibility is to utilise the heat effects associated with adsorption, by using the heat liberated by adsorption of a reaction product to the heat demands of a dehydrogenation, for example [3].

PL-5

Figure 1: Temperature and loading profiles for CO-Oxidation with and without 'desorptive cooling' at different times for an initially uniformly loaded adsorbent.

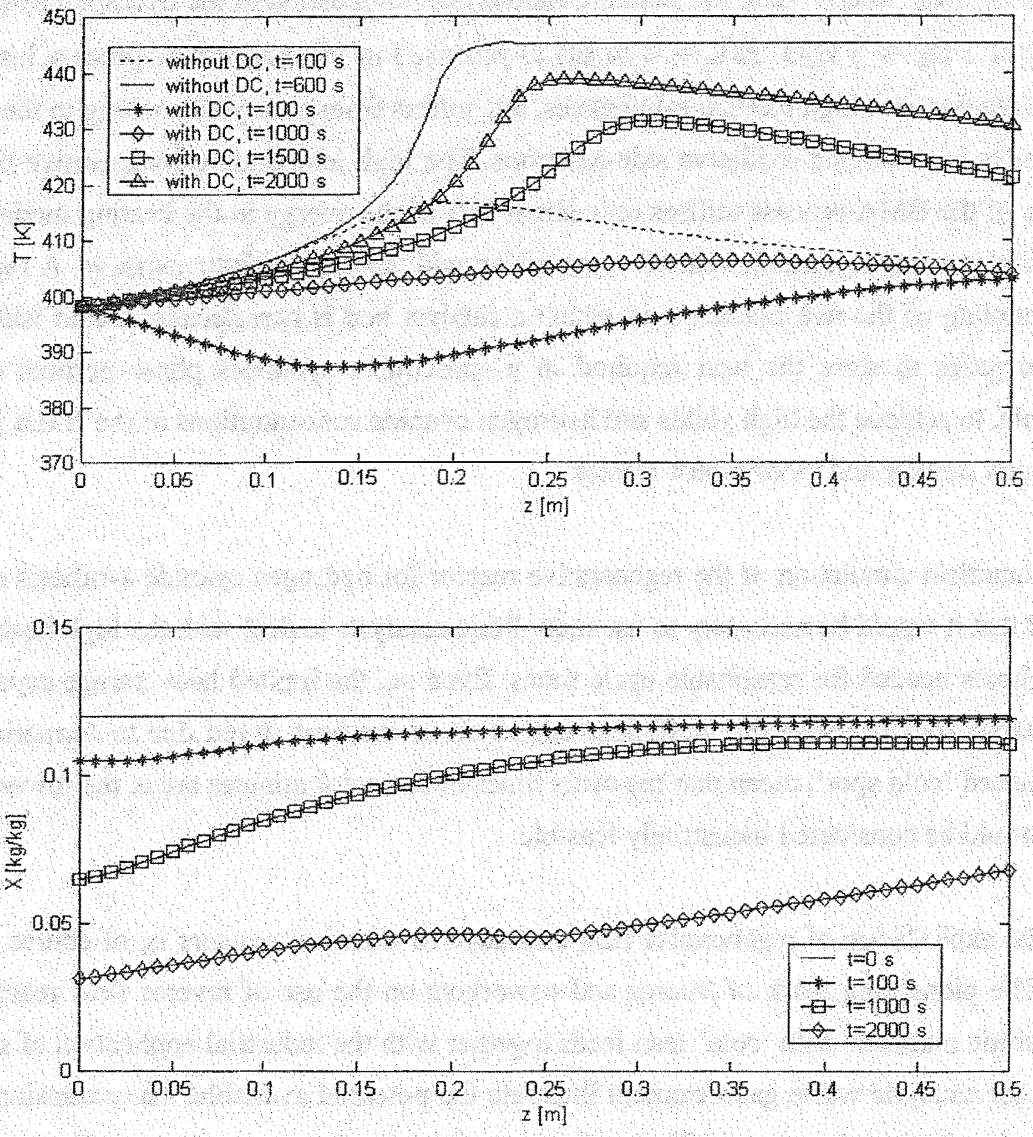

The desorption of previously adsorbed inert material from a mixed fixed bed of adsorbent and catalyst can give rise to uniform temperature profiles over considerable periods for exothermic reactions in an otherwise adiabatically operated reactor. The heat of reaction can removed very effectively and in a largely self-regulating process by such 'desorptive cooling' techniques, as illustrated in figure 1 with experimentally based model calculations for CO-oxidation on a fixed bed comprising Palladium catalyst and 3A zeolite loaded with water [4]. In this particular instance, the cycle duration could be increased by a factor of ten from 100 to 1 000 s with respect to the purely regenerative base case.

When using regenerative adsorptive processes to modify reactor concentration profiles the expedient realisation of the desorption process often poses greater difficulties than the integration of the adsorptive separation step into the reactor. An example of is provided by the single-stage adsorptive Claus process, in which the water formed in the reaction ($2\ H_2S + SO_2 \leftrightarrow 3/8\ S_8 + 2H_2O$) is adsorbed on 3A zeolite incorporated in the catalytic fixed bed [1]. The adsorption of this by-product offers both a more effective means of displacing the equilibrium than the conventional interstage sulphur removal and, together with reverse flow operation, permits a simple tandem regeneration process.

Should no suitable adsorbent be available for a reacting component under reaction conditions, one can introduce a coupled reaction to redefine the separation problem in a more accessible form. This technique can be illustrated using the reverse hydrolysis reaction for producing hydrogen cyanide from carbon monoxide and ammonia. Whilst there are no suitable adsorbents for the water vapour formed at the prevailing reaction temperatures of 400-500°C the inclusion of the water gas shift reaction by modifying catalytic activity enables one to adsorb the carbon dioxide formed in this secondary reaction to achieve the same effect. Problems with maintaining catalytic activity under strongly reducing conditions have so far impeded the development of this concept.

The direct integration of coupled secondary reactions to manipulate concentration and temperature profiles is an extremely challenging task as it is seldom possible to suppress unwanted chemical interactions. Even with reactive-recuperative techniques, in which the two thermally coupled reaction systems are spatially segregated by a catalytically active heat exchange surface, it is difficult to ensure that reactions take place at compatible locations [5].

The use of such hybrid processes exploiting two or more of the four fundamental options represents a logical and promising extension of the concept, as does the simultaneous manipulation of concentration and temperature profiles, in the regenerative unsteady-state Deacon process for hydrogen chloride oxidation, for example [6]. Measures for localising individual functionalities and intensifying recuperative processes within the reactor can similarly be employed to advantage.

[1] Chem.Engng.Sci. 54(1999):1299-1305
[2] Chem.Engng.Sci. 49(1994):5585-5601
[3] Chem.Engng.Sci. 53(19989.691-696
[4] Diploma Thesis, University of Dortmund, April 2001
[5] Chem.Engng.Sci.55(2000):5945-5967
[6] R'97 Proceedings, February 1997 Geneva VL45-VL50

PL-6

REACTION KINETICS – BASIS FOR MODELLING OF CATALYTIC PROCESSES

Mikhail G. Slin'ko and Dmitry Yu. Murzin*

Karpov Institute of Physical Chemistry, Moscow, 103064, Russia
**Laboratory of Industrial Chemistry, Process Chemistry Group, Åbo Akademi, Biskopsgatan 8, FIN-20500, Turku/Åbo, Finland*
ph: +358 2215 4985, fax: +358 2215 4479, e-mail: dmurzin@abo.fi

Introduction

Heterogeneous catalytic reactions constitute around 90% of all processes in chemical industry. Physico-chemical understanding of catalytic processes is thus essential for the proper reactor modelling. According to the very definition of catalysis it is a kinetic process, and thus reliable kinetic models, which describe the rate of catalytic reactions, are of vital importance for solving applied problems in mathematical modelling, design and intensification of chemical processes. The necessity of kinetic investigations in heterogeneous catalysis is closely connected to the tasks, which a chemical engineer has to deal with, e.g.

- Catalyst selection, comparison of activity and selectivity as well as long-term stability in the conditions which are optimal for each catalyst
- Estimation of the required amount of catalyst to meet specified conversion and selectivity
- Determination of all the possible by-products
- Calculation of the needed amount of heat to be provided to the catalytic reactor (or withdrawn from it) in order to have an optimal regime depending on conversion
- Investigation of the impact of heat and mass transfer processes on catalytic reaction, and based on it selection of the optimal pore structure, geometrical shape and size of catalysts
- Selection of the reactor type and the structure of reaction unit, which provides the closest approach to the optimum conditions
- Construction of bifurcation diagrams and determination of the steady-state multiplicity and stability, as well as parametric sensitivity and the impact of fluctuations on the steady-state regime
- Investigation of the feasibility of running a process in dynamic non-stationary conditions
- Determination of start-up/ shut down and transient regimes of catalytic reactors

- Characterization of catalyst deactivation
- Combination of catalytic processes with separation process, e.g. reactive (catalytic) distillation, multifunctional reactors, etc.

  Analysis of catalytic reactions, processes, reactors and reactor units based on non-linear dynamics

Physico-chemical basis for kinetic studies in catalysis

Any reactor design is thus starts from reactions kinetics and, therefore from the reaction mechanism, which means understanding of the reaction on the molecular level.

The most often used approach in the present day kinetic research in heterogeneous catalysis is by no means the Langmuir model of uniform surfaces. This concept applies, that all the surface sites are identical and binding energies of the reactants are the same independent the surface coverage. However, the model of an ideal adsorbed layer disagrees with a number of experimental data. Thus, differential heat of adsorption is not constant as a rule but decreases with surface coverage, and rate of adsorption and adsorption equilibrium are not described by the Langmuir equation or the Langmuir isotherm correspondingly. In several the kinetics of catalytic reactions disagrees with the equations obtained on the basis of the model of ideal adsorbed layers. For example, kinetics of ammonia synthesis obeys well-known Temkin-Pyzhev equation (e.g. kinetics for nonuniform surfaces). Adsorbed molecules not only participate in the surface reactions, but also change the structure and catalytic properties of the solids; therefore, the rates of elementary reactions depend on the spatial arrangement of atoms and molecules on the surface, their neighbours and the spatial arrangement of catalyst atoms. Hence, it is not enough to study heterogeneous catalytic reactions only by kinetic methods, but various physico-chemical methods (TPD, FTIR, LEED, HREELS, etc.) should be applied as well, providing the possibility to extract information about the elementary steps, which constitute a reaction mechanism.

Nonstationary kinetics

In chemical industry the majority of processes are conducted in stationary conditions. Therefore, it is not surprising that the steady-state kinetics is mainly studied. In the steady-state the surface concentration of reactants is time independent. Investigation of reaction kinetics in gradientless reactors further simplifies the experimental routine. The main drawback of kinetic models, based only on steady-state data, is associated with the fact, that start-up and transient regimes cannot be reliably modelled. Kinetic models for nonstationary conditions

are applied also for the processes in fluidised beds, reactions in riser (reactor) – regenerator units with catalyst circulation, as well as for various environmental applications of heterogeneous catalysis, when the composition of the gas to be treated changes permanently.

Understanding of nonlinear behaviour in nonideal adsorbed layers (oscillations, autowaves, formation of dissipative structures and deterministic chaos) can be achieved only on the basis of kinetic models for nonstationary conditions.

It is important to mention that deactivation is also an nonstationary process, however, in many cases dynamic kinetic models, which include deactivation as well are nonexistent. In fact reactor design should be arranged in a way, that provides the optimum of predefined parameters (accumulated yield, etc.) during the whole catalyst life-time, thus including modelling of deactivation.

Complex reactions

Historically the theory of catalytic kinetics was developed based on large-scale processes, like ammonia and methanol synthesis, production of sulphuric acid. More recently heterogeneous catalysis started to be widely used in the field of so-called classical organic chemistry, e.g. for the production of fine chemicals. However, in the fine chemicals applications, despite the increasing significance of heterogeneous catalysis in this area, kinetic studies are rather sparse. It can be understood, bearing in mind, that research in fine chemicals synthesis was and still is dominated (in major part) by pure organic chemists. One of the most important requirements for heterogeneous catalytic reactions in fine chemicals applications is proper selectivity, which in broad sense should be understood as chemo-, regio- and enantioselectivity. Kinetic analysis of complex reaction schemes, where the proper selectivity dependence is the key point of analysis, is still more an exception, than a rule.

The main objective is to bridge the knowledge of chemical reaction engineering of heterogeneous catalytic reactions to organic chemistry, in particular stereochemical and enantioselective reactions.

Case studies

In the lecture the concept "from reaction mechanism and kinetics to reactor design" will be illustrated by several examples.

PROCESS DEVELOPMENT IN THE FINE CHEMICAL INDUSTRY

Esko Tirronen, Tapio Salmi*

Kemira Oyj, Espoo Research Centre, P.O. BOX 44, FIN-22071 Espoo,
e-mail: Esko.Tirronen@kemira.com
**Åbo Akademi, Process Chemistry Group, Laboratory of Industrial Chemistry,*
FIN-20500 Turku, e-mail: Tapio.Salmi@abo.fi

Abstract

Fine chemicals are an important group of products consisting of pharmaceuticals, agrochemicals, dyes, photographic chemicals and intermediates of all these groups as well as chemicals for the textile industry. They are typically high value-added products. The processes for manufacturing these products are mostly batch and semibatch processes. The development of kinetic models for complex chemical reactions occuring in the fine chemical processes and including these models into batch and semibatch reactor models for scale-up are presented. A methodological approach to the modelling of these complex systems and the estimation of model parameters is proposed. The methodologies were applied to two case studies: reductive N-alkylation of an aromatic amine with homogeneous reactions and a heterogeneously catalyzed reactions and Claisen condensation as organic liquid-solid reaction.

Keywords: Process development, Dynamic models, Kinetics, Reductive alkylation, Claisen condensation

1. Introduction

In today's competitive environment, one of the key issues for fine chemical companies is to reach the market with new products as quickly as possible to guarantee a competitive edge over the other players in the field. This means that the whole chain from the idea via R&D activity to the commercialization and marketing has to form a fluent workflow to meet the project targets according to the pre-determined timescale.

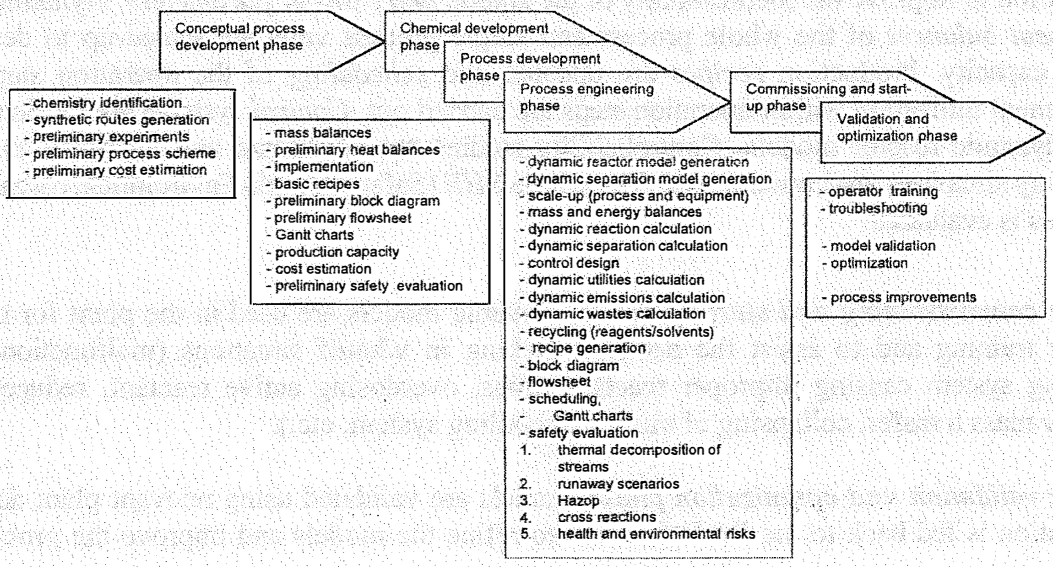

Figure 1. Workflow and tasks for the development of a fine chemical manufacturing process.

The tasks in the process development are executed more or less in parallel in different parts of the development organisation and efficient information generation and exchange and technology transfer are of the greatest importance.

The main activities in the ***conceptual chemical phase*** are the identification of different chemical routes and the generation of alternative chemical synthesis pathways and process schemes. Relevant routes are evaluated experimentally and preliminary cost estimations are performed to select the best alternative for further development

In the ***conceptual process development phase***, which is iteratively linked to the chemical development phase, the process concept for the selected chemical route is evaluated, *mass balances, preliminary heat balances* and *basic recipes* are generated for the process. *Block diagrams* and preliminary *flowsheets* are produced and the process is implemented to the existing production facility or a new production line is designed. In this procedure, *short-cut models for the reactions and separations* are used. This phase also involves an introductory *safety evaluation* of the process. A preliminary *scheduling* of the operation steps is performed and *Gantt charts* are generated to characterize interrelated time dependent operations and to identify process's bottlenecks. The production capacity is calculated and basic cost estimation is performed to obtain the feasibility of the process. This is the major decision point in the continuation of the development of the process.

The ***chemical development, process development and process engineering phases*** proceed both consecutively and parallel. In the unit process and equipment levels, the reactions and separations of the process are studied more thoroughly in laboratory and bench-scale by the chemists. Reaction enthalpies are estimated or measured with reaction calorimetry. The thermal stabilities of raw materials, products and other process streams, especially distillation residues are determined. *Dynamic mechanistic reactor models* and dynamic separations models (i.e. batch distillation models) are developed for scale-up in co-operation with chemists and chemical engineers. *Kinetic models* are derived or extracted from existing *model library*. *Mass- and heat balances* for the reactor configurations are generated and reaction kinetics is included in the balance models. *Mass transfer and heat transfer correlations* are introduced into the reactor models as needed. Systematic *experimental planning* is utilized in experimentation to improve the identifiability of the *kinetic and transfer parameters*. Dynamic *mass and heat balances* of the whole process and single process units are scaled-up to designed plant capacity. Production *recipes* are updated and *scheduling* of the operation steps and equipment utilization within operation steps are carried out. *Control* systems are implemented into dynamic reactor models. Controllability studies are performed and measures to avoid runaway situations are implemented. The whole *SHE* (*S*afety-*H*ealth-*E*nvironment) area of the process is evaluated.

In the ***commissioning and start-up phase***, dynamic models are used in the plant for the operator training and to assist the decision making in what/if situations (malfunctioning of feeding system causing improper reactant ratios, overdosing active reactant, reduced heat and/or mass transfer, collapsing of mixing or cooling system, etc.).

In the ***validation and optimization phase***, models are validated using relevant plant data. Information is fed back to the R&D function to refine the models and improve the process for

future production campaigns. Single operation steps and process units are optimized after validation and the optimal conditions are linked to overall process and plant optimization. Evolutionary process improvements should be carried out through the whole life cycle of the process.

In the presented fine chemical process development work flow this contribution is focused on the methodologies in the development of dynamic mechanistic kinetic and reactor models, on the methods for generating reliable and consistent data for modelling purposes and on the tasks required in the estimation of parameters for those models. The procedures and modular tools for dynamic modelling are presented in Fig. 2. The application of these procedures is illustrated with two case studies: reductive N-alkylation of an aromatic amine and a Claisen condensation reaction.

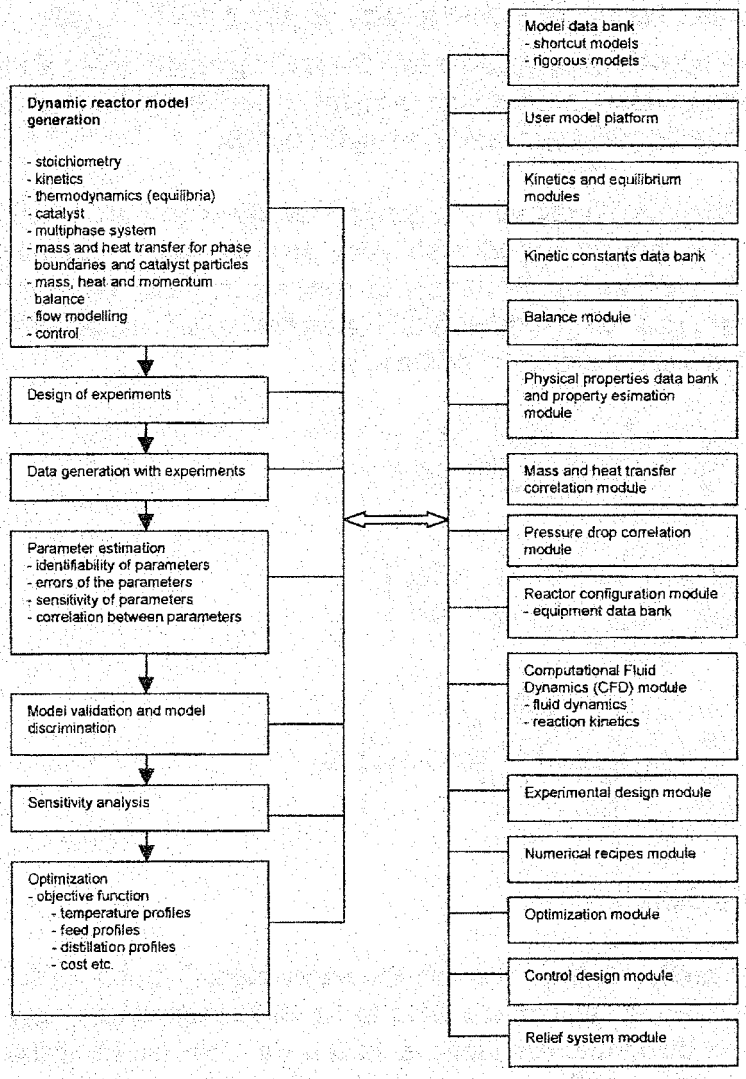

Figure 2. Procedures and tools for dynamic modelling.

2. Kinetic and reactor models

The reactions in the fine chemicals manufacturing are often very complex involving consecutive and parallel reaction steps, which take place simultaneously. This leads as such to complex and detailed kinetic rate equations with numerous adjustable parameters, which are

often correlated and difficult to identify accurately. In addition, many of the short-lived intermediates are not detectable by chemical analysis and so no information of their real concentrations in the reaction medium is available. A practical method of simplifying the kinetic equations for reaction systems with slow and fast reactions is to apply the *quasi-steady state* approximation i.e. To assume the intermediates to be very reactive and thus their generation rates to be approximately zero: $r_i = \sum_{j=1}^{n} \nu_{ij} R_j = 0$ (boudart 1968, laidler 1987). This approach enables the elimination of the concentrations of the intermediates from the generation rate equations of other components and the reduction of the number of adjustable parameters in the kinetic equations. An alternative method for simplifying the kinetic equation is to apply the *quasi-equilibrium* approximation for fast reactions or adsorption and desorption processes of reactive species at the catalyst surface. This treatment implies that the ratio of the forward and backward reaction rates is equal to 1: $R_{j+}/R_{j-} = 1$ for the fast reactions. The equilibrium ratio is introduced into the rate equations of the slow reaction steps enabling the elimination of non-detectable components, model simplification and reduction of the number of parameters by lumping them into single entities.

The reactors used in the manufacturing of organic fine chemicals are mostly multipurpose semibatch and batch reactors equipped with necessary auxiliary equipment for mixing, heating and cooling as well as for distillation or evaporation. The reactions typically take place in the liquid phase and only very seldomly gas phase reactions occur in these kind of systems. The reactor models are generally of the form:

Liquid phase :
$$\frac{d\mathbf{c}_L}{dt} = \mathbf{f}\left(\mathbf{c}_L, \mathbf{c}_G, \frac{d\mathbf{c}_L}{dl}, \frac{d^2\mathbf{c}_L}{dl^2}\right) \qquad (1)$$

Gas phase:
$$\frac{d\mathbf{c}_G}{dt} = \mathbf{g}\left(\mathbf{c}_G, \mathbf{c}_L, \frac{d\mathbf{c}_G}{dl}, \frac{d^2\mathbf{c}_G}{dl^2}\right) \qquad (2)$$

Catalytic reactions:
$$\frac{d\mathbf{c}_L}{dt} = \varepsilon_p^{-1}\left(\mathbf{D}_e \frac{d\left(\frac{d\mathbf{c}_L}{dr} r^s\right)}{r^s dr} + \mathbf{r}\rho_P\right) = 0 \qquad (3)$$

3. Experimental methodology

The proposed reactor model is the basis for the experimental design. The kinetic reactor model gives guidelines, which phenomena have to be studied experimentally to identify the necessary parameters in the model equations in such a way that the fit of the model and the identifiability of the parameters is good enough for the utilization purposes of the model during the lifecycle of the process. The preferable procedure is to try to separate the reaction kinetics from transfer phenomena and to carry out kinetic experiments under mass transfer free conditions to measure the real chemical kinetics and not the apparent mass transfer limited pseudo-kinetics. The model is validated by comparing the simulated results with the results of independent experiments preferably carried out under industrial conditions.

Typically laboratory (0.1-1 l) and bench-scale (1-2 l) reactors, equipped with PC-based data acquisition and control systems, are used in the kinetic measurements of fine chemcal

reactions. The reactors are usually operated batch or semibatchwise. The extent of the reaction is typically monitored using high pressure liquid chromatography (HPLC) and gas chromatography (GC). Modern in-situ UV, NIR, FTIR and Raman techniques enabling continuous monitoring of the spectral information from the reaction mixture, are the future trend in experimental reaction engineering.

4. Numerical methods and parameter estimation procedure

The mechanistic mathematical models for dynamic processes occuring in fine chemical manufacturing can be presented in the form of ordinary differential equations (ODE):

$$\frac{d\mathbf{y}}{dt} = \mathbf{f}(\mathbf{y}, t), \qquad (4)$$

with the initial conditions $\mathbf{y} = \mathbf{y}_0$ at $t = t_0$ where t is typically reaction time and $\mathbf{y}$ represents concentrations of chemical species. Software tools such as the MODEST software (Haario 1994) can be used in solving the ODEs (Hindmarsh, 1983, Marquardt, 1963).

The practical procedure for model building, experimental design, data generation and parameter estimation is summarized in Fig. 3.

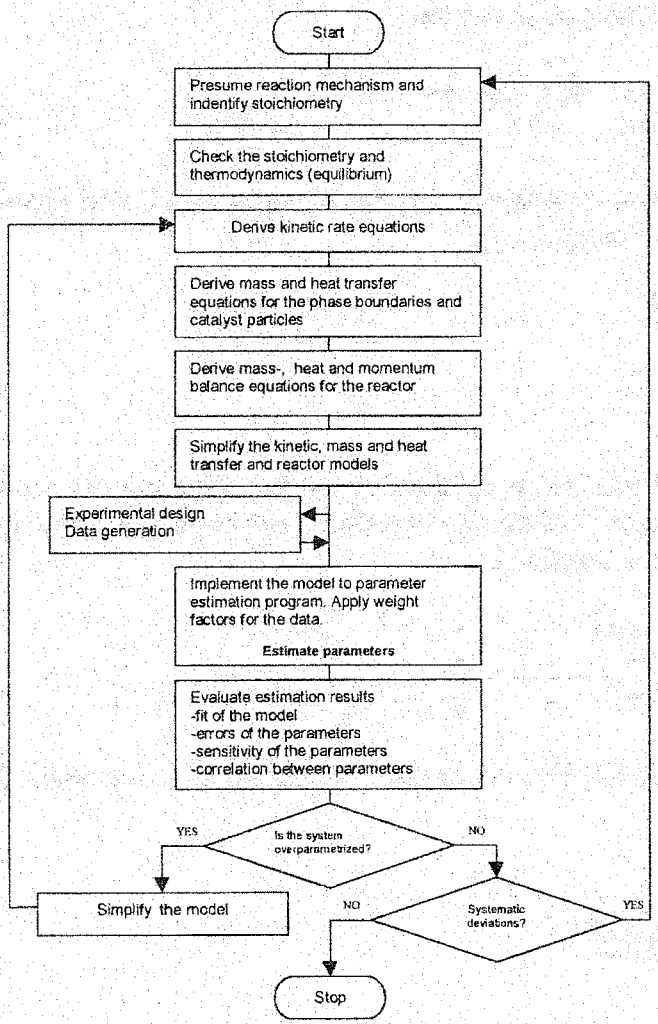

Figure 3. Practical procedure for modelling.

5. Case studies

Case 1. Reductive N-alkylation of an aromatic amine, a homogeneous-heterogeneously catalyzed reaction

Reductive N-alkylation of an aromatic amine is presented as an example of a complex reaction system involving homogeneous reactions and a heterogeneously catalyzed double bond reduction and/or hydrogenolysis (Malone and Merten, 1992, Lehtonen et.al., 1998).

Scheme 1. Reaction scheme for the reductive alkylation of aromatic amines.

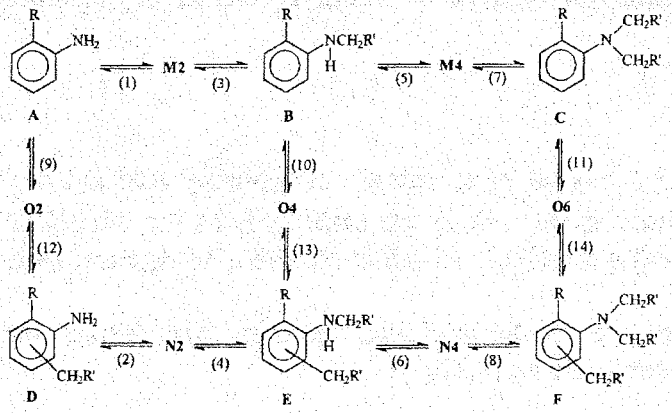

The initiating homogeneous steps can be written

$$\mathbf{A + R'CHO \Leftrightarrow I1} \qquad \mathbf{(I)}$$

$$\mathrm{I1} \Leftrightarrow \mathrm{I2} + \mathrm{H_2O} \qquad \mathrm{(II)}$$

The following kinetic equation is obtained for the homogeneous liquid phase reactions by applying quasi-equilibrium to the rapid step:

$$r_1 = k_1\left(c_A c_{R'CHO} - c_{I2} c_{H_2O} / K_1 K_2\right), \qquad (5)$$

where $K_1 K_2 = \dfrac{c_{I2} c_{H_2O}}{c_A c_{R'CHO}}$.

For the surface reaction that take place on the Pt catalyst, assuming dissociative hydrogen adsorption, consecutive hydrogen addition and product desorption, the following mechanism can be expressed to describe the reactions:

I2*	+	H*	→	I2 H*	+	*
I2 H*	+	H*	→	B*	+	*
I2*	+	2H*	→	B*	+	2* ,

where I2 can be M2, M4, N2, N4, O2, O4 or O6. We obtain a rate equation for the surface reaction:

$$r_3 = \frac{k'_3 c_{I2} c_{H_2}}{\left(1 + K_{I2} c_{I2} + \sqrt{K_H c_{H_2}} + \sum K_J c_J\right)^3}, \qquad (6)$$

where $k'_3 = k_3 K_{I2} K_H$.

The rate of formation or consumption of a component i is the sum of the homogeneous non-catalytic reaction and heterogeneous catalytic reaction:

$$r_i = \sum r_{j,noncat} + \left(\sum r_j\right) \eta \rho_B c_M , \tag{7}$$

The generation rates of chemical species ($\eta = 1$) are summarized below:

$$r_A = -R_1 - R_9 \tag{8}$$
$$r_B = -R_5 - R_{10} + R_3 \rho_B c_M \tag{9}$$
$$r_C = -R_{11} + R_7 \rho_B c_M \tag{10}$$
$$r_D = -R_2 + R_{12} \rho_B c_M \tag{11}$$
$$r_E = -R_6 + (R_4 + R_{13}) \rho_B c_M \tag{12}$$
$$r_F = (R_8 + R_{14}) \rho_B c_M \tag{13}$$
$$r_{M2} = R_1 - R_3 \rho_B c_M \tag{14}$$
$$r_{M4} = R_5 - R_7 \rho_B c_M \tag{15}$$
$$r_{N2} = R_2 - R_4 \rho_B c_M \tag{16}$$
$$r_{N4} = R_6 - R_8 \rho_B c_M \tag{17}$$
$$r_{O2} = R_9 - R_{12} \rho_B c_M \tag{18}$$
$$r_{O4} = R_{10} - R_{13} \rho_B c_M \tag{19}$$
$$r_{O6} = R_{11} - R_{14} \rho_B c_M \tag{20}$$

The reaction scheme was further simplified and the number of rate equations was reduced based on the experimental finding that the ring alkylation reactions are minor and so those reactions could be omitted in the final kinetic treatment.

An example of the fit of the kinetic model to experimental data is presented in Fig. 4.

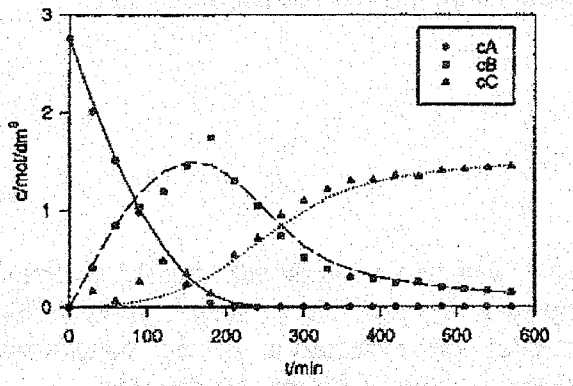

Figure 4. A comparison of experimental data and model simulation for reductive N-alkylation of aromatic amine with aldehyde.

PL-7

Case 2. Kinetics and mass transfer of organic liquid-phase reactions in the presence of a sparingly soluble solid phase

Claisen condensation is presented as an example of an organic liquid phase reaction, which takes place in the presence of a reactive, but sparingly soluble solid compound, in this case a methoxide (Tirronen, et.al., 2000).

Scheme 2. The reaction scheme of Claisen condensation.

Step 1

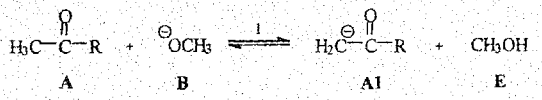

Step 2

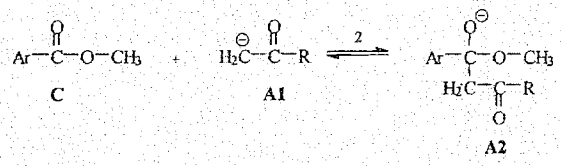

Ar = aromatic ring
R = alkyl chain

Step 3

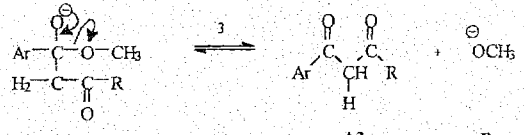

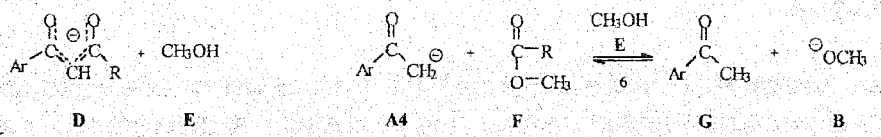

Steps 4, 5 and 6

Based on the simplified treatment of the reaction pathway, the elementary steps leading to the formation of the final product (D) and methanol (E) can be compressed to

A + B	⇔	A1 + E
A1 + C	⇔	A2
A2	⇔	A3 + B
A3 + B	⇔	D + E
A + B + C	⇔	D + 2E

Where A, B, C, D and E are analytically detectable compounds and A1 (carbanion), A2 and A3 are the reaction intermediates. Applying the quasi-steady state hypothesis on the reactive intermediates (A1, A2 and A3) enables the elimination of the concentrations of the intermediates and an analytical expression is obtained for the reaction rate:

$$r = k\left(c_A c_B c_C - \frac{c_E^2 c_D}{K}\right)\cdot\left(k_2 k_3 k_4 c_C + \left(\frac{k_2 k_3}{K_2 K_3} + \frac{k_2 k_4}{K_2} + k_3 k_4\right)\frac{k_1 c_E}{K_1}\right)^{-1} \qquad (21)$$

where $k = \prod_{j=1}^{4} k_j$ and $K = \prod_{j=1}^{4} K_j$.

For modelling purposes, eq. (21) was further simplified to improve the identifiability of the parameters in the estimation. The kinetic equation (22) was applied in the model for the main reaction scheme.

$$r = \frac{k_1 c_A c_B c_C}{c_C + K''' c_E} \tag{22}$$

The rate equations were coupled to the mass balances of the compounds in the reactor.

$$\frac{dn_i}{dt} = \dot{n}_{0_i} + N_i A + r_i V \tag{23}$$

In this particular case the compound (A) was fed into the reactor and the compounds (B, in this case sodium methoxide) existed predominantly in the solid phase due to its limited solubility. The mass transfer of B was rapid i.e. c_B was replaced with c_B^* in the rate expression.

An example of the fit of the model to experimentally measured concentrations is presented in Figure 5.

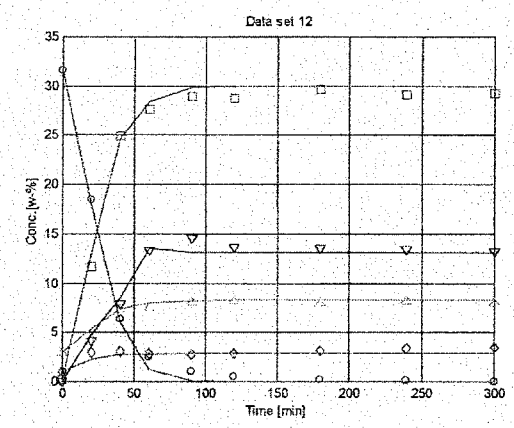

Figure 5. Comparison of experimental data and model simulation for Claisen reaction.

Symbols: A (∇), C (o), D (□), E (Δ), S21 (◊).

6. Conclusions

This contribution deals with the methodologies in the development of dynamic mechanistic kinetic and multiphase reactor models for batch and semibacth reactors for processes which take place in the manufacturing of fine chemicals. The practical methods for generating experimental data for the modelling purposes and the tasks required in the estimation of parameters for the models were covered. These methodologies are an essential part of the process development workflow concept and improve the utilization of models as tools during the process development cycle enabling a shorter development time and a higher performance of the new processes.

7. Notation

PL-7

A	mass transfer area or cross section
c	concentration
D	diffusion or dispersion coefficient
K	equilibrium constant
K', K'', K'''	lumped parameters
l	length coordinate
M	molar mass
m	mass
N	flux
n	molar amount of substance
$\dot{n}$	molar flow
R	reaction rate
s	shape factor
r_i	generation/consumption rate
r	particle radius
t	time
V	volume
y	state variable

Greek letters

ε	hold-up, void fraction
η	catalyst effectiveness factor
ν	stoichiometric coefficient
ρ	density

Subscripts and Superscripts

B	bulk
G	gas phase
i	component index
j	reaction index
L	liquid phase
p	particle
S	solid phase
0	inlet or initial condition
*	saturated state

8. References

Boudart, M., *Kinetics of Chemical Processes*, Prentice-Hall Inc., Englewood Cliffs, N.J.,1968, 67-70.

Haario, H., *MODEST-User's Guide*; Profmath Oy: Helsinki, 1994

Hindmarsh, A. C., A Systematized Collection of Ode-Solvers in Scientific Computing; Steple, R., et al., Eds.; IMACS North-Holland; Amsterdam, 1983, 55-64.

Laidler, K. J., *Chemical Kinetics*, Harpe&Collins, New York, 1987, 282.

Lehtonen, J., Salmi, T., Vuori, A. and Tirronen, E., (1998), On the Principles of Modelling of Homogeneous-Heterogeneous Reactions in the Production of Fine Chemicals. A case study: Reductive Alkylation of Aromatic Amines, Organic Process Research & Development, 2, 78-85.

Malone, R.J. and Merten, H.L., (1992), A Comparative Mass Transfer Study in the Reductive N-Alkylation of Aromatic Nitro Compounds, *Chem. Ind.*, **47**, 79-85.

Marquardt, D. W., An Algorithm for Least Squares Estimation on Nonlinear Parameters. *SIAM J.* 1963, 431-441.

Tirronen, E., Salmi, T., Lehtonen, J., Vuori, A., Grönfors, O., Kaljula, K., (2000), Kinetics and mass transfer of organic liquid-phase reactions in the presence of a sparingly soluble solid phase, *Organic Process Research & Development,* **4,** 323-332.

Tirronen, E., A Methodological Approach to process Development in the Fine Chemical Industry, Doctoral thesis, Åbo Akademi, Åbo, Finland, 2000.

Section I

PHYSICO-CHEMICAL AND MATHEMATICAL BASES OF PROCESSES OCCURRING ON CATALYSTS SURFACE

KINETICS AND MODELLING OF o-XYLENE HYDROGENATION OVER Pt/γ-Al_2O_3 CATALYSTS

A. Kalantar Neyestanaki, P. Mäki-Arvela, H. Backman, J. Wärnå, T. Salmi, D.Yu. Murzin, H. Karhu, T. Ollonqvist* and J. Väyrynen*

Laboratory of Industrial Chemistry, Process Chemistry Group, Åbo Akademi, Biskopsgatan 8, FIN-20500, Turku/Åbo, Finland,
ph: +358 2215 4985, fax: +358 2215 4479, e-mail: dmurzin@abo.fi
**Department of Applied Physics, Laboratory of Electron Spectroscopy and Surface Physics, University of Turku, Vesilinnantie 5, FIN-20014 Turku/Åbo, Finland*

Introduction

Catalytic hydrogenation of aromatics is used in oil refining industry to lower the amount of undesired aromatic hydrocarbon in diesel fuels. The rate of aromatic hydrogenation is strongly affected by steric factors as the hydrogenation rate decreases by substitution of alkyl groups to the aromatic ring. The kinetics of gas-phase catalytic hydrogenation of xylenes has been investigated over supported Ni, Pd and Rh catalysts [1-4]. However, there are no data on xylene hydrogenation over supported platinum catalysts. The aim of the present study was to investigate the kinetics of gas phase hydrogenation of o-xylene over highly dispersed Pt/alumina catalysts as well as stereoselectivity of the final products at temperature ranges of 430-520 K. Different characterization techniques were used to correlate the catalytic activity and selectivity as well as the understanding of the surface catalytic chemistry.

Experimental

Alumina supported platinum catalysts were prepared by impregnation of γ-alumina support (LaRoche) having a surface area of 220 m^2/g with solutions of H_2PtCl_6. The catalysts were washed and dried at 353 K. The activity of the catalyst were tested in a continuous flow tube reactor at WHSV of 116 h^{-1} and partial pressures of H_2 and o-xylene of 0.19-0.38 bar and 0.04-0.10 bar; respectively. Argon was used as make-up gas. Special experiments were carried out to ensure that the kinetics is measured in the absence of external and internal diffusion limitations. Prior to the experiments the dried catalysts (125-150 μm, 60 mg) were reduced *in situ* in H_2-flow at the pre-set temperature, followed by cooling to the reaction temperature at which point the reactants were introduced to the catalyst. The experimental set-up for the catalyst testing is illustrated in Figure 1.

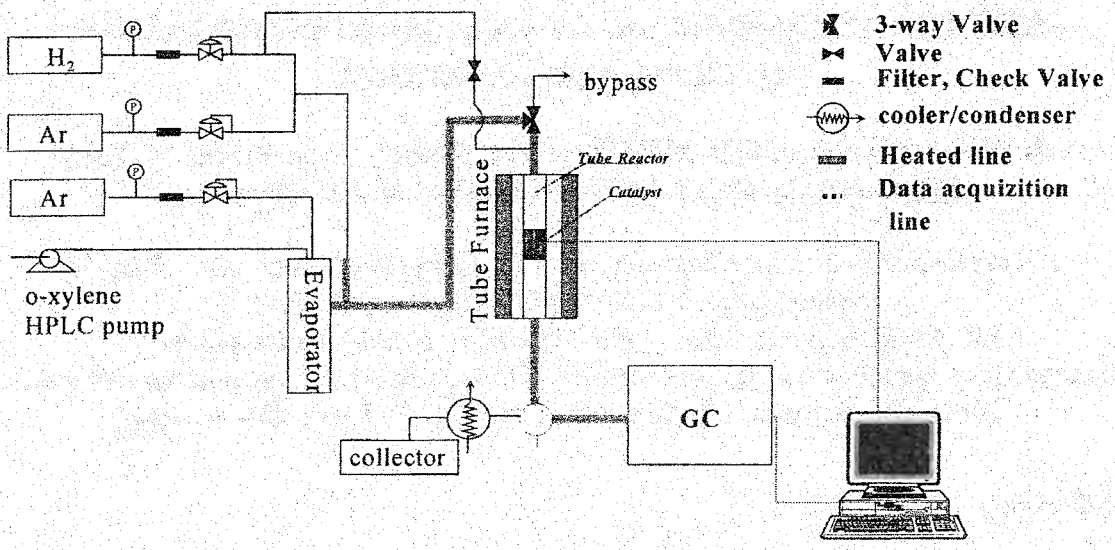

Figure 1: The experimental set-up for catalyst testing.

The products were analysed by GC and confirmed by GC-MS. The prepared catalysts were characterised by N_2-adsorption, H_2-adsorption, H_2/o-xylene-TPD and XPS.

Results and Discussion

The thermodynamic calculation for the gas composition and the operation temperatures used is given in Figure 2. A typical kinetic run is presented in Figure 3. As shown catalyst deactivation took place during the first 20 minutes and steady-state operation was reached. *Cis* and *trans* 1,2-dimethyl cyclohexane (1,2-DMCH) were the only hydrogenation products (i.e. no alkylcyclohexene was detected) and their ratio did not change during the initial catalyst deactivation. Table 1 presents the hydrogenation rate at different catalyst reduction temperature. The highest rate was obtained with the catalyst reduced at 673 K. The amount of H_2-desorbed from the catalyst surface from the TPD experiments was correlated to the hydrogenation rate (Table 1). The reduction of the catalyst at 673 K was therefore selected in kinetics experiments.

Figure 4 represents the hydrogenation rates as a function of temperature. The rates passes through a maximum at ca. 460 K. Thermodynamic calculations (Figure 2) indicates that the experimental data are obtained in the region very far from the equilibrium, therefore, the decrease in the hydrogenation rate above 460 K can be solely attributed to the hydrogenation kinetics.

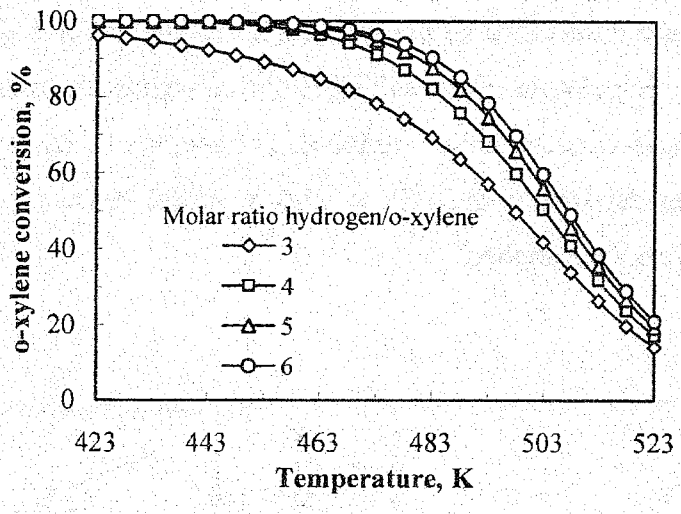

Figure 2: The thermodynamic calculation of o-xylene hydrogenation under the operation conditions.

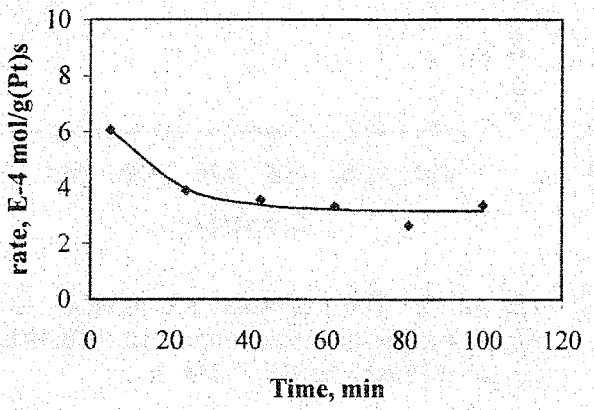

$r = a_3 + a_1 \exp(-a_2 t)$; [6]

where:

$a_1 = k_s r_0/(k_s + k_{-s})$

$a_2 = k_s + k_{-s}$ *and* $a_3 = k_{-s} r_0/(k_s + k_{-s})$

k_s & k_{-s}: rate constants for deactivation and self generation

r_0: rate in deactivation free conditions

Figure 3: The time on stream hydrogenation rate over the Pd/alumina catalyst. T = 470 K, p_{H2} = 0.38 bar, $p_{o\text{-}xyl}$ = 0.06 bar, WHSV = 116 h^{-1}.

Table 1: Comparison of the catalysts activity at 460 K. p_{H2}=0.38 bar , $p_{o\text{-}xyl}$=0.06 bar, WHSV = 116 h^{-1}.

Catalyst	$T_{reduction}$, K	$T_{reaction}$, K	Rate 10^{-4} mol/g(Pt)s	Amount desorbed*, mmol/g catalyst
1% Pt/Alumina	673	460	4.08	0.447
1% Pt/Alumina	623	460	2.04	0.389
1% Pt/Alumina	573	460	1.18	0.339

*- First H_2-desorption peak corresponding to H_2-desorbed from platinum [5].

The reaction orders in hydrogen and o-xylene partial pressures were determined in temperature ranges of 430-520 K with intervals of 10 K. The orders in o-xylene was found to be

close to zero at all the temperatures investigated. The order in hydrogen partial pressure increased with temperature from 0.9 at 430 K to 3 at 520 K, suggesting a decreased hydrogen coverage by increased temperature. The result indicated an increased *cis/trans* 1,2-DMCH ratio by increased hydrogen concentration. On the other hand, the *cis/trans* ratio decreased by increased operation temperature (Figure 5). A kinetic model based on advanced reaction mechanism was developed and applied.

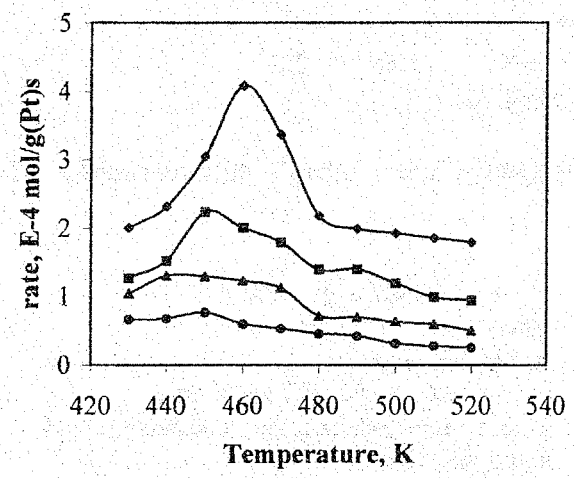

Figure 4: Hydrogenation rate as a function of temperature at p_{H2} : -♦- 0.38, -■- 0.31, -▲- 0.25, -●- 0.19 bars; $p_{o\text{-}xyl} = 0.06$ bar.

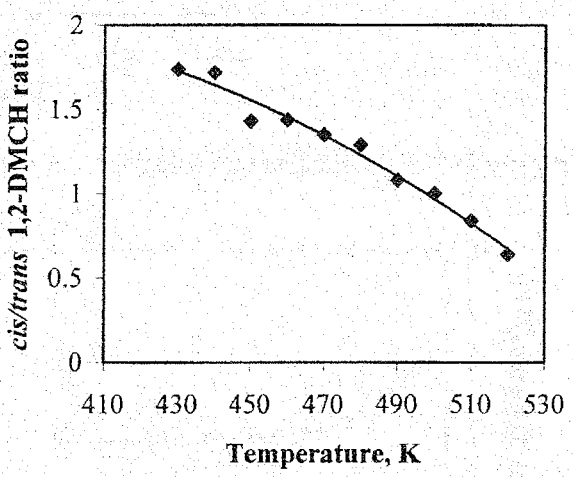

Figure 5: The *cis/trans* 1,2 DMCH as a function of reaction temperature. $p_{H2} = 0.38$ bar, $p_{o\text{-}xyl} = 0.06$ bar, WHSV = 116 h^{-1}.

References

1. S. Smeds, D. Yu. Murzin and T. Salmi, *Appl. Catal. A: General,* 253(**145**)1996.
2. S. Smeds, D. Yu. Murzin and T. Salmi, *Appl. Catal. A: General,* 141(**207**)1996.
3. M. A. Keane, *J. Catal.*, 347(**166**)1997.
4. M. V. Rahaman and M. A. Vannice, *J. Catal.*, 251(**127**)1991.
5. R. Kramer and M. Andre, *J. Catal.*, 287(**58**)1979.
6. M. Consoni , R. Touroude and D. Yu. Murzin, *Chem. Eng. Tech.*, 605(**21**)1998.

THE NEW PHYSICO-CHEMICAL APPROACHES TO REGULATE THE SURFACE OF CATALYST CARRIERS

K. Diblitz, T. Feldbaum, S. Maedje, M. Keung, K. Krause, A. Malyschew, T. Rappert[1]

Ueberseering 40, D-22297 Hamburg, SASOL Germany GmbH

As known from modern catalytic surface science the nature and quality of the carrier material is a key part of catalysis. Defined properties and consistent quality of the carrier material are key-requisites for a successful catalyst. This paper will demonstrate the possibilities and flexibility of CONDEA's alkoxide technology in terms of manufacturing aluminas, silica-aluminas, hydrotalcites and other mixed oxides as raw materials for the catalytic industry.

The CONDEA group operates two different types of processes for the manufacture of alkoxide derived aluminas and related products, the Ziegler-ALFOL process and CONDEA's On-Purpose Process. The Ziegler process is a co-production process of linear fatty alkohols and alumina, using alumo- organic compounds as intermediates, CONDEA's own On-Purpose technology is based on the formation of aluminum alkoxide from aluminum metal and alcohol. In both processes the formation of alumina is achieved by hydrolysis of aluminum alcoholates with water.

$$Al(OR)_3 + 2\,H_2O \longrightarrow AlOOH + 3\,ROH$$

Alumina from the hydrolysis of alcoholates is typically obtained in the form of boehmite or pseudoboehmite. It is important to mention that both processes give products of equivalent quality. Subsequent processing steps lead to a variety of different alumina products of high purity and defined physical properties such as

- boehmite aluminas of different crystallite size, porosity, particle size and peptisation or dispersion behaviour
- calcined aluminas of different phase compositions (gamma, delta/theta, alpha), porosities, surface areas, particle sizes and attrition resistance
- shaped carriers (spheres, extrudates, and tablets).

[1] Author for correspondence: thomas.rappert@condea.de; tel. ++49 40 6375 1236; fax ++49 40 6375 3626

OP-I-2

Besides boehmite and boehmite derived calcined alumina, bayerithe and η-aluminas are produced via this technology. Also accessible is an almost unlimited variety of high purity mixed oxides such as silica aluminas, hydrotalcites, and doped aluminas.

Alkoxide manufacturing technology for aluminas and related products as developed by the CONDEA group offers the following advantages to the catalyst manufacturer who is looking for high purity raw materials with defined physical properties.

- The alkoxide process allows close control over important physical properties and guarantees a consistent product quality at high purity level.
- Possibilities to tailor-produce properties like processing performance, pore size distribution, acidity and many more enable the catalyst manufacturer to adjust the desired performance of a catalyst.
- Besides pure alumina, other materials like doped aluminas, silica aluminas and hydrotalcites can be manufactured via the alkoxide process.

DEHYDRATION OF PHENYLETHYL ALCOHOL ON γ-Al_2O_3 BY MEANS OF THE ELECTRIC FIELD

A.A. Lamberov, I.G. Shmelev

Kazan State Technological University
K. Marx St., 68, 420015, Kazan, Russia, E-mail: rrg@kstu.ru

Our scientific interests lie in the sphere of the heterogeneous catalysis, the applied electrochemistry, the inorganic synthesis and the solid state physics. We study conditions for developing new catalysts and supports for the petrochemical and organic synthesis. A novel γ-Al_2O_3 technology with the use of the elements of the applied electrochemistry has been developed in our laboratory, which seems to be of significance. The application of our technology for the production of the dehydrating and desulfurization catalysts of diesel fuel has shown a number of advantages.

The industrial dehydrating of phenylethyl alcohol in styrene has been carried out under 250-300 °C on the γ-Al_2O_3 in the presence of steam. The research of the authors [1] showed, that the electrical conductivity of γ-Al_2O_3 increases in the presence of steam. The dehydrating of phenylethyl alcohol by means of the electric field increases the reactions speed as a result of increasing Fermi level in the catalyst [2, 3]. Both γ-Al_2O_3 and ZnO are known to be the n-type semiconductors; hence it was of great interests for us to study the dehydration of phenylethyl alcohol in the electric field. The installation used is in the Figure 1.

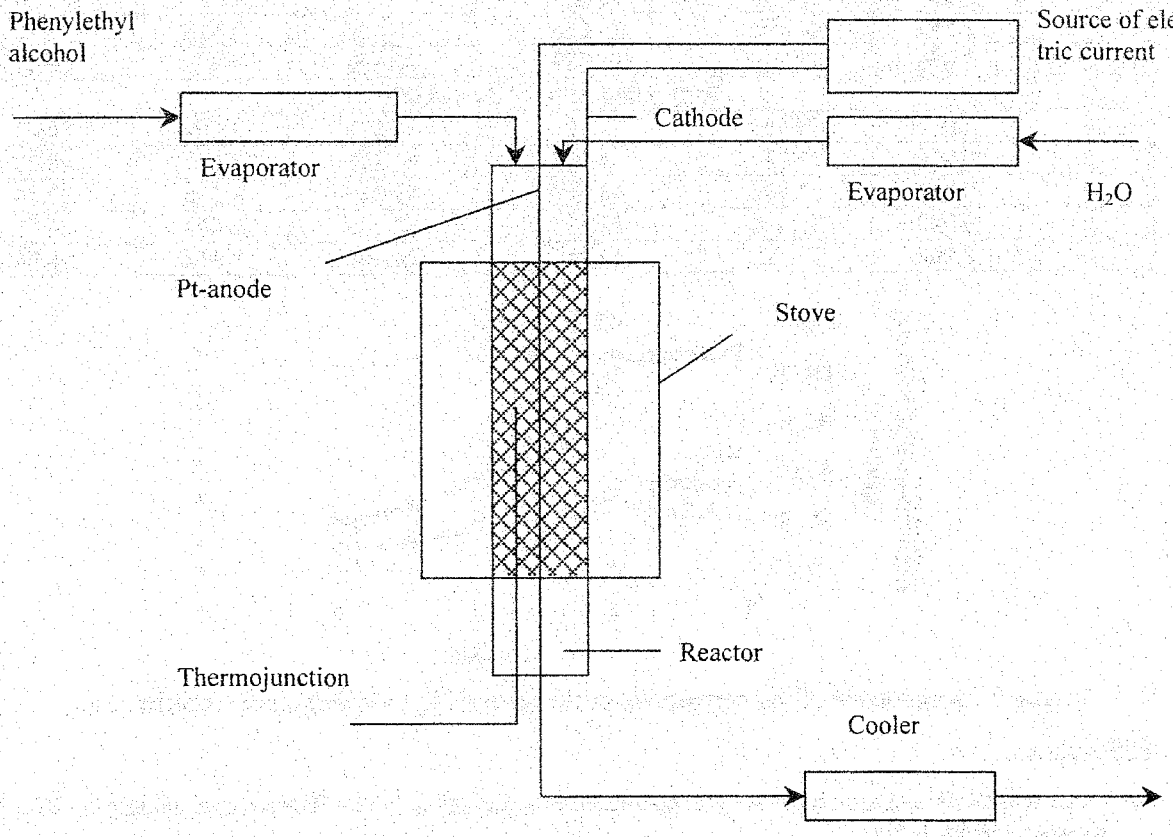

Figure 1. The installation for the dehydration of phenylethyl alcohol in styrene

OP-I-3

We have used 0.16-0.20 mm fraction of γ-Al_2O_3 as a catalyst. It can be seen that Pt-electrode was incepted into the center of the reactor. The reactor wall was used as a second electrode. The electric current up to 16 A run through the electrodes after the loading of the catalyst and the polarization of the electrodes. The electric current value greatly increases when the steam is passed through the catalyst. The introduction of the phenylethyl alcohol vaporous also increases the electric current value, but at a lass extent. The electric current value increases by 20 times when the steam and the phenylethyl alcohol vaporous are jointly passed in 1 : 1 relatively. The electric current value has been found to be constants upon the reactor operating. In the beginning of the polarization of the catalyst the conversion of phenylethyl alcohol increases by 260 %, and in the course of 6 hours it dropped to 18 %. The dependence of the conversion of the phenylethyl alcohol on the voltage is of the extreme character. There were found no changes in the composition of the reaction products during the polarization. The results obtained are presented in the Table 1.

Table 1. The results of catalytic research of γ-Al_2O_3 (T=180 °C; correlation phenylethyl alcohol:H_2O = 1 : 1).

Probe, hours	C_6-C_8, %	Styrene, %	Methylphenyl-cetone, %	Phenylethyl alcohol, %	C_{10+}, %	Conversion of phenylethyl alcohol, %
Initial fuel						
-	1.189	0.001	11.759	84.894	2.657	-
Without polarization of the γ-Al_2O_3						
2	2.110	24.906	13.482	58.155	2.574	31.50
3	2.113	10.571	12.770	72.898	1.647	14.13
4	2.034	17.424	12.902	67.017	2.522	21.06
5	2.555	6.316	11.666	77.484	2.878	8.73
6	1.876	6.217	14.783	76.390	2.433	10.02
With polarization of the γ-Al_2O_3						
2	1.060	67.466	12.071	16.012	3.389	80.41
3	0.999	37.237	14.987	41.871	1.647	48.78
4	0.897	27.584	16.010	51.310	4.198	37.24
5	0.940	21.420	13.978	60.179	3.383	26.38
6	0.868	17.415	12.242	66.406	3.068	18.76

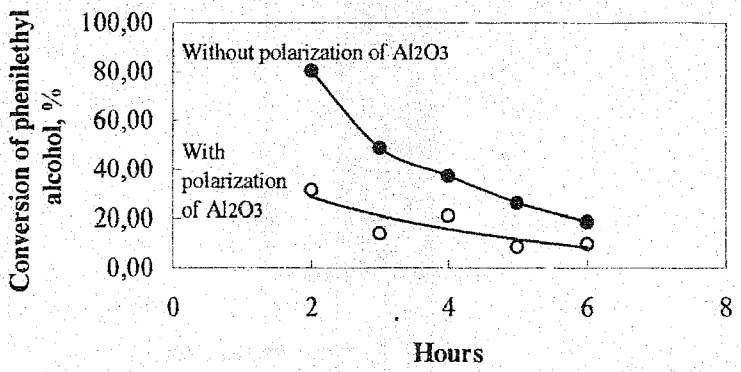

Figure 2. Dependence of the conversion of the phenylethyl alcohol on the reaction time.

References:

1. Fundamentals of provision of a catalytic operation. Proceedings of the IV International Congress, 1970, V. 1, Moscow, Nauka, 507 p.
2. N.P. Keier, E.P. Micheeva, L.M. Usoltseva. Kinetika I Kataliz, 1967, v. 8, N 5, p. 1199
3. V.F. Kiselev, O.V. Krylov. The electronic phenomena in an adsorption and catalysis on a semiconductors and dielectrics. 1979, Moscow, Nauka, 236 p.

A NEW TIME DEPENDENT MONTE CARLO ALGORITHM FOR STUDYING THREE-PHASE BATCH REACTOR PROCESSES

Giampaolo Barone and Dario Duca

Dipartimento di Scienze Farmaceutiche, Università di Salerno,
Via Ponte Don Melillo I-84084 Fisciano (SA), Italy

A time dependent Monte Carlo (tdMC) algorithm [1,2] for studying catalytic processes occurring in three-phase batch reactor has been developed and implemented in Fortran language. This tdMC code has been employed to mimic experimental results [3] of the industrially relevant [4] isobar and isotherm hydrogenation of 2,4-dinitro-toluene in ethanol solution in presence of Pd catalysts [5].

It has been found [5] that the latter reaction occurred via a complex network, originating product distributions influenced by several factors: temperature and pressure of the reaction system, concentration of reagents intermediates and products, morphology of the catalyst. However, due to the intrinsic complexity of the reaction, in our opinion the microscopic aspects of the title reaction were not achieved by the experimental approaches, interpreted by ordinary differential equation systems. Therefore, we tried to get microscopic details on the three phases 2,4-dinitro-toluene hydrogenation on Pd surfaces employing the tdMC algorithm above. Experimental findings were reproduced, modelling the activity-selectivity pattern of the reaction on a given Pd catalyst, by employing as fitting parameters the probability of occurrence of the simple events involved in the same reaction and using quantum-mechanical preliminary information.

Our tdMC code allowed us to state the role of all the intermediates present in the catalytic 2,4-dinitro-toluene hydrogenation, some of which not yet isolated by experimental procedures. Furthermore, the model predicted aspects not experimentally investigated and, reproduced the inmost physical and chemical characteristics of the same reaction system [3].

The simulations showed that the surface population occurring along with the hydrogenation, contrarily to what already claimed [5], cannot be explained by considering simply metal dispersion effects or a bi-dimensional analogous of the well-known 'random parking model'. Conversely, both the effects above have to be contemporaneously present, becoming more or less important depending on the particle morphology and on the involved surface reaction species.

Here, we report the relevant technical details of the model and the simulation procedures. The 36 different species we considered in the simulation were:

- in solution, 2,4-dinitro-toluene, 2,4-diamino-toluene and the seven possible intermediates,
- on the surface, three different arrangements for any of the adsorbed species above.

Fig. 1 shows, for the 2,4-dinitro-toluene molecule, the three possible arrangement of the surface species: fat constellation, **FC**, with the benzene ring parallel to the catalyst surface, and hindered-flag and free-flag constellation, **HFC** and **FFC** respectively, with the toluene derivatives interacting vertically to the Pd surface through the nitro, hydroxyamine or amine group in position 2 and 4, respectively. Incidentally, we have to stress that by the analysis of our findings, the role of the 2,4-dinitro-toluene **FC** species is generally shrunk with respect to the original interpretations [5].

The volume occupied by the species in water-ethanol solution, calculated using optimised geometries, by quantum mechanical calculations at HF level, was used to determine [3] the hitting probabilities of the solvated species. The hitting of the water molecules was used to synchronise the internal clock [1-3] employed in the tdMC simulations. The production of

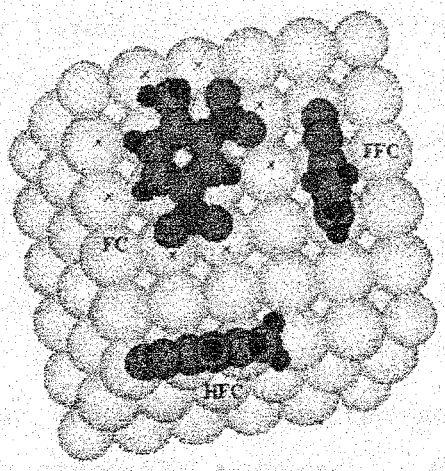

Fig. 1 2,4-di-nitro toluene molecules adsorbed in the fat, free flag and hindered flag constellation (FC, FFC and HFC) on a {100} plane of a Pd cluster. Legend: Pd atoms, light grey bigger spheres. C atoms, dark grey medium sized spheres. NO_2 fragments, light grey medium sized spheres. H atoms, black spheres. Dimensions of the spheres are normalised to the vdW radii of the atoms. Sites labelled by x are hindered, following the adsorption as mimicked in the tdMC simulations.

water occurring along the reaction did not affect the timing progression. This evidence induced us to allow the algorithm to change the sizes of the time unit when, due to the surface species distribution, the only possible events became the hitting of the solvated species. This procedure dramatically shortened the simulation time.

The molecular volumes were also employed to determine the surface sites hindered by the different species. Following the adsorption in the three different modes, the hindered sites were: 3 for **FFC**, 4 for **HFC** and 12 for **FC** (see Fig. 1). The steric hindrance of the hydrogen surface species, as usual, was considered null [6]. Quantum mechanical calculations performed on Pd_4 and Pd_6 clusters interacting with C_6H_6 or other model molecules composed by

the fragments $-C_6H_5$, $-NO_2$, -NHOH and $-NH_2$, gave an estimate of the energy needed for the desorption processes involving the same species.

Adsorption (hitting followed by sticking), desorption and reaction events of the different species were taken into account. To each of these steps, an occurrence probability was assigned for given reference time and number of metal surface sites. The tdMC code automatically updated solution and surface population, dynamically changing along the simulated reaction. The catalytic system was fully reproduced by normalising the values of the experimental extensive variables to the number of the surface sites considered. Actually, the reaction system was modelled as represented in Fig. 2. From the whole solution we isolated a micro-portion constituted by a metal particle of 10000 sites centred in a drop of solution. The volume of the drop was normalised to the area of the metal particle sites, knowing the experimental total exposed metal surface area and the whole solution volume.

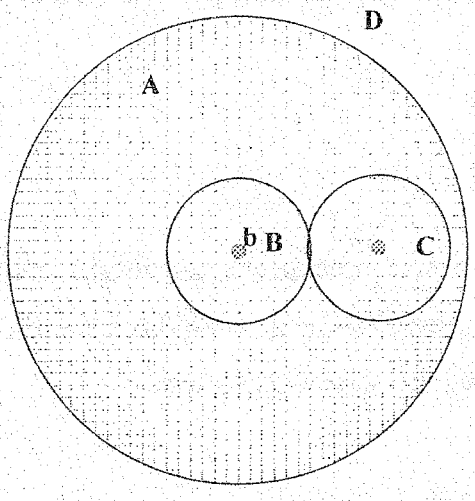

Fig. 2 Reactor Model: A, solution phase; B and C, micro-portions of solution, centrally including one grain of catalyst (e.g. b sphere); D, gas phase. Rays of the spherical regions are not scaled down. Metal surfaces can be considered spherical due to the periodic boundary conditions introduced.

This model assumes chemical regime conditions, which indeed were verified both in experimental [5] and simulative [3] sessions. Besides the H_2 concentration, fixed in the solution phase, the chemical characteristics of the drop changed dynamically along the reaction whereas its temperature was maintained constant.

The tdMC took account of all these characteristics. The metal particle, reproduced by 100 x 100 squared matrices, mimicking a mixing of adequately balanced {100} and {111} fcc Pd faces, was characterised by periodic boundary conditions. Different metal dispersion values were also modelled, introducing a proper number of gaps on the surface (matrix) [2]. Available surface energy, ASE, distributions [2] were not explicitly taken into consideration. However, the necessity to consider ASE distributions stood out, as expected, analysing the simulation results, and this will be the subject of next tdMC studies. The present algorithm allows one to calculate in two different ways the TOF values, considering either the transfor-

mations of the surface species or directly the concentration changes of the solution reagent and intermediate species. The program could also account of the water and ethanol sticking and of the surface deposit formation.

In order to reduce the number of parameters to be considered in reproducing experimental results the code can group together homologous actions hence their occurrence probabilities (e.g. probabilities of reaction of $-NO_2$ fragments in different positions or different surface species). Moreover, the desorption probabilities of the different toluene species can be obtained assuming independent probabilities of desorption of single fragments composing the whole molecule. Since surface hydrogen atoms are considered as ghost species [2,3,6], events of H species were not explicitly considered in the model. Diffusion of toluene derivatives did not influence the computational results on the whole reaction, hence, after preliminary studies, they were not considered. Initially, the events occurrence probabilities were taken from the "ceiling". Subsequently, a fit procedure was used to refine these parameter values. To obtain fit parameters the following function was minimised:

$$F = \frac{1}{n}\sum_{i=1}^{n}\left|\frac{\delta_{p_i}}{\varepsilon_{p_i}}\right|$$

where δ_p and ε_p are the differences found between simulated and experimental results and the experimental error of the i^{th} point, respectively. Values of F close to 1 validated the fitting model. Fitted points were related to the experimental activity-selectivity pattern.

References

1. D. Duca, L. Botár and T. Vidóczy, *J. Catal.*, 162 (1996) 260.
   D. Duca, P. Baranyai and T. Vidóczy, *J. Comp. Chem.*, 19 (1998) 396.
2. D. Duca, G. La Manna and M.R. Russo, *Phys. Chem. Chem. Phys.*, 1 (1999) 1375.
   D. Duca, G. La Manna, Zs. Varga and T. Vidóczy, *Theor. Chem. Acc.*, 104 (2000) 302.
   D. Duca, G. Barone, Zs. Varga and G. La manna, *J. Mol. Struct. (Theochem)*, 000 (2001) 000.
3. G. Barone and D. Duca, *J. Catal.*, submitted.
4. C.L. Thomas, in "Catalytic Processes and Proven Catalysts" Academic Press, New York, 1970.
5. G. Neri , M.G. Musolino, E. Rotondo and S. Galvagno, *J. Mol. Catal. A: Chem.* 111 (1996) 257.
   M.G. Musolino, C. Milone, G. Neri, L. Bonaccorsi, R. Pietropaolo and S. Galvagno, *Stud. Surf. Sci. Catal.*, 108 (1997) 237.
6. D. Duca, G. Barone and Zs. Varga, *Catal. Letters*, 000 (2001) 000.
   G. La Manna, G. Barone, Zs. Varga and D. Duca, *J. Mol. Struct. (Theochem)*, 000 (2001) 000.

Corresponding author:
Professor Dario Duca, Tel: ++39-089-962648, FAX: ++39-089-962828, e-mail: dduca@unisa.it

APPLICATION OF MATRIX ELIMINATION METHODS IN PROCESS SIMULATION

Mark Lazman

AEA Technology Engineering Software Hyprotech Ltd
707 – 8th Avenue SW Suite 800,
Calgary, Alberta CANADA T2P 3V3
MarkL@Hyprotech.com

"Matrices are forever" was a title of review on applied mathematics in chemical engineering. Engineers tend to think in terms of matrices when dealing with linear or linearized problems. We will also discuss this conventional domain: sparse elimination methods in flowsheet simulation and optimization. The second part of presentation deals with more intriguing subject: matrix elimination methods in non-linear situation. This technique allows effectively solve non-linear steady-state problems.

1. Simultaneous approach to real time optimization

The flowsheet is a set of interconnected unit operations and process streams. Flowsheet optimization requires the solution of non-linear programming problems. Recent developments in process simulator architecture resulted in simultaneous modular optimization procedure.

The flowsheet is subdivided into disconnected blocks. Additional constraints and variables represent their connectivity conditions. HYSYS™ flowsheet simulator supports this decomposition. Speed and reliability of optimization strongly depend on efficiency of derivative estimation. The efficiency problem becomes critical for complicated unit operations like distillation columns that require intensive iterative calculations. Slow calculation of column partial derivatives may diminish benefits of modular solution. Column should be solved at least n times to estimate the derivatives by n parameters even in case of simplest forward difference derivative approximation. Calculation of numerical derivatives requires tight column tolerances. This results in slower and less stable individual calculation. Cost of repetitive runs makes prohibitive calculation of optimal finite difference interval.

Application of analytic differentiation addresses all these issues. It is sufficient to solve column once to find n derivatives. HYSYS™ allows different methods of simulation and solution of column balances including simultaneous method. Sparse Continuation Solver combines homotopy continuation with Newton type algorithm based on Sparse linear elimination technique applied to the block diagonal type linear problem (fig 1).

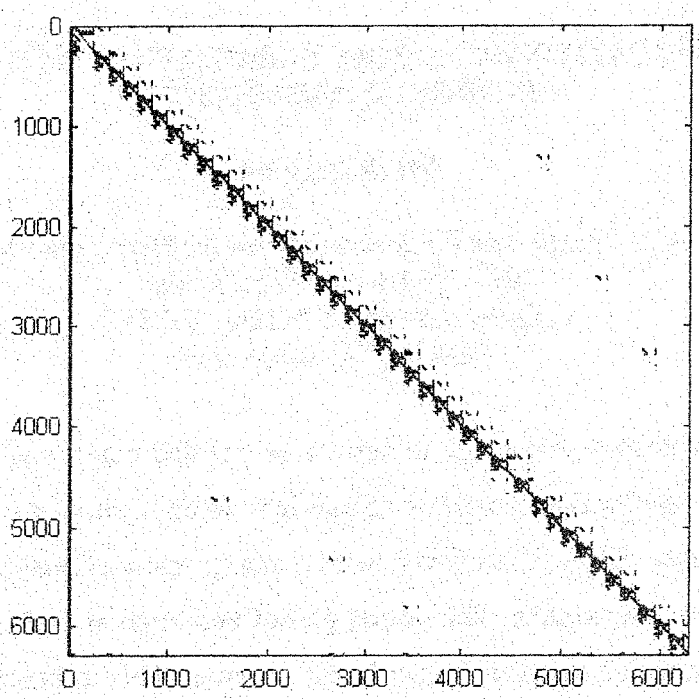

Fig.1 Jacobi matrix of Column model

Simultaneous solver allows the analytic derivatives. Implementation of analytic derivatives reduces calculation time. Furthermore, derivative calculator produces acceptable derivatives applying standard tolerances.

2.Polynomial elimination in kinetic problems

Quasi Steady State approximation

Equations of chemical kinetics in closed lumped system with complex reactions have form

$$dc/dt = \Gamma^t u \qquad (1)$$

where c is vector of components concentrations, Γ is stoichiometric matrix, and u is normalized vector of reaction stage rates. Classic kinetics assumes Mass Action Law (MAL) for rate of reaction stage. Common method of reaction rate equation derivation is based on Quasi Steady State Approximation (QSSA). QSSA is based on zero order approximation of integral manifold of the fast processes. Correspondent differential equations are simply replaced with algebraic equations

$$\Gamma^t u = 0, \qquad (2)$$

Matrix Γ accounts now for the fast components only.

Let Γ be $S \times J$ matrix (S is the number of reactions, J is the number of intermediates). Equation (2) can be presented in the equivalent form

$$u = NW, \qquad (3)$$
$$L(z) = 0,$$

where matrix N is composed of $P = S - (J - B)$ vectors of stoichiometric numbers ν. Symbol $L(z)$ represents B linear balances of catalyst active sites. Each ν vector corresponds to the reaction path. Vector W is composed of P reaction path rates.

Explicit solutions of system (3) in terms of reaction graph were obtained for linear reaction mechanisms.

Kinetic polynomial

The breakthrough in understanding of non-linear case happened in early 80'. We applied polynomial elimination theory to (3). New invariant of system (3) was discovered. It is a polynomial in terms of reaction rate w - kinetic polynomial [1]. Kinetic polynomial is resultant of system (3) in w. Vanishing of resultant is necessary and sufficient condition of system (3) solvability.

However, solution of many important problems including numerical calculation of zeroes does not require the explicit expression of resultant. The matrix can be built instead. The vanishing of its determinant is condition of system (3) solvability.

Matrix form of kinetic polynomial

Vanishing of the determinant of the following matrix is necessary and sufficient condition for w to be the steady state rate of two-stage impact mechanism.

$$\det \begin{vmatrix} 0 & r2 & -f2 & 2f1 & 0 & -2r1 \\ -1 & 1 & 1 & 0 & 0 & 0 \\ 0 & -1 & 0 & 1 & 1 & 0 \\ 0 & 0 & -1 & 0 & 1 & 1 \\ 2w & r2 & -f2 & 0 & 0 & 0 \\ 0 & 2w & 0 & r2 & -f2 & 0 \end{vmatrix} = 0 \qquad (4)$$

or

$$2\,(4(r1 - f1)\,w\text{^}2 + ((f2+r2)\text{^}2 + 4(f1f2 + r1r2))\,w + r1r2\text{^}2 - f1f2\text{^}2) = 0, \qquad (5)$$

where $f1, f2, r1, r2$ are kinetic parameters (reaction weights) of stages.

OP-I-5

Equation (5) is equivalent to the kinetic polynomial expression from [1] to multiplier independent of w.

We will discuss the properties [2] of family of matrices similar to matrix (4) as well as methods of their generation.

References:

[1] M.Z. Lazman, G.S. Yablonskii. Kinetic polynomial: a new concept of chemical kinetics, Patterns and Dynamics in Reactive Media, Springer-Verlag 1991, p.117

[2] M. Lazman. Effective Process Simulation: Analytical Methods. 16th IMACS World congress 2000 on Scientific Computation, Applied Mathematics and Simulation. Lausanne, Switzerland, August 21-25, 2000. M. Deville, R. Owens, eds.

OP-I-6

INTENSIFICATION OF PROCESSES OF TECHNOLOGY OF ZEOLITES WITH THE HELP PULSATION STRING TYPE REACTORS

A.V. Shumovsky, L.S. Nam, B.K. Nefedov*

Ministry of industry, science and technology of Russia, Moscow
**«Formika-R», Belgorod*

In master schedules of production of zeolites the agitators with a mechanical agitation with lacks, inherent in them, - nonuniformity mass- and heat interchange on volume basis of reactionary bulk are widely applied, that largely influences quality of termination products.

The authors carried out jobs on technology of zeolites with use on operations of crystallization and neutralization string type pulsation reactors. The tests in conditions of a pilot plant have shown their high performance. It has allowed at making industrial technologies of productions of zeolite such as and for operations of crystallization and neutralization of suspension of zeolite to develop and to introduce pulsation string type reactors.

In pulsation string type reactor being a means of theoretical replacement, the reciprocation of hydrogel on cut is converted in rotational, and the sign of rotation of a medium on each next plate is opposite. It promotes shaping of conditions of its homogeneity on chemical composition and temperature in all reactionary volume. The homogeneity of a medium on it, defining arguments of crystallization of zeolites, causes also uniform internal diffusive masstransfer, resulting in to shaping of chips, rather close on the sizes. In particular, the contents of fragments from 1 up to 5 microns will increase up to > 60 % as contrasted to 40 % at crystallization in a means with an agitator.

The kinetics of crystallization of zeolites is limited by internal diffusion, and the intensity of stirring renders influence only on repressing of influence internal diffusive factor, close to nongradient the temperature schedule of pulsation crystallization results also in acceleration of process of mass transfer and propagation of chips and, thereby, to a diminution of duration of process. The received outcomes have shown, that the time of crystallization of zeolite can be reduced till 1,0-1.5 hours.

The effect of homogenization mass- and heattransfer at crystallization of zeolites in a pulsation reactor revealed in the present job, allows to recommend it as the equipment, most applicable for accomplishment of master schedules of receiving of zeolites.

The use conditions of zeolites as adsorbents, catalyzators or ionexcangers require their express preparation after a stage of hydrothermal crystallization; separation of zeolite from

exuberant alkali and scrubbing action. As a rule, it is considered acceptable, if the hydrogen ion exponent of an aqueous extract of zeolite after this operation pH = 10,5-11, that corresponds to percentage by weight NaOH 0,3-0.6 g/l.

The most widespread method of separation of zeolite from alkali is the decantation, filtrating and scrubbing action. The experience displays, that for achievement of demanded completeness of scrubbing action it is necessary to utillize rather fair quantities of water: at scrubbing action on the packed bed not less than 6-8 volumes it is per unit mass of zeolite, at decantation 10-12 and more. In outcome the major volumes an alcalinous waste code containing aluminium and silicium in the diluted kind are formed. The processing and salvaging of such outlet requires essential capital investments, more energy consumption and is ecologically unsafe.

The authors have applied a pulsation string with a distributive nozzle to realization of process of neutralization of suspension of zeolite such as and flue gases containing dioxide of carbon. The passage through suspension of flue gases containing 10 % about was established, that. CO_2, is not accompanied by a little noticeable exothermic effect, in outcome pH was reduced up to 10.2-11.0. For development of industrial technology this alternative, as most economically favourable and simplifying instrument decor of the site of neutralization was elected.

The complex of the carried out explorations has allowed to create on Shebekino chemical factory the plant on production of zeolite NaA - component synthetic detergents, start-up and assimilation by which one have confirmed serviceability of pulsation meanses. The new production technology of zeolite NaA differs by the reduced specific consumption of materials, diminution energy and expenditures of labour, possibility of organization of a continuous process, sharp intensification of the basic stages of process. She provides receiving zeolite NaA, property, having a complex indispensable for use it in quality a component of detergents.

Special Workshop on the INTAS Project

EXPERIMENTAL AND THEORETICAL STUDIES OF TEMPORAL AND SPATIAL SELF-ORGANISATION PROCESSES IN OXIDATIVE REACTIONS OVER PLATINUM GROUP METALS: AN APPROACH TO BRIDGE THE GAP BETWEEN SINGLE CRYSTALS AND NANO-SIZE SUPPORTED CATALYST PARTICLES (Ref. No 99-01882)

TRANSITION TO CHAOS IN THE OSCILLATING CO OXIDATION ON ZEOLITE SUPPORTED Pd

M.M. Slin'ko, A.A. Ukharskii, N.V. Peskov*, N.I. Jaeger**

Institute of Chemical Physics, Russian Academy of Science, Moscow 117334, Russia, E-mail: Slinko@polymer.chph.ras.ru
**Department of Computational Mathematics and Cybernetics, Moscow State University, E-mail: peskov@cs.msu.su*
***Institut für Angewandte und Physikalische Chemie, FB 2, Universität Bremen, D-28334 Bremen, Germany, E-mail: jse@zfn.uni-bremen.de*

Introduction

The investigation of chaotic reaction rate oscillations can provide additional information about the reaction mechanism. The identification of the transition from regular to chaotic oscillations is one of the most significant problems in this field. While all three well-known routes to chaos were successfully detected in the homegeneous catalytic Belousov- Zhabotinskii reaction, it is more difficult to observe and examine the transition to chaos in heterogeneous catalytic systems. The main reason is the drift of the catalyst activity which makes it difficult to follow and analyse the phenomenon unambiguously. Another reason could be the very small region of experimental parameters in which the transition to chaotic behaviour can take place. The first and up to now the only identification of a transition to chaos via period doublings has been demonstrated for kinetic oscillations in the catalytic CO oxidation on a well-defined Pt(110) surface under UHV conditions [1]. The present work is devoted to the study of the transition to chaos during CO oxidation on a supported Pd catalyst at atmospheric pressure.

Experimental Results and Discussion

The dynamic behaviour of the system has been studied in a continuous flow glass reactor under conditions of good mixing. The catalyst was applied under shallow bed conditions on a glass frit in the reactor. The reaction mixture was fed into the reactor with a flow rate of 150 cm^3/min. The outlet CO, CO_2 concentrations were measured by IR analyser URAS 10E. The data obtained for CO, CO_2 concentrations and catalyst temperature were digitised with a sampling time 0.1 s.

The catalyst consisted of palladium dispersed within the cavities of a Faujasite X type zeolite. The average diameter of the Pd particles was 10 nm. The Pd loading was 0.05 wt %. Details of the experimental procedure can be found in reference 2.

Regular oscillations have been observed at 503 K in the case of an oxidised catalyst, when the reaction mixture contained 0.3 vol.% CO, 20 % of O_2 and N_2 as a balance. The CO

concentration played the role of a bifurcation parameter and increasingly complex oscillatory behaviour has been detected after a slow increase of the CO inlet concentration with very small steps (0.02-0.04%).

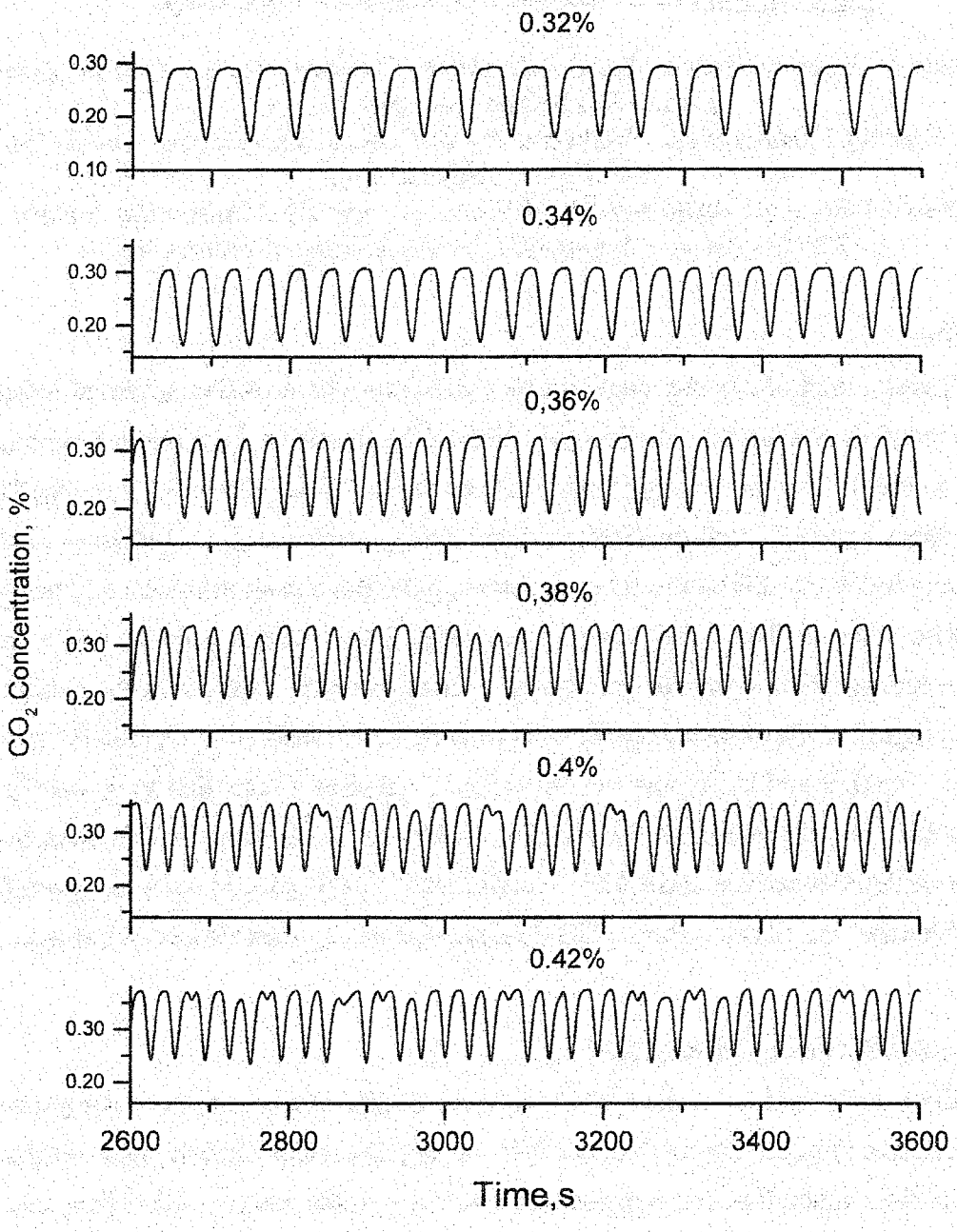

Figure 1. Increasing complexity of the reaction rate oscillations with increasing CO concentration.

Fig. 1 demonstrates that the system undergoes a sequence of transitions from regular to more complex temporal behaviour. The regular oscillations destabilize at C_{CO}= 0.34% , when the periodic state seems to be randomly disrupted by short "burst". It can be seen, that with increasing CO concentration the irregular bursts become more and more frequent until fully developed aperiodic behaviour is eventually reached at CO concentration equal to 0.4%. The calculations of the largest Lyapunov exponent λ by the Rosenstein method for the time series,

corresponding to 0.4% CO produce a value λ=0.08 bit/s. The positive value of λ indicates an exponential divergence of nearby trajectories on the attractor, which is the main characteristic of chaos. No signs of the torus destruction or the period doubling can be detected by visual inspection of the time series, presented in Figure 1. This suggests intermittency as a candidate for the route to chaos. The intermittency scenario is characterised by the existence of regular (laminar) phases along the evolution of a system variable, interrupted by bursts of irregular behaviour. Figure 2 shows Fourier power spectra, corresponding to the time series, presented in Fig. 1.

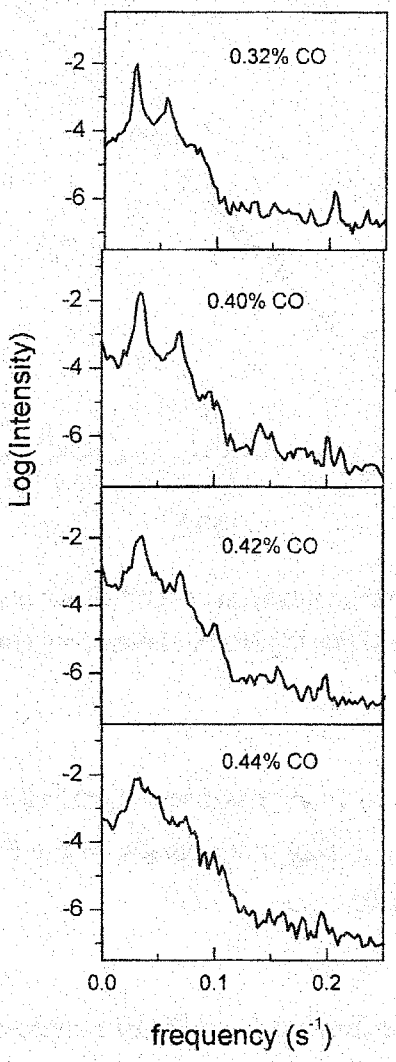

Figure 2. Fourier power spectra, corresponding to the time series, presented in Fig. 1.

Figure 2 shows that during the transition from regular to chaotic oscillations with increasing the inlet CO concentration no new peaks appear in the spectrum. This is an identification of the transition to type I intermittency chaos, during which the power spectrum changes continuously from a delta function to a broadened peak [3]. All types of an intermittency route to chaos can also be distinquished by the analysis of a one-dimensional reduced

IN-1

Poincare map. The main characteristic of an intermittency type I route to chaos is the tangent bifurcation due to which the system switches back and forth between a "ghost" periodic orbit and sudden bursts of chaotic behaviour. The return map for this case can be approximated by a quadratic polynom. Figure 3 demonstrates, that the overall shape of the reconstructed next-minimum map for the 0.4% CO time series is almost the same as the theoretical model map for type I intermittency.

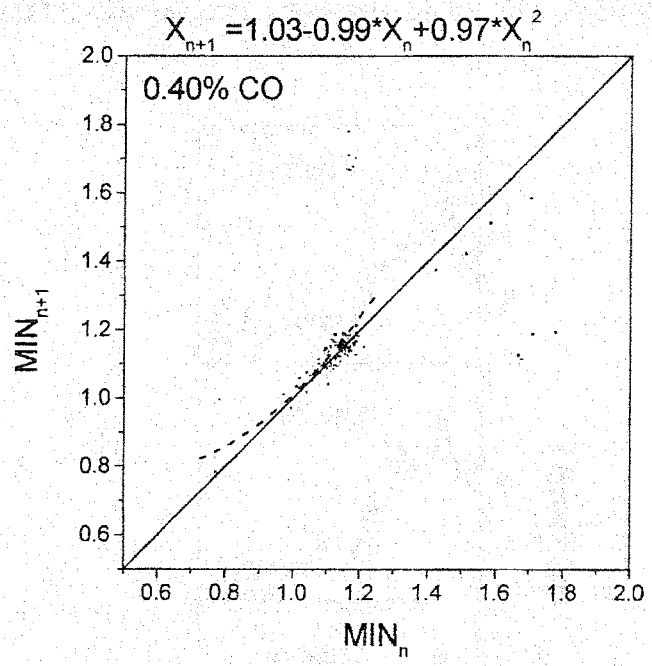

Figure 3. The next minimum maps for the time series 0.4%.
The dashed line depicts the fitting polynom.

Conclusions

The intermittency I type route to chaos has been identified in the case of the CO oxidation over a Pd zeolite catalyst by analysing the variation of the Fourier power spectra and the Poincare section with the CO concentration.

Acknowledgement

The work was supported by the Russian Fund for Basic Research (Grant № 00-03-32125) and by INTAS-2000 (project № 1882)

Literature

[1] M.Eiswirth, K.Krischer, G.Ertl, Surf.Sci., 202, 1988, 565

[2] M.M.Slinko, N.I.Jaeger, P.Svensson, J.Catal.,118, 1989, 349

[3] J.E.Hirsch, B.A.Huberman, D.J.Scalapino, Phys. Rev. A., v.25, N1, 519-532

SPIRAL WAVES IN THE MONTE CARLO MODEL OF CO OXIDATION OVER Pd(110) CAUSED BY SYNCHRONIZATION VIA CO_{ads} DIFFUSION BETWEEN DIFFERENT PARTS OF CATALYTIC SURFACE

E.I. Latkin, V.I. Elokhin, V.V. Gorodetskii

Boreskov Institute of Catalysis, Novosibirsk, 630090, Russia
Phone: 007-3832-344770, Fax: 007-3832-343056, e-mail: elokhin@catalysis.nsk.su

The mechanism of synchronization of local oscillators is one of the fundamental problems arising when studying the oscillatory behavior of heterogeneous catalytic reactions [1]. The isothermal kinetic oscillations in different oxidation reactions are observed as a rule [1,2] on the supported metals and on metal tips considered as a superposition of the interrelated single crystal nanoplanes. In this case the surface diffusion of the adsorbed species can be responsible for the synchronization of local oscillators. In our contribution we shall consider the possible consequences of the several catalytic surface sections coupling (in our case that is the surface of Pd(110)) exhibiting the surface wave behavior with some time shift in the period of oscillations. The analysis should be provided by means of statistical lattice modeling (dynamic Monte Carlo - DMC) of the CO oxidation reaction over Pd(110). The following reaction mechanism based on our FEM data was used in simulation [3]:

1) $O_{2(gas)} + 2* \rightarrow 2O_{ads}$
2) $CO_{gas} + * \leftrightarrow CO_{ads}$
3) $CO_{ads} + O_{ads} \rightarrow CO_{2(gas)} + 2*$
4) $O_{ads} + *_v \rightarrow [*O_{ss}]$
5) $CO_{ads} + [*O_{ss}] \rightarrow CO_{2(gas)} + 2* + *_v$
6) $CO_{gas} + [*O_{ss}] \leftrightarrow [CO_{ads}*O_{ss}]$
7) $[CO_{ads}\ O_{ss}] \rightarrow CO_{2(gas)} + * + *_v$

In this model the oscillations and surface waves of adsorbed species are determined by purely kinetic reasons and are not associated with trigger switching of catalytic and adsorption properties in the course of the reaction. The density of $[*O_{ss}]$ in the adsorbed layer controls the reaction behavior due to the change of O_2 or CO priority during the competition of their adsorption. Diffusion of CO_{ads} over the centers $*$ and $[*O_{ss}]$ is very important for the synchronization between local parts of the surface. The slow steps of formation (step 4) and especially consumption of subsurface oxygen (steps 5 and 7 restoring the centers for O_2 dissociative adsorption) play the decisive role in the appearance of oscillatory dynamics. Both the surface waves of adsorbed species and the presence of the narrow reaction zone between

the moving islands of adsorbates had been observed by simulation of the dynamics of this model [ref. 3, where the details of the simulation algorithm can be found].

The following simulation experiment had been carried out to prove the possible consequences of the synchronization between several catalytic surface parts coupled with CO_{ads} diffusion as was found experimentally on the Pt tip surface [4]. The whole model surface (800x800 active centers) was divided initially into four square parts «opaque» to surface diffusion: north-west (#1), north-east (#2), south-east (#3), south-west (#4). Contrary to [3] the lattice has no periodic boundary conditions, therefore it can serve as a model for a palladium tip with four separate Pd(110) faces. Let us imagine that the oscillations on these faces start with the time shift equals to 1/4 of the period. At the chosen set of the parameters (see the caption to the Fig. 1) the period of oscillations has the value ~ 500 Monte Carlo steps [1] and so the reaction in section #1 starts at 0 MCs, in section #2 - at 125 MCs, in section #3 - at 250 MCs, and in section #4 - at 375 MCs (Fig. 1). Then the reaction oscillates separately over the time of 2000 MCs (Fig. 1). In the course of this time interval the autowave processes in sections 1-4 were observed with a shape of propagating oxygen islands (high reaction rate) changing by the CO_{ads} coverage blocking the surface (low reaction rate). The overall reaction rate on the whole surface W_{int} in this time remains approximately constant (Fig. 1). But after the 2000 MCs we eliminate the borders between the sections and make it «transparent» for the CO_{ads} diffusion.

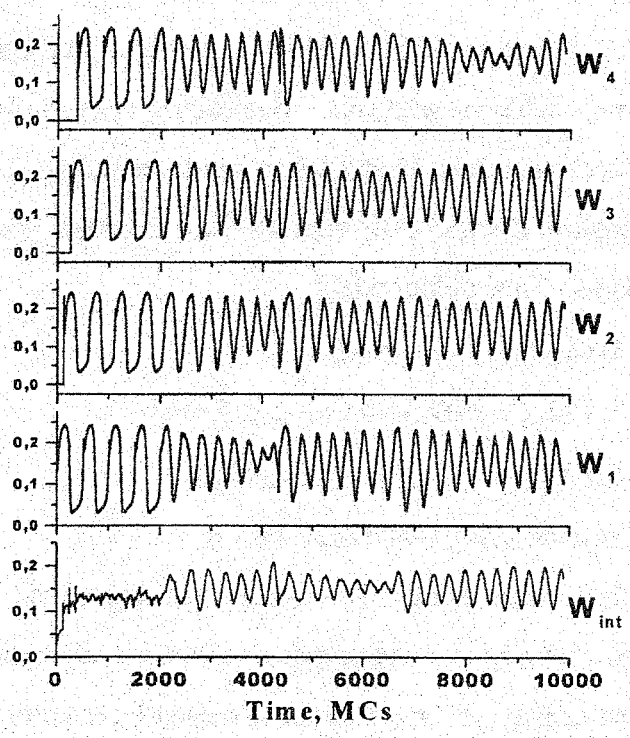

Fig. 1. Dynamics of the specific rate of CO_2 formation on the separate sections of the surface ($W_1 \div W_4$) and on the whole surface (W_{int}) at $k_1 = 1$, $k_2 = 1$, $k_{-2} = 0.2$, $k_4 = 0.03$, $k_5 = 0.01$, $k_6 = 1$, $k_{-6} = 0.5$, $k_7 = 0.02$ (s^{-1}). The reaction 3 proceeds immediately as soon as O_{ads} and CO_{ads} appear in the situation of nearest neighborhood. Parameter of the diffusion cycle M = 50.

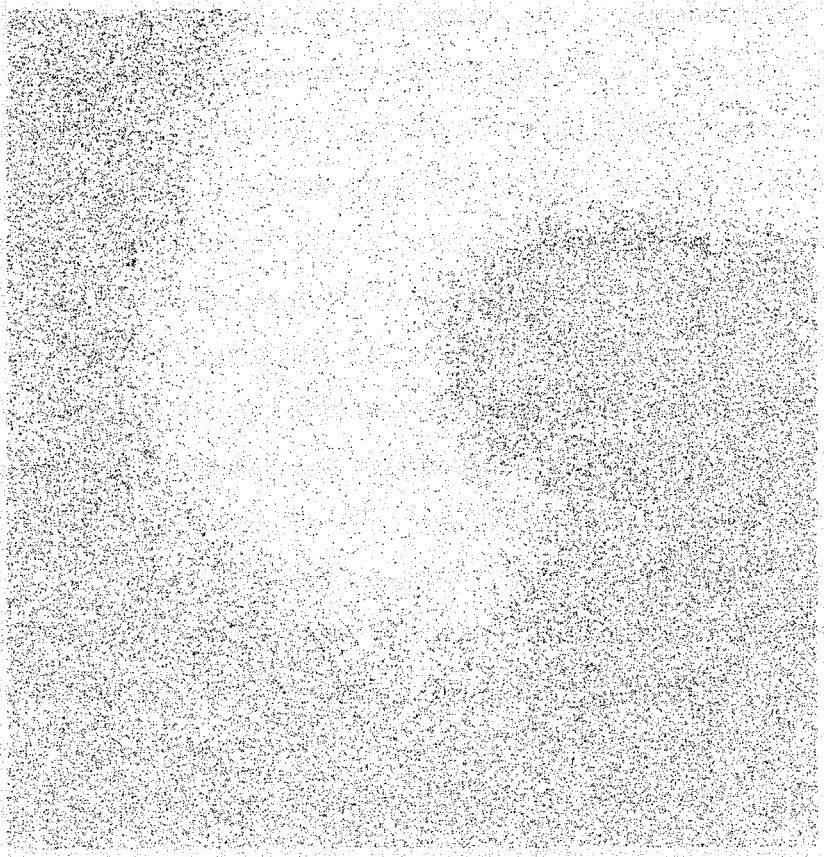

Fig. 2. The local intensity of CO_2 formation at the 5000 MCs

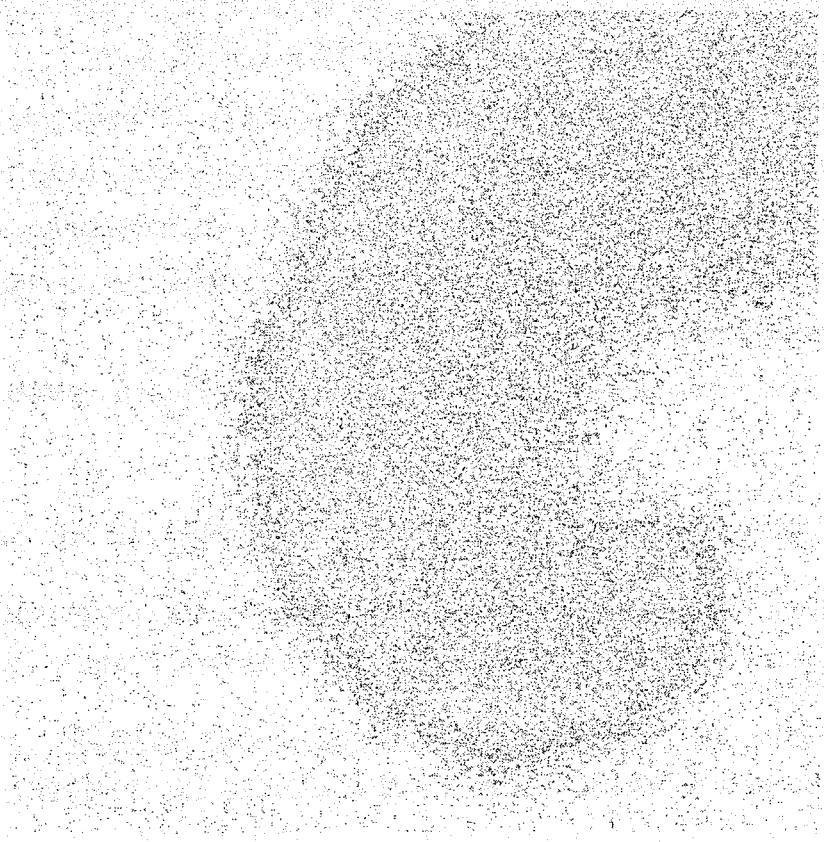

Fig. 3. The local intensity of CO_2 formation at the 9750 MCs

The synchronization leads, first, to the decreasing by 1.5-2 times of the period of oscillations (Fig. 1), and second, to the appearing of spiral waves over the whole surface (Figs. 2 and 3). It should be emphasized that this is exclusively the consequence of our simulation strategy described above. If from the very beginning we started the simulation on the whole surface without boundaries between different parts, we should obtain the synchronous oscillations with the same period ~ 500 MCs accompanied with autowave processes over the whole surface (propagating O_{ads} islands altering by CO_{ads} blocking). The spiral motion arises in our model from the time shift in the period between different parts of oscillating catalytic surface when to the moment of the communication via CO_{ads} diffusion the neighboring sections have differing composition of the adsorbed layer. The colliding oxygen islands propagating from one section to another form the spiral waves on the surface.

The shape of the spiral waves is represented in Figs. 2 and 3. The local distribution of the intensity of CO_2 formation is depicted in these figures (the rate intensity is reflected by the greyscale), but it could imagine the composition of the adsorbed layer corresponding to these figures. The CO_2 formation rate is minimal within the CO_{ads} adlayer, it is intermediate within O_{ads} adlayer, and the maximal intensity of CO_2 production exists right in the «reaction zone» - on the boundaries of the propagating oxygen islands where the local concentration of the free active centers is maximal. The existence of the «reaction zone» was found experimentally (field ion probe-hole microscopy technique with 5 Å resolution) in [5].

In this work a comparison of non-linear phenomena in CO oxidation on a flat Pd(110) surface and several independent parts of Pd(110) surface coupled by CO_{ads} diffusion has been presented in an attempt to bridge the gap between single crystals and supported metals.

The presentation will be accompanied by the experimental and computer movies illustrating the non-linear dynamics on the catalytic surfaces.

INTAS Grant # 99-01882 and RFBR Grant # 99-03-32433 supported this study.

References

[1] V. Gorodetskii, J. Lauterbach, H.-H. Rotermund, J.H. Block, G. Ertl. *Nature,* 370 (1994) 276.

[2] J. Lauterbach, G. Bonilla, T.D. Pletcher. *Chem. Eng. Sci.,* 54 (1999) 4501.

[3] E.I. Latkin, V.I. Elokhin, A.V. Matveev, V.V. Gorodetskii. *J. Molec Catal. A, Chemical,* 158 (2000) 161.

[4] V. Gorodetskii, J.H. Block, W. Drachsel, M. Ehsasi. *Appl. Surface Sci.,* 67 (1999) 198.

[5] V.V. Gorodetskii, W. Drachsel. *Appl. Catal. A: General,* 188 (1999) 267.

THE LOW-TEMPERATURE REDUCTION OF Pd-DOPED TRANSITION METAL OXIDES SURFACE WITH HYDROGEN

V.M. Belousov, M.A. Vasylyev, L.V. Lyashenko, N.Yu. Vilkova, B.E. Nieuwenhuys*

Institute of Metal Physics NASU, Kiev, Ukraine
**Leiden Institute of Chemistry, Leiden University, Leiden, The Netherlands*

Effective hydrogen absorbers, operating under vacuum and low-temperature conditions, are necessary in cryogenic technology. Mainly systems using Ag, Pd or Pt oxides are suggested as such getters. The use of transition metal oxides is promising for these purposes. The main interest to the metal oxide doping with noble metal is due to its effect on activity and selectivity in heterogeneous catalytic reaction.

In the present paper the effect of Pd has been shown over a number of transition metal oxides in hydrogen reduction in the temperature range of 77-330 K. Hydrogen absorption was studied in a static vacuum apparatus from the pressure drop in a known volume with removal of the reaction product (H_2O) by freezing a trap at 77 K.

The role of Pd has been investigated with respect to the oxides characterised by weak and rather strong oxygen-lattice bond alike. MoO_3, WO_3, Cr_2O_3, Fe_2O_3, CuO, V_2O_5, MnO_2 have been chosen. Pure oxides, Fe_2O_3 and Cr_2O_3, commence getting reduced at 470 K, MoO_3, WO_3 and V_2O_5 – at 700 K. As follows from Table 1, promotion of 0.3-0.5 wt.% Pd results in the oxides initial hydrogen reduction temperature plummeting by hundreds degrees, and they became capable to react with hydrogen at temperatures 293 K (Table 1), introduction of 0.5 wt. % Pd leads to grow of capacity in 15-100 time.

The state of Pd on the surface of Co_3O_4 has been investigated by *X*-ray photoelectron Spectroscopy (XPS) technique and electron microscopy in conjunction with an energy-dispersive spectroscopy. Pd on the surface of the oxides has been found to be uniformly distributed as clusters no larger than 40 Å in size. Using XPS technique it has been shown, that initial state of the Pd is PdO_2 (binding energy 337,4 eV). Upon exposure to hydrogen the binding energy for Pd ($3d_{5/2}$) is 335,7 eV, which is higher than that for the metallic Pd but lower than that for Pd^{+}. On the data obtained the conclusion is drawn that catalytically active form is an oxide cluster incorporating partially reduced Pd chemically bonded to the oxide. During the initial interaction of Pd-doped oxides and hydrogen a partial reduction of Pd occurs. In this form an oxide Pd cluster makes a catalyst. Measurements of the reduction rates of oxides containing oxidised or reduced Pd clusters bears out the conclusion. Hydrogen adsorp-

tion kinetics on the oxides surveyed in the range of 230-330 K obeys the first-order equation in hydrogen $-dP/d\tau=KP$.

It is known that at high temperatures the bond energy of surface oxygen increases with an increase of degree of oxide reduction and the rate of its removal decreases. Our data obtained for CuO, Co_3O_4, MnO_2 shows that analogous regularities are also observed at reduced temperatures and pressures. For example, rate of hydrogen reaction with oxide depends significantly on the oxygen content in surface layer: removal from the CuO surface at room temperature of all 0.02 % of the monolayer lowers by 2 times the specific reaction rate constant. The activation energy of the reaction increases from 31 kJ·mole^{-1} for the oxidised sample to 47 kJ·mole^{-1} upon removal of 0.08 % of an oxygen monolayer. A value of E_{act}, equal to 60 kJ·mole^{-1}, is presented for a stable operating copper oxide surface and a value of 72 kJ·mole^{-1} is presented for a partially reduced surface (1 % of the monolayer was removed). This indicates the pronounced heterogeneity of the copper oxide surface: evidently according to data of the stable operating CuO surface has an 0,08 % degree of reduction.

For Co_3O_4 the activation energy increases, which is due to the surface oxygen energy nonuniformity and the bond of the oxygen to be removed became increasingly stronger as the oxide is reduced. For Pd-Co_3O_4, when 6-8 percent of the oxygen monolayer is removed the reaction rate constant doubles, with the activation energy falling from 39 to 8 kJ/mol. Such reduction process of Pd-doped oxides indicates the catalytic character of the action Pd exerts in the range of 230-330 K (Table 2). We watched similar effect for MnO_2 and Pd-MnO_2 (Table 3).

Two regions are clearly traced in the studied temperature range with different dependence of the reaction rate on temperature: the normal Arrhenius dependence in the region 230 – 330 K and an anomalous dependence at 77-220 K. The reaction rate not only does not decrease in the second region with a decrease in temperature, but remains constant, and in certain cases even slightly increases.

The activation energy of the pure cobalt (II, III) oxide reduction in the interval of 230-330 K amounts to 12-18 kJ·mole^{-1}, while it is 8-10 kJ·mole^{-1} for the palladized sample; in the interval of 77-230 K zero or even negative activation energy is observed on both samples, the value of which is in the limits of the measurement accuracy of this quantity. Similar effect for Pd-MnO_2 for x (reduction steps)=100 % (Table 3).

At sufficiently low temperature (77-210 K) the change in pressure with time occurs according to the law $P=A\ln\tau$. The observed kinetics of the process in low-temperature region is

characteristics for processes, occurring by a tunnel mechanism. Adsorption of hydrogen on the synthesized Co_3O_4 can occur on O^- defects, cationic vacancies, or geometrically corresponding Co^{3+}-O^- centres.

On palladized Co_3O_4 and MnO_2 samples the reaction rate in the region of reduction by a tunnelling mechanism is 4-5 times greater than on the pure sample as a result of facilitation of atomisation of hydrogen on the partially reduced Pd ions. The nature of tunnelling particles (electron, proton, and hydrogen atom) can be determined from data on the kinetic isotope effect. In the case of tunnelling of a proton or hydrogen atom substitution of hydrogen by deuterium should lead to a sharp decrease in the reduction rate and to an increase in the kinetic isotope effect by several orders of magnitude.

Experiments, carried out with deuterium, showed that the kinetic isotope effect does not change significantly upon going from high (270-330 K) to low (77-220 K) temperature both for pure Co_3O_4 and for the Pd-containing sample: K_D:K_H =1.4-2.0. The hypothesis concerning tunnelling of an electron also agrees with the quite broad range of the tunnel effect (77-220 K). The obtained data do not exclude the spillover of hydrogen from Pd oxide clusters to the oxygen.

In our view this process can be seen a follows: hydrogen activation occurs on the oxide cluster containing partially reduced ions of Pd - Pd°... Pd^+-O-Me^{4+}: 1) $H_2 \xrightarrow{Pd^+ - O - Me^{n+}} 2H^-$; 2) $H^0+Pd^+ \rightarrow Pd^0+H^0$ (H+*e*). Then proton passes via spillover to the oxide's oxygen: 3) $H^+ + O^{2-}$ ------ OH^-; 4) $H^+ + OH^-$ ------ H_2O. Reduction of the oxide metal. Me^{n+} occurs during electron tunnelling from Pd° to Me^{n+}: 5) $Pd^0 + Me^{n+}$ ------ $Pd^+ + Me^{(n-1)+}$.

In all appearances, in the case of Pd-doped oxides, it is precisely electron tunnelling that governs the reduction rate at 77 - 220 K; disruption of Pd-H linkage and hydrogen-to-oxide's oxygen spillover probably play a minor role in this temperature region.

Table 1.

Oxide	Surface *S*, m^2/g	The temperature initial period reduction, K		Capacity H_2, $cm^3/g(P_{H2}$=0.700 kPa)
Pd- WO_3	2,5		293	0,01
MoO_3	3	700		
Pd- MoO_3	3		293	0,01
V_2O_5	11	693		
Pd- V_2O_5	11		293	0,01
CuO	100	300		3
Pd-CuO	100		293	50

IN-3

Co_3O_4	140	293		15
Pd- Co_3O_4	135		293	180
MnO_2	180	293		2,5
Pd- MnO_2	180		293	286
PdO	-		293	110
Ag_2O	1,3		293	1,5

Table 2.

X, %	Co_3O_4		Pd-Co_3O_4	
	$K \cdot 10^4$, c^{-1} m^{-2}	E_{akt}, kJ/mole	$K \cdot 10^4$, c^{-1} m^{-2}	E_{akt}, kJ/mole
0	20,0	18,0	16,0	39,0
0,3	15,2	-	17,1	-
1,0	11,3	25,7	18,4	25,7
2,5	7,2	31,8	20,6	18,0
5,0	3,8	39,0	22,5	11,6
8,5	2,2	43,0	23,0	9,0
10,0	1,2	45,1	24,8	8,1
....	....	....	....	....
160	0,8	45,0	25,1	8,0

Table 3.

T, K	X, %	MnO_2		Pd- MnO_2	
		$K \cdot 10^4$, c^{-1} m^{-2}	E_{akt}, kJ/mole	$K \cdot 10^4$, c^{-1} m^{-2}	E_{akt}, kJ/mole
295	0,0	13,00	17,6	35,6	38,0
	0,4	3,60	27,3	36,2	25,6
	0,7	-	-	58,0	24,2
	1,9	2,20	-	60,0	25,0
	2,4	0,40	-	-	-
	3,3	0,10	-	61,7	25,0
	5,1	0,08	37,6	68,8	21,2
	10,0	0,04	41,8	72,2	21,2
	12,0	0,00	-	102,0	24,0
	23,4	0,00	-	138,0	19,0
	100,0	-	-	290,0	15,0
273	100,0	-	-	206,0	-
206	100,0	-	-	148,0	15,0
163	100,0	-	-	52,0	-
77	100,0	-	-	36,0	0,5

Acknowledgements

This work was supported by Program INTAS 99 (Grant # 01882).

NUMERICAL INVESTIGATION OF NONLINEAR PROBLEMS BY CONTINUATION PARAMETER METHOD. SOFTWARE AUTOMATED PACKAGE BPR-Q FOR MATHEMATICAL MODELING OF THE CATALYTIC PROCESSES

S.I. Fadeev, V.V. Kogayi & V.K. Korolev

Sobolev Institute of Mathematics
4, pr. Acad. Koptyug, Novosibirsk, Russia
e-mail: fadeev@math.nsc.ru,
Tel.: 7-(3832) 33-33-87,
Fax: 7-(3832) 33-25-98

Let us consider a nonlinear boundary value problem, which has the following vector form:

$$x \in [a,b],\ dy/dx=f(x,y,Q),\ g(y(a),y(b),Q)=0. \quad (1)$$

Here f and g are sufficiently smooth vector functions on their arguments, Q is a scalar parameter depending on which the solution of the boundary value problem y(x,Q), $Q \in [Q_0, \bar{Q}]$ has been investigated. Introducing the spatial curve L_Q for every $Q \in [Q_0, \bar{Q}]$ the plots y(x,Q) in (N+1)-dimensional Euclidean space (x,y) are believed to form the surface S by continuous variation Q parameter. Then the same value Q may correspond to several spatial curves L_Q belonging to the surface S. In this case the square σ of the strip S bounded by plots of the solutions $y(x,Q_0)$ and y(x,Q) plays the role of the universal parameter of the problem, so y(x,σ) is a one-valued vector function.

We propose the following algorithm of continuation by a parameter. In accordance with the concept of the orthogonal sweep method by S.K.Godunov, we split the interval [a,b] on x into m parts:

$$a = x_1 < x_2 < \ldots < x_{m+1} = b, \quad (2)$$

and consider a number of the Cauchy problems:

$$dy/dx=f(x,y,Q),\ y|_{x=x_i} = p^{(i)}, \quad (3)$$

$$dV/dx=A(x)V,\ V|_{x=x_i} = I, \quad (4)$$

$$dw/dx=A(x)w+R(x),\ w|_{x=x_i} = 0, \quad (5)$$

$$x \in [x_i, x_{i+1}],\ i=1,\ldots,m,$$

where $A(x) = f_y(x,y(x,Q),Q)$, $R(x) = f_Q(x,y(x,Q),Q)$, I is an identity matrix. By the multiple shooting method we require that the functions $y(x,Q,p^{(i)})$ determined by the Cauchy prob-

lems (3) should represent the solution to the boundary value problem (1), i.e. satisfy the boundary conditions as well as those of continuity in the mesh points (2). As a result, we have nonlinear equation systems,

$$\Phi^{[1]} = g(p^{(1)}, p^{(m+1)}, Q) = 0,$$
$$\Phi^{[i]} = y(x_i, Q, p^{(i-1)}) - p^{(i)} = 0,$$
$$i=2,3,\ldots,m+1,$$

or

$$\Phi(p,Q) = 0, \qquad (6)$$

to determine the components $p_j^{(i)}$ of the vectors $p^{(i)}$, i=1, ..., m+1, j=1, ..., N. Here p is a combined vector formed by the vectors $p^{(1)}$, ..., $p^{(m+1)}$ and Φ is a combined vector formed by the vectors $\Phi^{(1)}$, ..., $\Phi^{(m+1)}$. If the plot of the solution to the boundary value problem (1) y=y(x,Q) is the smooth surface in the (N+1)-dimensional space, the plot of solution to the system (6) p=p(Q) will be a smooth spatial curve Γ_Q. The Cauchy problems (3) – (5) enable the solution to the system (6) by Newton's method to be found. Regular choice of the current parameter among the components of vector p in the process of solution continuation, i.e. parameterization, permits one to construct Γ_Q numerically including the possible "turning" points for several values Q.

The method proposed is used as a basis for software package BPR-Q, the first version being developed in 1985. Many problems, demanding the immediate adaptation of the numerical method for various applications, including the stationary catalytic processes in the catalytic particle and the reactors brought about the development of BPR-Q-package. The totality of experience has proved high efficiency of this package. For details, see [Fadeev et al, 1998]. List of references points to the comprehensive practice of using the BPR-Q package in applications.

The other packages for the numerical study of nonlinear problems are known to exist. Here alternative methods are used for the construction discrete models (for example, collocation methods with the orthogonal polynomials) and solution continuation. Comparison of various complexes is hampered, in particular, due to the lack of access to the program texts. Nevertheless, we can point to a number of mathematical models studied by BPR-Q as tests for comparison of various approaches. They are boundary value problems with multiple solutions, inner boundary layers moving in the process of solution continuation, determination of the initial approximation, and the choice of the initial position, etc. Such peculiarities of the mathematical models can hamper the application of the software complexes in which the pa-

rameterization or mesh adaptation or transition from one model parameter to another, etc. are not provided.

At present we can offer the modern BPR-Q-package version designed in standard WINDOWS-style with the detail "help". The user interface has been developed by means of Integrated development environment (IDE) DELPHI.

Acknowledgements

The work is supported by the Russian Foundation for Basic Research grant Ref. No 99-01-0035 "Nonlinear dynamics of gas-liquid catalytic systems" and the INTAS grant Ref. No. 99-01882, "Experimental and theoretical studies of temporal and spatial self-organization processes in oxidative reactions over platinum group metals: An approach to bridge the gap between single crystals and nano-size supported catalyst particles."

References

1. V.P.Doronin, S.I.Fadeev, R.G.Lukyanova. "Numerical Construction of All Solutions to Boundary Value Problem for the System of Nonlinear Differential Equations". Computational Systems, 72. Novosibirsk, (1972). (in Russian)
2. V.S.Sheplev, S.I.Fadeev, R.G.Lukyanova. "Calculation of Exothermal First Order Reaction over the Catalyst Particle". Computational Systems, 87. Novosibirsk, (1981). (in Russian)
3. S.I.Reshetnikov, V.S.Sheplev, S.I.Fadeev. "Methods for Finding Steady-State Solutions of Mathematical Models for Chemicothechnological schemes." React. Kinet. Catal. Lett. Vol.30, No 2, (1986).
4. E.A.Ivanov, S.I.Fadeev. "Study of Bifurcation of Steady-State Solutions to Two-Phase Diffusion Model of Fluidized Bed". Mathematical Modeling of Catalytic Reactors. Novosibirsk, Nauka, (1989). (in Russian)
5. E.A.Ivanov, S.I.Reshetnikov, S.I.Fadeev. " Numerical Method for Construction of Steady-State Regimes in Catalyst Particle". Mathematical Modeling of Catalytic Reactors. Novosibirsk, Nauka, (1989). (in Russian)
6. E.A.Ivanov, S.I.Fadeev. "Parameterization for Solving the Nonlinear Equation System with Parameter". Chemical Technology, Kiev, Naukova dumka, (1991), 95 – 100. (in Russian)

IN-4

7. E.A.Ivanov, S.I.Fadeev. "Numerical Study of Parametric Sensitivity for Chemical Technology Problems". Computational Technologies, Novosibirsk, (1993), v.2, N 6. (in Russian)
8. S.I.Fadeev, R.G.Lukyanova, V.M.Khanayev, V.A.Kirillov. "Mathematical modeling of Fisher-Tropsch Process in Suspension Reactors." Computational Systems, 159. Novosibirsk, (1997), 126 – 148. (in Russian)
9. S.I. Fadeev, "Organization of Numerical Experiment for Investigation of Nonlinear Boundary Value Problems by the Method of Continuation of Solution with respect to Parameter." Sib.J.Diff.Equation, Vol. 1, No 4, pp.321-350, Nova Science Publishers, Inc., N. Y., U.S.A (1998).
10. V.A.Kirillov, V.M.Khanayev, V.D. Mescheryakov, S.I. Fadeev, and R.G. Lukyanova. "A Mathematical Model of Fisher-Tropsch Synthesis in a Slurry Reactor." Natural Gas Conversion V, Studies in Surface Science and Catalysis, v. 119, edition by A.Parmaliana, Proceedings of the 5th International Natural Gas Conversion Symposium, Giardini Naxos-Taormina, Italy, September 20-25, (1998), 149 - 154.
11. Fadeev S.I., Khanaev V.M., Kirillov V.A. "Existence of Steady-State Regimes for Fischer-Tropsch Synthesis in Suspension Reactor". Sib. Zh. Industr. Matem., 1 (1998) pp. 182-188 (in Russian)
12. Kazhikhov A.V.,Reshetnikov S.I., Fadeev S.I. Non-Steady Catalysis and its Hydrodynamic Aspects "Integration Programs of Fundamental Studies", SB RAS, (1998).
13. Kirillov V.A.,Fadeev S.I.,Kuzin N.A.,Kulikov A.V. "Catalytic Oxidation of C3-C4 Hydrocarbons on a Porous Permeable Plate with Countercurrent or Cocurrent Feed of Reactants." Teor. Osn. Khim. Tekhn. (Theor. Found. of Chem. Engin.), 32 (1998) pp. 164-174 (in Russian)
14. E.A.Ivanov, S.I.Reshetnikov, S.I.Fadeev, A.Yu.Berezin, I.A.Gainova. "Mathematical Modeling of Processes under Periodic Impulses". Sib. Zh. Industr. Matem., 2, (1999), pp.1-11 (in Russian).
15. Kirillov V.A., Khanaev V.M., Meshcheryakov V.D., Fadeev S.I., Luk'yanova R.G. "Numerical Analysis of Fischer-Tropsch Processes in Reactors with a Slurried Catalyst Bed", Theor. Found. of Chem. Engineering, 33 (3), pp. 270-278 (English version) (1999)
16. S.I.Fadeev & V.V.Kogayi. "Continuation Parameter Method on the Basis of Multiple Shooting Method for Numerical Study of Nonlinear Boundary Value Problems". Sib. Zh. Industr. Matem., 1, (2001) (in Russian).

SOFTWARE AUTOMATED PACKAGE STEP FOR NUMERICAL INVESTIGATION OF AUTONOMOUS SYSTEMS OF GENERAL TYPE. MATHEMATICAL MODELING OF THE CATALYTIC PROCESSES

S.I. Fadeev, A.Yu. Berezin & I.A. Gainova

Sobolev Institute of Mathematics
4, pr. Acad. Koptyug, Novosibirsk, Russia
e-mail: fadeev@math.nsc.ru,
Tel.: 7-(3832) 33-33-87,
Fax: 7-(3832) 33-25-98

Mathematical models describing various catalytic processes, as a rule, belong to the class of autonomous equation systems. An important stage of investigation of such models is determination of key characteristics of their behavior for appropriate model parameters. It is necessary to apply the specific methods and techniques.

In this paper, we describe the software package STEP designed for the complex study of nonlinear equations systems and autonomous systems of general type. Problem of numerical study of autonomous systems is used in many applications such as the mathematical modeling of catalytic reactions, biological processes, physical problems and mechanics. The basic purpose therewith is to detect the nonlinear phenomena described by the mathematical model, namely detection of the model parameters, characterized by the oscillations, investigation of stationary solutions (i.e. solutions to nonlinear equations systems), multiplicity of solutions and high parametric sensitivity in their neighborhood, etc. Thorough parametric analysis of autonomous system behavior including the determination of the stationary solutions is possible only for some models. In general, investigation of autonomous systems for N ordinary differential equations

$$dy/dt=f(y,\alpha), \qquad (1)$$

where α is a model parameter, bear a numerical experiment character. The methods not accounting for the specific nature of right-hands of system, allow :

- to construct numerically the dependence $y(\alpha)$ of stationary solutions to the system

  $$f(y,\alpha)=0, \qquad (2)$$

  by the continuation parameter method and to find simultaneously the α-regions of multiple solutions;
- to determine their stability and locate the points on the stationary solutions diagram where unstable stationary solution passes into a stable limit cycle (Hoph bifurcation);

- to obtain the oscillations by integrating the autonomous system or to seek of the start stationary solution by the continuation parameter method;
- to detect α-regions, in which all stationary solutions are unstable. For autonomous system it means the self-excitation of oscillations for arbitrary initial data.

The software package STEP represents a powerful tool for realization of above-mentioned points. This package was developed by research group headed by professor Fadeev. The package STEP is based on the original algorithms suggested in the Sobolev Institute of Mathematics (Novosibirsk), including the method of continuation of stationary solutions by a parameter, technique of determination of stationary solution stability and integration of stiff autonomous system.

Brief description of algorithms

Nonlinear system (2) is supposed to be presented by the smooth spatial curve S and, therefore, only singular points of "turn" type take place there in numerical constructing S. Here the Jacobi matrix $f_y(y,\alpha)$ is degenerated. Since under the assumption that the rank $(N \times (N+1))$-matrix $[f_y(y,\alpha), f_\alpha(y,\alpha)]$ would be always equal to N in the neighborhood of S, then by the implicit function theorem such component μ of combined vector (y,α) could be found that $f_x(x,\mu) \neq 0$, where x is a vector (y,α) without the component μ. It means that the solution to system (2) can be continued to one step by the parameter μ, which will be called a current parameter. If the solution is found for the current parameter λ, then the choice of novel current parameter μ is stipulated by the normalization of the solution derivatives with respect to λ. Let

$$| dx_k/d\lambda | = \max (|dy_1/d\lambda|,|dy_2/d\lambda|,...,|dy_N/d\lambda|,|d\alpha/d\lambda|).$$

Then $\mu=x_k$. Herewith, the quantities

$$| dy_i/d\mu | = |dy_i/d\lambda| / |dx_k/d\lambda|, \ i=1,2,...,N, \ |d\alpha/d\mu| = |d\alpha/d\lambda| / |dx_k/d\lambda| ,$$

are less or equal to 1. Further, the derivatives found with respect to current parameter μ are used for prediction of the initial approximation in the neighborhood of μ by the Newton's method, etc.

We have used a numerical κ-criterion by Godunov-Bulgakov to determine the stability of stationary solutions in the package. It is based on the effective technique of determining the matrix norm H of the solution to Liapunov matrix equation

$$HA + A^*H=I,$$

where $A = f_y(y,\alpha)$. The STEP package contains the methods well suited for the stiff initial value problems as well, namely the semiimplicit Rosenbrock method of the 2-nd order and, also Gear algorithm. For details, see [Fadeev et al, 1998]. List of references points to comprehensive practice of using the STEP package in applications.

Package STEP runs on IBM-compatible personal computers. In order to construct the mathematical model it is required to input the expressions for right-hands of system, i.e., the elements of vector function $f(y,\alpha)$. The elements of matrix $[f_y, f_\alpha]$ are evaluated numerically on the basis of the Richardson approximation. Due to this fact the volume of input information is considerably decreased, and the model correction related to numerical investigation of system (2) depending on a parameter proceeds with a minimum efforts. In essence, it is only necessary to find out a model parameter that would play a role of a parameter α. Then it is required to input the elements of the matrix $f_y(y,\alpha)$ for the studying of stability of autonomous system stationary solutions.

Software package STEP has been tested on a great number of problems from different areas of the applied mathematics, such as: mathematical simulation in biology and chemical technology, non-linear oscillations and many other mathematical models, describing the processes, where hysteresis is possible. Package STEP meets the world standards with respect to efficiency and possibilities in study of the non-linear problems. It is applied at the Boreskov Institute of Catalysis, Siberian Branch of the Russian Academy of Sciences, Novosibirsk; Karpov Physicochemical Institute, Moscow; Semenov Institute of Chemical Physics, Moscow; and other Institutes (Russia) for the chemical processes study. This package is also used in educational process at the Novosibirsk University (Russia) on speciality "Engeneering Chemistry of the Catalytic Processes".

Acknowledgements

The work was supported by the INTAS grant Ref. No. 99-01882, "Experimental and theoretical studies of temporal and spatial self-organisation processes in oxidative reactions over platinum group metals: An approach to bridge the gap between single crystals and nano-size supported catalyst particles."

References

1. V.I. Savchenko, E.A. Ivanov and S.I. Fadeev, "Kinetic model of CO oxidation of heterophaze surface analyzed regarding CO_{ads} spillover. I. Homotopic method. Effect of temperature and CO pressure." React. Kinet. Catal. Lett. Vol.57, No 1, 55-60 (1996). Jointly publyshed by Elsevier Sciense B.V., Amsterdam and Akademiai Kiado, Budapest.

IN-5

2. V.I. Bykov, S.I. Fadeev and T.P.Pushkareva, "Parametric analysis of kinetic models, XI. Influence of the nubber of activesites." React. Kinet. Catal. Lett. Vol.57, No 1, 133-140 (1996). Jointly publyshed by Elsevier Sciense B.V., Amsterdam and Akademiai Kiado, Budapest.
3. V.I. Savchenko, E.A. Ivanov and S.I. Fadeev, "Kinetic model of CO oxidation of heterophaze surface analyzed regarding CO_{ads} spillover. II. Homotopic method. Effect of ml surface portion." React. Kinet. Catal. Lett. Vol.58, No 1, 79-84 (1996). Jointly publyshed by Elsevier Sciense B.V., Amsterdam and Akademiai Kiado, Budapest.
4. V.I. Savchenko, E.A. Ivanov and S.I. Fadeev, "Kinetic model of CO oxidation of nonuniform surface analyzed with regard to CO_{ads} spillover, III. Homotopic method. Effect of the reaction mixture composition." React. Kinet. Catal. Lett. Vol.59, No 1, 67-73 (1996).
5. Fadeev S.I, Ermakova A.,Ivanov E.A.,Gudkov A.V. "Calculation of Thermodynamic Equilibria in Gas-Phase Processes by the Continuation Method." Teoret. Osn. Khim. Tekhn. (Theor. Found. of Chem. Engineer.), 31 (1997) 62-69 (in Russian)
6. Fadeev S.I.,Gainova I.A.,Berezin A.Yu.,Yermakova A., Pai Z.P., Gudkov A.V. "Chemical" Model of a Liquid-Phase Claus Reaction: Transient and Steady States." Teor. Osn. Khim. Tehn. (Theor. Found. for Chem. Engineer.), 31 (1997) 440-446 (in Russian)
7. A.Ermakova, Z.P.Pai, A.V.Gudkov, S.I.Fadeev, I.A.Gainova, A.Yu.Berezin, "Chemical" Model of a Liquid-Phase Claus Reaction: Model parameters, numerical analysis, comparison with experiment". Teor. Osn. Khim. Tehn. (Theor. Found. for Chem.Engineer.), 31 (1997) 516-523 (in Russian) (Основы "химической" модели жидкофазной реакции Клауса. Параметры модели, численный анализ, сравнение с экспериментом)
8. Fadeev S.I.,Gainova I.A.,Berezin A.Yu.,Yermakova A.,Pai Z.P., Gudkov A.V. "Chemical" Model of a Liquid-Phase Claus Reaction: Steady States with a Partial Replenishment of the Solution." Teor. Osn. Khim. Tehn. (Theor. Found. for Chem. Engineer.), 31 (1997) 634-638 (in Russian)
9. S.I. Fadeev, V.I. Savchenko, A.Yu. Berezin, "The analysis of oscillations of CO oxidation reaction on a nonuniform surface consisting of two types of sides, coupled CO_{ads} diffusion." React. Kinet. Catal. Lett., (1998).
10. S.I. Fadeev, "Organization of numerical experiment for investigation of nonlinear boundary value problems by the method of continuation of solution with respect to parameter." Sib.J.Diff.Equation, Vol. 1, No 4, pp.321-350, Nova Science Publishers, Inc., N. Y., U.S.A (1998).
11. S.I.Fadeev, S.A.Pokrovskaja, A.Yu.Berezin, I.A.Gainova, "Software package STEP for numerical investigation of systems of nonlinear equations and autonomous systems of general type. Description of operation of the package STEP on examples of problems from the course "Engineering chemistry of catalytic processes" Novosibirsk State University (1998).
12. C.W.Gear, "Numerical initial value problems in ordinary differential equations." Prentice-Hall, Englewood Cliffs, N.Y. (1973).
13. E.Doedel, "Numerical analysis and control of bifurcation problems." Montreal: Concordia university, Department of computer science, (1988), 159 p.

RELAXATION OSCILLATIONS IN CATALYTIC HYDROGEN OXIDATION INCLUDING A CHASE ON FRENCH DUCKS

G.A. Chumakov and N.A. Chumakova*

Sobolev Institute of Mathematics, SB RAS, 630090 Novosibirsk, Russia
E-mail: chumakov@math.nsc.ru
**Boreskov Institute of Catalysis, SB RAS, 630090 Novosibirsk, Russia*
E-mail: chum@catalysis.nsk.su

Introduction. Investigation of relaxation and chaotic oscillations in different catalytic systems has been developed very rapidly during recent years [1,2]. Our renewed interest in relaxation oscillations [3] arose from the introduction and use of Non-Standard Analysis in the study of singular perturbations and in applied problems. A major claim to fame for Non-Standard Analysis is the discovery of a new phenomenon in relaxation oscillations which a group of french mathematicians have called "Les Canards" or "Ducks".

In our paper the French Ducks will be chased in one of the mathematical models of oscillating heterogeneous catalytic system. The phenomena of chaotic behavior of the heterogeneous reaction rate which concerns the nature of catalytic system, the mechanism of chemical interactions [2] and the influence of the global error in long-term numerical integration of ordinary differential equations [4] as a source of stochastic effects will also be discussed. One of the most important properties of the deterministic chaos is "a sensitive dependence on initial conditions".

Let us consider the mechanism of the heterogeneous reaction of hydrogen oxidation on metallic catalysts [5,6]:

$$\begin{gathered} H_2 + 2\,[Me] \leftrightarrow 2\,[H\,Me] \\ O_2 + 2\,[Me] \leftrightarrow 2\,[O\,Me] \\ 2\,[H\,Me] + [O\,Me] \rightarrow 3\,[Me] + H_2O \\ H_2 + [O\,Me\,] \rightarrow [Me] + H_2O \\ [Me_v] + [H\,Me] \leftrightarrow [Me_v\,H] + [Me] \\ [Me_v] + [O\,Me] \leftrightarrow [Me_v\,O] + [Me] \end{gathered} \qquad (1)$$

Here [Me] and [Me_v] are a vacant active site on the catalyst surface and an atom in the subsurface layer, respectively, [H Me], [O Me] and [Me_v H], [Me_v O] are hydrogen and oxygen atoms adsorbed on the surface and dissolved into the subsurface layer of the catalyst. We shall study the case when the activation energies of the third and fourth reaction steps may

depend linearly upon the reagents concentrations in the subsurface layer and upon the concentration of oxygen adsorbed.

Mathematical Model. The dynamic behavior of the catalytic system is described by a set of 6 ordinary differential equations, presenting the concentrations of hydrogen and oxygen adsorbed on the metal surface (x_1 and x_2), dissolved into subsurface layer (x_3 and x_4) and being in the gas phase (x_5 and x_6):

$$\begin{aligned}
\dot{x}_1 &= 2[k_1 x_5(1-x_1-x_2)^2 - k_{-1}x_1^2 - k_3(\mathbf{x})x_1^2 x_2] - \beta_1 \dot{x}_3,\\
\dot{x}_2 &= 2[k_2 x_6(1-x_1-x_2)^2 - k_{-2}x_2^2] - k_3(\mathbf{x})x_1^2 x_2 - k_4(\mathbf{x})x_5 x_2 - \beta_2 \dot{x}_4,\\
\dot{x}_3 &= k_5 x_1(1-x_3) - k_{-5}x_3(1-x_1-x_2),\\
\dot{x}_4 &= k_6 x_2(1-x_4) - k_{-6}x_4(1-x_1-x_2),\\
\delta\,\dot{x}_5 &= -\delta\beta\,[k_1 x_5(1-x_1-x_2)^2 - k_{-1}x_1^2 - k_4(\mathbf{x})x_5 x_2] + x_{50} - x_5,\\
\delta\,\dot{x}_6 &= -\delta\beta[k_2 x_6(1-x_1-x_2)^2 - k_{-2}x_2^2] + x_{60} - x_6.
\end{aligned} \tag{2}$$

Moreover, the rate constants of the 3rd and 4th steps are as follows

$k_3(\mathbf{x})=k_{30}\exp(\mu_{32}x_2+\mu_{33}x_3+\mu_{34}x_4)$, $k_4(\mathbf{x})=k_{40}\exp(\mu_{42}x_2+\mu_{43}x_3+\mu_{44}x_4)$,

where the parameters k_{30}, k_{40} are positive and μ_{ij} are real numbers. Note that the gradients of dissolved reagents are suggested to be small.

After some simplifications we can obtain several reduced models keeping the physical and chemical sense of the catalytic system dynamics and peculiarities being of high importance to the complex irregular behavior. In that meaning, a general simplified kinetic model looks as follows:

$$\mu\dot{x} = f(x,y), \qquad \dot{y} = g(x,y,z), \qquad \dot{z} = \varepsilon h(x,y,z). \tag{3}$$

Relaxation oscillations arise when μ and ε are small parameters, and $x=x_1$, $y=x_2$, $z=x_4$ (or $z=x_3$) are identified as fast, intermediate and slow variables, respectively.

We shall first study a one-parameter dynamical system

$$\mu\dot{x} = f(x,y), \qquad \dot{y} = g(x,y,z) \tag{4}$$

with the parameter z, $0 \le z \le 1$.

We shall establish that canard configuration indeed occur when $0.445017 < z < z_c$ with $z_c = 0.445233121773$ and we shall give an asymptotic expansion for the trajectories that run along the stable and unstable manifolds. It turns out that there are two breeds of canards.

Supercritical and Subcritical Ducks. The main features of the phase-portraits are as given in Fig. 1. A singular point of the system (4) is now stable and there are supercritical ducks as the one-parameter family of stable limit cycles (curves 2-5, Fig. 1) with growing subcritical ducks without heads as unstable limit cycles inside the stable manifold (curves 2'-5', Fig. 1). As we increase z further the two cycles coalesce at z_c between curves 5 and 5'. It is not difficult to see that for $z>z_c$ trajectories spiralize toward the singular point.

In the paper some reasons of chaotic behavior appearence in the system (3) are given as well (see Fig. 2). We would like to point out:

(i) an attractor of a special structure is presented in the phase space of the system;

(ii) a subregion on the attractor exists with a high sensitivity to the initial conditions;

(iii) infinite times the trajectory comes back into this subregion.

Acknowledgement. This research was supported in part by the International Association for the promotion of co-operation with scientists from the New Independent States of the former Soviet Union - INTAS grant No. 99-01882.

References:

1. M.M. Slinko and N.I. Jaeger. Oscillating Heterogeneous Catalytic Systems. (Studies in Surface Science and Catalysis; 86). Elsevier Science B.V., 1994.
2. G.A. Chumakov and M.G. Slinko: Kinetic Turbulence (Chaos) of Reaction Rate for Hydrogen Oxidation on Metallic Catalysts, *Dokl. Acad. Nauk USSR,* 1982, vol. 266, No 5, p.1194-1198. (in Russian)
3. G.A. Chumakov and N.A. Chumakova: French Ducks in Kinetic Model of a Heterogeneous Catalytic Reaction. IN: *4th Siberian Congress on Industrial and Applied Mathematics "INPRIM-2000".* Book of abstracts. Part IV. – Novosibirsk, IM SB RAS, 2000, p.26. (in Russian)
4. G.A. Chumakov and N.A. Chumakova: On a Global Error Estimate in Long-Term Numerical Integration of Ordinary Differential Equations, *Selcuc Journal of Applied Mathematics,* 2001, vol.2, No 1, pp.27-46.
5. G.A. Chumakov, M.M. Slinko, V.D. Belyaev, and M.G. Slinko: Kinetic Model of an Autooscillating Heterogeneous Reaction, *Dokl. Acad. Nauk USSR,* 1977, vol. 234, No 2, p.399-402. (in Russian)
6. G.A. Chumakov: Analysis of Mathematical Models of the Reaction Rate Oscillations in Heterogeneous Catalytic Reactions. PhD thesis, Novosibirsk, 1985. (in Russian)

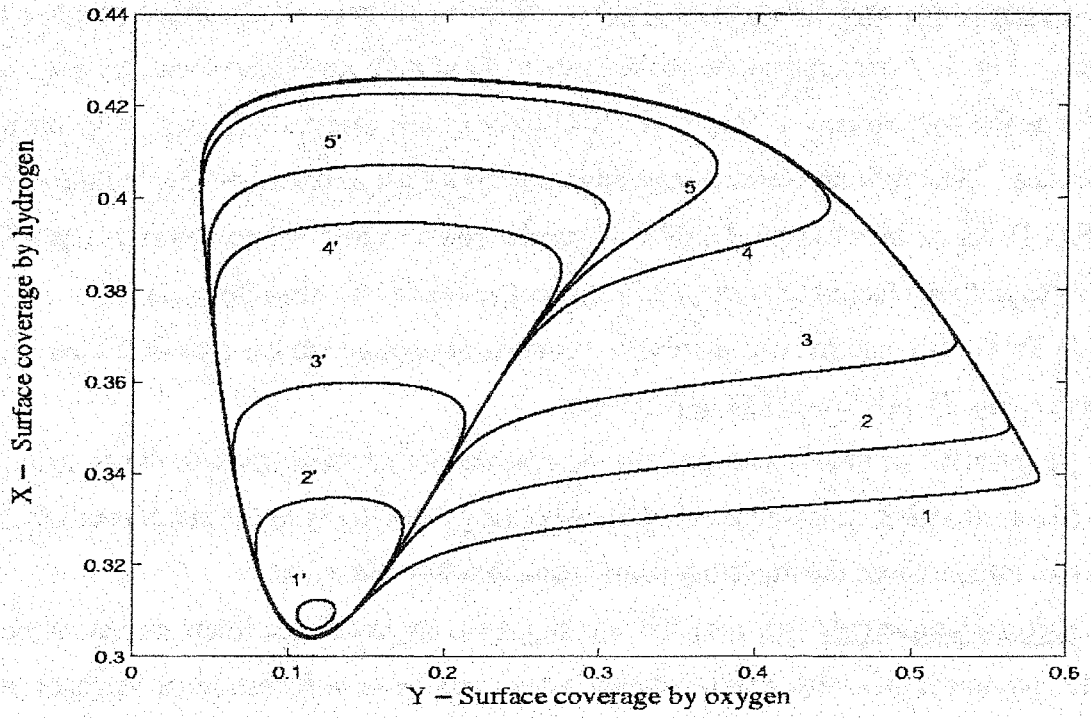

Figure 1. French Ducks for Z = 0.445017 (1,1'), 0.445224 (2,2'), 0.445233 (3,3'), 0.44523312 (4,4'), 0.445233121770 (5,5') in the model (4).

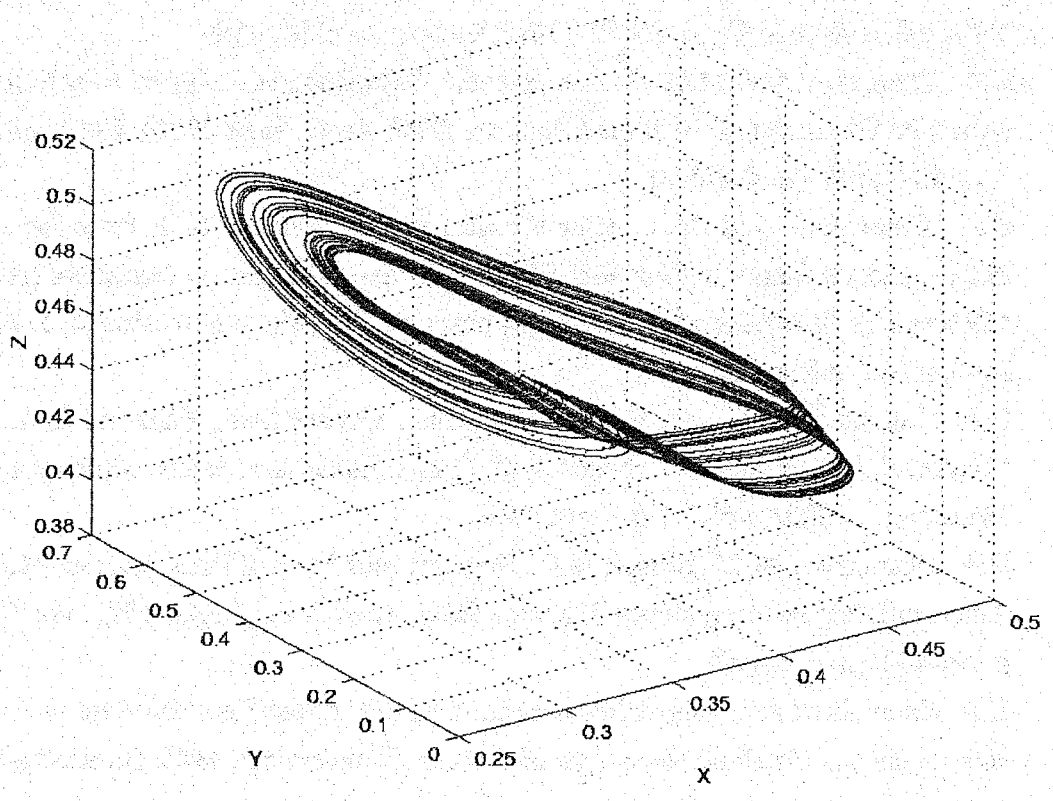

Figure 2. Phase-portrait of the chaotic behavior in the system (3).

THE OSCILLATORY BEHAVIOUR OF NO_x (x = ½ AND 1) REDUCTION REACTIONS OVER Pt, Ir AND Rh SINGLE CRYSTAL SURFACES

B.E. Nieuwenhuys, C.A. de Wolf, R.J. H.Grisel, S. Carabineiro

Leiden Institute of Chemistry, Leiden University,
P.O.Box 9502, 2300 RA Leiden, The Netherlands
tel. (31) 71 5274545; fax (31) 71 5274451
email: b.nieuwe@chem.leidenuniv.nl

Various kinds on non-linear behaviour have been observed, including oscillations in rate and selectivity, hysteresis phenomena, surface explosions, chaotic behaviour and spatiotemporal pattern formation.

The non-linear processes were followed both by gas phase analysis (MS) and surface analysis. Fast XPS experiments using the synchrotron facilities at Trieste were used to measure the nature and concentration of the relevant species on the surface during non-linear processes on Ir, Rh and, very recently, on Pt surfaces. This part of the project was done in collaboration with A.Baraldi, S.Lizzit and M.Kiskinova (Trieste).

In addition to experimental studies using various techniques, mathematical modeling have been applied to elucidate the mechanisms of the non-linear processes. Up to now the non-linear processes have been studied on Pt(100), various single crystal surfaces of Rh and Ir, Ru(0001), supported Pt-ceria catalysts and, in addition, on Rh, Ir, Pt and Pd field emitters.

In the present lecture the emphasis will be on:

a) the spatiotemporal pattern formation observed with almost atomic resolution by field electron and ion microscopy (FEM and FIM);

b) the differences observed in non-linear behaviour on Rh, Ir and Pt surfaces, differences in experimental conditions at which rate synchronized oscillations occur, differences in oscillations in selectivity (N_2, NH_3 and N_2O) and;

c) in particular, the differences in mechanisms, which have come to light directly as a result of studying this non-linear behaviour.

In the case of Rh, non-linearity is related to periodic transitions between N- and O-rich surfaces, with O destabilising the N-adlayer and causing an acceleration in N_2 production. However, in the case of Pt, the important step involves the creation of vacant sites required for NO dissociation, whereby products leaving the surface facilitate an autocatalytic rise in the concentration of such vacancies and, hence, reaction rate. Ir positions itself between the former two, because oscillations have been observed in two different regimes. Both a lower-temperature Pt-like and higher-temperature Rh-like behaviour have been observed on different It surfaces. New results gained from FEM and FIM measurements are presented to consolidate the lower-temperature Pt-like behaviour, and confirm the dualistic natures of Ir. No oscillations in rate have been observed over Pd(111) or Ru(0001). The Ru surface exhibits selectivity to N_2 of almost 100% even in large excess of hydogen.

Section II

PROCESSES IN CHEMICAL REACTORS

NONLINEAR CRYSTALLIZATION BEHAVIOR OF HIGHLY SUPERSATURATION SYSTEM

I.V. Melikhov, A.Ya. Gorbatchevski

Lomonosov Moscow State University, Chemical Dept., Vorob'evy Gory, Moscow 119899, Russia. E-mail: Gorba@radio.chem.msu.ru, Fax: (095) 9328846

Crystallization is one of the basic technological phenomenon. The experimental works demonstrated that the crystallization in highly supersaturated system is characterized by set of nonlinear processes leading to the formation of a nanocrystaline phases. These processes has not yet been fully investigated, but a qualitative picture has been generally established. This work outlines approaches to the qualitative description of rapid crystallization.

Model of processes. Crystallization involves a set of processes leading to cluster formation, growth, and transformation into crystallites, which then move in the medium.

The system contains different types of particles: clusters differing in epy number of molecules in a particle, individual crystallites, and aggregates composed of different numbers of crystallites. The state of any particle is characterized by its weight, spatial coordinates, and center-of-mass velocity (external coordinates), as well as by the habitus and other internal coordinates. Particles of each kind are characterised by their own distribution function, related to the properties of the medium $\{u_j\}$: $\varphi_k(x_j,t)=\partial^p N_k/\partial x_1...\partial x_p$, where N_k is the number of particles of kind k with state parameters no greater than $\{x_j\}$per unit volume at time t, p is the number of permanently varying state parameters under consideration.

Without *a priori* limitations it should be taken that a particle can, with a certain probability, pass from any one state to any other state. Then

$$-\frac{\partial\varphi_k}{\partial t}=\sum_{j=1}^{p}\frac{\partial}{\partial x_j}\left\{G_{j1}\varphi_k-\sum_{i=1}^{p}\frac{\partial}{\partial x_i}\left(G_{j2}\varphi_k-...\right)\right\}+Q_k(x_j,u_j), \qquad (1)$$

where G_{j1} is the rate of the X_j parameter change, G_{j2} is the fluctuation coefficient, $Q_k(x_j,u_j)$ is the rate of the transformation of particles of kind k into another kind of particles within the allowed range. It should also be taken that particles of a given kind can nucleate at the lower boundary of the allows interval with the rate

$$\Im(u_j)=\left[G_{j1}\varphi_k-\sum_{i=1}^{p}\frac{\partial}{\partial x_i}\left(G_{j2}\varphi_k-...\right)\right]_{x_j\to x_{jL}}. \qquad (2)$$

For clusters $\Im(u_j)=0$. For crystallites

$$\Im(u_j) = \Im_0(u_j)\left[\left(\frac{C}{C_\infty}\right)^m - 1\right]\varepsilon\Delta + N_0\delta(t) + \sum_k W_k, \qquad (3)$$

where $\Im_0(u_{ji})$ is the characteristic rate of spontaneous nucleation, C and C_∞ are the current and equilibrium concentrations (or activities) of molecules of the substance to be crystallized, m is the kinetic order of nucleation, ε is the volume fraction occupied by the medium, $\Delta = 0$ at $C < C_\infty$ and $\Delta = 1$ at $C > C_\infty$, N_0 is the number of foreign molecules that can serve as nuclei, W_k is the nucleation rate for particles of kind k.

Relations (1)–(4) should be supplemented with equations describing the variations of $\{u_j\}$ (concentration C, temperature T, and velocity $\vec{v}$) and the intensities of external fields. For concentration, we have

$$-\frac{\partial(\varepsilon C)}{\partial t} = \mathrm{div}[(\vec{v}C - D\,\mathrm{grad}\,C)\varepsilon] + \sum_k \int_{x_{jL}}^{x_{js}} (\Omega - \nu)\rho_k\, dx_j \qquad (4)$$

where D is the diffusion coefficient for molecules of the substance to be crystallized, Ω and ν are the frequencies of attachment and detachment of molecules. The solubility of such crystallites is given by

$$C_l = C_\infty exp\left[\frac{\sigma V_0}{kT(l + l_0)}\right], \qquad (5)$$

where σ is the average surface energy, V_0 is the molecular volume, k is the Boltzmann constant, and l_0 is the Tolman length. The growth rate, and the fluctuation coefficient for the size of a particle can be written in the form

$$G_{11} = \frac{12\sqrt[3]{V_0}\,q l^2}{1 + 6l^2\sqrt[3]{(q/f)^2}}, \qquad G_{12} = \frac{\sqrt[3]{V_0}\,G_{11}}{\left(1 + 6l^2\sqrt[3]{(q/f)^2}\right)}, \qquad (6)$$

with

$$q = q_0\left[(C/C_l)^{m_1} - 1\right] \qquad f = f_0\left[(C/C_l) - 1\right] \qquad (7)$$

where q_0 and f_0 are the characteristic rates of two-dimensional nucleation and lateral layer propagation, m_1 is the kinetic order of two-dimensional nucleation.

The G_{11} and G_{12} of aggregates and $Q_k(x_j,u_j)$ are given by the frequency of pair collisions.

By solving equations (1)–(7), we find that, if crystallization occurs in a homogeneous suspension, only one solid phase is formed, aggregates are loose enough for the crystallites to grow further, and $(q/f)^{1/3} >> 1$ at all l, then, after a 95% decrease in supersaturation, the average crystallite size is

$$\bar{l} = 0.69\sqrt[4]{\frac{C_\infty \sqrt[3]{V_0 q_0 f_0^2}}{\Im_0 \rho_0}} S_0^{-P_0}(1+P_0),$$

where $S_0 = C_0/C_\infty$, $P_0 = 0.25(m-(m_1+5)/3)$, C_0 is the initial solution concentration. The maximum crystallite size (the largest for the crystallites constituting 95% of the total number of crystallites) $l_{max} = 1.67\bar{l}$.

Local crystallization. The tendency toward localization within a small region of the system is typical of rapid crystallization processes. In this case, the region of high supersaturation and excitation levels, where crystallites are formed, is small in comparison with the volume of the system: energy accumulation in a large volume is prevented by dissipation. It has been demonstrated by the solving of the equations (1)- (7). These equation was used to analyze crystallization $BaSO_4$, $BaCO_3$, $CaSO_4 \cdot 0.5\ H_2O$ in a flowing supersaturated solution in tubular crystallizer.

By solving these equations under appropriate boundary conditions and realistic assumptions as to the character of the suspension motion in the pipeline, we find that, in a stationary process, nucleation and crystal growth are localized and part of the pipe - line of length

$$Y = \frac{1.2 v_m}{\sqrt[4]{\rho_k V_0 q_0 f_0^2 \Im_0 / C_0}} S_0^{-(m+m_1+1)/4} \qquad (8)$$

where v_m is the flow velocity at the outlet of the crystallizer.

Relation (8) describes local crystallization in moving systems. Localisation of crystalline depots studied in [1-6].

Stages of process. In highly supersaturated medium, crystallization involves several stages. In the first stage, nucleation and crystal growth occur, while the second and subsequent stages involve the formation of primary, secondary, etc., ordered aggregates. All these processes superimpose on the formation of disodered flocks, within which the crystallites remain free to move and grow almost as rapidly as in the unaggregated state.

Equation (1)- (7) are aplicable to each stage. As a result of multistage process, the crystallizing product has a multilevel, hierarchic structure, where each level reflects a particular stage of the process, as found in studies of the crystallization behavior of many substances. For example, during crystallization of $CaSO \cdot 0.5\ H_2O$ from a 7.3 M H_3PO_4 solution with S = 2.6 (353 K) and vigorous stirring, solution concentration was found to change in three stages . In the first stage, we observe nucleation and growth of prismatic crystallites, which attain 100 nm in size within 6 s. The aggregation process is accompanied by morphological selection of

densely packed configurations; as a result, the aggregates take the form of prisms. These prisms unite into secondary aggregates, which have a regular shape. After etching or fracturing, the secondary aggregates are seen to be composed of primary aggregates, which are in turn made up of crystallites.

In our studies, we also observed facing of aggregates of $BaSO_4$, CaF_2, NH_4Br, and CsI crystallites. Kinetic of crystallization in multiphase system studied in [7].

The general rule. In highly supersaturated systems, crystallization involves a few, kinetically self-similar stages. The origin of the self-similarity is that each stage is dominated by the nucleation and growth of only one kind of particles.

The possibility of different paths being realised concurrently reflects the general feature of crystallization - variability of this process, which implies that crystallites with different properties may coexist in the system under seemingly identical conditions, in combination with fluctuations of the crystallization rate.

This work was supported by the Russian Foundation Basic Research (№ 00-03-32644)

Literature

1. Melikhov, I.V., Kelebeev, A.S., and Bacic, S., Electron Microscopic Study of Nucleation and Growth of Highly Dispersed Solid Phase, *J. Colloid Interface Sci.*, 1986, vol. 112, no. 1, pp. 54–65.
2. Melikhov, I.V., On the Basic Law of Spontaneous Crystallization, *Zh. Fiz. Khim.*, 1989, vol. 63, no. 2, pp. 476 -482.
3. Melikhov, I.V., Elementary Crystallization Events in Highly Supersaturated Media, *Izv. Akad. Nauk SSSR, Ser. Khim.*, 1994, no. 10, pp. 1710–1718.
4. GorbatchevskiA.Ya., Melikhov, I.V., Vabishchevich P.N., Churbanov A.G. Influence de la forme du reacture sur la formation de depots sur ses parouis. In: Generation des solides et traitement des solides divises. Paris, 1997, vol. 11, no. 54. pp. 55-60.
5. A.M. Kutepov, Melikhov, I.V., A.M. Bylatov, Gorbatchevski A.Ya., Vabishchevich P.N., A.G. Churbanov. Processes of solid deposit formation on the surfaces of heat – transfer devices. Russian Chemistry Industry, 1997, vol. 29, no. 5, pp. 60-64.
6. Gorbatchevski A.Ya., Kutepov A.M., Melikhov I.V., Churbanov A.G. Simulation formation and evolution deposition in chemical apparatus : nonlinear aspects. CD ROM of full text of 14 th Int. congress of Chemical and processEngineering CHISA 2000, Praga Process Engineering Publisher, Praha, 2000. ISBN 80 – 86059 30 – 8, p.1 – 18
7. Melikhov, I.V., Gorbatchevski A.Ya., Vabishchevich P.N. Mechanism of successive formation of phases during crystallization in multiphase system. Theor. Foundation. Of Chem. Engineering, 1994, vol. 28, n0, 6, pp. 578- 582.

SIMULATION OF CONJUGATE HEAT/MASS TRANSFER IN CRYSTALLIZER WITH ARMATURE AND DEPOSITS ON ITS WALL

A.Ya. Gorbatchevski, I.V. Melikhov, A.J. Maroko, A.G. Churbanov*, A.M. Kutepov**

Lomonosov Moscow State University, Chemical Dept., Vorob'evy Gory, Moscow 119899, Russia, E-mail: gorba@radio.chem.msu.ru, Fax: (07 095) 9328846
**Institute for Mathematical Modeling RAS, 4 Miusskaya Square, Moscow 125047, Russia E-mail: chur@imamod.ru, Fax: (07 095) 9720723*
***Moscow State University of Environment Ecology. Moscow 107884, Staraya Basmannaya 21/4 Russia, Fax (07 095) 2677531*

The mathematical model describing this technological process involves the incompressible Navier-Stokes equations for the suspension flow as well as concentration transport and deposition law. So, it is necessary to consider in the conjugate formulation the strongly coupled process in: the suspension flow; solid walls of the reactor of complicated form; incrustations depositing on the internal surfaces.

Mathematical model. The mathematical model describing this technological process involves the incompressible Navier-Stokes equations for the suspension flow as well as concentration transport and deposition law. So, it is necessary to consider in the conjugate formulation the strongly coupled process in: the suspension flow; solid walls of the reactor of complicated form; incrustations depositing on the internal surfaces and heaving porous media properties.

Heat & Mass Transfer. The processes of convective mass transfer are considered here in the framework of the following assumptions. Analysis of conjugate heat and mass transfer is conducted in 2D formulation on the basis of dimensionless incompressible Navier-Stokes equations coupled with equations of convective transport for temperature and concentration:

$$\frac{\partial v_1}{\partial t}+\frac{\partial\left(v_1^2\right)}{\partial x_1}+\frac{\partial\left(v_1 v_2\right)}{\partial x_2}=\frac{1}{\mathrm{Re}}\left[\frac{\partial}{\partial x_1}\left(\mu\frac{\partial v_1}{\partial x_1}\right)+\frac{\partial}{\partial x_2}\left(\mu\frac{\partial v_1}{\partial x_2}\right)\right]-\frac{\partial p}{\partial x_1}-f_1 v_1 \qquad (1)$$

$$\frac{\partial v_2}{\partial t}+\frac{\partial\left(v_1 v_2\right)}{\partial x_1}+\frac{\partial\left(v_2^2\right)}{\partial x_2}=\frac{1}{\mathrm{Re}}\left[\frac{\partial}{\partial x_1}\left(\mu\frac{\partial v_2}{\partial x_1}\right)+\frac{\partial}{\partial x_2}\left(\mu\frac{\partial v_2}{\partial x_2}\right)\right]-\frac{\partial p}{\partial x_2}-\frac{Gr}{\mathrm{Re}^2}\Theta-f_2 v_2 \qquad (2)$$

$$\frac{\partial\left(c_p\rho\Theta\right)}{\partial t}+\frac{\partial\left(v_1 c_p\rho\Theta\right)}{\partial x_1}+\frac{\partial\left(v_2 c_p\rho\Theta\right)}{\partial x_2}=\frac{1}{\mathrm{Re}\,\mathrm{Pr}}\left[\frac{\partial}{\partial x_1}\left(\lambda\frac{\partial\Theta}{\partial x_1}\right)+\frac{\partial}{\partial x_2}\left(\lambda\frac{\partial\Theta}{\partial x_2}\right)\right]+Q_\Theta \qquad (3)$$

$$\frac{\partial C}{\partial t}+\frac{\partial\left(v_1 C\right)}{\partial x_1}+\frac{\partial\left(v_2 C\right)}{\partial x_2}=\frac{1}{\mathrm{Re}\,Sc}\left[\frac{\partial}{\partial x_1}\left(D\frac{\partial C}{\partial x_1}\right)+\frac{\partial}{\partial x_2}\left(D\frac{\partial C}{\partial x_2}\right)\right]+q_C \qquad (4)$$

where t is the time, x_1,x_2- cartesian coordinates, v_1,v_2 - velocity components, μ - dynamic viscosity, p- pressure, Θ - temperature, C and ρ - concentration and density of the solution, λ - heat conductivity, D - diffusivity c_p.- heat capacity at fixed pressure, $Q\Theta$ and q_C - sources of heat and mass. Here Re, Pr, Sc - Reynolds, Prandtl and Schmidt numbers, respectively, whereas additional terms in momentum equations (1), (2) describing hydrodynamical drag are introduced in order to construct homogeneous computational algorithms for complex domains using the porous body model.

Model growth. The process of deposition involves the mechanism of layer-by-layer growth with 2-dimensional nucleation. Nucleation rate dependence is proportional to the power of local oversaturaion and its dependency on inverse temperature is exponential. The shape of monocrystals changes because of material deposition on their surface, which is described by the mass flow density. The problem is considered in an element of periodic structure including halfs of two neighbor domain:

$$D\frac{\partial C}{\partial x_1} = G(\rho_k - C), G = h\sqrt[3]{\Im f^2}, \Im = \Im_0\left[\left(C/C_s\right)^m - 1\right]\exp\left[-\left(u_\Im\right)/k\Theta\right] \qquad (5)$$

$$f = f_0\left[\left(C/C_s\right)^m - 1\right]\exp\left[-u_f/(k\Theta)\right], \qquad (6)$$

where G is linear local normal crystal growth rate, h – monolayer thickness, To and f_0 – characteristically nucleation rate and tangential crystal growth rate, m – kinetical order of nucleation, u_t, u_f energies of activation and growth, local solubility in the curved site of the facet is given by $C_S = C_\infty \exp\left[\left(\sigma \quad v_0\kappa\right)/(k\Theta)\right]$, where κ – local surface curvature, s – surface energy, v_0 volume of a molecule in solid phase, k – Boltsman constant. The temperature equation is solved in the conjugate formulation simultaneously in the whole problem domain involving the moving solution and rigid bodies of variable geometry.

Numerical algorithm. To solve equations (1)-(4), an efficient homogeneous numerical algorithm has been developed. The algorithm allows to solve the above conjugate problem in the whole domain under consideration varying its form in time due to the deposition process. It is based on the fictitious domain method in the variant with continuation of equation coefficients at lower derivatives where drag terms are introduced into hydrodynamics equations similar to porous body model [1-3].

Numerical results. Computations have been conducted in the element of periodic structure including incoming solution and halfs of two neighbouring crystals changing their forms due to material deposition process from the solution.

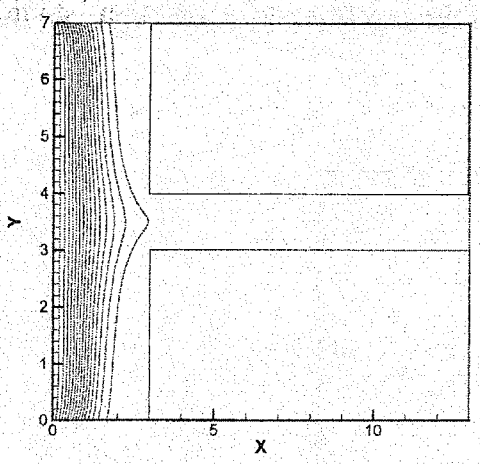

Fig.1. Concentration field at t=0.8

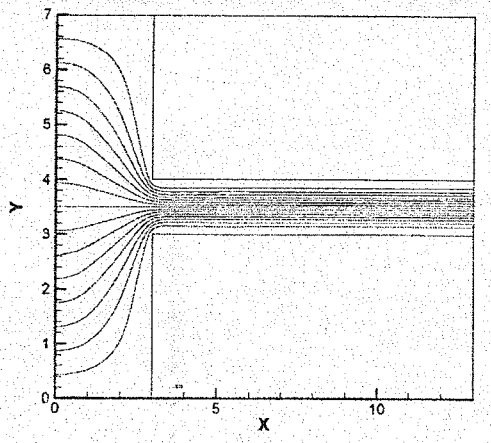

Fig.2. Flow pattern at t=0.8

The initial stage of the transient process is characterized by accelerating of the solution and downstream distribution of the impurity. Figures 1 and 2 demonstrate, correspondingly, isoconcentrations and flow pattern (streamlines) at the character time moment t=0.8 when the concentration contour with the value equals solubility C_s=0.01 for the first time achievs crystal surfaces, i.e. deposition does not yet start and crystals have the rectangular form. After this time there is appeared the material deposition from the solution resulted in changing of crystal forms and its further joining. Peculiarities of this process are governed by value $\Im_0$.

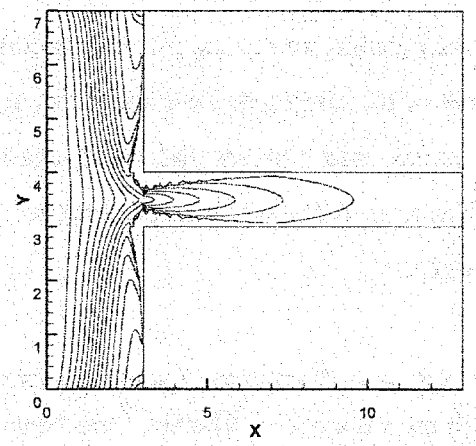

Fig.3. Concentration field at t=1.7 (betta=0.05)

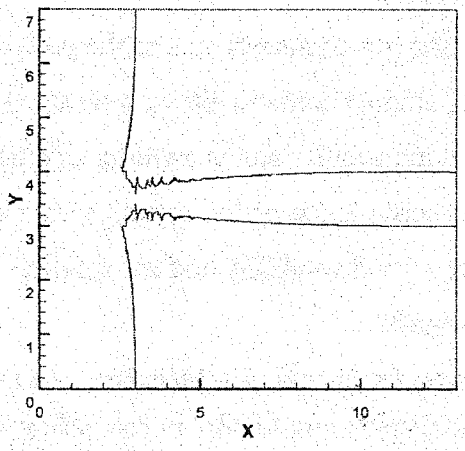

Fig.4. Channel form at t=1.7 (betta=0.05)

Figures 3 and 4 show the state of this process at moment time t=1.7 for b=0.05 when the gap width is about 80% from the initial value in the most narrow its part. The first picture (Fig.3) demonstrates the concentration field whereas in the second one (Fig. 4) there is depicted forms of the crystals. At this fast regime of deposition the growth takes place, in fact, in the vicinity of crystal corners and yields decreasing of the impurity concentration in the

downstream region. Thus, we have essentially nonuniform material deposition along the crystal surfaces that results in the transformation of the gap from the plane form into the lens form.

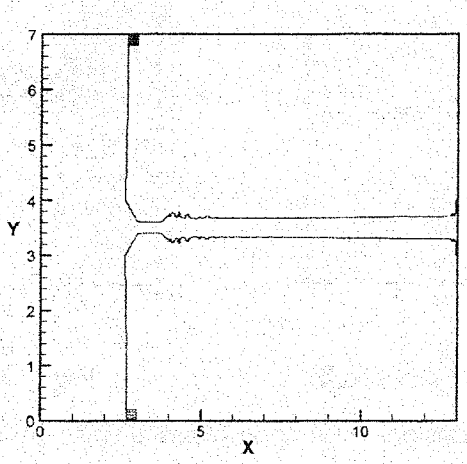

Fig.5 Channel form at t=11.4 (betta=0.0005)

A more slow deposition regime with b=0.0005 indicates a more uniform growth process. Figures 5 show crystals forms at the moment t=11.4, which is characterized by the same value of the gap width about 80% in the most narrow its part in compare with the initial state as in the previous case. It is clear that the crystal growth here is practically uniform for both vertical and horizontal faces.

Conclusions

The primary characteristics of the process of crystal joining in the incoming solution flow have been studied numerically via solving the problem of the conjugate heat and mass transfer in the solution and rigid growthing crystals. The considered process indicated essentially nonlinear dependence of the crystal form time-variation on the governing parameters of the deposition - local solubility and the solution temperature.

Reference

1. A.Ya.Gorbatchevski, I.V.Melikhov, A.M.Kutepov and A.G.Churbanov. Convective heat and mass transfer... In: CD Room Proceeding of the 13th Int. Congress of Chemical and Process Engineering CHISA'98, Praha 1998, Czech Republic, pp.1-18.
2. A.G.Churbanov and A.Ya.Gorbatchevski. Mathematical modeling of conjugate heat and mass transfer in a chemical reactor with incrustations. In: Proc. 2nd Int. Conf. On Finite-Difference Methods: Theory and Applications (CFDM98) (Ed. A.A.Samarskii), pp.80-84. Minsk, Belarus, 1998.
3. A.M. Kutepov, I.V. Melikhov, A.Ya. Gorbatchevskii, and A.G. Churbanov. Deposit Growth on Chemical Reactor Walls and the Associated Heat and Mass Transfer // Theoretical Foundations of Chemical Engineering, Vol. 34, No. 6, 2000, pp. 537–546.

SIMULATION OF LOW MACH NUMBER FLOWS USING THE QUASI-GAS-DYNAMIC SYSTEM

B.N. Chetverushkin and N.G. Churbanova

Institute for Mathematical Modeling, RAS
4 Miusskaya Square, 125047 Moscow, Russia
Fax: (095) 972-0723, E-mail: nata@imamod.ru

Numerical simulation of viscous compressible gas flows at low Mach number is of great practical interest. Many industrial problems deal with such kind of flows: these are, for example, flows in combustion chambers of a reciprocating engine and other combustion chambers, environmental problems, flows in chemical reactors etc. In the present study heat and fluid flow phenomena in chemical catalysis reactors are studied numerically. The natural gas is now available in many parts of the world and so, becomes in wide use for simple molecule synthesis. The mathematical model developed for this process includes both chemical mechanisms and hydrodynamical transport. The dynamical processes are characterized by low Mach numbers (0.01-0.1), large Reynolds numbers (500-1000) and strong temperature gradients in the boundary layer.

In this work there is presented a new approach to simulation of flows in dense gases and liquids. The quasi-gas-dynamic system (QGDS) of equations was successfully used during many years for efficient modeling of complex transonic and supersonic flows [1]. This system uses the classic Boltzmann equation or the Bchatnagar_Gross-Kruck model to describe the distribution function for gas molecules. It is correct enough for the gases of usually and weak rarefied density. It seems to be more successful to use another assumptions in the case of dense gases.

This paper deals with the similar quasy-gas-dynamic system based on the Enskog kinetic model for dense gases [2]. The Enskog equation for the distribution function was used instead of Boltzmann equation. The finite-difference scheme was used for computer simulation of gas flows in the horizontal chemical reactor. Predictions have been performed in the 2D cartesian formulation on the basis of the dimensionless QGDS-equations. The computational domain is the rectangular.

The left boundary of the computational domain is the inlet with the Poisseilue velocity profile and fixed temperature, the right boundary is the outlet with the open boundary conditions (zero normal derivatives for velocity components and temperature), the upper and lower boundaries are thermally-insulated rigid walls (no-slip, no-permeability velocity conditions)

with heated Segments of a fixed temperature and unit length located at the unit distance from the inlet. The calculations were performed with Re=500, M=0.1 and different temperature regimes (different temperature drops between the inlet and heated segments). The structure of the resulting heat and fluid flow and the resulting temperature gradients and their dependence on different boundary conditions was studied.

REFERENCES

1. T.G.Elizarova, B.N.Chetverushkin. Kinetically-consistent difference schemes for modeling flows of a viscous heat-conducting gas. J.Comp.Math. and Math. Phys., No.11, 64-75.(1988)
2. L.W.Dorodnicyn, B.N.Chetverushkin, N.G.Churbanova. Kinetically-consistent difference schemes and quasi-gas-dynamic system for modelling dense gas and liquid flows. J.Comp.Math. and Math. Phys. (to appear).

CFD SIMULATIONS OF CONTINUOUS PRECIPITATION OF BARIUM SULPHATE IN A STIRRED TANK

Zdzislaw JAWORSKI[1,2], Alvin W. NIENOW[2]

[1] *Faculty of Chemical Engineering, Technical University of Szczecin, Poland*
[2] *School of Chemical Engineering, University of Birmingham, UK*

1. Introduction

The precipitation reaction of barium chloride and sodium sulphate was used as a model reaction since it has been widely investigated experimentally and reported in the literature. In a recent study, Wong et al. (2000) showed that, in the concentration range applied, impeller speed had a small effect on crystal size and morphology. This result means that the contribution of mixing to the overall kinetics was marginal. Hence, micromixing effects have not been included in the current modelling.

In the last decade, pioneering CFD work was done for simple precipitator geometries. The first report of a successful CFD simulation of precipitation in a stirred tank was by Wei (1997), followed by a series of papers by Wei and Garside. In other studies, e.g. Van Leeuwen (1998), significant difficulties in obtaining fully converged CFD solutions for stirred tank precipitators were reported.

2. Precipitation model

The precipitation model was based on numerical solutions of a set of the differential transport equations of momentum, chemical species and the crystal size distribution moment form of the population balance for the $BaSO_4$ crystals with the boundary conditions for a model precipitator.

2.1. Precipiation reactor

A continuous flow stirred tank reactor (CSTR), of dimensions identical to those applied by Wei (1997), was modelled in this study. The tank had a diameter of T=0.3m and a flat bottom and was filled with solutions up to H=0.3m. It was equipped with 4 standard baffles and a 6-bladed Rushton turbine impeller of diameter D=0.10m, located at H/2. Four impeller speeds were applied; N= 200, 400, 600, 950 rpm. Two feed tubes were simulated for feeding with 0.1M solutions containing either $BaCl_2$ or Na_2SO_4. The feed rates of the two solutions were always the same and in the first part of this study were set to 18 ml/s. With the net working volume of 21.2 dm^3, the mean residence time was then about 20 minutes (1180 sec-

onds). The same CSTR was modelled in the second part of this study with a higher feeding rate, resulting in the mean residence time of reactants of 100 seconds, which was identical to that in the study of Wei (1997). The feed tubes were located at the free surface, on the opposite sides of the shaft, mid-way between two neighbouring baffles and roughly half way between the tank axis and wall. The reaction mixture exit was located in the centre of the tank bottom.

2.2. Model equations

The standard set of the Reynolds Averaged Navier-Stokes equations, accompanied by the continuity equation and the standard k-ε turbulence model with wall functions were applied for momentum transfer. The transport equations for all chemical entities, of molar concentration C_i (i = Ba, Cl, Na, SO_4, $BaSO_4$), were solved for the steady-state conditions. The equations had the general form of Eq. (1).

$$\mathrm{div}\left[\rho u C_i + \Gamma_{ef}\,\mathrm{grad}\left(\rho C_i\right)\right] = S_{Ci} \qquad (1)$$

The source term, S_{ci}, for the non-reacting ions (Cl, Na) was set to zero. For the other three entities, the source terms were equal to the crystal growth rate, S_g, with (+) for $BaSO_4$ and with (-) for the Ba and SO_4 ions. Following the approach by Baldyga et al. (1995), the crystal growth rate was related to the second moment of the crystal size distribution, m_2, and the crystal shape factor k_v, Eq. (2).

$$S_g = (3m_2 G)\,k_v\,\frac{\rho_{BaSo4}}{M_{BaSo4}} \qquad (2)$$

Five crystal size distribution moments, from the 0^{th} to the 4^{th}, were computed from a set of 5 equations of the population balance, Eq. (3)

$$\mathrm{div}\left[u m_j + \Gamma_{ef}\,\mathrm{grad}\left(m_j\right)\right] = 0^j J + j\,m_{j-1} G \qquad (3)$$

The crystal growth rate, G, and the nucleation rate, J, were computed from literature correlations (Baldyga et al., 1995) as functions of the local supersaturation ratio. Local values of that ratio were determined from local concentration of barium and sulphate ions computed from the iterative CFD solution of the transport equations (1).

2.3. Numerical solution

The CFD code used in this study was the structured Fluent™ code, version 4.2 and a specialized preprocessor MixSim™ for stirred tanks. The velocity (u) and turbulence fields were

obtained in the first stage of the CFD simulations, assuming a liquid density and viscosity equal to those for water. The momentum transfer stage was done using the multiple reference frame option and a direct definition of the impeller geometry. After reaching convergence, at the sum of normalised residuals below 10^{-4}, the solution was transferred to the stationary frame of reference and kept unchanged for the rest of the simulations. The same approach was used in the macromixing simulations (e.g., Jaworski et al., 2000).

Simultaneous solution of five equations for the chemical entities (1) and five equations of the crystal population balance (3) was obtained in the second stage of simulations. The physical constants for the equilibrium and kinetic equations were taken for the temperature of 20 °C. The convergence process of the numerical solution was unstable, rather slow and resulted in a relatively high number of iterations to satisfy the convergence criterion of normalized residuals lower than 10^{-7} and stable, final residual plateau for all concentration and moments. The required iteration number increased with increasing impeller speed, N, ranging from about 35,000 for 200rpm to about 90,000 for 950rpm. On average, each 10,000 iterations required about 9 CPU hours on the computationally intensive Digital server.

3. Modelling results

3.1 Long residence time

Above 99% conversion of reactants into the crystal, solid form of $BaSO_4$ was obtained in the exit stream from the precipitator for all the impeller speeds used. Equivalent figures for the conversion of barium and of sulphate ions and for the formation of solid barium sulphate were between 99.2 and 99.5% for all the impeller speeds and can be regarded as essentially constant. However, such values were significantly higher than those obtained by Wei (1997) for a residence time about 20 times shorter. Estimates of the obtained crystal mass, based on the m_3 moment and the crystal shape factor of $k_v=k_a/6=348$ (Baldyga et al., 1995), resulted in the values from 103% (200rpm) to 114% (950rpm) of the sum of the inlet mass flux of Ba and SO_4. The volume averaged crystal size (L_{43}) in the exit stream converged in the range from 11 to 18 microns. The simulation results suggest that the mean crystal size slowly increases with increasing impeller speed. However, the calculated values depend very much on the crystal shape factors used.

3.2 Short residence time

The same simulation programme was repeated for the mean residence time of 100 seconds, as used in Wei's (1997) study. About 1% lower conversion was obtained compared to

the long residence time cases, but still much higher than that found by Wei. The conversion data were between 98.1% and 98.4% for the barium and sulphate ions as well as for the solid barium sulphate. Other characteristics were also similar to those for the long residence time.

4. Concluding remarks

A continuous precipitation process of barium sulphate was successfully simulated in a model stirred tank. The calculated level of conversion into solid barium sulphate was significantly higher than in the previous work of Wei, which may be due to a substantially lower level of residuals being used to satisfy the convergence requirements of the iteration process in this study.

5. Literature cited

1. Bałdyga J., Podgórska W. and Pohorecki R., 1995, Mixing-precipitation model with application to double feed semibatch precipitation. *Chem. Engng Sci.* 50, 1281-1300.
2. Jaworski Z., Bujalski W., Otomo N., Nienow A.W.: CFD study of homogenization with dual Rushton turbines – comparison with experimental results. Part I: Initial studies. Trans IChemE, **78**, Part A, 327-333, April 2000.
3. Wong D.C.Y., Jaworski Z., Nienow A.W.: Effect of ion excess on particle size and morphology during barium sulphate precipitation: an experimental study. ISCRE-16 Book of Abstracts, pp. 112-113, September 2000, Cracow, Poland, accepted for publication in Chem. Eng. Sci.
4. Wei H., 1997, Application of Computational Fluid Dynamics techniques to the modelling of precipitation processes. PhD Thesis, UMIST.
5. Van Leeuwen M.J.L., 1998, Precipitation and mixing, PhD Thesis, Technical University Delft.

Acknowledgements

EPSRC financial support for ZJ and the use of the Digital Unix server of the University of Birmingham are gratefully acknowledged.

THE PHENOMENON OF ENERGY CONCENTRATION IN COMBUSTION WAVES AND ITS APPLICATIONS

V.S. Babkin, I. Wierzba* and G.A. Karim*

Institute of Chemical Kinetics and Combustion RAS
Novosibirsk 630090, Russia
**Department of Mechanical and Manufacturing Engineering*
The University of Calgary, Calgary, Alberta, Canada, T2N 1N4

Combustion processes are commonly controlled by chemical and physical parameters of the reacting mixture (such as mixture composition, chemical kinetics, etc.) and also by the parameters controlling the thermal, aerodynamics and other physical characteristics of combustion. These conventional methods are well known, but tend to be substantially limited. Therefore, non-conventional methods of control based on tendencies of flames to self-organization and particularly to the formation of excess enthalpy in combustion zones, commonly known in the literature by the term of "excess enthalpy", (EE), are of interest. The problem of excess enthalpy in combustion systems has been discussed in many papers but mainly in relation to combustors [1,2]. However, the phenomenon of EE is encountered more frequently in nature than has been thought previously [3] and there is a need for further analysis of combustion processes with EE to establish general trends and develop the physical and chemical foundations for various applications.

The present contribution analyzes some aspects of the phenomenon of "excess enthalpy flames" (EEF) and defines the systems, methods and elementary processes controlling EEF formation as well as the prospects for its use in practical devices (e.g. burners and reactors), and in other different technologies. Cellular flames, the propagation of combustion waves in porous media, spiral combustion, combustion with longitudinal auto-oscillations and diffusion flames will be also considered. In addition to the usual combustion processes with EE other processes will be considered in which the enthalpy excess is produced artificially, as for example in regenerative and tunnel burners, reverse-processes with gas-phase reactions and catalytic reactions and combustion of energetic materials with heat conducting elements. It can be shown that the energy concentration in combustion zones is essentially occurring in all systems in which combustion is possible. Hence, combustion processes involving excess enthalpy can be observed in laminar, turbulent premixed and diffusion flames, in stabilized combustion as well as in propagating waves in homogeneous or in multiphase disperse and other systems. It is interesting to note that the EE phenomenon produces in some cases the

appearance of uncommon type of flames such as cellular, spin and oscillating flames. In "filtration" combustion for example, unique features are displayed such as non-equilibrium and super adiabatic temperatures, a capability to propagate through channels with a characteristic size less than the critical distance, etc.

The mechanisms of energy concentration in combustion systems can be quite different. For example, there are two different modes of heat recuperation which create the EE effect - external and internal where all components of complex heat exchange, (i.e. conduction, convection and radiation) mass exchange processes are of importance. The effects of preferential diffusion (Lewis number), gas compressibility (Mach number), mass forces (Rayleigh number), phase transitions, filtration processes etc. play an important role. The effects of EE can be manifested in changes in temperature, mixture composition or pressure which reflect changes in both the thermal and chemical parts of enthalpy.

An increase in the reactivity of the mixture due to energy concentration can occur both over the whole flame front and locally in separate hot spots and cells. The EE features appear to be particularly noticeable near the critical conditions such as those at the flammability and stability limits. Additional thermal energy in the combustion products can be used not only in the preheating of the reactive mixture but also in other processes, such as evaporation, gasification and formation of combustible mixtures above the surface of a liquid fuel. However, for maximum energy concentration, optimum conditions are needed and the effectiveness of EEF applications is dependent on finding these optimal conditions.

It should be also noted that although the term "excess enthalpy" in flames is often used in the scientific literature, its physical meaning is not clearly defined except for the simplest case of the premixed laminar flame. In general terms, EE can be defined as a spatial concentration of energy during combustion. This definition can be made more specific by indicating the source of energy, i.e. whether internal from the inner resources of the combustible mixture or external from outside of the system. This definition can be narrowed further by specifying the part of the flame in which the energy is concentrated. For example, to control the combustion process by changing the chemical reaction rate, it is important that EE is concentrated in the zone of chemical reactions. Furthermore, in principle, different forms of excess energy are possible (e.g. thermal, chemical, compression, etc.). However, usually the thermal part of energy has been the main one considered.

These definitions tend to be rather inprecise as they concern only some aspects of the EE phenomenon. Also, the existence of some reference level of enthalpy is implied by the term

"excess enthalpy" and has to be specified. There are also other uncertainties in the concepts of flames with excess enthalpy where anomalously high combustion rates with wide regions of their existence, some "exotic" structures of flame fronts, etc. are encountered. Moreover, cellular and spinning flames with a three-dimensional structure of combustion zones are strongly non-linear and require adequate methods of analysis. At present, the theory of EEF is not sufficiently advanced and tends to fail to answer many questions concerning the structure, stability, extension of the flammability limits and blow-off characteristics of such flames.

Based on the examples discussed in the present contribution it can be concluded that there is a wide range of possible applications of the EEF's. The unusual features and characteristics of these flames are rather attractive for use in chemical reactors and in combustors operating as sources of thermal incinerators of dangerous and toxic substances. There is a great potential for such applications mainly due to the absence of the conventional link between the composition of a combustible mixture and its flame temperature. This is particularly important in the consideration of fire and explosion safety where the flame temperature and flammability limits play a significant role.

It is to be shown that further research is needed to improve our understanding of excess enthalpy flames, their peculiarities, conditions of existence and other characteristics including their rates and mechanisms of their propagation and limits, so as to effect suitable theories and contribute to the development of effective novel burners, reactors and technologies for various purposes.

References:

1. J. Masters and R. J. Webb, "The Development of a Recuperative Burner for Gas-Fired Furnaces", *Proc. Roy. Soc.*, Lond. A 393, 19-49 (1984).
2. F. J. Weinberg, "Combustion in Heat-Recirculating Burners", In: Advanced Combustion Methods, Academic Press, 183-236 (1986).
3. F. J. Weinberg, "A Brief Survey of "Excess Enthalpy" Combustion and Some Recent Developments", 1-st International School-Seminar "Modern Problems of Combustion and Its Applications", Minsk (1995).

OP-II-6

EXPERIMENTAL AND ANALYTICAL INVESTIGATION OF THE PREIGNITION REACTIONS OF n-HEPTANE – AIR MIXTURE UNDER STEADY FLOW REACTOR CONDITIONS

Ghazi A. Karim and E. Khalil

Mechanical Engineering - University of Calgary
2500 University Drive, N.W.- Calgary –Canada T2N 1N4

The oxidation reactions of the typical higher normal alkane, n-heptane, in air is simulated analytically, via a detailed chemical kinetic mechanism made up of 1950 elementary reaction steps and 380 species. The simulation of the preignition and post ignition processes was made for homogeneous fuel lean to stoichiometric reacting mixtures within externally heated steady flow tubular reactor under constant pressure conditions. A reduced version of the kinetic scheme was also formulated and tried. The simulation could display in detail the major features of the combustion process including the associated single and multi-stage ignition reaction phenomena.

The paper will present computed results of the simulation and will discuss the roles of the various design and operating variables on the progress of the reaction, the associated energy release rates and the temporal variations in the composition of the reacting flow.

Comparison of the simulation results with corresponding experimental data obtained in a laboratory set-up, was made showing good qualitative agreement; however, some quantitative differences could be observed. The possible reasons for such deviations are to be discussed. It is to be shown also that the employment of the reduced scheme in the modeling process could produce excellent agreement in the behavior of the key operational variables and the temporal changes in the major reactive species, with the corresponding values obtained using the full kinetic scheme in the modeling while effecting significant reductions in computing time.

The implication of these findings to improving the control of the combustion process and reducing exhaust gas emissions in industrial applications will be highlighted.

THE CATALYTIC OXIDATION OF HEATED LEAN HOMOGENEOUSLY PREMIXED GASEOUS FUEL-AIR STREAMS

I. Wierzba and A. Depiak

Mechanical Engineering – University of Calgary
2500 University Drive, N.W.-Calgary-Canada T2N 1N4

There is much interest in being able to oxidize lean mixtures in air of common gaseous fuels such as natural gas, at relatively low temperatures so as to reduce exhaust emissions of oxides of nitrogen, unburned hydrocarbons and carbon monoxide while maintaining high combustion and fuel conversion efficiencies. This would be particularly very attractive if relatively cheap non-noble catalysts are used instead of platinum.

The paper describes the results of an experimental laboratory investigation of the oxidation reactions within a packed bed tubular reactor, of heated low velocity streams of homogeneous lean mixtures of gaseous fuels in air at atmospheric pressure, in the presence of non-noble metal catalysts. The main fuel considered is methane. Comparative tests were also made using other common fuels that included ethylene, carbon monoxide, propane and hydrogen. The main catalysts employed were chromium and cobalt oxides and their mixtures. These were selected mainly because of their relatively high thermal stability.

The investigation examined the effects of changes in flow rate, and hence residence time, for different initial mixture temperature, (from 425K) and feed equivalence ratio on the exhaust composition, the course of the reaction and the associated energy release development within the catalytic bed. The associated light-off temperatures of the catalysts were also established. Corresponding tests were made throughout, using platinum catalytic beds for comparative purposes.

It is to be shown for these applications, there is an optimum ratio of cobalt to chromium oxides and catalytic bed loading that could yield significant improvement to the low temperature oxidation of the lean mixtures and the resulting emissions. However, these catalysts remain significantly less effective than platinum.

OP-II-8

SELECTIVE CATALYTIC HYDRATION OF ETHYLENE AND PROPYLENE OXIDES

V.F. Shvets, M.G. Makarov, R.A. Kozlovskii, A.V. Koustov

D.I.Mendeleev University of Chemical Technology of Russia, Moscow, Russia

The reaction of ethylene oxide hydration is the main industrial way of production of ethylene glycol which is one of the most large scale product of industrial organic synthesis, with a world annual volume of production above 15 million tons [1]. The reaction of ethylene oxide hydration proceeds on a serial-parallel route resulting in formation of glycol homologues:

$$H_2O \xrightarrow[k_0]{C_2H_4O} HOCH_2CH_2OH \xrightarrow[k_1]{C_2H_4O} HO(CH_2CH_2O)_2H \xrightarrow[k_2]{C_2H_4O} \text{and so on} \qquad (I)$$

Where k_0, k_1, k_2 – rate constants of series stages.

The reaction (I) is subjected to acid, base and nucleophilic catalysis [2, 3] and at the temperature higher 120°C proceeds with enough high speed without any catalysts. Till now all ethylene glycol in industry is produced by a noncatalyzed reaction. The product distribution in the reaction (1) is regulated by ethylene oxide - water ratio in the initial reaction mixture. The rate constants ratio of series stages of noncatalyzed reaction (I) is unfavorable for formation of ethylene glycol (distribution factor for a noncatalyzed reaction $b=k_1/k_0$ according to different sources is equal to 1.9-2.8 [2]). For this reason to increase the ethylene glycol yield in industry 15-20 multiple molar (or 6-9 multiple mass) excess of water in relation to ethylene oxide is usually used. It results in considerable power expenses at the stage of final products isolation.

One of the ways to increase the selectivity of ethylene glycol formation and, therefore, to decrease the excess of water is the application of the catalyst accelerating only the first stage of reaction (I). We have found that such catalysts are the anions of salts of some weak acids [3]. Other publications on this subject later have appeared [4-8]. A kinetics and mechanism of oxides hydration at a homogeneous catalysis by salts are studied by us in detail [3, 9, 10]. The obtained kinetic data have shown, that at concentration of some salts about 0.5 mol/l distribution factor $b=k_1/k_0$ is reduced in 10 and more time (till 0.1-0.2). It enables to receive ethylene glycol with high selectivity at molar ratio water - ethylene oxide of close to unit. The found properties of the mentioned above homogeneous nucleophilic catalysts we have used hereinafter for creation of industrial heterogeneous catalysts of selective hydration of ethylene and propylene oxides by an immobilization of anions on heterogenous carriers [11-16]. The main

world producers of ethylene glycol (Shell [17-19], Union Carbide [20-22] and Mitsubishi [23]) conduct researches on creation of selective hydration catalyst in the same direction.

For one heterogeneous catalyst, representing bicarbonate ions, immobilized on anionites, we constructed mathematical model of the reactor and carried out its experimental testing on laboratory tubular reactor with a diameter of the tube 4 mm.

The mathematical model was based on the kinetics of homogeneous catalytic reaction. When pH value is below 9, ethylene oxide (EO) reacts through noncatalytic reactions (1) and through reaction, catalysed by bicarbonate ion with rate constant K_{cat}. The rates for the consumption of EO and water and obtaining of monoethylene (MEG) and diethylene (DEG) glycols are equal accordingly:

$$\begin{aligned} r^{EO} &= C^{EO}*(C^{H2O}+1.84*C^{gly})*(K_0*(C^{H2O}+b*C^{gly})+K_{cat}*[HCO_3^-]) \\ r^{H2O} &= C^{EO}*(C^{H2O}+1.84*C^{gly})*(K_0*C^{H2O}+K_{kt}*[HCO_3^-]) \\ r^{EG} &= C^{EO}*(C^{H2O}+1.84*C^{gly})*(K_0*(C^{H2O}-b*C^{EG})+K_{cat}*[HCO_3^-]) \\ r^{DEG} &= C^{EO}*(C^{H2O}+1.84*C^{gly})*K_0*(C^{EG}-b*C^{DEG}) \end{aligned} \qquad (2)$$

where $K_0=\exp(-3.656-9720/T)$ $l^2/mol^2 \cdot sek$ – noncatalytic reaction rate constant, $K_{cat}=\exp(4.404-10568/T)$ $l^2/mol^2 \cdot sek$ – rate constant of the reaction catalysed by bicarbonate ion, $b= K_0 / K_1$, C^{gly} – total glycol concentration in the mixture.

The term $(C^{H2O}+b*C^{gly})$ in the equation (2) is caused by the solvatation of EO with water and glycols hydrogen bonding. As it follows from the equation (2), catalyst accelerate the reaction of the MEG formation.

The homogeneous reaction model was transformed for continous plug flow reactor, filled with anionites in the bicarbonate form. The calculations and direct measurements of temperature in the catalyst layer have shown, that in the experimental conditions the divergence of temperature along tube length because of exothermal process can be neglected. Transforming for these conditions of the equation (2) for plug flow reactor, we suggested, that in the liquid phase the only noncatalytic reaction proceeds, and in the ionite phase the noncatalytic reaction is accompanied by catalytic one, that is considerably faster.

In the equations of the mathematical model for plug flow reactor index $_i$ refers to ionit, index $_l$ refers to liquid phase; $\alpha=V_i/V_r$ – ionit part in total tube volume; C^i – concentration of i-component, mol/kg.

As tube reactor may be considered with very good precision as plug flow reactor, the equation for EO hydration in the presence of the ionit can be written $dF^i=dV*(\alpha*r_и+(1-\alpha)*r_ж)$ or $dC^i/d\tau==(\alpha*r_и+(1-\alpha)*r_ж)/\rho_o$, where $\rho=G_p/W_o$– density of the rection mixture, G_p and W_o –

mass and volume flow of the reaction mixture, $\tau=V/W_o$ – holding time. In the liquid phase only noncatalytic reaction take place, therefore

$$r^{EO}_{ж}=C^{EO}_{ж}*(C^{H2O}+1.84*C^{gly})_{ж}*K_{нк}*(C^{H2O}_{ж}+b*C^{gly}_{ж})$$

$$r^{H2O}_{ж}= C^{EO}_{ж}*(C^{H2O}+1.84*C^{gly})_{ж}*K_{нк}*C^{H2O}_{ж}$$

$$r^{EG}_{ж}= C^{EO}_{ж}*(C^{H2O}+1.84*C^{gly})_{ж}*K_{нк}*(C^{H2O}_{ж}-b*C^{EG}_{ж})$$

$$r^{DEG}_{ж}= C^{EO}_{ж}*(C^{H2O}+1.84*C^{gly})_{ж}*K_{нк}*(C^{EG}_{ж}-b*C^{DEG}_{ж})$$

For ionite phase the equation is more complex:

$$r^{EO}_{и}=C^{EO}_{и}*(C^{H2O}+1.84*C^{gly})_{и}*(K_{нк}*(C^{H2O}_{и}+b*C^{gly}_{и})+K_{kt}*[HCO_3^-])$$

$$r^{H2O}_{и}= C^{EO}_{и}*(C^{H2O}+1.84*C^{gly})_{и}*(K_{нк}*C^{H2O}_{и}+K_{kt}*[HCO_3^-])$$

$$r^{EG}_{и}= C^{EO}_{и}*(C^{H2O}+1.84*C^{gly})_{и}*(K_{нк}*(C^{H2O}_{и}-b*C^{EG}_{и})+K_{kt}*[HCO_3^-])$$

$$r^{DEG}_{и}= C^{EO}_{и}*(C^{H2O}+1.84*C^{gly})_{и}*K_{нк}*(C^{EG}_{и}-b*C^{DEG}_{и})$$

We approximated the solvation term by sum $C^{H2O}+1.84*C^{gly}$, but it is possible that in the ionit phase the composition and solvation ability of the reaction mixture can differ from that of the liquid phase. It seems evident that we must include the correction factor. Notifying that in the kinetic equations there are making $C^{EO}*(C^{H2O}+1.84*C^{gly})$, that is why we can include first parameter $\delta_1=(C^{EO}*(C^{H2O}+1.84*C^{gly}))_i/ (C^{EO}*(C^{H2O}+1.84*C^{gly}))_l$ taking into account the difference in the reaction mixture in two phases. Let $\delta_2=C^{H2O}_i/C^{H2O}_l$, $\delta_3=C^{gly}_i/C^{gly}_l$, and we make a rather probable suggestion that the parameters for MEG and polyglycols are equal. The interpretation of this assumption may be of the two kinds. In the first case, if we assume complete equilibria between liquid phase and ionite, these parameters are equilibria constants for the substances. Alternative is the quasiequilibria because of equality of the rates of diffusion and chemical reaction. It follows from both assumptions that parameters δ_1-δ_3 cannot be > 1 and only slightly depends on temperature (for solubility heats for substances in the phase are similar and diffusion rates also slightly depends on temperature). It is impossible to distinguish these two assumption without special physicochemical investigations, nevertheless this model can be used successfully.

Thus this system of equations is the full mathematical model for EO hydration in the tube reactor in the presence of ionite.

The experimental results on checking the model are represented in the table 1. In this table there are also the results of calculations of the composition of the reaction mixture in the outlet of the reactor according to the suggested model and known initial conditions. The part of ionit is calculated as ratio of ionit volume and tube volume, multiplied on the infilled coefficient 0.7. For fitting experimental data we change mostly parameter δ_1.

Table 1. Experiments in the tube reactor. Concentration in % weight, calculated values in the denominator.

τ, sec	EO	EG	DEG	A	δ_1	δ_2	δ_2
Ionit SBR, 2 ml, 95 oC, eff.exchange cap. 5.08 mmol/g, 12% wght EO							
690	0.57/0.671	14.36/15.86	0.094/0.088	0.609	0.9	0.7	0.7
Ionit MSA-1, 2 ml, 95 oC, eff.exchange cap. 4.42 mmol/g, 12% wght EO							
690	0.77/0.73	14.11/15.76	0.109/0.095	0.609	1.0	0.7	0.7
Ionit MSA-1, 1.7 ml, 95 oC, eff.exchange cap. 3.22 mmol/g, 12% wght EO							
1099	0.81/0.95	15.46/15.37	0.16/0.167	0.458	1.0	0.7	0.7
Ionit SBR, 1.5 ml, 95 oC, eff.exchange cap. 4.70 mmol/g, 12% wght EO							
987	0.44/0.46	15.57/16.11	0/0.12	0.458	1.0	0.7	0.7
Ionit MSA-1, 2 ml, 105 oC, eff.exchange cap. 2.39 mmol/g, 12% wght EO							
792	0.99/0.69	15.14/15.67	0.15/0.22	0.458	0.95	0.7	0.7
Ionit SBR, 1.7 ml, 105 oC, eff.exchange cap. 3.19 mmol/g, 12% wght EO							
1910	0.12/0.14	16.54/16.21	0.16/0.42	0.189	1.0	0.7	0.7
Ionit SBR, 1.7 ml, 105 oC, eff.exchange cap. 3.50 mmol/g, 20% wght EO							
1269	0.81/1.02	25.59/25.55	0.70/0.99	0.189	1.0	0.7	0.7

The analysis of the data of table 1 shows, what the offered model adequately describes the experimental data which have been carried out in a wide enough range of the initial conditions, and parameter δ_1=1 practically is constant for all experiments. Let's note also, that the model describes not only EO conversion, but also the composition of the reaction mixture, i.e. selectivity of process. Last two experiments show, that even at a small part of the ionit in the tube the basic reaction goes in the ionit phase, that provides high selectivity of process.

In the conclusion it is possible to say, that the mathematical model for EO hydration in the tube reactor in the presence of ionit is built and may be used to design and operate the installations of selective EG synthesis.

Literature

1. Noor-Drugan, Natalie, Testing Times for Ethylene Glycol Makers, Chemical Week, March 3, 1999, p.32.
2. Dyment O.N., Kazansky K.S., Miroshnikov A.M., Glycols and other derivatives of ethylene and propylene oxides. Moscow, 1976.

3. Lebedev N.N., Shvets V.F., Romashkina L.L., // Kinetics and catalysys (rus), 1976, v.17, №3, page 576.
4. Japanese Patent JP 57-139026, (1982).
5. Masuda T., Asano K.H., Naomi Ando S., US Patent 4937393; Mitsui Toatsu Chemicals, Incorporated, (1990).
6. Keen B.T., US Patent 4578524; Union Carbide Corp. (1985).
7. Keen B.T., US Patent 4571440; Union Carbide Corp. (1986).
8. Odanaka H., Yamamoto T., Kumazawa T., JP Patent 56090029 A2; Nippon Shokubai Kagaku Kogyo Co., Ltd., (1981).
9. Lebedev N.N., Shvets V.F., Romashkina L.L., // Kinetics and catalysys (rus), 1976, v.17, №3, page 583.
10. Lebedev N.N., Shvets V.F., Romashkina L.L., // Kinetics and catalysys (rus), 1976, v.17, №4, page 888.
11. Shvets V.F., Makarov M.G., Suchkov Yu.P. and others Russian Patent 2001901 (1993)
12. Shvets V.F., Makarov M.G.,Koustov A.V. and others Russian Patent 2002726 (1993).
13. Shvets V.F., Makarov M.G.,Koustov A.V. and others Russian Patent 2122995 (1998)
14. Shvets V.F., Makarov M.G.,Koustov A.V. and others Russian Patent , PCT/RU99/00087, WO 97/33850, (1997)
15. Shvets V.F., Makarov M.G.,Koustov A.V. and others Russian Patent , PCT/RU99/00087, WO 99/12876, (1999)
16. Shvets V.F., Makarov M.G.,Koustov A.V. and others Russian Patent 2149864 (2000)
17. Reman W.G., Van Kruchten Eugene M. G. A., US Patent 5488184; Shell Oil Company, (1996).
18. Van Kruchten Eugene M. G. A., US Patent 5874653; Shell Oil Company, (1999).
19. Van Kruchten Eugene M. G. A., WO Patent 9923053 A1; Shell Internationale Research Maatschappij B.V., (1999).
20. Soo H., Ream B.C., Robson J.H., US Patent 4967018; Union Carbide Chemicals and Plastics Company Inc., (1990).
21. Soo H., Ream B.C., Robson J.H., US Patent 5064804; Union Carbide Chemicals and Plastics Company Inc., (1990).
22. Forkner M.W., US Patent 5260495; Union Carbide Chemicals & Plastics Technology Corporation, (1993).
23. Iwakura T., Miyagi H., JP Patent 11012206 A2; Mitsubishi Chemical Industries Ltd., Japan. (1999).

PARAMETRIC SENSITIVITY OF THE METHANOL OXIDATION PROCESS AS A SOLUTION OF A BOUNDARY VALUE PROBLEM WITH A PARAMETER

Andrew I. Madyarov and Natalia A. Chumakova

Boreskov Institute of Catalysis, Pr. Akad. Larentieva, 5, Novosibirsk 630090, Russia
phone: 383 2 34 12 78 fax: 383 2 34 18 78 E-mail: chum@catalysis.nsk.su

The behavior of chemical reactors depends on variations in the inlet conditions, as well as in other physicochemical parameters of the system. We will develop a new approach to parametric sensitivity studies of a catalytic fixed-bed operation [1-2]. This approach allows estimating the influence of space-nonuniform conditions on technological process characteristics in a real fixed-bed reactor by means of relatively simple one-dimensional model consideration.

1. Mathematical model

An adiabatic catalytic fixed-bed reactor with the irreversible exothermic two-stage methanol oxidation reaction of $A \rightarrow B \rightarrow C$ type, where A is methanol, B is formaldehyde being a target product, and C denotes water and other deep oxidation products, is concerned.

An one-dimensional quasi-homogenous plug-flow mathematical model of the process has a form of an ordinary differential equations system [2]:

$$\frac{dX}{d\xi} = F(X, v, \varepsilon). \qquad (1)$$

Here $X = (x_1, x_2, P)^T$ are concentrations of the substances A and B, and pressure drop, v is the gas flow velocity, ε is the porosity of the bed, i.e. void volume fraction in the reactor volume (its effect is of practical interest, because the temperature profile along the bed length depends strongly on ε), ξ is the dimensionless axial coordinate. In traditional statements [3] the gas velocity v is considered as a known value and the initial value problem (IVP) is posed for the system (1):

$$X(0) = X_0 = (x_{10}, x_{20}, 0)^T. \qquad (2)$$

The parameter v in (1) presents an averaged value of the gas velocity through the fixed bed.

In another model [1-2] v is an unknown parameter and the pressure drop on the bed is supposed to be known, i.e. a boundary value problem (BVP) is considered with three conditions at the left bound $\xi = 0$ and one at the right bound $\xi = 1$ as follows:

$$X(0) = X_0, \qquad X_3(1) = \Delta P. \qquad (3)$$

In such case the parameter v corresponds to a local gas flow velocity in the catalyst bed.

Note that in case of more complex reaction of many stages, reactants and products we can obtain a similar system consisted of N equations:

$$\frac{dX}{d\xi} = F(X, v, \theta), \qquad X = (x_1, \ldots, x_N)^T, \tag{4}$$

where the last equation defines the pressure drop. For such systems the approach suggested in [2] leads also to the BVP with N conditions at the left bound and one condition at the right one:

$$X(0) = X_0(\theta), \qquad X_N(1) = \Delta P(\theta). \tag{5}$$

Here θ means a selected parameter of the model, sensitivity analysis to which is of practical interest.

The objective of our work was to develop an algorithm for the numerical construction of the BVP solution and the sensitivity functions of this solution to the model parameter θ. For the methanol to formaldehyde oxidation process as an example, the process sensitivity to the structure parameter ε was studied and comparative sensitivity analysis of solutions of the BVP (1), (3) and the IVP (1)-(2) was carried out.

2. Algorithm

To solve the BVP (4)-(5) with the parameter v we use Newton's method, and on each iteration the linearized BVP for function $\tilde{X}(\xi) = X(1-\xi)$ and parameter v arises:

$$\frac{d\tilde{X}}{d\xi} = -F_X(\tilde{X}^0, v^0)\cdot\tilde{X} - [F(\tilde{X}^0, v^0) - F_X(\tilde{X}^0, v^0)\cdot\tilde{X}^0] - F_v(\tilde{X}^0, v^0)\cdot(v - v^0), \tag{6}$$

$$\tilde{X}_N(0) = \Delta P, \qquad \tilde{X}(1) = \tilde{X}_0,$$

where $\tilde{X}^0$ and v^0 are the previously found approximations for vector $\tilde{X}$ and parameter v.

It is suggested to solve the linearized problem (6) numerically with the Godunov orthogonal factorization method [4], application of which to a BVP with a parameter was studied in detail in [5]. The main idea of the algorithm is as following. The interval [0, 1] is divided into several subintervals by a proper way, an orthogonal basis of the subspace satisfied the left boundary condition is determined and after the numerical integration along each subinterval this basis is orthogonalized again at the subinterval right end. It allows avoiding an effect of basis "squashing" and finding the solution more accurate in regions of high gradients.

3. Parametric sensitivity functions

To analyze the sensitivity of the BVP (4)-(5) solution X and v with respect to the selected parameter θ, we introduce parametric sensitivity functions:

$$Z = \frac{\partial X}{\partial \theta}, \qquad u = \frac{\partial v}{\partial \theta}.$$

Differentiation of (4) and (5) with respect to θ gives:

$$\frac{dZ}{d\xi} = F_X(X, v, \theta)\cdot Z + F_\theta(X, v, \theta) + F_v(X, v, \theta)\cdot u, \tag{7}$$

$$Z(0) = \frac{\partial X_0}{\partial \theta}, \qquad Z_N(1) = \frac{\partial(\Delta P)}{\partial \theta}. \tag{8}$$

Hence we obtain the linear BVP for the vector function Z and the parameter u, which after the substitution $\widetilde{Z}(\xi) = Z(1 - \xi)$ has the same form as the linearized BVP (6). Therefore we can apply the orthogonal factorization method too.

4. Numerical results

A universal Fortran code was developed to solve the BVP with a parameter and construct the solution sensitivity functions to some model parameter. Using this code, the concentrations, temperature and pressure losses profiles and the sensitivity functions to the porosity ε were obtained for the problem (1), (3). Fig. 1 shows A and B concentrations x_1, x_2 versus the axial coordinate as the BVP (1), (3) solution for different porosity values.

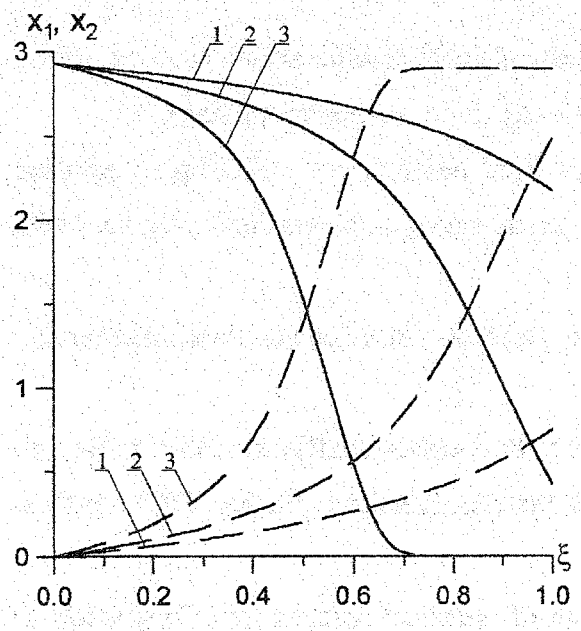

Fig. 1. Methanol and formaldehyde concentrations along the axial coordinate ξ. ΔP=0.0179 *atm*, ε = 0.45 *(1)*, 0.4 *(2)*, 0.35 *(3)*. Solid lines – x_1, dash lines – x_2

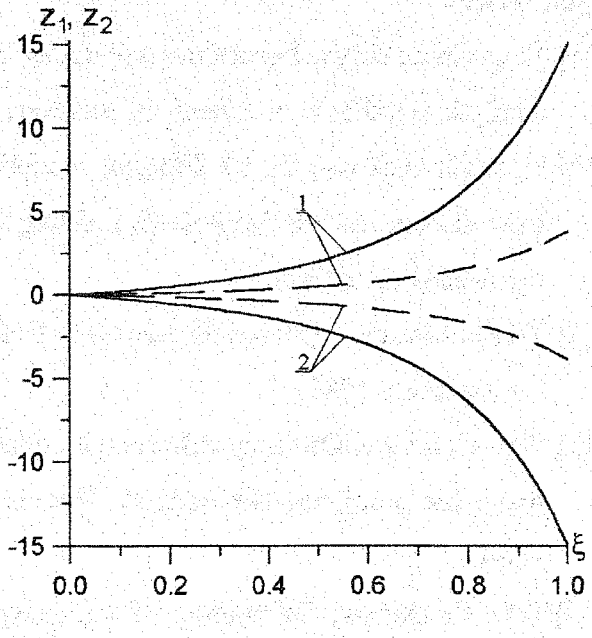

Fig. 2. Concentrations sensitivity functions z_1, z_2 to ε in the BVP at ΔP=0.0179 *atm* (solid lines), and in the IVP at v = 1.112 *m/s* (dash lines); ε = 0.45.

In order to compare the parametric sensitivity functions of BVP and IVP solutions in a correct way it is necessary in the BVP to take ΔP value in (3) as one corresponded to the gas

flow velocity in the IVP. That means the identity of the technological modes in the reactor models considered. As a result we obtained that the module of the solution sensitivity functions of the BVP (1), (3) is much bigger than the absolute magnitude of the IVP (1)-(2) solution sensitivity functions (Fig. 2), what is more compatible with practical surveys.

5. Conclusion

The BVP with a parameter for the system of N ordinary differential equations with N conditions at the left boundary and one condition at the right one was considered. The algorithm for numerical solution of such problem was developed and its software implementation was made. The algorithm was based on the Godunov orthogonal factorization method and was used for construction of the solution and sensitivity functions to one of system parameters.

Sensitivity functions to the porosity ε were obtained for the particular catalytic process and it was shown that the parametric sensitivity of the BVP (1), (3) solutions was higher than sensitivity of the corresponding IVP (1)-(2) solutions. Similar conclusions are valid with respect to other control parameters (e.g. the feed temperature, the inlet reactant concentration, the pressure drop over the bed, the catalyst activity, etc.).

References

[1] N.A. Chumakova, Parametric sensitivity of formaldehyde free methanol production in a catalytic fixed bed. In: *Chemical Industry*, 1997, No. 2, pp. 43-50 (In Russian).

[2] N.A. Chumakova, Yu.Sh. Matros, Modeling of fixed-bed reactors at fixed pressure drop over the bed. In: *Mathematical modeling of catalytic reactors*. Novosibirsk: Nauka, 1989, pp. 5-26 (In Russian).

[3] Yu.Sh. Matros, Unsteady Processes in Catalytic Reactors. Elsevier Sci. Publ., Amsterdam – New York, 1985.

[4] S.K. Godunov, Ordinary differential equations with constant coefficients. Part 1: Boundary value problems. Novosibirsk, Novosibirsk State University publisher, 1994 (In Russian).

[5] S.V. Kuznetsov, Calculating of stationary front of chemical reaction. In: *Computational problems in mathematical physics. IM SB RAS Proceedings*, 1988, vol. 11, Novosibirsk: Nauka, pp. 93-100 (In Russian).

SELF-ORGANIZED CRITICALITY IN INDUSTRIAL ETHYLENE OXIDE REACTORS

B.B. Chesnokov, B.Ya. Stul, A.V. Derugin, M.G. Slin'ko

Scientific Research Institute "SYNTEZ", Moscow

Industrial production of ethylene oxide by oxygen oxidation of ethylene, which is considered to be one of the most heat-strained process, is conducted in high capacity tubular reactors with fixed bed of expensive silver catalyst. Stable work of industrial reactors is the base for execution of strict production safety standards. However, in reality sometimes during reactor operation thermal runaways take place. The analyses of such thermal runaways, the study of the causes of their appearance, development and ways of their prevention, modelling of the situations play very important role [1,2].

During the study of the reasons of large natural and technical accidents new nonlinear phenomenon was discovered - self-organized criticality. Small accidential deviations from stationary conditions can lead to accidents. Self-organized criticality appears and forms during the evolution of nonlinear system. Here usually many self-developing mutually connected reasons of deviations from stable conditions appear, and then after small perturbation, disturbance takes place. It develops in accordance with its inner laws, which do not depend on external control. Then such process as chain reaction appears, and nonlinear system itself evolution to critical conditions and passes to accident [3,4].

Catalytic reactors for strong exothermal reactions, widely used in chemical industry, are typical open dynamic nonlinear system. For example, ethylene oxide reactor has up to 13000 tubes with diameter 21-27 mm and length 7-9 meters. Stationary stable conditions depend on reaction mixture composition (oxygen and ethylene) and concentration of promoter in it, temperatures of heat carrier and gas at inlet of the reactor, amount of circulating heat carrier and reaction gas mixture. All these factors stipulate ethylene oxidation reaction rate and are mutually connected by value of the selectivity of the process of ethylene oxidation into ethylene oxide, because heat relcase during the reaction of partial oxidation into ethylene oxide is approximately 10 times less than during full oxidation (32,9 kcal/mole and 330 kcal/mole respectively). Besides that, while the temperature is increasing, internal diffusion braking takes place, which increases the temperature of the grain and so decreasing the selectivity and increasing heat of reaction.

We studied the influence of different factors on parametrical sensitivity of the reactor, such as heat carrier and inlet gas temperature, heat exchange conditions, ethylene and oxygen content in initial gas mixture, uniformly of gas flow distribution in tubes with catalyst and heat carrier along intertube space, initial catalyst activity dispersion and its distribution along the reactor and so on. High heat strain of the process and discovered parametrical sensivity of

the reactor to fluctuation of technological parameters and to changes of catalyst performance, especially with its unhomogenious desactivation in time, can lead to reactor process failure, thermal runaway and emergency shut-down [5,6,7]

The analyses of thermal runaways of existing reactors showed that, as a rule, hot spot occurs in one of the tubes, mainly in peripheral areas, where the most of catalyst poisons build up (they make the performance of catalyst worse) and where there are difficulties with heat removal. Then hot spot spreads to adjacent tubes and while developing it moves in the direction of the gas flow motion or in the opposite direction, causing thermal runaway or exceeding of flammability limits of reaction gas mixture outside the catalyst layer in the space of top or bottom reactor cover. Catalyst temperature in these tubes in the area of hot spot approaches 700-800 °C, it is desactivated and begins to differ sharply from the rest catalyst in respect of its performance. Heat withdrawing surface can become coked, and it creates difficulties to the further reactor operation.

As the prevention of thermal runaway in reactor is the base of stable safe operation of industrial ethylene oxide plant, in order to study the reason of thermal runaway, its development, the ways of discovery and prevention we carried out experimental test runs in one-tube experimental reactors-elements of industrial reactor in the process of oxygen or air ethylene oxidation into ethylene oxide at different catalysts.

A series of test runs with catalysts of different activity and with variations of technological parameters was carried out at the test unit in reactors-elements of industrial reactor, in tubes with diameter 21 mm with heat removal by organic heat carrier and gas sample and temperature measurement after each one meter of catalyst bed length. Actual industrial gas mixture was used at pressure up to 20 atm. The analyses of the gas mixture and reaction products was carried out by chromatographic and mass-spectrometric methods.

Thermal runaway was initiated by step-by-step heat carrier temperature increasing or heat carrier supply decreasing, up to full supply stopping, while the temperature and amount of supplied gas mixture kept was constant.

Before the moment of thermal runaway beginning and during its development temperature and gas mixture components concentration profiles were measured. We controlled also the formation of new, typical for thermal runaway admixtures - ehylene pyrolysis products.

During normal reactor operation temperature profile in catalyst layer usually reaches peak on the bed length 4-6 m (from total length of catalyst bed - 7 m). While increasing of heat carrier temperature and load (heat of the reaction, heat release) or decreasing of heat carrier supply (heat removal) the value of maximum temperature Tmax increases, but remains stable up to the definite extent. However, in the moment of thermal runaway beginning Tmax value doesn't stop but increases continuously with typical curve point in time. The temperature in hot spot approaches 600-700 °C. In gas mixture the concentration of oxygen fell up to zero

point (oxygen was fully consumed) with formation of propylene (up to 500-750 ppm) and 2-methylpropylene (up to 200 ppm).

The results of these tests are given as an example in table and in the figure 1. After creation of stationary conditions of reactor operation thermal runaway was initiated by step-by-step heat carrier temperature increasing (figure 1 and table, experiment A) or by stopping of heat carrier circulation (table, experiment B).

Expirement A. When increasing the temperature from 234 to 236 °C thermal runaway occured, and the temperature at the height of catalyst bed of 2 m increased up to 350 °C. And then it moved gradually along the gas flow and reached the maximum more than 600 °C on the length of 4 m (55 min) and on the level of 5 m it was 380 °C (230 min). At that propylene and also 2-methylpropylene, which usually appear in the hot area, formed in the reaction products.

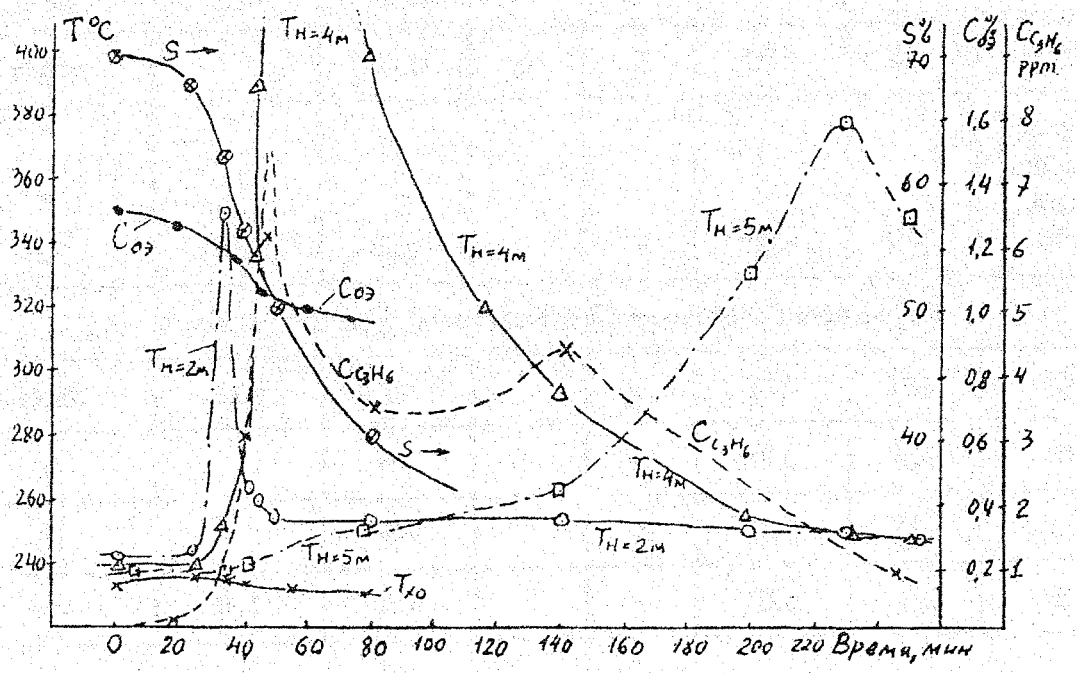

Figure 1. Beginning and development of thermal runaway in test tube (heat carrier temperature was increasing step-by-step from 230 °C, initial ethylene concentration was 15%, and oxygen - 5,5% vol.

Txo – temperature of heat carrier, °C; T_H – temperature of bed at H=2 m, 4 m, 5 m.

C_{EO} – concentration of ethylene oxide, %vol., C_{C3H6} – concentration of propylene, ppm.

S – selectivity, %.

Table 1.

Thermal runaway experiments with mass-spectrometric analyses of reaction products.

Content after reactor of

Time of runaway develop-ment, min.	T_{XO}, °C	Tmax, °C	Lmax, meter	Selec-tivity %	Ethylene oxide % vol.	Propylene, ppm	2-methyl-propylene, ppm
Experiment A. Runaway after step-by-step hear carrier temperature increasing							
0	233	248	3	78	1,28	abs.	abs.
50	234	252	4	76	1,38	abs.	abs.
108	236	261	4	74	1,61	traces	abs.
120	240	370	3	68	1,84		traces
Runaway develop-ment 126	240	>600	2		2,2	268	12
Experiment B. Runaway after heat carrier circulation stopping							
0	220	245	6		1,2	abs.	traces
10	225	530	6		1,6		5
13	228	570	5		1,9		10
25	230	622	2		1,0	730	140

Experiment B. After stopping of heat carrier supply to reactor, by that Tmax began quickly increasing and in 10 minutes it reached 530 °C and continued to increase.

During experiments it was determined that hot spot either moved along the gas flow motion at rate up to 5-10 cm/min. or met it at rate up to 50 cm/min. When stopping heat carrier supply "hot" front always met the gas flow towards inlet to the reactor. When heat carrier temperature increasing - the direction of motion depended on several factors such as heat removal surface state (for example, tubes coked in the place of hot spot) and catalyst activity. As a rule, in the tube with fresh, more active catalyst hot spot met the gas flow. This is more dangerous case, because it moves into the side of gas mixture with more high concentration of oxygen and ethylene. In any case temperature difference between gas at the outlet from the

reactor and heat carrier inlet to the reactor, quickly increases, so this value is used for blockage at thermal runaway beginning. When block system working, supply of oxygen and ethylene stops.

At thermal runaway in one tube in gas mixture at outlet the concentration of formed propylene is more than 700 ppm. In industrial reactor, containing more than 10 thousands tubes, hot spot from one tube through heat carrier increases the temperature of adjacent tubes, the heated area widens and reaches free space of top or bottom reactor cover. But even before thermal runaway of the whole reactor the content of propylene (or 2-methylpropylene) in gas mixture at reactor outlet will be 0,2-0,3 ppm because of gas dilution from normally operating tubes, and it can be fixed by continuously operating gas analysers. Timely interference and decreasing of reactors production let us prevent thermal runaway in the reactor and not to allow block systems operation and membrane rupture.

Mathematical modeling of the reactor using plug-flow model with consideration of internal diffusion in catalyst grain, correlared with regard of actual concentration and temperature profiles in test tubes, let us discribe actual conditions in reactors of Ethylene oxidation into Ethylene Oxide, causes of beginning and moment of thermal runaway start in the reactor [5]. By this, reserve resistance of the starting steady-state regime to runaway for the heat carrier temperature (ΔT = Trun -Tnorm), for normal thermal condition, calculated on base of computing experiment, in practice coincided with experimental. This allows to give reliable estimate of the conditions of stable safe operation of industrial reactors of ethylene oxidation into ethylene oxide. Together with fixing of generally used technological parameters of reactor operation, operative current control for appearance of byproducts (propylene for example) let us timely prevent appearance of thermal runaway of existing industrial reactors when non-uniformity appearing and developing in catalyst performances or state of the reactor and its heat removal surfaces.

In the figures you can see as an example, the results of some computing experiments on organization of conventional thermal runaway in industrial ethylene oxide reactor by step-by-step heat carrier temperature increasing as dependence of catalyst bed temperature upon the lengthes of the bed for different heat carrier temperatures (fig.2) and as dependence of specific heat of catalyst volume unit for the same heat carrier temperatures (fig.3).

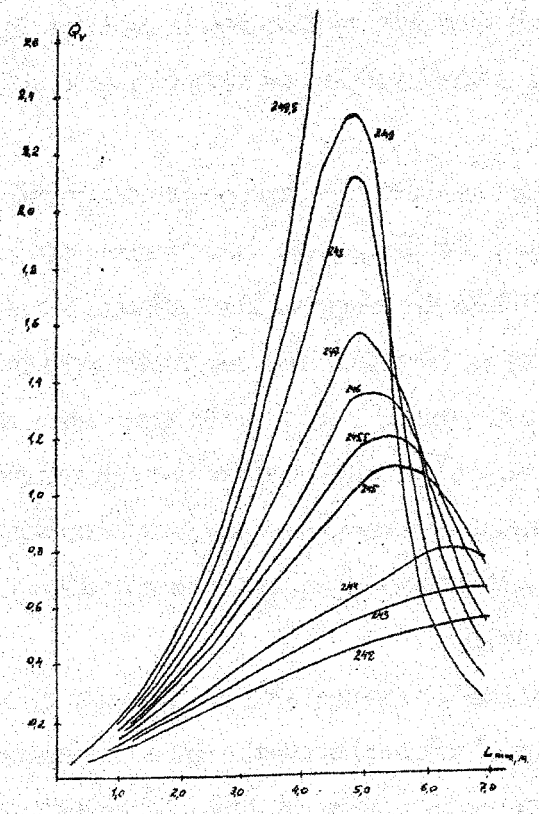

Fig. 2 Appearance and development of thermal runaway: dependence of temperature in catalyst bed over the length of the bed of catalyst for different heat carrier temperatures (from 241,7°C to 249,5°C)

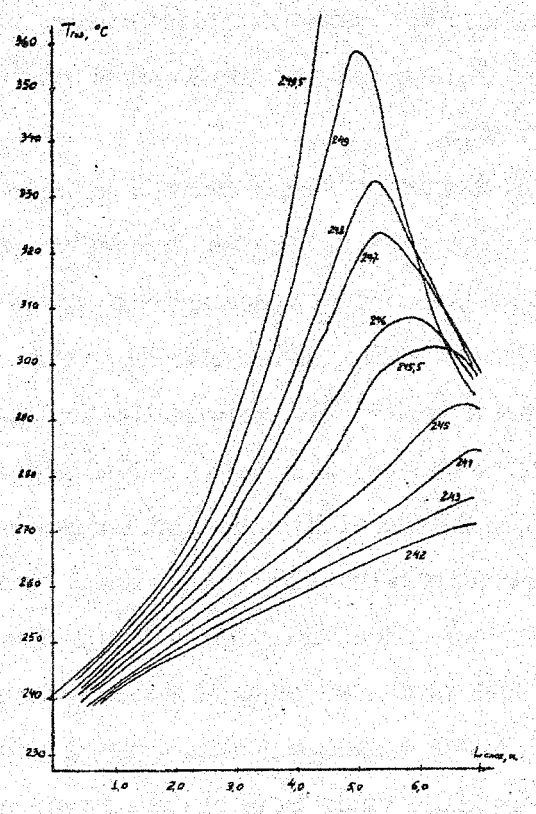

Pic.3 Appearance and development of thermal runaway: dependence of the specific heat release over the length of the bed of catalyst for different heat carrier temperatures (from 241,7 °C to 249,5°C)

By analogy thermal runaway develops in the reactor not only when heat carrier temperature increasing, but at any parameters deviations, leading to bed temperature increasing, selectivity decreasing and heat of the reaction (heat release) intensification. When some value increasing, called "parameter reserve resistance for runaway", the thermal runaway will sure take place. The possible parameters are as follows:

- oxygen concentration in initial mixture
- ethylene concentration in initial mixture
- promoter concentration in initial mixture
- heat carrier temperature
- inlet gas temperature
- gas mixture supply rate
- heat carrier supply rate
- appearance of different nature unhomogeneities

Deviations from some of these parameters are more dangerous, but all of them can be controlled and monitored, excluding the last one. In this case there is "vulnerability window",

when weak perturbations and small deviations should not lead to the runaway, however transition to critical conditions is forming during the evolution of the catalytic system itself. This phenomenon of appearing self-criticality is developing as chain branching process, when the deviation leads to certain temperature increasing, causing speed up of the reaction, heat of the reaction intensification, selectivity decreasing and, in one's turn, to the greater temperature increasing, selectivity decreasing, temperature increasing with swift intensification of reaction heat and temperature increasing up to thermal runaway and emergency shut down of the process.

At existing ethylene oxide plants some cases took place, when the process was conducted at small, but minimally sufficient reserve resistance of technological parameters for runaway. In spite of this, without any reasons, thermal runaway appeared and developed rapidly. Following examinations showed, that, for example, small active mass (dust) loss from the surface of catalyst led to certain increasing of catalyst bed resistance ΔP and decreasing of gas flow rate in one tube, which, in one's turn, led to temperature increasing, selectivity and heat transfer coefficient decreasing and so on up to thermal runaway, having a character of chain reaction.

Comparing the results of natural and computing experiments, mathematical model of the process was corrected and the conditions, which can lead to thermal runaway, were found with the purpose of prediction and prevention of thermal runaways in industrial reactors.

Literature

1. 1.Mathematical modeling and analyses of existing industrial ethylene oxide reactors' operation. // B.B.Chesnokov, B.Ja.Stul, A.V.Deryugin, M.S.Gabutdinov, M.G.Slin'ko // Transactions of International conference "Chemical reactor -13". Novosibirsk, 1996.
2. Researches of thermal runaway in industrial ethylene oxide reactors // B.B.Chesnokov, B.Ja.Stul, A.V.Deryugin, M.G.Slin'ko // Transactions of International conference "Chemical reactor-14". Tomsk, 1998.
3. Self-organized criticality. // G.G.Malinetsky, N.A.Mitin. // Physical chemistry journal, 1995, v.69, No 8, p.1513-1518.
4. Paradigm of self-organized criticality. Hierarchy of models and prediction limits. // G.G.Malinetsky, A.V.Podlazov. / High schools news, Applied nonlinear dynamics, v.5, N5, 1997, p.89-106.
5. Mathematical modeling and experimental study of the ethylene oxide synthesis reactor with small-porous catalyst. // B.B.Chesnokov, V.S.Kolobashkin, B.Ja.Stul et al. // Khimicheskaja Promyshlennost, vol.22, No 8, pp.457-460,1990 (Soviet Chemical Industry, Vol.22, No 8, pp.6-11, 1990)
6. Analysis of the operation of an industrial ethylene oxide synthesis reactor with consideration of variation in the heat removal system // B.B.Chesnokov, V.S.Kolobashkin, V.N.Stobetskii et al., // Khimicheskaja Promyshlennost, vol.23, No 12, pp.707-709, 1991 (Soviet Chemical Industry, Vol.23, No 12, pp.1-5, 1991).
7. Deactivation of silver catalysts used in the process of ethylene oxidation. // B.B. Chesnokov, V.S.Sokolov, V A Davydov et al., // Khimicheskaja Promyshlennost, vol. 20, No 5, pp.14-15, 1988 (Soviet Chemical Industry, Vol. 20, No 5, pp. 7-9, 1988).

OP-II-11

INVESTIGATION OF RADIAL HEAT TRANSFER IN BEDS PACKED BY REGULAR AND SHAPED PARTICLES

I.A. Zolotarskii, V.A. Kuzmin, A.V. Muzykantov, E.I. Smirnov

Boreskov Institute of Catalysis SB RAS
pr. Akad. Lavrentieva, 5, 630090 Novosibirsk, Russia.
Tel.: +7 3832 344491, fax: +7 3832 341878, e-mail: kva@catalysis.nsk.su

The experiments with measuring heat transfer parameters – effective radial heat conductivity and wall heat transfer coefficient of granular beds were performed with the following types of particles:

Table 1. Type of particles that were used in the experiments.

Number	Description	Number	Description
Spherical particles		Shaped particles:	
1	d = 3.2mm, glass	Rashig rings	
2	d = 16mm, steel	6	d=14mm, d_{hole}=12mm, h=14mm
3	d = 19mm, glass	7	d=14mm, d_{hole}=7mm, h=14mm
Cylindrical particles		Wheels with 6 spokes	
4	d = 10mm, h = 10mm	8	d=18mm, h=16mm,δ_{wall}=2mm
5	d = 19mm, h = 19mm	9	d=15mm, h=7mm,δ_{wall}=1mm

Experimental setup had an inner diameter of test section of 84 mm. Range of superficial air velocities studied is 0,2÷2,0 m/s. Temperature field was measured in 12 points by radius and in 12 angle positions with 30° step for different bed height. The program utilizing a square deviation minimization method to fit heat transfer parameters of standard heat dispersion model to measured temperature field was used.

For particles of regular shape – spheres of different diameters and cylinders with diameter equal to height, correlations of effective radial heat conductivity and wall heat transfer coefficient on gas velocity have been obtained and compared with literature data.

The wall Nusselt number was defined according to formula:

$$Nu_w = \frac{\alpha_w d_p}{\lambda_g} \qquad (1)$$

where d_p – diameter of sphere with volume equal to the volume of the grain, λ_g – heat conductivity of gas, α_w – wall heat transfer coefficient, defined from the relation:

$$\alpha_w = \frac{q_R}{T_R - T_W} \tag{2}$$

where q_R – heat flux at the wall, T_R – gas temperature near the wall, T_W – wall temperature.

The new formula for the wall Nusselt number was obtained in assumptions, that a) a temperature jump occurs in thin pre-wall layer with a thickness of Ad_p, b) a heat flux is constant in this layer and c) a heat conductivity changes linearly in this layer from the gas heat conductivity λ_g at the wall to effective radial heat conductivity in the bed core λ_{er} :

$$Nu_w = \frac{\lambda_{er}^*}{A(\ln \lambda_{er}^* - 1)} \tag{3}$$

where $\lambda_{er}^* = \lambda_{er}/\lambda_g$ and the parameter A was found to be independent on gas velocity and diameter of regular particles (spheres and cylinders) and equal to 0.54.

Because the correlation for an effective radial heat conductivity has the form:

$$\lambda_{er}^* = \lambda_{bed}^* + K\mathrm{RePr} \tag{4}$$

where $\mathrm{Re} = \frac{ud_p}{\nu}$, u – superficial gas velocity, ν - cinematic gas viscosity, formula (3) can be transformed to the form:

$$Nu_w = \frac{\lambda_{bed}^* + K\,\mathrm{Re}\,\mathrm{Pr}}{A(\ln(\lambda_{bed}^* + K\,\mathrm{Re}\,\mathrm{Pr}) - 1)} \tag{5}$$

Fig. 1 shows the comparison of formula (5) with our experimental data.

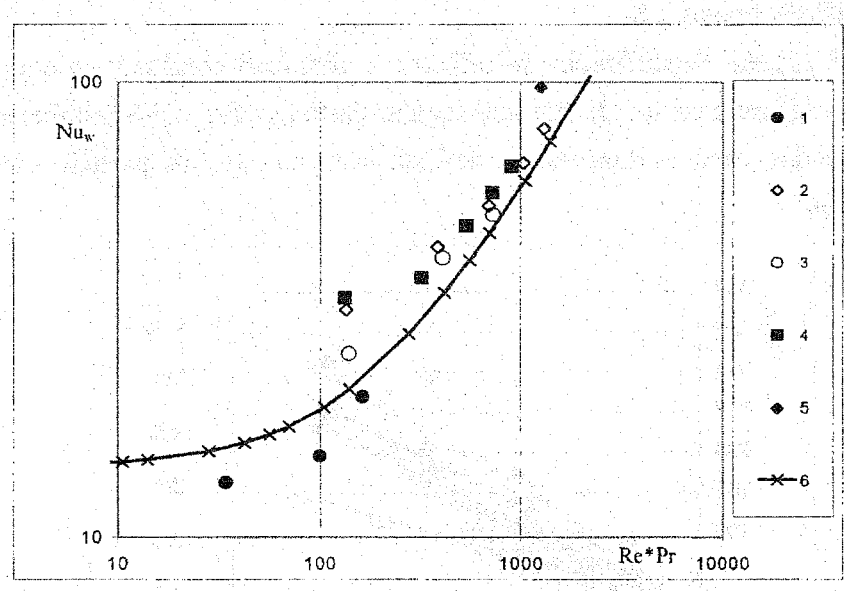

Fig.1. Dependence of wall Nusselt number on Re*Pr for different particles of regular shape in comparison with formula (5). 1 – 5 numbers of particles according to Table 1. 6 – formula (5) (parameters values: A=0.54, K=0,11; $\lambda_{bed}^* = 10$; Pr=0,7)

Fig.2 shows a good agreement of formula (5) with most reliable literature data.

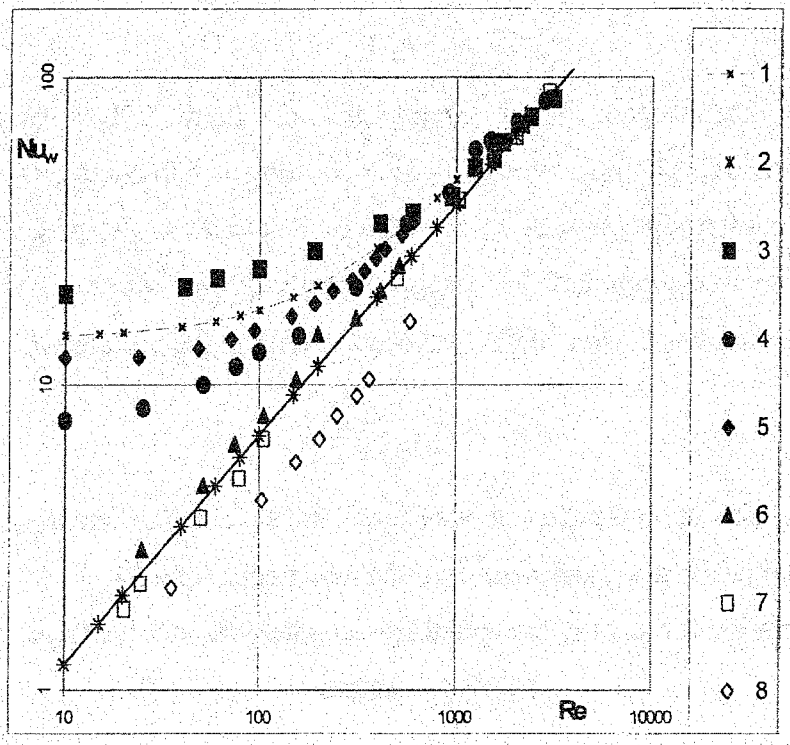

Fig.2. Dependence of wall Nusselt number on Reynolds number. 1 – formula (5) (parameters values: A=0.54, K=0,11; $\lambda^*_{bed} = 10$; Pr=0,7), 2 – Nu_w=0,24 $Re^{0,75}$ $Pr^{1/3}$, Kunii D., Suzuki M.[1], 3 – Martin H., Niles M. [2] 4 - Speccia V., Baldi G. [3], 5 – Yagi S., Kunii D. [4], 6 – Dixon A.G. [5], 7 – Li C.H., Finlayson B.A. [6], 8 - Chalbi M. [7].

For beds packed by shaped particles, the dependencies of heat transfer parameters on Reynolds number have been obtained as well. As shaped particles there were used cylindrical particles with different channels.

Fig. 3 and 4 present dependencies of effective radial heat conductivity and wall Nusselt number on Reynolds number for shaped and regular particles. Reynolds number in this case is based on an effective particle diameter d_p defined from an external particle volume without excluding hollows.

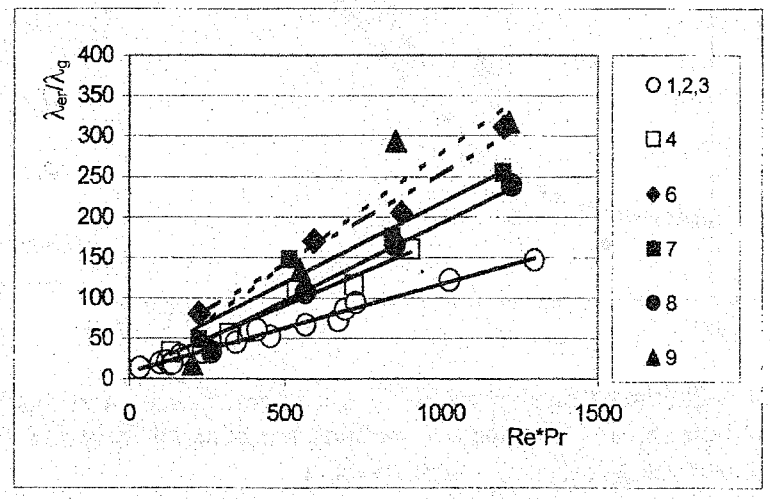

Fig.3. Dependence of effective radial heat conductivity on RePr for different particles. 1 – 4, 6 – 9 - numbers of particles according to Table 1.

Results of fitting procedure according to equation (4) are shown on Fig.3. Table 2 presents the corresponding values of parameter K for these correlations.

Table 2. Values of parameter K from the equatiopn (4) for shaped particles.

Particle number according to Table 1	1,2,3	4	6	7	8	9
K	0.108	0.163	0.226	0.198	0.192	0.279

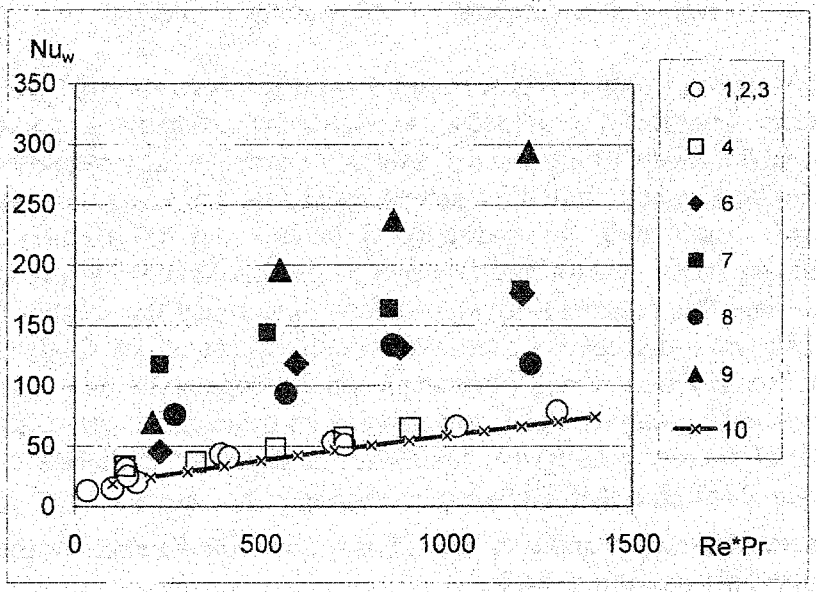

Fig.4. Dependence of wall Nusselt number on RePr for different particles. 1 – 4, 6 – 9 - numbers of particles according to Table 1, 10 – formula (5) (parameters values: A=0.54, K=0,11; $\lambda^{*}_{bed}=10$; Pr=0,7).

As one can see, shaped particles with channels have much higher values of radial heat transfer parameters than bulk particles. It corresponds to results of Bauer and Shlunder [8] for Rashig rings. In our understanding, this fact is explained by higher effective mixing length for shaped particles. Generalized correlations for such particles are to be developed in order to model tubular catalytic reactors.

The work is performed under support of the NATO grant SfP 972557.

LITERATURE

1. Kunii D., Suzuki M., Proc. *Symposium on heat and mass transfer, Minsk, 1968.*,
2. Martin H., Niles M, *Chem. Ing. Tech. 65(1993)1468-1477,*
3. Speccia V., Baldi G., Sicardi S., *Chem. Eng. Comm., 3(1980)361-380,*
4. Yagi S., Kunii D., *AIChE Journal, 6(1)(1960)97-104,*
5. Dixon A.G., *Chem. Eng. Comm., 71(1988)217-237,*
6. Li C.H., Finlayson B.A., *Ind. and Chem. Eng. Fund., 32(1977)1055-1066,*
7. Chalbi M., Castro J.A., Rodrigues A.E., Zoulalian A., *Chem. Eng. Journal 34(1987)89-97.*
8. Bauer R., Schlunder E.U., *International Chem. Eng. 18(2)(1978)181-188.*

OP-II-12

ELEVATION OF PERFORMANCE OF GAS-LIQUID REACTORS ON SOLID CATALYST

E.F. Stefoglo, V.I. Drobyshevich*, V.A. Semikolenov, I.V. Kuchin, O.P. Zhukova**

Institute of Coal and Coal Chemistry, Rukavishnikov, 21, Kemerovo, 650610, Russia
**Institute of Computational Mathematics and Math. Geoph.,. Novosibirsk, 630090, Russia*
***Boreskov Institute of Catalysis, Pr. Lavrentieva, 5, Novosibirsk, 630090, Russia*
Fax: 7 3842-281838, E-mail: chem@kemnet.ru

The behaviour of the gas-liquid process on a solid catalyst was studied using different modes of the reactor operation. The practical importance is to study the influence of the initial conditions on the performance of the reaction system: the preliminary saturation of a reaction solution have to hydrogenated before the reactor (continuous) or before the reaction (in batch) in comparison with "usual" mode of operation. In the last case the solution (suspension) is saturated with the gas in the reactor and this process is simultaneously accompanied by the catalytic reaction. And the conversion changes slower than when the solution is presaturated by gas. It should be noted that the concentration of gas reagent on the catalyst surface might influence the reaction direction. Thus, for example, the hydrogenation on hydrogen-"poor" instead of hydrogen-"rich" catalysts can involve hydrogenolysis and isomerization but not the reduction [1]. It is of interest to compare the conversion degrees x achieved at these different modes of operation. Assuming that the hydrogenation reaction rate is $r = k\,C_{cat}C_{HL}^{1}$, in a batch reactor at a constant temperature and pressure. Thus the material balance for the gas dissolved in the suspension and the liquid reagent is:

$$\frac{d\overline{C}_{HL}}{dt} = 1 - \overline{C}_{HL} - M \cdot \overline{C}_H \quad (1) \qquad \frac{d\overline{X}_L}{dt} = -\frac{d\overline{C}_L}{dt} = Q \cdot M \cdot \overline{C}_H \quad (2)$$

where: $\overline{C}_{HL} = C_{HL} / C_H^*$, $\overline{C}_L = C_L / C_{Lo}$, $t = \beta_{G-L} \cdot \tau$, $r = M \cdot \overline{C}_{HL}$, $t = \tau \cdot k_L a$, $Q = C_H^* / C_{L_0}$, $M = k \cdot C_{cat} / \beta_{G-L}$. The process may take place at two different initial conditions: 1) $t = 0, \overline{C}_{HL} = 0, \overline{C}_L = 1$; 2) $t = 0, \overline{C}_{HL} = 1, \overline{C}_L = 1$ the gas before the reaction start preliminarily saturates the suspension. Solving (1) with two initial conditions and putting the derived expression from eq.1 for $\overline{C}_H = f(t, M)$ to (2) then integrating it we find the X_{L_1} and X_{L_2} expressions as functions of M, Q and t for two different process modes. Then we determined: $\Delta X = X_{L_2} - X_{L_1} = \frac{M \cdot Q}{1+M} \cdot \left(1 - e^{-(1+M)t}\right)$ (at t→∞ and $M \to \infty$ so $\Delta X \to Q$). Thus, first, at the steady state region we have the limiting maximal value of the ΔX gain, but it does not exceed the Q value equal to C_H^* / C_{L_0}. This phenomenon is presented in Fig.1,2. The mathematical analysis of the proposed model shows that this gain (ΔX) is the greater the higher the reaction rate M ($k \to \infty$). Thus if the reaction rate is high or there is mass transfer limitations $k_L a \to 0$ and thus ($M \to \infty$) the greater the pressure (Q) the higher the ΔX value.

The experimental data of ethyl ether of para-nitrobenzoic acid hydrogenation over Pd/C in a batch stirred reactor with different initial conditions at a high pressure showed good agreements with the theoretical results (Fig.3,4). The obtained mathematical simulation has showed that for a continuous reactor this phenomenon is also the same and the analytical expression for ΔX calculation also are found for different kinds of the rate equation. Thus it is obviously experimental fact the high is the pressure the bigger is the profit in the conversion and it is the greatest when the gas absorption controls the reaction but is negligible in the kinetic regime.

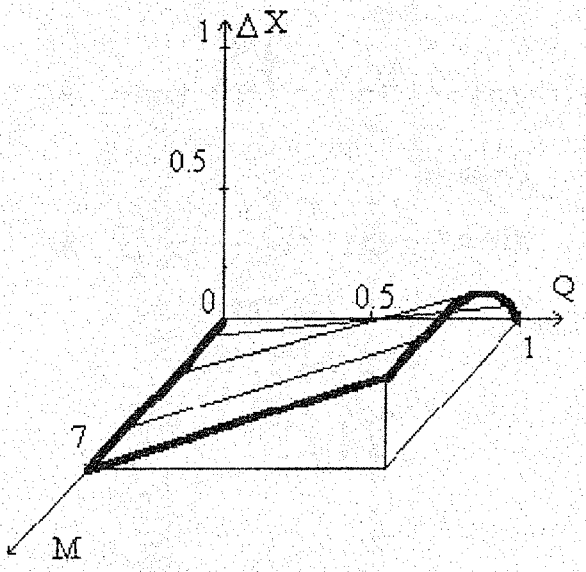

Fig.1 The general view of $\Delta X = f(Q, M)$ at t→∞ for the reaction of $r = -kC_{cat}C_{HL}$.

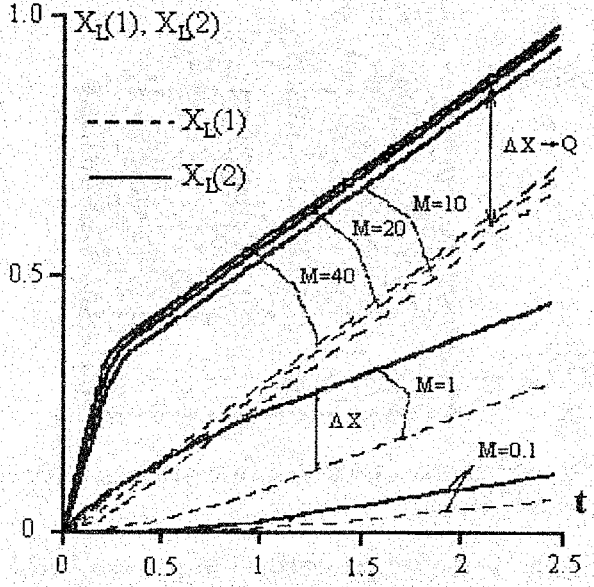

Fig.2 An unsteady state conversion behavior at a high pressure (Q=0.25) for the reaction $r = kC_{cat}C_{HL}$ at a different initial condition for a liquid batch type reactor.

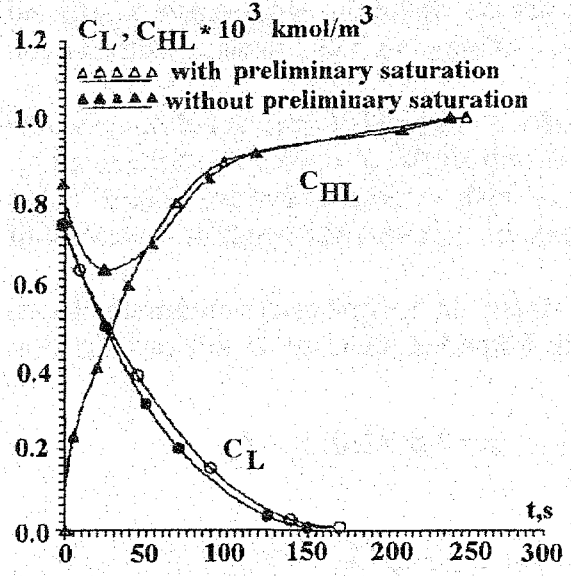

Fig.3 Hydrogenation of EEpNBA (ethyl ether of para-nitrobenzoic acid) with different initial conditions (T=100 °C at P= 2.5 bar at C_{cat}=0.083 kg_{pd}/m^3).

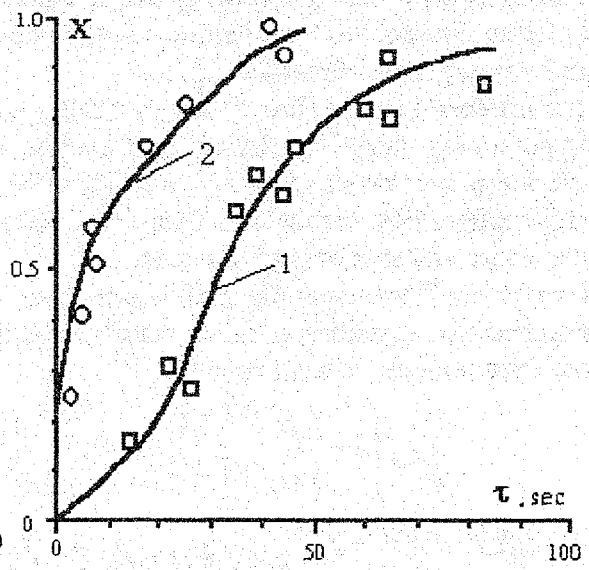

Fig.4 A high pressure (P_{H2}=40 bar) hydrogenation of EEpNBA, T=100° C, C_{cat}=0.083 kg_{pd}/m^3, Langmur-Hinshelwood mechanism for both gas and liquid components. 1-reaction without presaturation, 2- reaction with presaturation.

One of reactor construction where the preliminary saturation effect can be used is the trickle-bed reactor (Fig. 5). Gas from the bottle under pressure feeds the reactor and enters into the rise tube. Liquid in the tube is lifted by gas bubbles on the principle of air lift. Movement of gas is caused by pressure drop $\Delta p = p_1 - p_2$ (p_2 lower than p_1 due to gas consumption on reaction). During the lifting in the tube gas dissolves in liquid. Saturated with gas liquid reaches the top of reactor and flows down over the catalyst particles in a thin film where chemical conversion takes place. Further the liquid flows down to the bottom of reactor and again enters the rise tube. So the reactor operates cyclically and does not need any pumping.

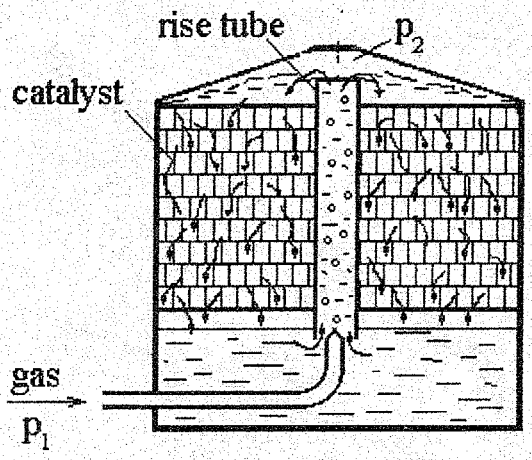

Fig. 5. Scheme of trickle-bed reactor operating without pumping.

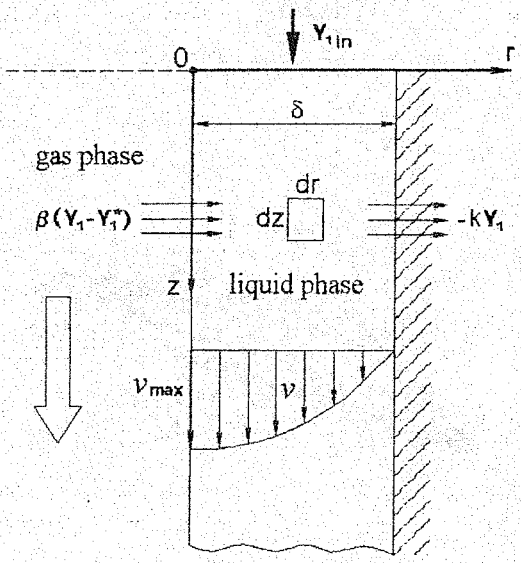

Fig. 6. Simplified presentation of gas and liquid flows and distribution of velocities in liquid film.

Mathematical model describing the behavior of gas dissolved in liquid flowing down through the catalyst bed was developed. Reaction has the first order with respect to gas and zero order with respect to liquid component. Direction of gas and liquid flows and distribution of liquid velocities are shown in Fig. 6.

It is assumed that the flow geometry of the model is represented by series of zero volume mixing points separated by relative short lengths of vertical flat plates (e.g. dumped or structured packing) over which the liquid flows [2]. These small sections (units) can be regarded as very short falling film contactors. Their expected number per unit bed length is dependent of the type, shape and size of packing used.

Two types of mathematical models can be developed. In the first one (equilibrium model) it is assumed that equilibrium exists between gas and liquid at interface. In this case the simple equilibrium model is written as [3]:

$$v_{\max}\left(1-\left(\frac{r}{\delta}\right)^2\right)\frac{\partial Y_1}{\partial z}=D_L\frac{\partial^2 Y_1}{\partial r^2} \qquad z=0\ \&\ r\geq 0: Y_1=Y_{1in}$$

$$z\geq 0\ \&\ r=0: Y_1=Y_1^*;\ z\geq 0\ \&\ r=\delta:\ S_{ud}D_L\frac{\partial Y_1}{\partial r}=-k'' Y_1;\ z=0, z=\mathrm{Hi}, i=1,\ldots,4;$$

$$i=1:\ z=0\ \&\ r\geq 0: Y_1=Y_{1in};\ i=2,3,4:\ z=0\ \&\ r\geq 0: Y_1=\frac{1}{\delta}\int_0^{\delta} Y_1(H_{i-1},r)\,\partial r$$

At not very high values of gas-liquid mass-transfer coefficient and at high velocity of liquid, concentration of gas dissolved in liquid near the interface is lower than its equilibrium value. Then the simple non-equilibrium model is written as:

$$v_{\max}\left(1-\left(\frac{r}{\delta}\right)^2\right)\frac{\partial Y_1}{\partial z}=D_L\frac{\partial^2 Y_1}{\partial r^2} \qquad z=0\ \&\ r\geq 0: Y_1=Y_{1in}$$

$$z\geq 0\ \&\ r=0: S_{ud}D_L\frac{\partial Y_1}{\partial r}=\beta_{lg}(Y_1-Y_1^*);\ z\geq 0\ \&\ r=\delta:\ S_{ud}D_L\frac{\partial Y_1}{\partial r}=-k'' Y_1$$

$$z=0, z=\mathrm{Hi}, i=1,\ldots,4;\ i=1:\ z=0\ \&\ r\geq 0: Y_1=Y_{1in};$$

i =2,3,4: $z=0\ \&\ r\geq 0: Y_1=\frac{1}{\delta}\int_0^{\delta} Y_1(H_{i-1},r)\,\partial r$

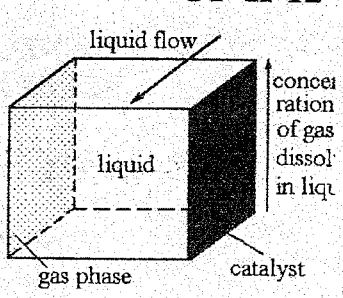

The results of numeric solution of given models are presented Fig. 7.

In real process gas dissolved concentration diminishes along catalyst bed not only due to chemical conversion, but due to pressure decreasing as well as.

Equilibrium model Non equilibrium model

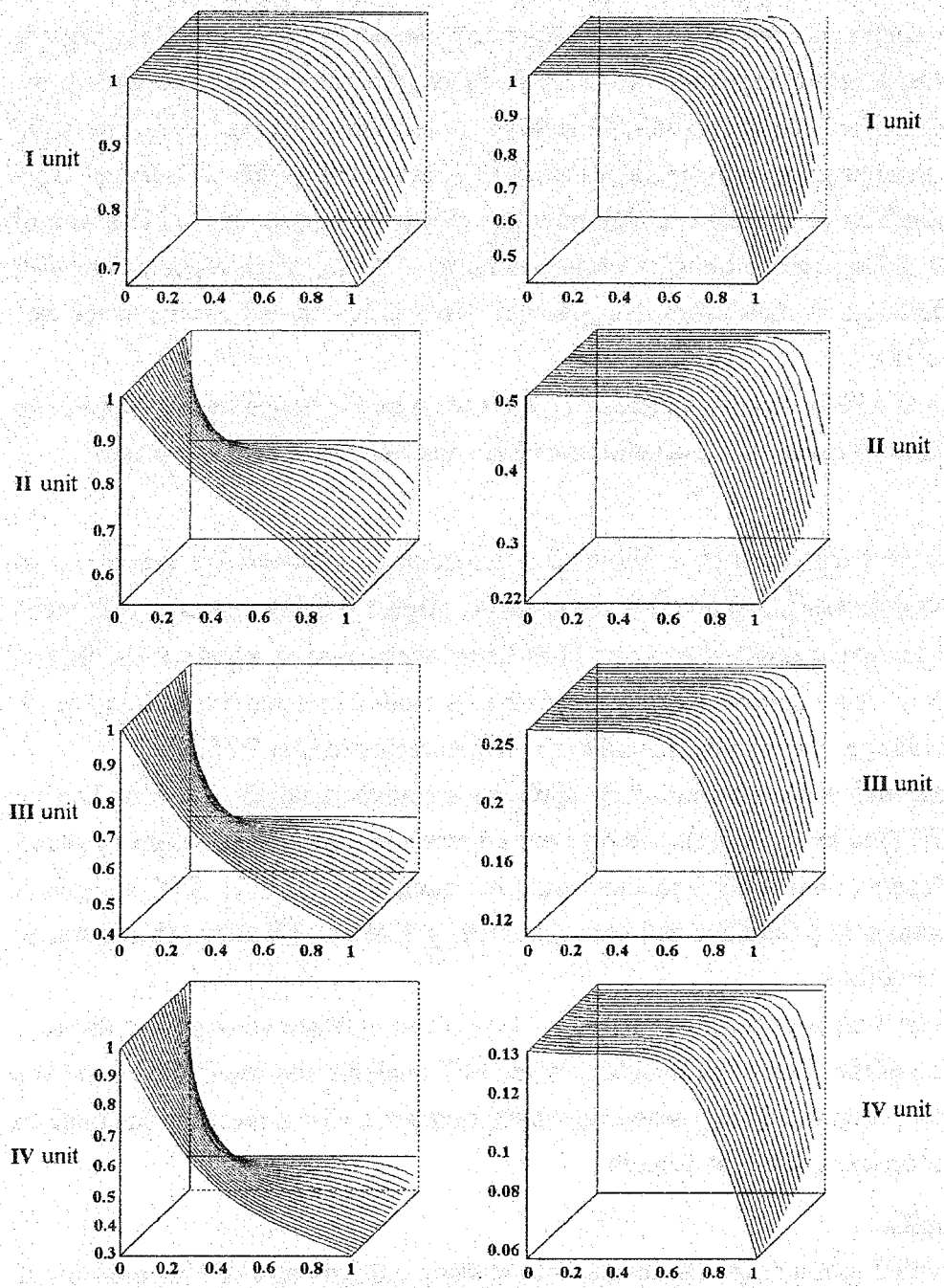

Fig. 7. Results numeric solut of equilibri and non- equi rium models.

References

1.P.N. Rylander, in Catalytic hydrogenation in organic synthesis. Ac. press, N-York, 138-152
2. G. Astarita and W.J.Beek Chem.Eng.Sc. 17 (1962), pp.665-674
3. G.F.Versteeg at al, Chem.Eng.Sc., Vol. 52 (1997), pp.4057-4067

OP-II-13

STUDIES ON THE ONSET VELOCITY OF TURBULENT FLUIDIZATION FOR ALPHA-ALUMINA PARTICLES

V.N. Kashkin, V.S. Lakhmostov, I.A. Zolotarskii, A.S. Noskov, J.J. Zhou*

Boreskov Institute of Catalysis Novosibirsk, Russia
**Solutia Inc. Pensacola, Fl 32560, USA*

Introduction.

Fluidized bed reactors are among the most important reactors for heterogeneous catalysis in chemical industry. Many commercial gas-solid fluidized bed reactors are operated in the bubbling or turbulent fluidization regimes. Compared to bubbling fluidized beds, gas-solid contact efficiency and chemical conversion are usually higher in the turbulent fluidized. Turbulent fluidized beds have also the advantage of being able to be scaled up with less loss of reactor efficiency [1]. However, a transition from bubbling to the turbulent regimeis not well defined due to differences in measurement techniques, test equipment and experimental data processing methods [2].

Alpha-alumina is widely used as a catalyst support for many heterogeneous reactions. In the this work the onset of turbulent fluidization for alpha-alumina particles was studied.

Experimental.

Experiments were carried out in a fluidized bed reactor of 150 mm ID and of 2.3 m height at atmospheric pressure and ambient temperature. Alpha-alumina particles with mean particle size of 50 μm and particle density of 2100 kg/m^3 were used in experiments. Settled bed height was 0.5 m. Air supplied to the reactor went through a moisturizing column to reduce electric static charge. The relative humidity of air was maintained at 70-80%.

Fluidization regimes were determined by applying a statistic analysis and Fast Fourier Transformations (FFT) to both absolute and differential pressure fluctuations measured at different locations. Details of the statistic method could be found elsewhere [3]. FFT analysis of the pressure fluctuations in a fluidized bed was also used by Trnka and Vesely [4] to determinate fluidized bed condition.

Turbulent fluidization is generally characterized by low-amplitude voidage and pressure fluctuations because of the absence of bubbles. When FFT analysis was used, transition from bubbling to turbulent regime occured when dominant frequencies of a pressure fluctuations started to disappear on increasing gas velocity.

Experimental results.

For the differential pressure measurement, both statistic analysis and FFT method reveal a similar transition velocity U_c indicating the onset of turbulent fluidization. The transition velocity, U_c, was found to be only slightly affected by the axial distance between two pressure

ports where measurements were taken. The results are in agreement with the empirical correlation $U_c=1.24*Ar^{0.45}$ suggested by Bi and Grace [3].

The transition velocity determined from absolute pressure fluctuation varried with the axial locations. Generally, they are lower than those obtained from differential pressure measurements.

As shown in Table 1, the ttransition velocity determined by statistic analysis agreed well with that from FFT analysis.

Table 1. U_c determined by different data processing methods.

	U_c (FFTmethod)	U_c (Statistical method)
APF	0.6 m/s	0.6 – 0.8 m/s
DPF	0.8 m/s	0.8 m/s

APF- absolute pressure fluctuation measurements

DPF- differential pressure fluctuation measurements

An example of amplitude spectra of pressure fluctuations is represented on the **Fig. 1**. At low gas velocities (U=0.06 m/s) dominant frequencies of 5 Hz shows bubbles passing the tip of pressure probe. At gas velocity of 0.8 m/s, dominant frequencies decreased to1-2 Hz. It indicates the presence of large bubbles. At gas velocities of 1.0 m/s, dominant frequency band is relatively wide. Further increase in gas velocity to1.3 m/s led to a substantial decrease in the amplitude of pressure fluctuation.

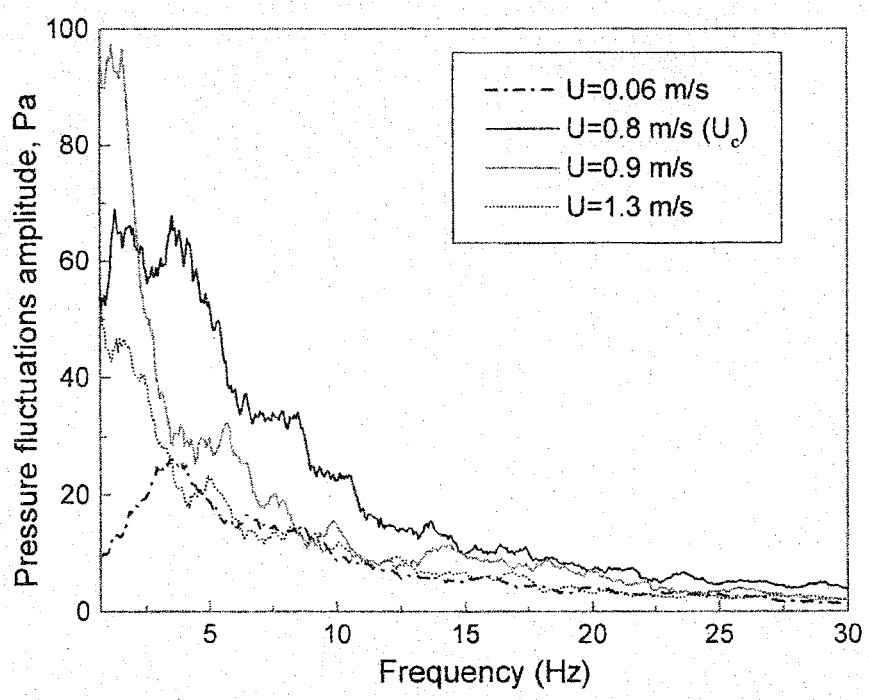

Figure 1. Amplitude spectra of the differential pressure fluctuations measured at 0.31-0.41 m over the distributor.

REFERENCES

1) **A.A Avidan, F.J. Kramberk, C.K. Lee and M.N. Lo:** *Predicting fluid-bed reactor efficiency using adsorbing gas tracers*; **AIChE J.** v.33, No 10, **1987.**

2) **H.T. Bi, N. Ellis, I.A. Abba and J.R Grace:** *A state-of-the-art review of gas - solid turbulent fluidization*; ***Chem. Eng Sci.***, v.55, **2000.**

3) **H.T. Bi and J.R Grace**: *Effect of the measurement method on the velocities used to demarcate the onset of turbulent fluidization*; ***Chem. Eng. J.***, v.57, **1995**.

4) **O. Trnka and V. Vesely:** *Identification of the state of a fluidized bed by pressure fluctuations*; **AIChE J**, v.46, **2000.**

THE EXOTHERMIC CATALYTIC REACTION IN A SINGLE PARTIALLY-WETTED POROUS CATALYST PARTICLE

V.A. Kirillov, I.A. Mikhailova, S.I. Fadeev*, M.G. Slin'ko**

Boreskov Institute of Catalysis, 5, Pr.Lavrentieva, Novosibirsk, Russia, 630090
e-mail: v.a.kirillov@catalysis.nsk.su
**Institute of Mathematics SB RAS, Novosibirsk, Russia*
***SRC "Karpov NIPCI", Moscow, Russia*

Catalytic processes in multiphase reactors are often considered to be very prospective for industrial applications. This induce the particular attention to the study of a multiphase catalytic reactions on a single particle level. Numerous experimental studies [1–3] report the multiplicity of catalyst particle states in conditions of a steady-state catalytic process. In our recent research such a multiplicity was studied for the case of the α-methylstyrene hydrogenation [4]. Data being reported in the cited papers evidence, that

(i) the catalyst particle can be either dry, either filled with liquid (wetted) or partially wetted, as well;

(ii) phase transitions (vaporization and condensation) inside the catalyst particle can be very intensive;

(iii) consideration of the capillary forces is significant, for it causes the imbibition of the liquid phase.

These three statements seem to be important and ought to be considered, when making the numerical experiments. Several models, which were suggested earlier [5–10] mark the significant progress in this field. However, each of these models includes certain assumptions, which limit the set of its applications. Thus, it is important to relax some of the assumptions of the previous models.

The objective of the present research is to develop the complete mathematical model of stationary catalytic process on the porous catalyst particle in the system "gas-liquid-solid" in the exothermic reaction conditions, as well as to perform the numerical experiments.

Numerical experiments are performed in the frame of the one-dimension model, where:

1) catalyst particle is a porous plate and distribution of pores by radii is given by a density function $f(r)$;
2) the left side of the plate contacts with the gas-liquid flow, the right side – with the gas-vapor flow;

3) every elementary volume (l; $l+dl$) is considered to consist of the gas phase and of the liquid phase with gas hold up $\alpha_1(l)$ and liquid hold up $\alpha_2(l)$ ($\alpha_1+\alpha_2 = 1$); gas and liquid hold up, α_1 and α_2, temperature, pressure and other parameters and variables are considered for each l as average values for all elementary volumes (l; $l+dl$).
4) temperature $T = T(l)$ is equal for the co-existing phases in every point of the plate; heat transfer is performed by thermal conductivity and convective motion of liquid and gas;
5) exothermic catalytic reaction occurs in both gaseous and liquid phases, kinetic parameters differ for gas-phase and liquid-phase reaction;
6) rates of the phase transitions are determined by the molecular-kinetic theory;
7) mass-transfer in gas phase follows the "dusty gas" model [11]; mass-transfer in the liquid phase is a superposition of diffusion and convective motion (incl. imbibition); phase transitions and catalytic reaction are taken into account in the equations of mass-transfer;
8) boundary conditions include: (i) mass-transfer in gas phase deduced from the Stefan-Maxwell equations at both boundaries of the plate; (ii) heat-transfer at both boundaries of the plate; (iii) mass-transfer in liquid phase at the left boundary; (iv) the fixed value of external wetting efficiency.

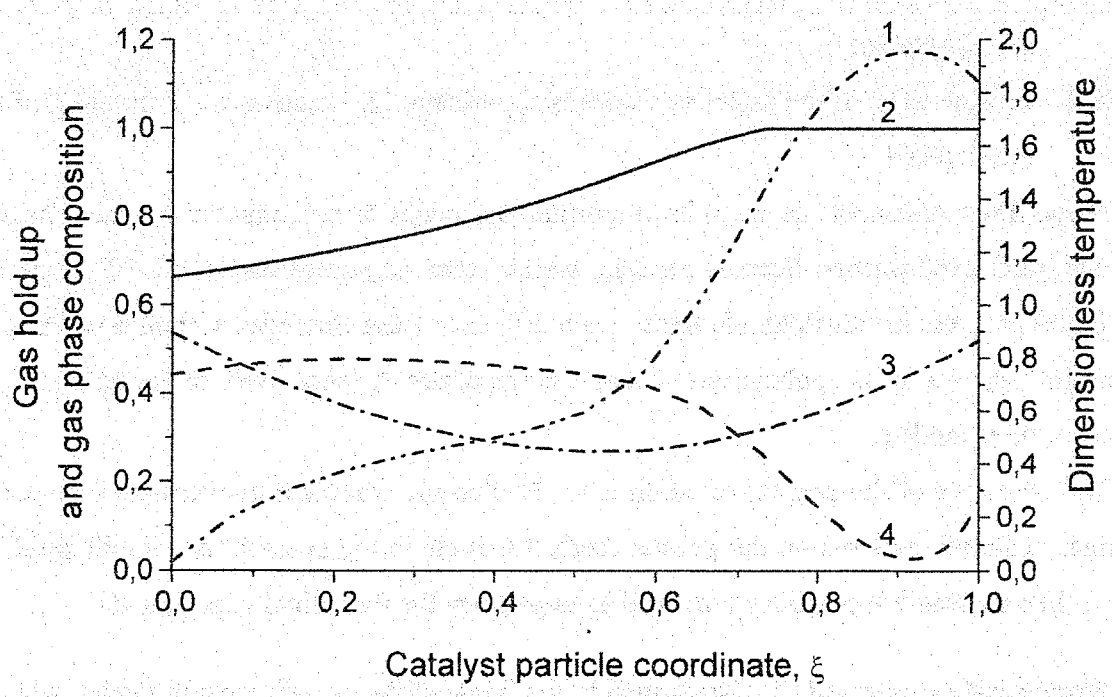

Figure 1. Example of the calculated profiles along the catalyst plate:

1 – dimensionless temperature, 2 – gas hold up,

3 – mole fraction of H_2 in gas phase,

4 - mole fraction of α-methylstyrene in gas phase.

Numerical experiments gave stationary profiles of liquid imbibition velocity, temperature, pressure, gas (or liquid) hold up, gas phase and liquid phase compositions along the catalyst particle. Some examples of the calculated profiles are represented at Figure 1.

The results of the experiments allowed to study the effect of external wetting efficiency, heat efficiencies of exothermic reaction and phase transitions, overall rates, average radius of the catalyst pores, and other parameters, which characterize imbibition of liquid, intraparticle and external transport processes on the state of the particle. The effect was assessed by examining the dependencies of catalyst effectiveness, all the profiles, width of the gas-filled ("dry") zone, and other characteristic values of the process on the specific catalyst activity. It is presented at Figure 2, as an example, the dependence of catalyst effectiveness on the catalytic activity for different values of external wetting efficiency.

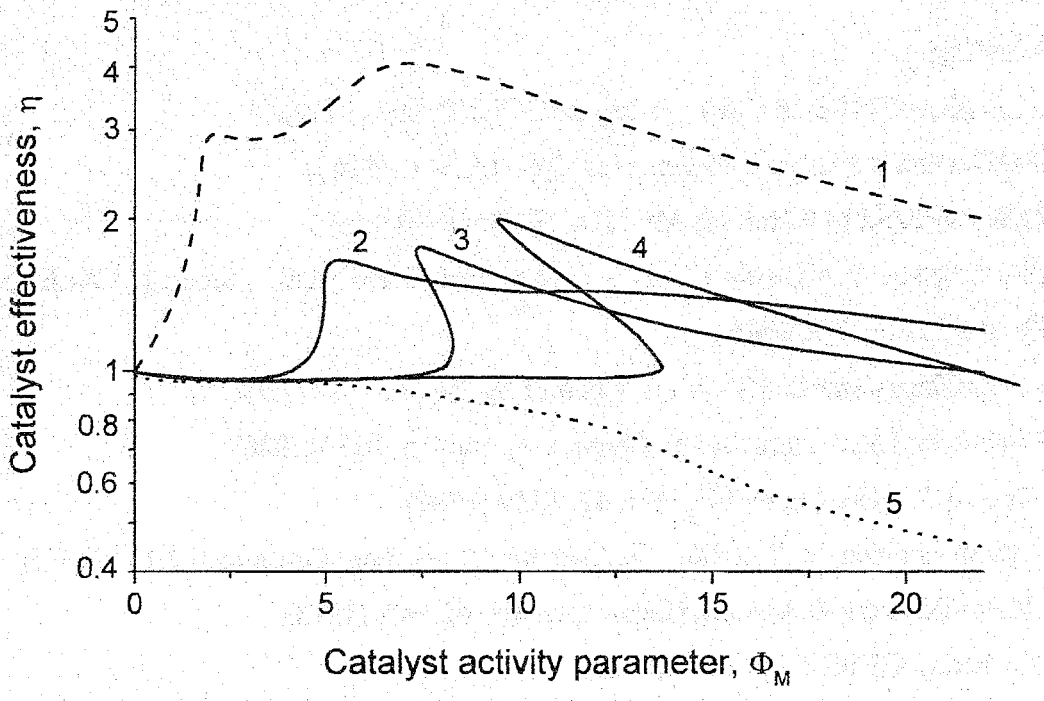

Figure 2. The effect of the external wetting efficiency, $\alpha_2\ (l = 0)$, on the dependence of catalityc effectiveness, η, on catalyst activity: 1 - $\alpha_2\ (l = 0) = 0$; 2 - $\alpha_2\ (l = 0) = 0.2$; 3 - $\alpha_2\ (l = 0) = 0.26$; 4 - $\alpha_2\ (l = 0) = 0.34$; 5 - $\alpha_2\ (l = 0) = 0.62$.

Numerical results established three different types of stationary states of the catalyst particle, when the particle constitutes:

I. practically non-wetted porous structure, where liquid contacts only external surface of the particle and is vaporized in thin boundary layer;

II. completely liquid-filled porous structure, where liquid is filtered through the particle;

III. partially wetted (and partially gas filled) porous structure.

In the case of partially wetted catalyst particle interaction between exothermic catalytic reaction and phase transition leads to the multiple steady solutions. The regions of the multiple solutions were determined.

The obtained results of the numerical experiments allow to analyze the role of the mass-transfer and heat-transfer phenomena (incl. the phase transitions and liquid imbibition due to the capillary forces) in the multi-phase catalytic process on the partially-wetted catalyst particle and to evaluate their impact on the overall catalyst performance.

Acknowledgements – This research is supported by RFBR № 99-01-0035.

REFERENCES

1. G.A.Funk, M.P.Harold and K.M. Ng, AIChE J. 2, 202 (1991).
2. D.N.Kim and Y.G.Kim, J. Chem. Eng. Jpn. 14, 311 (1981).
3. P.C.Watson and M.P.Harold, AIChE J. 39, 989 (1993).
4. M.G. Slin'ko, V.A.Kirillov, A.V.Kulikov, N.A.Kuzin, A.B. Shigarov, Doklady RAN 373, 355 (2000) in Russian.
5. J.V.Yentekakis and C.G.Vayenas, Chem. Eng. Sci. 42, 1327 (1987).
6. P.L.Mills and M.P.Dudukovich, Chem. Eng. Sci. 35, 1557 (1980).
7. R.Hu and T.C.Ho, Chem. Eng. Sci. 42, 1239 (1987).
8. V.I.Drobyshevich, V.A.Kirillov, N.A.Kuzin, Chem. Eng. Commun. 22,151 (1983).
9. M.P.Harold and P.C.Watson, Chem. Eng. Sci. 48, 981 (1993).
10. S.K.Bhatia, AIChE J. 35, 1337 (1989).
11. Mason E.A. and A.P.Malinauskas. "Gas Transport in Porous Media: The Dusty Gas Model". Chem. Eng. Monographs 17, Amsterdam: Elsevier (1983).

THE CALCULATION NON-STATIONARY OF INDUSTRIAL METHANOL SYNTHESIS AT FORECASTING

A.V. Kravtsov, A.A. Novikov, A.A. Saifulin

Tomsk Polytechnical University, Tomsk. Russia

The calculation in the computer analysis dynamics of a catalytic activity in time allows to solve a number of the actual tasks:

- elaboration of the optimal technological parameters of the industrial methanol synthesis change strategy in view of catalyst deactivation;
- consequences of short-lived overheats of the catalyst;
- usage efficiency of modified flow diagrams and catalysts forecasting.

Thus, the calculation of non-stationary at mathematical model of industrial methanol synthesis development is the important problem.

Development of non-stationary kinetic model of the methanol synthesis.

The numerous researches have shown that irreversible deactivation of active centres during the methanol synthesis can happen as a result of passing the synthesis reaction:

$$[A] + CO + 2H_2 \rightarrow [A] + CH_3OH$$
$$[A] + CO + 2H_2 \rightarrow [D] + CH_3OH \qquad (1)$$

A – active centre

D – deactivated centre.

In compliance with that the rate of activity changing can be featured by the equations:

$$\frac{da}{dt} = -k_a^* \cdot G \qquad \text{(2) for catalyst layer}$$

k_a^* - temperature coefficient;

G - productivity of a catalyst layer.

Numerical integration of this equations allows to define change of a catalytic activity dynamics, however, the main difficulty is a definition of current relative productivity on each integration step.

In this work as main toolkit of forecasting calculations is the computer complex 'SYNTEZ' [1] was used. Using of this computer complex with adequate kinetic models (with

parameters) allows to define relative productivity (G) of a catalyst bed and, therefore, activity ratio, 'a' on each integration step.

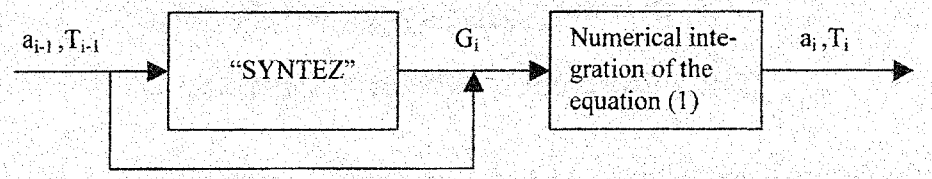

Fig. 1. Algorithm of a differential equation numerical integration.

Indispensable stage of the catalyst deactivation modelling is the definition of parameters of the temperature coefficient k_a^*. For long-lived exploitation of the catalyst this task was solved on the basis of the big-volume aggregate methanol synthesis M-750 (ICI-process) design data.

Thus was marked, that:

- in accordance with operation of the catalyst the activity it falls nonuniformly on layers;
- the main parameter influential in catalyst layer productivity under conditions of falling of its activity, is temperature;

For kinetic parameters of a temperature coefficient k_a^* of model of "sluggish" deactivation on layers definition with using of the computer "SYNTEZ" unit was calculated average value of T, G, a. The design dependence of activity ratios of catalyst layers on time is enough precisely approximated by simple functions, on the basis of which one the time dependence of deactivation rate and as a result numerical values of a temperature coefficient of deactivation on a beginning, middle and extremity of campaign were obtained.

At some dispersion of the obtained points (Fig.2) the linear dependence describing data on all catalyst layers is tracked from which one there are values of parameters of coefficient of model of "sluggish" deactivation:

$$k_0^* = 4.52\ 10^6\ [м^3_{CAT}/\ kg_{Met}], \qquad E^* = 138769\ [Joule/Mole].$$

Integrating model of deactivation, it is possible to solve the following tasks:

- calculation of activity decreasing and relative productivity of the catalysts layers under constant technological parameters;
- the analysis of different technological parameters change influence for dynamics of activity decreasing and relative productivity of the catalyst;
- forecasting of the catalyst overload periods.

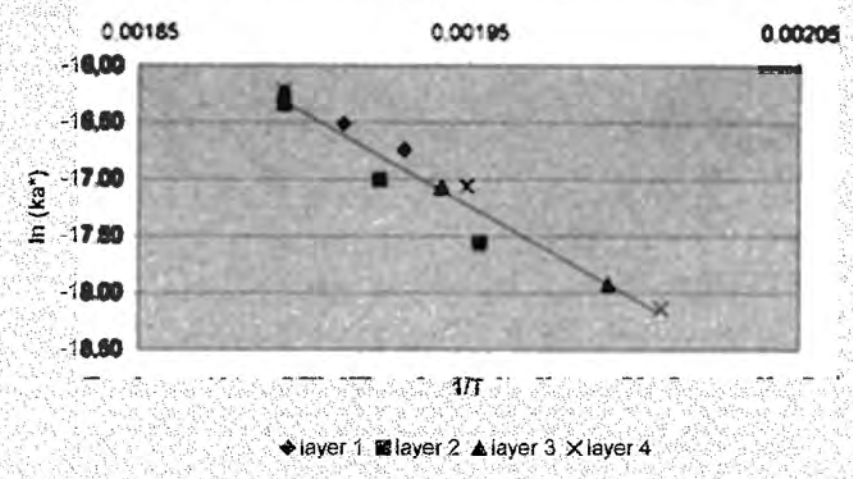

Fig. 2. ln (k_a^*) vs.1/T

Forecasting of industrial methanol synthesis

At the analysis of design data it was revealed, that in accordance with decreasing a catalytic activity all controlling parameters vary, providing constant productivity of aggregate. In such conditions the development of the common strategy controlling parameters change in time considerably becomes complicated. Two main variants of the strategy of support of the process were reviewed:

1) Stabilizing in time of all controlling parameters;
2) Programming entry temperature on catalyst layers.

In actual conditions the implementation of the first variant is possible on a particular time before reaching some critical values of the process metrics with their subsequent step change.

In the second case — programming entry temperature on catalyst layers is yielded by by-pass streams tuning at a time-varying catalytic activity.

Parsing outcomes held model forecasting calculation with increase of time of exploitation, decrease of a temperature drop on catalyst layers was marked. Though catalyst layers activity ratio, as well as common productivity on methanol is slashed, the relative productivity's on catalyst beds undergo interesting changes: the reallocation of offload with upper on low catalyst layers is watched.

As it is visible from a fig. 3, at an identical catalytic activity common catalyst productivity, in case of programming entry temperatures, is much higher.Thus, outcomes of the analysis forecasting calculations allows to draw a conclusion, that the most reasonable criterion of the optimal strategy of industrial methanol production is maintaining constant productivity of the reactor block

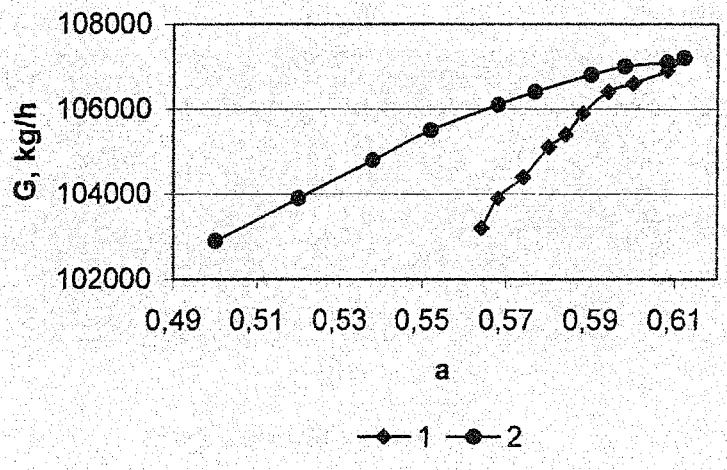

Fig. 3. Link of an average catalytic activity and productivity of the reactor block at matching variants with fixed values of data-ins (1) and with programming of entry temperature on catalyst layers (2)

Thus, during this work the non-stationary model of methanol synthesis taking into account of the catalyst deactivation at the regulated mode of his exploitation was designed. On the basis of non-stationary model the methodology is proposed. Also, the analysis of catalytic activity change dynamics and operational characteristics of layers four-ledge industrial methanol synthesis reactor operation under different conditions of its exploitation is held.

1. A.V. Kravtsov, A.A. Novikov, P.I. Koval, D.V. Ivolgin. Computer analysis of the methanol synthesis based on the natural gas chemical-engineering system. Abstracts o the XIV International conference on Chemical Reactors CHEMREACTOR-14. Russia, Tomsk 1998. 109-110 p.

CATALYTIC PROPERTIES OF NANOPARTICLES OF NOBLE METALS WITH EMPHASIS ON THE SELECTIVE OXIDATION OF CO IN THE PRESENCE OF HYDROGEN

B.E. Nieuwenhuys, C.A. de Wolf, R.J. H.Grisel, S. Carabineiro

Leiden Institute of Chemistry, Leiden University,
P.O.Box 9502, 2300 RA Leiden, The Netherlands
tel. (31) 71 5274545; fax (31) 71 5274451
email: b.nieuwe@chem.leidenuniv.nl

CO oxidation and NO_x reduction (by hydrogen and CO) over small Pt and Au particles supported on alumina.

In particular the selective oxidation of CO in the presence of a large excess of hydrogen will be discussed. This part of the research project is motivated by the search for catalysts that can remove traces of CO in the presence of hydrogen. These catalysts are required for the generation of electric energy by using PEFC fuel cells.

Gold has long been regarded as catalytically inactive. The era of miniaturization, however, gave access to new technologies that made it possible to manifacture and characterize small Au nanoparticles (<5 nm). It became clear that very small Au particles, highly supported on suitable metal oxides (MO_x) do exhibit extraordinarily high activity in, e.g., low-temperature CO oxidation. From here new investigations around Au supported systems arose and the research in Au catalysis took a giant leap.

The catalysts used in our studies consist of Pt and Au on γ-Al_2O_3 and on MO_x/ γ-Al_2O_3 (M = Mg, Cr, Mn, Fe, Co, Ni, Cu and Zn). The preparation of supported Au catalysts is crucial, in order to obtain highly active Au nanoparticles. Several preparation techniques to deposit Au on γ-Al_2O_3 are compared. The most critical steps in the manufacture of these catalysts, as well as the effect of MO_x on the preparation and stability of small Au particles will be considered and discussed. The catalysts were characterized on Au content (AAS), Au particle size and size distribution (XRD, HRTEM), and the possible presence of ionic/metallic Au surface species (XPS, MES). The effect of the gold particle size and the effect of the presence of MO_x on the activity and the selectivity will be discussed. It will be shown that for CO oxidation by O_2 both the presence of very small gold particles and the presence of MO_x are of great importance to obtain a high activity. The behaviour of gold based catalysts in the relevant reactions will be compared with those of other noble metal catalysts.

On the basis of our results we propose a formulation for a novel catalyst for the selective oxidation of CO. In addition, a mechanism is proposed for the relevant processes.

OP-II-17

NUMERICAL RESEARCH OF MASS TRANSFER ON THE HONEYCOMB CHANNEL WALLS

V.P. Zakharov, I.A. Zolotarskii and V.A. Kuz'min

Boreskov Institute of Catalysis, 630090, Novosibirsk, Russia
E-mail: xap@catalysis.nsk.su

Nowadays honeycomb monolith catalysts find more and more application in modern industry [1]. Particularly, they are used as the second stage in reactors for ammonia oxidation in nitric acid plants [2]. In this case they substitute a part of platinum gauzes served as the first oxidation stage, rectilinear monolith channels being orthogonal to the gauze pad and parallel to the reactor axis. Mass transfer in honeycomb monolith catalysts is an important factor of their efficiency.

As a rule, a longitudinal dependence of mass transfer in monolith channels is evaluated according to a classic [3] or more novel [4] correlations. All these correlations originate from a theoretical consideration of a gas flow about a plate of zero thickness, mass transfer coefficient being dependent on an axial coordinate z as $\sim z^{-1}$ or $\sim e^{-z}$. But there are experimental data on mass transfer in gas flow about a thick plate in free conditions disproving above correlations [5]. In literature there is no at all data on mass transfer study in case when burrs exist. Such burrs partially block the inlet of each channel and caused by peculiarities of honeycomb monolith manufacturing technology.

The aim of the present study is to elucidate the effect of burr length on mass transfer in honeycomb monoliths with walls of significant thickness.

A calculation problem corresponding to a gas flow through honeycomb catalyst (essentially three-dimensional object) is very sophisticated. But it may be reduced to a much simpler single-plate geometry problem. In accordance with that, the catalytic system is considered as a two-dimensional infinitive flat-periodic structure consisted of an alternating sequence of parallel plates (walls of block cells) and slit channels. One space period includes one solid impenetrable plate of finite thickness.

Mathematical formulation of the problem is based on two-dimensional Navier-Stokes equations coupled with a mass balance equation for a key reagent. The mass balance equation accounts for a diffusion in both directions. Boundary conditions of periodicity were used. Gas flow is considered to be viscous, laminar, isothermal, and incompressible. Only heterogeneous reaction takes place. Catalyst activity is assumed to be extremely high thus providing a zero concentration of a key reagent at a catalyst surface. As a result of a numerical procedure, two-dimensional in space, time-depending fields of gas flow velocity vector components, pressure and key reagent concentration are obtained.

The equations were approximated with regard to primitive physical variables on the base of Galerkin finite element principle. The velocity components and concentration were represented in piecewise-bilinear basis, pressure – in piecewise-constant basis. System time integration was performed using the second-order accuracy Rounge-Cutta's scheme with decoupling of particular model equations. An implicit Euler scheme was used to approximate the diffusion terms. The discrete diffusion/convection equations were solved using a version of the ORTHOMIN method. The pressure field was determined by an original SIMPLE-like procedure. To provide a convergence of iteration algorithms, the SLAE scaling was applied.

Calculations were performed for a grid with a uniform spatial step h equal to 0.05 mm. The resulted number of nodes is 741×141. Thus, the total number of unknown variables, including two velocity vectors, pressure and concentration fields achieves a value about 310 000. A value of a time step was chosen to be 1×10^{-5} s. Because a resulting solution was non-stationary often, time-averaging was necessary to calculate effective mass transfer rates. Up to 10^5 time steps were needed to reach an accurate averaging at times.

Model parameters used in calculations correspond to the typical reactor for ammonia oxidation at high-pressure nitric acid plants: pressure - *7 atm* and temperature - *900°C*. A plate thickness was equal to 2 mm, a distance between plates was 5 mm. These values correspond exactly to a wall thickness and a square channel size of a commercial monolith catalyst. The burr thickness was equal to 0.1 mm.

In our study [6] we have shown that a platinum gauzes pad has perfect refractive properties. This means that the first catalyst stage extinguishes a transverse velocity component, gas flow leaving the pad in parallel to monolith channels of the second catalyst stage. For this reason, we have studied the cases of only longitudinal orientation of gas flow running over a plate. An uniform velocity profile was fixed at a distance equal to a gap between two catalyst stages.

The following results were obtained.

An increase in the burr length ζ provides a non-monotonic change in the nature of plate flowing about (fig. 1). In absence of burrs, the flow is eddy and steady state (fig. 1a). An increase in the burr length is accompanied first by an elongation of the shadow recirculating zone located just behind the burr (fig. 1b), then a mobility appears in its stern part. With further burr length increase, this flow fluctuations amplitude increases, and eventually, as ζ reaches some critical value, the recirculating zone transforms completely into a series of non-steady vortexes. The plate surface free of burrs is characterized by an eddy zone which is always presented on the plate edge. One more zone with counter-clockwise gas recirculation first appears and then disappears downstream at this plate surface. Figure 1c corresponds to the maximal length of this zone and simultaneously to the maximal length of the shadow zone behind the burr. As the flow transforms into the fluctuating mode, the effective length of the

shadow zone significantly decreases (figs. 1d and 2a), an additional embedded recirculating zone being formed within it (fig. 1d).

Effect of a burr dimension on the integral mass transfer corresponds well to the non-monotonous change of flow behavior. As the burr size increases, mass transfer rate is first suppressed (fig. 1b corresponds to its minimum), then it significantly increases (fig. 2b) due to appearing of non-steady vortexes. Prior to the increase in mass transfer, a considerably higher conversion occurs on the undersurface of the plate. Then, the process is more intensive on the top surface. The average mass transfer rate on the frontal surface is several times higher than that on the lateral surfaces. Mass transfer is non-uniformly distributed along the lateral surfaces (fig 3). Dotted curves correspond to calculations performed with a zero thickness of the channel wall of the monolith and without a burr. It is evident that a consideration of the wall thickness in calculations affects significantly the character of mass transfer. Features of the curves (minimum or maximum) shown in fig. 3 can be explained by analyzing the processes of convection-diffusion mass transfer. Local mass transfer rates on the plate surface without a burr correspond to data of reference [5] qualitatively.

Thus it was shown that a bur strongly effects mass transfer in the monolith channels serving as a turbulator of gas flows.

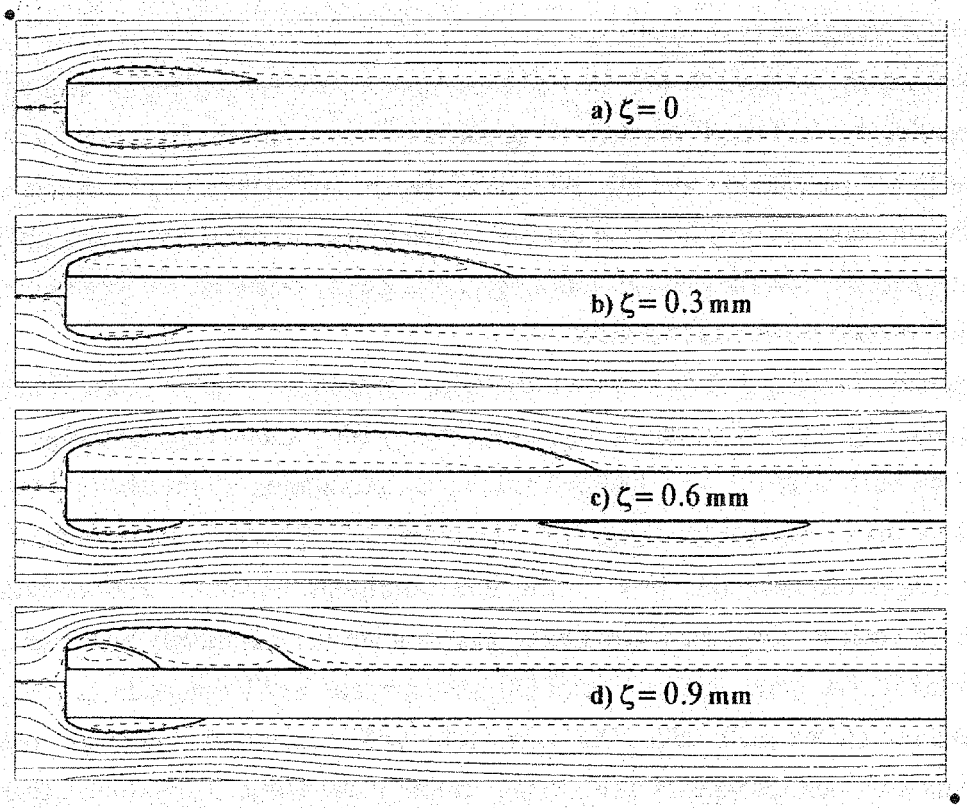

Fig.1 Time-averaged streamlines. Gas flow is directed from left to right.
The burrs are located on left upper edges (ς denotes burr dimension).

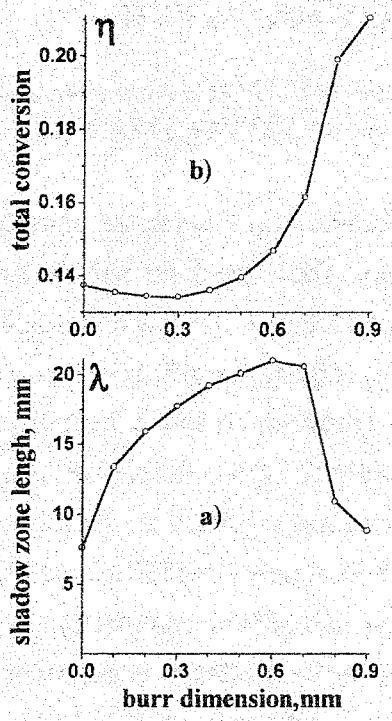

Fig.2 Time-averaged processes characteristics.

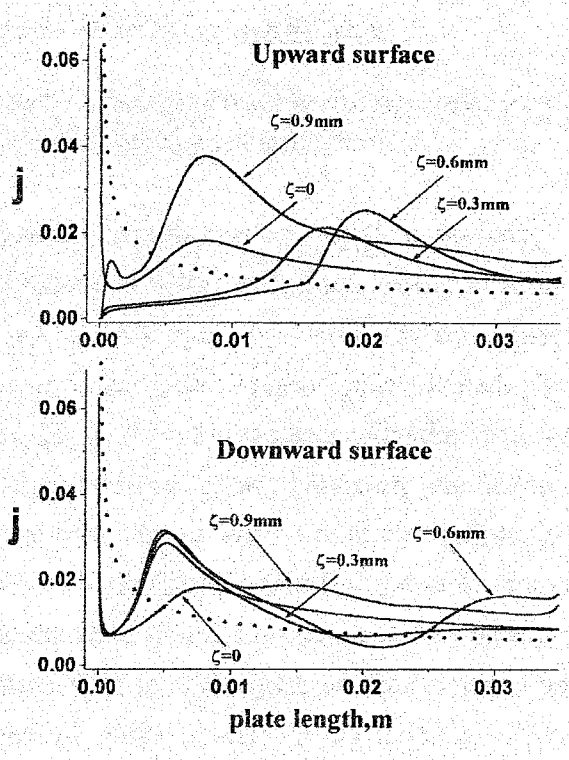

Fig.3 Time-averaged local dimensionless mass transfer rate **j**.

References

1. Structured catalyst and reactors// Edited by A.Cybulski and Jacob A.Mouljin, Marcel Dekker Inc., 1998.
2. V.A. Sadykov, L.A. Isupova, I.A. Zolotarski, L.N. Bobrova, A.S. Noskov, V.N. Parmon, E.A. Brushtein, T.V. Telyatnikova, V.I. Chernyshev, V.V. Lunin, Oxide catalysts for ammonia oxidation in nitric acid production: properties and perspectives // Appl. Catal.: A General, **204,** Issue 1(2000), pp.59-87.
3. Shlichting H. Grenzschicht-theorie.- Karlsruhe, 1951.
4. Hayes R.E., and Kolacszkowski S.T. A study of Nusselt and Sherwood numbers in a monolith reactor// Catalysis Today, 47 (1999), pp. 295-303.
5. Hwang K.S., Sung H.J., and Hyun J.M. Mass transfer measurements from a blunt-faced plate in an uniform flow// Int. J. of Heat and Fluid Flow, 1996, vol.17, No.2, pp. 179-182.
6. Zakharov V.P., Zolotarskii I.A., and Kuz'min V.A. Computational Study of Gas Flow through "Gauze-Pad - Honeycomb" Catalytic System// Ibid.

OP-II-18

MODELLING OF CRITICAL PHENOMENA FOR THE LIQUID/VAPOR- GAS EXOTHERMIC REACTION ON A SINGLE CATALYST PELLET

A.B. Shigarov, A.V. Kulikov, N.A. Kuzin and V.A. Kirillov

Boreskov Institute of Catalysis, Prosp. Akad. Lavrentieva 5, 630090, Novosibirsk, Russia
e-mail: shigarov@catalysis.nsk.su, phone/fax: (0073832)341187

The essential part of industrial multiphase (gas-liquid-solid) heterogeneous catalytic reactions is carried out in the trickle-bed adiabatic reactors. These reactions may be rather exothermic and volatility of the liquid phase may be also noticeable. A typical example of such reactions is hydrogenation of hydrocarbons. So far, the problem, attracting both the academician and industrial interest is how to escape hot spots (resulting in low selectivity, cocking, sintering and runaway) and meanwhile to keep productivity of the trickle-bed reactor. The challenging task is to understand the intrinsic mechanism for transition from the well-known normal trickling operation (liquid phase reaction on the internally liquid filled catalyst) to the abnormal one (gas phase reaction with vaporisation on partially or completely dry pellets). The experimental investigations of alphametilstyrene (AMS) (Germain et.al., 1974) and cyclohexene (Ruzicka & Hanika, 1994) hydrogenation in a laboratory trickle-bed reactor revealed hysteresis/multiplicity of steady states and the impact of vaporisation, gas phase reaction and liquid distribution. Unfortunately no models were suggested because the local picture was unclear. Watson & Harold (1994) were the first to establish multiplicity for cyclohexene hydrogenation on pellet scale, though only for the case when the gas flow contained no vapor and the liquid flow rate was constant. Recent experimental research (Slin`ko et.al., 2000; Kulikov et.al., 2000) has pointed out temperature hysteresis phenomena with a varying liquid flow rate during AMS hydrogenation on a single catalyst pellet. A mathematical model of the half-side wetted and partially liquid filled catalyst slab was developed (Harold, 1993), but it was not compared with experimental data. Both the theoretical and experimental study of the gas phase hydrogenation of hydrocarbons on the dry catalyst pellet under external transport control (Kirillov et.al., 2000) partially elucidates the earlier obtained experimental data. The goal of this paper was to develope mathematical models for undrestanding the critical phenomena, which were experimentally observed for the AMS hydrogenation on the partially wetted catalyst pellet (Slin`ko et.al., 2000; Kulikov et.al., 2000). Althougth our attempts to construct the unique model to simulate all the experimental data were not successful, we consider two rather crude but highly nonlinear mathematical models with lumped parameters, corresponding to different gas flow composition. The models are based on the different physical assumptions, which are briefly mentioned in the discussion chapter (to satisfy the paper volume restrictions).

1. Case of hydrogen flow, completely saturated with the AMS vapor at gas temperature.

$$\beta_{dry}(1-f)C_0Q_p = \alpha(1-f)(T_{dry}-T_0)+\alpha_{int}f(T_{dry}-T_{wet})$$

$$\alpha_{int}(T_{dry}-T_{wet}) = \beta_{wet}[C-C_0]H_{ev}+\alpha(T_{wet}-T_0)$$

$$G_{AMS} = \beta_{wet}Sf[C-C_0]M_{AMS}$$

Here $C_0 = \frac{P_{vap}(T_0)}{RT_0}$; $C = \frac{P_{vap}(T_{wet})}{RT_{wet}}$; $\alpha = \frac{Nu\lambda}{d}$; $\beta_{dry} = \frac{D^0Sh(D^0)}{d}$; $D^0 = \left(\frac{x_0}{D_{23}}+\frac{1-x_0}{D_{12}}\right)^{-1}$

(see Kirillov et.al., 2000); $\beta_{wet} = \frac{D_{12}Sh(D_{12})}{d}$; $\alpha_{int} = \frac{\lambda_p}{d}$, $x_0=P_{vap}(T_0)/P_{tot}$, R=8.31 J/(mole K), d=5 mm, $\lambda(x_0,\lambda_{ams},\lambda_{H2})$ - Brokay gas mixture conductivity correlation (Reid et.al.); λ_p= 0.33 W/(m K); $D_{23}= 5\times10^{-6}$ m^2/s; $D_{12}= 7.5\times10^{-5}$ m^2/s; Sh = 2 + 0.6 $Re^{0.5}$ $Sc^{0.33}$; $Nu = 2 + 0.6\ Re^{0.5}\ Pr^{0.33}$.

2. Case of pure hydrogen flow (without vapor).

$$W_{reac}Q_p = W_{ev}H_{ev}+(\alpha S+Cp_{AMS}G_{AMS}/M_{AMS})(T-T_0)$$

$$\frac{G_{AMS}}{M_{AMS}} = W_{ev} = \frac{S\beta_{12}D^*_{12}/h_{dry}}{\beta_{12}+D^*_{12}/h_{dry}}C^*$$

where $C^*=P_s(T)/RT$; $\beta_{12} = \frac{D_{12}\,Sh(D_{12})}{d}$.

$$W_{reac} = W^{(1)}_{reac}+W^{(2)}_{reac}$$

$W^{(1)}_{reac} = 0$ and $h_{dry} = 0$ if $\frac{G_{AMS}}{M_{AMS}} > \beta SC^*$;

$W^{(1)}_{reac} = Sh_{dry}r_i(T,P_{H_2})$ if $h_{dry} < h^{(1)}_{reac}$;

$W^{(1)}_{reac} = G_{AMS}/M_{AMS} = W_{ev}$ if $h_{dry} > h^{(1)}_{reac}$.

$h^{(1)}_{reac} = \frac{G_{AMS}/M_{AMS}}{Sr_i(T,P_{H_2})}$; $r_i = k_0\exp\left(-\frac{E_1}{RT}\right)P^{0.8}_{H_2}$; $r_2 = k_0\exp\left(\frac{-E_2}{RT}\right)P^{0.63}_{H_2}$

see (Germain et.al., 1974); $W^{(2)}_{reac} \approx S(\overline{D}_{12}r_2C_{H_2})^{0.5}$; $C_{H_2} = \frac{P_{H_2}}{RTHe}$.

$Q_p=109\times10^3$ J/mole; $H_{ev}=43\times10^3$ J/mole; Cp=200 J/(mole K); M_{AMS}=118 kg/mole; $S=1.25\times10^{-4}$ m^2; β=0.036 m/s; α=100 Wt/(m^{2}K); $D^*_{12} = 5\times10^{-6}$ m^2/s; $\overline{D}_{12} = 5\times10^{-9}$ m^2/s; $E_1=37.8\times10^3$ J/mole; $E_2=41.8\times10^3$ J/mole; He=15;

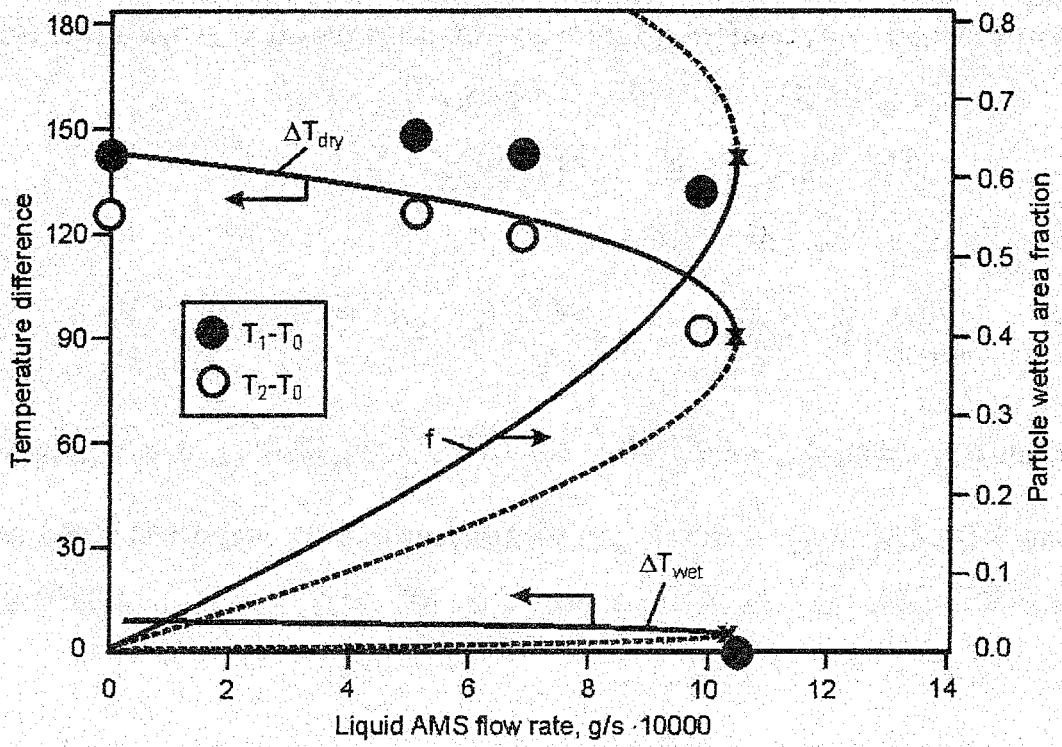

Fig. 1. Experimental extinction phenomenon and modelling in case of hydrogen flow, saturated by AMS vapor at T_0 = 125°C; cylindrical pellet 4.8 mm × 5.7 mm with egg-shell catalyst 15%Pt/$\gamma - Al_2O_3$; T_1 -measurements at pellet centre, T_2 - under particle top side, dotted curves - unstable steady states, continuous curves - stable, cross symbols - points of theoretical extinction.

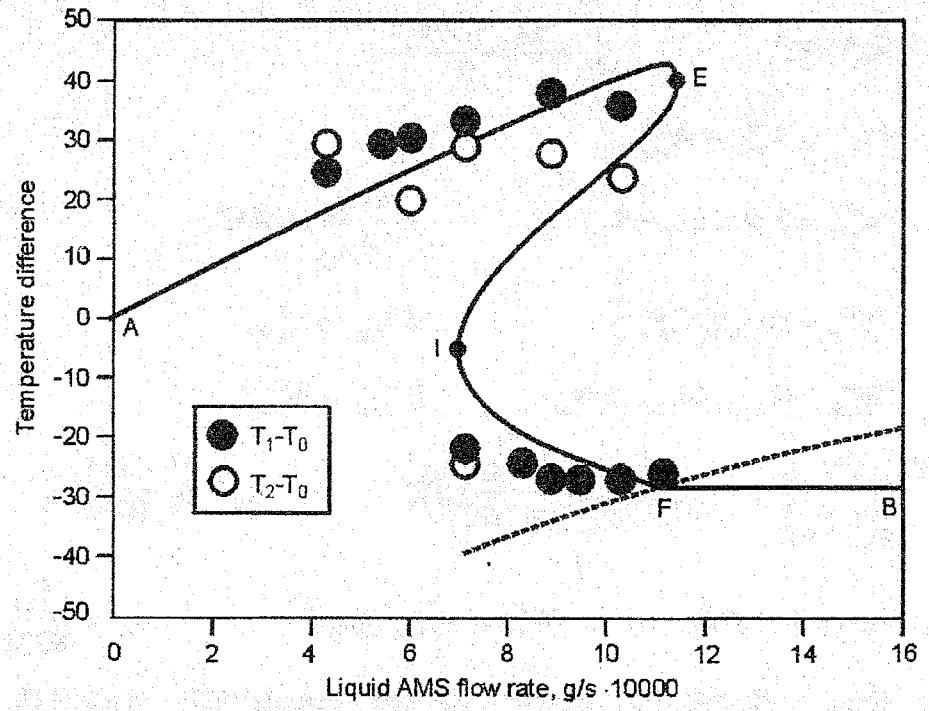

Fig. 2. Experimental hysteresis phenomenon and modelling under pure hydrogen gas flow at T_0=110°C. AE -upper stable branch (total AMC vaporisation and conversion), IB -lower stable branch (FB-pellet filled by liquid, no gas reaction but evaporation), EI -unstable branch, I -ignition point, E -extinction point.

Discussion

The mathematical models successfully simulate the experimental data on the critical phenomena observed for the catalyst pellet, which is fed with liquid AMS and blown either with AMS-vapor saturated or pure hydrogen. In the first case (Fig.1), the extinction conditions are controlled by fraction f of the pellet wetted surface and by intensity of heat transfer through the particle, that is, by linear size and thermal conductivity of the pellet. In the second case (Fig.2), the model displays hysteresis. The nature of this hysteresis is associated with interaction between the pellet drying and the gas phase hydrogenation proceeding in the dried subsurface layer of the pellet. For lower stable branch IFB liquid is evaporated not far from the external pellet surface and AMS vapor conversion is negligable, and so flow-pellet temperature difference is negative. If liquid flow rate decreases, the thikness of dry layer increases resulting in ignition via the gas phase reaction. The vaporisation/reaction front shifts deep inside the porous pellet. This state corresponds 100% AMS conversion on the upper stable branch AE when thickness of the gaseous reaction zone (assuming zero AMS order) is much smaller than that of the dry layer. If this unequality reverses with the increasing liquid flow rate and conversion becomes unsufficient, the catalyst pellet extinction occurs.

Our results may be helpful for analysing the accumulated experimental data concerning the problem of hot spots and runaway in the multiphase reactors.

Acknowledgments

The authors wish to thank the Netherlands Organization for Scientific Research (NWO) Grant 047-011-000-01 and the Russian Fund for Fundamental Investigations (RFFI) Project 99-01-00035 and are grateful to prof. K.R.Westerterp, Dr. A.Kronberg and prof. M.G.Slin`ko for their interest to this research.

References

1. Germain A.H, Lefebvre A.G., L'Homme G.A. // Adv. Chem. Ser. 1974. 133. p. 164.
2. Ruzicka J., Hanika J. // Catalysis Today. 1994. V.20. P.467.
3. Watson P.C., Harold M.P. // AIChE J. 1994. V.40. N 1. P.97.
4. Slin`ko M.G., Kirillov V.A., Kulikov A.V., Kuzin N.A., Shigarov A.B. // Doklady Academy Nauk. 2000. V.373. N.3. P.359 (in russian).
5. Kulikov A.V., Kuzin N.A., Shigarov A.B., Kirillov V.A., Kronberg A.E., Westerterp K.R. // Proceedings of the 3-rd International Symposium "Catalysis in multiphase reactors", Naples, Italy, May 29-31, 2000, P. 81. // Catalysis Today, 2346, 1-8 (2001).
6. Harold M.P. // Chem.Engineering Sci. 1993. V.48. N 5. P.981.
7. Kirillov V.A., Kuzin N.A., Kulikov A.V., Lukyanov B.N., Hanaev V.M., Shigarov A.B. // Theor. Found. of Chem.Technology. 2000. V.34.N.5.P.526 (in russian).

OP-II-19

INVESTIGATION OF STEADY STATES MULTIPLICITY IN HETEROGENEOUS CATALYTIC REACTIONS KINETICS

N.I. Koltsov* and F.J. Keil

**Department of Physical Chemistry, Chuvash State University, Moskovskii prospekt 15, 428015 Cheboksary, Russia, phone: (+78352)498792, e-mail:koltsov@chuvsu.ru*
Department of Chemical Engineering, Technical University of Hamburg-Harburg, Eissendorfer Strasse 38, D-21073 Hamburg, Germany, phone: (+49040)428783042, e-mail: keil@tu-harburg.de

One of the current problems in kinetics is the investigation of the multiplicity of steady states (MSS) and the shapes of the phase portraits in heterogeneous catalytic reactions. Some important results in this field of research is reviewed in this paper. We will first discuss the shapes of the kinetic curves which reveal multiplicity. MSS of reaction rates are investigated as a function of one parameter (concentration of one reactant, temperature, flow rate of one reactant etc.). These dependencies are characterized by the existence of some different stable regimes of reaction proceeding under the same conditions. Typical shapes of kinetic phase planes which are characterized by MSS are given in Fig. 1.

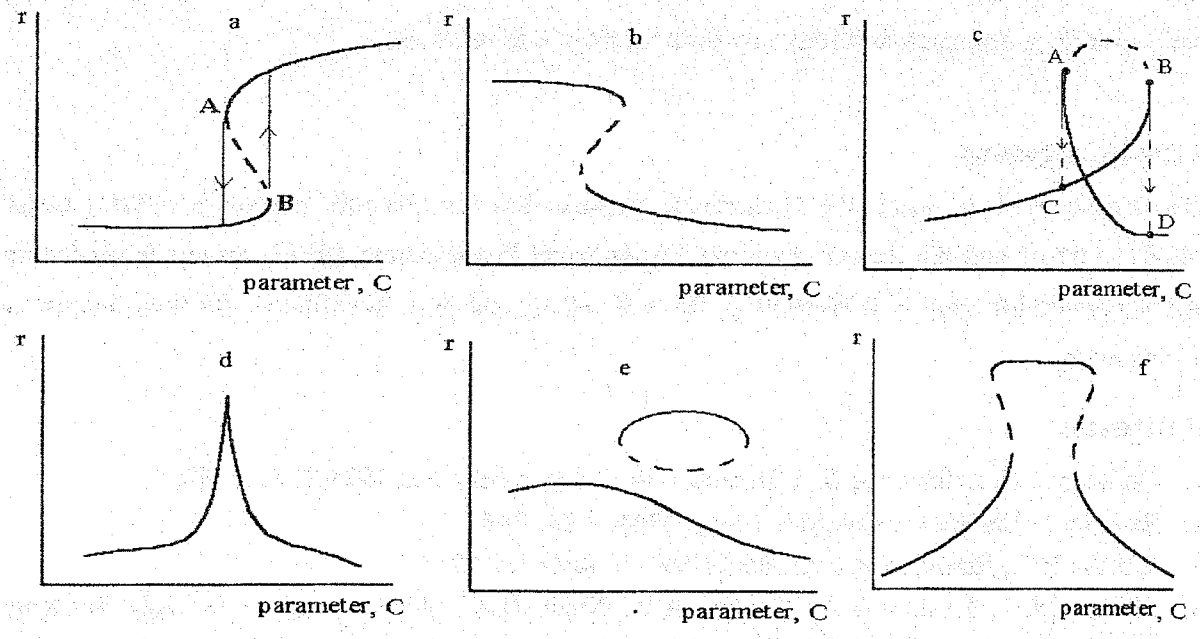

Fig. 1. Multiplicity shapes of steady states: a - "anticlockwise" hysteresis, b- "clockwise" hysteresis, c- self-crossing ("loop"), d- breakdown , e - isola, f - mushroom (solid lines-steady stationary states, broken lines-unsteady stationary states)

S-shaped hysteresis. Examples of MSS of heterogeneous catalytic reactions given in the form of S-shaped hysteresis are the oxidation of hydrogen, carbon monooxide etc. In most cases for the description of hysteresis in the above-mentioned reactions, the mechanisms characterized by interraction of adsorbed components on a catalyst surface were used. The most effective approach finding of MSS is the mathematical criterion offered in paper [1]. The criterion allows on the basis of the stoichiometric matrix of intermediate and basic components of a reaction scheme, to detect unequivocally the existence of MSS, and also to define a set of stages ensuring MSS on kinetic properties of an investigated catalytic reaction, as function of the concentration of intermediate components. The criterion includes the necessary conditions of existence of MSS for reversible and irreversible stages respectively

$$\left(W-\sum_j a_{i,j}^{+}V_j-\sum_k b_{i,k}^{+}U_k\right)\left(\sum_j\left(a_{i,j}^{+}-a_{i,j}^{-}\right)V_j+\sum_k\left(b_{i,k}^{+}-b_{i,k}^{-}\right)U_k\right)>0 \quad \text{for } \omega_{-i}\neq 0, \qquad (1)$$

$$W=\sum_j a_{i,j}^{+}V_j+\sum_k b_{i,k}^{+}U_k \quad \text{for } \omega_{-i}=0. \qquad (2)$$

The sufficient conditions of MSS are

$$\exists i,j:\ V_i<0<V_j. \qquad (3)$$

$$U_l\le 0\le U_p\le W \text{ or } U_l\ge 0\ge U_p\ge W, \qquad (4)$$

where $\omega_{\bar{i}}$ - refers to the number of stages in reverse directions; $a_{ij}^{\pm}$, $b_{ij}^{\pm}\ge 0$ $(\sum_j a_{ij}^{+}=\sum_j a_{ij}^{-})$ - stoichiometric coefficients of intermediates X_j and basic A_l substances; $V_j=\ln\frac{x_j^{(2)}}{x_j^{(1)}}$, $U_k=\ln\frac{C_k^{(2)}}{C_k^{(1)}}$, $W=\ln\left(\frac{r^{(2)}}{r^{(1)}}\right)$. On the basis of the description of a MSS criterion one can conclude that there is MSS only when at least two different sets of concentrations of intermediate compounds $x_j^{(1)}$, $x_j^{(2)}$ and concentrations of basic substances $C_k^{(1)}$ and $C_k^{(2)}$ with corresponding nonzero values of process $r^{(1)}$ and $r^{(2)}$ $(r^{(1)}\neq r^{(2)})$ exist. For a catalytic reaction of carbon monooxide oxidation on platinum [2] proceeding according to the scheme

1. $O_2+2K=2KO$, 2. $CO+KO+K\rightarrow CO_2+2K$

where K and OK are free and occupied by oxygen catalyst surface centres, respectively, MSS according to the relations (1) and (2) will occur under the following conditions:

$$(2V_1 + U_1 - W)(2V_2 - 2V_1) > 0,\ W = V_1 + V_2 + U_2.$$

The relations (1) and (2) are carried out, for example, for $W = 2$, $V_1 = 6$, $V_2 = -2$, $U_1 = -13$, $U_2 = -2$ (the parameters U_1 and U_2 correspond to substances of O_2 and CO). The given values satisfy the vector components V and U, and also the inequalities (3), (4).

Self-crossing. Another shape of MSS is a kinetic curve with self-crossing (Fig. 1c). This critical phenomenon is characterized by the fact that the graph of reaction rate, dependent on one parameter, crosses itself at one point. This leads to a kinetic "loop". It is worth to note that at the self-crossing point, which is characterized by various values of intermediate substance concentrations on a catalyst surface, the reaction rate has the same value. The equations of the MSS criteria (1), (2) in case of self-crossing will be written down in the following way:

$$\sum_j a_{i,j}^{+} V_j \left(\sum_j (a_{i,j}^{-} - a_{i,j}^{+}) V_j\right) > 0, \qquad (\omega_{-i} \neq 0) \tag{5}$$

$$\sum_j a_{i,j}^{+} V_j = 0, \qquad (\omega_{-i} = 0) \tag{6}$$

The simplest mechanism satisfying to this criterion for $A_1 \Leftrightarrow A_2$ reaction is

$$1.\ A_1 + X_1 + X_2 = 2X_1 + A_2, \qquad 2.\ X_1 + 2X_2 = 3X_2, \tag{7}$$

Breakdown. As can be observed, under certain conditions points A and B in Fig.1c with self-crossing can exist very close to each other, which leads to a kinetic curve with breakdown. The kinetic behavior of this form was obtained for reactions of carbon monooxide and hydrogen oxidation on platinum metals. Besides these examples the appearence like breakdown were obtained at joint oxidation of carbon monooxide and nitrogen oxide. In works [3,4] the criterion of occurrence of a breakdown is offered at the certain values of rate constants of stages. It is shown that the relations of the criteria of a breakdown are equivalent to basic relations of criteria of self-crossing of kinetic dependences. This researche shows that kinetic dependences with self-crossing and with a breakdown are determined by identical states in reaction stoichiometry, although they are different shapes of MSS. Therefore for describing breakdown it is quite sufficient have reaction schemes giving self-crossing of kinetic curves. Fig. 1d illustrates breakdown for scheme (7). The most simple schemes of catalytic hydrogen oxidation reaction describing MSS in the form of breakdown (or with self-crossing) kinetic dependencies are the following:

$$1.\ O_2 + 2K = 2KO,\ 2.\ H_2 + K = KH_2,\ 3.\ KO + KH_2 \rightarrow 2K + H_2O.$$

Isola (Fig. 1e). The existence conditions of this shape for a non-isothermal reaction of the first order are formulated in paper [5]. The basic cause of appearance of isola is a process of

"rolling - unrolling" of a mushroom curve in Fig. 1f, which is described in papers [6,7]. The isola in dependence graph r(C) can be obtained from a kinetic curve having "a special point" [5,8]. If one of the parameters changes slightly, this point becomes an isola. The simplest model of a kinetic curve with isola realization is a $A \Leftrightarrow D$ reaction proceeding via an intermediate B according to the following scheme,

$$1.A + 2B + X_1 = X_2 + 3B, \quad 2.B + 3X_1 + X_2 = 4X_1 + D,$$

for which shows posibility of existence of isola on the dependence $r(C_B)$.

Mushroom. Mushroom behavior (Fig. 1f) can be considered as a monoparameter kinetic curve which consists of two S-shaped hysteresis branches. This MSS shape rarely appears. The mushroom shape is a transitional one between isolated and selfcrossing kinetic curves. The mushroom shape is connected with existence of "a special point". The investigation of stoichiometric conditions of "special point" existence of the kinetics showed some interesting results. For example, the $B_2 \Leftrightarrow 2B_1$ reaction proceeding via the following scheme

$$1.B_2 + X_1 = X_2 + B_1, \quad 2.X_2 = X_3 + B_1, \quad 3.2X_1 + X_3 = 3X_1,$$

describes the kinetics with isola under certain conditions (Fig. 1e). If the conditions change, approaching and blending of the isola with a monotonous branch takes place. Thus, self-crossing appears (Fig. 1c) which turns into a mushroom form (Fig. 1f).

The conditions and criteria of MSS and its different shapes are mathematical relations which contain stoichiometry, concentrations of components and kinetic parameters. The solution of these algebraic equations for catalytic reactions proceeding via multiple stage schemes it can be done by applying computers [9].

REFERENCES

1. N.I. Koltsov, V.Kh. Fedotov and B.V. Alexeev, Dokl. Akad. Nauk SSSR, 1988, 302(1), 126-131 (in Russian).
2. L.F. Razon and R.A. Schmitz, Catal. Rev.-Sci. Eng., 1986, 28(1), 89-164.
3. B.V. Alexeev, N.I. Koltsov and V.Kh. Fedotov, Dokl. Akad. Nauk SSSR, 1991, 317(1), 147-151 (in Russian).
4. N.I. Koltsov and B.V. Alexeev, Ibid., SSSR, 1989, 307(6), 1407-1410 (in Russian).
5. Ja.B. Zeldovich and Ju.A. Zysin, Zhurn. Phys. Chem., 1941, 11 (6), 501-508 (in Russian).
6. V. Hlavacek and P.V. Rompay, Chem. Eng. Sci., 1981, 36(10), 1730-1731.
7. P. Gray and S.K. Scot, Ibid., 1983, 38(1), 29-43.
8. V.Kh. Fedotov, N.I. Koltsov and B.V. Alexeev, Chem. Kinetics in Catalys. Theoret. Problems of Kin. Chernogolovka, 1985, 89-95 (in Russian).
9. B.V. Alexeev, I.V. Kozhevnikov and N.I. Koltsov, Comput. and Chem., 1999, 23, 69-74.

OP-II-20

DYNAMIC BEHAVIOR OF SELECTIVE HYDROGEN SULFIDE OXIDATION IN A FLUIDIZED BED

A. Balaev, E. Konshenko, S. Spivak, F. Ismagilov

Institute of Petrochemistry and Catalysis of Bashkir Academy of Sciences
450075, Russia, Ufa, Prospekt Oktyabrya, 141
Fax: 3472-312750
E-mail: spivak@bsu.bshedu.ru

The analysis of three kinetic models of selective hydrogen sulfide oxidation over metal oxide catalyst was carried out and the kinetic parameters of the mechanism of the reaction were found. From a comparison of calculated and experimental data for consequent simulation of the process it was selected the scheme of transformations which took into account the dissociative adsorption of oxygen.

This kinetic model considers formation of sulfur not only as a S_2 structure, but also its transformation into S_4, S_6 and S_8 structures, these were in a thermodynamic equilibrium. In addition, it is assumed the catalyst deactivation by the formation of sulfur deposits on an active surface.

For simulation of the process the transient two-phase dispersion model of fluidized bed reactor was developed. The model take into account heat- and mass- transfer in a dense phase at the expense of a thermal conduction and longitudinal diffusion, transports in a dense phase and phase of bubbles by convection streams and also by Stefan stream, which arises because of a decreasing of mole number during a chemical reaction. The computing of hydrodynamic and transport parameters was made by the use of the empirical criteria equations.

The model equations of mass and energy balances for the dense and gas phases for an adiabatic reactor are given by

$$\varepsilon q\frac{\partial y_i}{\partial t}+qU\frac{\partial y_i}{\partial l}=D\frac{\partial^2 y_i}{\partial l^2}+f(\beta_м S_u+\mu)(x_i-y_i)+f\sum_{j=1}^{J}(\nu_{ij}-y_i\delta_j)\frac{W_j}{C_0}$$

$$\varepsilon(1-q)\frac{\partial x_i}{\partial t}+(1-q)U\frac{\partial x_i}{\partial l}=f(\beta_м S_u+\mu)(y_i-x_i)$$

$$\mu=-(1-q)\sum_{j=1}^{J}\delta_j\frac{W_j}{C_0}-\frac{\varepsilon_0}{\varepsilon(1-\varepsilon)}\frac{Ud\varepsilon}{\varepsilon dl}$$

$$\varepsilon C_k\frac{\partial\Theta}{\partial t}+qU\frac{\partial\Theta}{\partial l}=\lambda\frac{\partial^2\Theta}{\partial l^2}+f(\beta_т S_u+\mu)C_p(T-\Theta)+f\sum_{j=1}^{J}Q_j W_j$$

$$\varepsilon(1-q)\frac{\partial T}{\partial t}+(1-q)U\frac{\partial T}{\partial l}=f(\beta_T S_u+\mu)(\Theta-T)$$

The initial and boundary conditions are:

$t = 0$: $U = U_o$, $y_i = 0$, $x_i = x_i^o$, $T = T_o$, $\Theta = \Theta_o$;

$l = 0$: $U = U_o$, $x_i = x_i^o$, $T = T_o$ $\qquad D\frac{\partial y_i}{\partial l}=qU(y_i-x_i^0)$, $\quad \lambda\frac{\partial \Theta}{\partial l}=qU(\Theta-T_0)$,

$l = H$: $\lambda\frac{\partial \Theta}{\partial l}=D\frac{\partial y_i}{\partial l}=0$

With the help of reactor model it was carried out the computing experiment and conditions of the optimum process operation were found. The calculations were made in the temperature range 100...330°C, in the H_2S concentration range 5...30% (vol.) and at atmospheric pressure.

One of the important problems for practical realization of selective hydrogen sulfide oxidation process is the determination of maximal initial value of hydrogen sulfide concentration, as its exceeds thatlts in "heat explosion".

It was established, that the initial hydrogen sulfide concentration should not exceed 25 % (vol.). Otherwise it is impossible to remove enough of heat amount, therefore at beginning of the bed "heat explosion" actually happens (see fig.1). Under these conditions there is complete hydrogen sulfide oxidation with sulfur dioxide production.

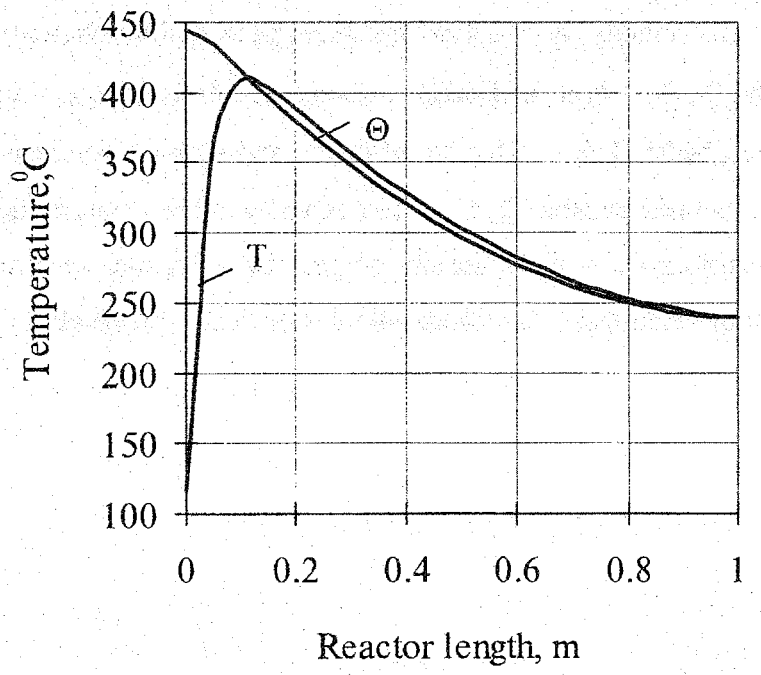

Fig. 1. Temperature profiles of dense (Θ) and babble (T) phases at the "heat explosion" conditions (initial hydrogen sulfide concentration is 25%(vol.), surface of heat removing is 16 $м^2/м^3$)

For initial hydrogen sulfide concentrations 12...19%(vol.) it was calculated a transition range up to the steady states with high (more than 99%) hydrogen sulfide conversion.

There were computed also the ignition temperatures of process T_o in dependence on initial temperature of the catalyst Θ_o and initial hydrogen sulfide concentration $[H_2S]_o$ (see tabl.1).

Table 1

$[H_2S]_o$	10% (vol.)				15% (vol.)			
Θ_o, °C	171	169	168	167	170	169	167	166
T_o, °C	60	65.1	70.2	79.8	55	59.7	70	80

The following optimum modes of operations of a reactor of length 3 m and diameter 0.4 m was found, which was loaded with 250 kg of catalyst.

For $[H_2S]_o$=10% (vol.) - G_{gas}= 180 m^3/h; T_o = 70°C; Θ_o = 168°C.

For $[H_2S]_o$=15% (vol.) - G_{gas}= 180 m^3/h; T_o = 60°C; Θ_o = 169°C.

Notation

y_i and x_i – compound concentration in the dense and babble phase; W_j – rate of chemical reactions; U – local gas velocity; q – fraction of stream, passing through dense phase; μ - rate of the Stefan stream; β_T, β_M – heat- and mass-exchange coefficients; ε, ε_o – void fraction of the fluidized and fixed beds; D, λ – effective diffusion and thermal conductivity; Θ, T – temperature of dense and gas phases; $C_к$, C_p – heat capacity of the catalyst and gas; 1/f – coefficient of bed expansion; C_o – mole density of gas; S_u – external specific catalyst particle surface; Q_j – heat of reactions; l, H – longitudinal coordinate and height of the fluidized bed; t – time.

CATALYST DEACTIVATION MODELS BASED ON STAGE MECHANISMS

N.M. Ostrovskii

Boreskov Institute of Catalysis, Omsk Department, Russia

It is demonstrated how deactivation equations can be derived using the Bodenstain principle of quasi-steady state. A common equation for any linear mechanism is suggested as well as equations for some nonlinear (binary) mechanisms. Equation for "qualitative deactivation", when an active center is transformed to another one, is discussed. Several examples are given regarding various reaction mechanisms and reactions. Some rules are proposed for interpreting deactivation experiments.

Deactivation has to be considered as an unsteady state irreversible process of catalyst evolution in a quasi-steady state reaction occurring on the catalyst.

The Bodenstain's principle of quasi-steady state is valid for deactivation as:

$$\frac{d\Theta_j}{dt} \approx \frac{d\Theta_j^o}{dt} = 0, \quad j=1,..N; \quad \frac{d\Theta_{Pi}}{dt} \neq 0, \quad i=1,...M; \qquad \sum\Theta_j = 1 - \sum\Theta_{Pi} \tag{1}$$

where Θ_j are concentrations of intermediates (coverage), participating in the catalytic cycle; Θ_{Pi} refers to coverage excluded from the catalytic cycle due to deactivation.

Quasi-steady state application is possible due to the fact, that deactivation rate (r_P) is significantly lower in comparison to reaction rate (r). In turn aging rate (r_A) is slower than deactivation rate: $r >> r_P >> r_A$. Just this fact allows us to show that at quasi-steady state approximation each coverage Θ_j decreases proportionally to its initial value, Θ_j^o, and to active surface ($1-\Theta_P$) [1]:

$$\Theta_j(t) = \Theta_j^o\,[1 - \Theta_{Pi}(t)], \quad j = 1,...N \tag{2}$$

In the quasi-steady state the initial (r^o) and current (r) reaction rates are equal to the rate of any step ($r = r_j$) of reaction mechanism:

$$r^o = w_j\Theta_j^o - w_{-j}\Theta_{j+1}^o, \qquad r = w_j\Theta_j - w_{-j}\Theta_{j+1}, \tag{3}$$

where w_j - is corresponding step weight ($w_j = r_j/\Theta_j$).

Since relative activity is $a = r/r^o$, the combination of (2) and (3) gives:

$$r(t) = r^o\,a(t), \qquad r(t) = r^o\,[1 - \Theta_P(t)], \qquad a(t) = 1 - \Theta_P(t) \tag{4}$$

Linear mechanisms. Using (2,4) one can derive deactivation kinetics equations for any linear mechanism. It may be presented as a catalytic cycle with reaction rate r (see 5). Deactivation and self-regeneration are assumed to be slow steps external to catalytic cycle:

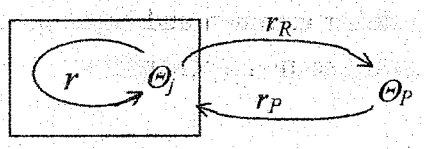

$$\frac{d\Theta_P}{dt} = w_P\Theta_j - w_R\Theta_P \tag{5}$$

where r, r_P, r_R - are the rates of reaction, deactivation and self-regeneration (for example by H_2 in reforming or by H_2O in CH_4 conversion); $w_j = r_j / \Theta_j$ are the weight of steps, which are the functions of concentration and temperature.

According to (2) $\Theta_j = \Theta_j^o$ (1- Θ_P), and Θ_j^o may be expressed through the rate and weight of the j-th step $\Theta_j^o = r_j^o / w_j$. In quasi-steady state $r^o = r_j{}^o$, therefore

$$\Theta_j = \frac{r^o}{w_j}\left(1-\Theta_P\right), \quad \text{and} \quad \frac{d\Theta_P}{dt} = \frac{r^o}{w_j} w_P\left(1-\Theta_P\right) - w_R\Theta_P \tag{6}$$

Since from (4) $a = 1 - \Theta_P$, then $da = - d\Theta_P$, and consequently

$$\frac{da}{dt} = -\frac{r^o}{w_j} w_P a + w_R(1-a) \tag{7}$$

In case of reversible deactivation (i.e. at self-regeneration by H_2, H_2O etc.) activity reduces to some stationary level (a_S), but not to zero. This level is attained at time $t \geq t_S$ when deactivation rate (r_P) becomes equal to the rate of self-regeneration (r_R). So in (7) at $t = t_S$: $(r^o / w_j)\, w_P a_S \approx w_R (1 - a_S)$. Therefore, we may exclude parameter w_R from equation (7), and to replace it by a_S, which is more useful as is determined from experimental data. The equation obtained has the structure that is common for any linear mechanism:

$$-\frac{da}{dt} \approx \frac{r^o}{w_j} \quad \sum w_{Pj} \quad \frac{a - a_S}{1 - a_S} \tag{8}$$

$f_o(C,T)$ - function of main reaction

$f_d(C,T)$ - function of deactivation

$f_a(C,T)$ - function of activity

Nonlinear mechanisms. The same approach can be applied to some nonlinear mechanism. Because of a very low probability for more than two species to interact on the surface, most nonlinear mechanisms can be reduced to binary interactions in the adsorbed layer. Only three types of nonlinear binary mechanisms can be formulated:

Double-center adsorption	Surface dimerization	Surface disproportionation
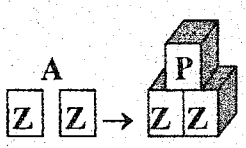	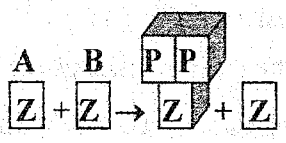	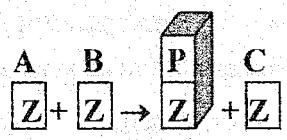

AZ, BZ are precursors of poison or coke, **PZ** is blocked center.

In the first case 1 precursor molecule poisons 2 active sites. In the second case 2 molecules poison 1 site, and in the third case 1 molecule poisons 1 site.

For these nonlinear mechanisms one can also obtain rather common and rigorous equations, that are different for linear (9a) and nonlinear (9b) main reaction mechanisms:

$$\frac{da}{dt} = -w_P f_1(r^o)\, a^2, \qquad \frac{da}{dt} = -w_P f_2(r^o)\, a \quad a, \qquad (9a,b)$$

Equations for reversible deactivation (with self-regeneration) are presented as (10a) for linear, and (10b) for nonlinear mechanism of the main reaction (example of acetylene hydrogenation). In each case the "surface dimerization" as a mechanism of deactivation was assumed.

$$-\frac{da}{dt} = \frac{k_P}{1-a_S}\left(a^2(1-a_S) - a_S^2(1-a)\right), \quad -\frac{da}{dt} = \frac{2k_P}{1-a_S^2}\left(a^2 - a_S^2\right)a \quad \overline{a}. \qquad (10a,b)$$

"**Qualitative deactivation**" is an another nonlinear phenomenon. It means that during deactivation some active sites, that are poisoning or blocking, can also transform into another type sites. On such sites the reaction also occurs, but with a different rate. Schematically it can be presented as some catalytic cycle on Z - type sites (reaction rate r_Z) with slow deactivation (r_P) and slow transformation (r_F) of Z to X - type sites (reaction rate r_X):

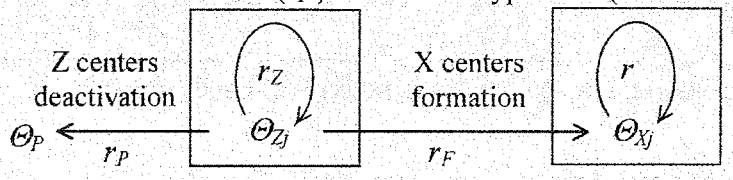

(11)

If the rate of reaction on initial sites is higher than on new sites ($r_Z > r_X$), activity falls continuously. In the opposite case ($r_Z < r_X$) activity initially grows and then decreases due to deactivation. Using the approach described above it is possible to derive a common equation for "qualitative deactivation". Activity (a) in this case is the function of activities of Z and X sites: $a = (r_Z + r_X) / r_Z^o = a_Z + a_X\, a_m = 1 - \Theta_P - \Theta_X(1 - a_m)$, where $a_m = r_X^o / r_Z^o$. Therefore

$$-\frac{da}{dt} = r_Z^o\left(\frac{w_P}{w_{ZP}} + \frac{w_F}{w_{ZF}}\right)\left(a - \frac{\gamma}{1+\gamma}\, a_m\right), \qquad (12)$$

where $\gamma = w_F w_{ZP} / w_P w_{ZF}$; w_j are the weights of deactivation steps (w_P) and new sites generation (w_F), and of steps where sites Z are consumed, Θ_Z, that take part in r_P (w_{ZP}) and in r_F (w_{ZF}). Similar approach was applied to dynamics in the process of HDS-HDA of motor fuels on a sulfide catalyst [2], and in complete oxidation of aromatics on oxides.

Analysis of experimental data. In practice and in the literature one can find several typical mistakes in experiments interpreting. The main mistake consists in using the relationship $a = X / X^o$ for relative activity instead of $a = r / r^o$. Such a ratio of current and initial conversion is valid only for zero order reaction and only in gradientless reactor. Indeed the relation $a = f(X)$ is defined by reaction kinetics and by type of reactor, but it does not depend on deactivation kinetics. The corresponding formulas are listed in table 1.

Another mistake comes from interpretation of deactivation curves $a(t)$ and $X(t)$ since their shapes usually differ. Furthermore, it was shown in this work that $X(t)$ - curves have the flex-points even in the simplest case, when $da/dt = -k_P\, a$. The coordinates of the flex-points and corresponding equations are listed in table 2. It is important that flex-point usually disappears if $X^o < X_m$. In the integral reactor the analysis and interpretation of experiments is complicated, because of activity gradient in catalyst bed.

Table 1. The relations of activity vs. conversion.

Reaction order	Gradientless reactor	Plug flow reactor
Common case	$a=\frac{(1-X^o)^n}{X^o}\frac{X}{(1-X)^n}$	$\langle a\rangle=\frac{(1-X)^{1-n}-1}{(1-X^o)^{1-n}-1}$, $n\neq 1$
$n=0$:	$a=X/X^o$	$\langle a\rangle=X/X^o$
$n=1$: (irreversible)	$a=\frac{1-X^o}{X^o}\frac{X}{1-X}$	$\langle a\rangle=\frac{\ln(1-X)}{\ln(1-X^o)}$
$n=1$: (reversible)	$a=\frac{X_P-X^o}{X^o}\frac{X}{X_P-X}$	$\langle a\rangle=\frac{\ln(1-X/X_P)}{\ln(1-X^o/X_P)}$
$n=2$:	$a=\frac{(1-X^o)^2}{X^o}\frac{X}{(1-X)^2}$	$\langle a\rangle=\frac{1-X^o}{X^o}\frac{X}{1-X}$

X_P - equilibrium conversion, $\langle a\rangle$ -average activity of catalyst bed.

Table 2. Flex - point coordinates X_m in curves of $X(t)$. $\gamma=k_P C_A^o$.

Type of deactivation	Gradientless reactor	Plug flow reactor
Independent $da/dt=-k_P a$	$dX/dt=-\gamma(1-X)X$ $X_m=0.50$	$dX/dt=\gamma(1-X)\ln(1-X)$ $X_m=0.63$
By initial substance $da/dt=-k_P C_A a$	$dX/dt=-\gamma(1-X)^2X$ $X_m=0.33$	$dX/dt=-\gamma(1-X)X$ $X_m=0.50$
By product $da/dt=-k_P C_B a$	$dX/dt=-\gamma(1-X)X^2$ $X_m=0.67$	$dX/dt=\gamma(1-X)[X+\ln(1-X)]$ $X_m=0.80$

However, the problem can be solved in a case of linear kinetics, using terms of average activity of bed: $\langle a\rangle=\int a(\xi)\,d\xi$. Then equations for conversion $x(\xi,t)$ and activity $a(\xi,t)$, that are change with time (t) and coordinate (ξ), can be reduced to one equation for conversion at the exit of reactor: $X(t)=x(1,t)$. The corresponding equations are listed in Table 2.

For reversible deactivation, accompanied by self-regeneration:

$$\frac{dX}{dt}=\left(1-\frac{\ln(1-X_S)}{\ln(1-X)}\right)\Psi_j(X) \qquad (13)$$

where X_S - is stationary conversion that corresponds to $\langle a_S\rangle$; $\Psi_j(X)$ - function represents type of deactivation: $\Psi_1(X)=\gamma(1-X)\ln(1-X)$ - independent; $\Psi_2(X)=-\gamma(1-X)X$ - by initial substance; $\Psi_3(X)=\gamma(1-X)[X+\ln(1-X)]$ - by product. Here $\gamma=k_P C_o$.

1. *Ostrovskii N.M., Yablonskii G.S.* - React. Kinet. Catal. Lett., 39, 287-292 (1989).

2. *Ostrovskii N.M., Gulyaev K.S., Startsev A.N., Reutova O.A.*. - Canadian J. Chem. Eng., 74, 445-456 (1997).

CHEMICAL REACTIONS IN SUPERCRITICAL SOLVENTS. FUNDAMENTALS AND APPLICATIONS

Vladimir I. Anikeev, Anna Yermakova

Boreskov Institute of Catalysis, Pr. Lavrentieva, 5, Novosibirsk 630090, Russia
Fax: 7 383 23974 47, E-mail: anik@catalysis.nsk.su

Supercritical fluids (SCFs) or solvents with unique properties are widely used in different applications for separation and extraction of substances for a long time. However, only for the last decade the SCFs were seriously considered as the reactive media for different processes: complex organic and new materials synthesis, utilization of toxic and harmful substances, utilization of municipal and industry waste, conversion of low-quality fuels, etc.

Very important for industry are processes, which are carried out at high pressure and temperatures, including area of supercritical parameters of process. The examples of such processes are ammonia and methanol production, high alcohols synthesis, hydrocarbon synthesis by the Fischer-Tropsch reaction, hydrogenation of unsaturated organics in supercritical solvents, and also many other processes. It is known, that in the supercritical conditions the properties of the reaction mixture differ strongly from the properties of the ideal gas, and these deviations cannot be neglected at calculation of the kinetic, equilibrium constants. For this reason, the choice of adequate thermodynamic model for the description P-V-T of properties of not ideal mixes plays an important role at calculation of kinetics and chemical equilibrium.

An effect of the non-ideal reaction mixture on the Fischer-Tropsch (FT) synthesis reaction rate in the supercritical propane and n-hexane is reported. Using the experimental data on kinetic of the Fischer-Tropsch reaction, obtained for the commercial precipitated promoted iron catalyst, the kinetic model is designed. In this model, the effect of nonideality of the reaction medium on the reaction rate is taken into account by introducing fugacity coefficients derived from a modified Redlich–Kwong–Soave equation of state.. The equations for description of two Anderson-Shultz-Flory distributions dependent from the carbon monoxide and hydrogen fugacities in the reaction mixture are given for saturated and unsaturated hydrocarbons. The proposed kinetic model is applicable at T = 523–623 K and P = 6–100 atm. A method based on the calculated critical parameters of the reaction mixture is proposed for the selection of suitable supercritical solvent and for the optimization of its concentration. The reaction rate and the total yield of C_nH_{2n} ($n \geq 2$) olefins (including the desired fraction C_5–C_{11})

under supercritical conditions were demonstrated to be essentially higher than those for the reference process carried out in the absence of solvent.

Effect of Supercritical Water Density on the Rate of 2-propanol Dehydration Reaction

The new experimental technique to study kinetics and thermodynamics of chemical reactions in supercritical solvents is suggested. Kinetics and mechanism of 2-propanol dehydration reaction in supercritical water (SCW) in the batch reactor are investigated. It has been shown, first, that the mechanism of the dehydration reaction essentially differs from the reaction mechanism in the presence of the homogeneous acid catalyst; secondly, the rate of reaction depends considerably on the SCW density. In the result of experimental researches of hydrolysis and hydrogenation reactions of the main products of reaction of 2-propanol dehydration, the basic mechanism of 2-propanol dehydration in supercritical water is offered. The experimental data are well described by the first order reaction. Kinetics of 2-propanol dehydration has been investigated, the values of the first-order rate and equilibrium constants have been found.

It has been shown, that CSW density can be used as parameter for control kinetics and selectivity of chemical reaction.

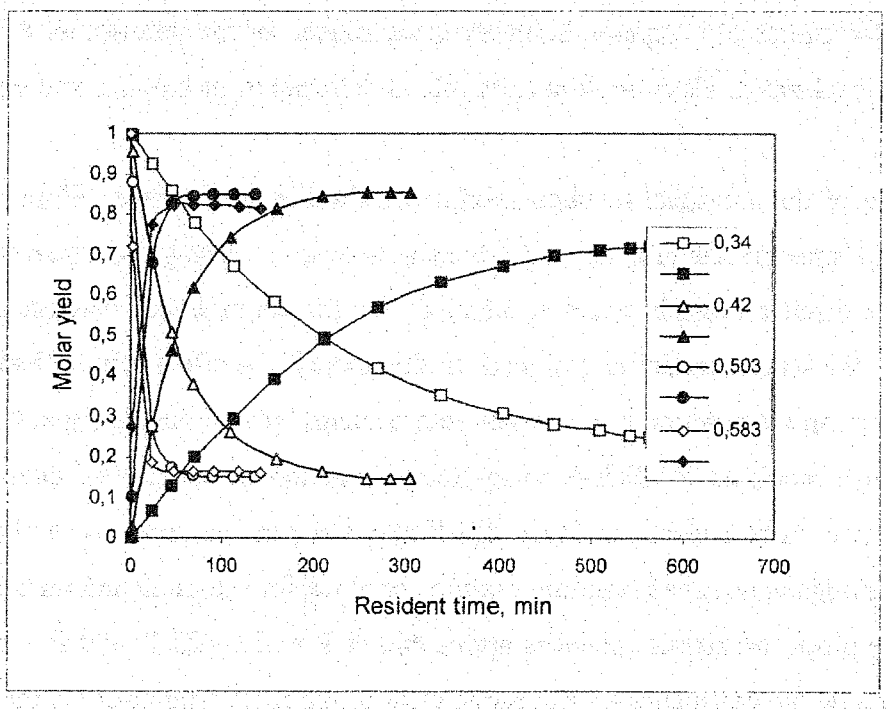

Molar yield of 2-propanol and propane versus the resident time by different SCW densities. Temperature 393° C

Section III

NEW TYPES OF CHEMICAL PROCESSES AND REACTORS

SIMULATION OF TUBULAR REACTOR FOR NITROUS OXIDE PRODUCTION

A.S. Noskov, I.A. Zolotarskii, S.A. Pokrovskaya, V.N. Korotkikh, V.N. Kashkin, V.V. Mokrinskii, E.M. Slavinskaya

Boreskov Institute of Catalysis, Novosibirsk, pr. Akademika Lavrentieva, 5, Russia
Phone: 007-3832-344491; fax: 007-3832-341878, E-mail: pokrov@catalysis.nsk.su

Nitrous oxide is widely known as a mild oxidizer for the partial oxidation of hydrocarbons, consider for example the process of benzene oxidation to phenol jointly developed by the Boreskov Institute of Catalysis and Solutia [1,2]. Widespread commercial adoption of this process requires an inexpensive process for producing nitrous oxide. This report presents the joint efforts of the Boreskov Institute of Catalysis and Solutia towards the development of a catalytic process for ammonia oxidation to nitrous oxide in a tubular reactor. The report addresses lab-scale kinetics studies, mathematical reactor modeling and pilot-scale trials of this process.

Catalyst

A $MnO_2/Bi_2O_3/Al_2O_3$ catalytic system has been shown to provide high selectivity of ammonia oxidation towards nitrous oxide [3]. Batches of this catalyst shaped as spheres were prepared for a pilot reactor.

Kinetic study

Lab-scale studies of the catalyst properties in an isothermal plug flow reactor and in a continuous stirred tank reactor reveal that nitrous oxide selectivity grows with increasing ammonia conversion. Increasing the oxygen and water concentrations in the system also leads to higher N_2O selectivity. In the optimal operating temperature range, 310-370°C, the nitrous oxide selectivity reaches 90-92 % (See Fig.1) while nitrogen oxide selectivity remains in the range 0.3-0.5 %.

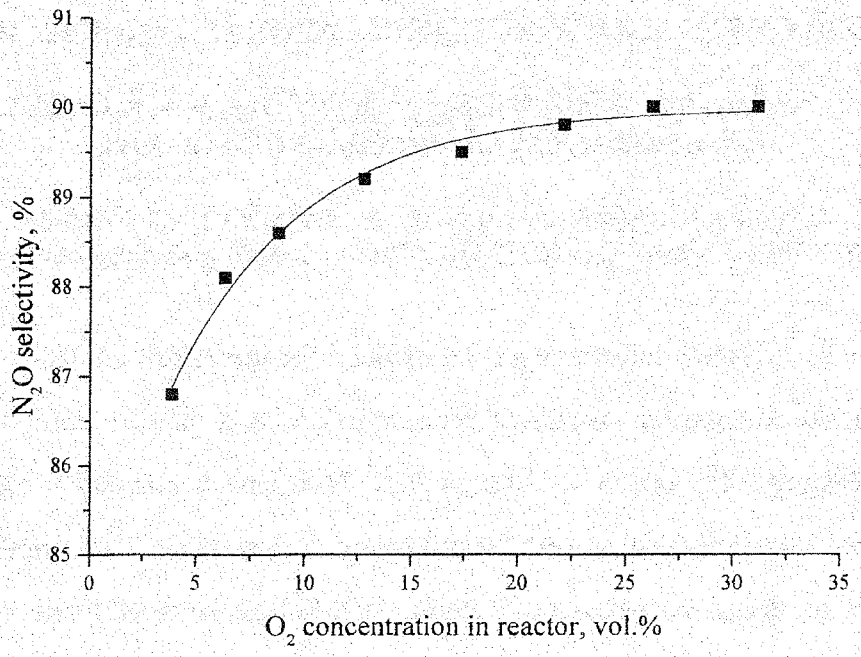

Fig.1. N_2O selectivity versus oxygen concentration at temperature 350°C.

Reactor modelling

A quasi-homogeneous model of heat and mass transfer along the tube radius was developed to find the optimal operating regimes for pilot and industrial reactors. The model used reaction rate constants and activation energies determined from experiments in the lab scale reactors. Special experiments flowing an ammonia-free gas in a reactor were used to correct the heat transfer parameters. The optimal operating regime for the pilot reactor was chosen based on restrictions imposed by the hot spot temperature, pressure drop, and hot spot temperature sensitivity to cooling agent temperature. The modeling allows one to determine optimal pilot reactor dimensions, choose optimal operation regimes, and find optimal catalyst activity and geometry. Additionally, the model provides a guide for the experimental efforts.

Pilot reactor testing

The process was piloted in a single-tube reactor as a model of part of a multi-tubular industrial reactor. The reactor tube was placed in a fluidized sand bed for cooling. The operating conditions are given in Table1.

Table 1.

Pilot Reactor Conditions

Catalyst height	1.8 – 4 m
Gas superficial velocity	2.0 – 3.5 st m/sec
Inlet NH_3 concentration	4 – 5 vol. %
Temperature	250 – 400°C
Average pressure	1.5 – 2.5 atm
Catalyst Load	1.0 – 2.3 liters
Catalyst Particle Diameter	5 – 6 mm

Nitrous oxide selectivity of 87-89% was obtained with almost complete conversion of ammonia.

Comparisons of the temperature profiles measured and calculated using the mathematical model with and without reaction are in good agreement (about 15°C accuracy). Fig.2 shows a comparison of the measured and calculated temperature profiles. The accuracy of the model gives confidence that it can be used successfully for optimizing an industrial multi-tubular reactor.

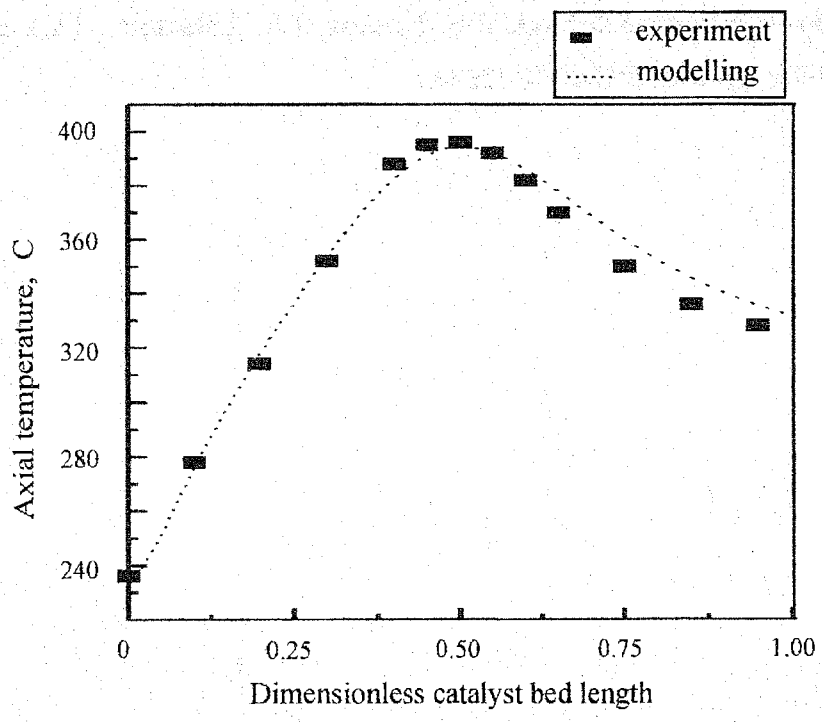

Fig.2. Steady-state axial temperature profile in N_2O synthesis.

Conclusions

The characteristics for industrial reactor with the ring-shaped catalyst were determined on the basis of modeling and pilot testing. The modeling studies showed that an inlet ammonia concentration up to 7-8 % could be used in a tubular reactor packed by a Rashig ring catalyst. In addition, for the conditions considered the hot spot temperature in the reactor does not exceed 400°C (a rise of 160°C above the inlet temperature as compared to the theoretical adiabatic temperature rise of 550- 650°C). An N_2O selectivity of up to 88-90% could be achieved with ammonia conversion 98-99.5% and a catalyst productivity of 3.5-4 ton N_2O/m^3/day. Additionally, the catalyst shows good stability, operating at the above conditions for 700 hours.

References

1. Uriarte A.K., Rodkin M.A., Gross M.J., Kharitonov A.S., Panov G.I. Direct Hydroxylation of Benzene to Phenol by Nitrous Oxide. 3rd World Congress on Oxidation Catalysis, San Diego, USA. R.K. Grasselli, S.T. Oyama, A,M. Gaffney and J.E.Lyons (Editors). Elsivier, 1997, p. 857-864.
2. Panov G.I., Uriarte A.K., Rodkin M.A., Sobolev V.I. Generation of active oxygen species on solid surfaces. Opportunity of novel oxidation technologies over zeolites. Catal. Today, 1998, vol. 41, p.365-385.
3. V.V. Mokrinsii, E.M. Slavinskaya, A.S. Noskov, I.A. Zolotarsky, PCT Int. Appl. WO 9825698 (1998), priority: RU 96-96123343.

NOVEL MEMBRANE MICROREACTOR FOR PROPANE DEHYDROGENATION

L. Kiwi-Minsker, O. Wolfrath, A. Renken

Laboratory of Chemical Reaction Engineering,
Swiss Federal Institute of Technology (EPFL), CH-1015 Lausanne, Switzerland
Phone: +41-21-693 31 82; Fax:+41-21-693 31 82, e-mail: lioubov.kiwi-minsker@epfl.ch

The increasing demand for propene and propene derivatives requires further development of available technologies taking into account the process efficiency, environmental impact and operating simplicity. Production of propene via non-oxidative catalytic dehydrogenation of propane has technological constrains because:

- the reaction is highly endothermic
- the conversion is limited by the thermodynamic equilibrium
- at the reaction temperature required, thermal cracking occurs leading to coke deposition on the catalyst surface and lowering the selectivity.

To burn off the coke, the catalyst is exposed to cyclic operation by alternating propane and oxidative atmosphere. Any development of catalytic propane dehydrogenation technology has to consider:

- the supply of a big amount of heat
- to minimise the bed pressure drop as possible
- to optimise catalyst formulation for working in the temperature range and keeping reasonable operational catalyst lifetime
- to burn off coke from the catalyst without altering its activity/selectivity.

Therefore, reactor development has to be closely integrated with catalyst design. Herein, we report a novel reactor design for non-oxidative dehydrogenation of hydrocarbons. Our reactor concept combines the advantages of membrane reactors (to shift the equilibrium and to lower the working temperature) with optimal fluid dynamics ensuring laminar flow and narrow residence time distribution during periodic operation of the reactor. This specific reactor design calls for a special catalyst structure in the form of long-length fibrous threads.

The catalyst used in this study are filaments consisting of a silica core covered by a γ-alumina layer with 0.5%Pt/1%Sn as active phase[1]. This catalyst shows a good selectivity towards propene in combination with acceptable stability and relatively slow deactivation.

[1] I. B. Yarusov, E. V. Zatolokina, N. V. Shitova, A. S. Belyi, N. M. Ostrovskii, "Propane Dehydrogenation over Pt-Sn Catalysts", 1992, Catalysis Today, **13**: 655-658

Threads of the catalyst were placed parallel in the cylindrical tube reactor. The catalytic bed arranged in this manner with about 300 filaments per cm^2 of tube diameter presented a low pressure drop. Indeed, the size of the filaments leads to a hydraulic diameter of some micrometers, like in a micro-channel reactor, ensuring a laminar flow and a short diffusion time from the gas-phase to the catalyst surface. Therefore, a narrow residence time distribution close to those of an ideal plug-flow reactor is obtained.

The catalyst performance was tested first in a quartz tube plug-flow reactor at the temperature of 823K. The equilibrium conversion (24% under the reaction conditions used) was reached at the beginning of the propane dehydrogenation over fresh catalyst with a propene selectivity of 90%. Other products detected in the effluents were methane, ethane and ethane (Fig. 1).

Coke formation on the catalyst surface decreases its activity and thus, regeneration with oxygen was needed. The regeneration of the catalyst in a flow of N_2 with 5% of O_2 (7.5 Nml/min) took about 160 min.

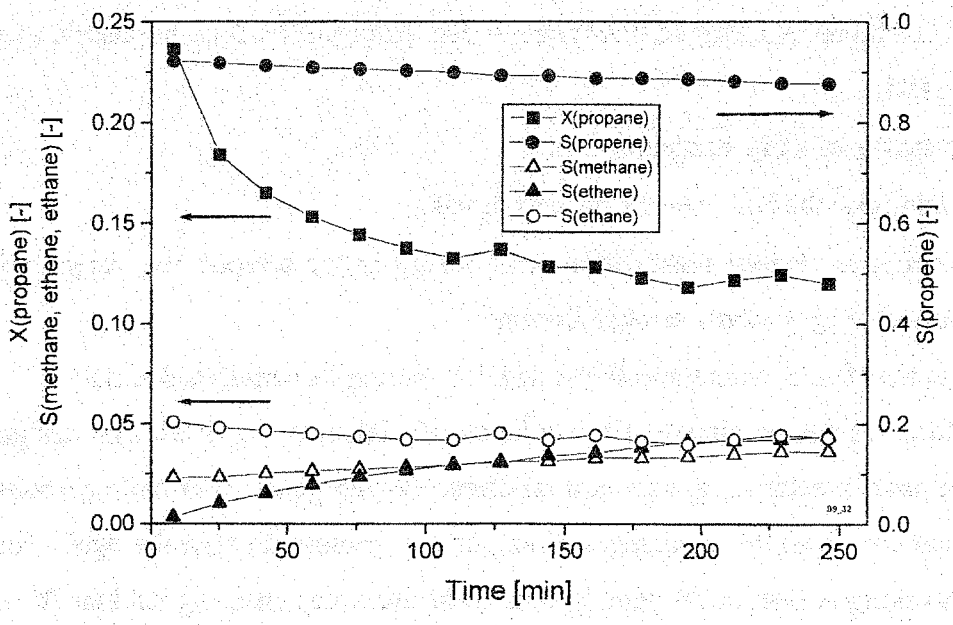

Fig. 1. Product selectivities and propane conversion over 0.5%Pt/1%Sn/ASF, residence time τ=4.9s, 823K, 1.4 bar, inlet 100% propane with flow rate 7.5 Nml/min

Fig. 2 presents the scheme of the membrane reactor used in the second step of this study. On one side of the membrane (zone **I**), the dehydrogenation takes place with simultaneous coke formation on the catalyst surface and diffusion of hydrogen through the membrane wall. On the other side of the membrane (zone **II**), the hydrogen is oxidised by oxygen (5% in N_2),

simultaneously the catalyst is regenerated by oxidising the coke. Oxidation of carbon and hydrogen generates heat along the reaction zone and guarantees a permanent hydrogen concentration gradient and autothermal reactor operation. The flows of propane and oxygen are switched periodically from zone **I** to zone **II,** thus leading to a high average catalytic activity and selectivity.

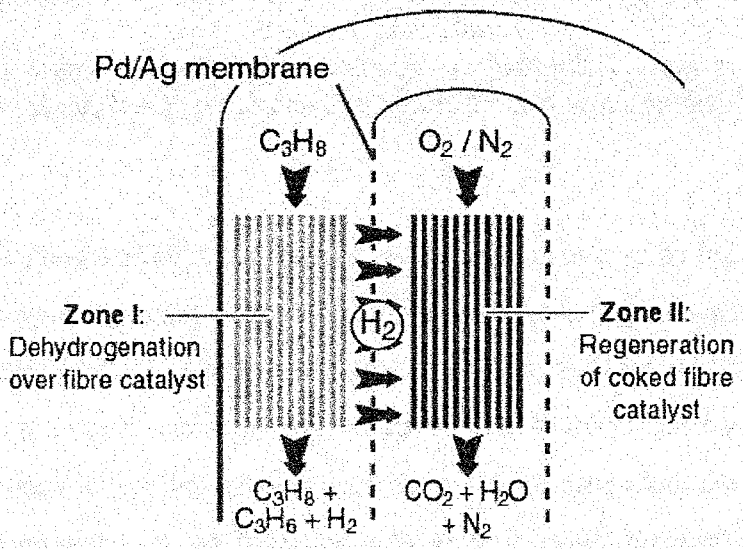

Fig. 2. Schematic presentation of the membrane reactor operation.

Kinetic simulations have shown that with a flow 3 Nml/min of pure propane, a catalytic bed of 15 cm (ε=0.83) and a Pd/Ag tube membrane of ID 6mm and wall thickness 70μm, the conversion of 75% can be reached over fresh catalyst instead of 24% corresponding to the equilibrium value. The conversion can be even more increased by using a longer catalytic bed.

OP-III-3

ISOMERIZATION OF α–PINENE OVER ION-EXCHANGED NATURAL ZEOLITES

Fehime Ozkan*, Oguz Akpolat**, Dmitry Yu. Murzin*, Gonul Gunduz and Nurgun Besun**

Dept. of Chemical Engineering, Ege University, Bornova/Izmir, Turkey
**Laboratory of Industrial Chemistry, Process Chemistry Group, Åbo Akademi University, Turku/Åbo, Finland*
***Dept. of Biology Engineering, Ege University, Bornova/Izmir, Turkey*
****Dept. of Engineering, Izmir Institute of Technology, Çankaya/Izmir, Turkey*

Introduction

The isomerization of α-pinene is generally carried out at reflux temperature over acidic catalysts in the absence of water. Various types of catalysts prepared from titanium dioxide, clays, halloysite, natural zeolites, activated carbons, synthetic zeolites and silica supported rare earth oxide have been reported in the literature for the isomerization of α-pinene [1-7]. It is well known that the difference in acidity of the catalyst used in the reaction influences selectivity in α-pinene isomerization. Over solid acidic catalysts, the main product is camphene which is of particular interest as an intermediate in the synthesis of camphor. Tricyclene is always obtained with camphene as an equilibrium product. The main by-product of the isomerization are p-menthedienes, which are collectively referred to as dipentene in the trade. The most important terpene resins are made from limonene or dipentene. Reactants are presented in Fig.1

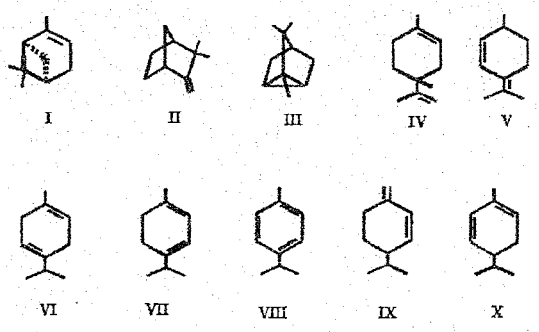

I-α-Pinene, II - Camphene, III. Tricyclene,
IV - Limonene, V- Terpinolene,
VI γ-Terpinene, VII- α-Terpinene,
VIII. p-Cymene, IX.β-Phellanderene,
X. α-Phellanderene

Isomerization of α-pinene over ion-exchanged zeolites is less studied [8]. The objective of the present work is to study the catalytic properties of ion exchanged (NH_4^+, Ba^{2+} and Pb^{2+}) clinoptilolite based natural zeolite tuffs.

Experimental

Prior to ion exchange zeolite tuffs rich in clinoptilolite obtained from Bigadic (Balikesir/Turkey) were reduced into a grain size of ca. 0.5 mm. Zeolite samples of 5 g removed from impurities and dissolved in water were suspended in 100 ml of an aqueous solution of NH_4Cl at different concentrations ranged from 0.25 M to 6 M at 25°C for 24 hours. After filtration, the samples were washed with distilled water until Cl^- free and calcined at 400°C for 4 h.

Pb rich-zeolite was obtained via cation exchange from 0.1M or 0.5M nitrate solutions. 1 g of NH_4^+-zeolite prepared with 0.5 M or 1.5 M NH_4Cl solution was contacted with 20 ml of 0.1 M or 0.5 M $Pb(NO_3)_2$ solution at 25°C for 24 h. Similarly 2 g of zeolite samples removed from impurities dissolved in water were contacted with 50 ml of $BaCl_2$ in different concentration (0.1, 0.5 and 1 M) at 25°C for 7 days. After filtration, the samples were washed with distilled water until Cl^- free and dried in vacuum at 160°C for 24 h.

Additionally different amounts of PbO (1; 5 and 10 % in weight) or BaO (1.3; 3.3 and 10 % in weight in the mixture) were mechanically mixed with natural zeolite in a glass reactor. The mixture prepared was stirred vigorously, the speed of the stirrer was kept constant but the direction of angular velocity was changed periodically to prevent the mixture to be heaped at the surface of the reactor.

Prepared catalysts were tested in the isomerization reaction of α-pinene. Reaction was carried out at atmospheric pressure under nitrogen flow in a glass reactor with a reflux condenser, an efficient stirrer and a temperature controller. 1 g of catalyst and 50 ml of wood terpentine (Ortas, Edremit, Turkey) containing 85 wt % α-pinene were charged in the reactor. The reaction was started by adding the catalyst and all experiments were carried out under isothermal (155 °C) conditions. Samples of the reaction mixture were taken during the course of the reaction and analyzed by GCMS. A kinetic run took three hours.

Surface areas and pore volumes were obtained from the nitrogen adsorption isotherms measured at 77 K in a static volumetric apparatus (Coulter Omnisorp 100cx) up to P/Po~0.95.

Residual solutions obtained during the catalyst preparation were analyzed by atomic absorption spectrometer (Varian 10 plus) to determine % removal of ions in the zeolite catalyst samples. The chemical analysis of the catalyst samples was done by atomic absorption except of gravimetrically analysis of SiO_2 and water.

IR-Spectra of the zeolite catalysts were recorded on KBr wafers (1.2 mg catalyst and 150 mg KBr) with a Shimadzu 470 Instrument at room temperature and atmospheric pressure.

OP-III-3

Pyridine adsorption was carried out to identify the acid centers of the catalysts prepared. X-Ray diffraction studies were done with some catalyst samples.

Results

The main products of α-pinene isomerization on all the ion-exchanged clinoptilolite based catalysts are camphene, tricyclene, limonene, fenchene, terpinolene, p-cymene, α- and γ-terpinene.

Activity of catalyst (e.g. total conversion of α-pinene) increases with increasing concentration of NH_4^+-solution and complete conversion of α-pinene is obtained over the catalysts prepared by ion-exchange with NH_4^+>4M. Although slight increase in conversion to camphene is observed with increasing concentration of ion-exchange solution, the highest conversion to camphene is obtained over the natural zeolite untreated with NH_4^+-solution. A sharp decrease in limonene conversion was obtained with increasing concentration of ion-exchange solution, so that the amount of limonene in the reaction mixture after a reaction duration of 3 h was much less than that in the initial mixture, probably due to the secondary reactions of limonene. In lead exchanged zeolites, although a drastic decrease in limonene amount is observed in the reaction mixture after 3 h, the results obtained are not consistent and comparable with each other. Mixing of PbO with natural zeolite mechanically causes a large decrease in catalytic activity, an important decrease in camphene conversion, but less decrease in conversion to limonene compared to those obtained over natural zeolite. For zeolites containing Ba the increase in limonene amount with $BaCl_2$ concentration increase was found, due to the increase in the acidity.

In the present study, α-pinene consumption kinetics was investigated over the zeolites exchanged with NH_4^+. A first order dependency was observed. Reaction rate constant was found to be 1.2885 h^{-1} with a correlation coefficient of R^2=0.86.

The IR spectrum for the H-rich zeolites showed ammonium deformation band at 1400 cm^{-1} after thermal treatment at 400 °C for 4 h. Nitrogen adsorption isotherms for original and modified natural zeolites are classified to be type 2 according to Brunauer. The maximum amounts of nitrogen adsorbed on all modified zeolites at maximum relative pressure P/P_0=0,9 are clearly lower than that on original zeolite with an exception of Pb rich-zeolite. Nitrogen adsorption data were evaluated and monolayer surface area and half width of zeolites were calculated by using Langmuir and D-A methods, respectively. Ba, H and Pb rich zeolites have lower monolayer surface areas and pore size diameters than that of original zeolite.

Acidic OH groups were identified with IR spectroscopy via the wave number of the OH stretching band. In this study, pyridine was used as proton acceptor. The density of the sites was evaluated by the intensity (absorbance) of the respective bands. It was observed in accordance with literature data that camphene and bicyclic products are formed on the Lewis sites while monocyclic products such as limonene are formed on the framework Bronsted. As the acidity of the catalyst decreases, limonene formed by isomerization also decreased in contrast to the increase of camphene amount with decreasing acidity. But, in general, it can be said that limonene production is more affected by the change of acidity of the catalyst prepared with respect to camphene production on the same catalysts.

Conclusions

Activity of catalyst in α-pinene isomerization accompanied with a sharp decrease in limonene conversion was observed with increasing concentration of NH_4^+-solution in the preparation of ion exchanged natural zeolites. The acidity studies indicated, that the Bronsted acidity decreases with NH_4Cl concentration, whereas the Lewis acidity is not affected. This observations together with catalytic data suggest that camphene and bicyclic products are formed on the Lewis sites, monocyclic products such as limonene are formed on the framework Bronsted sites.

Acknowledgements

Funding for this work from TUBITAK (Turkish Scientific Research Council) through Grant MISAG-120 and from EBILTEM (Ege University Research Fund) through Grant 98Muh018 is gratefully acknowledged.

References

1. Popov, A.A., and V.A. Vyrodov, Lesokhim Prom-St. 6, 18 (1979).
2. Findik, S., JAOCS, 74 (9), 1145 (1997).
3. Allahverdiev, A., G. Gunduz and D.Yu. Murzin, Ind. Eng. Chem. Res., 37, 2373 (1998).
4. Allahverdiev, A., N.A. Sokolava, G. Gunduz, and N.V. Kul'kova, Russ. J. Phys. Chem. 72, 1647 (1998).
5. Severino, A., A. Esculcas, J. Rocha, J. Vital, and L.S. Lobo, Appl. Catal.A.Gen., 142, 255 (1996).
6. Yamamoto T., Matsuyama T., Tanaka T., Funabaki T., Yoshida S., Phys. Chem. Chem. Phys., 1, 2841 (1999).
7. AllahverdievA.I., S., Irandoust, D.Yu. Murzin, J. Catal., 185, 352 (1999).
8. Stefanis, A.D., Perez, G. and Tomlinson, A.A.G., Appl. Catal.A.Gen., 132, 353 (1995).

OP-III-4

METAL OXIDES ON WIRE GRIDS AS EFFECTIVE STRUCTURED COMBUSTION CATALYSTS

I. Yuranov, N. Dunand, L. Kiwi-Minsker, A. Renken

Laboratory of Chemical Reaction Engineering , Swiss Federal Institute of Technology
CH-1015 Lausanne, Switzerland
Phone: +41-21-693 31 82; fax +41-21-693 31 90, e-mail: igor.iouranov@epfl.ch

Catalytic combustion, an alternative to conventional flame combustion, has received considerable attention during the last decades [1]. The incinerators based on catalytic combustion typically operate at temperatures below 400°C and at GHSV from 1,000 to 100,000 h^{-1}. Therefore, highly active catalysts are desirable leading to complete oxidation within short residence times with the pressure drop in converters as low as possible.

The catalysts used for combustion are mainly noble metals or transition metal (Cu, Co, Cr, Fe, etc.) oxides supported on pellets, honeycomb monoliths, fiber pads and sintered metals. Catalytic fixed-bed reactors are know to have some drawbacks like high pressure drop in the bed, flow maldistribution and susceptibility to fouling by dust. The incinerators based on structured catalytic beds are considered as a most suitable alternative to the former ones [2]. At present a variety of ceramic and metal monoliths are used for this purpose. The catalytic efficiency of these catalysts is improved compared to conventional pellet catalysts since pore diffusion limitation during combustion is smaller due to shell-like design of active outer layer. The main drawbacks of ceramic monoliths in use are their high weight to volume ratio, rather high manufacturing cost and their susceptibility to thermal and mechanical stress.

The catalytic materials made from metal wire grids can be efficiently used for structured catalytic beds as an alternative to metal monoliths. Similar to metal monoliths, the specific surface of the grids has to be increased to get effective catalysts. Usually metals are covered by oxide washcoat. The main problem of these composite materials is poor adhesion between metal and ceramic oxide layer leading to flaking off ceramics, especially under vibration.

In the present work a novel metal–metal oxide composite catalysts for the combustion have been proposed. High porous oxide outer layer on metal grids was prepared by Raney-type coating technique [3]. Nickel and copper grids were used as starting support materials. After the preparation of the skeletal outer layer, the support was oxidized, resulting in high porous oxide layer strongly bounded to the surface. Metal oxide catalysts were obtained by impregnation of outer porous layer with different metal salts followed by calcination in air.

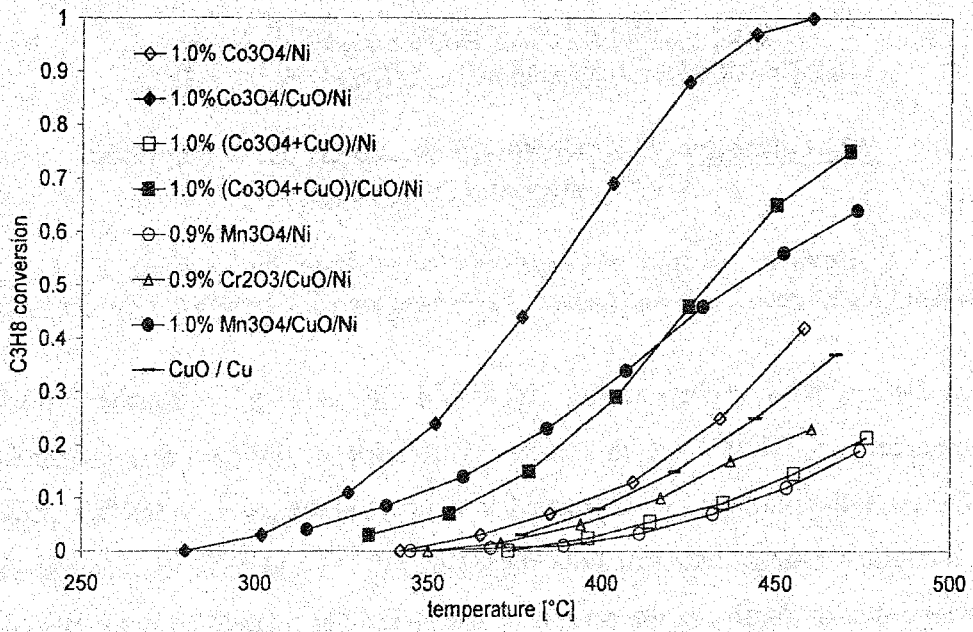

Figure. Temperature dependence of C_3H_8 conversion over metal oxides supported on metal grids (GHSV=20'000 h^{-1} (STP), C_{O2}=10 vol.%, C_{C3H8}=0.5 vol.%).

The catalysts were tested in the propane total oxidation (see Figure). Cobalt oxide based catalysts were observed to be the most active. The influence of chemical composition of active phase and the catalyst pre-treatment on its activity and long-term stability was studied. Kinetics of C_3H_8 oxidation was investigated and the kinetic parameters were determined. All catalysts were characterized by SEM, XRD, ESCA and BET methods.

[1] R. E. Hayes and S. T. Kolaczkowski, "*Introduction to Catalytic Combustion*", Gordon & Breach Sci. Publ., Amsterdam, 1997.

[2] *"Structured catalysts and reactors"*, ed. by A. Cybulski, J. Moulijn, Chemical Industry, v. 71, 1998.

[3] B. Zong, M. Muhler, G. Ertl, in *"Studies in Surface Science and Catalysis"*, ed. by B. Delmon and J.T. Yates., Elsevier, Vol.118, 1998, p.331-340.

OP-III-5

CATALYTIC HEATING ELEMENT FOR AUTONOMOUS DOMESTIC HEATING SYSTEMS

B.N. Lukyanov, V.A. Kirillov, N.A. Kuzin, M.M. Danilova, A.V. Kulikov and A.B. Shigarov

Boreskov Institute of Catalysis, Prosp. Akad. Lavrentieva, 5
630090 Novosibirsk, Russia E-mail: lukjanov@catalysis.nsk.su; Fax: 34 11 87

Combustion of hydrocarbon fuels (both liquid and gaseous) is routinely performed in flame burners at 1100-1700°C which results in formation of nitrogen and carbon oxides. By contrast, the catalytic combustion, performed at lower temperatures (to 900°C), provides efficient conversion of energy and low concentrations of CO and NO_x in waste gases. At the Boreskov Institute of Catalysis, the design of catalytic heat generating elements (CHGE) of different generated heat is in progress. Such elements provide surface combustion of natural gas (methane) during one stage to yield heat for heat carriers which are used in autonomous domestic heating systems.

Design of the efficient CHGE of heat output ranging from 3 to 30 kWt upwards involves two steps. At the first step, the below problems were to be solved: development of the method for preparing the reinforced catalysts both with additions of supported platinum group metals and based on the oxides systems, development of the regimes for thermal treatment and sintering of the catalytically active layer, study of thermal stability, activity, operation life, and safety of the catalysts. The main problems to be solved at the second step are as follows: design and improvement of CHGE, their components, provision of homogeneous distribution of the gas-air mixture in the catalyst bed, determination of the optimal consumption characteristics of CHGE and the range of generated power variations, and choice of a startup of CHGE.

Method for Catalyst Preparation

Pd and Pt based systems and Mn_2O_3+Cr_2O_3/Al_2O_3 (or Ti-Al-Si) were used as an active component of the catalyst. The compositions of the support and catalyst are as follows:

65-70 wt.% Ni (or Ti) + 35-25 wt.% Al + 5 wt.% (1 wt.% Pd or Pt/Al_2O_3)

61 wt.% Ti + 30 wt.% Al + 0.1 wt.% Pd + 8.8 wt.% Mn_2O_3.

Both the catalyst and support are deposited on the stainless steel net (net cell 0.4 x 0.4 mm, wire diameter 0.25 mm). Dispersion of the supported platinum (palladium) does not decrease if the regime of sintering of the reinforced catalyst is observed. The formed catalyst

layer possesses high mechanical strength and is strongly bound to the metal net. According to bench tests, the catalyst preserves its activity for 1500 hours.

Design of the Catalytic Heat Generating Element

A design of CHGE depends on the required boiler capacity and geometry of the boiler furnace volume. The element is designed as a cylinder, consisting of a tubular heat exchanger built as a ring which contains a gas-distributing tube for feeding the gas-air mixture (Fig. 1).

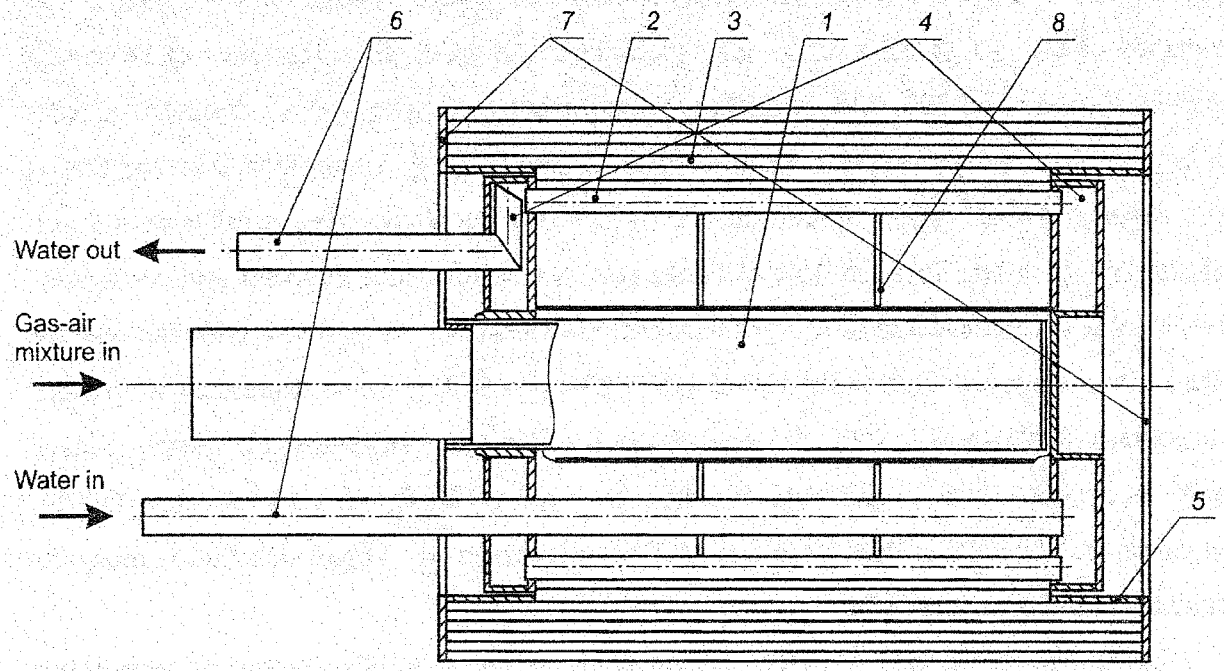

Fig. 1. General view of CHGE: 1- GDT, 2 – connecting tube of the inner water-cooled heat exchanger, 3 – catalytic plate, 4 – water collector, 5- end-face ring, 6 – inlet and outlet water tubes, 7 – flange, 8 – stiffening rib

The surface of the tube is corrugated and one side of it is plugged. By choosing the number and diameter of corrugation holes, the gas mixture is uniformly distributed along the tube length and flows from the holes into the intertubular area. The catalyst, formed of flat and corrugated plates, is wound on the tubes of the heat exchanger and cylinder surfaces and sintered with them. The plates are arranged so that the odd rows are corrugated and the even rows consist of flat plates. The plates form the catalytically active channels in which the gas-air mixture is oxidized on the walls to yield water and carbon dioxide. The oxidation products are removed through the channels into the surroundings. By choosing the thickness of the catalytically active layer, one can obtain the conditions providing no CO and NO_x in waste gases. The reaction heat is partly removed from the catalyst layer to the environments, including IR

radiation. Some part of heat is transferred to water circulating in the heat-exchanging tubes. The heat-exchanger tubes and headers built a circular cylinder-type system supplied with cold water meant for heating.

At the Institute of Catalysis, the catalytic heating elements of 0.75, 3-5, 10, 20-30 kWt power have been designed.

Testing of CHGE

The gas distributing tube, corrugated along the length with a particular pitch, is an important part of CHGE. The number and diameter of holes, and corrugation pitch control distribution of the gas-air mixture. In our experiments, the gas-distributing tubes of 18 and 28 mm in diameter and 300, 400, and 500 mm long were used. The optimal diameter of holes (1.5 mm) and corrugation pitch were determined. The value of nonuniform consumption of gas depends on the ratio between the area of all holes and the cross section of the gas-distributing tube and does not depend on the rate of gas flow, tube diameter and corrugation length. We have elucidated how a gas distributor, a catalyst layer, and the oxidation reaction affect on the pressure drop in the CHGE of 25 kWt power. For the total pressure drop under operation conditions of CHGE, the contributions of the gas-distributing tube, catalyst layer, and reaction are 70, 20, and 10% respectively. We have designed a CHGE providing the pressure drop not higher than 60 mm H_2O if the inhomogeneity of gas distribution along the surface is not higher than 8%.

Thermalphysic testing of CHGE permitted us to determine distribution of temperature along the length and thickness of the catalyst layer, heat conductivity of the layer, and coefficients of heat exchange. The catalyst can be irreversibly deactivated because of the local overheatings observed inside the catalyst bed. The water-cooled heat exchanger of CHGE, the outer layer surface, and waste gases release respectively 31-53, 32-39, and 12-36% of the total generated power. The catalytic elements exhibit stable operation over the entire range of the heat flux density 70-130 kWt/m^2 (estimated operation regime of CHGE).

On combustion of the mains natural gas, the concentration of CO is 5-10 ppm, methane 10-20 ppm, and NO_x – traces in waste gases.

According to the long-term tests (more than 1500 h), the catalyst operation is stable.

The versions of CHGE of 20-30 kWt power, used in floor and wall-type domestic heating boilers, are very profitable and ecologically compatible.

THE Pt,Pd-CONTAINING CATALYSTS ON A BASE OF FIBER GLASS WOVEN SUPPORTS - A NEW ALTERNATIVE FOR TRADITIONAL V-CATALYSTS IN SO_2-OXIDIZING PROCESS

B. Balzhinimaev, L. Simonova, V. Barelko*, A. Toktarev, V. Chumachenko**

Institute of Catalysis SB RAS, Novosibirsk, Russia
**Institute of Problems of Chemical Physics RAS, Chernogolovka, Russia*
***JSC "Catalyst Company", Novosibirsk, Russia*

It was investigated the fiber glass woven catalysts doped by Pt and Pd (0.003-0.5%) in reaction of SO_2-oxidizing. As a support material it was used two types of glasses: silica glass fiber matrix and borum-silicate one with value of SSA 1-150 m^2/g. It was shown that Pt(Pd) accepted by glass matrix have essentially more high activity than the metals on surface of the glass. Technological estimation of the fiber glass woven catalytic materials showed that the systems have serious advantages in comparison with traditional granulated V-catalysts especially for high temperature processes:

- high activity (decreasing of process temperatures by 40-50 °C and decreasing of SO_2-content in tail gases);
- advanced reactor design (decreasing of the catalyst loading on a reactor shelf by 1-1.5 order);
- high thermoresistance up to 700-750 °C.

OP-III-7

GAS-PHASE FLUORINATION OF FLUOROETHANS WITH ELEMENTAL FLUORINE IN A GAS PREMIX BURNER REACTOR

D.S. Pashkevich, D.A. Muhortov, Yu.I. Alekseev

RSC "Applied Chemistry", St.-Peterburg, Russia

At present there is a strong trend towards growth of fluorocarbons and hydrofluorocarbons, particularly fluoroethanes, consumption in diversified industrial sectors. This is due first of all to the necessity of ozone-depleting chlorinated substances phaseout required by the Montreal protocol.

Fluoroethanes have found numerous applications in industry as refrigerants, propellants, fire-extinguishants, dielectric media, and reagents for plasmochemical processing in manufacture of super-large integral circuits, etc.

Currently available industrial methods for fluoroethanes production make use of organochloric raw materials that must be phased out. On the other hand, the world capacity for fluorine production totals over dozen thousand tons per year. This is why the idea to develop a technology for fluoroethanes production via fluorination of fluoroethanes-predecessors with elemental fluorine became one of the central problems in chemical industry.

By now the methods of organofluoric substances manufacture with the help of elemental fluorine were not widely used in chemical technology. This was due to high chemical activity of fluorine and also to considerable heat release in the process. However, if studied from methodological point of view, in terms of the combustion theory, the process of gas-phase fluorination may become applicable in industry.

We have developed a no-waste technology intended for full-scale manufacture of fluoroethanes through gas-phase fluorination of 1,1-difluoroethane and 1,1,1,2-tetrafluoroethane, both being now produced in industry.

The kinetic dependencies of fluoroethanes gas-phase fluorination with elemental fluorine were investigated using 1,1,1,2-tetrafluoroethane as an example, and the reaction was shown to be a degenerate branch chain process, its activation energy being 50 kJ/mole. Our computations proved that having in mind the activation energy there would be no point in using any reactor operated at stationary heating regime, because the length of the reactor would be technically unthinkable (more than thousand meters).

From our studies on interactions between fluoroethanes and fluorine within a self-propagating heat wave it may be deduced that if the concentration of fluorine is below 30 %

by volume then destruction of fluoroethane carbon skeleton does not occur. The process selectivity for fluorination of a molecule-precursor containing N fluorines reaches 90% for the product containing (N+1) fluorines.

Our study resulted in development of a new gas premix burner reactor. The reactor may be easily scaled, and flow rate may be increased without any changes in the reactor design. The reactor is very easy in manufacture and operation, and the required construction materials are not expensive.

Both the proposed synthesis method and the reactor have successfully undergone tests at our pilot plant.

OP-III-8

MOVEMENT OF FINELY DISPERSED HEAT CARRIER THROUGH THE FIXED CATALYST BED

L.V. Barysheva, E.S. Borisova, V.M. Khanaev

Boreskov Institute of Catalysis, Novosibirsk, Russia

In the present paper we give experimental results and modeling data related to the disperse phase filtering through the catalyst bed.

The fine particles used as heat carrier in the fixed bed catalytic reactor is of interest for performing chemical processes with large endo- and exo-effects. In the case of endothermic reactions dispersed phase heats the catalyst and gaseous reaction mixture to required temperature and provides additional heat supply to reaction zone thus decreasing the energy capacity of the process. In order to estimate the efficiency of heat supply by the disperse phase, one must know the uniformity of particle distribution over the bed, their residence time beside the coefficients of heat and mass exchange between the fine particle and the bed.

When studying disperse phase filtering through the fixed particulate catalyst bed we used various experimental methods 1) bed permeability method, 2) residence time method 3) NMR-tomography. Thus we determined main parameters affecting the residence of particles in the bed.

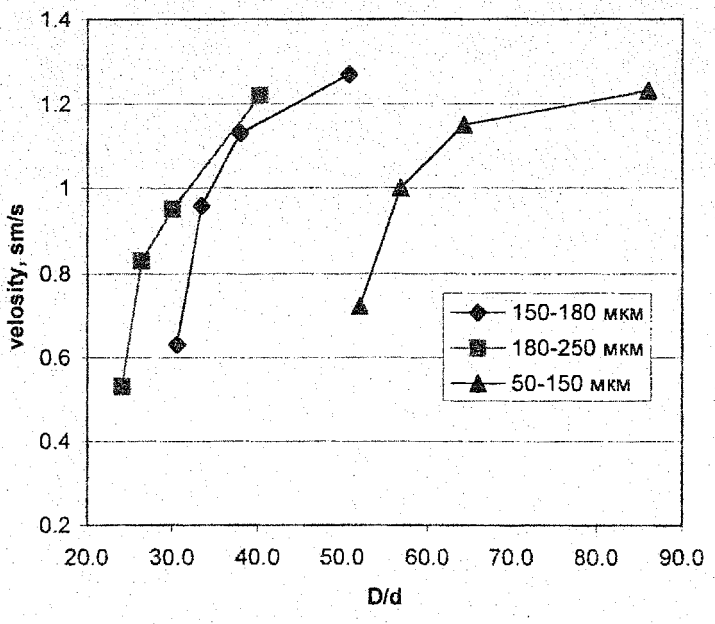

Fig. 1. Disperse phase poring rate versus the size ratio of packing and particulate phase

Figure 1 shows data obtained with the bed permeability method. Alpha-alumina served as finely disperse phase, fixed bed particles size and material was varied.

In order to "observe" the filtered phase with tomography it is necessary to saturate this phase with a proton containing liquid. Experimental adjusted concentration of this liquid on one hand allowed a high enough method sensitivity and on the other hand had no effect on the hydrodynamic parameters of filtering. The radial distribution of fines in a fixed bed detected by ^{1}H NMR microimaging technique.

When modeling we have used the following assumptions: 1) fine particles move in the space between spherical fixed particles, 2) fine particles do not interact with each other, 3) their movement is determined by such parameters as gravity, aerodynamic resistance, inelastic collision with the spheres.

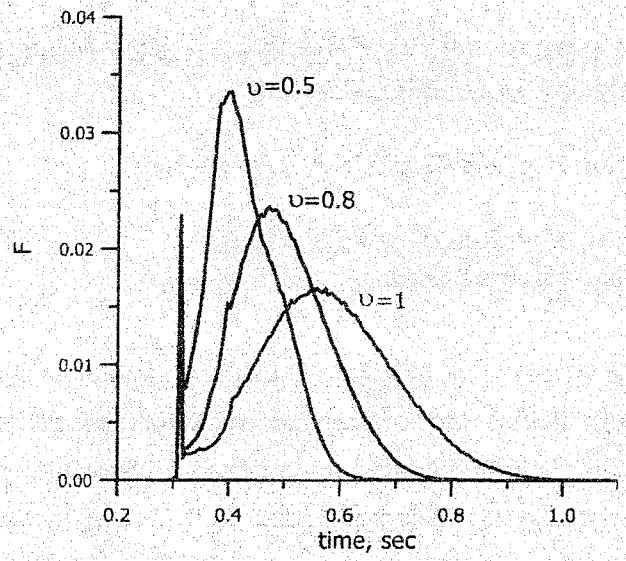

Fig. 2. Collision coefficient effect on the residence time at elastic collision

Figure 2 shows how the relative number of particles at the bed outlet depends on the time of their residence in the bed. $\nu=V_+/V_-$ - is the coefficient of small particle impact against the grain, V_-, V_+ - is the normal constituent of velocity before and after collision respectively.

Using the Lagrangian approach we have built a mathematical model, which describes particle movement through particular bed considering collisions and particle sliding over the catalyst grain and reactor walls. A numerical algorithm has been designed for calculating statistical values characterizing this process such as particle residence time distribution and average particles distribution along the apparatus radius. Despite the fact that calculation of each particle trajectory is not stable by initial data, main parameters calculated for the disperse flow are statistically stable.

According to modeling results one may divide the filtered flow into the central flow and adjacent to walls flow, which differ by the residence time and rate. Figure 3 shows the distribution of relative particles flow along the radius at various heights. Curve 1 corresponds to inlet distribution, while curve 6 shows the outlet distribution.

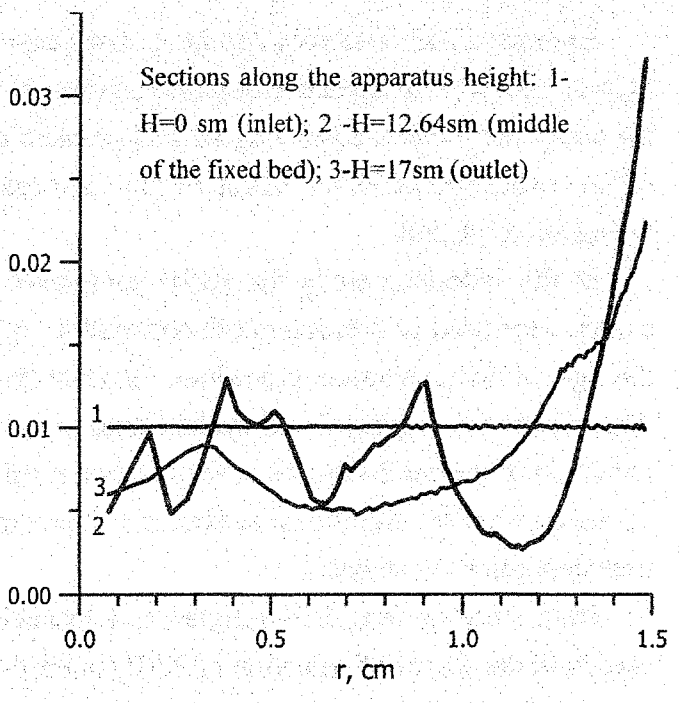

Fig. 3. Distribution of relative particles flow along the apparatus radius

Conclusions

1. Determined are main parameters affecting particles residence time in the bed. Bed porosity, disperse particles size, packing size and disperse phase pouring rate essentially influence the hydrodynamics. Disperse phase density and gas flow rate appear to impose a less effect on the particles movement.
2. Model analysis regarding parameters we obtained the one of essential importance, which is impact coefficient at particles collisions with the grains of catalyst and with reactor walls.

OP-III-9

NOVEL CATALYTIC SYSTEMS FOR PRODUCING ALKOHOLS AND KETONES *VIA* O_2/H_2 OXIDATION OF HYDROCARBONS

N.I. Kuznetsova, L.I. Kuznetsova, N.V. Kirillova, V.A. Likholobov

Boreskov Institute of Catalysis, Novosibirsk, 630090, Russia,
E-mail: kuznina@catalysis.nsk.su.

Conversion of hydrocarbons to oxygenated products proceeded under the action of hydrogen peroxide or other peroxy compounds in the presence of transition metal compounds as catalysts. Owing to the peroxide decomposition, the processes are, in general, characterized by low selectivity relatively to the peroxide compound. "Monooxygenase-like" catalysts are capable of oxidating hydrocarbons with dioxygen in the presence of a suitable reducing agent [1], the preferable one is hydrogen. The appropriate catalytic systems have been described for hydroxylation of aromatics [2-3], oxygenation of methane [4] and other hydrocarbons [5-6], and the knowledge in this field have been permanently growing because of great commercial interest to this problem.

In the present study oxygenation of cyclohexane, saturated and aromatic hydrocarbons with O_2/H_2 gases was carried out in the catalytic systems based on Pd or Pt and heteropoly compounds

Homogeneous version of this kind of systems included Pd(II) complexes with $PW_{11}O_{39}^{7-}$ anions. Reaction proceeded in 2-phase mixture of substrate benzene and aqueous solution of the complexes. When contacting with H_2-containing gas, Pd(II) was reduced, but kept in solution owing to stabilizing effect of anions surrounding. Oxidation of benzene resulted in formation of phenol.

In the following study the Pd(II) complexes with $PW_{11}O_{39}^{7-}$ and $PW_9O_{34}^{9-}$ heteropoly anions were used as precursors of supported samples. When the complexes were kept spared throughout the preparation procedure, the resulting silica supported samples catalyzed oxidation of benzene to phenol and cyclohexane to cyclohexanol and cyclohexanone. Progressive reduction of the solid samples in the reaction medium was accompanied by increasing rate of oxidation reaction. Additional activation of these samples arose from very mild reductive pretreatment prior to catalysis.

Both systems thus demonstrated that formation of the active in catalysis species proceeded in the course of reduction of Pd(II) in Pd-P-W-oxides.

Analogous systems were composed of Pt metal catalyst and heteropoly acid solution in organic medium. Catalytic activity in hydrocarbons oxidation was developed as a result of heteropoly anions adsorption on the Pt surface.

The action of a number of heteropoly acids (HPA) in cyclohexane oxidation was tested (Table 1).

Table 1.

Results of oxidation of cyclohexane on the 1%Pt/SiO_2 catalyst (50 mg) suspended in HPA solution (6 mg) in CH_3CN: C_6H_{12}:CH_3CN = 0.1:1.0 ml, O_2:H_2 = 1:2, 35°C, 1 hour.

HPA	Products, μmol		O_2/H_2 consumed, μmol
	Cyclohexanol	Cyclohexanone	
$H_3PMo_{12}O_{40}$	25,2	1,1	2860
$H_6P_2Mo_{18}O_{62}$	26,7	3,2	1520
$H_3PMo_6W_6O_{40}$	6,5	0,6	1740
$H_3PW_{12}O_{40}$	3,8	0,7	2050
$H_5PW_{11}Ti^{IV}O_{40}$	4,1	6,7	1120
$H_5PW_{11}Zr^{IV}O_{40}$	13,9	5,8	315
$H_4PW_{11}V^{V}O_{40}$	11,9	1,2	1295
α-1,2,3-$H_6PW_9V_3O_{40}$	19,8	1,6	940
$H_5PMo_{10}V_2O_{40}$	74,4	3,5	1830
$H_4PMo_{11}VO_{40}$	55,7	2,1	1695
$H_6PMo_9V_3O_{40}$	6,5	-	1295

Maximum yield of oxygenated products was obtained in the presence of P-Mo and P-Mo-V heteropoly acids which known as catalysts of radical-type oxidation with hydrogen peroxide.

The active species of identical composition were created in solid samples which represented (1) Al_2O_3 impregnated with Pt(IV) chloride and $H_3PMo_{12}O_{40}$ acid, and (2) a complex salt of Pt(II) with P-Mo heteropoly anions of composition$\{Pt(NH_3)_4(H_2[PMo_{12}O_{40}])_2\}$ $7H_2O$. Both materials were carefully calcined and treated with H_2, that resulted in reducing Pt(II) to Pt(0) and minor transformation of heteropoly anions. Results of the catalytic tests shown in Fig.1 exhibited advantage of the solid samples in comparison with the composition of the solid Pt-containing catalyst with dissolved HPA.

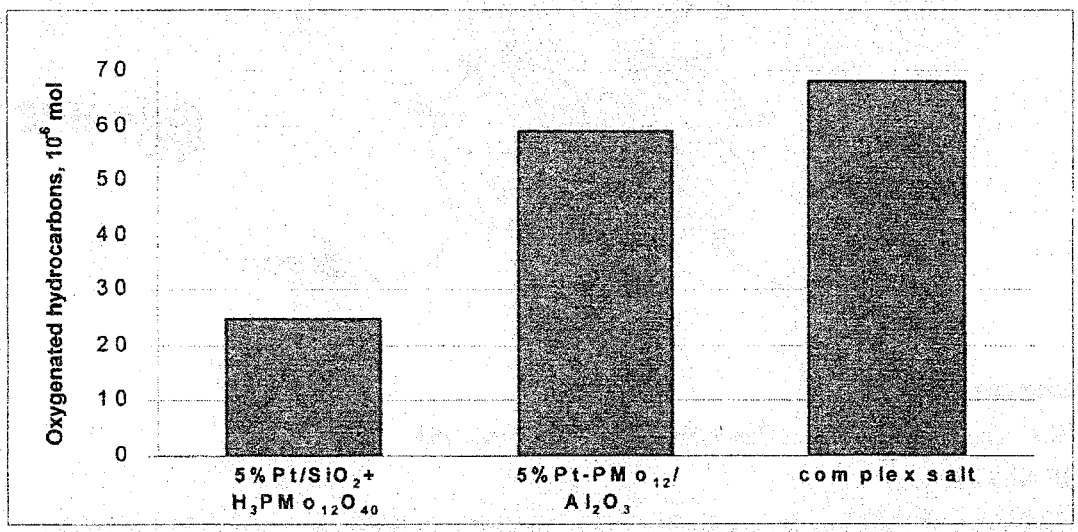

Fig.1. Comparative activity of the catalytic systems: (1) 5%Pt/SiO_2 (10 mg) + $H_3PMo_{12}O_{40}$ (6 mg); (2) 5%Pt-20%PMo_{12}/Al_2O_3 (10mg); (3) complex salt $\{Pt(NH_3)_4(H_2[PMo_{12}O_{40}])_2\}$ $7H_2O$ calcined and reduced (10 mg). C_6H_{12}:CH_3CN = 0.1:1.0 ml, O_2:H_2 = 1:2, 35°C, 1 hour.

OP-III-9

Optimal conditions of the process were determined by variation of solvents, temperature, catalyst to substrate ratio, composition of gas. Comparative activity of different hydrocarbon substrate was demonstrated by the yields of hydrogenated products (Fig.2), which were iso-alkohols and ketones in the case of saturated hydrocarbons and phenols in the case of aromatics.

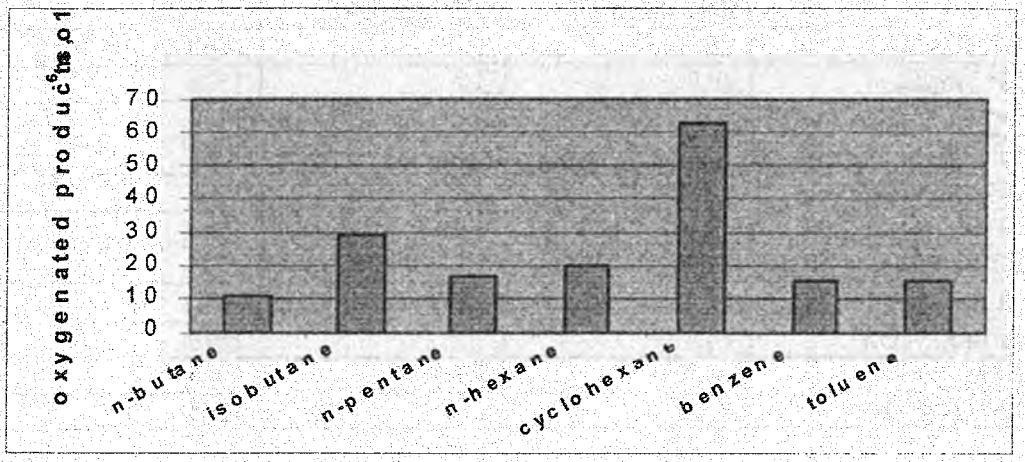

Fig.2. The yield of oxygenated products. Conditions: 10mg of $Pt(NH_3)_4(H_2[PMo_{12}O_{40}])_2\}$ $7H_2O$ calcined and reduced, hydrocarbon:CH_3CN = 0.1:1.0 ml, O_2:H_2: C_4H_{10} = 0.5:0.5:1 for butane and O_2:H_2 = 1:2 for other hydrocarbons, 35°C, 1 hour.

The redox processes in the system under study are schematically described below.

Specifically organized Pt and Pd species are capable to produce hydrogen peroxide or other peroxide compounds. Oxygen transfer to the hydrocarbon substrate is assisted by heteropoly compound.

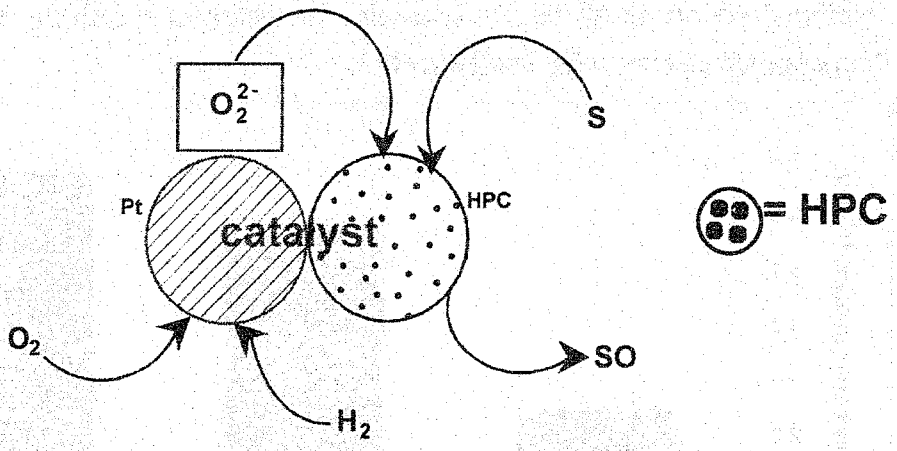

References

1. M.G.Clerici, P.Ingallina, Catalysis Today 41 (1998) 351.
2. JP No5-4935.
3. T.Miyake, M.Hamada, Y.Sasaki, M.Oguri, Applied Catalysis A: General 131 (195) 33.
4. Y.Wang, K.Otsuka, J. Chem. Soc., Chem. Commun. (1994) 2209.
5. S.-B.Kim, K.-W.Jun, K.-W.Lee, Chem. Lett. (1995) 535.
6. Y.A.Kalvachev, T.Hayashi, S.Tsubota, M.Haruta, J. Catal. 186 (1999) 228.

MODELING OF PRODUCTION OF FILAMENTOUS CARBON FROM METHANE ON THE IKU-59-1 CATALYST IN VARIOUS-TYPE ISOTHERMAL REACTORS

Sergei G. Zavarukhin and Gennadii G. Kuvshinov

Boreskov Institute of Catalysis, Pr. Akad. Lavrentieva, 5, 630090 Novosibirsk, Russia

Production of filamentous carbon from gas hydrocarbons is a very promising way for processing of gases, such as methane, natural gas, casing head gases etc. into valuable carbon materials [1].

Development of the process is directed towards the creation of catalysts, study of the mechanism and kinetics of the process, design of reactors, optimization of the operation regime of reactors, and mathematical modeling. The catalysts providing the synthesis of filamentous carbon as mesoporous granules, 3-5 mm in diameter and the concentration of carbon being to 99.7 %, are described elsewhere [2-7]. The reactors are described in [8-10]. The granular filamentous carbon was produced in the laboratory [1-9] and pilot reactors [1,10] (3 kg of carbon per one operation cycle). The kinetic features of production of filamentary carbon from a mixture of methane and hydrogen in the presence of the IKU-59-1 catalyst (Ni 88 mass.% [4]) were studied at the below parameters: concentration of hydrogen 0 – 40 %, temperature 490 –590 °C and pressure of the gas mixture was atmospheric [11,12]. The experimental results were generalized to a mathematical model describing the kinetics of formation of filamentous carbon from a methane-hydrogen mixture with a regard for deactivation of the catalyst [13]. The model regards the possibility of the catalyst deactivation during the finite time and the fact that the amount of the formed carbon and the time of catalyst deactivation increase as temperature decreases and the concentration of hydrogen in the gas mixture increases.

Because the opportunity of commercialization of the filamentous carbon production is in sight, the key problem is to develop methods for calculating the process performed in different reactors. Mathematical modeling permits one to calculate properties of the process and to design the optimal reactor and operation conditions. When the process involves a periodic loading of the catalyst and is performed up to the complete deactivation of the catalyst, one may calculate the amount of the produced carbon and time of the catalyst deactivation versus temperature, composition and consumption of the initial gas mixture. To simulate the process performance in the existing [8-10] and candidate reactors, it seems interesting to consider the below model reactors:

(1) a reactor with a perfectly stirring of catalyst particles and gas (model 1);

(2) a reactor with a perfectly stirring of catalyst particles and a gas plug flow (model 2);

(3) a reactor with a steady-state catalyst layer and a gas plug flow (model 3);

(4) a reactor with a perfectly stirring of catalyst particles, a gas plug flow, and a gas flow recirculation (model 4);

(5) a two-phase reactor with a perfectly stirring in the dense phase and a plug flow in the bubble phase (model 5).

Model 1 permits one to describe processes performed in the laboratory kinetic set-ups with a fluidized catalyst bed which are used to study kinetics of processes and to certify catalysts [5,11,12]. Figure 1 shows the calculated specific yield of carbon c_m (per 1 g catalyst) versus temperature T [14] and the experimental data (dots) [11]. The process was performed at the below conditions: constant composition of the gas medium and pure methane (lower line) and the concentration of hydrogen was 15 % in the methane-hydrogen mixture (the upper line). For pure methane, T = 823 K and c_m = 48 kg/kg. Figure 2 shows the calculated degree of methane conversion x versus time t [14] and the experimental data (dots) obtained [5] at the following conditions: Q = 120 m^3/(kg·h), T = 823 K, methane being pure. The difference between the calculated and experimental c_m (165 and 145 kg/kg, respectively) is less than 15 %.The calculated and experimental time of complete catalyst deactivation are 18 and 16 h, respectively. The calculated and experimental average degrees of methane conversion x are 0.141 and 0.143, respectively.

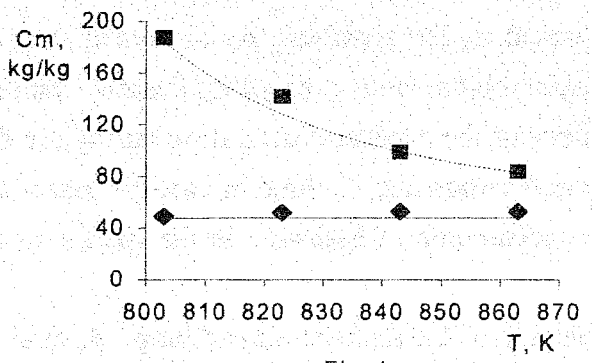

Fig. 1

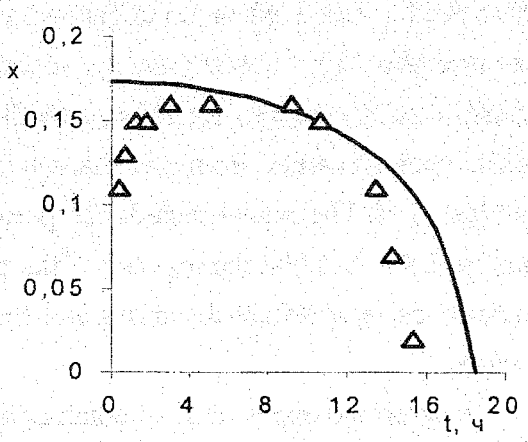

Fig. 2

Model 2 can be considered as a first approximation on modeling the process performance in a pilot reactor with a fluidized catalyst bed [10] in which the degree of vibration is an order of magnitude lower than in the laboratory reactor [11]. For pure methane the calculated yield of carbon is 111 kg/kg at Q = 120 m^3/(kg·h) and T = 823 K [13]. This indicates that the specific yield of carbon decreases by a factor of 1.5 as one passes from a laboratory reactor to the pilot one.

The aim of the present work is to develop methods for calculation processes in models 3-5 and to compare the models.

Model 3 can simulate processes in a pour-type reactor [8] with a co-current catalyst-gas upward and downward flows. The process is distinguished by the wave of catalyst deactiva-

tion which moves along the reactor. For the reactor with a rather large catalyst loading, the wave profile is stabilized and the wave moves at a constant rate. The wave profile and dependence between the wave rate versus temperature and concentration of hydrogen in the initial mixture are calculated. For the reactor with a finite catalyst loading, the profiles of carbon concentration and degree of methane conversion along the reactor are calculated for different periods of the process. After the catalyst deactivation, the concentration of carbon increases when one moves from the reactor inlet. For pure methane at Q = 120 m^3/(kg·h) and T = 823 K, the average concentration of carbon $\bar{c}_m$ is 97 kg/kg. For small and large loadings, $\bar{c}_m \rightarrow$ 48 and $\bar{c}_m \rightarrow$ 125 kg/kg, respectively.

The drawback of plug reactors (models 2 and 3) is that the catalyst contacts with the initial gas mixture which is not enriched with hydrogen. As hydrogen concentration decreases, the rate of catalyst deactivation increases, and the yield of carbon decreases. This problem can be eliminated by re-circulating the gas flow. As a result, the catalyst contacts with the gas mixture enriched with hydrogen and the yield of carbon increases.

Model 4 is supplied with a gas circulation as in model 2. Figure 3 shows the calculated c_m versus circulating factor n for pure methane (Q = 120 m^3/(kg·h) and T = 823 K). As the circulating factor increases, the reactor approximates to the reactor with an ideal stirring of catalyst particles and gas (model 1).

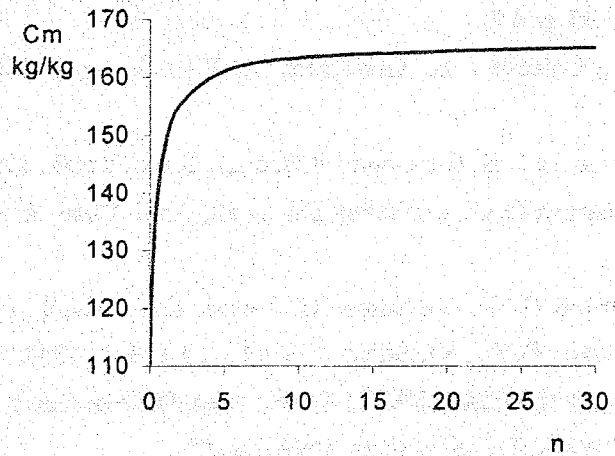

Fig. 3

Model 5 can describe processes in the reactor with a fluidized catalyst bed. Since the ideal mixing of particles and gas is assumed for the dense phase, model 5 describes the process occurring in it. Introducing the mass-transfer resistance between the dense and bubble phases results in the increase in hydrogen concentration in the solid phase compared to model 1, and correspondingly, to increase in the carbon yield. In Fig. 4, c_m is shown as a function of coefficient of mass transfer (β) between the phases of pure methane (Q = 120 m^3/(kg·h) and T = 823 K). For $\beta \rightarrow \infty$, model t transforms into model 1. In contrast to model 5, c_m in model 1 can be increased by decreasing the flow rate of the initial mixture.

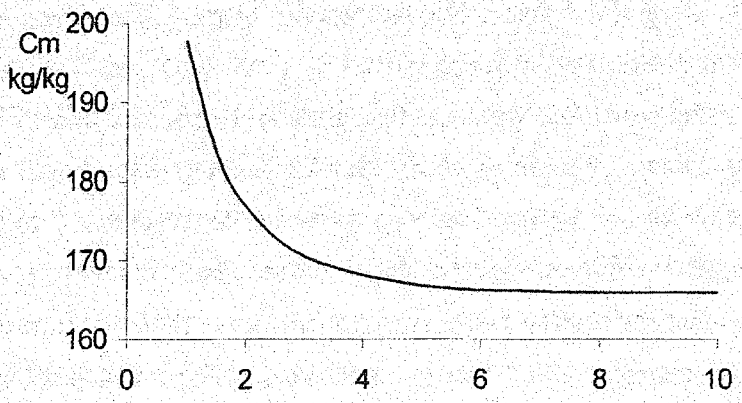

Fig. 4

A comparison of the process data calculated with different reactor models shows that in order to maximize the carbon yield, one should provide the maximum mixing of catalyst particles and gas, which can be obtained by re-circulation of the gas flow or using a fluidized catalyst bed.

References

1. Kuvshinov G.G., Avdeeva L.B., Goncharova O.V. et al., International Meeting on Chemical Engineering and Biotechnology. Thermal Process Engineering. ,ACHEMA`94, 1994, p. 96.
2. Avdeeva L.B., Kuvshinov G.G., Goncharova O.V. et al., 1st World Congress Environmental Catalysis, Pisa (Italy), 1995, p. 459.
3. Shaikhutdinov Sh.K., Avdeeva L.B., Goncharova O.V et al., Appl. Catal. A: General, 1995, v. 126, p. 125.
4. Goncharova O.V., Avdeeva L.B., Fenelonov V.B. et al., Kinet. Katal., 1995, v. 36, No 2, p. 293.
5. Avdeeva L.B., Goncharova O.V., Kochubey D.I. et al., Appl. Catal. A: General, 1996, v. 141, p. 117.
6. Ermakova M.A., Ermakov D.Yu., Kuvshinov G.G. et al., Kinet. Katal., 1998, v. 39. No 5, p. 791.
7. Ermakova M.A., Ermakov D.Yu., Kuvshinov G.G et al., J. Catal., 1999, v. 187, p 77.
8. Investor's Certificate No 16008207 (USSR). Discoveries. Developments, 1990, No 43.
9. Russian Patent No 2064831, Developments, 1996, No 22.
10. Kuvshinov G.G., Zavarukhin S.G., Mogilnykh Yu.I. et. al, Khim. Prom-st, 1998, No 5, p. 300.
11. Kuvshinov G.G., Mogilnykh Yu.I., Kuvshinov D.G. et. al, Khim. Prom-st, 1997, No 4, p. 270.
12. Kuvshinov G.G., Mogilnykh Yu.I., Kuvshinov D.G. et al, Carbon, 1998, v. 36, p. 87.
13. Kuvshinov G.G., Mogilnykh Yu.I. and Kuvshinov D.G., Catal. Today, 1998, v. 42, p. 357.
14. Zavarukhin S.G., Mogilnykh Yu.I., Kuvshinov G.G., Khim. Prom-st, 1999, No 10, p. 641.
15. Kuvshinov G.G., Zavarukhin S.G., Zhdanova E.S., Vestnik NGTU, 1999, No 2, p. 127.

VANADIUM HONEYCOMB CATALYST FOR THE CASSETTE REACTOR

V.I. Vantchurine, A.N. Kabanov, A.V. Bespalov, V.S. Beskov

D.I.Mendeleyev University of Chemical Technology of Russia
Miusskaya Sq.9, 125047 Moscow, Russia
E-mail : Kabanov_Alexandr@mail.ru

The technology of preparing the vanadium honeycomb catalyst is developed by using the stage of the preliminary formation of the contact carrier based on aerosil or white ashes. The moulding mass composition is following: matrix, petrolatum, olein acid with ratio as 60:16:1.

The vanadium honeycomb catalyst was extruded as hexagonal prism with square thin-walled (0.3 –0.4 mm) channels (2 x 2 mm). The free surface of the prepared catalyst is about of 70 %.

Thermal treatment was carried out by the gradual temperature augmentation up to 900-950 °C. Specimens of the prepared catalyst were kept under this temperature for 2-3 hours. The contact carrier was modified.

Characteristics of the vanadium honeycomb catalyst are given in table 1.

Table 1

Contact carrier	Content of the active constituent % MASS.		Activity under standard conditions, %		Mechanical durability, MPA	Specific surface, M^2/G
	V_2O_5	K_2O	420°C	485°C		
Aerosil	5,44	5,61	30,2	84,8	1,4	13,6
White ashes	6,51	6,33	32,4	86,1	1,6	10,7

The vanadium honeycomb catalyst was tested in the pilot cassette reactor. This reactor worked under adiabatic conditions. The gas warmed up to 440 °C was conveyed into the pilot cassette reactor. The gas consumption was 5-35 nm^3/h. The sulfur dioxide concentration was 9,5 – 10,5 % vol. The dust concentration in the gas reached 0.07 – 0.09 g/nm^3. The gas was conveyed into the reactor by an injector under the pressure of 6 atm.

The results of the tests of the vanadium honeycomb catalyst in the pilot cassette reactor are given in table 2.

Table 2

Gas rate, m/s	1,35	1,68	2,02	2,36	2,69	3,50	5,6
Contact time, s	0,54	0,43	0,36	0,31	0,27	0,21	0,13
Degree of oxidation (calculated), %	69,0	62,0	55.3	45,0	37,0	26,0	15,0
Degree of oxidation (experimental), %	50,0	47,5	45,0	40,5	33,0	22.5	11.5

Comparison of the obtained data on the vanadium honeycomb catalyst in the pilot cassette reactor with the same indices of the vanadium catalyst of the irregular layer shows the advantages of the first one.

OXIDATION OF DUSTED SULFUR DIOXIDE IN THE CASSETTE REACTOR

A.N. Kabanov, A.V. Bespalov, V.I. Vantchurine, V.S. Beskov

D.I.Mendeleyev University of Chemical Technology of Russia.
Miusskaya Sq. 9, 125047 Moscow, Russia
E-mail: Kabanov_Alexandr@mail.ru

The cassette reactor and fixed-bed reactor with the irregular catalyst layer (filtering reactor) were tested in industrial conditions in production of sulfuric acid. Sulfur dioxide is catalytically oxidized to sulfur trioxide. The content of sulfur dioxide is rich in the dust.

The main indices of the work are the pressure drop and the degree of sulfur dioxide oxidation. The change of the sulfur dioxide concentration was determined in cross-section of the cassette experimentally and by simulation.

Geometrical parameters of the pilot cassette reactor were the following: the length of the cassette – 600 mm, the width of the cassette – 50 mm, the distance between the cassettes 30 mm. The cassettes were filled with grained catalyst IC-1-4, diameter of granules – 5 mm and length - 10-15 mm.

The rate for the both reactors was about 0,38 nm/s. The concentration of the suspended ashes particles in sulfur dioxide was measured by the method of the inner filtration (0.07 – 0.1 g/m^3) and sulfur dioxide concentration – by Reich method (9-10 % vol.)

The long-term test have proved numerous advantages of the pilot cassette reactor over the filtering reactor. First, the initial pressure drop for the cassette reactor is much lower than that for the filtering reactor. Second, the pressure drop for the cassette reactor does not change. Third, dust sedimentation does not take place in the cassette reactor.

The distribution of the sulfur dioxide concentration was simulated. The main equation of the proposed model is given

$$v\frac{dc}{dx} - D\frac{d^2c}{dx^2} = w. \qquad (1)$$

The boundary conditions are the following:

$x = 0$ (the center cassette): $dc/dx = 0$;

$X = X_O$ (surface of the cassette): $c = c_o$, (2)

where c and c_o - initial SO_2 concentration and current SO_2 concentration, respectively; v - transversal constituent of the SO_2 flow rate (the following assumption is also considered reasonable for the present system: some SO_2 quantity is filtered throw the packing of the cas-

sette); D – effective coefficient of diffusion of SO_2 in the irregular layer; w – chemical reaction rate.

As the reaction rate constant of SO_2 oxidation does not change considerably under high temperature one can write:

$$w = -k(X^* - X), \tag{3}$$

where k – reaction rate constant of SO_2 oxidation; x^* - equilibrium degree of oxidation; x – degree of oxidation.

Thus differential equation (1) with the boundary conditions (2) has analytical solution:

$$\mathbf{c} = \frac{\lambda_1 \, exp(\lambda_2 \mathbf{x}) - \lambda_2 \, exp(\lambda_1 \mathbf{x})}{\lambda_1 \, exp(\lambda_2 \mathbf{x}_0) - \lambda_2 \, exp(\lambda_1 \mathbf{x}_0)} \mathbf{c}_0 \mathbf{X}^* + (1 - \mathbf{X}^*)\mathbf{c}_0, \tag{4}$$

where $\lambda_1 = \dfrac{v + \sqrt{v^2 + 4k\,D/c_0}}{2D}$; $\quad \lambda_2 = \dfrac{v - \sqrt{v^2 + 4k\,D/c_0}}{2D}$.

The agreement between the experimental and calculated values justifies the suitability of the proposed model in particular for low values of c_o. The obtained data have proved efficiency of active packing of the cassette (SO_2 concentration in the central part of the cassette was higher than in the equilibrium one).

APPLICATION OF HONEYCOMB STRUCTURE IN REACTOR OF AMMONIA OXIDATION

V.I. Vantchurine, V.S. Beskov, A.V. Bespalov, A.N. Kabanov

Mendeleyev University of Chemical Technology of Russia
Miusskaya Sq.9, 125047 Moscow, Russia

The deviation of local speed values of ammonia-air-mixtures (AAM) from average value in the reactor of ammonia oxidation can reach 30-40 %. Because of unsatisfactory distribution of a gas flow uniformity of a temperature mode in cross section of platinoid grids is not achieved, their vibration and wear increases and degree of conversion of ammonia decreases.

The distribution devices such as metal lattices, grids, grain layer of grain material and etc. do not much improve distribution of AAM. Besides the distribution devices can provoke collateral reactions, that increases consumption factor on ammonia.

Use of the honeycomb structure after a package of platinoid grids should in all cases result in improvement of gas distribution in the reactor of ammonia oxidation and accordingly techno-economic parameters of the reactor of ammonia oxidation.

The efficiency of application of the regular packing of honeycomb structure made from cordierite neutral to a reaction mixture was shown during industrial tests at Cherepovets joint-stock company "NITROGEN". The regular packing consisted of elements of honeycomb structure (size of cells 3,5 × 3,5 mm, thickness of a wall 0.6 mm) in the form of a parallelepiped with the basis 75 × 75 mm and height of 20 mm and was prepared according to technology we developed.

It is obvious that due to the stabilizing function of the regular packing made of elements of honeycomb structure the decrease of platinoides losses reaches 12-18 %.

The industrial tests of the nonplatinoide catalyst of honeycomb structure were carried out at Gorky joint-stock company "Styrol". The nonplatinoide catalysts of honeycomb structure were made from the industrial moulding mass of the ferric oxide and had the form of square prisms with the basis 100 × 100 mm and height of 50 ± 5 mm (size of cells 3,0±0,5 × 3,0±0,5 mm). The nonplatinoide catalysts of honeycomb structure stacked on a grid under a package of platinoid grids with size of a backlash not exceeding 0,5 from the size of an individual cell. The quantity of platinoid grids thus was reduced up to eight instead of usually used twelve.

The nonplatinoide catalysts of honeycomb structure were spreaded on the lowered fire bars and above the nonplatinoide catalysts of honeycomb structure directly on them a package of platinoid grids was placed. After 3800 hours of work of the reactor of ammonia oxidation the platinoids loss was 0,128 g par ton of a nitric acid (the norm standard – 0,155 g par ton). Visual survey of platinoid grids and the nonplatinoide catalysts of honeycomb structure has shown that they were well kept and are suitable for further operation. A gain of a degree of conversion of ammonia has made about 0,3 %.

After regeneration the platinoid grids in the reactor of ammonia oxidation have worked 1420 hours.

Section IV

CHEMICAL REACTORS FOR SOLVING THE FUEL AND ENERGY PRODUCTION PROBLEMS

HEAT RECOVERY FROM DILUTE METHANE EMISSIONS USING THE CH4MIN TECHNOLOGY

Hristo Sapoundjiev and Francois Aubé

Natural Resources Canada, CANMET Energy Diversification Research Laboratory
1615 Lionel-Boulet Blvd, P.O.Box 4800, Varennes, Quebec, Canada, J3X 1S6
Phone: (450) 652 5789; Fax: (450) 652 5994, E-mail: hsapound@NRCan.gc.ca

Introduction

Throughout the world, anthropogenic methane emissions account for 19% of all greenhouse gas emissions. A major fraction of these methane emissions is at low concentration (0.1-1.0 v/v% methane in air). Mainly these dilute methane emissions comes from industrial activities such as underground coal mining, natural gas and petroleum and petrochemical primary and secondary production, agriculture sector etc.

Until now no technology has offered satisfactory economic viability for treatment of these lean methane gases below 1 v/v%. Currently, NRCan is developing the CH4MIN technology to economically process large flows of industrial air emissions, containing dilute methane (0.1 – 1.0 v/v %).

This paper describes the operating principles of CH4MIN technology and the experimental work done with a 500 mm pilot unit for estimating the efficiency of the extracted heat from lean (0.1-1.0 v/v%) methane gases. A mathematical model and a computer program were developed for numerical simulation of the technology. The simulation results are in good agreement with the experimental data. A preliminary economic analysis is presented in the case of industrial application of the CH4MIN technology.

Operating principle of CH4MIN technology

The scheme of a typical CH4MIN process is shown in Figure 1. It consists of a reactor, two pairs of valves and a heat removal system in the central region separating the catalyst bed in two parts. At both ends of the reactor, an inert material bed is present and acts as a thermal capacity. The flow reversal is controlled by the sets of valves. When valves 1 are opened and valves 2 are closed, the reaction mixture flows from left to right (direct flow operation). After a certain period of time, inverting the position of the valves reverses the flow direction. The reaction mixture flows from right to left (reverse flow operation). Before initiation of the process the inert and the catalysts beds are preheated by an external heat source to an appropriate temperature. During normal operation the system is energy autonomous and the preheating

system is switched off. In direct flow operation the reaction mixture enters the reactor from the left. It heats up, going through the hot left inert bed and enters the catalyst bed at a sufficient temperature for the oxidation of methane to occur and further heat the air. The hot gas heats the right inert bed before exiting to the atmosphere. During direct flow operation, the left inert bed, which was initially hot, cools down while the right inert bed, which was relatively cool, heats up. The process switches to reversed flow when the temperature of the gas mixture entering the left catalyst bed nears the low-temperature set point, below which catalytic oxidation is less efficient. The incoming feed gas now enters from the right, heats up while rising through the right inert bed, reacts in the catalyst section and heats the left inert bed before leaving the reactor. Direct flow is re-established at the end of the reverse flow. The heat generated in excess by the exothermic chemical reaction is withdrawn by the heat removal system in the mid-section of the reactor.

Experimental demonstration

A 500-mm pilot-scale unit was built to demonstrate the technical ability of the technology. A set of thermocouples has been installed along the central axis for temperature registration. Methane conversion was measured by gas chromatography, analysing the methane concentration in the feed gas stream, mid-section gas withdrawal and the outlet gas from the reactor. Methane is totally converted by the chemical reaction. Because of the low oxidation temperature (below 800°C), the outlet gas and extracted hot air in the mid-section not contain nitrogen oxides.

The pressure drop of the air stream through the experimental reactor pipes and valves remains below 400 mm of water.

The heat recovery efficiency of CH4MIN was evaluated on basis of the temperature and flow rate of the extracted gas in the case of hot air withdrawal. Results show that the reactor operates in autothermal regime (without external heat) even if the concentration of the methane in air is only 0.1 v/v %. Heat recovery is possible with higher concentrations. For concentrations between 0.3 and 1.0 v/v % of methane the heat recovery efficiency of the CH4MIN technology is between 50 – 95%. For a typical coal mine concentration (0.5 v/v% of methane), the efficiency is 75%.

The benefits of the CH4MIN technology for every 100 m^3/s (0.5 v/v% of methane) of coal mine ventilation air are:

- Heat recovery: 14 $MW_{therm.}$ or (425 000 GJ/ year) thermal energy.
- Reduced greenhouse gas emissions: 208 000 equivalent tonnes of CO_2/year.

Numerical simulation

A mathematical model and computer programs were developed for the study and design of CH4MIN reactors. A transient two-dimensional heterogeneous model is combined with a numerical method allowing the fast formulation of new reactor designs. The program has been validated with experiments performed with a 500-mm reactor. Good agreement with the experiments was observed. The dynamic behavior of the CH4MIN reactor can be predicted accurately by the model for a wide range of conditions including small reactor diameter and low air flow rate. Good agreement between the model and the experiments was observed for two configurations of heat removal by means of hot air withdrawal from the mid-section of the reactor and for a configuration including conventional heat exchanger installed of the mid-point of the reactor.

Time evolution of temperature profiles and distribution along the reactor length are shown on Figure 2(a-c) for the hot air withdrawal configuration.

Figure 2a shows the temperature evolution along the reactor length during the first half-cycle. The flow direction is from left to right. The initial temperature profile is shown as a dashed line. The circles and the solid line represent the temperature distribution and the predicted profile along the reactor length at the end of the first half-cycle (200 s). The flow direction is then reversed. The evolution of the heat front during the second half-cycle is shown on Figure 2b (200 s to 400 s) as the difference between the solid and hollow circles. Hot air extraction in the mid-section implies adjusting operations conditions in order to achieve complete methane combustion in the upstream catalyst bed and thus avoiding the presence of methane in the withdrawn air. This restriction imposes shorter cycle duration and leads to the formation of two peaks on the axial temperature profile, both located at the catalyst beds. Figure 2(c) shows temperature profiles after 15 cycles (6950 s). For this case, the reactor operates in stable regime and 52% of the heat generated by the chemical reaction is removed by air withdrawal in the central region of the reactor. The flow rate of the extracted hot air was kept constant, with an average temperature around 700°C.

Conclusion

The development of the CH4MIN technology and its application to the elimination of methane and recovery of heat from underground coal mine ventilation air has been shown to be a technically viable solution to a major global warming problem. The recovered heat can be used to produce electricity, which can then be transmitted to user sites. When direct use of the CH4MIN-generated heat is envisaged, consumption of the heat must be carried out near

the mine site. The CH4MIN technology is being shown to constitute a low capital and low operating cost solution when mine ventilation air contains over 0.5 v/v % of methane. The CH4MIN technology can also be implemented for elimination of lean methane emissions from the other sources as well as natural gas and oil industry etc.

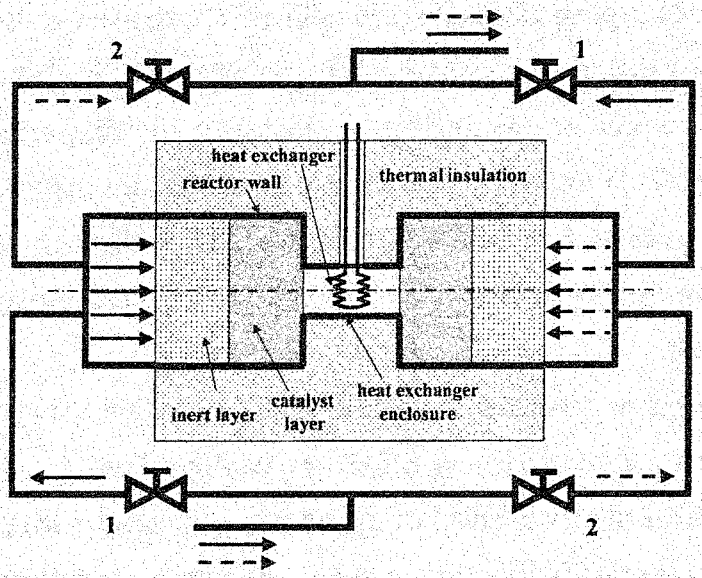

Fig. 1. Flow diagram of the CH4MIN reactor

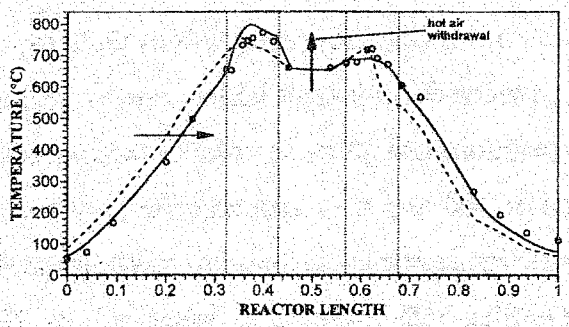

Fig. 2a First half-cycle (t=0 and 200 s)

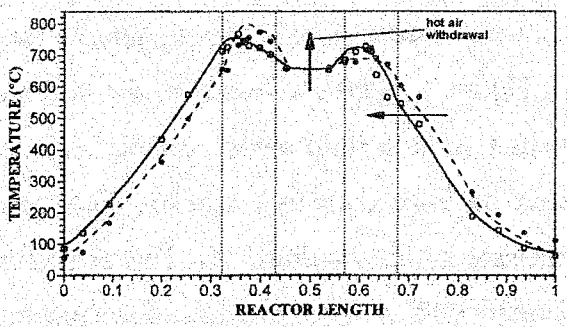

Fig. 2b Second half-cycle (t=200 and 400 s)

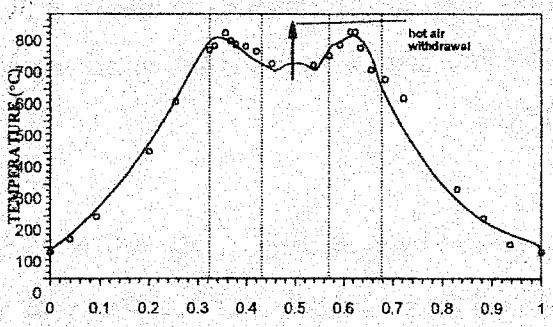

Fig. 2c After 15 cycles (t=6950 s)

Fig. 2. Comparison between the model simulation and experiments performed with 500-mm ID reactor. v=0.65 m/s, 0.3% v/v of methane, hot air withdrawal.

CLEAN CATALYTIC COMBUSTION OF LOW HEAT VALUE FUELS FROM GASIFICATION PROCESSES

J.J. Witton, J.M. Przybylski, E. Noordally

Combustor & Heat Transfer Technology, School of Mechanical Engineering, Cranfield University, Cranfield, Bedford MK43 0AL.
Tel/Fax 44 (0)1234 754636. e-mail: j.j.witton@cranfield.ac.uk

The conversion of biomass, coal and some waste materials by gasification offers an opportunity to utilise such fuel sources cleanly. Many of the aggressive species inherent in the fuel precursors can be retained in process, but one exception is nitrogen, which appears in the derived fuel gas generally as ammonia. Amounts of ammonia can be large, up to 3-4000 vppm from biomass. Heat values of the derived fuel gases depend on the process, but are typically one-tenth to one-half that of natural gas. Although the derived gases can be water washed to give low contaminant (especially ammonia) levels, typically 50 PPM, this creates a waste stream for disposal and represents a thermodynamic loss to the cycle.

Efficient conversion of gaseous fuels to electrical power is accomplished in gas turbines, preferably in combined cycle mode, where thermal efficiencies can be greater than 65%. Open cycle, high pressure ratio machines can achieve efficiencies greater than 40%.

Primary issues for the gas turbine combustor when using gasification gases are:

1. Their large volumetric flows, and
2. The fuel-bound nitrogen content represented by the ammonia fraction.

The poster is concerned with the second issue.

Fuel-bound nitrogen conversion in flames can be large, even with stoichiometry control of the combustion process in the homogeneous phase, where reduction to atomic nitrogen can be achieved. The lowest levels of conversion reported in turbulent flames are of order 20% of the input fuel bound nitrogen content, and this will, in many cases, exceed the permitted range for nitrogen oxides emissions.

The poster describes experiments aimed at using catalytic combustion with reaction-specific catalysts to reduce the ammonia conversion rates, and so enable high levels of ammonia to be accommodated in the fuel gas without the disadvantage of waste disposal and thermodynamic loss to the engine cycle. The poster will show the outlines of a process and some results obtained at representative gas turbine conditions.

OP-IV-3

A NEW ONE-STEP CH_4 AND C_3-C_4 PARAFFINS CO-PROCESSING INTO AROMATIC HYDROCARBONS

Ts.Ts. Cherninov, V.V. Shevlyuk, B.I. Sokolov, G.V. Echevskii*, A.S. Noskov*, V.N. Parmon*

JSC "Tomskgasprom", Russia, 634009, Tomsk, Bolshaya Podgornaya, 73
**Boreskov Institute of Catalysis, Russia, 630090 Novosibirsk, pr. Akad. Lavrentieva, 5*

Tomskgasprom was established in 1995 by the well known Russian company Gasprom as its affiliate specialized in development of the local natural gas reserves in Tomask region. At present, the Myldzhinskoye gas/condensate field is operated by Tomskgasprom with annual production rate of 2 billion m^3 of gas, 200 000 tons of condensate, and about 100 000 tons of hydrocarbons C_3-C_4. The annual production rate of about 10 billion m^3 gas and 1 million tons condensate is expected by 2010.

Insufficient transportation systems and high cargo tariff make it economically vital to locate the processing facilities immediately to hydrocarbon production sites. For example, it is highly desirable for processing of C_3-C_4 hydrocarbons, which are hardly transportable, or for conversion of natural gas into liquid hydrocarbon fuels.

A typical problem for Russia is necessity of raw a hydrocarbons processing under severe transport limitations directly at the place of their extraction. For example, it is necessary to process C_3-C_4. hydrocarbons (which are hard for transportation) or to convert the natural gas into liquid hydrocarbon fuels. Small scale (with annual capacity up to 100 thousand tons) plants producing motor fuels and built in the regions with hydrocarbon reserves are able to satisfy the local demand in automotive and diesel fuels.

A commonly accepted two-stage processing of methane, which is the main component of natural gas, into liquid hydrocarbons including gasoline and diesel fuel has some disadvantages for operation on industrial scale. First of all, it involves an intermediate energy consuming conversion of light hydrocarbons into syngas, which is then followed by the catalytic synthesis of desired fuels. Nevertheless, basing on the modern Russian space-jet technologies, a leading Russian rocket-jet manufacturer PO "Energomash" together with chemical institutes of the Russian Academy of Sciences have designed movable unit plants for this two-stage natural gas processing. These plants are based on the modular mobile syngas generators with a flexible process scheme, each module converting 80 thousand tons of natural gas per year. As a target synthetic fuel, the plant allows production of, e.g., fuel alcohols, high octane

gasoline, diesel fuel or dimethyl ether using catalytic technologies developed at either the Boreskov Institute of Catalysis or other chemical institutes of Russia.

At the same time, till now there were only few attempts to develop simple technologies for the processing of hard to transport C_3-C_4. hydrocarbons directly at the place of their extraction. Indeed, there is no problem to convert light hydrocarbons into easy to transport methane, but it is not economically profitable owing to the lower price of methane in comparison to the C_3-C_4. hydrocarbons.

This report presents recent results related to the design of a new process of one-step co-processing of methane and the paraffin C_3-C_4. hydrocarbons into aromatic hydrocarbons on modified solid catalysts. Under the lab scale conditions, the yield of aromatic hydrocarbons at the process with respect to the converted C_3-C_4. hydrocarbons attains 90%.

Another way to use the propane-butane mixture is its direct involvement into reforming of oil to produce additional high octane gasoline. The experimental results show that such co-processing of light hydrocarbons with heavier oil hydrocarbons gives an increase in the gasoline yield up to 10-15% by the expense of C_3-C_4..

Just at the hydrocarbons extraction place, it is also possible to convert light hydrocarbons into valuable solid carbonaceous materials, for example, into filamentous carbon via catalytic pyrolysis of hydrocarbons. Under consideration are modern results on the simultaneous production of filamentous carbon and hydrogen over heterogeneous catalysts.

One may expect that the new one-step catalytic processes under discussion can open new ways of the natural gas and gas condensate conversion into valuable chemical products just near hydrocarbon sources in the not very well developed areas.

Section V

WASTE DETOXICATION AND PROCESSING

DEVELOPMENT OF MULTI-REACTOR PROCESS FOR CATALYTIC DESTRUCTION OF HIGHLY TOXIC ROCKET FUEL 1,1-DIMETHYLHYDRAZINE

Z.R. Ismagilov[a], M.A. Kerzentsev[a], V.A. Sazonov[a], I.Z. Ismagilov[a], V.N. Parmon[a], G.L. Elizarova[a], O.P. Pestunova[a], Yu.V. Ostrovsky[b], Yu.L. Zuev[c], V.N. Eryomin[c], N.V. Pestereva[c], L.N. Rolin[c], V.A. Shandakov[d]

[a]Boreskov Institute of Catalysis, 639090, Novosibirsk, Russia, phone: +7(3832) 34-12-19, fax: +7(3832)39-73-53, e-mail:zri@catalysis.nsk.su
[b] Novosibirsk Exploratory Design Institute VNIPIET, Novosibirsk, Russia
[c]State Rocket Center "Academician V.P.Makeyev Design Bureau", Miass, Russia
[d]Federal Research and Production Center "Altai", Biysk, Russia

Reduction and conversion of weapons productions in Russia have made extremely urgent the problems of development and implementation of environmentally safe and efficient processes for disposal of rocket fuels. One of the most pressing problems is the development of the disposal process for extremely toxic 1,1-dymethylhydrazine (unsymmetrical dimethylhydrazine - UDMH) and industrial wastes containing UDMH.

The problem of UDMH utilization can be solved by creation of a treatment plant based on UDMH oxidation in a fluidized catalyst bed. The unique feature of this method of fuel and waste combustion, elaborated in BIC is the possibility of total oxidation of organic compounds in *stoichiometric* ratio with oxygen at relatively low temperatures (500-750°C), which suppresses formation of nitrogen oxides. This is achieved by the use of highly active catalysts in a fluidized bed which also allows the efficient removal and possible use of reaction heat. Pilot and industrial plant tests have shown high efficiency and environmental safety of this technology in treatment of various hazardous organic wastes: organic solvents, chemical industry wastes, nitrogen-containing compounds, used scintillation fluids, mixed organic wastes containing radionuclides, etc [1, 2].

UDMH is the most toxic of rocket fuels currently used. Its maximum allowable concentration is 0.001 mg/m^3 in air and 0.01 mg/L in water. Therefore, a treatment facility should provide special measures for total UDMH destruction.

The problem of UDMH treatment is further complicated by its high reactivity resulting in formation of numerous intermediate and side products. The research on UDMH vapor catalytic oxidation carried out in BIC over a number of solid catalysts $Cu_xMg_{1-x}Cr_2O_4/\gamma$-$Al_2O_3$, Fe_2O_3/γ-Al_2O_3, Cu/(ZSM5+TiO_2+Al_2O_3)/Al_2O_3-SiO_2 Pt/γ-Al_2O_3 and Pd/γ-Al_2O_3 at temperatures 200-400°C showed that along with the prevailing non-toxic products of deep oxidation

(H_2O, CO_2 and N_2), about 10 intermediate and side products, such as methane, formaldehyde, dimethylamine, formaldehyde 1,1-dimethylhydrazone, NO and NO_2 are formed during UDMH catalytic oxidation [3-5]. This research allowed to chose an optimum catalyst $Cu_xMg_{1-x}Cr_2O_4/\gamma$-$Al_2O_3$, providing the highest selectivity to desirable products (H_2O, CO_2 and N_2), and minimum formation of toxic side products.

For necessary reduction of concentrations of residual UDMH and toxic side products a multi-stage process diagram was developed (Fig. 1).

It includes the following apparatuses: catalytic fluidized bed reactor, cyclone, two jet scrubbers, absorber-condenser.

The principal apparatus is the fluidized bed catalytic reactor (1). It is intended for conducting the main reaction - total catalytic oxidation of UDMH to CO_2, water and N_2. The catalytic reactor is made of stainless steel, its height is 2000 mm, and the inner diameter is 120 mm. Air for fluidization and UDMH oxidation is supplied through a perforated gas distributing plate. UDMH is injected into the bed through a nozzle. The reaction products are removed through the upper, wider part of the apparatus. Due to the widening entrained catalyst particles separate out of the gas stream. Along the height of the reactor, at a pitch of 50 mm, horizontal tubes are located for thermocouple wells, gas sampling and pressure gauges. The reaction proceeds over the catalyst $Cu_xMg_{1-x}Cr_2O_4$, supported on strong spherical γ-Al_2O_3 granules (1.4-2.0 mm).. The process takes place at temperatures of 600-700°C and air-fuel equivalence ratio 1-2. The fluidized bed provides uniform temperature across the bed and efficient heat removal by a coil water heat exchanger (2) immersed in the bed, decreasing the temperature of the exhaust gas at the exit of the reactor to 450-350 °C.

The cyclone (3) placed after the main reactor is used for removal of large-sized dust particulates (>30 μ) formed due to catalyst crushing and attrition in fluidized bed.

The jet scrubbers (5, 6) placed downstream the cyclone are intended for further purification of off gas from low-sized particulates (3-30 μ) and for removal from the gas stream of traces of UDMH and its incomplete oxidation products. The surface of contact is provided in these apparatuses by intensive oppositely directed liquid jets forming a foam layer with large surface area [6, 7]. The jet scrubbers also serve to provide cooling of the gas to 35-40°C. The parameters of jet scrubbers were calculated by methods described in [7].

In the jet scrubber No 2 (6) complete oxidation of traces of UDMH absorbed in scrubbing liquid (water) is conducted over special powder catalysts for liquid phase UDMH oxidation [8-9]. If necessary, additional air or hydrogen peroxide can be fed into the scrubber.

After this scrubber, the gas saturated with water vapor enters the absorber-condenser (7). The operation of this unit is based on removal of admixtures from the off-gas by a screen of water droplets sprayed by the nozzle [10]. In this apparatus the gas purification from low-sized particles (<3 μ) takes place with final removal of trace amounts of UDMH and gas cooling to 25-30°C.

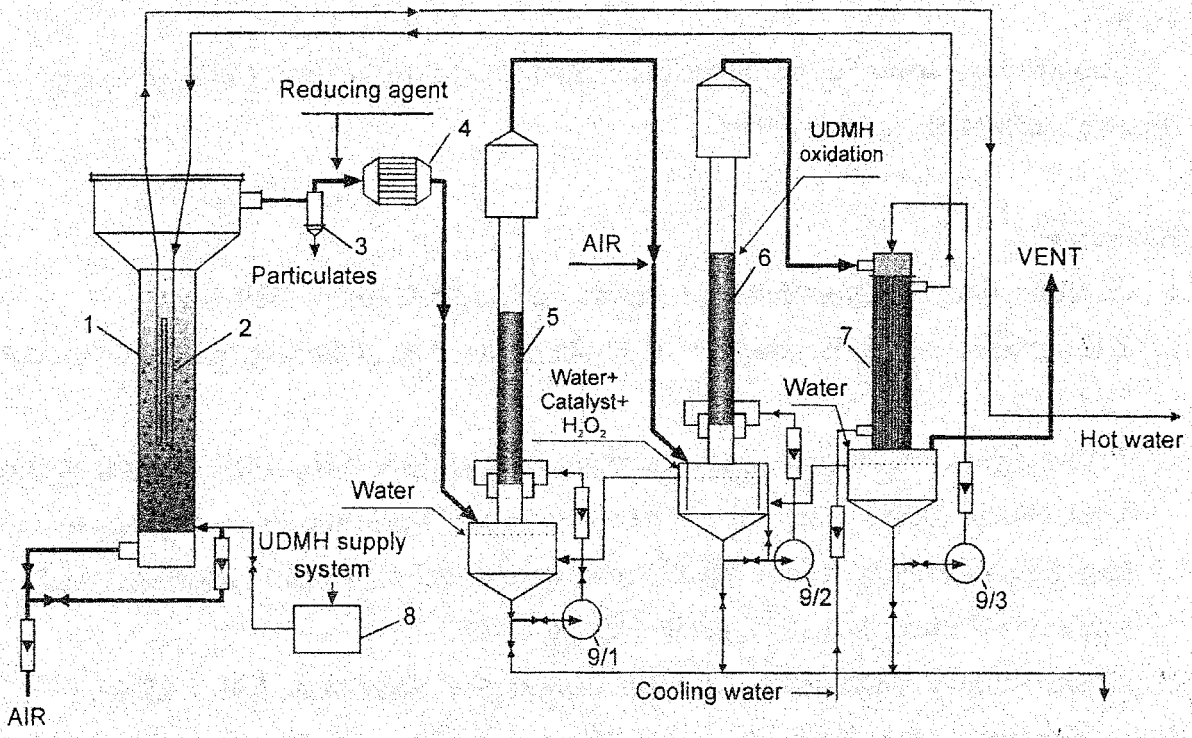

Fig. 1. Flow diagram of the pilot plant for catalytic treatment of udmh: 1 - catalytic fluidized bed reactor; 2 - water heat exchanger; 3 - cyclone; 4 - scr reactor; 5,6 - jet scrubber; 7 - absorber-condenser; 8 - tank for udmh; 9/1-9/3 – circulation pumps

Preliminary experiments on UDMH oxidation in a fluidized catalyst bed at 600-700°C showed that in addition to high selectivity of transformation of fixed nitrogen to N_2 (>90%), the formation of some nitrogen oxides was detected. Therefore a deNOx stage was added into the flow diagram, based on selective catalytic reduction of NO_x with ammonia over monolithic honeycomb catalyst.

The experimental installation for UDMH destruction in a fluidized catalyst bed with a capacity of 2 kg/h was designed and fabricated at the State Rocket Center, and experiments on UDMH catalytic oxidation in this installation were carried out. These experiments showed high efficiency and environmental safety of the technology developed. The process was carried out in a fluidized bed of catalyst at a temperature of 600-700°C. The main reaction products were CO_2, water and nitrogen. Under optimum operation regimes the UDMH

concentration at the outlet of the main reactor is below maximum allowable limit in industrial areas (0.1 mg/m^3). Trace amounts of UDMH in the off gas are efficiently oxidized over catalysts in aqueous solutions in the jet scrubber.

Full set of results of industrial exploitation of the pilot plant as well as design and construction of the mobile unit for processing of UDMH at distant military locations will be presented.

Acknowledgment: To the International Science and Technology Center for support of this work under ISTC project # 959.

References

1. Z.R.Ismagilov, M.A.Kerzhentsev, Catalysis Today, 1999, vol. 47, 339-346.
2. Z.R. Ismagilov, M.A. Kerzhentsev, R.A. Shkrabina, et al., Catalysis today, 2000, vol.55, 23-43.
3. Z.R.Ismagilov, V.N.Parmon, M.A.Kerzhentsev, et al. Proc. Scientific-Technical Seminar "Problems in Methodology of Utilization of Solid Propellants, Production Wastes, and Liquid Fuel Residues in Missilery Objects" Research&Production Corporation "ALTAI", Biysk, 16-17 November, 1999, Biysk, 2000, p. 13-27.
4. I.Z.Ismagilov, V.V.Kuznetsov, M.A.Kerzhentsev, V.A.Shandakov, Ibid, p. 28-35.
5. V.N.Parmon, O.N.Pestunova, G.L.Elizarova, M.A.Kerzhentsev, I.Z.Ismagilov, V.A.Sazonov, V.V.Kuznetsov, Z.R.Ismagilov, Proc. Prof. V.V.Popovsky Memorial Seminar "Regularities of deep oxidation of substances over solid catalysts", Boreskov Institute of Catalysis, Siberian Branch of RAS, Novosibirsk, May 22, 2000, p. 235-240.
6. Yu.V.Ostrovsky, G.M.Zabortsev, Heat and mass-exchange apparatus, Patent of Russian Federation No 2123375 (1998).
7. Yu.V.Ostrovsky, G.M.Zabortsev, Russian Journal of Applied Chemistry, 1998, vol.71, No 11, 1836-1839.
8. G.L.Elizarova, L.G.Matvienko, O.P.Pestunova, et al., Kinet. Catal. Engl. Tr., 1998, Vol. 39, 44-50,
9. O.P.Pestunova, G.L.Elizarova, V.N.Parmon, Russian Journal of Applied Chemistry, 1999, vol.72, 1209.
10. Yu.V.Ostrovsky, G.M.Zabortsev, Z.R.Ismagilov, M.A.Kerzhentsev, Evaporation-condensation apparatus, Patent of Russian Federation No 2123375 (2000).

CATALYTIC DETOXICATION OF WET GAS EMISSIONS OVER OXIDE CATALYSTS IN ISOPRENE PRODUCTION

E.V. Alexandrovich, V.A. Chumachenko, T.V. Andrushkevich, V.M. Bondareva and G.Ya. Popova

JSC "Katalizator", Novosibirsk, Russia
Boreskov Institute of Catalysis SB RAS, Novosibirsk, Russia

Introduction

At present time oxide catalysts and catalysts, containing precious metals, including platinum, are widely used in the processes of industrial waste gases neutralization.

In this paper the possibility of using oxide catalysts for combustion of industrial waste gases, containing large amounts of water vapors, is being explored. Proposed is a solution for the problem of replacing expensive catalysts, containing precious metals, by much less expensive ones. Kinetic studies, mathematical modeling of the process and process optimization are the steps of this work. Results of the work are implemented at industrial plants.

The source of emissions and technology of purification

One of the most widespread technologies of isoprene production as a monomer of synthetic polyisoprene rubber (SPR) is a two-stage synthesis from isobutene and formaldehyde through intermediate formation of dimethyldioxane (DMD). DMD is then splitted on calcium-phosphate catalyst at 370-390 °C. After this cycle is completed, the reactor is purged by water steam, and the cycle of oxidative regeneration of catalyst starts again. The process of regeneration is periodical, it results in variation of volumetric flow of gases that are fed then to purification unit ("regeneration gases").

Table. Regeneration gases in isoprene production

№	Parameter	Value
1.	Flow rate, Q [Nm^3/h], ...	25000-30000
	U [Nm/s], ...	0.44 – 0.61
	including: 1) water steam, Q_1, [ton/h]..	16 – 18
	2) air R_1, Q_2 [Nm^3/h]	3000-8000
	3) air R_2, Q_3 [Nm^3/h]	600 – 2000
	4) air R_3, Q_4 [Nm^3/h]	1500
2.	Temperature, [C]	360 – 550
3.	Total content of impurities, [g/m^3]	1.3 – 4.5
4.	Efficiency of purification [%] over catalyst IP-62 (theoretical)	appx. 99

Regeneration gases, which are emitted in isoprene production, contain admixtures of organic compounds (isoprene, isobutylene, formaldehyde etc.), carbon monoxide as well as large amount of water vapors, see the table.

Fig. 1. **Technological flowsheet of purification unit**

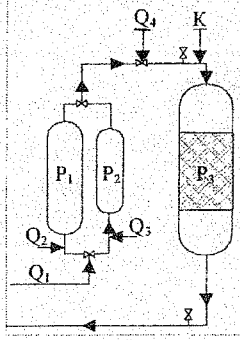

K – cooling condensate;
R_1, R_2 – large and small reactors for regeneration of calcium-phosphate catalyst by water steam;
R_3 – catalytic-reactor for detoxication of regeneration gases.

Purification of regeneration gases from toxic admixtures consists in their complete oxidation to carbon dioxide and water that is occurred on Pt-containing catalyst. The principle diagram of catalytic purification unit is shown on Fig. 1. Reactor is 4.5 m in diameter, height of the catalyst layer is 0.38 m, weight of catalyst is 3.9 tons.

Substantial losses of Pt from the catalyst were observed, due to high filtration speeds, elevated temperatures etc.

Kinetic studies

For kinetic studies were chosen carbon monoxide (CO) as the major and the most difficult-to-treat component of regeneration gases and formaldehyde (CH_2O) as the most toxic one.

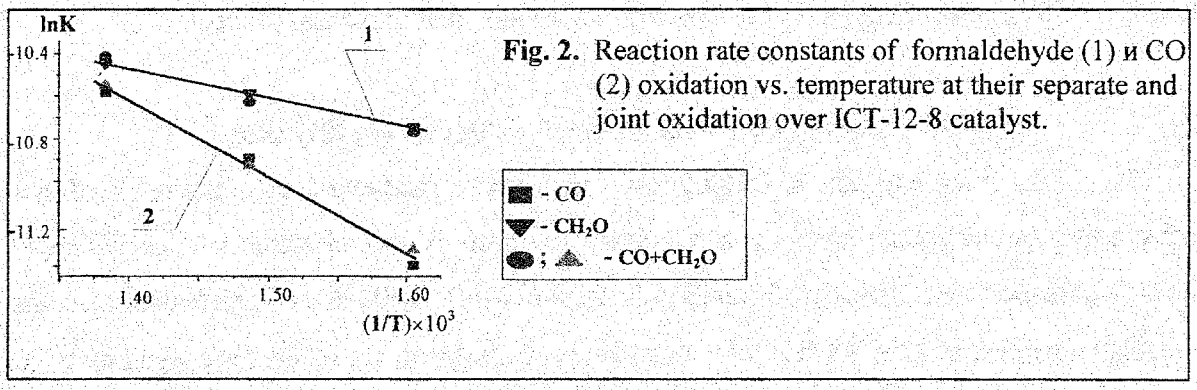

Fig. 2. Reaction rate constants of formaldehyde (1) и CO (2) oxidation vs. temperature at their separate and joint oxidation over ICT-12-8 catalyst.

To study the comparative working stability of various oxide catalysts under long-term hydrothermal treatment, we tested copper-chromium-alumina catalyst ICT-12-8 and manganese-alumina catalyst ICT-12-40 in reaction of CO oxidation. Experimental conditions in isothermal flow reactor were as follows - gas mixture content: H_2O = 70%, CO = 0.3%, air balance; τ = 0.92 s; T = 450 °C; time of hydrothermal treatment was more than 107 hrs. According to tests, ICT-12-8 catalyst was chosen as the most active and stable.

The kinetic studies of CO and CH_2O oxidation (both separately and jointly) in large excess of water vapors were carried out over industrial samples of selected ICT-12-8 catalyst (rings, 7 and 15 mm in dia.) and Pt-containing catalyst IP-62 (0.6% Pt, 2.8 mm in dia.). Experimental conditions in isothermal gradientless circulation flow reactor were as follows - gas mixture content (%): $H_2O/CO/CH_2O$ = 70/(0.28÷0.3):(0.5÷1.0), air balance; T = 350÷550 °C. At given conditions, the 1st order kinetic law was determined in oxidation of individual CO

and CH_2O, interference of CO and CH_2O was not noticed. Kinetic parameters in diffusion-control region were measured and presented in Fig. 2 for 15-mm rings.

Mathematical modelling and economic evaluation

Mathematical modelling of the process was made using quasistationary one-dimensional model of a fixed bed catalytic reactor, that considers processes of mass and heat transfer along the catalyst bed.

To meet legal regulations for content of toxic components in regeneration gases emission, the efficiency of purification over any type of catalyst should be no less than 99%.

Calculations for inlet gas temperature T=450 °C, total inlet content of toxic components Co=2.9 g/m^3, gas velocity U=0.52 Nm/s (considered as nominal entry conditions) let to determine the minimum bed heights of ICT-12-8 catalyst (rings, 7 or 15 mm in dia.) that provide effective CO conversion in regeneration gases (X_{CO} = 99%).

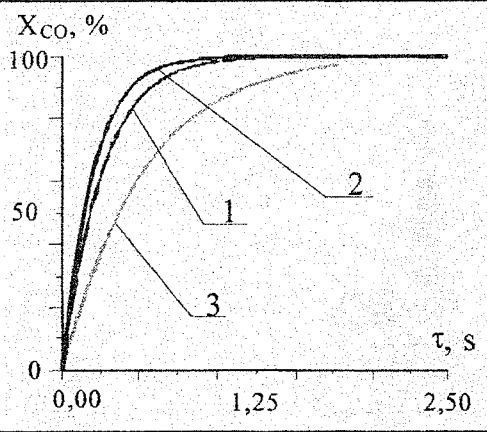

Fig. 3. Dependence of carbon monoxide conversion X_{CO} vs. contact time τ at various regimes.

Catalyst ICT-12-8 bed height H=1.1 m; rings 15 mm in dia.
1 – total content of impurities C_0 = 2.9 g/m^3 (incl. C_{CO} = 1.4 g/m^3), inlet temperature T_0 = 450 °C, linear velocity U=0.52 Nm/s (nominal regime);
2 – C_0 = 4.5 g/m^3 (incl. C_{CO} = 2.4 g/m^3), T_0 = 550 °C, U=0.44 Nm/h;
3 - C_0 = 1.4 g/m^3 (incl. C_{CO} = 0.4 g/m^3), T_0 = 360 °C, U=0.61 Nm/h.

All inlet technological parameters are subjected to strong variations during industrial work. Modeling of the process of CO and CH_2O oxidation and selection of optimal technological regimes were performed under parameters within ranges: inlet temperature 360-450 °C, content of impurities 1.3-4.5 g/m^3, volume gas rates (25-35)·10^3 Nm^3/h. Some of the results are shown in Fig. 3.

According to results of technological parameters evaluation there had been performed a calculation of economical characteristics of oxide catalyst operation compared to Pt-containing catalyst IP-62. It was assumed, that catalyst life-time, effectiveness of purification and payments for gas emissions into atmosphere remains unchanged. The process of purification is conducted at the same reactor unit, without additional capital costs. Thus,

economical efficiency of replacement IP-62 catalyst by ICT-12-8 catalyst is mainly determined by the difference in the installed cost of both catalysts.

Results

For effective purification of regeneration gases the optimal height of ICT-12-8 catalyst d=7 mm and d=15 mm should be, accordingly, 1 and 1.15 m. Due to a higher activity of smaller rings, its loading is less, compared to larger rings. However, pressure drop of 7-mm rings exceeds the one of initial IP-62 catalyst (Fig. 4). Installed cost for IP-62 catalyst is more than 5 times higher than for ICT-12-8. Thus 15-mm rings ICT-12-8 catalyst is optimal for replacement. Assuming the bed's height 1.15 m and bulk density 0.65 g/cm^3, the optimal load of catalyst is 12 tons, which is about 3 times more than that of initial IP-62 catalyst.

Industrial application of the process

An industrial experiment at one of SPR plants in Russia was effected with respect to our recommendations. Pt-containing catalyst IP-62 (4 tons) was replaced by 15-mm ring-shaped oxide catalyst ICT-12-8 (12 tons).

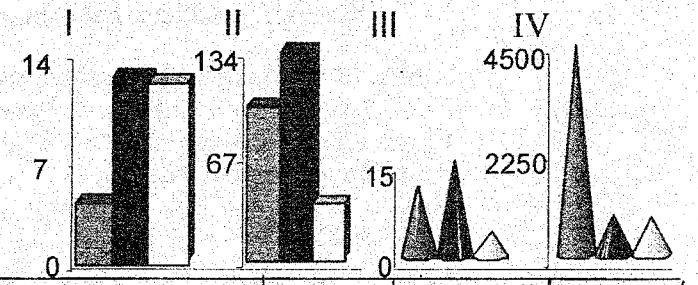

	I	II	III	IV
IP-62	3,9	98	11	4415
ICT-12-8 d=7mm	12,2	134	15	792
ICT-12-8 d=15mm	11,8	36	4	816

Fig.4. Comparison of technical and economical parameteres for catalysts IP-62 and ICT-12-8

I – catalyst loading, tons;
II – pressure drop, mm H2O;
III – annual operational costs (as electricity), thous. RUR;
IV – annual installed cost for catalyst, thous. RUR

The results of the long-term industrial experiment proved the fact that ICT-12-8 catalyst guarantees practically full degree of regeneration gases purification from CO and considerably high elimination of formaldehyde and other organic compounds. This allows to meet all requirements of maximum allowable emissions set for the given source of pollution.

AEROSOL CATALYSIS: A NEW LEAD IN DISPOSAL OF INDUSTRIAL WASTES

M.A. Glikin, D.A. Kutakova, E.A. Pavlyuk, I.M. Glikina, R.Y. Perestoronina

"Khimtekhnologiya" Institute, Ukraine, 93400, Severodonetsk, st. Vilesov, 1
Fax: (38 06452) 25367

In recent years the problem of decomposition of industrial and municipal wastes has become very actual. Nowadays it concerns not only specialists and scientists.

One of the methods for waste detoxication is incineration in special incinerators. Among shortcomings of this method are significant consumption of additional fuel due to insufficient calorific value of wastes to make a flare and severe operating regime of major equipment. Technology of waste oxidation in flame requires high capital and operating costs. It is widely known that flame treatment of a number of wastes does not comply with environmental safety requirements concerning effluents into atmosphere because thermal nitrogen oxides, carbon monoxide and carcinogenic compounds are generated in flame. During treatment of chlorine-containing wastes dioxines are produced which maximum permissible concentration is 0.1 ng/m^3. Removal of toxic components off the effluent requires additional after-treatment stages that complicate the process and practically double capital and operating costs.

As alternative to incineration technology of catalytical treatment of industrial wastes can be proposed. Classical catalysts present a system containing porous carrier and active component. Micro- and macropore ratio of carrier provides for a developed contact surface. Catalysis is widely used in treatment of gaseous wastes. Sometimes liquid wastes are evaporated and sent to a fixed catalyst bed. After evaporation there always remains concentrated liquid or solid sludge which are to be incinerated. Fluidized catalyst bed is known to be used for incineration of liquid wastes. However, presence of salts and considerable catalyst attrition make this technology unperspective. Use of the catalysts having carriers is connected with certain limitations, i.e.:

- compulsory preliminary evaporation of liquid wastes and unsolved problem of high-boiling wastes subjected to resinification;
- catalyst surface poisoning and coking by reaction products leading to loss of catalyst activity;
- intradiffusional retardations of reaction rate;
- high requirements to mechanical strength and heat resistance of the catalyst;
- difficulties connected with production of carriers;

– impossibility to treat liquid salt-containing and solid wastes.

One of catalysis applications is aerosol catalysis technology for waste treatment developed by 'Khimtekhnologiya' Institute (Severodonetsk, Ukraine). It is based on finely dispersed catalytically active component (without carrier) in form of solid aerosol. Particulate sizes amount down to nanometers. Elimination of carrier allows to avoid all above mentioned problems. A variant of this technology employs fluidized bed of inert material to provide high dispersity of catalyst particulates. Simultaneously high surface activity is attained due to mechanical activation in situ. Thus a complex problem of optimal surface and catalyst activity can be solved. Transfer from macroparticulates to micro- and nanosizes leads to changing in a number of significant for catalyst surface properties: adsorption, electric conductivity, surface energy, surface tension, electronic work function, electromagnetic effect, etc. Evidently, by this fact one can explain increase in reaction rate by 10^4 - 10^5 per 1 g of catalyst. Activity of aerosol particulates in a medium of solid salts and coke is kept due to mechanical activation. Fluidized bed of solid inert particulates acting as a ball mill is constantly renewing the surface of catalyst particulates. Equal accessibility to surface provides a complete oxidation of organic compounds of wastes to form thermally stable products such as carbon dioxide and water.

Systematic studies of aerosol catalysis efficiency were carried out in flow-type units. Major piece of a laboratory scale unit was reactor of 1 m in height and 50 mm in diameter. Pilot scale reactor was of 200 mm in diameter and 6.5 m in height. In reactor reaction zone a fluidized bed of inert particulates is combined with continuously moving flow of catalytically active material. Air was used as an oxidizing and fluidizing agent. Investigations were carried out for individual materials, model mixtures and real wastes. If required, oxidizing and fluidizing zones can be alternated along reactor height.

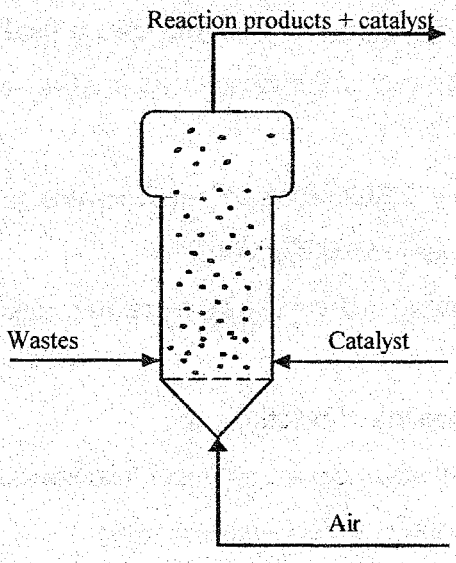

The results obtained showed that the new catalysis organization results in significant increase in catalyst activity. The problem of decrease in catalyst thermal stability and strength has been eliminated and catalyst preparation procedure has been simplified. The catalyst is completely suitable for reuse that allows to organize recycling. The outcomes obtained under aerosol catalysis conditions have been confirmed by performance of the pilot unit. Aerosol catalysis method of waste treatment has no limitations either on aggregate state of wastes or their quality and quantity structure.

To summarize all above said one can make a conclusion that aerosol catalysis technology will provide the following:

- increase in catalyst aerosol activity compared to classical catalysts using carriers;
- equal access to active surface;
- simplified catalytical system;
- continuous mechanical activation of the catalyst inside reaction zone;
- catalyst concentration control within reactor volume.

OP-V-4

SLP-As TECHNOLOGY FOR PURIFICATION OF WASTE GASES AND WATERS FROM SULFUR AND ARSENIC COMPOUNDS

Zinaida P. Pai

Boreskov Institute of Catalysis, Prosp. Akad. Lavrentieva, 5, 630090, Novosibirsk, Russia, E-mail: zpai@catalysis.nsk.su

High toxic arsenic compounds (AsH_3, As_2O_5, $AsCl_3$, As_2O_3, and As_2S_5 etc.) produced by different metallurgical enterprises give rise to a number of ecological and process problems.

About 70 thousand tons of arsenic are annually obtained together with raw materials for production of tin, lead, zinc, copper, gold, and other non-ferrous metals. Unfortunately, only 2.5% arsenic is utilized and 97% arsenic is discharged into atmosphere. It should be noted that 10% arsenic is discharged as industrial waste and 87%, as stored waste [1].

In industry, arsenic waste is routinely utilized by the below methods:

- production of low-toxic arsenic compounds such as As_2S_3, As_2Me_3, As, $AsMe_3$, $FeAsO_4$ etc;
- binding into astringent composites and slags (concretes, cements, polymers, and alloys with sulfur etc.);
- use of water-proofing materials (encapsulation, adsorption coverings, chemically bound coverings).

On processing of sulfide ores in metallurgy, the problem of complex utilization of sulfur and arsenic compounds (dioxide sulfur and arsenic dioxide), formed at the stage of high-temperature ore processing, becomes urgent. Waste gases containing the above compounds are very dangerous for environment.

Studies, performed at the Boreskov Institute of Catalysis for several years, permitted a design of the sulfur liquid purification (SLP) process which was used for design of SLP-2 and SLP-3 meant for purification of gases from SO_2 to produce elemental sulfur as a commercial product [2].

The process is based on the Claus reaction performed in the aqueous phase under mild conditions (40-60°C, 1 atm, pH = 4-6) in the presence of a homogeneous catalyst:

$$2\,H_2S + SO_2 \rightarrow 3\,S + 2\,H_2O$$

Despite the fact that stoichiometry of interaction between H_2S and SO_2 in the aqueous medium is similar to that of the gas-phase Claus reaction, the process chemistry differs much because of intermediates (sulfides, sulfites, hydrosulfite, thiosulfite, polythionates) providing sulfur generation on their reduction. Since the above intermediates can also interact with dissolved As_2O_3 to form non-toxic arsenic sulfide, we studied the kinetics and mechanism of the Claus reaction in the presence of As_2O_3 in the reaction mixture. Based on the study results, "SLP-As" for complex cleaning of metallurgical gases from sulfur and arsenic oxides was developed. The process provides almost a complete SO_2 and As_2O_3 (99.98%) removal from sorption solutions.

"SLP-As" belongs to the first version of the above methods for processing of arsenic waste (production of low-toxic arsenic compounds) into As_2S_3. Besides it has the elements of the second version (binding of the obtained arsenic sulfite by its sintering with elemental sulfur, which is also the final product of gas purification from SO_2). At present, the following work has been performed for developing and commercialization of "SLP-As":

1. Laboratory development;
2. Pilot testing of the method using the actual gases of tin production (the flow rate of purified gas, 300 l/h);
3. Commercial testing of the process using the actual plant at "Novosibirsk Tin Plant". The plant capacity with respect to the purified gas ranges from 8 to 20 thousand m^3/h.
4. Process regulations for preparing Feasibility Report on the plant (N = 80 thousand m^3/h) for a complex cleaning of waste gases from SO_2 and As_2O_3.
5. The Feasibility report for alternative purification methods suggested for consideration to the "Novosibirsk Tin Plant" Directorate:
   a) limestone method for purification of gases from SO_2 (developed by the State Institute of Nonferrous Mettalurgy, Moscow);
   b) electron beam method (developed by the Institute of Nuclear Physics, Novosibirsk);
   c) "SLP-As" (developed by the Boreskov Institute of Catalysis).

   The experts of "GIPRONIKEL" of "NORILSKNIKEL" (St. Petersburg) have shown that "SLP-As" is a profitable and environmentally safe process.
6. Jointly with the Central Research Institute of Tin (TsNIIOLOVO, Novosibirsk), we have studied potentials for further utilization of the purification products (sulfur and AsS). In particular, we proposed for commercialization:

- *the method of sulfur refining by alkaline allocation;*
- *the method of AsS utilization by its sintering with sulfur.*

7. The process of gas purification from SO_2 and As_2O_3 is covered by the Russian patent [3].

Investigation of As_2S_3 formation during interaction between As_2O_3 and thiosulfate and polythionates indicates that the method can be used for utilization of arsenic from sewage water produced by different ferrous-metal enterprises. Distribution of As in the gas, liquid and solid phases on processing of ferrous metals is shown in Table 1 [4].

Table 1.

Concentration of As in nonferrous metal ores

Production	Content of As	Extraction of As, %	
	in feed stock, %	With gases and dust	With waste water and solid wastes
Copper	0,2-2	70-90	5-16
Nickel	0,05	~ 15	49-45
Zinc	0,01-0,3	15-20*	70-80
Lead	0,05-1	5-10	10-25
Tin	3-7		10-30
traditional furnace		70-85	
in a boiling layer		90-95	
Antimony	0,1-1	20-35	5-15

** Extraction of As with a solution on leaching of burnts carried out in two stages.*

In spite of the fact that the original "SLP-As" method was designed for utilization of SO_2 and As_2O_3 from fuming gases of tin productions, the above data show that similar problems exist in different ferrous metal productions. Moreover, the problems of following utilization of cakes and electrolyte solutions containing arsenic compounds are acute (see Table 2). It should be noted that the concentration of arsenic in the electrolyte solutions can be 10-15 g/l (for Cu production) and 20 mg/l (for Ni production) etc.

Table 2.

Distribution of As on the electrolyte refinement of metals

Production	Fraction of As (%) transition ints		
	metal	waste water	solid waste
Copper	1-2	70-75	20-25
Nickel	0,1	80-85	1-2
Lead	-	2-10	10-25

For zinc production, the requirements imposed on arsenic isolation from solutions are especially rigid. The zinc production involves stages of solid waste leaching. At the acidic leaching stage, the concentration of As in the solution is 10-100 mg/l. At the neutral stage, 1 mg/l. Note that the concentration of As should not exceed 0.1 mg/l in the solution supplied for electrolyte zinc precipitation.

Thus, "SLP-As" can be used for purification of waste industrial gases and for isolation of As from sewages formed on production of copper, nickel, zinc, tin, lead, and antimony.

REFERENCES

1. Maksimov I.E. Problems arsenic in nonferrous metallurgy // Novosibirsk. - Institute of GIDROCVETMET. -1991.-18 p.
2. Pai Z.P., Yermakova A. Utilization of Industrial sulfur of Gases on the basis of SLP // CHEMREACTOR-13 - Part I.- Novosibirsk.- 1996.- P. 219-223.
3. Patent Russian Federation № 2077932 "Method of purification of industrial gases from SO_2 and As_2O_3" // Pai Z.P., Yermakova A., Kundo N. N. et al. -1997. -Bull.Izobr. - № 12.
4. Pai Z.P. Scientific creation of catalytic complex liquid-phase purification methods of gases from SO_2, NO_x, As_2O_3, H_2S, COS and HCN // Thesis for a Doctor's degree/ Novosibirsk.- 2000.- 421 p.

OP-V-5

CATALYTIC INCINERATION OF MUNICIPAL SEWAGE SLUDGE

O.V. Sumenkova, A.D. Simonov, N.A. Yazykov

Boreskov Institute of Catalysis, SB RAS
Novosibirsk, 630090, Russia
Fax (383 2)343269, e-mail: sumenk@catalysis.nsk.su

Annual amount of sludge resulting from municipal wastewater treatment facilities in Russia exceeds 2.5 million tons [1]. Wastewater sludge is a slurred organic-mineral substance showing high wetness (99.5-99.7%) and containing a wide variety of chemical elements, including heavy metals. A lot of organic compounds contained in the sludge posses mutagenic activity. Besides, sludge is a substrate containing pathogenic microorganisms threatening human health [2]. For this reason, agricultural use of the sludge is problematic.

The main method to neutralize municipal wastewater sludge, used both in Russia and abroad, consists in its storage in dewatered plants. Because of high sludge wetness, the systems occupy vast territories. Existing sludge-storage systems are overloaded. As a result, toxic compounds and heavy metals accumulate in the ground, infiltrate into ground waters; come into atmosphere with dust.

More reliable method to neutralize toxic deposits consists in their high-temperature combustion, for example, in layered fire-chambers, torch furnaces, fluidized-bed furnaces loaded with inert material. However, this leads to air pollution with toxic combustion products (CO, NO_x, SO_x, benzapirens, etc.).

A novel process for catalytic fluidized-bed incineration of various fuels and wastes has been developed at the Boreskov Institute of Catalysis. The process is free from the major disadvantages of high-temperature combustion. Moreover, it allows:

- autothermal operation when incinerating sludge of <75% wetness and thus provides essential fuel savings;
- more then 20 times decrease of reactor dimensions and metal-intensity in comparison with known burning technology;
- sharp decrease of toxic emissions, including organic substances, nitrogen oxides, sulfur oxides, carbon oxide.

Indeed, flue gas, resulting from the incineration of solid wastes in a fluidized sand bed reactor (Tsukishima Kikai, Japan) at Ust-Ilimsk Timber-Processing Complex, contains 800

mg/m^3 NO_x, 1500 mg/m^3 CO, 1000 mg/m^3 SO_x, while catalytic combustion emits only 50 mg/m^3 NO_x, 60 mg/m^3 CO and 5 mg/m^3 SO_x [3].

The results of sludge incineration at Municipal Unitary Enterprise «Gorvodokanal» in the city of Novosibirsk are discussed below.

Organic substances, including sulphur and phosphorus, constitute 37.46% of the sludge. Table 1 presents elementary composition of the organic sludge fraction.

Table 1

Elements' content in organic fraction of sewage sludge

C^c, wt. %	H^c, wt. %	N^c, wt. %	P^c, wt. %	Cl^c, wt. %	O^c, wt. %	S^c, wt. %	A^c, wt. %	Total, wt. %
18,25	2,54	1,90	0.40	0.21	13,39	0,77	62,54	100

The analysis of mineral part of dry sludge shown about 20 various elements in it.

Table 2

The data of analysis of sewage sludge by X-ray fluorescence (XRF) method

Contents, wt.%	Elements
10-50	Fe, Si, Zn
1.0-10	Al, Ca, K
0.1-1.0	Zr, Y, Sr, Rb, Cu, Ni, Cr, Mn, Ti, S,
<0.1	Pb, Hg, Cl, P

Analysis of mineral part of dried sludge revealed the presence of 20 chemical elements. According to the data of XRF analysis, Fe, Si, and Zn were the main elements in the mineral sludge fraction, the content of Al, Ca and K was evaluated by several percents. The content of other elements, including heavy metals, sulfur, phosphorus, was represented by tenths and hundreds parts of percent.

Incineration of sludge sample was performed in a lab-scale catalytic unit (see Fig. 1). The reactor of 40 mm in diameter, fitted with distributing grid, was charged with 400 cm^3 of Al-Cu-Mg-Cr catalyst with an average particle size of 1.5-2.0 mm; the flow rate of fluidizing air was 3 m^3/h; consumption of deposit for incineration – 360 g/h. The contact time is 1.5 sec. The gas rate in reactor - 0.7 m^3/s. Experimental run was accompanied by the analysis of deposit, flue gases, and solid combustion products.

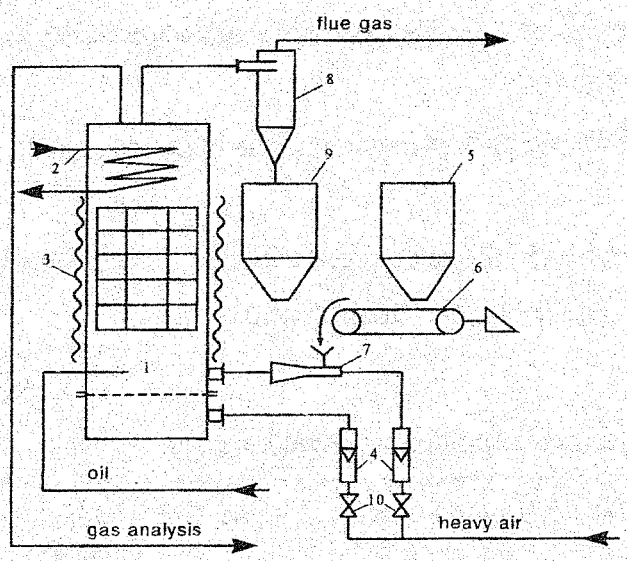

1. Reactor
2. Heat-exchanger
3. External electric heater
4. Rotameters.
5. Tank for solid fuel or wastes
6. Transporter
7. Ejector
8. Cyclone
9. Ash collecting tank
10. Regulating valves

Fig. 1. Layout of lab-scale catalytic incineration unit.

Fig. 2 shows how the burning-out degree and ash content of communal sludge sample changes with temperature. It is seen that at 500°C the burning-out degree attains 94%. As the temperature increases to 700°C, the burning-out degree rises to 98.2%. The ash content in the sample also increases with temperature (from 87% at 500°C to 98% at 700°C). It shows that the light-oxidation components are in the basis of organic fraction of the sludge.

Chromatographic analysis of flue gases made on gas chromatograph with limit inferior of detection less than 10 ppm. The analysis of flue gases resulting from combustion at 700°C proved the absence of CO, CH_4 and SO_2. As the process temperature decreased to 500°C, the CO concentration in the exit gas flow increased gradually to 0.22 vol.%, while NO_x concentration lowered from 131 mg/m^3 to 42 mg/m^3 (Fig. 3).

In order to determine the HCl and P_2O_5 concentration in the reactor flue gas, the latter was bubbled through distilled water. Analysis of the obtained solution provided data for the calculation of toxic compounds content in the flue gas. It was found that at the process temperature of 700°C the flue gases contained 50 mg/m^3 of HCl and 0.22 mg/m^3 of P_2O_5.

The comparison of elements content in the organic part of municipal wastewater sludge (Table 1) with that of the mineral deposit (Table 2) proves that the most amount of chlorine and phosphorus associate with organic substances. The data of Table 1 and the amounts of Cl and P in flue gas suggest that P_2O_5 bounds with mineral part most completely (bounding degree 99.98%); the degree of HCl bounding with mineral deposit equals 77.20%.

Mercury compounds (sulfates, chlorides, oxides) are very dangerous, because they decompose even at 400°C releasing atomic mercury. Mercury content in the initial deposit and solid combustion products was determined by XRF with multiple amplification.

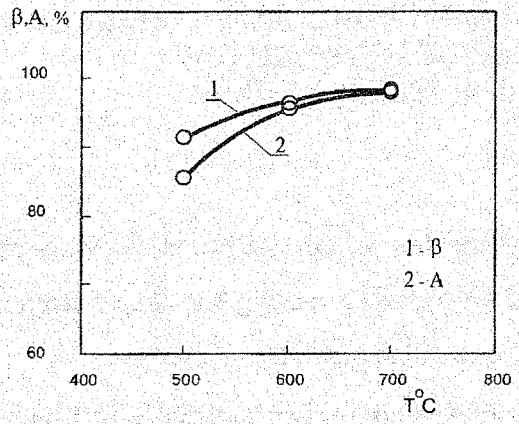

Fig. 2. Changing of the burning-out degree and ash with temperature

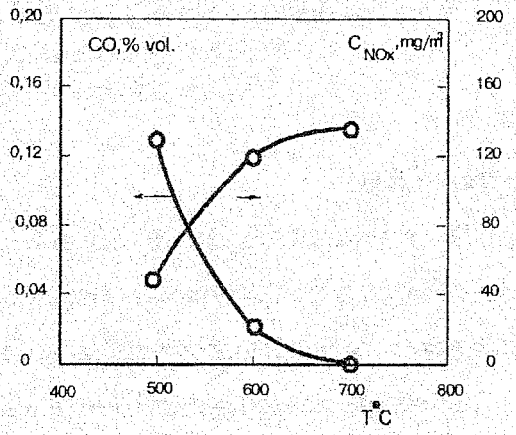

Fig. 3. Changing of concentrations of CO and NO_x in flue gases with different temperatures

It was found that initial deposit contained $7 \cdot 10^{-4}$ wt.% Hg, solid combustion product - $5 \cdot 10^{-4}$ wt.%, that is, mineral part bounds 46% of Hg. The maximum permissible emission of Hg in Russia is $2.33 \cdot 10^{-3}$ g/s [4]. The emission of Hg resulting from catalytic incineration of municipal wastewater sludge sample was $1.08 \cdot 10^{-3}$ g/s that is better then the permissible concentration limit.

Thus, the results obtained demonstrate that the process of catalytic incineration of municipal wastewater sludge provides permissible concentrations of toxic compounds in flue gases and therefore is recommended for practical use at municipal purification facilities.

References:

1. Rusakov N.V., Merzlaya G.E., Afanas'ev R.A, etc., Gigiena i Sanitariya, 1995, №4, pp. 6-10 (in Russ.)
2. Latypova V.Z., Selivanovskaya S.Yu., Ecological Chemistry, 1999, v. 8, № 2, pp. 119-129 (in Russ.)
3. Siminov A.D., Chemistry for Sustainable Development, 1998, v. 6, pp. 227-292 (in Russ.)
4. Bespamyatnov G.P., Bogushevskaya K.K., Bespamyatnova A.V., etc. Permissble concentration limits of toxic compounds in air and water, Leningrad, Khimiya, 1975, pp.10-19 (in Russ.)

OP-V-6

CATALYTIC OXIDATION OF POLLUTANTS IN INDUSTRIAL WASTE WATERS

Nikolay M. Dobrynkin, Marina V. Batygina and Aleksander S. Noskov

Boreskov Institute of Catalysis of Siberian Branch of Russian Academy of Sciences,
Pr. Ak. Lavrentieva, 5, Novosibirsk-90, 630090, RUSSIA
Fax: + 7-3832-341878, E-mail: dbn@catalysis.nsk.su

Introduction

The subject of the present research is the determination of the conditions for an effective realization of the oxidation reactions of organic and inorganic polluting substances from multicomponent technological solutions and wastewater of the industrial enterprises.

Among pollutants, nitrogen - containing (up simple compounds - ammonia, acetonitrile to aromatics), oxygen - containing (alcohols, acids and ethers of a various structure), chlorine - containing (tetrachloromethane, dichlorethane and chlorobenzenes), sulphurous compounds (sulfide, thioles and others) are widespread. The concentrations of individual substances are from 0.01 up to 100 g/l ordinarily. An opportunity of the application of the methods of biological treatment is limited by the toxicity of many substances. The application of the burning or the separation of substances is economically inefficient for the concentrations up to 100 g/l. The most expedient way for the treatment of similar wastewater is the process of oxidation (by air, oxygen or hydrogen peroxide) in a liquid phase at the increased temperatures and pressures using specially designed solid catalysts.

The modern catalysts [1-5] in this case allow to abatement inorganic and organic substances from wastewater by transformation of N- and O-containing organic compounds to nitrogen, carbon dioxide and water, realizing the total mineralization of the dissolved components. Sulfurous compounds oxidize into sulfates, Cl- containing - to chlorides.

Experimental

The experiments were carried out (1) in a perfectly mixed batch reactor, and (2) in a fixed-bed upflow reactor (batch reactor volume is 200 ml, solution volume - 100 – 150 ml, catalyst weight - 1 g, time - 1 h) at T = 373 K and P = 1.0 MPa for Na_2S, 403-473 K and 1.5-3.6 MPa for C, H, O-containing compounds, 423- 533 K and 2.0-4.6 MPa for N-containing compounds, 473-513 K for Cl-containing compounds.

Solutions. The model solutions of chlorine- and nitrogen containing substances and real wastewater of chocolate factory and alcohol plant (oxygen-containing compounds), petrochemical plant (sulfurous substances), chemical-recovery plant (ammonia, sulfurous sub-

stances) were tested. Initial concentrations of contaminants were up 0.1 to 60 g/l, pH were up 6.0 to 14.

As *catalysts* we tested:

I. various types of commercial graphite-like materials Sibunit with different physico-chemical properties; platinum-palladium catalysts supported on fiber glass and Sibunit;

II. metal (Pt, Pd) and metal-oxide (M = Mn, Cr, Fe) supported systems - the typical catalysts of complete oxidation in gases;

III. sulfides of cobalt, nickel, rhenium, molybdenum and tungsten supported on Sibunits (in the reaction of sulfide oxidation).

Analysis. Typical gas chromatographic analysis (gas chromatograph CVET –560, TCD + FID) was used to determine both the concentrations of the main organic components in water solutions and a composition of gas phase (O_2, CO_2, CO, N_2, N_2O, NO, NH_3). The analysis of intermediates formed in the liquid-phase oxidation was performed by chromato-mass-spectrometry on a VG-7070. We used HPLC to follow NO_3^-, NO_2^-, CO_3^{2-} and SO_4^{2-} ions (Millichrom-1), an iodine titration to follow sulfide, sulfite and thiosulfate ions. Additionally routine chemical analysis was applied to determine the concentrations of separate ions and total content of the contaminants.

Results and discussion

It is defined, that:

Among the different types of the catalysts the graphite-like carbons - sibunit and Ru/sibunit are most active and selective in the reactions of oxidation of the heteroatomic molecules.

For the oxidation of ammonia in pure solutions it is defined that N_2 formation very strongly depends on reaction temperature (Fig. 1). The absence of NO_3- and NO_2- in a liquid phase and NO_x and N_2O - in gas phase point out for high selectivity of NH_3 oxidation to N_2.

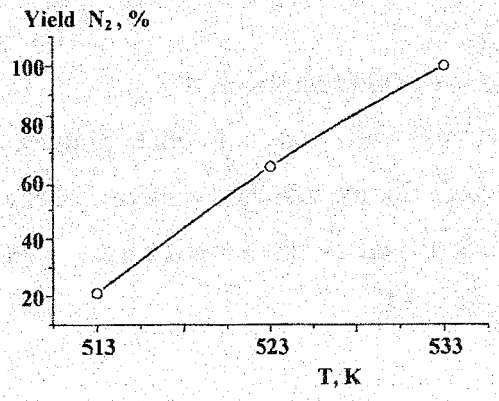

Fig. 1. Ammonia oxidation (C_{NH3} = 1 g/l) in the presence of 5% Ru/sibunit catalyst. P_{O2}= 10 atm, t= 1h.

Table 1.

Ammonia oxidation (C_{NH3} =1 g/l) at T=523 K, P_{O2} = 10 atm. Batch reactor, t = 0.5 - 1h.

Catalyst	pH		P_{total}, atm	Yield N_2, %	
	initial	final		t = 30 min	t = 60 min
Sibunit-4	10,6	7,2	44	82,0	100,0
Sibunit-3	10,6	10,0	38,4	36,0	91,0
5%Ru/ Sibunit-3	10,6	7,2	46,0	87,0	100,0

For wastewater containing N-C- compounds is shown, that:

1. Ammonia is a main product for a noncatalytic liquid-phase oxidation, whereas the use of 4.8 wt.% Ru/Sibunit-3 and the various types of Sibunits allow to realize a selective oxidation to molecular nitrogen without the formation of ammonia.
2. The conversion and selectivity to N_2 essentially depend on the type of Sibunit:
   A) The conversion and CO_2 yield is an average pore size dependent: the more an average pore size, the higher conversion and CO_2 yield.
   B) The conversion and selectivity to N_2 is a dependent of the concentration of carboxylate fragments on the Sibunit surface: the higher concentration, the higher conversion and selectivity to N_2.
3. The stability of the catalysts depends on the type of Sibunit. The more average pore size, the higher a degree of Sibunit destruction as a result of an oxidation to CO_2.
4. The introducing of Ru in Sibunit allows not only to increase of the catalytic activity, but also to raise an upper bound of their temperature stability, that is an important for N- containing compounds, those an effective oxidation take place at T = 493-533 K.

For the oxidation of wastewater containing H-C-O - compounds is shown, that:

– The conversion increases with an increase of the ratio C/MW (where C is the weight of carbon composed of one molecule, MW - molecular weight).

For the oxidation of chlorine-containing organic compounds is shown, that:

– Both for chloroform and dichloroethane, CO_2 and HCl are the basic products of oxidation. Track amounts of formic and acetic acids are detected. The experiments performed demonstrate that the use of sibunit as catalyst remarkably increases the yield of CO_2. The complete oxidation of this substances take place at T=493-513 K.

For the oxidation of Na_2S is shown, that:

Liquid-phase oxidation of sodium sulfide to sodium sulfate on Sibunits in an alkaline medium goes totally in one stage via transfer of 8 electrons (S^{2-} to S^{6+}) by electrochemical mechanism with a rate ~ 10^2 mol $O_2/L \cdot s \cdot m^2C$, and end in milliseconds. The rate of electrochemical Na_2S oxidation by molecular oxygen is determined by the mass exchange of oxygen in system gas-liquid-solid catalyst. According to the calculated data *oxygen transportation through interface liquid-catalyst is the limiting process* of sodium sulfide oxidation on the studied diapason of starting parameters. Mass and heat transfer parameters, oxygen supply are estimated for the process design with liquid circulation. Optimal process conditions were defined.

Long-term tests of catalyst performance show that graphite-like carbon is not only active and selective, but also a rather stable catalyst.

References:

[1] Seiichiro Imamura. Catalytic and Noncatalytic Wet Oxidation, Ind. Eng. Chem. Ras., 1999, 38, 1743-1753.

[2] Batygina M.V., Dobrynkin N.M. and Noskov A.S Advances Environ. Res. J., 2000, vol. 4, p.123-132.

[3] Imamura S., Dol A., Ishida S., Ind. Eng. Chem. Prod. Res. Dev. 1985, 24, 75.

[4] Oba Y., Nakamura E., Kirihara T., Treatment of Oxidized Liquor from WAO Process by Catalytic Oxidation, Geseido Kyokaishi, 1985, 22, 69, Chem. Abstr., 1995, 122, 221805.

[5] Bal'zhinimaev B.S., Batygina M.V., Dobrynkin N.M., Likholobov V.A., Noskov A.S., et.al., 12th Int. Congr. on Catalysis, Recent Reports of the 12thICC, Granada, Spain, July 9–14, 2000. CD-ROM, RR035.

Acknowledgement

This study is financial supported by the Ministry of Education of Russian Federation within the project 02.01.039 under subprogram 207 "Ecology and rational nature management". The support is gratefully acknowledged.

Special thanks are due to Valerii Kuz'min and Viktor Korotkikh for their technical assistance.

POSTERS

KINETIC OF ESTERIFICATION OF ACRYLIC ACID WITH METHANOL AND ETHANOL

Miroslaw Grzesik and Mariusz Witczak*

Institute of Chemical Engineering, Polish Academy of Sciences, Baltycka 5, 44-100 Gliwice, Poland, Tel./Fax +48 32 2 310318, E-mail: rrgrzesi@cyf.kr.edu.pl
**Faculty of Food Technology, Agricultural Academy, Krakow, Poland,*

Introduction

Acrylates are primarily used to prepare emulsions and solutions of polymers. Acrylate polymer emulsions have found wide utility as coatings, finishes and binders for leather, textiles and paper [1]. Methyl and ethyl acrylate are ones of the most extensively used in industry.

The esterification of acrylic acid with aliphatic alcohols proceeds as an equilibrium reaction:

$CH_2 = CHCOOH + ROH \leftrightarrow CH_2 = CHCOOR + H_2O$

Some of the kinetic studies have described the esterification of acrylic acid with methanol [2,3], ethanol [2,4] catalysed by sulphuric acid. Malshe and Chandalia [2] found that the kinetic data for the H_2SO_4 – catalysed esterification of acrylic acid with methanol and ethanol could be satisfactorily correlated by an elementary reversible rate expression based on the classical kinetics. Rubinstein et al. [4] have shown that the reaction rate changes linearly with the sulphuric acid concentration. They carried out their studies in the closed vessels, at the range of temperatures 333-363 K. At these conditions they confirmed that the catalytic esterification of acrylic acid with ethanol was second order.

Because of the absence of stable and suitable conditions in various study from the standpoint of its reversibility (or irreversibility) seems to be the reason for the discrepancies between the various kinetic models given in the literature.

The aim of our study was to develop rigorous kinetic equations for the esterification of acrylic acid with methanol and ethanol in the presence of H_2SO_4 as catalyst.

Experimental

The apparatus used was three - necked glass flask of 0,1 dm^3 capacity with the heating jacket connected with a thermostat. This flask was equipped with a thermometer, a high-speed magnetic mixer, a head for collecting samples and a cooler. The following initial molar ratios of acrylic acid to methanol and ethanol were used: 1:2, 1:3, 1:4; the concentrations of sulphuric acid employed were 0.5, 1, 2, 3, 4 wt. %; the range of temperatures: 39-60 ^oC for

methanol and 45-75 °C for ethanol. Acrylic acid was purified by the distillation under vacuum. Hydroquinone (0.2 wt.%) was used as an effective polymerisation inhibitor.

Alcohol and sulphuric acid in exactly weighted amounts were placed in a three-necked flask and heated to the required temperature. Acrylic acid was then added and the mixture was stirred continuously. When the mixture reached the required temperature, a sample was taken and this moment was considered as the beginning of the experiment. Liquid chromatographic (HPLC) analysis didn't show any by-products in this reaction and the progress of the reaction was monitored directly by the determination of the acid number of samples taken from the reacting mixture.

The conversion α^{exp} of acrylic acid was calculated from:

$$\alpha(\tau) = 1 - \frac{LK(\tau) \cdot m_o}{n_{Ao} \cdot 56000}, \tag{1}$$

where n_{Ao} is the initial mole number of acrylic acid, m_o is total mass of reagents in reactor, $LK(\tau)$ is the acid number after the time τ and 56000 is an analytical factor.

The experimental values α^{exp} were compared with the values α, which were obtained by integrate the balance equation for the batch reactor:

$$\frac{d\alpha}{d\tau} = \frac{V \cdot r}{n_{Ao}}, \tag{2}$$

with initial condition $\alpha = \alpha_o$ for $\tau = \tau_o$, and where r is a kinetic equation of first order, second etc. In the next step the experimental values of acid numbers were compared with these values obtained by integration of the equation (2).

The criterion of fitting of the experimental data to the calculated results was the following objective function:

$$\sum_{j=1}^{M}\sum_{i=1}^{N} abs(\alpha_{ij}^{com} - \alpha_{ij}^{\exp}) / \alpha_{ij}^{\exp} \longrightarrow \underset{k_0,\, E \text{ or } k(M=1)}{\text{MIN}}, \tag{3}$$

where j refer to a set –experiment, i apply to the sampling with regard to time, M is the number of a set-experiments, N is a number of the samples.

The selection criterion of the true form of a kinetic equation was a small scatter of kinetic constants for several experiments which were taken at the constant temperature but at different initial molar ratios alcohol/acrylic acid. This discrimination was very efficient and permitted explicitly to determine the right kinetic order. The frequency factor k_0 and energy of activation E was calculated from the Arrhenius equation on the basis of the average reaction

rate constants at different temperatures after the kinetic order and the form of kinetic equation have been determined. In the last step the calculations were taken for all set-experiments again. The values k_0 and E estimated in the previous step were taken as a start point. The Marquardt method was used for the determination of minimum of the function (3). The fitting of experimental data to the mathematical model has been realised with the least square method.

Results and Discussion

Unexpectedly, both studied reactions seem to be of a forth order - second order with respect to acid and second order with respect to alcohol for the forward reaction and also forth order for the backward reaction with respect to ester and water in the presence of sulphuric acid as a catalyst (double square kinetics). The rate of reactions are proportional to the catalyst concentration.

Final kinetic equations are listed below (R = 1.987 cal/mol K, T - temperature):

acrylic acid + methanol (A-acrylic acid, M-methanol, E-ester, cat-sulphuric acid):

$r = k\, c_{cat} (c_A^2 c_M^2 - c_E^2 c_W^2/K_M^2)$, where $K_M = 2.5\ 10^6 \exp(-8980\pm50/RT)$

and $k = 1.88\ 10^{-6} \exp(-15200\pm200/RT)$ $[m^{12}/(mol^4\ min)]$

acrylic acid + ethanol (Et-ethanol):

$r = k\, c_{cat} (c_K^2 c_{Et}^2 - c_E^2 c_W^2/K_{Et}^2)$, where $K_{Et} = 2.7\ 10^4 \exp(-6490\pm50/RT)$

and $k = 4.83\ 10^{-6} \exp(-15900\pm100/RT)$ $[m^{12}/(mol^4\ min)]$

Results from the comparisons between theoretically calculated (solid lines) and experimentally measured (individual symbols) acid numbers are shown for the esterification of acrylic acid with methanol (Figures 1-3), and for the esterification of acrylic acid with ethanol (Figures 4-6).

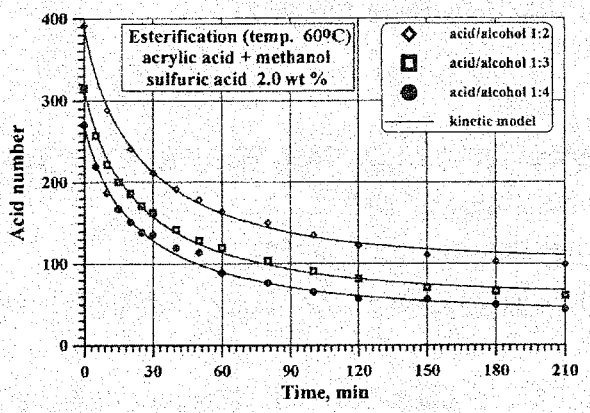

Fig.1.

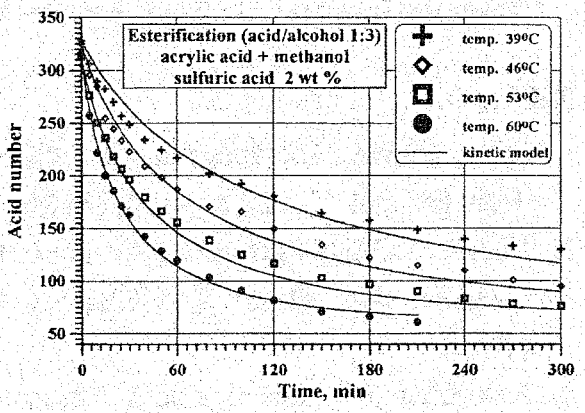

Fig.2.

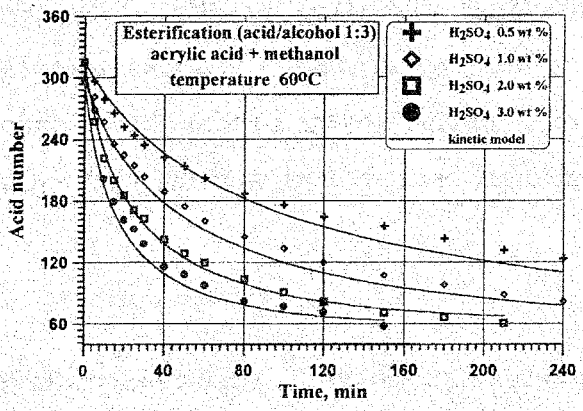

Fig.3.

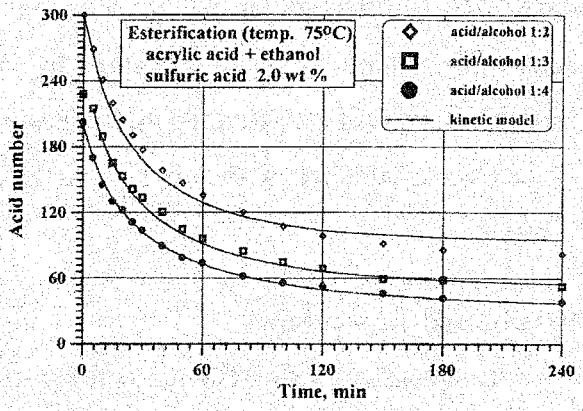

Fig.4.

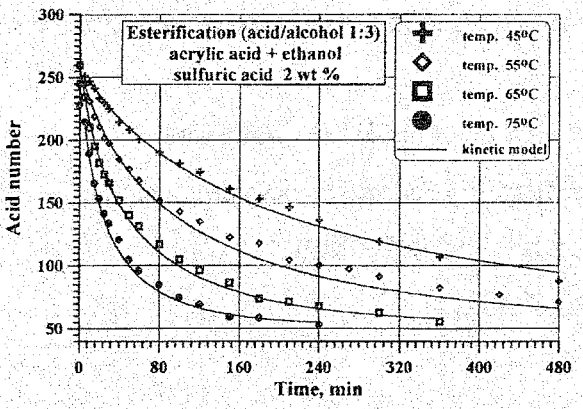

Fig.5.

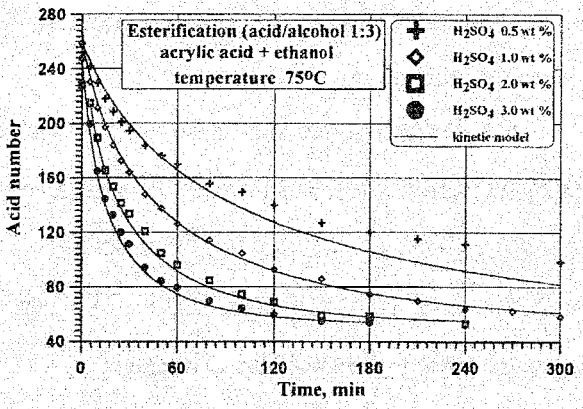

Fig.6.

Conclusions

(1) The liquid phase esterification of acrylic acid with methanol and ethanol in the presence of sulphuric acid as a catalyst follows non elementary, reversible kinetics.

(2) The kinetic model proposed gives the results which fit well experimental data.

(3) Obtained kinetic equations can be utilised in a process of designing and in optimization of industrial chemical reactors for a synthesis of aliphatic alcohols esters.

References

1. Kirk - Othmer: The Encyclopaedia of Chemical Technology, (John Wiley & Sons, Eds.), 4-Th. ed., Vol. 1, p. 288, New York, Chichester, Toronto 1991.
2. Malshe V.C. and Chandalia S.B., Chem. Engng. Sci., *32*, 1530 (1977).
3. Czubarov G.A., Danov S.M., Logutov W.I., Starikova O.A.: Zh. Prik. Chim., *55*, 1204 (1982).
4. Rubinstein B.I., Leontiev Ja.A., Butakova T.V., Tomashchuk V.I., Morozov L.A., Zh. Prik. Chim., *45*, 214 (1972).

MULTICOMPONENT MASS TRANSPORT EFFECT IN A PELLET OF THE METHANOL SYNTHESIS CATALYST

Miroslaw Grzesik and Jerzy Skrypek*

**Institute of Chemical Engineering, Polish Academy of Sciences, Gliwice, Poland*
Faculty of Food Technology, Agricultural Academy, 31-425 Krakow, Al. 29 Listopada 46, Poland, Fax: +48 12 4 117753, E-mail: rrgrzesi@cyf.kr.edu.pl

Introduction

Internal mass transport in porous pellets can have a considerable influence on processes occurring in chemical reactors. In many situation this phenomenon produces an undesirable effect resulting in decrease of the overall process rate. However, in certain special cases, especially in multicomponent and multireaction systems the effect of intraparticle diffusion becomes equivocal. For certain parameters regions the overall process rate increases, while for others decreases (Skrzypek et al., 1985).

In this work we study the multicomponent mass transport effect in a pellet of the methanol synthesis catalyst. The attention is focused not only on the effect of the pellet size (internal resistance to mass transport) on the reactants concentration /profiles in the pellet and on the values of the effectiveness factors, but also, on the influence of the variable initial composition of the gaseous mixture. This, we believe, should enable us to better understand the phenomena taking place in a pellet of the$CuO-ZnO-Al_2O_3$-catalyst.

Mathematical model

Methanol is one of the most important products of the organic synthesis. The process, according to the modern low-pressure technology, is carried out over a porous copper catalyst. A number of studies suggest that during the synthesis of methanol over a Cu-type catalyst, methanol is produced directly from carbon dioxide rather than from carbon monoxide, according to the following stoichiometric equation:

$$CO_2 + 3H_2 \Longleftrightarrow CH_3OH + H_2O \qquad (1)$$

with the conversion of carbon monoxide as a side reaction:

$$CO_2 + H_2 \Longleftrightarrow CO + H_2O \qquad (2)$$

This reaction progresses from the left-hand side to the right provided the reactants do not contain CO.

In the papers by Skrzypek et al., 1991 extensive kinetic studies have been carried out dealing with the methanol synthesis over a domestic $CuO-ZnO-Al_2O_3$-catalyst. The analysis of the experiments led to kinetic equations of the Langmuir-Hinshelwood type:

$$R_1 = k_1 K_{H2}^2 K_{CO2} \frac{\left\{p_{H2}^2 p_{CO2} - p_{CH3OH} p_{H2O} / (p_{H2} K_{P1})\right\}}{(1 + K_{H2} p_{H2} + K_{CO2} p_{CO2} + K_{CH3OH} p_{CH3OH} + K_{H2O} p_{H2O} + K_{CO} p_{CO})^3}, \quad (3)$$

$$R_2 = k_2 K_{H2} K_{CO2} \frac{\left\{p_{H2} p_{CO2} - p_{CO} p_{H2O} / (p_{H2} K_{P2})\right\}}{(1 + K_{H2} p_{H2} + K_{CO2} p_{CO2} + K_{CH3OH} p_{CH3OH} + K_{H2O} p_{H2O} + K_{CO} p_{CO})^2}, \quad (4)$$

The values of model parameters are given in Skrzypek et al, 1991.

The above equations were employed in a general model describing multicomponent mass transport together with accompanying it isothermal chemical reactions in a porous catalyst pellet (Grzesik, 1988). The model is defined by the following equations, corresponding to a two-reaction, seven component system analysed (inerts: CH_4 and N_2):

$$\frac{d\Lambda_1}{dl} = l^m R_1(x), \quad (5)$$

$$\frac{d\Lambda_2}{dl} = l^m R_2(x), \quad (6)$$

$$\frac{dx_i}{dl} = \frac{1}{l^m}\left(\sum_{k=1}^{2} \Lambda_k \sum_{j=1}^{7} \nu_{jk} F_{ij}\right), \quad (7)$$

$$\frac{dP}{dl} = -\frac{RT}{l^m W}\left(\sum_{i=1}^{7} \frac{1}{D_i} \sum_{k=1}^{2} \nu_{ik} \Lambda_k\right) \quad (8)$$

subject to the following boundary conditions:

$$\Lambda_k \qquad for \quad l = 0, \quad k = 1,2, \quad (9)$$

$$x_i = x_{io} \qquad for \quad l = a, \quad i = 1,2,...,6, \quad (10)$$

$$P = P_o \qquad for \quad l = a, \quad (11)$$

where

$$x_7 = 1 - \sum_{i=1}^{6} x_i,$$

$$\Lambda_k = \Omega_k l^m, \quad k = 1,2$$

$$\sum_{k=1}^{2} \nu_{ik} \Omega_k = N_i, \quad i = 1,2,...,7$$

The model may be used in the reactor calculations only after it has been supplemented with the relations defining the effectiveness factors for a catalyst pellet:

$$\eta_1 = \left|\frac{r_{ov1}}{R_1(x)}\right| = \frac{m+1}{a^{m+1}}\left|\frac{\Lambda_1 a)}{R_1(x_o)}\right|, \quad (12)$$

$$\eta_2 = \left|\frac{r_{ov2}}{R_2(x)}\right| = \frac{m+1}{a^{m+1}}\left|\frac{\Lambda_2 a)}{R_2(x_o)}\right|. \quad (13)$$

Results and discussion

In order to solve the two-point boundary-value problem for the set of ordinary differential equations (5-11) an optimization method was employed.

The numerical simulation has been performed using frequency factors corresponding to one of the levels of catalyst activity measured under industrial conditions:

k_{o1} = 1.709 10^{10} [kmol/(kg kat h)]= 0.807 10^{13} [mol/(m^3s)]

k_{o2} = 8.326 10^{9} [kmol/(kg kat h)]= 3.932 10^{12} [mol/(m^3s)]

The selected values of process parameters are given below:

temperature: 475 K; total pressure: 50 atm; pellet geometry: sphere (m = 2); initial concentrations: $x_{CO}(a)$=0-0.25; $x_{CO2}(a)$=0-0.25, $x_{H2}(a)$=0.6-0.7; $x_{H2O}(a)$=0-0.1; $x_{CH3OH}(a)$=0; $x_{N2}(a)$=var; pellet radius: a=0.001-0.015 m; pellet density: = 700 kg/m^3; average pore radius: r=8 nm.

Some of the numerical results are presented in Figs 1 - 4:

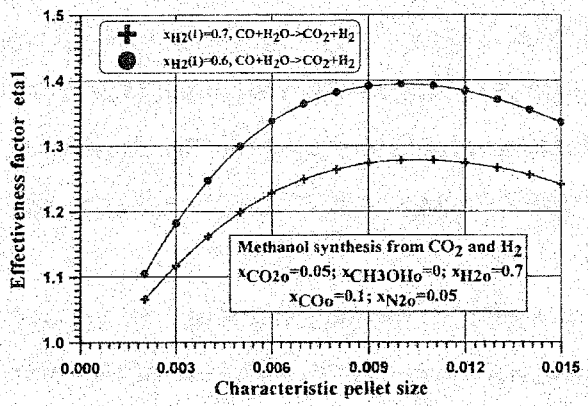

Fig.1.

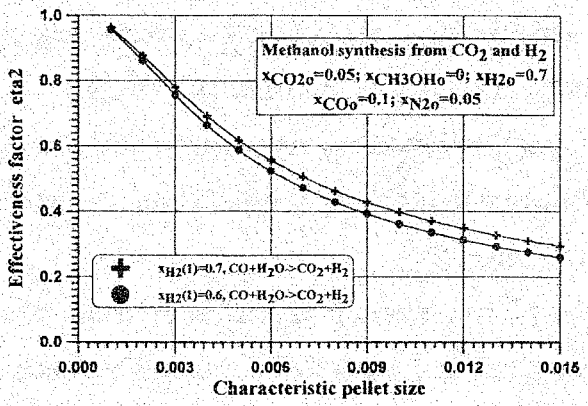

Fig.2.

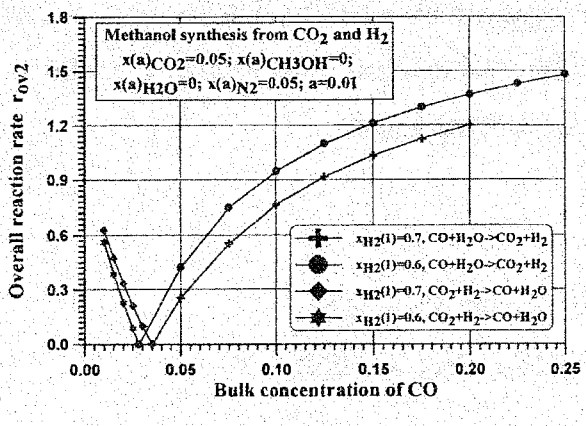

Fig.3.

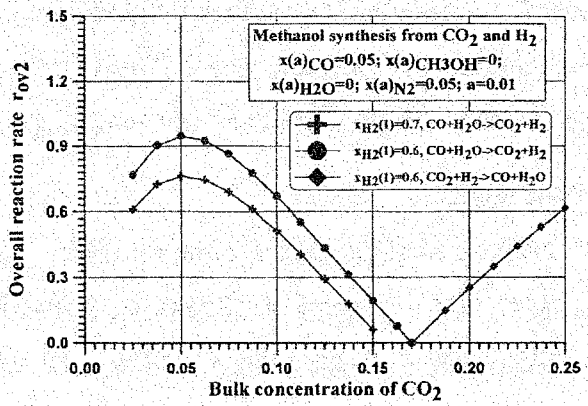

Fig.4.

The discussion of the numerical results shown in the figures led to the following conclusions:

(1) When the reaction products appear in the gaseous mixture on the pellet surface (deeper layers of the bed) the increase in the pellet radius leads initially to the increase in the effectiveness factor η_1; upon reaching a maximum η_1 begins, however, to decrease. This does not concern η_2, whose dependence on the radius is a decreasing function. It should be noted that η_1 may assume values greater than unity, despite the fact that the calculations dealt only with isothermal pellet.

(2) Due to the increase in the concentration of CO on the pellet surface, the overall rate r_{ov1} increases only slightly, while the increase in the overall rate r_{ov2} is relatively high. In both cases, large increase is observed for small concentrations of carbon monoxide. The change in the H_2 concentration on the pellet surface affects much more the value of r_{ov2} than that of r_{ov1}

(3) The increase in the concentration of CO_2 on the pellet surface produces initially a relatively high increase in the overall rate r_{ov1}; then, however, upon reaching a maximum value, it rapidly diminishes. The reverse is true for $r_{ov2}=r_{ov2}\{x_{CO2}(a)\}$, which is a increasing-decreasing-increasing function. At a minimum point, however, where $r_{ov2}=0$, the direction of the reaction (2) changes from "from the right-hand side to the left" to "from the left-hand side to the right".

(4) The diminishing character of the curve of $x_{CO}(l)$ for medium and large pellets, with $R_2(x_o)>0$, is a proof that a cross-effect occurs in a pellet, namely the transport of CO from lower to higher concentrations.

(5) The results obtained pave the way for the intensification of the synthesis of methanol over $CuO\text{-}ZnO\text{-}Al_2O_3$ -catalyst by means of, say, optimum choice of the inlet composition of the gaseous mixture, variation of the pellet size along the reaction path, controlled modification of concentration of the reaction products along the reactor, etc.

References

1. Grzesik M., DSc Thesis, Krakow 1988.
2. Skrzypek J., Grzesik M., Szopa R., Chem. Eng. Sci, 40, 671 (1985).
3. Skrzypek, J., Lachowska, M., Moroz, H., Chem. Eng. Sci., 46, 2809 (1991).

CHEMICAL EQUILIBRIA IN DIRECT SYNTHESIS OF DIMETHYL ETHER

Miroslaw Grzesik and Anna Ptaszek

Faculty of Food Technology, Academy of Agriculture, Al. 29 Listopada 46, 31-425 Krakow, Poland, Tel. +48 12 4119395, Fax +48 12 4117753, E-mail: rrgrzesi@cyf-kr.edu.pl

Introduction

Dimethyl ether (DME) is an important chemical and a chemical intermediate. It might be applied as a fuel for diesel engines or a fuel additive and also as a refrigerant instead of the freons [1,2].

Dimethyl ether can be obtained either from methanol [1], or directly from the synthesis gas [2,3,4]. Because of the process economics, the preferred method of synthesis is a direct, one-step process, that can be conducted using two-functional, or hybrid, catalysts [1,2,3]. These catalysts have two kinds of active centers: one kind is responsible for the synthesis of methanol (MeOH), and the other is responsible for the dehydration of MeOH. Therefore in one catalyst bed, DME can be obtained as a result of the following reactions:

$$CO + 2H_2 \leftrightarrow CH_3OH, \qquad \Delta H_1 < 0 \qquad (1)$$

$$2\,CH_3OH \leftrightarrow CH_3OCH_3 + H_2O, \qquad \Delta H_2 < 0 \qquad (2)$$

and the associated with it synthesis of the water-gas shift reaction:

$$CO + H_2O \leftrightarrow CO_2 + H_2. \qquad \Delta H_3 < 0 \qquad (3)$$

The fundamental advantage of the ether synthesis is that it moves the equilibrium of the methanol synthesis (1). Reactions (1-2) create a system, where one reaction follows the other. Thus, according to the le Chatelier's principle a continuous depletion of MeOH in reaction (2) causes its increased production in reaction (1).

The purpose of present study is to determine the effect of process parameters as temperature, pressure, and the initial molar ratio of H_2 to CO on equilibrium yield and selec-tivity of DME in the reaction system (1-3).

Process modelling

The conversion degrees were defined as follows (n - number of mole):

$$\xi_1 = \frac{|\Delta n_{CO}|_1}{F_{on}}, \quad \xi_2 = \frac{|\Delta n_{DME}|_2}{F_{on}}, \xi_3 = \frac{|\Delta n_{CO}|_3}{F_{on}}, \qquad (4)$$

where

$$F_{on} = \sum_i n_i^o = n_{CO}^o + n_{H_2}^o + n_{CO_2}^o.$$

Making use of above equations the mole fractions of each component of reaction mixture (1-3) can be easily obtained:

$$y_{CO} = \frac{y^o_{CO} - \xi_1 - \xi_3}{\delta}, \quad y_{H_2} = \frac{y^o_{H_2} - 2\xi_1 + \xi_3}{\delta}, \quad y_{MeOH} = \frac{\xi_1 - 2\xi_2}{\delta},$$

$$y_{DME} = \frac{\xi_2}{\delta}, \quad y_{H_2O} = \frac{\xi_2 - \xi_3}{\delta}, \quad y_{CO_2} = \frac{\xi_3}{\delta}, \quad \delta = 1 - 2 \cdot \xi_2 . \tag{5}$$

For each of reactions (1-3), an equilibrium expression can be written that relates the conversion degrees ξ_1, ξ_2, ξ_3 to an equilibrium constant, K_{api}, $i = 1,2,3$. They are of the form:

$$\frac{y_{MeOH}}{y_{CO} y^2_{H_2}} \cdot p^{-2} - K_{ap1} = 0,$$

$$\frac{y_{DME} y_{H_2O}}{y^2_{MeOH}} - K_{ap2} = 0, \tag{6}$$

$$\frac{y_{CO_2} y_{H_2}}{y_{CO} y_{H_2O}} - K_{ap3} = 0,$$

where (T - temperature in K)

$$K_{apj} = exp(a_j \cdot T^{-1} + b_j \cdot (lnT - 1) + c_j \cdot T + d_j \cdot T^2 + e_j \cdot T^3 + f_j), \quad \text{j=1,2,3} \tag{7}$$

and y_i, i = CO, CO_2, H_2, MeOH, DME and H_2O are given by (5).

The value of coefficients $a,b,c.d,e$ and f are presented in Table 1 [5].

Table 1. Coefficients in equation (6)

Reaction	a	b	c	d	e	f
Reaction 1	9204.2	-7.6927	3.920	0.5127	-0.311	14.294
Reaction 2	2820.07	0.83543	2.3526	-1.8736	0.516075	-8.065189
Reaction 3	4766.3	-1.9434	5.623	-2.17	0.4117	3.1519

Results and discussion

The system of nonlinear equations (5-7) were solved with respect to equilibrium conversion degrees ξ_1, ξ_2, ξ_3. In order to calculate the equilibrium yield and selectivity of DME the following formulae were used:

$$Y_{DME} = \frac{2 \cdot \xi_2}{y^o_{CO}}, \tag{8}$$

$$S_{DME} = \frac{2 \cdot \xi_2}{\xi_1 + \xi_3}. \tag{9}$$

The effect of temperature (400-700 K), pressure (1-10 MPa) and initial molar fraction of CO (0.2-0.5) on the equilibrium yield and selectivity of DME has been evaluated in detail and the selected results are presented in Figures (1-6).

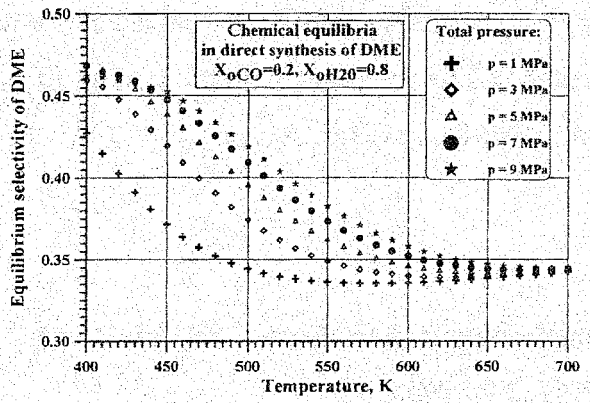

Fig.1.

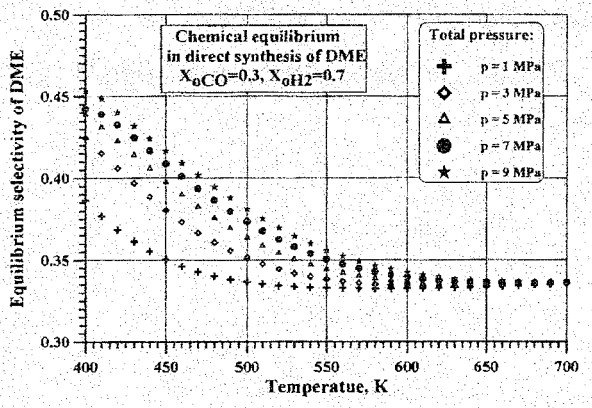

Fig.2.

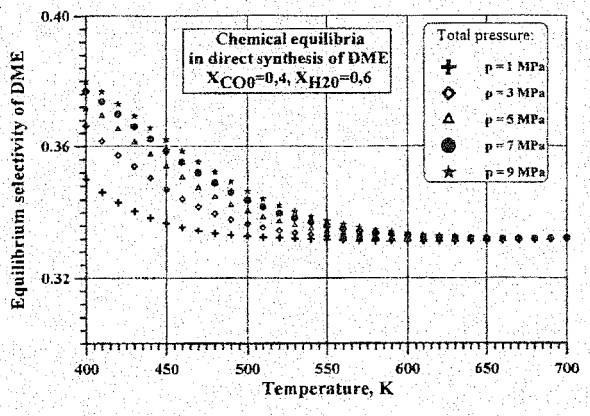

Fig.3.

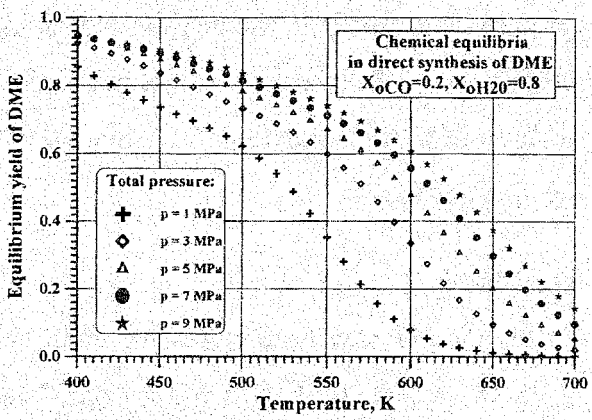

Fig.4.

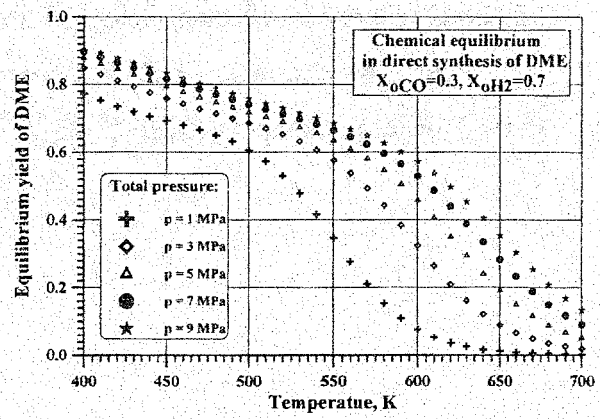

Fig..5.

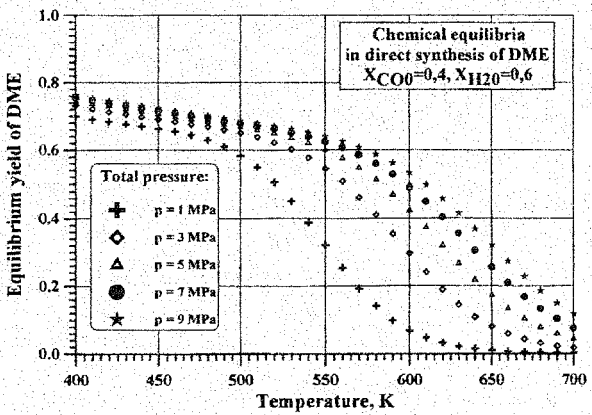

Fig.6.

Both temperature and pressure have a considerable effect on the equilibrium yield and selectivity of DME. Pressure influences strongly the selectivity of DME in low temperatures as 400-600 K and has rather moderate effect in higher ones. On the contrary, pressure effects on the equilibrium yield of DEM in the whole temperature range studied. An increase in temperature decreases both the equilibrium yield and the equilibrium selectivity, however in low pressure as 1-3 MPa a slight minimum is observed in equilibrium selectivity curve. The effect of the initial mole fraction of CO on the equilibria in the reaction system of (1-3) is also highly significant.

References

1. M. Xu, J.H. Lunsford, D.W. Goodman, A. Bhattacharyya, Appl. Catal., 149, 289 (1997).
2. Q. Ge, Y. Huang, F. Qiu, S. Li, Appl.Catal., 167, 23 (1998).
3. J.L. Li, X.-G. Zhang, T. Inui, Appl. Catal., 147 23 (1996).
4. T. Shikada, Y. Ohno, T. Ogawa, M. Ono, M. Mizuguchi, K. Tomura, K. Fujimoto, „Natural Gas Conversion", Elsevier Science Publishers B.V., Amsterdam, 1998.
5. R.C. Reid, J.M. Prausnitz, T.K. Sherwood, „The Properties of Gases and Liquids", Mc Graw-Hill Book Company, New York, 1977.

NUMERICAL INVESTIGATION OF THE PECULIARITIES OF THE KINETIC OSCILLATIONS IN THE CO OXIDATION REACTION IN THE POROUS CATALYST LAYER

E.S. Kurkina, E.D. Tolstunova

Department of CM&C, Moscow State University, Moscow 119899, Russia,
e-mail: kurkina@cs.msu.su

A new distributed mathematical model of heterogeneous catalytic reaction proceeding in the oscillatory mode in the thin layer of the granular catalyst is suggested. The model is examined on the example of CO oxidation reaction over Pd-zeolite catalyst. Observed in the experiments were various types of reaction rate oscillations, including nearly harmonic and relaxation ones, as well as chaotic and complex mixed-mode regimes, depending on conditions of experiments [1 – 3].

In the efforts to explain the nature of the observed dynamic behavior, several mathematical models of CO oxidation on Pd-zeolite catalysts were developed [4, 5]. However, each of these models considers the process of the reaction in some approximation, accounting for the influence of only few factors capable of limiting the reaction rate, and neglecting other ones. Therefore, all complex oscillations obtained as a result of simulation did not correspond to physical conditions of the experiment.

The suggested model is more complete compared to former ones. It takes into account simultaneously a number of factors capable of limiting the reaction rate in the conditions of the experiment. Provided respective assumptions as to the experimental conditions, the formulated model is reduced to the above models [4, 5]

The complete model is the hierarchical nested system of models. Each level of model description corresponds to a certain spatial-temporal scale: 1) At the lowest level, the mechanism of reaction on the surface of a single palladium cluster is modeled. 2) At the level of catalyst pellet containing a large number of Pd clusters, the processes of reaction and CO diffusion in the pellet pores are considered. And finally, 3) at the macro-level, the complete catalyst layer consisting of a large number of pellets is considered, and the processes of mass and heat transfer between the pellets and passing of gaseous flows through the layer are taken into account.

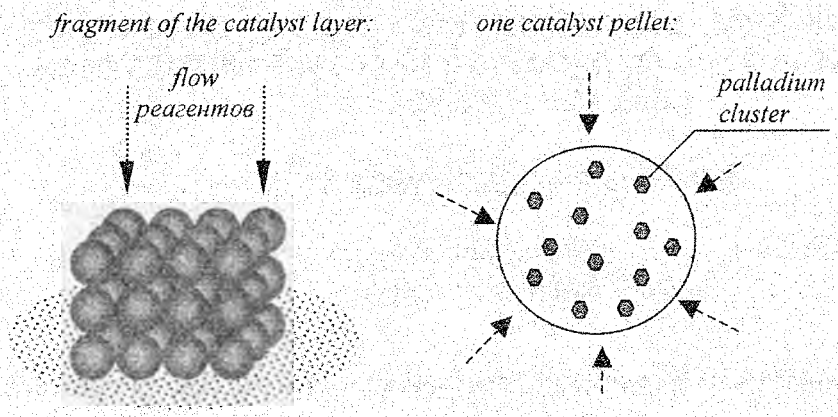

The new distributed model was investigated in various approximations, including homogeneous layer approximation, CSTR, *etc*. The present research enabled to clarify the area of applicability of these approximations [6]. The influence of different factors, such as diffusion rate in pores of zeolite, flow rate, sizes of pellets, Pd loading, thickness of the layer, and others, on the dynamics of system were examined. Various types of reaction rate oscillations were obtained at the values of parameters corresponding to experimental conditions. In particular, the wide area of chaos and complex mixed-mode regimes was found. The examples of the oscillations obtained are demonstrated in Fig. 1.

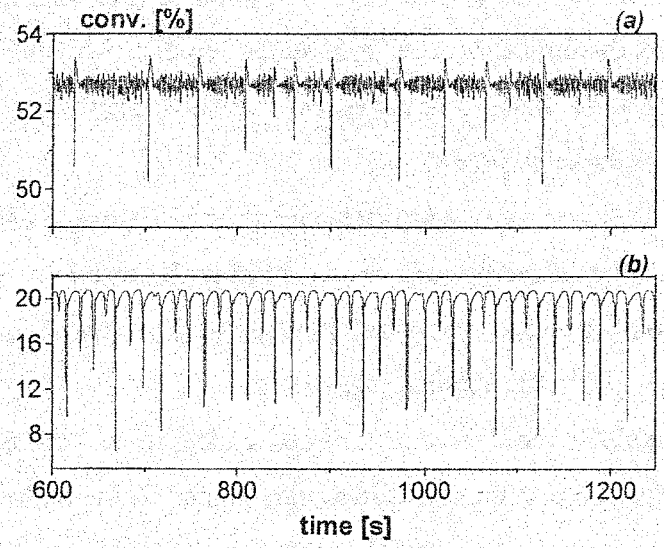

Fig.1 . *Chaotic time series at flow rate F = 2.5 cm³/s , and (a) P_{co} = 3.67 Torr, (b) P_{co} = 0.28 Torr.*

References

1. Jaeger N.I., Moller K., Plath P.J. // J. Chem. Soc: Faraday Trans. Pt II, 1986, V. 82, p. 3315-3330.
2. Slinko M.M., Jaeger N.I., Svensson P. // J. Catal., 1989, V. 118, p. 349-359.
3. Liauw M., Plath P.J., Jaeger N.I. // J. Chem. Phys., 1996, V. 104 (16), p.6375-6386.
4. Kurkina E.S., Peskov N.V., Slinko M.M. // Physica D, 1998, V. 118, p. 103-122.
5. Slinko M.M., Kurkina E.S., Liauw M.A., Jaeger N.I. // J. Chem. Phys., 1999, V. 111 (17), p. 8105-8114.
6. Kurkina E.S., Tolstunova E.D. //In the book «Applied mathematics and informatics», №5 – M.: Moscow State University, Department CM&C, 2000 (in Russian).

PULSE BIFURCATION AND TRANSITION TO SPATIOTEMPORAL CHAOS IN REACTION-DIFFUSION MODEL OF NO+CO/Pt(100)

E.S. Kurkina

Moscow State University, Department of Comput. Mathematics § Cybernetics (BMK), Moscow, 119899, Russia, E-mail: kurkina@cs.msu.su

Recent investigations with the photo-emission electron microscope (PEEM) have revealed a rich variety of spatiotemporal concentrations patterns on the Pt(100) single crystal surface during the NO+CO reaction [1] A four-variable mathematical model of the reaction-diffusion type previously developed [2] was studied to describe the self-organization phenomena. Lateral interactions in the adlayer are an essential feature of the model and play a crucial role in the adequate simulation of the experimental data. It was shown that this model exhibits pulses, fronts, chemical turbulence and others spatiotemporal patterns. In this paper we investigate pulse bifurcations upon temperature or pressure NO variations. In particular it was found two different scenario of the apparent loss of stability pulse solution and transition to spatiotemporally chaotic dynamics. Numerical studies have revealed that the attractor in the resulting turbulent state has positive Lyapunov exponents. Travelling solutions of the PDE are studied in a co-moving frame as the solution to a set of ODEs. Structures in the ODEs phase space such as fixed points, periodic orbits, homoclinic and heteroclinic connections correspond to homogeneous solutions, travelling waves, pulses and fronts. The path-following algorithm was used to study the bifurcations of homoclinic orbits corresponding to solitary pulses. The bifurcation analysis allows to detect the existence regions of pulses and to study different bifurcations of these solutions. However, the stability of ODEs structures cannot be resolved in the ODE framework and was investigated in the full PDE system.

Figure 1 shows the stable solitary pulse solution simulated in the model. Figure 2 illustrates one type of the transition from stable pulses to spatiotemporally chaotic behavior. The homoclinic connection corresponding to pulse solution annihilates through collision with unstable fixed point (fig. 2a) at the bifurcation value of parameter. The progection on one of the phase plane of the resulting chaotic regime is shown on fig. 2b.

References

1. G. Veser and R. Imbihl // J. Chem. Phys. **100** (11), 8483 (1994).
2. E.S. Kurkina, A.V. Malykh, *et. al.*//Moscow.: depart. CM&C MSU, p. 44-63, 1997 (in Russian).
3. Kurkina E.S., Malykh A.V. // Preprint "Dialog-MGU" - MSU, 2000 (in Russian).

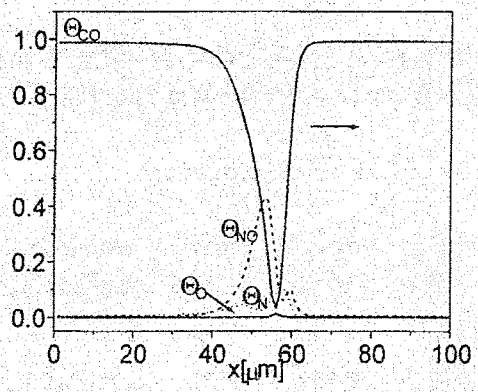

Figure 1. *The solitary pulse simulated in the model of the reaction of NO+CO/Pt(100) (P_{NO}=4.0*10^{-7} mbar, P_{CO}=3*10^{-7} mbar, T=380 K).*

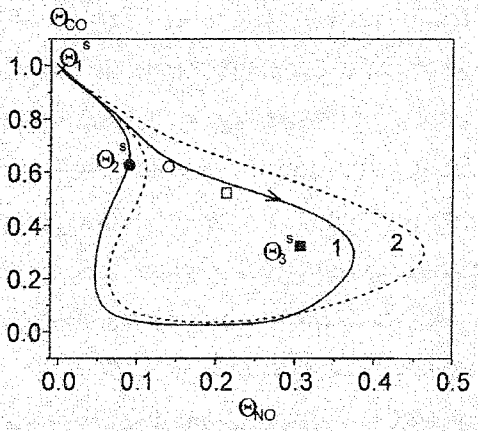

Figure 2a. *The projections of homoclinic orbits and stationary fixed points on phase plane (θ_{NO},θ_{CO}) for two values of parameter pressure P_{NO}: 1) P_{NO}=3.5*10^{-7} mbar, 2) P_{NO}=5.0*10^{-7} mbar. × - the stable fixed point θ_1^s, ● ○ - the unstable fixed point θ_2^s, ■ □ - the unstable fixed point θ_3^s. The dashed line corresponds to P_{NO}=5.0*10^{-7} mbar. The solid line corresponds to the bifurcation value of parameter P_{NO}=3.5*10^{-7} mbar.*

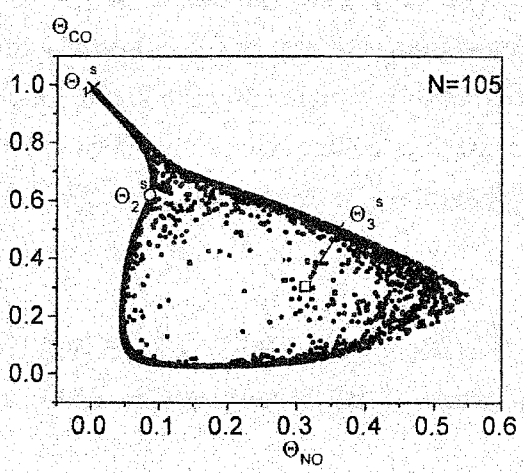

Figure 2b. *The projection of strange attractor on the phase plane (θ_{NO}, θ_{CO}) at P_{NO}=3.4*10^{-7} mbar, T=380 K, P_{CO}=3.0*10^{-7} mbar.*

THE MECHANISM OF THE LOW TEMPERATURE NITROGEN DESORPTION FROM IRIDIUM SURFACE

E.S. Kurkina, N.L. Semendyaeva, A.I. Boronin*

Faculty of CM&C, Moscow State University, Moscow, 119899, Russia; E-mail: NatalyS@cs.msu.su
**Boreskov Institute of Catalysis SB RAS, pr. Akad. Lavrentieva, 5, Novosibirsk, 630090, Russia; E-mail: boronin@catalysis.nsk.ru*

New mathematical model of the nitrogen temperature recombination on Ir(111), Ir(110) and polycrystalline Ir surface has been developed to explain the complicated N_2 temperature programmed desorption (TPD) spectra from an (N+O) layer. Model takes into account the structural defects of the surface, their modification by subsurface oxygen and the morphology of adsorbed layer. TPD simulation reproduces successfully the main experimental features including the appearance of the low-temperature TPD peak. Both deterministic and stochastic approaches are used for mathematical modelling of N_2 TPD spectra.

Introduction. There are reliable experimental evidences that catalytic reduction of NO with CO on Ir surfaces under low pressure conditions is characterized by CO_2 and N_2 product formation [1,2]. Usually, the mechanism of CO_2 formation as an important part of NO+CO reaction is studied. However, another part of this reaction - the process of N_2 recombination- has also the complicated reaction kinetics [3-6]. The rate of the N_2 recombination depends essentially on the surface structure and presence of adsorbed oxygen. In the present paper the new mathematical model describing the specific features of the N_2 TPD spectra from Ir surfaces is proposed.

Experimental results. Experiments were performed in an electron spectrometer "VG ESCA-3" equipped with TPD and XPS facilities. The N_2 desorption from an (N) or (N+O) adsorbed layer on Ir(111), Ir(110) and polycrystalline Ir surface has been studied in the temperature range 300÷1200 K. Desorption of atomic nitrogen from an (N) layer occurs at T_p = 750÷760 K independently on the surface structure (Ir(111), Ir(110) or polycrystalline Ir surface). The N_2 TPD spectra from a mixed (N+O) layer on polycrystalline surface have the low temperature peak at T_p = 550÷560 K. Its intensity depends on the oxygen coverage (Fig.1).

In order to explain experimental findings the following assumptions were used. We take into consideration two states of oxygen: adsorbed on a surface and penetrated to upper layer of metal. The oxygen penetration significantly depends upon the surface structure and takes place on the structural defects of a surface and on the opened (like Ir(110)) single crystal

planes. The subsurface oxygen modifies electronic and geometric structure of the nearest adsorption centers and changes the rates of elementary surface reactions.

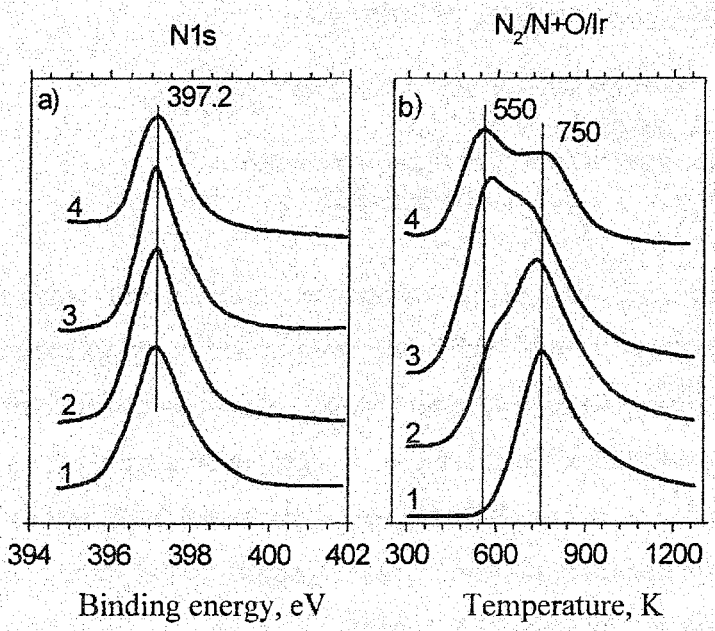

Fig.1. a) XPS-spectra N1s of nitrogen adsorbed over polycrystalline Ir surface and b) N_2 TPD spectra depending on nitrogen concentration C_N [at/cm^2] and oxygen concentration C_O [at/cm^2];
curve 1: $C_N=3\times10^{14}$, $C_O=0$;
curve 2: $C_N=3\times10^{14}$, $C_O=2.5\times10^{14}$;
curve 3: $C_N=3\times10^{14}$, $C_O=3.5\times10^{14}$;
curve 4: $C_N=2\times10^{14}$, $C_O=7\times10^{14}$

Mathematical model. The description of the kinetics of N_2 TPD is carried out in the framework of multi-component lattice gas model and the theory of absolute reaction rates. An iridium surface is presented by two-dimensional lattice of nonequivalent sites: modified by subsurface oxygen (m) and non-modified (n). The process of N_2 desorption from an (N+O) layer is described by

$$(N)^n + (N)^n \Rightarrow (*)^n + (*)^n + (N_2)\uparrow, \quad (R_{nn}), \tag{1}$$

$$(N)^m + (N)^m \Rightarrow (*)^m + (*)^m + (N_2)\uparrow, \quad (R_{mm}), \tag{2}$$

$$(N)^n + (N)^m \Rightarrow (*)^n + (*)^m + (N_2)\uparrow, \quad (R_{nm}), \tag{3}$$

$$(N)^n + (*)^m \Leftrightarrow (*)^n + (N)^m, \tag{4}$$

$$(N)^n + (*)^n \Leftrightarrow (*)^n + (N)^n, \tag{5}$$

$$(O)^n + (*)^n \Leftrightarrow (*)^n + (O)^n, \tag{6}$$

$$(N)^m + (*)^m \Leftrightarrow (*)^m + (N)^m. \tag{7}$$

Two different approaches are used for the solution of this problem: the stochastic approach using dynamic Monte Carlo type algorithms and the deterministic approach using systems of two coupled ordinary differential equations. The mathematical description in both cases depends on the space configuration of the modified active sites. Some examples of the space distributions of non-modified sites located in terraces and modified sites located in structural defects like steps are shown in Fig.2.

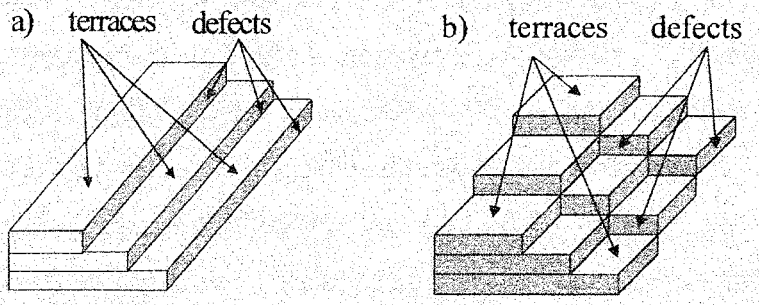

Fig.2. Some models of a polycrystalline surface:
a) "monosteps",
b) "hauberk"

The deterministic approach assumes a macroscopically homogeneous distribution of adsorbed species on the equivalent adsorption sites.

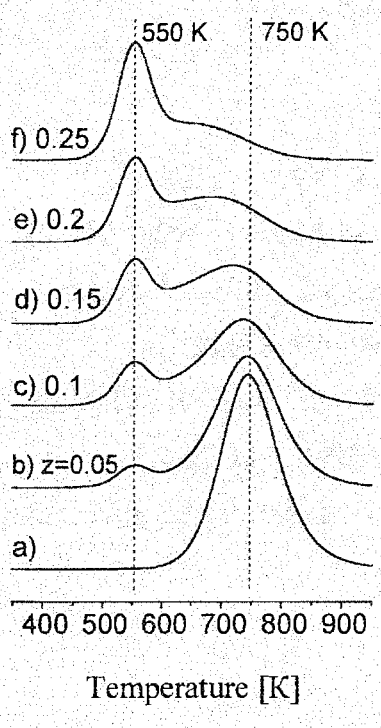

Fig.3. The N_2 TPD spectra depending on the concentration of modified sites z calculated in the framework of the deterministic approach using the model of the polycrystalline surface of "monosteps"-type (curves b-f); curve a) – the ideal adsorbed layer approximation on a homogeneous surface; $\theta_N(t^0)$=0.25, $\theta_O(t^0)$=0.2

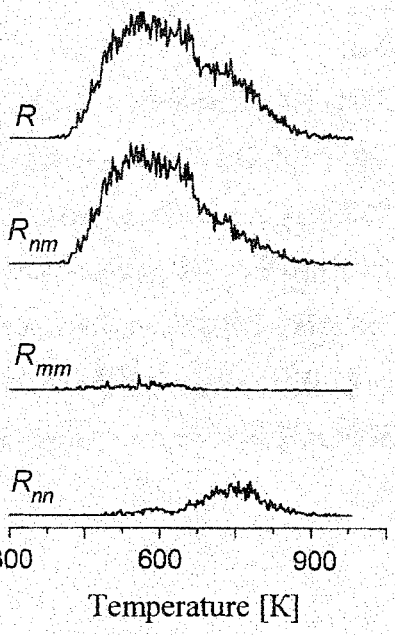

Fig.4. The structure of a total N_2 TPD spectrum $R=R_{nn}+R_{nm}+R_{mm}$ from a polycrystalline surface of "monosteps"-type, z=0.1; the stochastic approach using lateral interactions in the adsorbed layer [Kcal/mol]: $\varepsilon_{NN}^{1}=\varepsilon_{NO}^{1}=\varepsilon_{OO}^{1}=-1.6$, $\varepsilon_{NN}^{2}=\varepsilon_{NO}^{2}=\varepsilon_{OO}^{2}=0.8$; $\theta_N(t^0)$=0.25, $\theta_O(t^0)$=0.2; 90x90 sites, 10 realizations

Results of simulation. The results simulation show that the proposed mathematical model can give a good description of the main experimental data concerning the N_2 temperature recombination on Ir surfaces (Fig.3,4).

Numerical investigations demonstrate that the appearance of multiple peaks may be due to the occurrence of distinct oxygen states altering the activation energies of N_2 desorption. The dominant requirement for successful simulation of N_2 TPD spectra is the small rate of the elementary stage (4) describing the movement of N_{ads} from non-modified to modified site and backwards. A strong dependence of the total N_2 desorption rate on the heating rate and the initial N_{ads} distribution was revealed. A detailed discussion of simulated results can be found in Ref. [7]. Further experimental investigations are necessary to confirm all predictions of the model.

Acknowledgements. This work was supported by the Russian Foundation for Basic Researches (Grant № 00-01-000587).

References.

1. P.A.Zhdan, G.K.Boreskov, A.I.Boronin et al. // J. Catal., 1979, v.60, p.93.
2. C.A. de Wolf, B.E.Nieuwenhuys, A.Sasahara et al. // Surface Sci., 1998, v.411, p.L904.
3. P.D.Cobden, B.E.Nieuwenhuys, F.Esch et al. // Surface Sci., 1998, v.416, p.264.
4. O.Kortuke, W.von Niessen. // Surface Sci., 1998. v.401. N2. p. 185.
5. M.Hirsimaki, S.Suhonen, J.Pere et al. // Surface Sci., 1998, v.402-404, N1-3, p.187.
6. H.Wang, R.G.Tobin, G.B.Fisher et al. // Surface Sci., 1999, v.440, p.429.
7. E.S.Kurkina, N.L.Semendyaeva, A.I.Boronin // Kinet. Katal., to be published [in Russian].

AUTO OSCILLATIONS IN CSTR

V.I. Bykov, L.S. Trotsenko*

Institute of Computational Modelling of the Siberian Branch of the Russian Academy of Sciences, 660036, Krasnoyarsk, Russia, e-mail: bykov@cc.krascience.rssi.ru.
**Krasnoyarsk State Technical University,*
660074, Krasnoyarsk, Kirenskogo, 26, Russia, tel: (3912) 497210

With realization catalytic reaction in CSTR there is an additional nonlinearly, which can result in complication of the observable phenomena.

Let's consider conversion scheme:

$$\begin{aligned} &1)\ A + Z \Leftrightarrow AZ; \\ &2)\ B + 2Z \Leftrightarrow 2BZ; \\ &3)\ AZ + BZ \Rightarrow 2Z + AB, \end{aligned} \qquad (1)$$

where: B, A, AB - observable substances; Z - active center of a surface of the catalyst; AZ, BZ - substance adsorbed on the active site (AZ, BZ - intermediate substances).

The scheme (1) does not contain autocatalytic stages of A+X⇒2X type, therefore for interpretation plenty steady state (st.s.) three stages and two independent substances are necessary as a minimum. The kinetic model adequate to (1), in the assumption of constancy of concentration of observable substances, is elementary catalytic trigger, that is system, in which can be three st.s. (two steady and one unstable)

The scheme (1) corresponds to non-stationary kinetic model:

$$\dot{a} = -k_1 \cdot a \cdot z + k_{-1} \cdot x + v(a_0 - a) \qquad (2)$$

$$\dot{b} = -k_2 \cdot b \cdot z^2 + k_{-2} \cdot y^2 + v(b_0 - b)$$

$$\dot{x} = k_1 \cdot a \cdot z - k_{-1} \cdot x - k_3 \cdot x \cdot y \qquad (3)$$

$$\dot{y} = 2k_2 \cdot b \cdot z^2 - 2k_{-2} \cdot y^2 - k_3 \cdot x \cdot y,$$

where: a, b, x, y - concentration of observable and intermediate substances; $z = 1 - x - y$; a_0, b_0 - concentration at the entrance of reactor; v - rate of submission of a reactionary mixture to the reactor; k_i - rate constant of stages. If a, b = const, then the kinetic subsystem (3) can have three st.s.

Choosing suitable meanings v and b_0, it is possible to create conditions of unique and unstable st.s., that provides existence of autofluctuations in system. Probability of occurrence of fluctuations is higher, the closer is the point of crossing to a point of transition from area of existence of a steady stationary condition, to area of an unstable stationary condition. For ex-

ample, with a≡const the decision oscillation with a set of parameters k_1=0.3; k_{-1}=0.0005; k_2=0.1;

k_{-2}=0.0005; k_3=1; v=0.65·10^{-3}; b_0=1. With increase b_0 or reduction v, the fluctuations become fading and further disappear. The fluctuations disappear also with change of constants of rates k_{-1} and k_{-2}. The area of existence of auto fluctuations in space of parameters v, b_0, k_i is rather narrow.

Knowing meanings a_0, b_0 is possible to determine a condition of existence of autofluctuations and in initial model (2), (3). For example, with meanings of parameters k_1=0.3; k_{-1}=0.0003; k_2=0.08; k_{-2}=0.0002; k_3=1; v_1=0.68·10^{-3}; v_2=0.02·10^{-3}; b_0=1; a_0=0.004 system (2), (3) has autofluctuations.

The assumption about autocatalysis allows to receive the most simple scheme, with kinetic model admits plenty of st. s. (autocatalytic trigger):

$$1)\ A + Z \Leftrightarrow X; \qquad (4)$$
$$2)\ X + 2Z \Rightarrow 3Z + B,$$

where: A, B - observable substances (substance in a gas phase); X - intermediate substance (adsorbed substance on a surface of the catalyst Z).

The scheme (4) answers kinetic model flowing catalytic reactor:

$$\begin{aligned} \dot{a} &= k_1 \cdot a \cdot z - k_{-1} \cdot z + v(a_0 - a); \\ \dot{x} &= k_1 \cdot a \cdot z - k_{-1} \cdot z - k_2 \cdot x \cdot z^2, \end{aligned} \qquad (5)$$

where: a - concentration of substance A; x - concentration (degree of a covering) substance X; z = 1-x; a_0 - concentration A on an entrance reactor; v - speed of submission of substance A in reactor. In model (5) parameters are a_0, v and constant speeds of stages k_i.

St.s. for (5) are determined as the decision of the cubic equation. Let's find from equation an obvious kind of expression for functions return to parametrical dependence.

The parametrical dependence's of speed of submission and initial concentration of substance A are most interesting to us. Under the analysis of parametrical dependence's is possible to make conclusions, that:

- with reduction of initial concentration of substance, area of existence unique unstable st.s. grows;
- area plenty of st. s. brightly is expressed with v aspiring to infinity and practically disappears with v = 1;
- Diagrams of parametrical dependencies are most sensitive to changes of coefficient k_{-1}.

On a basis (5) and critical conditions the expressions for bifurcation curves can be written down. With the help of the analysis of parametrical dependence's and bifurcation curves was determined area of existence unique unstable st.s., that guarantees presence of fluctuations, for example k_1=0.026, k_{-1}=0.01, k_2=0.001, v=0.0135, a_0=0.017.

In the given work is shown, that the interaction of a gas phase with a surface of the catalyst is essentially nonlinear process, which can result in critical effects. The parametrical analysis of mathematical models flowing catalytic system in approach of ideal mixture is spent and the auto oscillatory modes of its work are received which cannot exist in the scheme without flow. Accounts flow give an additional degree of freedom and nonlinearly, that results in the greater variety of the critical phenomena.

Elementary kinetic models describing autofluctuations, in such systems are the equation (2), (3) or (5). In quality elementary catalytic subsystem here acts the catalytic and autocatalytic trigger.

PP-8

THE PARAMETRIC ANALYSIS OF ARIS-AMUNDSON'S MODEL FOR ARBITRARY ORDER REACTION

V.I. Bykov, S.B. Tsybenova*

Institute of Computational Modelling of the Siberian Branch of the Russian Academy of Sciences, 660036, Krasnoyarsk, Russia, e-mail: bykov@cc.krascience.rssi.ru.
**Krasnoyarsk State Technical University,*
660074, Krasnoyarsk, Kirenskogo, 26, Russia, tel: (3912) 497210

The parametric analysis of classical model of the theory of chemical reactors - model of a continuous stirred tank reactor (Aris-Amundson's model) is carried out. For reaction of first order the results of the analysis of local bifurcations of steady states, including Andronov-Hopf bifurcations are received. The curves of a multiplicity and neutrality of steady states are written in an obvious view for various combinations of dimensionless parameters. The requirements are received, at which the diagram of Van Heerden can be for a geometrical stability criterion of steady states. The sample parametric and phase portraits of dynamic system are given. The fields of parameters responding safe modes of installation of the solutions and steady points - to modes without dynamic springs are allocated. The description of designed system of the software of the parametric analysis and bank of models are given.

The mathematical model of a continuous stirred tank reactor (CSTR) is traditional object of research in Chemical Engineering Science. Taking into account the considerable contribution by R. Aris and N. Amundson to the theory of chemical reactors, the relevant class of models we called of Aris-Amundson's models. For one exothermal reaction of the first order

$$A \rightarrow B,$$

where A - starting substance, B - finished product of reaction.

The mathematical model CSTR:

$$\begin{aligned} V\frac{dX}{dt} &= -Vk(T)X + q(X^0 - X), \\ C_p\rho V\frac{dT}{dt} &= (-\Delta H)Vk(T)X + q\rho C_p(T_0 - T) + hS(T_X - T), \end{aligned} \qquad (1)$$

where $k(T) = k^0 \exp(-E/(RT))$. Agrees [1], we shall enter the following dimensionless parameters and variable:

$$Da = \frac{V}{q}k(T_0), \quad \gamma = \frac{E}{RT_0}, \quad \beta = \frac{(-\Delta H)X^0}{\rho C_p T_0}, \quad y^* = \frac{T_x}{T_0},$$

$$x = \frac{X^0 - X}{X^0}, \quad s = 1 + \frac{hS}{q\rho C_p}, \quad \tau = \frac{q}{V}t, \quad y = \frac{T}{T_0}.$$

The system (1) is conversed to a dimensionless view:

$$\frac{dx}{dt} = f(y)(1-x) - x = f_1(x,y),$$
$$\frac{dy}{dt} = \beta f(y)(1-x) - s(y-1) = f_2(x,y), \qquad (2)$$

where $f(y) = Da\exp(\gamma(1-1/y))$.

Usage modern mathematical and software has allowed even more penetrating to advance in the analysis of all variety of nonlinear properties of dynamic system (2). Characterizing a state of a problem of the parametric analysis of nonlinear dynamic models such as (2), we allocate two directions [2]. To the first direction it is possible to attribute works, in which the enough thin mathematical technique of the analysis Lyapunov coefficients, of global bifurcations and other characteristics of model with the purpose of its research «deep into» will are used [3]. Thus more often relevant the curves of bifurcations are given diagrammatically, as the modifications of phase portraits occur at change of parameters in 5-7 significant digits. Such narrow fields of parameters from the engineering point of view are unessential, and have only mathematical sense. The second direction of works can be characterized as research «in widely» [2,4]. The most significant phase portraits allocated in here, are created basic the curves of bifurcations in various planes of parameters, all technology of the parametric analysis is made as information-calculation system, with purpose making bank of models. We demonstrate not technique of a mathematical analysis, and results influence of parameters on dynamic properties of concrete model (2). The parametric analysis includes definition of steady states (st.s.)., their stability, building of dependencies st.s., from parameters, curves of a multiplicity and neutrality st.s., parametric and phase portraits, time dependence of the solutions of model (2). For reaction of first order (1) usages of specificity of system (2) allow many results to receive in an obvious view, that from the computing point of view essentially simplifies the procedure of the parametric analysis. If obvious expressions for the curves of local bifurcations to receive it fails, it is possible to use the geometrical approaches based on building of the diagrams of dependence st.s. one of parameters at variation of second parameter. Moreover, if not it is possible to receive and obvious expressions for parametric dependencies, but the conditions of a stationary are reduced to one equation, it is possible to offer the simplified variant of the method of continuation on parameter [4].

The mathematical Aris-Amundson's model for arbitrary kinetics:

$$\frac{dx}{d\tau} = f(y)g(x) - x = f_1(x,y),$$
$$\frac{dy}{d\tau} = \beta f(y)g(x) - s(y-1) = f_2(x,y), \qquad (3)$$

where f (y) =Daexp (γ(1-1/y)) - temperature dependence, g(x) - arbitrary kinetic function. The program of the parametric analysis is implemented and for system (3). In particular, the cases are specially allocated; $A+O_2 \rightarrow B$; $nA \rightarrow B$; $nA+O_2 \rightarrow B$. The program - software for a surveyed class of models, including all the basic stages of the parametric analysis of systems such as (3) is created.

REFERENCES

1. Aris R. Method in the Modelling of Chemical Engineering Systems. Academic Press, New York, 1979.
2. Bykov V.I., Pushkareva T.P. The simple models of critical phenomena in the kinetic region and their parametric analysis // Chem. Eng. Sci., 1999, Vol. 54, №20, p.4529-4533.
3. Sheplev V.S., Treskov S.A., Volokitin E.P. Dynamics of a stirred tank reactor with first-order reaction // Chem. Eng. Sci., 1998, Vol. 53, №21б p. 3719-3728.
4. Tsybenova S.B. The parametric analysis of base models of the chemical reactor theory and combustion theory. Ph. D. Thesis. Krasnoyarsk, 1999.

MATHEMATICAL MODELING OF REGENERATION OF THE CATALYST FOR TETRAFLUOROETHANE AND PENTAFLUOROETHANE PRODUCTION

S.I. Reshetnikov, N.M. Ostrovsky*, G.S. Litvak, V.A. Sobyanin, N.A. Davydov and A.N. Ilyin

Boreskov Institute of Catalysis, Novosibirsk 630090, Russia
fax: +7(3832) 343056, E-mail: resh@catalysis.nsk.su
**Omsk Department of Boreskov Institute of Catalysis, Omsk 644040, Russia*

Regeneration of coked catalysts (to restore their activity) is an important part of a great number of catalytic processes. This is especially true for catalysts, containing chromium (+3) and fluorides of Group II metals meant for production of ozone-safe chladones (R-134a, R-125 etc.) by gas-phase hydrofluorination of chloroethylenes. To restore a catalyst, coke deposits are burnt with oxygen. During a regeneration it is important to prevent a catalyst overheating, which may result in the catalyst sintering, and as a result, irreversible loosing of its activity.

The aim of the present work is to investigate regimes of the chromium-magnesium-fluoride catalyst regeneration in an adiabatic reactor.

Regeneration of the catalyst bed is an unsteady-state process. Moreover, in every catalyst section along a bed height, oxygen concentration and gas temperature "instantaneously" adjust to variations of coke concentration and catalyst temperature, hence they are quasi-stationary. Capacity of the solid phase with respect to a substance and heat is much higher than capacity of the gas phase. With respect to it, the mathematical two-phase model includes equations for changes of the below substances and temperature:

Coke fraction in a catalyst (g, *kg/kg*):

$$\frac{dg}{dt} = - r(g,x,T_k) , \qquad (1)$$

Oxygen concentration in a gas stream (y, m^3/m^3):

$$\frac{dy}{dz} = -\beta \tau (y-x) , \qquad (2)$$

Oxygen concentration in a catalyst pellet (x, m^3/m^3):

$$\beta (y-x) = B_m r(g,x,T_k) , \qquad (3)$$

Temperature of a gas stream (T_g, K):

$$\frac{dT_g}{dz} = - \tau B_g (T_g - T_k) , \qquad (4)$$

Temperature of a catalyst (T_k, K):

$$\frac{dT_k}{dt} = + B_k (T_g - T_k) + \frac{Q}{C_k} r(g,x,T_k) , \qquad (5)$$

Initial and boundary conditions:

$$\underline{z = 0}: \quad y = y_o , \quad T_g = T_{g\,o}; \quad \underline{t = 0}: \quad g(z) = g_o , \quad T_k(z) = T_{k\,o};$$

Where

$$\tau = \frac{V_p \rho}{G}, \qquad B_m = \frac{22.4 \nu_o \rho_k}{M_c}, \quad B_g = \frac{\alpha S_H}{\rho C_p}, \quad B_k = \frac{\alpha S_H}{\rho_k C_k},$$

$r(g,x,T_k) = k_0 \exp(-E/RT)\, g\, P_0\, x$ [1]; $z = l/L$ – dimensionless coordinate of a bed; τ – residence time, hour; V_p – reactor volume, m^3; G – air stream, kg/h; ρ, ρ_k – air and catalyst density kg/m^3; β - mass-exchange coefficient in a catalyst pellet, h^{-1}; ν_o – stoichiometry of the oxygen for coke burning, mol/mol; M_c –molecular weight of coke, kg/kmol; Q – heat of reaction, kcal/kg; C_p, C_k – heat capacity of a gas and a catalyst, kcal/kg; α - heat exchange coefficient between a catalyst surface and gas stream, kcal/m^2 h K; S_H – specific external surface of a catalyst pellets, m^2/m^3.

Oxygen is fed into the catalyst pellet by mass transfer. Under quasi-stationary regime, the rate of mass transfer is equal to the rate of combustion in the pellet (see Eq. 3). The coefficient of mass transfer β in the region of internal diffusion is a variable value, because the area of coke burning r_c moves from the pellet surface to its core. In addition, the catalyst porosity ε decreases on sintering, which change the value of surface through which mass transfer occurs ($3\varepsilon\,(1 - \varepsilon)/R_z$ cm^2/cm^3). For this reason, the summary expression for the coefficient of mass transfer can be written as:

$$\beta = \frac{3600\, D_E}{(R_z - 0.95 r_c)} \frac{3}{R_z} \in (1 - \varepsilon),$$

where R_z – radius of a catalyst pellet, cm; D_E – diffusion coefficient, cm^2/s; ε - porosity of a catalyst bed; $\in = V_\Sigma \rho_z$ - porosity of a catalyst pellet; V_Σ - pore volume, cm^3/g; $\rho_z = \rho_k/(1 - \varepsilon)$ – pellet density, g/cm^3; $r_c = R_z\, (g / g_o)^{1/3}$ – radius of coke burning in a catalyst pellet, cm.

In this work, the results of mathematical modeling are discussed. The optimal dynamic regimes for regeneration of the coked catalyst, temperature, gas flow rates and oxygen concentration were determined.

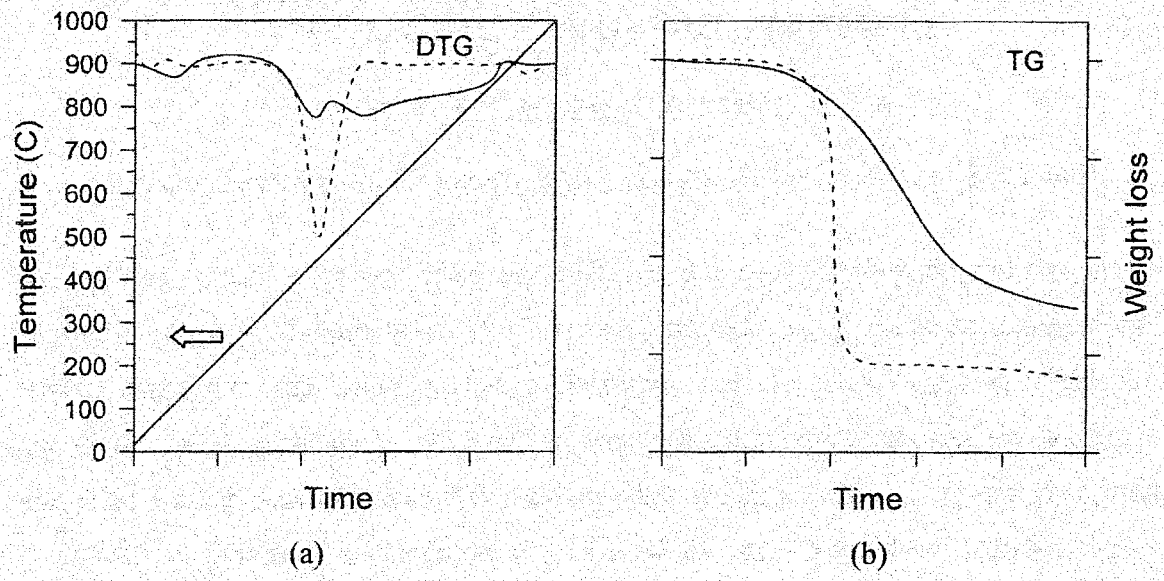

Fig.1. Temperature increasing *vs* time (a) and DTG, TG curves for the different catalyst pellet sizes: catalyst powder (dashed line) and catalyst pellet (solid line).

Parameters of the model, such as rate constant, reaction heat, reaction order, diffusion coefficient, activation energy, and coke composition, were determined from the experimental data obtained in the differential reactor and improved by mathematical modeling.

Analysis of the process occurring in the catalyst bed shows that coke burning proceeds in the region of strong diffusion limitations. This is confirmed by DTG and TG analysis data. Experiments were performed on DC and Q-1500D derivatographs. Fig. 1 shows the experimental results obtained for the deactivated catalyst, the samples are prepared as: (i) a fine-grained powder and (ii) catalyst particles 7.5 × 11 mm in size. On heating the fine-grained sample in air, coke is completely burnt out at 400-470°C. Whereas, coke burning on the large catalyst pellet proceeds much longer up to 900°C, at the same heating rate. Moreover, because the process of oxygen diffusion deep into the catalyst pellet is limited, an increase in temperature does not result in an increase in the rate of coke burning.

REFERENCES

1. Jonson B.M., Froment G.B., Watson J.M. *Chem. Eng. Sci.*, 1962. 17, 835.

PP-10

STUDY OF GAS PREPARING AND GAS CONDENSATE BY APPLYING OF INFORMATION-SIMULATING SYSTEM

A.V. Kravtsov, A.C. Maslov, N.V. Usheva

Tomsk Polytechnic University, Tomsk, Lenin avenue 30, E-mail:chtd@tpu.ru

At present low temperature separation (LTS) is the basic process of gas preparing. This process combines satisfactory gas preparing for transport, small capital expenses, simplicity and reliability in exploitation. At low temperature separation of gas two material currents(streams) are formed: commodity (dry) gas and unstable condensate. As a rule, at gas preparing they aspire to section a tabular mixture so that the components that are in lighter than propane should reach dry gas, and all the rest of the components - unstable condensate.

It is desirable, that fewer none-target components should reach in any above mentioned material. This meets the demands of product quality (condensation point on water and hydrocarbons, stress of saturated steams, water content and mechanical impurities), and economic reasons.

The information-simulating systems are the most effective for decision of such task, at changing input composition of a tabular mixture and carrying out technological process, and also at designing calculation of trade gas installations and gas condensate. A major part at making IMS is the creation of models for exact composition calculation and number of phases at variation of the basic technological arguments and compositions of input currents (streams). Here there are various complications because the process of gas preparing and gas condensate is carried out at high pressure and negative temperatures.

We have designed the model and the program for phase equilibrium calculation in a wide range of trade stresses and temperatures. The process description accuracy by given model has shown, that the error at fraction distillate calculation is no more than 2 %, compositions of a fluid phase 10-12 % and compositions of a steam phase 4-5 %.

In pressure range from 2 up to 12 MPa and temperatures from -30 up to 30^0C the isotherms of tabular mixture condensation of the Mildzino field were constructed. The dependence of distillate fraction on stress has the expressed exponential nature. In other words every mixture has certain pressure, after which the yield of a fluid phase begins to grow strongly. On the contrary, at high temperatures the dependence of distillate fraction on stress is much weaker. In this connection, the distillate fraction of fluid at high pressure to a greater extent is defined by separation temperature, and at low pressure – the separation pressure itself. The

separation temperature effect on distillate fraction at high pressure is 2-3 times is stronger, than at low pressure. The more this difference is, the more high-gravity hydrocarbons are in formation gas composition.

The studies of technological mode effects of the Mildzino field on gas condensate preparation processes were made. The summarized mass balance of mode variation in a separator of a final stage is given in table №1.

Table 1

The mass balance of installation complex gas preparing of the Mildzino field

Current(stream), kg/h	Conditions of a final stage of separation		
	P=5,0 MPa, t=-27°C	P=5,0 MPa, t=-33°C	P=5,0 MPa, T=-38°C
Input of formation gas	$5000*10^3$	$5000*10^3$	$5000*10^3$
Input of dry gas	3983872,0	3959616,2	3928008,5
– including C_3H_8 and C_4H_{10}	311662,1	290976,7	264229,3
– mass %	7,823	7,349	6,727
– including C_{5+}	2521,3	1445,3	876,7
– mass %	0,06	0,04	0,02
Yield of a unstable condensate	1015137,7	1038645,5	1068936,1
– including components are more lighter than C_3H_8	38898,9	41551,7	45214,8
– mass %	3,832	4,000	4,230
– including C_3H_8 and C_4H_{10}	116261,6	136930,1	162966,0
– mass %	11,45	13,18	15,24

The made study demonstrates as far as important correctly to choose a duty specially at a final stage of gas separation. Thus, at drop of separation temperature at a final stage the contents of none-target components in commodity gas has decreased on 1,14 %. In a unstable condensate the contents of none-target components has increased on 0,40 %. Therefore, the drop of temperature in a final separator is economically justified

The comparison of two alternatives separation schemas – one-stage and three-stage is made.

As a tabular mixture the gas from an apron of a bush of wells the Mildzino field of following composition (in molar percents) was taken: CO_2 - 0.43; N_2 - 2.59; CH_4 - 87.36; C_2H_6 -

4.36; C_3H_8 - 2.88; i-C_4H_{10} - 0.71; n-C_4H_{10} - 0.94; C_{5+} - 0.73. The charge on a yield in both cases has compounded 10000 kg/ч. So, the incremental value of an absolute extent of withdrawal of target components has compounded: 6,71 %.

Therefore, for more sharp separation of a tabular mixture on dry gas and unstable condensate resulting in to gain in yield of a condensate is more expedient all condensate, allocated on first stages, to submit on an input of last stage of separation.

Thus, the designed computer technologically shaped simulating system, allows carrying out calculation for engineering, optimization and forecasting of installation work of complex gas preparing.

1. Batalin O.U., Brusilovsky A.I, Zaharov M.U. Phase equilibriums in systems of natural hydrocarbons .M.: Bowels of the earth, 1992 -p.272.
2. R. Read, Dg. Praustniz, T. Shervud. Property of gases and fluids. L.: Chemistry.1982.-p.590
3. Stepanova G.S., Zaitsev I.U., Burmistrov A.G. Design of hydrogen sulfide containing oilfield of hydrocarbons. M.:Bowels of the earth,1986-p.163
4. Shilov V.I., Klochkov A.A., Yrishev G.M. Constant calculation of phase equilibrium of natural mixtures.//Oil economy,-1987.-№1, p.37-39
5. Kravtsov A.V., Maslov A.C., Usheva N.V., Moizes O.E., Kusmenko E.A. Computer analysis of technological modes of installation gas preparing and gas condensate. // Jubilee materials of a scientific - practical conference. Problems and paths of effective development of mineral-raw resources of Siberia and the Far East.2000.p.85-87.

PHYSICO-CHEMICAL AND TECHNOLOGICAL BASIS FOR COMPUTER FORECASTING AND OPTIMIZATION OF BENZINE PROCESSING

A.V. Kravtsov, E.D. Ivanchina, S.A. Galushin, L.V. Dyakonova

Tomsk Polytechnic University, Tomsk, Russia
E-mail: IED@ZMAIL.RU. Fax 415-235

Methological aspects of intellectual systems (IS) formation and their usage for forecasting of petrochemical processes and for training of university students and plant engineering staff on questions connected with physical-chemical and technological laws of industrial processes are considered. The objective necessity of IS using while preparation of engineers according to discontinuous and encyclopaedic principle is shown. The principles of IS creation and realization on the base of generalization of industrial units operation experience for special date processing in computer dialogue regime for users are expounded. Methods of forming of physical-chemical models of heterogenous catalytic processes counting catalyst deactivation are generalized.

The work sets new approach to the efficiency rising and optimization of commercial benzine production by use of computer modelling based on physical-technical and technological peculiarities combined with the data obtained from the existing production lines. Physical-chemical analyses with computer processing of experimental data from refineries offer solutions for the problems of catalyst tests varied due to peculiarities of raw material and technological process, optimal level for Pt-contact of acid and metallic activity, technological parameters stabilisation and catalyst regeneration period forecasting. A model for commercial benzines compounding based on calculation of molecular links intensity between the mixture components and efficiency of joint optimization on technological and production stages of refinery process have been set. A description of training system for both operational and emergency mode for refinery process has also been included.

The approach offered to development intellectual systems represents consecutive set of stages of formation of the adequate circuit of the mechanism of chemical-technological process with subsequent its kinetic description, on the basis of which non-stationary generalised model of contact apparatus and all chemical-technological system as a whole are formed. This model allows not only operative estimation of optimum modes of processes for the given raw material, but also to predict activity of the catalyst during period between regeneration and

general service life, to decide a problem of complex processing of petroleum raw material on ORF and modernisation of working plants.

The following intellectual systems developed on a physical-chemical basis in view of the mechanism and kinetic of transformations hydrocarbons on Pt-catalysts are introduced at the oil refining factory's of Russia:

1. Predicting system of optimum operation of the oil refining factories (ORF, Kirishi, Russia).
2. Computer program of testing of industrial catalysts on physic-chemical properties of processes reforming and isomerization (OC "YUKOS")
3. Computer program "the Adviser of the technologist" for definition of activity of catalysts reforming and distribution of the recommendations on technological modes, conditions of regeneration and development of Pt-catalysts (ORF, Achinsk, Russia)
4. Computer program according to efficiency of the complex technological benzine production (ORF, Kirishi, ORF, Achinsk, Russia)
5. Computer program of optimisation of manufacture commodity benzene in view of the effective additives (ORF, Omsk, Russia)
6. Computer training system for preparation and retraining of the technologists of the oil refining factories (ORF Kirishi, ORF Achinsk, ORF Omsk, ORF Myagikay, Litva)

SIMULATION OF THE PYROLYSIS OF THE WIDE FRACTION OF LIGHT HYDROCARBONS

A.V. Kravtsov, P.I. Koval, A.V. Agafonov

Tomsk Polytechnic University, Tomsk, Russia
E-mail:IED@ZMAIL.RU, Fax 415-235

Now the increase of polymeric products production is observed. The main raw materials for obtaining the polymeric materials are olefins, such as ethylene and propylene. The large-capacity source for producing the olefins is the pyrolysis of hydrocarbons. The hydrocarbon gases (such as ethane, propane and butane), the liquid fraction of oil (virgin gasoline, refined oil, naphtha and kerosene fractions, mazut) and their mixtures are used as the feedstocks for the pyrolysis process. Now many firms and plants are analysing different variants for using the wide fraction of light hydrocarbos (WFLH) as the feedstock for the pyrolysis process because of increasing extraction and production and its low price. If the raw material is changed it is nessesary to evaluate its aptitude and to determine the optimal techological rezhime for operating pyrolysis units. Solving this problems by making a pilot or laboratory unit requires large capital, material and labour inputs. A morden tool which is able to solve this and others problems and decrease probability of appearing an accident on a plant is computers' simulating systems (which include all mathematical description of the technological unit or the main node). Thus, at present creation of the mathematical model of the WFLH pyrolysis is a actual problem.

The main node in the technological scheme of the pyrolysis process is a block of furnaces working in parallel. Therefor, first of all it is nessesary to create the mathematical model of the pyrolysis furnace.

Simulating the pyrolysis process in the furnace is complicated by the number of physico-chemical processes taking place in it (such as heating gas-vapor mixture in the convectional zone of the furnace, thermal destruction of hydrocarbons in the coils, heat transfer through the coil wall, burning fuel in the radiant chamber and turbulent rezhime of the stream in the coil). Taking into account the construction peculiarities of the pyrolysis furnace coil (i.e. the coil diameter is much smaller than its length: $L/d>>50$ and the Reynolds' number is bigger than 10^5), the process may be described by the ideal forcing model.

The ideal forcing model of the reactor (coil) includes the equations of mass and heat balances and the equations for calculating pressure differential which describe changing the stream characteristics (such as temperature, substances concentrations) along the coil length.

Implicit Eiler's method is used for solving the rigid system of the differential equations. In order to obtane the iteration convergence the main cycle (along the coil length) consists of three embedded cycles in which the molar streams of the mixture components, the total molar stream and the temperature are selected.

358 reactions including 20 substances and 17 radicals are used for calculating the WFLH pyrolysis kinetics. The stream mixture characteristics (such as the mixture density, the stream velocity, the heat transfer intensity; enthalpy, heat capacity, heat conductivity, viscosity of the substances) changes along the coil length because of changing the stream composition, temperature and pressure. And therefor the equations correlating the characteristics were found. The viscosity are calculated by Raihenberg's method; the heat conductivity - by Reid-Sherwood one because these methods are the most exact.

The results are shown in fig. 1.

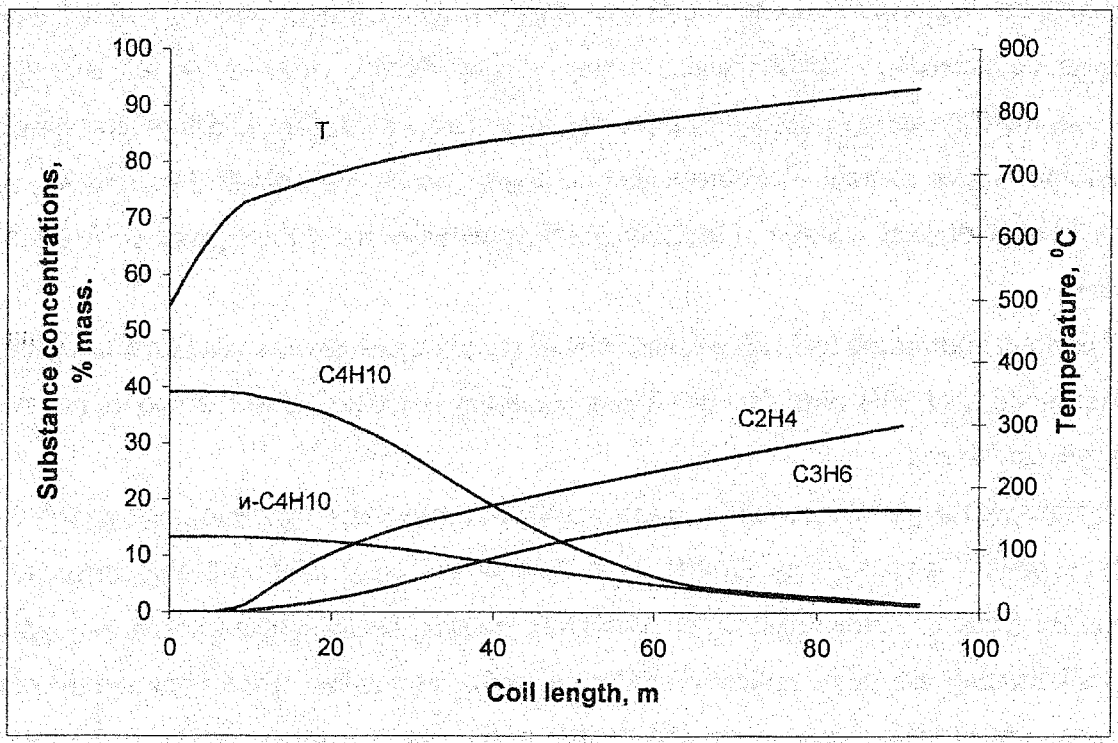

Fig. 1 – Temperature and concentrations changing along the coil length.

The model verification was made on basis of the experimental data collected on Tomsk Petrochemical Combinant. The calculation ratio error for the main hydrocarbons does not exceed 3%.

Table 1 – The program calculation results

Substance, % mass.	Composition, % mass.					
	Ethane fraction+propane fraction+propane-butane fraction			WFLH		
	Feed	Product (experiment)	Product (calculation)	Feed	Product (experiment)	Product (calculation)
H_2	–	1,57	1,54	–	1,39	1,26
CH_4	0,06	10,25	9,37	–	18,47	18,32
C_2H_4	0,44	35,13	35,94	–	31,8	32,1
C_2H_6	47,88	26,64	27,88	2,91	3,64	3,44
C_3H_6	0,09	10,30	9,44	–	17,32	18,05
C_3H_8	25,26	12,10	12,36	27,64	21,14	20,04
ΣC_4	26,27	3,36	3,12	52,43	3,92	3,87
ΣC_5	–	0,65	0,35	17,02	2,32	2,92

This program may be used for both teaching students and optimisation of the pyrolisis process.

PP-13

NEW TECHNOLOGY OF PROCESSING OF PHOSPHATE (MINERAL) RAW MATERIALS USING TOPOCHEMICAL REACTIONS

V.N. Rudin, V.E. Bozhevolnov*, I.V. Melikhov*

Scientific Research Institute of Mineral Fertilizings "NIIUIF",
Leninski prospekt, 55, Moscow, Russia
**Lomonosov State University, Moscow, Chemical Dept.,*
Vorob'evy Gory, Moscow 119899, Russia.
E-mail: Gorba@radio.chem.msu.ru, Fax: (095) 9328846

Most methods used in processing of mineral raw materials are based on two opposed processes: dissolving (evaporation) of desired ingredients of raw materials and crystallization of produced phases. Generally it does not require excessive power consumption. In this relation an idea comes to exclude dissolution and crystallization from the processing and to replace them by topochemical transformation of the primary raw materials. If the raw material has been underwent granulation, the topochemical process may be localized in the granule bulk. It results in new technological possibilities for controlling the process not only by conventional treatment (heat, changing the composition and the flow rates of solutions, on so on), but also by modification of the size, shape and inner structure of granules.

We have carried out a mathematical modeling of a conventional method for processing of raw material (through dissolving) and compared it with a topochemical process. It is shown that if raw material is processed through topochemical route of the chemical reaction, in this case higher technical (power saving) and ecological parameters (increased yield of a final product, possibility of direct utilization of production wastes) are achieved.

Based on the obtained data a technology for production of phosphoric acid has been developed in realizing a topochemical route in the processing phosphate raw materials (apatite). Technology involves a consecutive use of the following operations and apparatus: granulation of apatite in a granulator with treating the granulated material with sulfuric acid solution and covering the granules by porous layer of calcium sulfate and attaining the strength of granules ~ 10 kg/cm^2; realization of topochemical reaction in a countercurrent column –reactor giving granules of calcium sulfate washed from the phosphorus and produced phosphoric acid; separation of produced granules.

Phosphoric acid yield was shown to increase for 3-5% in comparison with conventional processes. Application of the topochemical technology results in decreased (3-4 times less) content of phosphorus in granules of phosphogypsum than in a conventional method. Such

content of phosphorus is ecologically safe in a storage of phosphogypsum in disposal areas. Moreover, produced granules of phosphogypsum may be used both in building industry and in production of ameliorants or ameliorant-fertilizers after impregnation of granules pores by feeding substances.

Application of the topochemical process results in series of advantages in comparison with conventional processes:

- operational time of the process is reduced twice decreasing metal consumption of installation;
- scheme excludes using traditional reactors with stirring devices having high power consumption;
- size of power consuming filtrating equipment decreases in 5-6 times.

All mentioned factors and taking into account an increased efficiency index of raw material processing as calculations show, decreases power consumption for 40-50%.

Thus, theoretical and practical data have shown that technologies based on topochemical transformations may find wide application in the chemical industry.

PP-14

COMPUTATIONAL STUDY OF GAS FLOW THROUGH "GAUZE-PAD - HONEYCOMB" CATALYTIC SYSTEM

V.P. Zakharov, I.A. Zolotarskii and V.A. Kuz'min

Boreskov Institute of Catalysis, 630090, Novosibirsk, Russia
E-mail: zol@catalysis.nsk.su

Qualitative and quantitative simulation results are reported and discussed for the problem of gas flow through a two-stage catalyst bed consisting of a gauze pad and honeycomb monolith bed. Monoliths channels are rectilinear, co-axial and orthogonal to a gauze pad. A reaction takes place on both parts of the catalytic system. Such system is currently used in ammonia oxidation at nitric acid plants [1].

For simplicity the honeycomb is considered as a two-dimensional flat-periodic structure, representing channel walls as solid impenetrable plates of finite thickness. Gas flow is considered to be viscous, laminar, isothermal, and incompressible, while pack of gauzes is isotropic and homogeneous. Catalyst activity is assumed to be extremely high thus providing a mass transfer limitation. At an inlet boundary of a calculation domain, gas flow is considered to be flat-parallel.

The numerical code used in calculations is based on a mathematical model represented by a set of partial differential equations. Resulting numerical solution are two-dimensional in space, time-depending fields of gas flow velocity vector, pressure and active reagent concentration. Gas flow dynamic interaction with the pack of gauzes is represented by a effective porous medium approximation. Thus stated equations set is solved in primitive variables, finite element approximation principle being applied. Pressure field is determined by an original SIMPLE-like algorithm.

Model constants corresponded to the air flow with operation parameters typical for reaction zone in a real catalytic reactor for ammonia oxidation in high pressure nitric acid plants. Geometry used for calculations is also real for the conventional monoliths and packs of platinum gauzes. Flat-periodic channel sizing is performed for a pair of different cases. One case is characterized by walls of the same thickness as in honeycomb. In another one a structure period has the same value as in a real monolith. A porosity of a flat structure is always the same as a porosity of honeycomb.

Effect of a distance between the pack of gauzes and the frontal surface of the honeycomb monolith was studied. Calculations show that extinguishing of the transversal component of

flow velocity in the porous gauze pack is so high that the flow exits the bed oriented almost parallel to channels walls. This means that gauzes pack in the reactor possesses practically absolute refraction property. This result is confirmed by an analytical estimation. This obstacle allows to study a case with the inlet flow direction parallel to the longitudinal axis of monolith channels only.

Numerical results show that a wall streamlining nature changes not monotonously with increasing a distance between two parts of a catalytic system. Flows may be as stationary and non-eddy, as pulsating with recirculation zones. For pulsating regimes time-averaged solutions were obtained. We have found that integral reagent conversion in a pack weakly depends on distance, being minimum when both compartments are attached. Longitudinal reagent diffusion leads to a 1-3% decrease of its concentration at the pack inlet. A distance between the monolith and the gauzes pack essentially effects pressure drop at the inlet of channels. This numerical result was confirmed by a special experiment.

As a result a recommendation for a commercial application of a two-stage catalytic system was obtained.

REFERENCE

1. V.A. Sadykov, L.A. Isupova, I.A. Zolotarski, L.N. Bobrova, A.S. Noskov, V.N. Parmon, E.A. Brushtein, T.V. Telyatnikova, V.I. Chernyshev, V.V. Lunin, Oxide catalysts for ammonia oxidation in nitric acid production: properties and perspectives // Appl. Catal.: A General, **204,** Issue 1(2000), pp.59-87.

PP-15

THE EFFECT OF THE CATALYTIC LAYER DESIGN ON OXIDATIVE DEHYDROGENATION OF PROPANE OVER MONOLITHS AT SHORT CONTACT TIMES

S.N. Pavlova, V.A. Sadykov, Yu.V. Frolova, N.F. Saputina, P.M. Vedenikin, I.A. Zolotarskii, V.A. Kuzmin

The Boreskov Institute of Catalysis, Siberian Branch of the RAS, Lavrentieva, 5, Novosibirsk, RUSSIA; 630090, Fax: (73832) 343766, E-mail: pavlova@catalysis.nsk.su

Introduction. The autothermal oxidative dehydrogenation of paraffins at short contact times over Pt-supported monolithic catalysts was recently shown to be quite efficient in the olefins, especially ethylene, production, [1-2]. For the propane oxidative dehydrogenation, the propylene yields are not sufficient for industrial catalytic process due to propylene cracking into ethylene and methane [2]. Tuning the chemical composition of supported monolithic honeycomb catalysts and the feed composition was shown to improve propylene selectivity and yield as compared with the earlier reported values [3-4]. For the reactor up-scaling the problem of optimal catalytic layer configuration affecting the mass and heat transfer is also very important. Furthermore, homogeneous or surface-enhanced homogeneous reactions are expected to appreciably affect the propylene yield. However, these questions were earlier not addressed properly for the case of experiments conducted with monolithic catalysts operating at short contact times in the autothermal mode. Hence, the present research aims primarily at filling these gaps in fundamentals of propane oxidative dehydrogenation at short contact times on honeycomb corundum monolith supported catalysts.

Experimental. The catalysts with active components based upon platinum or complex framework zirconium phosphates containing Co (Mn) supported onto corundum thin-wall micromonoliths were tested in the autothermal mode at high concentration of propane in air. The tubular reactor of the original design allowing to independently preheat the inlet feed and control the catalyst temperature was used. For tuning the longitudinal temperature profile, a reactor was additionally equipped with a heat exchanger allowing to cool the rear part of the monolithic catalyst. To take probes of the gas phase immediately after the catalyst, a specially designed tube sampler kept at a constant temperature to prevent the water condensation was used. For tuning the feed composition, water, carbon dioxide, carbon oxide, and hydrogen were added, and the propane/oxygen ratio was varied. The role of the gas-phase reactions was studied by varying the distance between the cooled sampler and the monolith end as well as by changing the distance between two monolithic pieces placed into the reactor. Available

data on the elementary steps of propane pyrolysis and homogeneous oxidation were taken into account.

Results and discussion. To optimize the catalytic layer configuration, the effect of the front and back heat shields on the performance of a monolithic catalyst was studied. The data obtained at similar values of propane conversions and operating temperatures show that adding of the back shield decreases propylene selectivity owing to its cracking, and this trend is more pronounced at higher operation temperatures. Without the front shield the propane and oxygen conversion decreases though the catalyst temperature measured at the end of monolith is somewhat higher than that with the front shield installed. The high outlet gas temperature and low propane and oxygen conversions suggest that without the front thermal shield, the temperature gradient along the monolith changes and its maximum transfers to the end of monolith. The front shield helps to keep heat generating at the catalyst and flattens the temperature gradient along the monolith length thus allowing to increase propane conversion and olefins yield. Therefore the temperature profile along the catalyst being dependent on processes of heat generation and transfer is very important.

To clarify the role of heat generation and its transfer along the monolith in the autothermal mode, the dependence of the catalyst temperature, propane conversion and products selectivity on the feed rate, monolith length and its position in the reactor was studied. The results obtained show the absence of any general relation between the propane conversion and contact time for monoliths of different length. Similarly, monolith position in the reactor, mean catalyst temperature and space velocity do not determine propane conversion and selectivity. Therefore, to compare results obtained in different reactors a catalyst bed configuration and gas velocities should be very similar. To decrease the catalyst overheating at the reactor outlet, the heat exchanger was demonstrated to be very efficient. However, comparable values of propane conversions and products selectivities for the catalyst performance in both types of reactors – with and without the heat exchanger, allows to conclude that in all cases they are mainly determined by the high temperatures developed in the inlet part of monolithic layer.

Comparison between performance of the catalyst fraction (0.25-0.5 mm) and monolithic piece shows that due to the gas flow turbulence and inhomogeneity in the packing of fraction within the layer, the degree of propylene cracking is higher in the former case. It suggests that cracking easily proceeds via thermally activated process in the gas phase. Hence, to minimize cracking, we must use straight-channel monoliths with very narrow channels, decrease the gas

residence time by increasing linear velocities while keeping the catalyst temperature at the optimum level by controlled preheat of gas and catalyst.

The impact of gas-phase reactions on the process of propane oxidative dehydrogenation at short contact times has been demonstrated by results of experiments with varying the empty space between the cooled sampler and the exit of monolith, as well as by experiments with the variably distance between two parts of the monolithic catalyst. As for the case of a big distance between the cooled sampler and monolith, propane conversion increases when the distance between the monolithic pieces is reasonably long (8 mm), suggesting the essential impact of the homogeneous reaction proceeding in the space between two monolithic parts, contribution of the homogeneous reaction being certainly higher for higher linear velocities (feed rates). Though propane conversion is higher, no gain in propylene selectivity was found. Hence, purely heterogeneous approach is certainly preferable.

Complex zirconium phosphates supported onto corundum micromonoliths were found to be able to support the autothermal mode of propane oxidative dehydrogenation at short contact times even without Pt addition. Tremendously important is the fact that these catalysts are not subjected to coking even for feeds with the excess of propane, and their performance is stable. For those systems, the propylene yield was higher than that for corundum supported Pt. In the autothermal conditions, in the reactor not equipped with the heat exchanger, the temperature usually increases with the feed rate due to higher rate of heat generation. As the result, propylene cracking into ethylene and methane prevails at short contact times. The cracking was found to be rather insensitive to the acid-base properties of the active component and mainly determined by the surface initiated radical reactions in the gas phase at high (> 750 ^{o}C) temperatures. A low ability of complex zirconium phosphates to combust propane limits the surge of temperature at the monolith inlet, thus decreasing cracking.

In general, cracking probability is determined by the relative abundance of n- propyl and secondary propyl radicals. While the latter is rapidly converted into propylene by the hydrogen atom abstraction, the former is splitted into methyl radical and ethylene. Heterogeneous route favors formation of secondary propyl radicals due to lower C-H bond strength for central carbon atom. The addition of hydrogen to the feed and presence of Pt in the catalyst help to convert i-C_3H_7 into n-C_3H_7 via hydrogenation of propylene, thus increasing cracking. Moreover, for Pt-containing catalysts, in the reactor equipped with the heat exchanger cooling the rear part of monolith, ethane appeared in the products due to ethylene hydrogenation.

Water and carbon dioxide added to the feed hinder hydrogen activation thus decreasing cracking.

By simultaneous tuning such parameters as the temperature profile along the monolith layer, the active component and feed compositions, the yield of olefins was increased to more than 40%, propylene dominating.

References

1. M. Huff and L.D. Schmidt. J. Catalysis, 149, 1994, 127.
2. A.S. Bodke, D.A. Olshki, L.D. Schmidt, E. Ranzi, Science, 285, 712 (1999)
3. V.A. Sadykov, S.N. Pavlova, N.F. Saputina, I.A. Zolotarskii, N.A. Pakhomov, E.M. Moroz, V.A. Kuzmin, A.V. Kalinkin, Catalysis Today, 61, 1-4 (2000) 93.
4. V.A. Sadykov, S.N. Pavlova, N.F. Saputina, I.A. Zolotarskii, N.A. Pakhomov, E.M. Moroz, V.A. Kuzmin, A.V. Kalinkin, A.N. Salanov, I.G. Danilova, E.A. Paukshtis. In: Studies in Surface Science and Catalysis, A.Corma, F.V. Melo, S.Mendioroz and J.L.Fierro (Editors), Elsevier, 2000, 130 B, 1907.

PP-16

PHOTOCATALYTIC OXIDATION OF BUTYRALDEHYDE IN AIR: BY-PRODUCT IDENTIFICATION AND MECHANISM

Cunping Huang, Daniel H. Chen*, Kuyen Li

Dept. of Chemical Engineering, P.O. Box. 10053,
**Lamar University, Beaumont, TX 77710, USA*
Tel.: (409) 880-8786, Fax: (409)-880-2197,
e-mail: address: chendh@hal.lamar.edu

Photocatalysis has gained much attention in air and water pollution control. The photocatalytic oxidation was carried out in various photoreactors such as thin-film reactor, fiber-optic reactor, or packed-bed reactor. Photocatalytic oxidation of VOC to a great extent mineralizes low concentrations of VOC to carbon dioxide and water at room temperatures under the activation of near-UV. It also produces some low-molecular mass by-products, which can be further oxidized and are amenable to bio-remediation. An activated carbon column and a glass bead column were used for by-product identification of butyraldehyde photocatalytic oxidation in air. The oxidation yielded carbon dioxide as the major product. The major by-products caused by C-C bond cleavage were propinonaldehyde, 1-propanol, ethanol, and acetaldehyde, whereas propyl formate and di-n-propyl ether were secondary by-products. The reductive coupling of propinonaldehyde and butyraldehyde may result in the formation of 3-heptene and some other related C7 olefins. Aldol condensation of the vapor phase aldehydes on TiO_2 surfaces may be partially responsible for the formation of some minor by-products.

INFLUENCE OF PARTIAL PRESSURES OF METHANE AND OXYGEN ON TEMPERATURE CONDITIONS OF METHANE DIMERIZATION PROCESS AND C_2-HYDROCARBON YIELD

S.I. Galanov, L.N. Kurina, I.A. Kurzina*

Tomsk State University, Tomsk 634050, Russia
Fax:+7 3822 415585; Phone:+7 3822 424257; E- mail: galanov@xf.tsu.tomsk.su
**Tomsk State University of Architecture and Building, Tomsk, Russia*
Fax: (3822)753362; Phone: (3822)753086; E-mail: kurzina99@mail.ru

Synthesis of ethylene by an oxidizing dimerization of methane (ODM) - one of promising methods of natural gas processing for production of ethylene and liquid fuel from non-oil stock [1, 2]. The ODM reaction proceeds efficiently at low partial pressures of CH_4 and O_2 reagents [1]. The rise of their contents in a reaction mixture leads to fall of selectivity and C_2-hydrocarbon yield. For clearing up the reasons of this effect we have investigated the influence of variations of partial pressures of CH_4 and O_2 on selectivity and C_2-hydrocarbon yield over Sn-containing catalysts.

In the present study we used the catalysts based on tin dioxide, promoted with 10 wt. % of lithium and potassium oxides. The CH_4:O_2 ratio was 3,5-4:1 in all experiments, O_2: N_2 ratio varied from 20 up to 0. The contact time was 0,5 sec, initial temperature in reactor - 760°C.

Table.

Influence of a dilution of reagents by nitrogen on a yield and selectivity on C_2-hydrocarbons (T_0=760°C; contact time 0,5 c).

CH_4: O_2:N_2 ratio	CH_4 conversion, %	Selectivity on C_2, %	C_2 yield, %	CH_4;O_2 pressure, 10^5 Pa
10 wt.% Li_2O/SnO_2 catalyst				
3,5:1:20	20,9	84,5	17,6	0,182
3,5:1:17	24,7	75,0	18,5	0,202
3,5:1:11	33,3	71,2	23,6	0,293
3,5:1:7,5	28,3	69,0	19,5	0,384
3,5:1:5	30,8	62,8	19,4	0,475
3,5:1:3	26,7	56,2	15,0	0,606
3,5:1:2	23,1	55,0	12,7	0,697
4:1:0	26,6	43,0	11,4	1,01
10 wt.% K_2O/SnO_2 catalyst				
3,5:1:3	9,0	73,0	6,57	0,606
4:1:0	9,2	71,9	6,6	1,01

Data of the table show that the rise of partial pressures of reagents when using the Li-containing sample leads to decreasing of selectivity to C_2-hydrocarbons. The growth of CH_4 conversion is observed up to a particular reagents/solvent ratio. The yield of C_2-hydrocarbons raises up to a maximum at dilution of a reaction mixture in 11 times, the further rise of methane and oxygen pressure results in lowering of C_2-hydrocarbon yield.

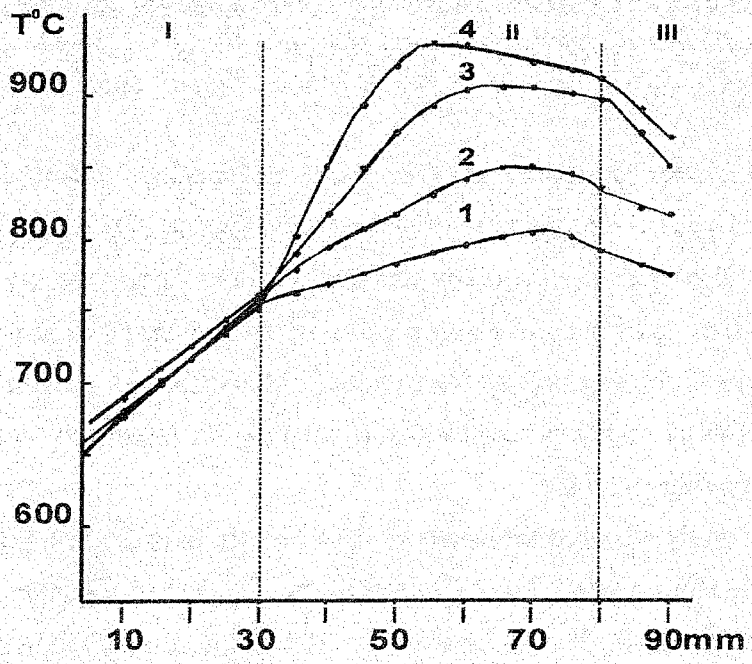

Fig. 1. Influence of partial pressures of methane and oxygen on change of temperature gradients on the catalyst layer:

I - preheat zone; II – catalyst layer; III – quartz layer.

P (CH_4; O_2) × 10^5 (Pa): 1- 0.29; 2 - 0.47; 3 - 0.70; 4 - 1.01

Dilution with N_2: 1 - in 11 times, 2 - in 5 times, 3 - in 2 times, 4 - without dilution.

The measuring of the temperature gradient on reactor length has shown that at low partial pressures of reagents and initial temperature of a reactor (760°C) catalyst layer is not heated up (Fig. 1). At ratio CH_4:O_2:N_2 = 3,5:1:11 temperature of the catalyst increases up to 790-800°C, the yield of a dimerization product is maximum. Usage of a reaction mixture at pressure of reagents near $0{,}475\times10^5$ Pa leads to spontaneous heating of the catalyst up to 840-850°C, that causes growth of selectivity, but the high C_2-hydrocarbon yield remains. The rise of the reagent pressures increases the temperature of the catalyst up to 900-920°C, and the maximum of temperature is shifted to an upper part of a catalyst layer. This leads to sharp fall of selectivity on C_2-hydrocarbons and, accordingly, their yield. Usage of the methane-oxygen admixture not diluted with nitrogen results in overheating of the catalyst layer up to 940-950°C with significant lowering of selectivity and yield of principal products (Fig.1, Table).

The substitution of the active 10 wt.% Li_2O/SnO_2 catalyst by less active 10 wt.% K_2O/SnO_2 sample does not lead to overheating of the catalyst layer and high selectivity on principal products remains at high concentrations of methane and oxygen (Table).

According to thermochemical data [3], at temperatures of ODM reaction (700-900°) the heat effect of basic reactions can be evaluated by the following data:

1. $2CH_4 + 0{,}5O_2 = C_2H_6 + 0{,}5H_2O$ $\Delta H = -176{,}8$ kJ/mol.
2. $C_2H_6 + 0{,}5O_2 = C_2H_4 + H_2O$ $\Delta H = -105{,}5$ kJ/mol.
3. $CH_4 + 2O_2 = CO_2 + 2H_2O$ $\Delta H = -803{,}9$ kJ/mol.
4. $C_2H_6 + 3{,}5O_2 = 2CO_2 + 3H_2O$ $\Delta H = -1490{,}2$ kJ/mol.
5. $C_2H_4 + 3O_2 = 2CO_2 + 2H_2O$ $\Delta H = -1329{,}7$ kJ/mol.
6. $C_2H_4 + O_2 = 2CO + 2H_2$ $\Delta H = -451{,}1$ kJ/mol.

The equations (1) - (6) show that even selective reactions of ethane and ethylene formation are exothermic and the heat emission of the reactions of deep oxidation considerably exceeds ΔH of target reactions. Accordingly, at increasing the partial pressures of the reagents an extreme overheating of the catalyst layer is observed, that results in rise of a part of unselective reactions. The raising of temperature at 100°C from optimal one (750-850°C) increases the rate of a deep oxidation of ethane and ethylene in 1,7 times [4]; the rate of thermal decomposition of ethylene increases in 3 times [5]. With temperature growth the rate constants of secondary reactions of synthesis-gas formation raises at interaction of hydrocarbons with O_2 and H_2O [3]. It can explain the fall of selectivity on C_2-hydrocarbons with rising of partial pressures of reagents [1].

The obtained results display that the commercial usage of the process will confront with the following difficulties: at usage of concentrated methane-oxygen admixtures strong heat development and warming up of the catalyst limits the methane conversion: no more than 10-15 % for one cycle of the reaction. The carried out study has shown that the presence of abundant oxygen in a gas phase does not lead to significant lowering of the selectivity on principal products, at keeping a thermal regime of a reaction.

References

[1] Otsuka K., Liu Q., Hatano M., Morikava A. // Chem. Lett. 1986. № 6. -P.903-906.

[2] Kurina L.N., Galanov S.I., Meltser L.Z. // Catal. Today. 1992. V.13, № 4. P. 537-542.

[3] Petrenko I.G., Philippova V.I. Thermodynamics of reactions of C_1-C_5-hydrocarbon transformation. Moscow: Chemistry, 1972, 152 p.

[4] Lane G.S., Wolf E.E.. // J. Catal. 1988. V.113, № 1. P.144-163.

[5] Taniewski M., Skutil K., Lachowicz R., et all. // Catal. Today. 1992. V.13, № 4, P.529-536.

PP-18

OXIDATIVE CATALYTIC CONVERSION – A NEW LINE IN HEAVY PETROLEUM FEED PROCESSING

R.R. Vezirov, S.L. Larionov, E.G. Telyashev, U.B. Imashev

Ufa State Petroleum Technical University
Russia, 450062, Ufa, Kosmonavtov, 1
The Institute of Petroleum Refining and Petrochemistry of the
Bashkortostan Republic Academy of Sciences
Russia, 450065, Ufa, Initsiativnaya, 12, Phone: (3472) 42-24-71, Fax: (3472) 43-31-17

Analysis of the up-to-date state of research in the field of thermocatalytic processing of high molecular weight petroleum feed has shown that the use of heavy petroleum fractions and residues as a catalytic processing feed has some difficulties explained by high content of asphaltic resinous materials and sulfur compounds as well as technological features of their processing (intensive coke formation and catalyst poisoning by metals). Use of the catalysts containing metal oxides including iron oxides in heavy petroleum feed processing makes it possible not only to obtain high yield of gaseous olefin hydrocarbons but also avoid the problems, connected with catalyst poisoning by feed metals and enlarged coke formation [1,2]. A peculiar feature of the catalysts, containing metal oxides of variable valence, is proceeding of reduction reactions on them, while hydrocarbons transformation takes place according to a stage mechanism with an intermediate carboxylate complex production which is either destructed with formation of O_2 and a less molecular mass hydrocarbon or desorbed from the catalyst surface with an oxygen-bearing compound formation [3].

The conducted researched works have shown that a supported catalyst, containing Cu and Cr oxides, has the maximum estimated by CO_2 yield oxidative activity among the other catalysts examined. It has been shown that content of oxidation products depends on the presence of active oxygen on the catalyst surface. As it is consumed, oxydative activity exponentially decreases and approaches a definite level caused by partial reduction of catalyst oxidative activity at the expense of steam oxidation. At the same time, the maximum selectivity in oxidative dehydration reactions with olefin formation, estimated by relation between the sum of olefins and the sum of paraffins in gas, is observed for the catalysts bearing iron oxides.

Nature, fractional and chemical composition of the feed influence proceeding of oxidative catalytic conversion. The maximum CO_2 formation rate at the initial moment is observed for a hydrotreated vacuum gasoil, and decreases according to the raw: hydrotreated vacuum gasoil, straight – run vacuum gasoil, fuel oil, road tar. The rate of CO_2 formation decreases

with time for all kinds of the feed and approaches a comparable level. The difference is explained by variation of sulfur compounds content which are strong oxidative exhibitors. As the quantity of feed sulfur compounds increases the rate of CO_2 formation goes down.

Iron oxide catalysts have a high selectivity in oxidative dehydration reactions, their selectivity depends on feed nature and process temperature. As temperature rises selectivity drops for all kinds of the feed. The maximum selectivity is observed for a hydrotreated vacuum gasoil.

Formation of the basic part of liquid products proceeds according to a stage mechanism with formation and subsequent destruction of intermediate carboxylate or sulphone complexes leading to appearance of hydrocarbon products and high content of oxygen-bearing compounds. During the process of oxidative catalytic conversion an essential increase of oxygen content takes place of the residue with EBP 350°C. The total yield of oxygen – bearing compounds decreases with increase of temperature which is explained by their low thermal stability and increase of complete destruction reactions part. At the expence of essential rearrangement of oxygen – bearing compounds advantageous formation of dicarbonic acids anhydrides, sulphoxides, phenols and ketons takes place, while the maximum ketone content coincides according to temperature extreme levels with the maximum content in liquid products [3,4].

In the process of coke formation during oxidative conversion of heavy petroleum feed take place such reactions as oxidation, dehydration, dealkylation, destruction, polymerization and polycondencation of asphaltic resinous substances.

Besides, oxidative consecutive transformation of coke deposits leads to a more deep chemical conversion as compared to a thermal transformation. Selective influence of the iron oxide catalyst on the process of burning- out of the basic elements of coke deposits has been found.

Iron oxide catalysts speed up hydrogen oxidation to a larger degree as compared to sulfur oxidation. Possibility of complete catalyst self-regeneration during oxidative catalytic conversion of vacuum gas-oil and partial self-regeneration during processing of a heavier petroleum feed has been shown [5,6].

During catalytic cracking alongside with catalytic processes, proceeding according to a carbonium-ionic mechanism, and thermal processes, having a radical mechanism, transformation due to oxidation – reduction reactions take place. The mechanism of interaction of sul-

fur compounds from a catalyst surface with formation and destruction of sulphone compex and SO_2 production has been proposed.

During catalytic conversion of a heavy petroleum feed, taking place in a large-scale catalytic cracking process, it is oxidation of sulfur compounds that takes place first. Feed sulfur compounds react with oxide catalysts oxygen with intermediate sulphone complex formation with finite gaseous oxidation products and sulphoxides formation. High molecular weight sulfur compounds of sulphide type have the largest inhibitory ability [7]. It was proposed and supported by pilot and full-scale tests that phenols formation during catalytic cracking proceeds mostly according to oxidation of feed alkylaromatic hydrocarbons by oxygen, induced into the reactor with a recovered catalyst.

The method of prevention of formation and proceeding of oxidation-reduction reactions in the catalytic cracking process has been proposed based on introduction of a reduction agent – hydrocarbon gas [8].

The established laws of oxidative catalytic conversion of a heavy petroleum feed [7] may be used not only in development of new technologies of petroleum residues conversion on oxide-type catalysts but also in improvement of existing processes proceeding with oxidative conversion.

REFERENCES

1. Valitov R.B., Telyashev E.G., et al. Catalytic Pyrolysis of Heavy Petroleum Fractions and Residues. M. TsNIITENeftekhim, 1988, p.38.
2. Valitov R.B., Telyashev E.G., et al. Production of the lowest Olefinic and Aromatic Hydrocarbons from High Molecular Weight Petrochemical Feed. Book "Synthesis on the Basis of Petrochemical Products" Novosibirsk. Nauka, 1990, p.p. 5-16.
3. Vesirov R.R. Neftepererabotka i neftekhimia, 1998, №9, p.p. 29-33.
4. Vesirov R.R., Yavgildin I.R. et al. Khimia i technologia topliv i masel. 1995, №6, p.p. 23-25.
5. Telyashev E.G., Vesirov R.R et al. See above, p.p. 28-30.
6. Vesirov R.R., Yavgildin I.R. et al. See above, p.p. 31-33.
7. Vesirov R.R., Larionov S.L. et al. Oxydative Catalytic Conversion of Heavy Petroleum Feed. Ufa, "Reaktiv", 1999, p. 132.
8. Vesirov R.R., Oukhova S.A. et al. Neftepererabotka i neftekhimia, 1998, №4, p.p. 17-21.

PERSPECTIVE TECHNOLOGIES OF ENVIRONMENT FRIENDLY GASOLINE PRODUCTION ON THE BASIS OF THE CRUDE HYDROCARBONS SELECTIVE PROCESSING PRINCIPLE

R.R. Vezirov, N.R. Vezirova

Ufa State Petroleum Technical University
Russia, 450062, Ufa, Kosmonavtov, 1
The Institute of Petroleum Refining and Petrochemistry of the
Bashkortostan Republic Academy of Sciences
Russia, 450065, Ufa, Initsiativnaya, 12, Phone: (3472) 42-24-71, Fax: (3472) 43-31-17

Production of environment friendly gasoline was generally associated with reduction of lead contents, having negative impact on the environment, in this connection application of reforming and isomerization processes, producing high-octane components, sharply has grown. Especially effective octane upgrading is reached by reforming of petroleum fractions. Improvement of process was conducted in the following directions:

- Increase of target conversion in the naphthenes dehydrogenation and paraffin's dehydrocyclization reactions with formation of high-octane aromatic compounds;
- Decrease of coke formation and deactivation of the catalyst;
- Reduction of gas fraction lower C_5 formation and increase of the reformate yields.

The increase of target conversion alongside with the application of bimetallic and polymetallic selective catalysts is promoted by increase of the process severity (mainly, pressure decrease), however it results in increased coke formation and fast deactivation of the catalyst. To solve this problem the technologies of continuous catalyst regeneration were developed which for want of severe mode of process (pressure 0.35 МПа) [1] and high capacity of regeneration allow to obtain the product which has RON up to 102-105. The reformate has the yields up to 83-88 % and contains up to 87 % of aromatics (depending on the content of paraffins in the crude) [2].

From the end of the 80-th the new ecological requirements to reduction of the aromatics content, and especially benzene content in fuels were developed, that has caused changes in technology of straight-run gasoline cuts processing. The variants of benzene reduction are divided into two types: preliminary fractionation of the reforming crude with elimination of the benzene precursors, or separation of benzene containing cut of reformate, with the consequent processing of these fractions [3,4].

The benzene reduction problem activated development of isomerization processes, which are considered now as perspective methods of ecologically pure high-octane components pro-

duction from gasoline cuts. The improvement of isomerization technology is mainly characterized by transition to active zeolite and amorphous catalysts and increase of selective conversion of paraffins through increase of recycle degree of non-transformed feed compounds. The increase of the hydrocarbons recycle degree through the catalysate rectification allows to increase isomerizate RON by 2-4 items as compared to once-through isomerization. The technology of separation with rectification is usually selected depending on the type of feed. So, if the processes feed has predominant pentane content the scheme with deisopentanizer is used, and with more heavy feeds catalizate deisohexanization is more preferable. The recycle of n-paraffins through isomerizate adsorption permits to reach isomerizate RON increasing by 8-9 units. The selectivity of processing using rectification is much lower, than that for adsorption, as in the first case a fair quantity of n-paraffins rests in isomerizate, and the reactor thermodynamic balance is worsened at the expense of the high isoparaffins content in recycle stream.

The higher degree of n-paraffins conversion in isoparaffins is reached by a combination of these two methods of separation. For example, when pentanes content is predominant in feed, the isomerization technology with upstream deisopentanization and adsorption of n-paraffins from isomerizate is offered, that allows to increase product RON up to 88-90, depending on catalyst used. The scheme with the combination of deisohexanizer and adsorption provides practically complete conversion of the feed in isocomponents (isomerizate RON achieves 92), in which not only n-paraffins, but also main part of methylpentanes are separated from the isomerizate and come back to reactor [5]. Maximizing the selectivity of processing using such schemes is provided by technologies with isoparaffins separation from process feed, that improves balance in reactor, the ballast content in feed is reduced and therefore, the catalyst consumption decreases. Non-transformed components recycle allows also using of zeolite catalyst in process, that is less active, but more convenient in operation, than amorphous one [6].

Thus, in gasoline production the tendency of raising of crude hydrocarbons processing selectivity is traced which assumes separating both feeds, and products of processing not only by boiling points, but also by chemical tag, i.e. by classes and groups of hydrocarbons (or even separation of individual compounds), and their processing, that allows to improve products quality and to increase processes efficiency.

On the basis of a principle of hydrocarbons selective processing, developed earlier [7], the technology of environment friendly high-octane gasoline blends obtaining from straight-run naphtha is developed: the fraction C_5-180 (200) is directed to hydrotreating for deleting

sulfur and other impurities, as well as saturating olefins. Then hydrogenated naphtha is fractionated on C_5-C_6 fraction and C_6+ cut. From the C_5-C_6 fraction isopentane is separated, which is used as a gasoline blend, then the fraction is fed to the isomerization process with n-paraffins and methylpentanes recycle, obtaining the product containing only high-branched high-octane isoparaffins C_5-C_6. Fraction containing benzene and its precursors is selected from the naphtha C_6+, which is exposed to severe hydrogenation and is directed together with C_5-C_6 cut to isomerization. On the other hand, the obtained heavy naphtha is divided into a paraffinic fraction and a naphthenic fraction (which also contains aromatic hydrocarbons). Naphthenic fraction moves to a soft mode reforming with continuous catalyst regeneration that gives the product containing up to 95 % and above aromatic hydrocarbons. If necessary, the benzene cut is selected from reformate, and is either processed together with the benzene predecessors, or alkylated by olefins. The paraffin fraction is exposed to isomerization with n-paraffins recycle in order to increase hydrocarbon conversion. The advantages of such approach to the gasoline production are the followings:

- First, the technology of existing processes becomes simpler because providing of conversion of all kinds of feed compounds is not required. So, for example, in catalytic reforming processes up to date the feed contains a fair quantity of paraffins, which are hardly converted to aromatics, therefore catalyst and technological mode are improved mainly to activate not only naphthenes dehydrogenation, but also paraffins dehydrocyclization. In a case of reforming of the only naphthene-aromatic feed it is possible to apply a soft mode of process (lower temperature, higher pressure) for complete conversion. That allows to reduce a cracking degree and coke formation and to increase an output of the target product, i.e. to increase gasoline pool;
- Secondly, the absence of ballast components passing through reactor, not undergoing conversion to target components, allows to reduce the capacity of units, i.e. to reduce appropriate capital and operating costs;
- Thirdly, the given approach allows to reduce considerably the content of aromatic hydrocarbons in comparison with all existing methods, without double processing, where the reactions have the opposite effect, as in the schemes, where to satisfy standards of the gasoline to benzene and total aromatics after naphtha reforming the catalysate or its fraction is hydroprocessed, i.e. return to delete aromatics takes place.

Thus, the technology developed on the basis of hydrocarbons selective processing principle allows to make qualitative jump in production of gasoline and to use in a new fashion conventional processes of petroleum refining, as reforming and isomerization.

REFERENCES

1. The directory of modern processes of petroleum refining, 1994 // Oil and gas technology, 1995. - № 3. - Pp. 39-62.
2. Anderson G., Felch D., Gray G., Haizmann R.S., McBride T., Rechford R., Raguram S. New approach to the platforming technology, directed on increase of flexibility and profitability of process. // UOP Refining Technology Conference. – Moscow, 1997. - Pp. 1-22.
3. Kisom U. H., Kuchar P. K. Combination of Penex and Platforming processes for more effective naphtha using and benzene management. // UOP Refining Technology Conference. - Moscow, 1997. - Pp. 1-16.
4. Bortov V.U., Georgiyevskiy V.U., Shipikin V.V., Tanatarov M.A., Akhmetov A.F. Obtaining of low aromatics containing high-octane gasoline blends // Khimicheskaya tekhnologiya topliv i masel. - Moscow, 1985. - № 5. – Pp. 8-10.
5. Kuchar P. K., Breaker J.S., Renault M.E., Haizmann R.S. Improvement of the paraffin isomerization process. // UOP Refining Technology Conference. - Moscow, 1997. – Pp. 1-14.
6. Dupra K., Minkkinen A. The advanced technology of paraffins isomerization with recycle scheme. // Neftepererabotka i neftekhimiya. - Moscow, 1999. - № 10. - Pp. 3 - 11.
7. Vezirov R.R., Vezirova N.R., Telyashev I.R. Perspectives of "chemical" fractionation in the petroleum processing technology. // Neftepererabotka i neftekhimiya. - Moscow, 997. - № 8. - Pp. 30 - 31.

EFFICIENCY ANALYSIS OF CATALYTIC TECHNOLOGIES FOR ELEMENTAL SULFUR PRODUCTION FROM HYDROGEN SULFIDE WITH THERMODYNAMIC MODELS

A.R. Mukhamedova, T.R. Zdanov, A.V. Podshivalin, E.G. Telyashev

Ufa State Petroleum Technical University
Russia, 450062, Ufa, Kosmonavtov, 1
The Institute of Petroleum Refining and Petrochemistry of the
Bashkortostan Republic Academy of Sciences
Russia, 450065, Ufa, Initsiativnaya, 12, Phone: (3472) 42-24-71, Fax: (3472) 43-31-17

Sulfur production by Claus method is a widely used at modern refineries petrochemical process of elemental sulfur recovery. A great variety of feed calls for different technologies and instrumental alternatives of this process. With deepending of petroleum processing new hydrogen sulfide sources are appearing (visbreaking, and coking gases, etc) promoting further development of the process. A moving force stimulating development of hydrogen sulfide utilization process lies in the necessity to increase sulfur recovery from a hydrogen sulfide – bearing gas and minimize sulfur compound emissions.

At a standard Claus unit hydrogen sulfide conversion does not exceed 96% vol. due to catalytic reaction equilibrium limits [1]. Increasing the number of stages makes it possible to increase conversion degree to 97-98% vol.

This work deals with several modifications of the Claus process permitting to solve the problems of the hydrogen sulfide conversion and creating an efficient system of technological process control on the basis of theoretical model calculations and real process data, realized at the joint-stock society «Bashkirian Petrochemical Co».

The thermodynamic models of three variants of the process have been developed for calculation of technological parameters, material and heat balances of the process. The first model is a standard Claus unit with two catalytic converters, operating with 90% and above H_2S content in acid gas. The second model constitutes a standard Claus unit supplied with three catalytic converters. The third model is a standard Claus unit with a reactor of direct hydrogen sulfide oxidation.

Model schemes of the process are shown at fig. 1. Comparative technological parameters of the models (designed) and the real processes (real) are given in the table below.

During model calculations thermodynamics of proceeding reactions and kinetics of sulfur formation in the catalytic reactions were taken into account:

$$2H_2S + SO_2 \rightarrow 3/nS_n + 2H_2O \qquad (1)$$

$H_2S + 0{,}5O_2 \rightarrow 1/nS_n + H_2O$ (2)

According to reaction (2) the basic sulfur forms, formed during operating conditions of the Claus catalytic converters (T÷250-350 °C), are S_6 and S_8, that's why only these component were taken into account.

The reaction of direct oxidation (2) is thermodynamically compete contrary to the Claus reactions, and has an exothermal character being conducted at one stage. In order to make reaction proceeding complete it is necessary to guarantee a constant concentration of hydrogen sulfide in the acid gas with minimum content of sulfur dioxide in the effluent gases. That's why a thermodynamic stage is conducted with an air shortage (the air-to-acid gas ratio being decreased by 10-15% against the normal). During this at catalytic stages of the process proceeds the reaction of interaction between hydrogen sulfide and sulfur dioxide with H_2S excess, permitting complete transformation of SO_2 into sulfur.

The calculations performed have shown that increase of catalytic stages does not lead to sharp increase of conversion – for a three stage variant conversion amounts to 97.5-98%. Capital costs are not proportional to the resultant quality. The total degree of hydrogen sulfide conversion at the Claus units with a direct oxidation reactor is 1.5 higher as compared to the Claus unit with three catalytic converters. Accordingly, the scheme of the Claus process with a direct oxidation reactor has more benefits against the standard three-stage Claus process.

According to IPNKHP recommendations in march 2000 a unit of effluent gases after-treatment according to the direct oxidation technology was put into operation. A full-scale test has shown that the total degree of hydrogen sulfide conversion at the unit ammounted to a stable value of 99%, while sulfur discharged decreased by 5-8 times in average.

The results of models testing have shown that the real degree of hydrogen sulfide conversion is somewhat lower against the designed one. In spite of it the developed models adequately describe operation of Claus units at different regimes.

Adequacy of the models to real of units makes it possible to use them with success in the algorithms of adaptive control of the process.

Use of adaptive control of the technological process permits to take into account possible process reactions and constantly adapt for process conditions in order to automatically maintain the optimum operation regime. The scheme of apparatus-program control complex is given at fig.1.

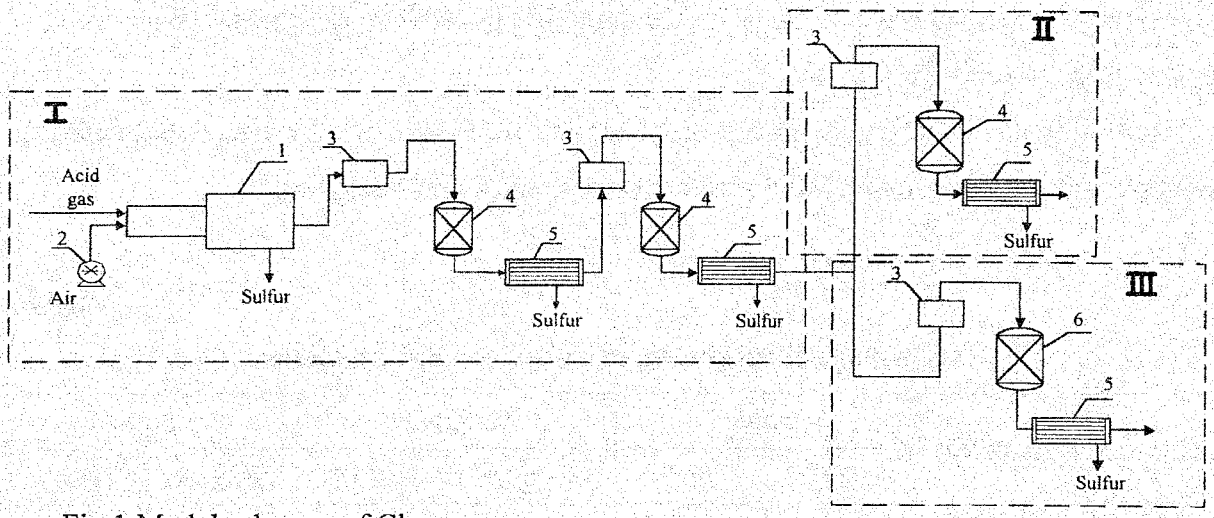

Fig.1 Model schemes of Claus process

I – a standard Claus unit; II – a standard Claus unit plus the third catalytic reactor; III – a standard Claus unit plus the direct oxidation reactor.

1 – a reaction furnace with waste heat exchanger; 2 – an air-blower; 3 – a reheaters; 4 – a Claus converters; 5 – sulfur condensers; 6 – a direct oxidation reactor;

Input and output data on the current technological parameters (pressure, temperature, gas content, etc) are directed constantly through a controller for computer processing, where the data base is created. The data base undergoes statistical processing and analyzed in order to find out possible laws of the process. Processing is conducted in a real-time scale with constant correction of statistical models parameters. An empirical model is made up after that, which is described by a system of non-linear differential equations showing interdependence between input flows rates and technological parameters. After that the initial system of non-linear differential equations of high-order is linearized and converted into a system of linear differential equations of the first and the second orders in the working area. The chosen model is tested for truth of the trial with the help of optimization criteria. A control algorithm is created, and controller tunings are found out on the basis of this model.

Tasks to local control systems are given according to calculated optimal values of feed flows rates and corresponding concentrations of basic effluent gases components. Such control actions as air input into a reaction furnace of the thermal stage and air rate at the inlet of the catalytic stage reheaters can be used.

The basic control criterion is maintaining constant H_2S/SO_2 ratio before the incinerator. In case of an irregular situation, if such appears, the complete mathematical model of the process is used for its analysis and giving recommendations. This model includes a sub-model,

describing the thermal stage of the process and models of catalytic converters, taking into account chemical reactions kinetics.

Use of the thermodynamic models together with the system of adaptive control makes it possible to increase operation flexibility and technological process control.

Table

Technological parameters of models and real processes

Controled parameter	Models I		Models II		Models III	
	designed	real	designed	real [4]	designed	real
Air-to-acid gas ratio before thermal stage	2,5 : 1	2,5 : 1	2,5 : 1	2,5 : 1	2,3 : 1	2,3 : 1
Temperature at reactor outlet, °C						
– the 1st stage	280	280-290	275	280-290	275	270-280
– the 2d stage	260	260-270	260	260-270	250	260
– the 3d stage	-		260	250-260	-	-
– direct oxidation	-	-	-	-	280	280-310
Hydrogen sulfide conversion into sulfur, %	96,0	94,5	98,0	97,5	99,5	99,0

REFERENCES

1. Grunvald V. R. Gas Sulfur Technology. M: Khimia, 1992, p. 272.
2. Avdeeva A. V. Sulfur Recovery from Gases. M: Metallurgia, 1977, p. 175.
3. Podshivalin A. V., Vesirov R. R., Zdanov T. R., Mukhamedova A. R. Operating Experience of the Effluent Gas After-treatment Unit of Claus Elemental Sulfur Recovery Process. Khimia nefti i gasa. Materials of the IVth International conference. Two volumes. Tomsk: "STT", 2000. V. 2, P. 470-471.
4. Gavin Mcintyre, Lili Lyddon "Claus Sulphur Recovery Options" Petroleum Technology Quarterly Spring, 1997, P.57-61.

IMPACT OF INTERACTION PARAMETERS ON SULFUR DISTRIBUTION IN COMPOSITIONS WITH PETROLEUM RESIDUES

I.R. Telyashev, S.A. Obukhova, Ju.M. Kut'in, E.G. Telyashev

Ufa State Petroleum Technical University
Russia, 450062, Ufa, Kosmonavtov, 1
The Institute of Petroleum Refining and Petrochemistry of the
Bashkortostan Republic Academy of Sciences
Russia, 450065, Ufa, Initsiativnaya, 12, Phone: (3472) 42-24-71, Fax: (3472) 43-31-17

In spite of a great number of research works devoted to behavior of elemental sulfur during its interaction with heavy petroleum residues there is no universal point of view on the processes proceeding during this phenomena.

Interaction of elemental sulfur with petroleum residues proceeds differently at high (above 180 – 200 °C) and at low (about 120-140 °C) temperatures [1]. At high temperatures dehydrogenation of petroleum residues accompanied by hydrogen sulfide release takes place. At low temperatures sulfur reacts with petroleum residues hydrocarbons without hydrogen sulfide release. During this stage it exists in three main conditions: chemically bound, dissolved and dispersed, while distribution between different forms of sulfur depends on introduction conditions, petroleum residues properties and quantity of the introduced sulfur.

Presence of sulfur in different hydrocarbons practically of all the classes has been confirmed by a great number of scientists. Bound sulfur in a polysulfide chains form is found in large quantities in alkyl substituents of asphaltenes and in smaller quantities – in resins [2,3]. Dissolved sulfur is found mainly in aromatic fractions [2]. Research works with electron microscopes have shown that during introduction of sulfur into bitumen its part is implanted into asphaltene structures changing reological properties of bitumen.

In order to obtain more stable systems, in which the largest part of sulfur exists in a bound condition, it is necessary to conduct the process for a long time. Contact conditions and quantity of the added sulfur also influence sulfur bounding process. Conversion of sulfur into a bound condition is necessary because unbound sulfur during future heating above 180 °C in the process of pre-treatment and laying of road coatings can dehydrate binder hydrocarbons with hydrogen sulfide formation. It may be supposed that it is the sulfur introduced into asphaltene structures that constitutes an efficient modificator of plastic properties of products produced [4] and has the largest thermal stability.

Interaction of elemental sulfur with different petroleum residues (visbit (bitumen from visbreaking unit), West-Siberian road tar, propane deasphaltization asphalt) has been studied.

PP-21

Different quantities of sulfur (up to 30 %) in a melted form were introduced into a petroleum residue (asphalt and road tar), the resultant mixture was subjected to mechanoactivation treatment by an ultrasonic dispergator (up to 30 minutes). The samples of road tar with sulfur also allowed to stand at 140 °C for 2 and 5 hours. Sulfur was introduced into visbit in a form of finely dispersed powder, the resultant mixture was mechanically mixed at 120 – 130 °C for about 20 minutes, a part of the samples was allowed to stand at 140 °C for 18 hours.

Group chemical compositions and sulfur content were determined for the resultant samples. Then asphaltenes were extracted from them, and their sulfur content was determined. X-ray photographs of the samples and of the extracted asphaltenes were taken. The asphaltenes extracted from asphalt and sulfur mixtures were allowed to stand in a special cell for 1 hour at 150 °C and 200 °C. Vapours were collected at the tip of a cooled trap and washed off by a solvent. Sulfur content was measured in the liquid residue and in the initial asphaltenes, then their X-ray photographs were taken.

The experiments have shown that addition of elemental sulfur leads to increase of asphaltene sulfur content against the initial product [5]. The influence of all three factors is felt – quantity of added sulfur, mechanical activation and thermotreatment duration. Addition of less than 10 % of elemental sulfur for the road tar and less than 5 % for the asphalt has little effect on sulfur content in asphaltenes, while influence of mechanical activation and thermotreatment effects became apparent – their growth leads to increase of asphaltene sulfur content, both these factors being interdependant [6].

Analysis of X-ray photographs of the extracted asphaltenes has shown that for several asphalt samples a crystalline sulfur signal appears. A standard mixture was prepared, and the quantity of asphaltene crystalline sulfur was measured for it.

It has been shown that during addition of a little quantity of elemental sulfur (5 %) and, accordingly, low sulfur content in asphaltenes no crystalline sulfur signal was observed. During increase of sulfur quantity to 15 % its asphaltene content grows to 20 – 26 % on the added sulfur, 6 % of which constitutes crystalline sulfur. At standing of asphaltenes for 1 hour at 200 °C sulfur content decreases, mainly at the expence of crystalline sulfur, which is partially sublimated while other part reacts with asphaltenes without hydrogen sulfide formation. When quantities of the added sulfur are large (up to 30 %) its content in asphaltenes increases to 37 –38 %, but during recalculation taking into account the added sulfur its quantity decrease to 13 –14 %. Crystalline sulfur passes into another modification, which makes its quantitative estimation according to the standard sample more difficult. Qualitative analysis shows that heating evokes decrease of crystalline sulfur quantity.

Crystalline sulfur signal was also observed for visbit samples which were not subjected to thermotreatment during addition of above 4 % of sulfur [7]. For thermotreated samples with the same quantity of added sulfur, crystalline sulfur signal was absent.

The data obtained made it possible to understand the picture of sulfur behavior during its interaction with petroleum residues. During sulfur addition at first its interaction with a dispersed media takes place. It is partially dissolved in the latter and partially reacts with polysulfides formation. Besides, there is a certain level of dispersed media saturation by sulfur, dependant on chemical composition and dispersed media quantity. Interaction of sulfur with dispersed phase (asphaltenes) takes place only when this level is achieved. Interaction with asphaltenes leads to sulfur introduction into crystal lattice of under-molecular asphaltene associates without chemical binding formation. The introduced sulfur may either react during further heating with asphaltenes with chemical binding formation or be extracted from asphaltenes and react with a disperse media. When a certain limit of asphaltene sulfur content is reached, introduction of sulfur into crystal lattice stops showing practically no effect on thermotreatment or mechanical activation. Further increase of sulfur quantity does not lead to its interaction with petroleum residue hydrocarbons, unbound sulfur being in a dispersed state in the system, and finely dispersed particle size depends mainly on contact conditions.

REFERENCES

1. Petrossi U., Bocca P. L., Pacor P. Reactions and technological properties of sulfur-treated asphalt. // Ind. And Eng. Chem. Prod. Res. And Develop., 1972. - V. 11. - № 2. - P. 214 - 219.
2. Costantinides G., Lomi C., Schromer N. Trattamento di bitumi con zolfo: considerazioni su eventuali reazioni. // Riv. combust., 1979. - V. 33. - № 1. - P. 1 - 13.
3. Bocca P. L., Petrossi U., Pacor P. Heavy hydrocarbons and sulfur: reactions, reaction products and technological properties. // Int. J. Sulfur Chem., 1972. - A 2. - № 3. - P. 241 - 242.
4. Peyrot Jean. Contribution de la microscopic electronicue a letude des melanges bitume-soufre and bitume-polymere. // Bull. liais. lab. ponts et chaunssees, 1981. - № 113. - P. 146 - 150.
5. Telyashev I.R., Obukhova S.A., Vezirov R.R., Telyashev E.G. Interaction Between Oil Dispersed System and Elemental Sulfur. // Dynamics of Multiphase Systems. Proceedings of International Conference on Multiphase Systems. - Ufa, 2000. – P. 475 - 478.
6. Telyashev I.R., Obukhova S.A., Vezirov R.R., Telyashev E.G. Optimization of the process of elemental sulfur introduction in asphaltene structures of heavy petroleum residues. // Bashkirskii Khimicheskii Zhurnal. – 2000. – Vol. 7. – № 5. – P. 62-63.
7. Telyashev I.R., Davletshin A.R., Obukhova S.A. // Neftepererabotka i Neftekhimiya. - 2000. - №1. – P. 31...34.

PP-22

COMBINATION OF MIXING AND DISPLACEMENT REACTORS IN SORPTION TREATMENT TECHNOLOGIES

S.L. Larionov, O.V. Arkhipova, V.R. Nigmatullin

Ufa State Petroleum Technical University
Russia, 450062, Ufa, Kosmonavtov, 1
The Institute of Petroleum Refining and Petrochemistry
of the Bashkortostan Republic Academy of Sciences
Russia, 450065, Ufa, Initsiativnaya, 12, Phone: (3472) 42-24-71, Fax: (3472) 43-31-17

The basic lines in sorption technology development are selection and improvement of the adsorbents and the methods of implementation of technological schemes of the process. Sorption process can be conducted differently – in mixing reactors (contact treatment) or in displacement reactors (percolation treatment). Different porous solid substances in finely dispersed or granular states are usually used as adsorbents.

The decisive factor of adsorption process is diffusion rate of adsorbate particles into adsorbent pores, depending on the nature of adsorbate and adsorbent pores diameter. Increase of diffusion rate in adsorption technologies can be obtained by decrease of flow rates of the products being separated, raise of temperature, use of solvents, modification of adsorbent surface including its crushing, etc [1].

The basic advantage of the mixing reactor using finely dispersed adsorbents consists in the fact that contact conditions become easier: diffusion difficulties are decreased, diffusion rate of adsorbate into adsorbent pores is increased and the time, necessary for displaying its full bleaching ability, is reduced; finely dispersed adsorbents are more easily kept in a weighted condition in the product being treated. Rather large diffusion rates and use of activated clays permit to conduct treatment under rather low temperatures.

The efficiency of displacement reactors is determinated by the ability to use a wide range of flow rates and temperatures, permitting to guarantee more deep treatment.

According to laboratory tests the most effective results of adsorption treatment of solid paraffins (with colour estimation) have been got during two-stage treatment combing treatment by a finely dispersed clays in mixing mode (contact treatment) and treatment by a granular synthetic adsorbent in displacement mode (percolation treatment). At the first stage – during contact treatment of a paraffins (colour - 11 units) with a clay in 5 % quantity and at the temperature 70 - 90 °C – the colour of 6 units was achieved, and at the second stage – during synthetic adsorbent treatment – the colour of the paraffin amounted to 3 units.

Two-stage treatment, combining advantages of both methods, can be realised at a full-scale unit of contact treatment, which operation consists in mixing a product being treated

with a finely dispersed adsorbents in the reactor-mixer with subsequent separation of the adsorbent at the system of filters.

The analysis of a mixer with an agitator operation as well as the mathematical calculation conducted using the model of ideal displacement have shown that adsorbent concentration in the mixer drops down practically to zero approximately after two hours or operation independently on its loading ratio [2]. Increase of its operation efficiency and contribution of the stage of adsorbent with product contact can be achieved at the expense of intensification of mixing device operation and guaranteeing conditions of ideal mixing, as well as by means of modernisation of adsorbent dosing system.

A great contribution in products treatment is put by filtration stage at disc filters, used for separation of the main quantity of adsorbent – in the process of accumulation of definite quantity of adsorbents on these filters formation of filters layers takes place working as percolation treatment in displacement mode.

The problem of percolation stage treatment consists in blocking up of disc filters and a short period of continuos operation of the unit. It can be solved by introduction into the reactor-mixer at the first stage of treatment together with clay some quantities of adsorbent with a more rigid lattice, synthetic as a rule, which decrease growth of pressure loss of the adsorbent layer at the disc filters and make it possible to increase their operation period before complete blocking up.

So, at the example of laboratory experiments and analysis of full-scale contact treatment unit it has been shown that combination of the mixing mode (at the first stage) and the displacement mode (at subsequent stages of treatment) have a positive effect on treatment degree. Intensification of operation of mixing and displacement reactors at the expense of elimination of operation short-comings of a full-scale unit of contact treatment and selection of active adsorbents makes it possible to organise a highly efficient two-stage process of sorption treatment with production of products of desirable purity.

REFERENCES

1. Keltsev N.V. Basis of sorption technology. – M.: Khimya, 1984. - p.592.
2. Larionov S.L., Arkhipova O.V., Vezirov R.R. Production of high-quality market petroleum products by contact treatment process. // Neftepererabotka i Neftekhimya. – 1998. - № 9. - P. 78-81.
3. Vezirov R.R., Larionov S.L. et al. Use of catalysis dust as an adsorbent for petroleum products treatment. // Neftepererabotka i Neftekhimiya. – 1998. - № 4. - P. 45-46.

PP-23

THE COMBINED TECHNOLOGY OF DIESEL FUELS PRODUCTION WITH LOW AROMATIC HYDROCARBONS CONTENT USING EXTRACTIVE AND CATALYTIC DEAROMATIZATION

S.A. Obukhova, D.E. Khalikov, A.A. Kulik, E.G. Telyashev

Ufa State Petroleum Technical University
Russia, 450062, Ufa, Kosmonavtov, 1
The Institute of Petroleum Refining and Petrochemistry of the
Bashkortostan Republic Academy of Sciences
Russia, 450065, Ufa, Initsiativnaya, 12, Phone: (3472) 42-24-71, Fax: (3472) 43-31-17

The main up-to-date tendency in diesel fuels production is increasing requirements to their aromatic hydrocarbons content. On the world market it does not exceed the level of 5-10 %. In Russia diesel fuels of DLAC-B and DZAC [1] grades are producing with aromatic hydrocarbons content not above 20 and 10 %, accordingly. These requirements make actual the problem of research and development of efficient and economically advantageous technologies of low aromatic hydrocarbons diesel fuels production.

The diesel fuel pool at a typical refinery consists of hydrotreated straight-run fractions and gasoiles of corresponding fractional composition, their content and nature of aromatic hydrocarbons being essentially different. Straight-run diesel fractions contain about 25-30 % of aromatic hydrocarbons [2], which are represented mainly by mono- and bicyclic structures with naphthene and alkyl radicals. Gasoiles are more aromatic. Catalytic cracking gasoil fractions, boiling in diesel fuel limits, contain more than 75-85 % of hydrocarbons with aromatic fragments, aromatics being represented by bi- and tricyclic hydrocarbons with short radicals which are the most undesirable in diesel fuel.

Extractive dearomatization permits to obtain the results, satisfying aromatic hydrocarbons content requirements, but the significant part (up to 30-40 %) of potential feed resource is lost. Gasoiles are similar to extracts of dearomatization from aromatics content point of view, and decrease of their aromatics content can be conducted only chemically, that is transition of aromatic hydrocarbons into paraffin-naphthenic ones, which can be achieved by catalytic hydrogenation. On the basis of the above mentioned facts the new combined technology of environment friendly diesel fuel production provides separate dearomatization of diesel fuels components, determined by their chemical composition (fig.).

Due to high process costs of extragent regeneration stage it is not profitable to subject to extractive dearomatization the entire straight-run diesel fraction.

Besides, the most undesirable diesel fuel components are bi- and tricyclic aromatic hydrocarbons. When the sum of aromatic hydrocarbons is withdrawn from the straight-run die-

sel fraction alongside with polycyclic aromatic hydrocarbons monoaromatic ones are also withdrawn, their molecules contain about 2/3 of paraffin and naphthenic structures. Bi- and tricyclic aromatic hydrocarbons [2] are concentrated in a heavy part of the straight-run diesel fraction, which also contain the main part of high melting paraffins. Dearomatization of only this heavy part, taken from the main atmospheric column, permits to decrease extractive dearomatization feed flow by 2-3 times and to increase selectivity of aromatic components removal preserving monoaromatic ones.

Hence, the part of the straight-run diesel fraction, containing the basic part of polycyclic aromatics, is subjected to extractive dearomatization with production of the raffinate – a component of market environment friendly diesel fuels and the extract – an aromatic hydrocarbons concentrate, which composition is close to that of gasoiles.

Extractive dearomatization processes of oil fractions is efficiently used in industrial practice (selective treatment of lubes, extraction of individual aromatic hydrocarbons from reformate, etc.). The main difference of diesel fractions extractive dearomatization process is the using extragent. The conducted research of several extragents [3,4] has shown that the extractive dearomatization with their use permits to obtain the necessary content of aromatic hydrocarbons (5-10 %) in the raffinate, and the extract aromatics content amounts to 75-90 %.

Extractive methods also permit to decrease sulfur content in dearomatizate because sulfur-bearing compounds (thiophenes and sulphides) [5] are simultaneously removed with aromatic hydrocarbons, which permits in some cases to exclude the raffinate hydrotreatment stage during diesel fuels production.

When this technology with separation of heavy part (about 30-50 % of entire diesel fraction) of diesel fraction as the extractive dearomatization feed is used at a typical refinery with capacity of 8 million tons of crude per year (a diesel fraction content in crude oil is 25 %), the volume of extractive dearomatization feed amounts to 0.6 – 1.0 million tons per year.

In order to preserve potential resource of market diesel fuel, products with high aromatics content (75-90 %) – the extract, catalytic cracking light gasoil, refinery processes gasoiles (500 – 800 thousand tons per year) are subjected to hydrogenation according to the known technologies.

The advantages of hydrogenation of high aromatized gasoiles and extracts as compared to entire straight-run diesel fraction hydrogenation are evident:

- only high aromatics content part of a diesel fraction (content of non-hydrogenated components – paraffins, naphthenes and monoaromatic hydrocarbons is low (10-15 %)) is subjected to hydrogenation, which permits to decrease unit feed flow by 3-4 times;

– hydrogenation of bi- and tricyclic aromatic hydrocarbons as compared to monoaromatic ones proceeds more easily, in less severe conditions and with greater efficiency [6].

At the hydrogenation stage, conducted under the pressure of 12-15 MPa, saturating and cracking of aromatic rings take place. The produced product with aromatics content below 5 % is compounded with the hydrotreated light part of straight-run diesel and raffinate.

Hence, the offered technology permits to guarantee high efficiency of market low aromatics diesel fuel production without essential losses of potential resource at the expense of combination of extractive and hydrocatalytic methods.

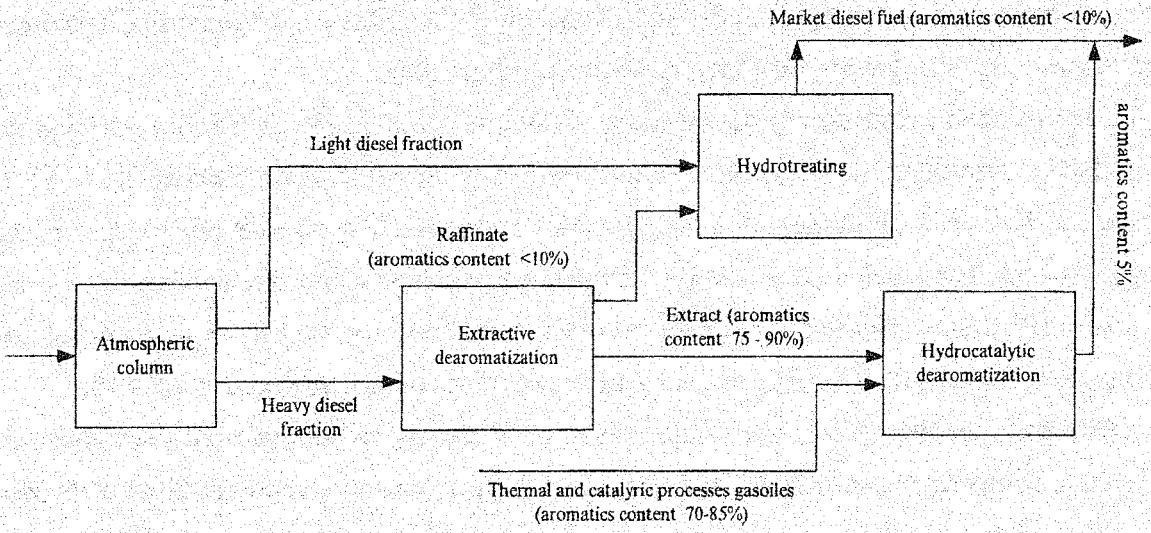

Fig. Basic flow scheme of environment friendly diesel fuel production with aromatics content 10-20 %.

REFERENCES

1. Anisimov I.G., Badyshtova K.M., et al. Fuels, lubricants, technical liquids. Range and application. M. "Tekhinform", 1999, P.98.
2. Olkov P.L., Gorelov V.S., et al. Impact of fractional composition on some operation characteristics of middle distillate //Neft i gas. –1985, No. 5, P. 45-48.
3. Khalikov D.E., Obukhova S.A., Vezirov R.R., Telyashev E.G. Rules of extraction of aromatic hydrocarbons during extractive dearomatization of a diesel fraction 270-340 °C // Materials of the Second Congress of Oil and Gas Manufactures of Russia (section B). Ufa, 2000, P.122.
4. Khalikov D.E., Obukhova S.A., Vezirov R.R. Optimization of diesel fuels extractive dearomatization using a numerical experiment method // Neftepererabotka i neftekhimya. 2000, No 1, P. 46-48.
5. Hydrocarbon Processing. – November 2000, P. 36-37.
6. Berg G.A., Khabibullin S.G. Catalytic hydrotreatment of petroleum residues. L.: "Khimya", 1986, p.57.

FEATURES OF PETROLEUM RESIDUES THERMOLYSIS IN AN UPWARD FLOW REACTION CHAMBER

S.A. Obukhova, A.R. Davletshin, D.E. Khalikov, R.R. Vezirov

Ufa State Petroleum Technical University
Russia, 450062, Ufa, Kosmonavtov, 1
The Institute of Petroleum Refining and Petrochemistry of the
Bashkortostan Republic Academy of Sciences
Russia, 450065, Ufa, Initsiativnaya, 12, Phone: (3472) 42-24-71, Fax: (3472) 43-31-17

One of the alternatives of qualified petroleum residues treatment is their participation in the visbreaking process with a removable upward flow reaction chamber aimed at thermal conversion in mild conditions with distillate fractions production.

The analysis of literature, experimental and industrial data has made it possible to assume that chemical behavior of products formation in a visbreaking upward flow reactor differs from the chemical behavior of visbreaking process realized according to other alternatives. These characteristic features are caused either by correlation of technological parameters of the process (temperature, pressure, residence time), influencing system thermodynamics, or by hydrodynamic flow regime in the reaction chamber.

Estimation of hydrodynamic flow regime of upward vapour – liquid flow in operating reaction chamber has been performed, and influence of technological parameters on its character has been studied [1]. In order to obtain varying with conversion characteristics of the flow passing through a reaction chamber the model of industrial reaction chamber (height- to diameter ratio 5 : 1) has been developed. For this purpose its height volume was divided into six sections. Composition and characteristics of each of six flows were determined taking into account temperature and pressure variations along the chamber height (see the table). Hiewitt – Roberts diagram for a vertical upward flow [2] has been used for determination of hydrodynamic section regime. Reduced velocities of vapour and liquid phases (Hiewitt parameters) have been calculated for each of eight flows (inlet, at six reactor sections and outlet).

The estimation performed has shown that in a reaction chamber feed pipe, when diameter is small and vapour phase ratio is not large, a bubble flow bordering with a disperse – circular one is realised which is characterised by distribution of the vapour phase in the form of separate bubbles in the continuous liquid phase. When reaction products from the feed pipe enter the reaction chamber their diameters and velocity sharply decrease. This leads to realisation of

transition slug – type regime when gas bubbles stick together with formation of large bubbles separated by liquid areas containing smaller gas bubbles.

Beginning from the second reaction section intensive formation of vapour phase takes place as a result of conversion leading to large bubbles destruction and transition to the churn regime characterised by vapour – liquid mixture uniform movement. But when diameters are large, as is the case, pulsation and unsteady vibrating flow may appear. The churn flow regime in our case is kept up to the reaction chamber top. At the exit during transition to smaller as compared to the reactor diameter the circular flow regime is realised when liquid flows along the walls while gas moves in the central part of the pipe.

To optimise reaction chamber operation providing necessary degree of conversion and long – term operation period it is necessary to maintain the regime approaching ideal displacement that is prevention of reverse mixing, stagnant zones formation and sintering. Formation of large quantities of the vapour phase may induce the churn regime destruction and its transition to the circular regime even in upper part of the reaction chamber. More intensive interphase mass exchange during the circular regime resulted from increase of the velocity disbalance of the phases promotes more intensive build-up of non-volatile viscous components on the reactor walls and coking of its upper part.

The performed estimate of technological parameters influence on the upward flow regime in the visbreaking reaction chamber has shown that the churn flow regime of piston type exists along the whole height of the chamber which is typical for an ideal displacement reactor.

According to traditional points of view visbreaking process, including the alternative with a removable reaction chamber and upward feed flow, is considered to be a variant of thermal cracking process realized in milder temperature conditions and longer residence time.

Analysis of technological balance parameters and product properties has made it possible to suppose that the processes, induced by addition reaction between light intermediate products of the vapour phase, take place besides thermal cracking processes. The thermodynamic preconditions of this phenomenon are: rather low temperature (400...450 °C) and high pressure (7-9 atm) in the reaction chamber including the reactions proceeding with volume decrease (condensation, coking and compounding) as well as lower activation energies of addition reactions as compared to cracking reaction [3].

Due to characteristics features of the hydrodynamic flow regime in a visbreaking reactor thermolysis is carried out in two phases – vapour and liquid, differing by fractional and chemical compositions of the hydrocarbons contained in it. Selective cracking of the most

high – molecular weight feed components takes place under mild temperature conditions. During this process low – molecular weight products of primary decay and alkyl radicals are easily "flied out" into the gas phase and do not take part in the secondary liquid phase reaction due to the huge phase division surface, provided by the hydrodynamic flow regime in the reactor. The liquid phase is enriched by long – term existing benzyl and phenyl radicals [4] at the expense of initial high - molecular weight hydrocarbons. These radicals take part in interphase thermopolycondensation reactions. This chemical behaviour of the processes proceeding in liquid phase prevents its destabilisation, asphaltene formation and coking due to maintaining high balance content of aromatic hydrocarbons and fragments. This is confirmed by practical absence of coke deposits in the visbreaking reaction chamber (coking in the upward flow visbreaking reaction chamber of the Arlan full – scale oil tar processing unit does not exceed 0.003%), while asphaltene content in the visbreaking vacuum residue fluctuates at the initial feed level (7 – 9%).

In the vapour phase, which volume in the reactor changes from 50 to 90% (see the table) at the expense of conversion addition reactions between saturated hydrocarbons, alkyl radicals and unsaturated hydrocarbons take place alongside with thermal cracking reactions. As a result the middle distillates having chemical properties close to those of the straight – run distillates (gasoline iodic number does not exceed 40-50g I_2/100g) are formed. Variation of produces fractional composition of the full – scale visbreaking process with a removable upward flow reaction chamber (see the fig.) confirms formation of visbreaking middle distillate products at the expense of addition reactions.

Table

Vapour and liquid flows characteristics in the reaction chamber

Parameter	Inlet	Section						Outlet
		1	2	3	4	5	6	
Temperature, °C	455	451	447	444	441	437	434	430
Diameter, mm	100	1800						400
Pressure, atm	9,0	8,9	8,7	8,6	8,4	8,3	8,1	8,0
Vapour								
Rate, % vol.	28,45	56,72	69,85	77,08	81,97	85,20	87,76	89,55
Hiewitt parameter, kg/m* c^2	124	0,02	0,05	0,09	0,16	0,24	0,35	192
Liquid								
Rate, % vol.	71,55	43,28	30,15	22,92	18,03	14,80	12,24	10,45
Hiewitt parameter, kg/m* c^2	29726	0,36	0,34	0,32	0,31	0,29	0,27	105

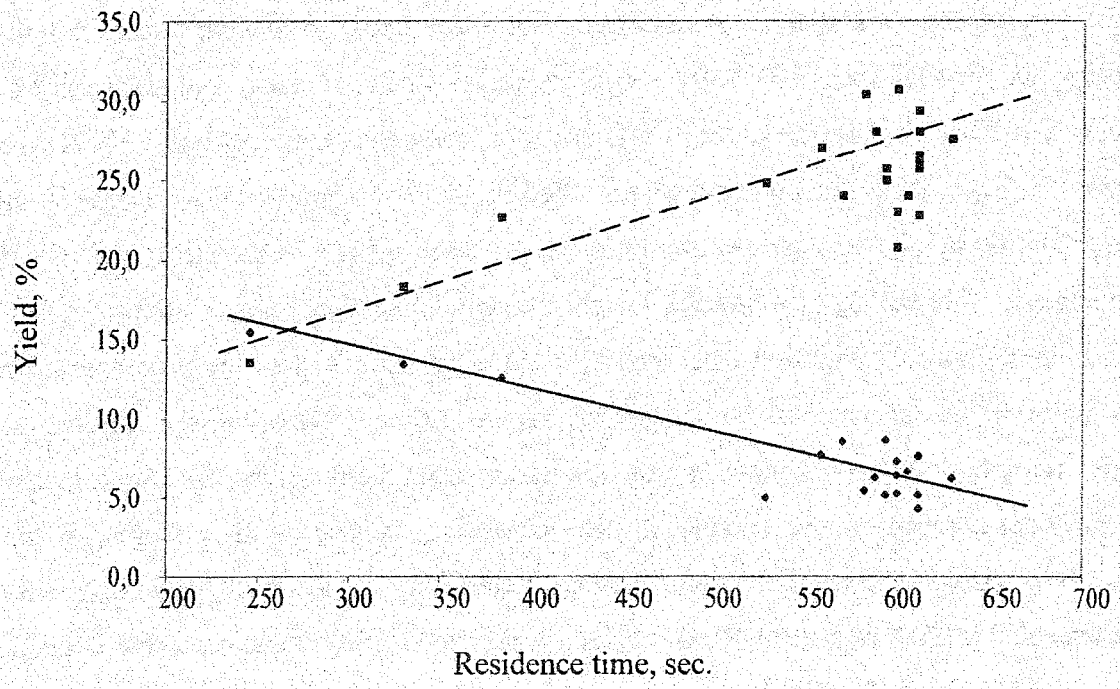

Fig. The relation between products distribution of the oil tar thermolises and residence time

◆ total gas yield + fraction IBP–160 °C

■ fraction yield 160 – 450 °C

Increase of feed residence time in the reaction chamber leads to increase of middle distillate products yield with simultaneous decrease of gas and gasoline yields. So, the hydrocarbons, boiling in the gasoline fraction limits, participate in the addition reactions with formation of large molecular mass hydrocarbons.

The research work conducted has shown that in visbreaking process with a removable upward flow reaction chamber the maximum selective conversion, as compared to the other variants of this process realisation, is provided by vapour phase addition reactions with formation of middle distillates.

REFERENCES

1. A.R. Davletshin, D.E. Khalikov, S.A. Obukhova, S.F. Urmancheev, R.R. Vezirov. The Chemical Journal of the Bashkortostan Republic. Ufa, Reactiv, 200, v. 7, p-p 44-45.
2. Reference book on heat exchangers. M., Energoatomizdat, 1987, v.1, p.p. 183.
3. R.Z. Magaril. Theoretical basis of Petroleum Refining Chemical Processes. M., Khimiya, 1976, p.p. 41-42.
4. S.A. Akhmetov. Physico – chemical technology of deep oil and gas processing, part 2, Ufa, UGNTU, 1997, p.38.

INFLUENCE OF PRECIPITATION TEMPERATURE ON THE TEXTURE OF COOL PRECIPITATION HYDROXIDE

A.A. Lamberov, O.V. Levin, S.R. Egorova, H.H. Gelmanov

Kazan State Technological University
Novokuibyshevsk Catalyst Plant
K. Marx St., 68, 420015, Kazan, Russia, E-mail: rrg@kstu.ru

The influence of precipitation temperature on the texture of aluminium hydroxide (AH) was investigated on the industrial samples, that were obtained in the plant laboratory using the technology of the periodic precipitation (sulfate version). Precipitation temperature is 20-80°C, pH=9.2-9.4. Results are presented in table 1 and figure 1-2.

Porous structure of hydroxide obtained by cool precipitation is rather labial, its changing during increasing of contact time of hydroxide and mother liquor at 30°C (Figure 1, sample 2) indicates this. In this case destruction of secondary pores occurs that is attended by growth of specific surface and decreasing of pore volume. S_{sp}=357m^2/g, V_p=0.38 cm^3/g). The texture is defined by maximums at 21Å (0.16 cm^3/g-47% V_p) and 36 Å (0.11 cm^3/g- 32% V_p). 99% of pore volume are defined by pores ≤ 150 Å, the most part of pore volume 0.29 cm^3/g -83% V_p) are pores with diameter ≤ 70 Å.

The further increasing of precipitation temperature up to 50°C (Figure 2, sample 1) results in hydroxide formation with less liable texture characteristics. Thus, keeping hydroxide at 50°C in mother liquor practically does not change its pore structure (S_{sp}=337 m^2/g, V_p= 0.77 cm^3/g), which is defined by maximum at 45 Å (0.31 cm^3/g-46% V_p). 99% of pore volume are defined by pores ≤ 150 Å, the most part of pore volume (0.43 cm^3/g - 63% V_p) are pores with diameter ≤ 70 Å.

At the same time very important fact is that the increasing of AH pore volume, synthesized at 50°C, is conditioned by the formation of secondary porosity. It is well presented in the figures. AH synthesized at 20°C and stabilized at 50°C (Figure 1, sample 3) and above mentioned hydroxide have close, almost monomodal pore distribution.

However, if in the first case volume of the pores with the diameter more than 70 Å makes 0.027 cm^3/g, in the second case it is 0.23 cm^3/g at a similar pore volume less than 70 Å (0.39 and 0.43 cm^3/g accordingly). It must be mentioned that secondary AH pore system, synthesized at 50°C, does not have maximum on the curve of pore distribution with diameter 60-120 Å.

Increasing of the precipitation temperature up to 60°C (Figure 2, sample 2) also produces hydroxide with stable structure. Keeping it in mother liquor at 50°C practically does not have influence on texture characteristics (S_{sp}=31 m^2/g, V_p=0.69 cm^3/g). Porometrical system is de-

fined by "shoulder" 22 Å (0.02 cm^3/g –3.5 % V_p), by maximums 35 Å (0.10 cm^3/g –18 % V_p), 45 Å (0.22 cm^3/g –39 % V_p) and 81 Å (0.12 cm^3/g –22 % V_p). 99% of pore volume are defined by pores ≤ 150 Å. The most part of pore volume (0.48 cm^3/g –86% V_p) pores with diameter ≤ 100 Å.

Transformation of pore system at the transition of precipitation temperature from 50°C to 60°C. Comparing the curves of pore distribution demonstrates the significant reduce of intensity of maximum pore distribution at 45 Å with 0.0415 cm^3/g – Å till 0.021 cm^3/g – Å and simultaneous appearance of maximum at 81Å. Intensity in the first case is 0.086 cm^3/g – Å and 0.015 cm^3/g – Å in the second. It can be interpreted by dimerization of particles ~ 45 Å with formation of pores of appropriate size (~80 Å).

Hydroxide synthesized at 80°C (Figure 2, sample 3) has stable texture characteristics (Ssp=218 m^2/g, Vp=0.66 cm^3/g) which are conditioned by two maximums of pore distribution: narrow – at 62 Å (0.28 m^2/g, - 43 %Vp) and wide ~150 Å (0.38 m^2/g, - 57 %Vp). Formation of pores with 62 Å can be conditioned by trimers of particles 21-22 Å, and with pore diameter 140-160 Å – by dimers of particles 81 Å.

Results reveal the following regularity:

Hydroxides formed at 20-40°C has liable porous structure, that destroys when deposit is keeping in the mother liquor with formation of closely packed deposit from particles ~ 21-22 Å and 36 Å. Such AH are characterised by high specific surface area 350-370 m^2/g and low V_p=0.38-0.39 cm^3/g, we can draw one conclusion that primary particles practically do not interact and secondary structure of deposit does not form.

At precipitation temperature increase till 50°C 21-22 Å particles disappear and ~ 44-45 Å particles appear, which probably are dimers, consisted of 21-22 Å particles. They exactly begin to coordinate intensively and form secondary porosity.

Further precipitation temperature increase leads to significant reduction of pore content - 44-45 Å, which is following by formation of 90 Å pores. More probably appearance of these pores becomes the result of particles dimerization with diameter 44-45 Å. In this case the increasing of pore volume practically does not occur – though secondary porous system gains a strongly pronounced maximum ~90 Å. It is interesting that transformation of ~36 Å pores practically is not observed. The intensity of this maximum slightly increase with the growth of precipitation temperature 20°C→ 40°C→50°C → 60°C from the point 0.017 → 0.020 → 0.022 cm^3/g Å.

From the practical point of view hydroxides synthesized at the temperature more than 50°C is of great interest because they have developed surface and sufficient pore volume.

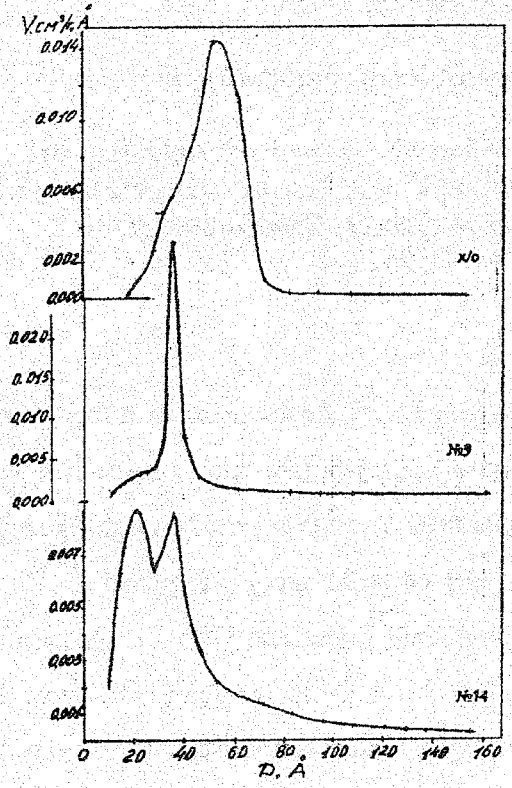

Figure 1. Curve of AH cool precipitation pore volume distribution, stabilized at 1-20°C; 2- 30°C; 3-50°C.

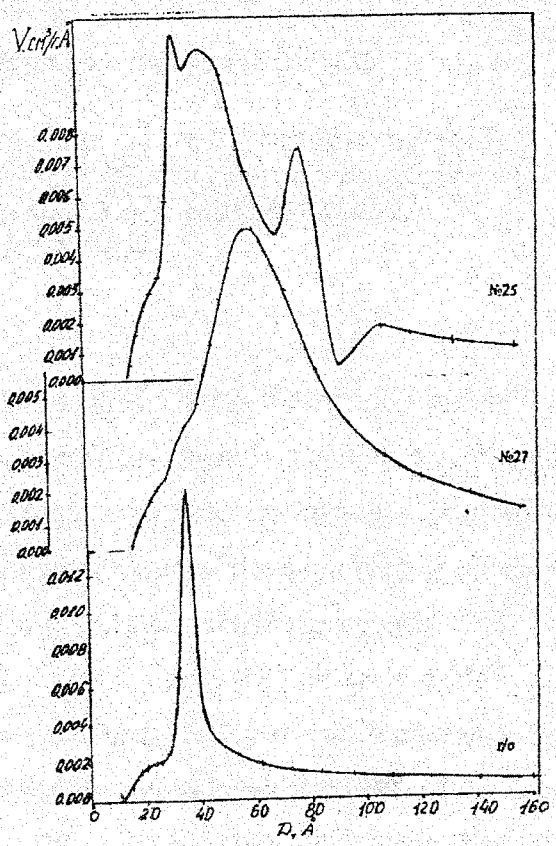

Figure 2. Curve of AH samples pore volume distribution, stabilized at conditions (Tpr\Tst): 1-50°C/50°C; 2- 60°C/50°C; 3-80°C.

Table 1

Influence of precipitation temperature on the texture of cool precipitation hydroxide

T	Maximum on the curve of pore volume distribution, Å				Intensity of maximum pore distribution, cm^3/g – Å 10^{-3}				Pore volume of maximum distribution, cm^3/g – Å 10^{-2}				S_{BET} m^2/g	Pore volume, cm^3/g	
	D_1	D_2	D_3	D_5	I_1	I_2	I_3	I_4	V_{D1}	V_{D2}	V_{D3}	V_{D4}		V_{BET}	V_{DES}
20	20,4	35,8	-	-	5.6	64.1	-	-	3.6	18.6	-	-	290,7	0,442	0,339
30	20,1	35,8	-	-	3.7	52.3	-	-	3.4	12.7	-	-	298,2	0,624	0,388
40	20,2	35,8	-	-	5.6	64.0	-	-	15.4	9.5	-	-	376,4	0,392	0,354
50	-	34,4	45,6	-	-	-	-	-	-	5.5	31.9	-	336,9	0,772	0,677
60	22,4	35,4	45,0	81,2	4.8	22.5	21.2	14.6	1.9	10.2	39.8	8.5	321,1	0,693	0,557

PP-26

UNSTEADY-STATE DOUBLE CONVERSION-DOUBLE ABSORPTION METHOD FOR SULPHURIC ACID PRODUCTION

Dimiter Dimitrov, Nikolai Konarev and Hristo Sapoundjiev*

KCM S.A. –Plovdiv, Bulgaria, 4009 Asenovrgradsko shosse. (e-mail: 314@kcm.bg).
**Natural Resources Canada, CANMET Energy Diversification Research Laboratory, 1615 Lionel Boulet Blvd, P.O.Box 4800, Varennes, Quebec, Canada, J3X 1S6*
(e-mail: hsapound@Nrcan.gc.ca)

Non-ferrous metallurgical plants emit SO_2 emissions with fluctuations in the flow rate and sulphur dioxide concentration. These variable conditions generate less or surplus of a reaction heat and create difficulties in autothermal operation of classical multi-stage fixed bed reactors. To perform a stable autothermal regime a costly control system is required.

To realise an autothermal operation of classical Double Conversion-Double Absorption (DC/DA) scheme the SO_2 concentration in the inlet gas should be above 6.0 v/v%. When the concentration of SO_2 is below the above value burning of sulphur is necessary to increase the content of SO_2 or additional energy should be add to the system to compensate the lack of the heat and keep autothermal operation of the system.

To avoid the above problems a new unsteady-state DC/DA system was designed and industrially proved in KCA S.A., Plovdiv, Bulgaria. Both oxidation stages operate in flow reversal regime. The inlet gas with SO_2 concentration 4.0 v/v % enters the first oxidation stage, where the SO_2 partially oxidise. Produced SO_3 is absorbed into intermediate absorber and unreacted SO_2 is directed to the second oxidation stage for final conversion. To adjust a proper SO_2 concentration (1.2 v/v/%) the strong SO_2 gas is delivered through bypass line. At that conditions both stages operate in autothermal regime.

During the first three months of industrial operation the new unsteady-state DC/DA system shows a stable autothermal operation in presence of fluctuations in the inlet SO_2 concentration. The final SO_2 conversion is over 99.0%. The SO_2 emissions to the atmosphere after the second oxidation stage are below 600 ppm.

CATALYTIC PERSPECTIVES OF "METAL WOOL"OF RAPIDLY QUENCHED FIBER MATERIALS PREPARED BY EXTRACTION OF FILAMENTS FROM MELTED MEDIA

B. Mitin*, V. Barelko, M. Serov*, M. Pasechnik*, V. Dorokhov, S. Serdyukov, T. Danilchuk**, L. Izmailov**, M. Safonov****

Institute of Problems of Chemical Physics RAS, Chernogolovka, Russia
**MATI-Russian State Technology University, Moscow, Russia*
***Moscow State University, Moscow, Russia*

The creation of chemical reactors on a basis of «metal wool» fiber catalysts prepared by method of the pedant drop of a melt, represents significant scientific and practical interest. The using of the specified systems of new generation for liquid phase processes of hydrogenation of organic connections will allow essentially promote the decision of such difficult questions, as branch high-dispersed catalysts from products, their regeneration and utilization.

The processes of a filtration and decantation are used, as a rule, for separation of particles of the catalyst from a liquid phase, that is connected with significant capital expenses and huge inconveniences in a work. The regeneration and utilization of the used catalyst are also difficult and toilful. The application of metal fibres will allow to proceed stationary working of liquid phase reactors as in this case the stage of a filtration is excluded. The heat treatment, acid and alkaline processing of catalysts as fibres will allow to carry out their regeneration easily. Thus installation simplicity of catalytic element and its dismantle is provided.

«Metal wool» fiber catalysts have good prospect of introduction in the industry because they have the mechanical durability and the stability to trituration higher in comparison with traditional catalysts, and also an opportunity of automation of preparation.

"Metal wool" fibers were obtained by a method the pedant drop of a melt. This method is based on the melting of the end of a vertically disposed rod with the formation of a pendant melt drop. The working edge of a rotating chilled disk – crystallizer contacts with the drop. The solidification of a melt takes place in the contact zone. Due to disk rotation the solidificated material is extracted from the melt in the form of fibres. In result rapidly quenched material gets microcrystalline structure. Thin (effective diameter up to 22 microns) homogeneous nickel fibres having insignificant disorder on thickness were obtained due to a variation of capacity of heating of the melt, the volume of a drop of the melt and the speed of rotation of a disk-crystallizer.

The cross section of fibres had the form close to an ellipse. The specific surface of the catalyst measured by method BET, was 0,5 m^2/g. The parameter of nickel fibres lattice determined by a X-ray diffraction method was 3,524 A. This corresponds to nickel of 99,96 % purity.

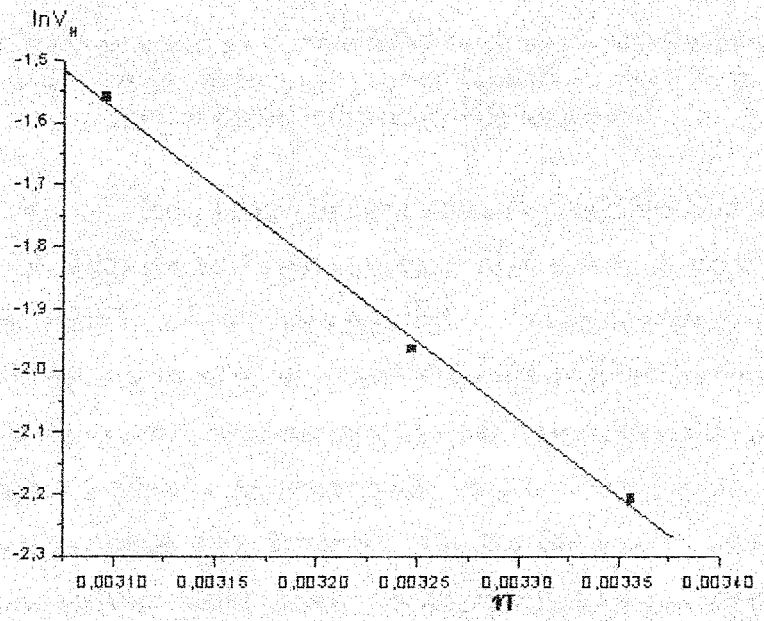

Fig. 1. The dependence of the logarithm of reaction rate on reciprocal temperature.

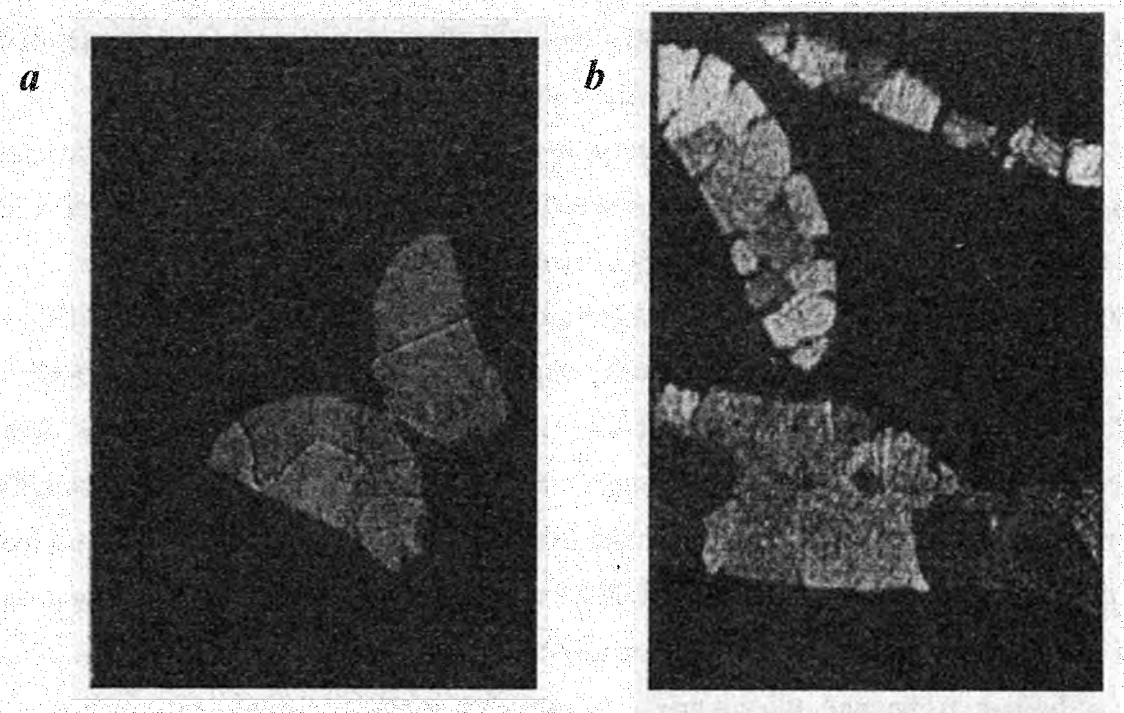

Fig. 2. (a) Microstructure of rapidly quenched fibres of nickel before carriage of catalytic reactions.
(b) Microstructure of rapidly quenched fibres of nickel after catalytic reactions.

Liquid phase catalytic hydrogenation of nitrobenzene and dinitrotoluene was carried out at the atmospheric pressure and the temperature 20 - 60 °C. The solvent of 90 %-water iso-propyl alcohol, weights of the substrate 0.5 - 1.0 g, weights of the samples of fibres varied within the limits of 1.0 - 6.0 g. Before tests the fibres have been cut on slices in length 1 - 1.5 cm, washed out in acetone and an ether and dried up at temperature 80 - 100 °C.

The experiences were carried out in a standard glass laboratory reactor. The speed of hydrogenation was measured by quantity of the hydrogen spent in unit of time. The researches have shown, that catalytic activity of the nickel fibres obtained by method of the pedant drop of a melt, is higher on orders than that of the metal, received by a traditional method of drawing.

The basic qualitative laws, which is characteristic for traditional catalysts, are shown at the presence of new investigated catalytic systems. The initial rate of absorption of hydrogen at hydrogenation are directly proportional to the weitght of the catalyst. The energy of activation of hydrogenation of nitrobenzen (Fig. 1) was 20 - 22 kJ/mole.

However, the induction period takes place in all experiences. The nature of this induction period for the present is not clear. It is probably connected with the metastable condition of the fibrous matrix produced by method of the pedant drop of a melt.

In the investigated hydrogenation conditions of both reactants specific catalytic activity of fibres is lower more than the order than one of traditional catalysts. However there is an opportunity of preparation of nickel-aluminium alloys basic treatment which will provide increase on orders of a specific surface and in result catalytic activity of "metal wool" inreases too.

Steam conversion of metane was carried out in flowing installation in a tubular reactor 10 mm in diameter with external electric heating. The temperature of a reactor was measured by the Cr-Al thermocouple. Converted gas was analyzed on chromatograph LCM-80, equipped with the detector on heat conductivity.

The temperature interval during experiences - 550-700^{0}C, pressure 1,0 - 1,3 atm. Ratio H_2O:CH_4 on reactor inlet was varied from 1:1 up to 4:1.

The increasing of catalytic activity was in 7 - 9 times after 60 hours. After catalytic reaction the sample of the catalyst represented fragile needles in length 0,5 - 5,0 mm covered by pyrolytic carbon.

The microstructural analysis of nickel fibres has shown, that destruction of metal occurs basically on borders of grains, beginning from a surface layer (fig. 2). The reason of destruction of nickel fibres can be the formation of pyrolytic carbon in space between grains.

Thus, steam conversion of metane on the investigated nickel fibres results in significant formation of pyrolytic carbon and loss of the mechanical durability of metal. A metastable state of rapidly quenched microcrystalline nickel can be the reason of this phenomenon.

However it is possible to expect, that preparation of metal fibres from nickel alloys will allow lower formation of pyrolytic carbon in a process of metane steam convertion.

In summary it is necessary to note, that metal fibres undoubtedly will find the applications in perspective autothermal reactors of metane steam conversion [1,2].

The work is supported by International Scientific Foundation"Science for Peace", Project No SfP 971897.

1. Safonov M.S., Granovskii M.S., Pozharskii S.B. Dokl. RAN, 1993, V.328, P.202.
2. Granovskii M.S., Safonov M.S., Patent RF No 2097314 (1997).

SOFTWARE "REACTOR" IN EDUCATION COURSE OF CHEMICAL ENGINEERING IN CATALYSIS

N.V. Vernikovskaya, V.I. Drobyshevich*, L.V. Yausheva*, S.A. Pokrovskaya, N.A. Chumakova

Boreskov Institute of Catalysis SB RAS, Novosibirsk, Russia
**Institute of Computational Mathematics and Mathematical Geophysics (Computing Center) SB RAS, Novosibirsk, Russia*

Some aspects of the modern specialists training in the field of Chemical Engineering were widely talked over in the 2nd Discussion Forum of the European Federation of Chemical Engineering in Prague, 1998. And one of the problems pointed out is the deficiency of the software packages that speak engineer's language without too much mathematics, are universal, use simplified but physically substantiated models. Besides that the packages input should consist of data easily available from routine sources – the reactor diameter, the diameter of the catalyst particle and so on.

A software package named "REACTOR" satisfies the requirements listed above. The computational algorithm and code were developed at the Institute of Computational Mathematics and Mathematical Geophysics (Computing Center), Novosibirsk, Russia [1,2]. This package allows carry out the mathematical modeling of a particular process in different catalytic fixed bed reactors: in a plug flow reactor, an adiabatic reactor or in tubular one. It is possible to carry out the mathematical modeling of the processes occurring on a single catalytic particle as well. The using of the package does not need high mathematical training. This package is universal and only knowledge's about parameters of the process under investigation are required.

One can carry out the mathematical modeling of different reactor types using the models with different complexity level. For example, the mathematical modeling of a tubular reactor can be carried out by means of:

- minimal (the simplest) model – two-dimensional pseudo-homogeneous model with uniform temperature and concentrations profiles inside the catalyst particles,
- maximal (complete) model – two-dimensional heterogeneous model accounting for intraparticle gradients,
- intermediate (between minimal and maximal) model – two-temperature or two-concentration mathematical model with/without accounting for intraparticle gradients.

To physically substantiate the simplification it is better at first to carry out the mathematical modeling of the process on a single catalytic particle. If there is no significant intra-

particle gradients, the homogeneous catalyst grain model can be used. If there is no interfacial gradients, one can use the homogeneous mathematical model and so on.

One can vary such process parameters as length and diameter of the reactor, grain diameter and void fraction of the bed, inlet concentrations and gas phase temperature, wall temperature, pressure and so on.

The temperature and concentration data obtained are dynamically mapped on the screen by means of a graphical system included. Besides that one can looking through the tables with the data obtained after the calculations finish.

The bank of physical-chemical properties, which was designed in GOSNIIMETANOLPROEKT (Severodonetsk) and the kinetic bank of catalytic reactions are the parts of the software "REACTOR". The bank of physical-chemical properties is easy to supplement and, at present, contains data of about 160 components. The kinetic bank of catalytic reactions contains its own dialogue component, which helps the user to fill up the kinetic bank himself.

On the base of the "REACTOR" package, one part of the computer course on "Chemical Engineering in Catalysis" was developed in Novosibirsk State University. It includes analysis of both the processes on a single catalyst particle and ones occurring in the different catalytic fixed bed reactors:

1. *Processes on a single catalyst particle.* The influence of both heat and mass transfer inside the catalyst grain and heat and mass transfer between the flow and the external surface of the grain on the catalytic reaction proceeding is investigated. One estimates the conditions when the resistance to mass and heat transfer inside the catalyst particle is negligible and/or the conditions when the interfacial gradients are absent.
2. *Processes in a plug flow fixed bed reactor.* Stationary temperature and concentrations fields in the reactor are under consideration and the dependencies of outlet temperature and component concentrations on different process parameters are studied.
3. *Processes in an adiabatic fixed bed reactor.* One can consider the influence of the next factors on the process performance:
   - axial heat conductivity and diffusion,
   - solid-gas heat and mass transfer,
   - mass transfer within the catalyst particle,
   - heat transfer from the reaction zone to the coolant.

   Students compare the process performance in adiabatic reactor with one in previously considered reactor. A particular process can be studied in both single-bed and multi-stage adiabatic reactors. The time evolution of temperature and concentration fields is displayed on the screen.

4. *Processes in a tubular fixed bed reactor*. One investigates the influence of the next factors on the process performance:
   - radial heat conductivity and diffusion,
   - solid-gas heat and mass transfer,
   - mass transfer within the catalyst particle,
   - heat transfer through the wall.

   Stationary temperature and concentrations fields in the reactor are analyzed under wide variation of process parameters. Students compare the process performance in tubular and adiabatic reactors.
5. *Processes in the combined fixed bed reactor*. Mathematical modeling of a catalytic system for a two-step process using a tubular reactor at the first step and an adiabatic bed at the second step allows compare the reactor operation for various designs and show ways to some improvements.

The present part of the computer course on "Chemical Engineering in Catalysis" permits students to learn the features of the particular process performance in catalytic fixed bed reactors of different design and to understand how one or another specific process parameter influences the process performance.

Moreover the software "REACTOR" can be used in the other fields:

- development of broad educational net for graduated engineers and other personal working in industry, science, etc. in the fields of catalysis, adsorption, chemical engineering, ecology,
- development of undergraduate and postgraduate computer chemical engineering courses with different complexity level,
- modeling of catalytic processes in catalytic fixed bed reactors for practical applications.

References:

1. V.I.Drobyshevich, L.A.Rapatsky, L.V.Yausheva. Interactive package "REACTOR" for program generation in unsteady process modeling of catalytic reactors. In: *Unsteady State processes in catalysis* (Yu.Sh.Matros, Ed.), pp.485-490, Utrecht-Tokyo: VNU Science Press (1990).
2. L.V.Yausheva, V.I.Drobyshevich, S.A.Pokrovskaya, Yu.V.Malozemov. Interactive computational package for specialists training in the field of catalytic processes modeling. In: *XIII International Conference on Chemical Reactors*, 18-21 June 1996, Novosibirsk, Russia. Abstracts, part 2, pp.162-163.

PP-29

MATHEMATICAL MODELING AND INDUSTRIAL IMPLEMENTATION OF UNSTEADY STATE METHOD FOR GAS PURIFICATION FROM NITROGEN OXIDES

Yu.N. Zhukov*, A.S. Noskov, E.S. Borisova, L.Yu. Zudilina

**Federal unitary enterprise "Biysk Oleum Plant"*
Boreskov Institute of Catalysis SB RAS

At present selective reduction of nitrogen oxides by ammonia is a widely used process for NOx abatement in industrial gases. Vanadium containing systems are conventional catalysts for the process. One of the earlier designed methods of process technology is based on a periodic change of filtered gas flow direction, as it passes through the reactor, ammonia being supplied into the central part of reactor. This technology was implemented at the Biysk oleum plant to purify the off-gases from explosives production. With time production technology was changed, and off-gases composition changed significantly, which required plant revamp. At present, NOx concentration in the off-gases ranges from 1.5 to 5.0 g/m^3. Therefore, reactor design requires the heating of filtered gases, as NOx concentration falls below 1.5-2.0 g/m^3.

Newly designed reactor is equipped with a kettle heater installed in the central part. Catalyst bed is divided into two parts connected with a tube. This tube also serves as a mixer for ammonia fed into the purified gases. Plant control system provides the automatic electric heater switch-on, as NOx concentration decreases and catalyst bed temperature decreases to 230-250 °C. Periodic gas flow reversal and electric heater installed in reactor center allows the minimum energy consumption on the gas heating. When NOx content in the purified gas is 1.0 g/m^3, and gas flow rate is 7200 m^3/h, apparent electric power required for gas heating does not exceed 5 kWt.

As based catalysts for the newly designed plant chosen were a) ring alumina-vanadium catalyst, b) cylinder extruded alumina-vanadium catalyst produced by AO "Katalizator" (Novosibirsk).

Calculated regimes for gas purification from NOx at a periodic reversal of filtering direction are given in the Table below:

catalyst	NOx content, vol.%	Time between reversals, min	Catalyst bed height, m	T_{max}, °C	NOx removal, %	P, mm H_2O
a)	0.15	7	2x0.35	316	96.7	343
a)	0.15	9	2x0.35	291	95.2	331
a)	0.30	25	2x0.35	385	97.0	335
a)	0.30	27	2x0.35	360	95.0	317
b)	0.15	7	2x0.44	364	95.2	548
b)	0.3	22	2x0.35	423	94.8	460

T_{max} is the maximum temperature in the catalyst bed
P is reactor pressure drop

At the first stage of industrial application cylinder extruded catalyst was used. Commissioning has shown the following. At an inlet NO_2 concentration of 3-4 g/m^3, gas flow rate 7-8 10^3 m^3/h and gas flow temperature 20-25 °C, purification degree is 98-99%, maximum temperature never exceeds 350 °C, while time between reversals is 20-22 min. In this case NOx residue after purification does not exceed 70 mg/m^3.

Comparison between calculations (see the Table above) and industrial performance parameters shows a good agreement by the main process parameters (maximum temperature, purification degree). Difference between the calculated and real values of time between reversals is provided by rector peculiarities (metal weight), which are not taken into account in the mathematical model.

Transfer to the ring catalyst will reduce catalyst loading by 30-40%, maximum temperature – by 40-50 °C, and reactor pressure drop – by 150-200 H_2O mm.

PP-30

SYNTHESIS AND CHARACTERIZATION OF SUPPORTED BIMETALLIC CATALYSTS FOR HYDRODECHLORINATION OF POLYCHLORINATED COMPOUNDS

V.I. Simagina, I.V. Stoyanova, V.A. Yakovlev, V.A. Likholobov

Boreskov Institute of Catalysis, Pr. Acad. Lavrentieva, 5, 630090, Novosibirsk, Russia, Fax: 007 3832 343056, E-mail: V.I.Simagina@catalysis.nsk.su

Polychlorinated organic compounds (PCOC) are environmentally persistent chemicals which are bioaccumulated in fatty tissue and show carcinogenic and mutagenic activity. Catalytic hydrodechlorination is one of the ways of detoxification of the PCOC, which excludes the formation of more toxic substances such as polychlorinated dibenzodioxins and dibenzofurans. This process is also a well-known method in synthetic organic chemistry [1].

The goal of this study is the preparation and investigation of effective and inexpensive catalysts, permitting to carry out hydrodechlorination of hexachlorobenzene and carbon tetrachloride under mild reaction conditions. It was decided to prepare bimetallic catalysts consisting of nickel, iron or copper associated to palladium, supported on a high surface area carbon "Sibunit" and TiO_2 [2]. We have studied the catalytic property of prepared catalysts and modification of catalytic surface under the influence of reaction medium..

The catalysts NiPd/C, CuPd/C and PdFe/C were prepared from metal salts and than reduced by $NaBH_4$. For increasing the reaction rate of liquid and gases phase hydrodechlorination carried out in a two-phase system (aqueous KOH and organic solvent) with the use of tetramethylammonium chloride as phase-transfer catalyst. The catalysts were characterized by chemical analysis, X-ray diffraction, electron microscopy.

It was shown that amorphous bimetallic catalyst supported on "Sibunit» alloy is very effective for hydrodechlorination of hexachlorobenzene and carbon tetrachloride.

Such palladium containing bimetallic compounds allow formation of C_1-C_5 hydrocarbon during hydrodechlorination of carbon tetrachloride.

It was shown that the effect of Pd content on the initial activity and stability is of great importance. On the other hand the metal precursor used have a decisive influence on the initial activity and deactivation of catalysts.

The kinetic study revealed that the reaction mechanism was the Langmuir-Hinshelwood type.

References

[1] Kovenklioglu S., Cao Z., Shan D., Farrauto R.J., Balko E.N.: *AIChE Journal*, 38, 7, 1003, (1992).

[2] Simagina, V. I.; Renouprez, A. J.; Bergeret, G.; Gimenez, M. T.; Stoyanova, I. V.; Egorova, M. B.; Likholobov, V. A., Organohalogen Compd., 40, 563, 1999.

NITRIC OXIDE FORMATION IN INDUSTRIAL HEATING FURNACE[1]

N.Y. Romanyukha, K.Y. Malikov* and B.N. Chetverushkin

Institute for Mathematical Modelling Russian Academy of Sciences,
4 Miusskaya Square, 125047 Moscow, Russia
Fax: (095) 972-0723, e-mail: rona@imamod.ru
**Ural State Techical University, Ekaterinburg, Russia*

The heat transfer processes and chemical mechanisms controlling nitric oxide formation under methane - air mixture combustion are investigated in specially designed rapid heating metallurgic furnace. The furnace is characterised by relatively low concentrations of nitric oxides concentrations, experimentally measured.

The design of the furnace may be briefly described as follows. The furnace is a consequence of several sections. The steel nozzles, inserted into the refractory walls and directed normally to the heating metal, supply the fuel-air mixture directly into the furnace space. The fuel-air mixture is well premixed and preheated up to the temperatures 600-800K. Each section has the local system for combustion products removing. The optimal choice of the distance between the nozzle and the workpiece (35 –50 calibres) is the key point of the furnace design.

The combustion process is characterised by high flame velocities - up to 300 m/s without causing flame instability. The combustion gas temperature ranges from 1400 to 1700K. The averaged temperature varies from one section to another (the difference is approximately 30 – 50K). The refractory walls are relatively cold, their temperature does nor exceed 1300K. The internal volume is occupied most of all (up to 99%) by the hot gases combustion products - water vapour and carbon dioxide. The cold jet cores occupy less than 1% of the furnace volume. Intense penetration of hot products into the cold core provides ignition and stabilise the flame. High velocities of combustion products lead to very effective mixing and consequently provide complete fuel combustion in the furnace. The main gas phase toxic substances produced in the furnace under these conditions are the nitric oxides.

The correct estimation of the temperature fields in the furnace is especially important for realistic evaluation of nitric oxide concentrations. The relatively simple numerical model for a single flame jet was developed. The aerodynamic and thermal structure of a homogeneous jet was numerically investigated. The model provides acceptable accuracy for engineering purposes. The model includes conservation equations for steady 2-D axisymmetric flow for mass, momentum, energy and species concentrations. The zone-node radiation exchange method was developed to estimate radiative heat transfer [1,2]. The main advantage of this method is the flexible coupling between the fluid part of the problem computed on a fine grid and the radiation part estimated on a coarse grid. The numerical experiments with the model supply

[1] The work is supported by Russian Foundation of Basic Researches, project 00-01-00291.

the data on the temperature fields, combustion products distribution and the estimations of characteristic times of gas dynamic processes inside the furnace. These data were used for numeric analyses of the processes controlling nitric oxides formation in the furnace.

The fuel used in industrial furnaces consists of more than 98% methane. The detailed chemical kinetic model including 198 forward and the same number of reverse reactions corresponding to methane – air combustion was developed and applied to estimate NOx concentrations [2]. Reactions corresponding to thermal and radical mechanisms of NO formation were considered.

The characteristic times of chemical kinetic processes controlling NOx formation were estimated for different ignition temperatures and equivalence ratios of methane- air mixture. These values correspond to respective values of temperature measured and numerically estimated for different sections of the furnace and equivalence ratio of mixture supplied into the same section. The numerically estimated characteristic times of kinetic processes and the times of removing the hot combustion products (1700K) from the reaction zone with the following cooling to at about 900K were compared. No gas phase reactions of NO formation occur under the temperature 900K. The comparison leads to the following conclusion. All the nitric oxide produced in the furnace is formed by 'prompt' mechanism only. That provides relatively low NO concentrations. The sensitivity analysis of the model for such parameters as equivalence ratio of methane – air mixture, ignition temperatures and initial concentrations of hot combustion products corresponding to different zones of the internal space of the furnace was fulfilled. It should be mentioned that the increase of concentrations of some intermediate products of methane oxidation (as radicals CH, CH_2 for example) in hot combustion products leads to significant amounts of nitric oxides. That's why, the complete fuel combustion reached in the furnace is very important for good ecological characteristics of the process.

The mean flame jet flow characteristics, temperature profiles and NO concentrations were not only numerically estimated but measured as well. The results of numerical modelling are in a good agreement with the measured quantities. The relatively low temperatures and good mixing conditions in the furnace lead to relatively low NOx emissions. The NO concentration in the final combustion products does not exceed 40ppm, that is quite low for metallurgic furnace. The relatively high impact of convective heat transfer in the furnace provides the improvement of the energetic and ecological characteristics of the furnace.

References.

1. Lisienko V.G. Malikov G.K., Malikov Y.K. Zone-Node Method for Calculating Radiant Gas Flows in Complex Geometry Ducts. Numerical Heat Transfer. An International Journal of Computation and Methodology. Part B: Fundamentals. 1992, vol.22, N1, pp.1-24.
2. K. Malikov, N. Romanyukha, B. Chetverushkin, Y. Malikov. Mathematical Modelling of Heat Transfer and Nitric Oxide Formation in Flame Jet Impingement Furnace, Proceedings of ECSBT2, Stuttgart, 2000, v1, pp.91-100.

SEPARATION OF METHANE – ETHANE GAS MIXTURES ON CARBON MICROPOROUS ADSORBENTS BY PRESSURE SWING ADSORPTION

V.N. Kashkin, M.S. Mel'gunov, A.I. Madyarov, S.A. Pokrovskaya, N.A. Chumakova, I.A. Zolotarskii, V.B. Fenelonov

Boreskov Institute of Catalysis, Pr. Akad. Lavrentieva, 5, Novosibirsk 630090, Russia
phone: 383 2 34 12 78 fax: 383 2 34 18 78 E-mail: kashkin@catalysis.nsk.su

Separation of methane homologues from a natural gas by the pressure swing adsorption (PSA) method is of importance from practical point of view. Carbon microporous adsorbents were shown to be feasible for this purpose [1-3]. In this work the results of numerical and experimental studies of PSA cycles for carbon microporous adsorbents of different properties are presented.

Modeling results.

The elementary steps that constitute a PSA cycle are: pressurization (with a product stream), feed (removal of the purified product during the high-pressure feed step) and depressurization (blowdown to the low pressure), followed by purge step.

A mathematical model of a PSA process consists of the mass conservation law equations for gas and solid phases with the corresponding boundary and initial conditions. For the feed step, a linear driving force approach is used to describe mass transfer resistance in the pellet. The adsorption equilibrium is described by Langmuir type dependencies for both gas components. The gas phase concentration profiles were modeled by a plug flow regime.

Detailed numerical simulation has been performed for the single-bed system. The algorithm is based on the method of lines. To obtain a system of ordinary differential equations, the spatial derivatives were approximated by finite differences. The average and dynamic properties of the process (such as refined product purity and recovery) were calculated and the evolution of concentration and gas velocity profiles were studied under various operating conditions.

Separation cycles were modeled for the samples of commercial carbon microporous adsorbents produced by «Chemviron Carbon» company (Belgium) and the Joint Stock Company «CHMZ» (Elektrostal, Russia). The adsorption properties of methane and ethane over these carbon microporous adsorbents were determined using the gas-chromatographic technique described elsewhere [4]. Intraparticle diffusivity constants of methane and ethane were found to be nearly equal.

In the numerical studies, the feed gas mixture consisted of 95% methane and 5% ethane to model a typical composition of natural gas.

Duration of the adsorption step and rate of the gas flow were chosen to provide a mole fraction of the refined methane to be not lower than 99, 99%. It was found that the quantity of the refined methane obtained per cycle diminishes with a decrease in ethane mass transfer rate at constant purity of the methane outlet flow. At constant gas flow rate a decrease of the ethane mass transfer rate leads to a decrease of methane outlet purity. The values of ethane mass transfer rate were determined which provide maximal quantity and purity of refined methane.

A numerical simulation of the PSA cycles has shown that the equilibrium regime of the PSA separation is realized for studied adsorbents. These adsorbents provide the purity of the refined methane about 99.99% with methane recovery of 40-60%.

At the same time it is possible to obtain simultaneously the concentrated ethane and pure methane from their mixture. The results of the numerical studies indicate that the ethane concentration in the gas phase during the blowdown step is not very high (is not higher than 12-14% vol.) due to strong ethane adsorption. However, the ethane fraction after blowdown step in the adsorbed phase is essentially high and reaches 75 - 80% vol. To release the concentrated ethane, the temperature should be increased during blowdown step.

Experimental results.

A dynamic adsorption set-up was used to realize a cyclic PSA regime. The operation conditions were as follows: temperature 25^0C, height of the adsorbent bed 35 cm, gas velocity 0.3 m/s, adsorption pressure 4.4 atm, desorption pressure 0.1 atm and cycle time 50 s.

Experimental data have confirmed the modeling results. The refined methane was obtained with a purity of 99,99% from the feed mixture that contained 95% vol. methane and 5% vol. ethane.

Conclusions:

- The possibility to obtain the refined methane with a purity of 99.99% vol. from the ethane-methane mixture by PSA method using carbon microporous adsorbents is demonstrated by experiments and modeling.
- The concentrated ethane with a ethane fraction of 75-80% vol. could be obtained by a temperature rise during the blowdown step.
- Comparison with experimental data confirmed the efficiency of the software developed for optimization of the operating PSA cycle conditions.

We express sincere thanks to V.D. Al'pern (Chemviron Carbon) and N.K. Kulikov (Joint Stock Company «CHMZ», Elektostal') for the supplied adsorbent samples.

References

1. D.M. Ruthven, «Pressure swing adsorption», VCH Publishers, Inc., 1994.
2. V.B. Fenelonov, "Poristy uglerod", Novosibirsk, 1995.
3. V.N. Kashkin, M.S. Mel'gunov, I.A. Zolotarskii, S.A. Pokrovskaya, N.A. Chumakova, V.B. Fenelonov and N.A. Baronskaya. Adsorption properties of methane and ethane over carbon microporous adsorbents, XIV International Conference on Chemical Reactors CHEMREACTOR, Tomsk, Russia, June 23-26, 1998, p.101-102.
4. K. Kawazoe, M. Suzuki; Chromatographic study of diffusion in molecular- sieving carbon; *J. Chem. Eng. Jap.* v.7, No3, p.151-157, 1974

The studies were performed with the grant support of Education Ministry of Russian Federation: "Fundamental Researches in the Field of Chemical Engineering", № 3H–247-99, № 3H–247-00.

PP-33

REACTOR FOR CATALYSTS SYNTHESIS BY PRECIPITATION AS A COMPLICATED HIERARCHICAL SYSTEM WITH INTERACTIVE LEVELS

Oleg P. Krivoruchko

Boreskov Institute of Catalysis SB RAS, Pr. Akademika Lavrentieva, 5, Novosibirsk 630090, Russia
Ph.: +7(383 2) 34 12 22; Fax: +7(383 2) 34 30 56; E-mail: opkriv@ catalysis.nsk.su

1. Introduction

Poorly soluble hydroxides are widely used to prepare catalysts, supports, adsorbents and other materials. An understanding of the mechanism of hydroxide formation at the level of sol-gel processes and gel evolution on its ageing in mother solutions permits one to control their properties such as phase composition, dispersion, and porous structure that are important for catalysis.

Principal peculiarity of systems with chemical reactions of poorly soluble hydroxides formation is their essential non-equilibrium (oversaturation of reagents to fresh phase reaches 5-15 orders), open character of systems and existence of feedback. Besides, it is well known that hydrolysis is always complicated by formation of polynuclear hydroxo - complexes (PHC) on the interaction between aqua - cations (III, IV) and bases.

We have established [1] a new, not known earlier mechanism of formation and crystallization of poorly soluble hydroxides and formulated the theoretical concepts, providing an explanation for relations and dependences between the stages of genesis of hydroxides and oxides on catalyst synthesis. Thus, we state that PHC of precipitated metals act as intermediate materials on hydroxide formation. As was shown, a limited number of complexes forms on polycondensation. In the course of mutual conversions, "key" polynuclear hydroxo complexes (KPHC) are formed and accumulated in solutions to produce sol particles. Consequently, the key complexes are not engaged in the formation of complexes with a different nuclearity and structure at the following steps of the hydroxide formation.

We have established a very important phenomenon of "inheritance" of the structure of key polynuclear hydroxocomplexes by hydroxides, which determines a genetic relation of the nearest order between gels of amorphous hydroxides and the structure of the corresponding PHC. The structure, chemical composition, and arrangement of the functional atom groups of the key PHC carry an information about the evolution of amorphous hydroxides on ageing up to the point when they transform to the crystal state. The number of crystal phases formed on ageing corresponds to the number of structurally and chemically detectable versions of amorphous hydroxides in precipitates. When one knows the structure of the key PHC and their concentration in the parental solution, it is possible to predict quantitatively a phase composition of the ageing products.

The state of physico-chemical processes and reactor for catalysts synthesis by precipitation is analyzed based on the proved mechanism of formation and crystallization of poorly soluble M(III) hydroxides.

2. Mechanism of formation and crystallization of poorly soluble M(III) hydroxides in reactor as hierarchical system with interactive levels

Aluminium hydroxides are extensively used to manufacture supports and catalysts. For this reason, they are the subject for numerous studies, primarily, of empirical nature. Nevertheless, the mechanism of formation and the structure of amorphous Al(III) hydroxides are not sufficiently elucidated.

For any method and precipitation conditions, the interaction between a precipitated metal salt and an alkaline, the system passes through a number a states which are characterized by various æ = $[OH^-]/[Al^{3+}]$. A particular distribution of Al(III) complexes with a different nuclearity corresponds to every æ. ^{27}Al NMR permits one to follow separately the complexes containing 1, 2, and 13 atoms of aluminium (Al_1, Al_2, and Al_{13}, respectively). On polycondensation of concentrated solutions of Al(III) salts, Al_p forms which is not observed in the ^{27}Al NMR spectra. We suggest the following experimentally substantiated structural and crystallochemical model of this complex in solution: $Al_7O_2(OH)_{14}(H_2O)_{10}^{3+}$ (denoted as Al_7).

For diluted salt solutions ([Al(III) < 0.3 mol/l), as æ increases, a fraction of α (Al_1 + Al_2) decreases and a fraction of the key complex α(Al_{13}) increases. The limiting value is 2.3. When æ is higher than the limiting value, primary particles (PPs) of hydroxide begin to form from the key PHC of Al(III). The products of polycondensation of aqua ions of Al(III) are different in concentrated solutions. Here, Al_7 is the key complex. However, polycondensation processes proceed in a similar way [1].

When a base is added to an aluminium salt solution, polycondensation may follow the routes:

$Al(H_2O)_6^{3+} \leftrightarrow Al_2(OH)_2(H_2O)_8^{4+} \leftrightarrow Al_{13}O_4(OH)_{24}(H_2O)_{12}^{7+} \rightarrow PPs_1 \rightarrow$aggregates of PPs_1 (1)

$Al(H_2O)_6^{3+} \leftrightarrow Al_2(OH)_2(H_2O)_8^{4+} \leftrightarrow Al_7O_2(OH)_{14}(H_2O)_{10}^{3+} \rightarrow PPs_2 \rightarrow$aggregates of PPs_2 (2)

Schemes (1) and (2) exhibit the limiting cases for diluted and concentrated solutions of Al(III) salts. In the general case, both KPHC of Al(III) exist on polycondensation in solutions. The key complexes of Al(III) form true solutions

It was found that the chemical nature of the initial salt anions affects essentially both the direction of polycondensation processes of aqua - cations and the whole ensuing evolution of hydroxides on their ageing. Thus, sulfate ions can completely suppress formation of Al_{13} complexes, when the concentration is sufficiently high. The effect of anions on the polycondensation of aqua - ions of Al(III) and the properties of gels decreases in a series: $SO_4^{2-} >> Cl^- = NO_3^- > ClO_4^-$.

PP-33

We have shown [1] that Al_{13} and Al_7 pass from the solution into gels of Al(III) amorphous hydroxides with no detectable changes in their structure and size (18 and 15 **Å**, respectively) at pH = 4-10 and T < 50 ^{0}C. Hence it follows that (i) a minimum, theoretically attainable size of PPs is determined by sizes of key complexes of precipitated metals, and (ii) gels of Al(III) hydroxides "inherit" the structure of key complexes of Al(III). Note that an interaction between several key complexes yielding particles of Al(III) hydroxide sols 30-50 **Å** in size is more typical.

At the close of gel formation at pH = 7-10, T > 60 ^{0}C, a series of complex physicochemical processes begins spontaneously. Crystallization of Al(III) hydroxides is the most important one. We have established the mechanism of crystallization of poorly soluble hydroxides[1]. Crystallization proceeds in a volume of every PP via the rearrangement of its polymer structure and growth of secondary crystals (SCs) and by oriented accretion of the primary, partially crystallized PPs over the similar faces of the other particles, rather than via dissolution of highly disperse PPs. The phase composition of crystallization products is determined by the nature of key complexes yielding an amorphous hydroxide gel. Thus, the gels obtained from Al_{13} or Al_7 transform into bayerite and pseudoboehmite, respectively, during ageing, the other conditions being the same [2].

The main stages of formation of amorphous hydroxides of Fe(III) are [3, 4]:

$Fe(H_2O)_6^{3+} \leftrightarrow Fe_2(OH)_2(H_2O)_8^{4+} \leftrightarrow Fe_p \rightarrow PPs \rightarrow$ disordered aggregates of PPs (3)

The key complexes of Fe_p composed of double chains of octahedrons [FeO_6] are joint at the edge. The composition of Fe_p complexes is $FeOOH \cdot H_2O$. When complexes Fe_p transfer to the volume of sol particles, their structure and composition do not practically change. Gels of amorphous hydroxides of Fe(III) are composed of disordered aggregates of PP with a narrow size distribution (35-45 **Å**). Analyzing the curves of radial atom distribution, and using the bright image and dark image of TEM techniques, we have discovered local, structurally ordered regions 10 **Å** in size. The atom distribution in such regions is characteristic of α-FeOOH (goethite) [3].

On the basis of the theoretical concept on the mechanism of crystallization of poorly soluble hydroxides, we have developed [4] an approximate kinetic model: $d\alpha/dt = K(1 - \alpha)^2$ (α is a fraction of the crystal goethite phase). This model adequately describes all experimental data on gel ageing in alkaline media at 25-90 ^{0}C. Parameters $K_o = 7.085\ 10^{11}$ and E = 76.8 ± 2.6 kJ/mol were determined elsewhere [4]. A knowledge of the mechanism and kinetics of crystallization of amorphous Fe(III) hydroxides permits one to manufacture (using one technological scheme) a wide range of hydroxides and even oxides with the following parameters: S = 20-500 m^2/g, the overall pore volume is 0.1-1.0 cm^3/g, size of pores ranging from 10 to thousands **Å**.

Hierarchical structure of physico-chemical processes and reactor of ideal mixture for catalyst synthesis by precipitation method may be represented as follows:

1. Aqueous solutions of M(III) salts [$M(H_2O)_6^{3+}$, $M(H_2O)_5An^{(3-n)+}$, An^{n-}, H_2O, H_3O^+ and bases [M(I), OH^-].
2. Products of hydrolysis and polycondensation $M(H_2O)_6^{3+}$ [$M(H_2O)_5(OH)^{2+}$, $M_2(OH)_2^{4+}$, key PHA $M(III)_i^{n+}$, H_3O^+ or OH^-, H_2O].
3. Primary particles (PP_s), disordered and/or ordered aggregates of PP_s of amorphous M(III) hydroxides in aqueous solutions.
4. Gels of amorphous and/or crystal M(III) hydroxides.
5. Reactor of ideal mixing; hydrodynamics, heat- and mass transfer of reagents and reaction products in the reactor volume.

The promising way for solution of problems of theory and practice of catalysts preparation by precipitation of poorly soluble substances is mathematical modeling of reactions, processes and reactors. Unfortunately, this scientific area still does not attract attention of researchers to the right degree. The experimental material which could be used for description of kinetic behavior of suggested five-level structure of processes and reactor for catalyst synthesis is very poor.

References

1. R.A.Buyanov and O.P.Krivoruchko, React. Kinet. Catal. Lett.,35(1987)293.
2. O.P. Krivoruchko, R.A. Buyanov, M.A. Fedotov and L.M. Plyasova, Zh. Neorg. Khim., 23(1978)1798 (in Russian).
3. T.A. Kriger, O.P. Krivoruchko and R.A. Buyanov, React. Kinet. Catal. Lett., 24(1984)401.
4. O.P. Krivoruchko, V.V. Malahov, A. Ermakova, R.A. Buyanov and L.F. Lokotko, Kinetika i Kataliz, 28(1987)442 (in Russian).

PP-34

APPLICATION OF GRADIENTLESS REACTORS WITH OUTSIDE MIXING DEVICES TO STUDYING KINETICS OF CATALYTIC PROCESSES

A.S. Bobrin, N.N. Bobrov

Boreskov Institute of Catalysis, Novosibirsk, Russia
Fax: 007 383-239-7363, E-mail: bobrin@catalysis.nsk.su

A key problem of experimental heterogeneous catalysis is evaluation of a catalytic activity of samples under investigation. The catalytic activity is typically measured as a specific rate of reaction referred to the catalyst amount (weight, volume, surface area) [1]. Because the rate is in dependence on experimental conditions, in practice, we measure the specific steady-state rate at given temperature, pressure and flow of reagents.

Laboratory techniques apply recycle reactors for the rate control. The gradientless regime is provided by intensive agitation of reagents by means of special units which may be installed inside or outside of the reaction vessel.

The recycle reactors with internal agitation are widely used now [2,3]. Along with positive characteristics of the internal agitation, there are some problematic moments. The essential drawback is impossibility of experimental control of the flow passed through the catalyst bed. Also a problem with heat removal can appear in a case of strongly exothermic reactions when the reactor is not supply with external cooling.

An external recycle reactor shown in Fig.1 was designed to overcome these drawbacks [4]. As seen in the scheme, incoming to the catalyst reagents are preheated to reaction temperature by means of heat

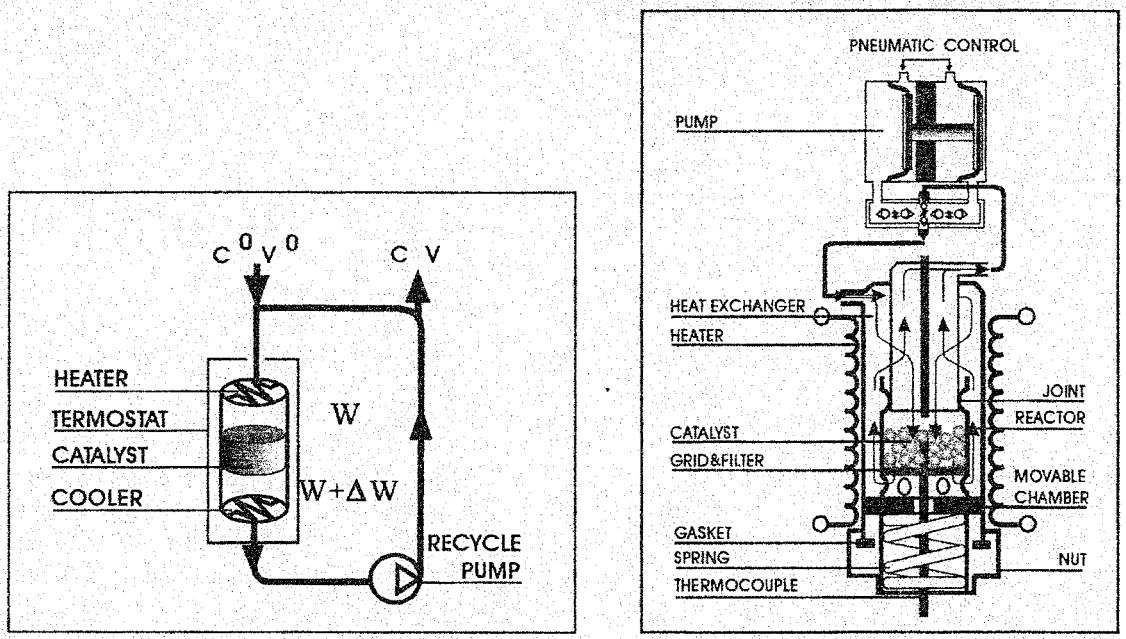

Fig 1. Recycle reactor configuration (to the left) and one of gradientless design with outside circulation (to the right)

exchange with outgoing gases, which, in turn, are cooled down to the working temperature of the circulating pump. The reactor design easily ensures attainment of isothermal condition for the catalyst bed, including the case of exothermic processes.

We used kinetic methods to control isothermal station of the catalyst bed. In Fig. 2 are presented steady-state reaction rates measured in the model exothermal process at specified composition of the reaction flow supplied and different amount of catalyst in the fixed reaction volume. When the catalyst amount was increased by 10 times, the reaction rate was still kept unchanged. This result indicated that the temperature was constant throughout the catalyst volume.

Thus, the catalytic activity is determined experimentally as the steady-state rate at specified temperature and composition of the reaction flow. At the first level of catalysts standardization we consider the catalytic processes from the formal kinetics standpoint. Hence, some standard and general methods for a kinetic control of the catalyst activity can be developed.

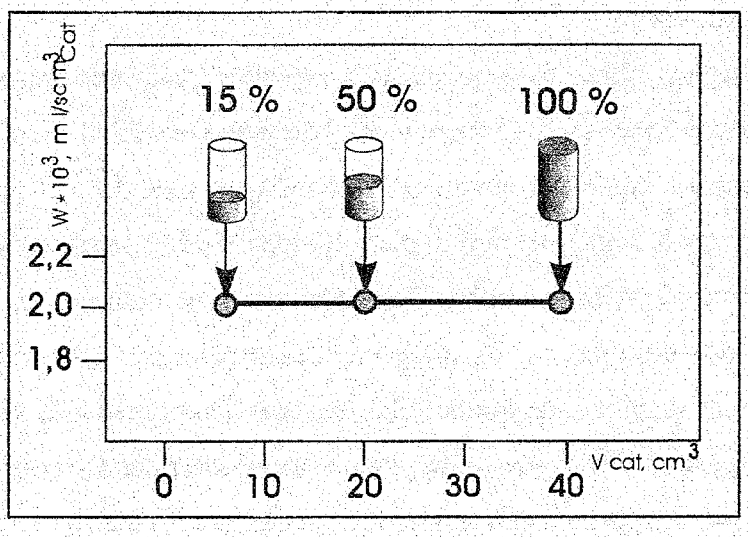

Fig.2 Dependence of the rate of methane oxidation on the catalyst amount, T=773 K

Concentration fluctuation within the catalyst volume was estimated according to equations for the complete oxidation of hydrocarbons.

$$W = \frac{C^0V^0 - CV}{100m} = \frac{(C^0 - KC)V^0}{100m} = \frac{C^0xV^0}{100m};$$

$$K = V^0/V; \qquad x = \frac{C^0 - KC}{C^0};$$

$$W = kC; \qquad G_{circulation} = 1000l/h;$$

$$\delta = \frac{W + \Delta W}{W} = 1 + \frac{V^0}{V} \cdot \frac{x}{1-x};$$

if: $V^0 = 1l/h;$ $x = 0.90;$ $\delta = 1.009;$
if: $V^0 = 50l/h;$ $x = 0.15;$ $\delta = 1.009;$

As determined, the gradientless regime was realized to a high precision at the normal discharge of recycle pump. It should be noted some fundamental features of gradientless reactors.

- Varying the rate of the reaction flow supplied into reactor, we change conversion of the key components, but did not create concentration gradients in the reactor.
- In any gradientless reactors composition of the reaction mixture contacting with the catalyst is practically equivalent to the composition of the outlet flow.

Basing on these facts we can measure the reaction rates at the different rates and composition of the flow supplied, and, as a result, determine the reaction rate at the desired composition of the contact mixture.

The reactor designed allowed us to perform effective precision measurements of the steady-state rate for a number of fundamental catalytic reactions [5,6]. The appropriate data processing was made by especially developed interpolation method. For instance, in Fig.3 there is a scheme of graphic interpolation method for single-route processes of complete oxidation of hydrocarbons. Varying incoming flow rate at a fixed composition of reagents, we obtained a set of steady-state rates at the different concentrations of a key component. In the following procedure of graphic interpolation the rate was determined at a desired concentration of the key component. For single-route processes characterized by nonzero order to key component the method was successfully applied as a rapid test of activity of new catalysts.

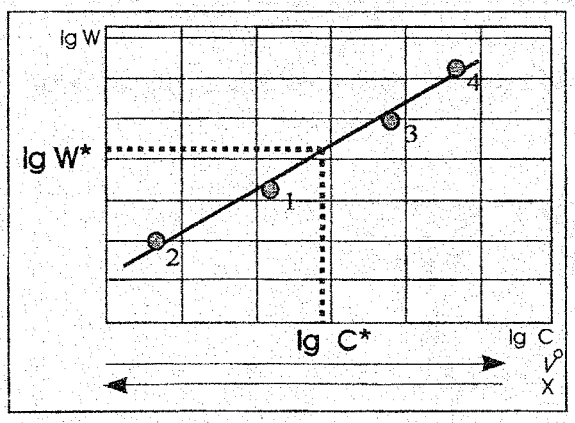

$$C_nH_m + (n + 0.25m)O_2 \rightarrow nCO_2 + 0.5m\,H_2O$$
$$(C^0,C) \quad (C^0ox,Cox) \qquad (Ccd) \quad (C\omega)$$

$$W = \frac{\sum_{i=1}^{4} Ki \cdot f(C,Cox,Ccd,C\omega)}{1 + \sum_{i=1}^{4} Ki \cdot f(C,Cox,Ccd,C\omega)};$$

Fig. 3 Scheme of determination of the catalytic activity.

Predetermined model and kinetic equation of the catalytic process simplified experimental work, because in this case it was sufficient to obtain only single point on the in Fig.3. In practice, this is the typical situation in the quality control of commercial samples. The reactor design and experimental procedure including computer control of the process and data processing, provided a high precision and reproducibility of results of the catalytic testing [5]. Standard measurements normally made every month gave deviation of the constants of no more than 7% from the average value.

The present study is a contribution to creating experimental department for control and investigation of the catalytic activity as a part of international center of catalysts investigation in BIC.

REFERENCES

1. Boreskov G.K., *Kinet. Catal.*, 1962, no. 3, p. 470.
2. Carberry J.J., *Ind. Eng. Chem.*, 1964, vol. 56, no12, p. 39.
3. J.M. Berty: Catal. Rev., 20, 75, 1979.
4. Bobrov N.N., *Experimental methods for catalytic properties investigations.*, NSU, Novosibirsk, 1989.
5. Bobrov N.N., Arakelyan V.V., *Methods and setups for industrial catalyst activity testing.*, Standardization of methods and devices for catalyst quality testing. Novosibirsk, 1991, p. 62-80.
6. Bobrin A.S., Sokolov V.P., Bobrov N.N., *React. Kinet. Catal. Lett..*, 1985,vol. 27, no. 2, p. 433-436.

PP-35

LAYERED DOUBLE HYDROXIDES AS NANOREACTORS

V.P. Isupov, L.E. Chupakhina, K.A. Tarasov

Institute of Solid State Chemistry and Mechanochemistry SB RAS,
Kutateladze-18, Novosibirsk, Russia, 6390128
Tel: 7-3832-36-38-37, Fax: 7-3832-32-28-47, E-mail: isupov@solid.nsk.su

Layered double hydroxides are a large group of compounds with the chemical formula $[M(II)_{(1-X)}M(III)_X(OH)_2]^{Y+}(A^{n-}_{Y/n})\cdot mH_2O$ (LDH-A), where M(II) are the cations of double-charged metals (Mg^{2+},Ni^{2+}, etc) and lithium, M(III) are the cations of triple-charged metals (Al^{3+}, Cr^{3+}, Fe^{3+}), An - are interlayer anions (Fig.1). These compounds are widely used as precursors to obtain complex oxides containing M(II) and M(III) metals, acid-base catalysts,

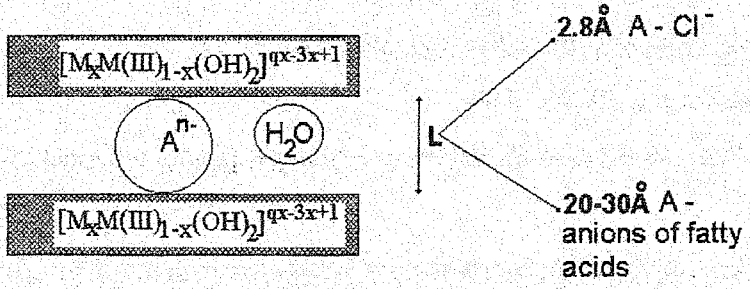

Fig.1. Structure of LDH.

drugs, sorbents as well as anion exchange matrices of the "anionic clay" type [1,2]. The structure of these compounds is formed by alternating charged brucite-like layers of the composition $[M(II)_{(1-X)}M(III)_X(OH)_2]_{(2\infty)}^{Y+}$ and the layers containing A- anions and water molecules at the same time. The thick of $[M_XM(III)_{1-X}(OH)_2]^{qX-3X+1}$ layer is approximatelly 5 Å. The distance between the layers (L) is determined by the nature of anion A^{n-} and varies from 3 Å for Cl^- to 20-30 Å for anions of flatty acids. The presence of two fragments of nanoscale thickness which differ sharply in composition, structure, and chemical properties makes it possible to employ these compounds as nanoreactors for chemical reactions of interlayer molecules. The chemical reactions of interlayer molecules can be conventionally divided in two groups. The first group includes reactions in which two-dimensional $[M_XM(III)_{1-X}(OH)_2]^{qX-3X+1}$ layers are conserved after reaction of interlayered molecules.

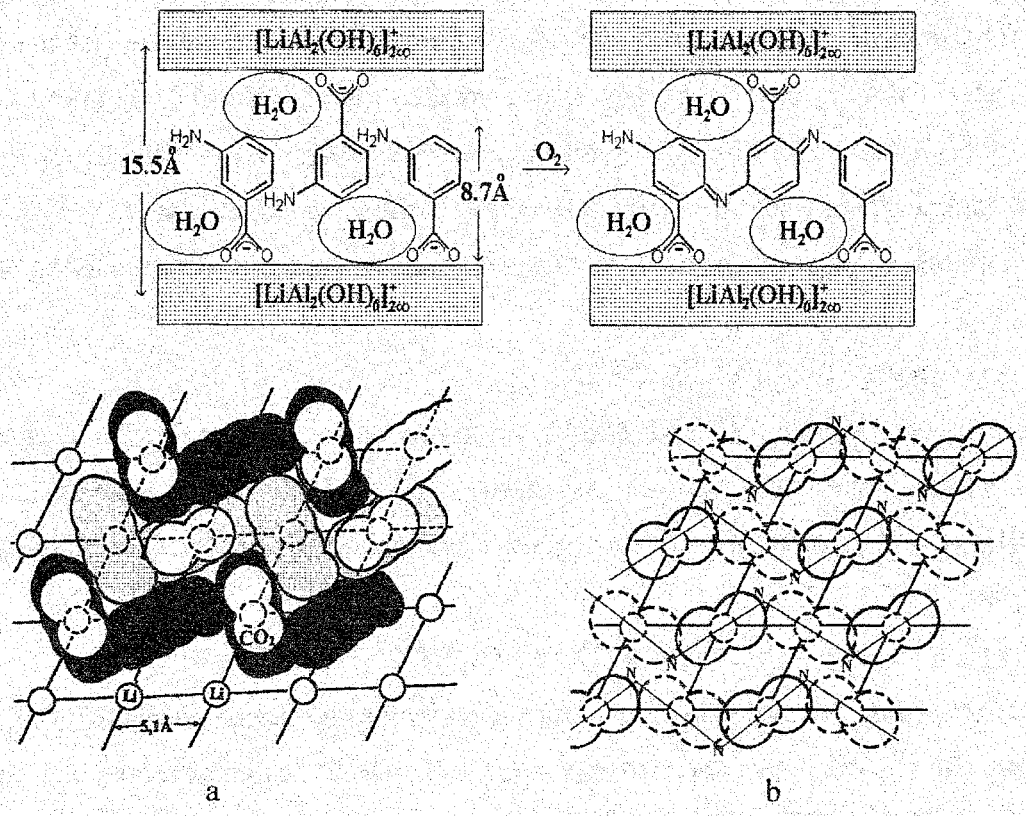

Fig.2. Interlayer polymerization of organic molecules. Structure of initial $[LiAl_2(OH)_6][m\text{-}NH_2C_6H_4COO]\cdot nH_2O$ (a), orientation of organic chains with respect to $[LiAl_2(OH)_6]^+$ (b).

The second group includes reactions in which two-dimensional layers are destructed.

Reactions of interlayered molecules with conservation of hydroxide layers of LDH.

Interlayer oxidation of unsaturated carboxylic anions.

The interaction of LDH-A containing unsaturated carboxylic anions ($(CH)_2(COO)_2^{2-}$, $(CH)_4(COO)_2^{2-}$) with aqueous solution of potassium permanganate has been investigated [3]. It has been found that the interaction results in the break of the double bonds of the organic anions and reduction of MnO_4^- to Mn^{4+}, the reduced manganese being fixed in the interlayer space. Thus obtained solid product allows to prepare, after heating in air, Mn-containing oxides that can be used as selective sorbents of lithium.

Interlayer polymerization of aromatic anions.

When heated in air, LDH containing m-aminobenzoic acid anions undergoes polymerization of the anions in the interlayer space resulting in the formation of polymeric, high oriented polyconjugated macromolecules between hydroxide layers. Polymerization mechanism includes the diffusion of oxygen molecules through the interlayer space of $[LiAl_2(OH)_6][m\text{-}$

$NH_2C_6H_4COO]\cdot nH_2O$ into the contact region of two anions, further oxidation of the anions and the formation of macromolecules (Fig.2). The repeating unit along the polymer chain (which is about 10 Å) is close to the parameter **a** for the initial LDH which should be 10.2 Å. The use of LDH makes possible to control the character of molecular contacts between the anions of aminobenzoic acids in interlayer space. This allows to control the possibility of the formation of polyconjugated chains during oxidative polymerization of intercalated organic anions.

Interlayer photolysis of $[Fe(III)(CN)_6]^{3-}$.

Photolysis of LDH$[Fe(III)(CN)_6]$ leads to the formation of nanoscale systems containing two-dimensional hydroxide layers separated by $[Fe(II)(CN)_6]^{4-}$ complexes and $[FeO_X(OH)_{6-X}]^{(3+x)-}$ clusters [4]. The photolysis of interlayer molecules may be described by the equation:

$$3\ [Fe(CN)_6]^{3-}, H_2O + h\nu \rightarrow 2\ [Fe(CN)_6]^{4-} + [FeO_6H_x]^{(12-3-x)-} + HCN\uparrow + (CN)_2\uparrow$$

Reactions of interlayered molecules with destruction of hydroxide layers of LDH.

During the vacuum thermal decomposition of LDH-X containing organic anions, X - $(CH_2)_2(COO)_2^{2-}$, $(CH)_2(COO)_2^{2-}$, $(CHOH)_2(COO)_2^{2-}$, $(CH_2)_8(COO)_2^{2-}$, $C_6H_4(COO)_2^{2-}$, $C_6H_5(CH)_2(COO)^-$, nanoscale particles of carbon and lithium aluminates are produced [5]. The size of carbon cluster depends on the type of the organic anion and on reaction conditons. In the case of nonaromatic acid anions the reaction forms linear polyconjugated system containing an odd number of carbon ($x<50$) and oxygen atoms. In the case of aromatic acid anions, polyconjugated system of the aromatic type with an odd number of carbon atoms forms. In the case of phtalate anions, there are no more than 50 carbon atoms, and the electron gase is nondegenerate. In the case of the cinnamic acid anion, there are more than 50 carbon atoms, ant the electron gas is degenerate.

Thermal decomposition of $[LiAl_2(OH)_6]_nX\cdot nH_2O$(X - Cl^-, Br^-, J^- and SO_4^{2-}) leads to formation of composites containing fine (5-10 nm) particles of alumina covered with a thin (3-5 nm) layer of lithium salts [6]. The presence of the point reflections on the microdiffractograms of the thermolysis products testifies that aluminium oxide particles are well ordered with respect to each other. Orientation of aluminium oxide particles to the matrix of the starting compound is such that the $(111)_{Al_2O_3}$ plane is parallel to the $(001)_{LDH\text{-}X}$ plane. This material possesses much higher conductivity than individual lithium salts. It can be used in chemical current sources as solid electrolyte with lithium conductivity.

Thermal decomposition of $[LiAl_2(OH)_6]_2[Medta{\cdot}4H_2O$ and $[LiAl_2(OH)_6]_2[M^I_XM^{II}_{1-X}$ edta]$\cdot nH_2O$ (M, M^I, M^{II} - Co, Ni, Cu) leads to the appearance of nanoscale (2-150 nm) metal particles distributed in a dielectric oxide matrix [4,7]. The data of HRTEM confirm formation of the round nickel particles (4-5 nm) with the narrow size distribution spread uniformly in the matrix upon the thermolysis of $[LiAl_2(OH)_6]_2[Niedta]{\cdot}4H_2O$. Thermal decomposition of LDH-Co leads to the formation of only large cobalt particles. According to the electron microscopy data, the particles have different shapes depending on whether they are located at the surface of the matrix flakes, or within their volume. The surface particles, having maximal sizes of 100-150 nm, exhibit tri- or six-angle shapes when observed normally to the basal sheets of the flakes, while the inner ones are lens-shaped. **This demonstrates that during metal particle growth the lamellar matrix exhibits itself as a template.** Thermal decomposition of LDH-Cu gives round copper particles, their size varying in the rather wide range from 2 to 80 nm.

In order to prepare nano-sized particles of binary alloys, we synthesised precursor compound of the type LDH-$Ni_{0.56}Co_{0.44}$. Nickel and cobalt form readily a continuous series of solid solutions. According to TEM, the size of the nickel-cobalt alloy particles formed after the decomposition of LDH-$Ni_{0.56}Co_{0.44}$ is about 11 nm. The surprising thing is that their morphology is close to that of the individual nickel but not of the cobalt.

References

1. F. Cavani, F.Trifiro, A.Vaccari, *Catalysis Today* **11,** 173-301 (1991).
2. W.T. Reichle, *J. Catal.* **94,** 547-557 (1985).
3. E.I.Bakchinova, V.P. Isupov, V.A. Poluboyarov and V.V. Boldyrev, Dokl. Academii Nauk **324**, 592-595 (1992) (in Russian).
4. V.P.Isupov et al. Solid State Ionics **101-103**, 265- 270(1997).
5. V.P.Isupov et al. Dokl. Academii Nauk **324**, 1217-1221 (1992) (in Russian).
6. N.F. Uvarov, B.B.Bokhonov, V.P.Isupov and E.F.Hairetdinov, Solid State Ionics **74**, 15-27 (1994).
7. V.P. Isupov, K.A. Tarasov, R.P. Mitrofanova and L.E. Chupakhina, Mat.Res.Soc. Symp. Proc., **457**, 539-544 (1997).

PP-36

PARTIAL OVERLOAD OF NATURAL GAS CONVERSION CATALYST IN TUBULAR PRIMARY REFORMER OF AMMONIA PLANT AM-1360

P.V. Ovsienko, N.P. Pavlova, T.Ye. Nefedova

"Khimtekhnologiya" Institute, Ukraine, 93400, Severodonetsk, st. Vilesov, 1
Phone: (38 06452) 93669; fax: (38 06452) 25367

Tubular primary reformer of natural gas is one of the most complex for operation among ammonia plant apparatus; its stable and efficient performance influences the work not only of syngas preparation section but of the plant as a whole. Among operating costs catalyst replacement in primary reformer is the most expensive step.

One of the ways to cut catalyst replacement costs is partial overload of primary reformer tubes. It means that catalyst is replaced only along a certain length, e.g. first 4-6 m of gas flow or diluted during replacement with inert material in the lower part of reaction tubes.

The object of this study is development of mathematical model for numerical predicting of reaction tube performance at partial replacement of catalyst bed in reaction tube. Results presented here relate to radiation chamber of reformers with top-fired furnaces. For other types of heating individual investigation is required.

Simulating procedure was based on assumption that all reaction and raising tubes are operated under conditions of uniform heat input from combustion zone. Reformer volume was divided into N number of equal vertical segments. In each elementary segment the law of heat and matter conservation was observed. Corresponding balance equations were set up for each zone, i.e. fuel gas combustion zone, reaction zone accounting for known kinetic relations, zone of raising tubes. Heat transfer was investigated within an elementary volume cross section. Initial data for calculations were the following:

1) design parameters of reformer;
2) inlet compositions, temperature; fuel gas, reaction mixture and air pressures, respectively;
3) degree of fuel burning off along flare length;
4) air surplus coefficient;
5) heat losses;
6) catalyst grain geometry;
7) parameter accounting for different catalyst activity along tube height, including zero activity, when catalyst is poisoned or substituted with inert.

The following resulting values were obtained:

1) exit compositions, temperature, pressures of reaction and flue gases;
2) temperature distribution of reaction and raising tubes along reformer height;
3) temperature distribution along flare length;

4) temperature distribution along catalyst bed;

5) concentration distribution of all components in reaction mixture along tube height;

6) change in convective heat transfer coefficient from combustion zone towards reaction tube walls along reformer height;

7) heat distribution along reformer height;

8) total heat input to reaction and raising tubes;

9) reformer resistance.

In the Table the calculated longitudal methane concentration in reaction tube is presented for normal process conditions accepted among primary reformers of ammonia plants AM-1360. One can see that within the first meters of tube length methane consumption is 3.5 times higher compared to the last meters. It means that major part of the feedstock is converted in tube upper part and contribution of lower catalyst beds into the total conversion degree is insignificant.

Calculated data for two most important process parameters, i.e. methane content at reaction tube exit and temperature of reaction tube external surface are presented. Calculations were done for two cases: a) normal operation b) operation of reaction tubes when non-overloaded catalyst portion of approximately 2 m in length has completely lost its activity (critical situation). We see that methane content increased from 4.74% to 5.93% (from 8.8% to 11.6% as dry gas), however such residual methane content is allowed by process norms and regulations. The temperature of reaction tube external surface also increased, but it didn't exceed the temperature of upper part or approach the limiting operating temperature of 930 °C.

Tube length	Methane content, vol.%		Tube wall temperature, °C	
	normal operation	critical regime	normal operation	critical regime
Inlet	18.2	18.2	-	-
0.63	17.35	17.35	810	810
1.26	16.41	16.41	844	844
1.89	15.16	15.15	867	868
2.52	13.76	13.76	883	884
3.15	12.36	12.35	893	894
3.79	11.05	11.03	887	888
4.42	9.87	9.89	880	881
5.05	8.85	8.83	872	873
5.68	7.96	7.94	867	869
6.31	7.19	7.17	866	866
6.94	6.53	6.50	864	865
7.57	5.96	5.93	858	858
8.2	5.49	5.93	851	866
8.83	5.05	5.93	848	874
9.46	4.74	5.93	846	880

In principle there are two critical situations which theoretically can occur during partial overload and serve as reasoning against this proposal:

1) overall loss of activity of non-overloaded catalyst portion;
2) excessive increase in reaction tube resistance due to destruction of non-overloaded catalyst tablettes.

The first situation was briefly described above and it was shown that no serious consequences would occur for production process. Real and serious risk may be possibility of destruction of old tablettes. This process cannot be theoretically predicted and only operating experience in using this catalyst can be a reliable basis.

In conclusion we give recommendations on measures required before you accept and use partial overload. We strongly advise to investigate reformer performance during 5-6 months prior to overloading date; continuous control of reformer performance is also desirable during the whole period of catalyst use.

Investigation measures include the following:

1. Visual control of reaction tubes external surface to determine the number of normal tubes, obviously overheated tubes and tubes having slight thermal spots on their surface. Mathematical models for each type of the tubes will have special characteristics.
2. Measurement of all reformer process parameters and longitudal temperature profiles of tube external surface.
3. Mathematical model adaptation to operating conditions of a particular unit.
4. Technological analysis of performance characteristics of natural gas conversion section as a whole is needed to distinguish between situations connected with conducting the process and those of inadequate catalyst behaviour.
5. Activity and mechanical strength testing of the catalyst discharged from critical levels of reaction tubes.
6. Analysis of the total information obtained and making decision as to overload type: complete overload, partial overload by catalyst replacement at upper levels of reaction tubes, overload by dilution of catalyst portion with inert.

Realization of this proposal will provide 10 to 70% savings of fresh catalyst.

TECHNIQUE OF DENSE CATALYST BED FORMATION IN TUBULAR REACTORS

V.M. Ivanov, V.V. Vladimirov, F.V. Kalinchenko, A.G. Deryabko*, V.N. Trukhanov*, Yu.Yu. Tur*

"Khimtekhnologiya" Institute, Ukraine, 93400, Severodonetsk, st. Vilesov, 1
Phone: (38 06452) 93408, E-mail: kalin@ixt.lg.ua
**"DneprAzot" plant, Ukraine, Dneprodzerzhinsk, st. Gorobtsa, 1, Phone: (38 05692) 78748*

Industrial practice of tubular reactors and reformers operating has shown that traditional catalyst charging by "socking" method or charging by portions through the upper tube part do not provide required catalyst bed density, uniformity and stability even when charging technology is strictly observed. Technologies used nowadays are based on improving or correcting measures of the system being formed, however, it is not always possible in narrow reaction tubes.

Thus, when catalyst portions are being charged into the tube by "socking" method, each portion is compressed by impact against tube surface. The procedure is repeated until tube and reactor filling as a whole has been completed.

Evidently, impact effect results in compression not only of a newly charged portion but also of lower bed layers which have been already formed, respectively. However the values of controlled charging parameters, that is bed height and hydraulic resistance cannot be used to characterize bed structure. Abrupt local narrowing of free section due to granule destruction and bed discontinuity resulting in voids in lower and middle parts of the tube are practically impossible to detect.

Over years "Khimtekhnologiya" Institute has been working on formation of catalyst beds in chemical reactors of different types. The main lead is formation of regular catalyst beds using spherical granules. Results obtained, techniques and devices developed in course of investigations have been published in journals, awarded patents and certificates of authorship; semi-commercial tests have been a success [1,2,3].

Approaches and procedures developed were shown to be applicable to form dense catalyst beds using non-spherical granules. This technique is based on immediate formation of a required bed structure unlike methods aimed at improving the structure which has been already formed in a random way. It is attained by layer-by-layer build-up of bed and giving time required for a granule to take a stable position and also by inputting into the system being formed the energy to fluidize granules of the upper monolayer.

PP-37

We have made comparative investigations on charging 32x3 mm tube with tabletted 5x5 mm catalyst by methods of a) charging by portions through the upper tube part; b) piston compression of small portions; c) impact effect on surface of the tube filled with catalyst; d) formation of bed using chargers developed in "Khimtekhnologiya" Institute. Results of investigations are presented in Table 1.

Table 1. Influence of bed formation method for 5x5 mm tabletted catalyst on hydraulic coefficient value $f = \frac{\Delta P g d}{2hyU^2}$ [4]

Air rate in tube (m/sec)	Values of dimensionless coefficient f of hydraulic resistance at charging			
	charging by portions through upper tube part	piston compression	impact effect	using chargers
0,2	11,5-11,9	15,1-16,0	14,7-21,7	20-21
1,0	6,3-6,9	12,1-12,3	7,8-10,4	10,4
3,2	2,7-3,1	3,4-3,7	3,2-4,1	4,0-4,2

From Table 1 one can see that beds formed by chargers provide the most dense and uniform structure reproducible at repeated formation.

During investigations carried out in tube of 72mm in diameter with K-905D-1 catalyst, 'socking' and charger techniques were compared. Results of bench investigations are presented in Table 2.

Table 2. Characteristics of ring support layers formed in tube of 72mm in diameter

№	Technique of bed formation	Number of tests	Bed height (m)	Air rate (m^3/hr)	Pressure drop (10^3 n/m^2)	Calculated bed porosity (m^3/m^3)
1	"socking"	5	3.2-3.5	41.0	8.7-9.4	0.495-0.479
2	charger	3	3.2	41.0	10.2-10.3	0.500

As we see from data in Table 2 the bed formed by "socking" technique with subsequent impact effect on tube surface has a lower calculated bed porosity at a lower drop of hydraulic resistance and poor reproducibility of charging parameters. It is the evidence of considerable ununiformity inside bed structure which may hinder performance of tubular reactor.

A bed formed by the chargers developed in "Khimtekhnologiya" Institute has a small value of porosity simultaneously with high uniformity and reproducibility of charging results.

Investigation results have been confirmed completely at industrial-scale charging of natural gas reformer at Dneprodzerzhinsk "DneprAzot" plant in 1999. It was made by specialists of "Khimtekhnologiya" Institute by means of five chargers. Deviations in hydraulic resistance drop along reformer tubes did not exceed 5%; all tubes were filled at first attempt without further corrections or improvements of the bed which had been formed.

A conclusion can be made that this technique of catalyst bed formation in tubular reactors and reformers is very promising. It provides for formation of dense stable systems, simplifies charging process, reduces costs and duration of overloading.

References.

1. R.Z. Adinberg, V.M. Ivanov, V.V. Dilman. Reports of Academy of Sciences, USSR, 1986, 288, (2), 425-428.
2. V.V. Dilman, R.Z. Adinberg, V.M. Ivanov et al. Chemical Engineering, 1988, (II), 617-621.
3. R.Z. Adinberg, V.V. Dilman, V.M. Ivanov et al. Chemical Engineering, 1990, (8), 23-26.
4. M.E. Aerov, O.M. Todes. Hydraulic and thermal bases of apparatus performance with fixed and boiling grain beds. L., Chemistry, 1968.

PP-38

SYSTEM OF OPTIMUM CONTROL OF BURNING PROCESS ON THERMAL POWER STATION

G.N. Abdullayev, R.M. Kasimov, E.M. Mamedov

Institute of Theoretical Problems of Chemical Technology of Academy of Sciences of Azerbaijan Republic

The results of experimental researches and system engineering of the optimum control of burning process on a thermal power station (TPS) are identified. The system provides the control of the charge of fuel and air acting in fire-place of TPS. For measurement of the charge of fuel as the primary converter is used jet meter, assembled on the consecutive circuit from three consistently connected jet triggers. The fluctuations of pressure, created on it, will be transformed with the help of the piezoelectric converter to electrical signals with frequency proportional to the measuring volumetric charge of fuel. On the existing TPS, the air acts in the fire-place through versatile pipelines. In this connection for measurement of speed of air submission in fire-place of TPS as the primary converter is used the fitting wing located in a flow under certain corner of attack. Both surfaces of fitter are connected by the internal pipe-line of small section, into which is entered similar jet meter, connected with the piezoelectric gauge. The readings of this meter are proportional to linear speed of air flow.

With the purpose of optimum mode maintenance of burning process in fire-place and re-duction of a pollution level of a atmosphere by toxic gases in system is stipulated adjustment and stabilization of ratio between the charge of air, fuel and degree re-circulation of burning products.

For processing of information, acting from gauges and the representations of the received results in appropriate manner and for maintenance of an exchange of the information with the personal computer are developed the appropriate electronic blocks of interface. The visual control of parameters of the charge of fuel, air and their ratio, and also re-circulation degree of burning products in system is stipulated.

THE CHOICE OF THE ACTIVE CATALYST FOR THE PROCESS OF OXIDIZING COMBINATION OF METHANE IN THE SYSTEM OF REACTORS

A.M. Aliyev, E.M. Mamedov, R.M. Kasimov, V.A. Rasulov

Institute of Theoretical Problems of the Chemical Technology of Azerbaijan AS.

Working out of the chemical-technological installation completed by the technical means of automation and ten reactors on basis of the personal computer enabled to examine in the institute an activity of the great number of catalysts for the process of oxidizing combination of methane.

In the reactors of automatized setting the examined- specimens of the catalysts were placed in the initial position and the temporary regimes of study of their activity were introduced by program into the electronic computer's memory.

The work of the reactors was carried out in the consecutive order.

When conducting the experimental tests they wed the synthesized metal zeolite catalysts obtained by the method of ion exchange from the natural zeolites: clinoptylolite and mordenite. They wed the samples of dealuminiumized form of natural clinoptylolite and mordenite with the diverse values of silicate modulus, synthesized on their base Ca, Mg, Sr, Ba- substilited metal zeolite catalysts of the different composition as well as metal zeolite catalysts with the additional amount of ions of Li put into them. The studies of catalytic activity have been carried out at the temperature range of 700-800 °C, at velocity of the reactionary mixture in 1800 $h.^{-1}$ and mole correlation of the reagents methane- oxygen 0,402 – 0,312. The comparative analysis of the obtained data has shown that the best results are achieved on aluminum forms of zeolites with silicate modulus in 10,8 and containing ions of calcium. With this, increase of calcium from 5% to 7% of zeolite weight substantially increases its activity However, further increase of calcium concentration to 10% has a slisht influence upon activity of the catalyst of this tupe. It is established that addition of ions of Zi. to it promotes increase of selectivity of the process of oxidizing transformation of methane as well as decrease of the process temperature by 100 °C with improvement of the yield of the end product. The optimal composition of the catalyst for reaction studied has been found by the investigations carried out. The most active are dealuminiumized clinoptylolite with silicate modulus in 10,8, modified by ions of calcium and lithium content of which makes up 7% and 8% uspectively of zeolite weight.

PP-40

FORMATION OF CATALYTICALLY ACTIVE COATINGS ON ALUMINIUM ALLOYS BY MICROARC OXIDATION IN ELECTROLYTIC SOLUTIONS

P.I. Butyagin*, A.I. Mamaev, Ye.V. Khokhryakov

Institute of Strength Physics and Materials Science of the Siberian Branch of the Russian Academy of Sciences, Tomsk, Russia
E-mail: aim@mai.tomsk.ru, mamaev@ispms.tsc.ru

Development of high-efficiency catalytic systems and new methods for their preparation are an important topical problem. It is known that anodization is used for the formation of oxide layers on aluminium followed by impregnation with solutions of transition metal salts. We have developed multipurpose oxide coatings over aluminium surface using microarc oxidation. This method provides catalytically active coatings without any impregnation of oxide layers on the aluminium surface. We have identified the formation mechanism for catalytically active coatings. The limiting stage of the formation process is found to be ion diffusion from electrolytic solutions to the microarc discharge region. It is shown that microarc discharge conditions at the electrolyte-aluminium interface give rise to the interaction between the electrolyte components and aluminium ions and oxide. X-ray diffraction shows that the coatings include a spinel structure and oxygenic compounds of chromium (14%), cobalt (2-4%), cerium (5%), manganese (25%), copper (3,5%) and iron (10%).

We have studied the catalytic activity of the coatings in the course of methane oxidation. Their activity is found to be comparable to that of magnesium-chromium catalysts. Impregnation of the oxide layers by platinum chlorate solution improves the activity of the coatings. The coatings produced are 100 - 300 μm thick. Thermocyclic loading tests show that the coatings withstand 40 cycles at 600 °C without destruction. The microhardness is 600-2500 kg/mm^2.

The proposed microarc oxidation technique makes it possible to apply porous coatings containing compounds of transition metals, which exhibit catalytic activity comparable with that of standard catalysts and high thermal stability. These facts indicate that microarc oxidation shows good promise for synthesizing catalytic coatings on aluminium and aluminium-alloy substrates.

REFORMING REACTOR BEHAVIOR IN VIEW OF CATALYST DEACTIVATION BY COKE

O.A. Reutova

Chemistry Department, Omsk State University, Russia
55-a, Pr. Mira, Omsk, Russia, 644077
E-mail: reutova@univer.omsk.su

Reforming process is carried in a series of four reactors. The temperature and concentration profiles are an important characteristic because it reflects a kinetics on the each process stage.

The coke deactivation influence on the reactor behavior is studied on the kinetic model because of the long-duration period between the regenerations (near one year).

For the reactor working prediction it is necessary to include many aspects into the full kinetic model:

1 - the goal reaction scheme accounting Pt/Al_2O_3 catalyst bifunctionality;

2 - the coked deposition mechanisms on each types of the active sites;

3 - the establishing of a dependence between the polyfunctional reaction rates and a total deactivation parameters (for instance, the coke content) and etc.

The crude (petrol) components were united to 15 ones. The dependence of the activity on time was derived and it was taken into account for the computations of concentration and temperature profiles in the reforming reactor cascade.

In the first reactor a temperature decrease is maximum because of the endothermic reactions (naphtenes $\rightarrow$ aromatics) proceeding primarily, so the concentration are flowing oppositely. Simultaneously an isoparaffine concentration increases.

In the second reactor the isoparaffine concentration is maximum, this fact is very interesting for a perspective engineering.

In the third reactor the exotermic reactions of hydrocarbon hydrocracking proceed; the temperature drop is minimum.

These profiles show that the catalyst deactivation staggers in the reactor beds. For the aromatics and naphtenes concentration curves shift upwards and downwards. During deactivation the temperature drops decrease in the first reactor and increase in the next ones.

This model was used for the analysis of the monitoring data of industrial catalytic reforming unit (Sibneft - Omsk NPZ).

The work was supported by Federal Program "Integration – 2000".

PP-42

FORMATION OF THE UPSRTEAM WAVES UNDER COKE BURNING IN A FIXED BED REGENERATORS

A.V. Balaev, I.M. Gubaidullin

Institute of Petrochemistry and Catalysis of Bashkir Academy of Sciences, Russia

The regeneration is characteristic of the topochemical process which determines the surface reaction rate. The proposed kinetic model considers the combustion of coke deposits of some stoichiometric form CH_n. In addition, the loss of catalyst weight and the adsorption of oxygen on a surface of coke deposits and its diffusion into a volume of the coke deposits are taken into account.

All components of a reaction system were classified into three groups:

$\overline{Z}$ - composition of coke deposits (Z_1 - hydrogen, Z_2 - oxygen, Z_3 – carbon);

$\overline{\theta}$ - overall surface of area fractions ($\Theta_{CH2}=\Theta_1$, $\Theta_{CO}=\Theta_2$, $\Theta_C=\Theta_3$);

$\overline{Y}$ - components of the gas phase (1 – oxygen, 2 – carbon dioxide, 3 – carbon monooxide, 4 – water).

On these assumptions the kinetic model of the coke deposits oxidation is given by

$2\,\Theta_C + O_2 \rightarrow 2\,\Theta_{CO}$	$W_1 = k_1(T)\theta_3^2 Y_1$
$\Theta_{CO} + O_2 \rightarrow \Theta_{CO} + CO_2$	$W_2 = k_2(T)\theta_2 Y_1$
$\Theta_{CO} \rightarrow \Theta_C + CO$	$W_3 = k_3(T)\,\theta_2$
$\Theta_{CH2} + O_2 \rightarrow \Theta_{CO} + H_2O$	$W_4 = k_4(T)\,\theta_1 Y_1$
$\Theta_{CO} + \Theta_{CO} \rightarrow 2\,\Theta_C + CO_2$	$W_5 = k_5(T)\theta_2^2$
$\Theta_{CH2} \Leftrightarrow \Theta_C + Z_{H2}$	$W_6 = k_6(T)(\theta_1^* - Z_1)$
$\Theta_{CO} \Leftrightarrow \Theta_C + Z_O$	$W_7 = k_7(T)(\theta_2^* - Z_2)$

For simulation of process a transient two-phase diffusion model of the coke combustion in a catalyst fixed bad has been developed. The model balance equations take into account the thermal conductivity in a dense phase and the heat and mass transfer in a gas phase by convection streams. In addition, account must be taken of Stefan's stream, which arises because of a increasing of mole number during a chemical reaction.

The model equations of mass and energy balances for the dense and gas phases for an adiabatic reactor are given by

$$\frac{dZ_m}{dt} = A_m \sum_{j=1}^{J} \nu_{mj} W_j, \qquad m=1...M$$

$$\Theta_k \Rightarrow \sum_{k=1}^{K} \nu_{kj} W_j = 0$$

$$\frac{\partial y_i}{\partial t} = \beta S_{ex}(x_i - y_i) + \mu Y_i + \sum_{j=1}^{J} \nu_{ij} \frac{W_j}{C_o}$$

$$C_d \frac{\partial \vartheta}{\partial t} = \lambda^* \frac{\partial^2 \vartheta}{\partial l^2} + \alpha S_{ex}(T - \vartheta) + \sum_{j=1}^{J} Q_j \frac{W_j}{C_o}$$

$$Y_i = (y_i \text{ if } \mu<0,\ x_i \text{ if } \mu>0)$$

$$\mu = -\sum_{j=1}^{J} \delta_j \frac{W_j}{C_o}, \qquad \delta_j = \sum_{i=1}^{I} \nu_{ij}$$

$$\varepsilon \frac{\partial x_i}{\partial t} + U \frac{\partial x_i}{\partial l} = (\beta + \frac{\mu + |\mu|}{2}) S_{ex}(y_i - x_i)$$

$$\varepsilon \frac{\partial T}{\partial t} + U \frac{\partial T}{\partial l} = \frac{\alpha S_{ex}}{C_g}(\vartheta - T)$$

The initial and boundary conditions are:

$t = 0$: $y_i = 0,\ x_i = x_i^o,\ T = T_o,\ \vartheta = \vartheta_o;$

$l = 0$: $U = U_o,\ x_i = x_i^o,\ T = T_o,\ \lambda^* \frac{\partial \vartheta}{\partial l} = \alpha_{in}(\vartheta - T_o);$

$l = L$: $\lambda^* \frac{\partial \vartheta}{\partial l} = 0$

Where: z_m – weight fraction of the *i*-th coke species; y_i and x_i – compound concentration in the catalyst and gas phases; W_j – rate of chemical reactions; ν – stoichiometric coefficients; U – local gas velocity; α, β – heat and mass transfer coefficients; μ - rate of the Stefan's stream; ε – void fraction of the fixed bed; λ^* – effective thermal conductivity; ϑ, T – temperature of the catalyst and gas; C_d, C_g – heat capacity of the catalyst and gas; C_o – mole density of gas; S_{ex} – external specific catalyst particle surface; Q_j – the heats of reaction; l, L – axial position in the bed and total bed length; α_{in} – heat exchange coefficient in beginning of bed; t – time; A_m – coefficients depending on the order of the chemical reactions.

A numerical analysis of oxidative regeneration of catalyst in a fixed bed was carried out. The effect of various parameters (initial coke weight fraction, oxygen concentration, inlet

temperature and volumetric flow rate) on the overall maximum temperature rise in a fixed bed was examined. Under any conditions there is the formation in a bed of the temperature and concentration profiles which creep along the bed at constant velocity without change of the gradients. A wave nature of coke burning gives rise to dynamic superheating in an adiabatic fixed bed.

The volumetric flow rate can a significantly effect the performance of the coke burning. In case when contact time (τ_c) is equal to 5-20 sec there takes place downstream creeping of the reaction zone, but in case τ_c is more than 100 sec there are upstream creeping of one. The computation results of the latter are presented in Figures 1 and 2. It is observed, that the oxidation of a condensed phase such as a coke deposits differs from the catalytic combustion of a gas phase. The latter have a continuous creeping of the profiles, but the former have some sharp shift of the temperature and concentration profiles from one to another positions of a fixed bed. This phenomenon may be explained by the influence of thermal conductivity witch warms up a bed above the reaction zone.

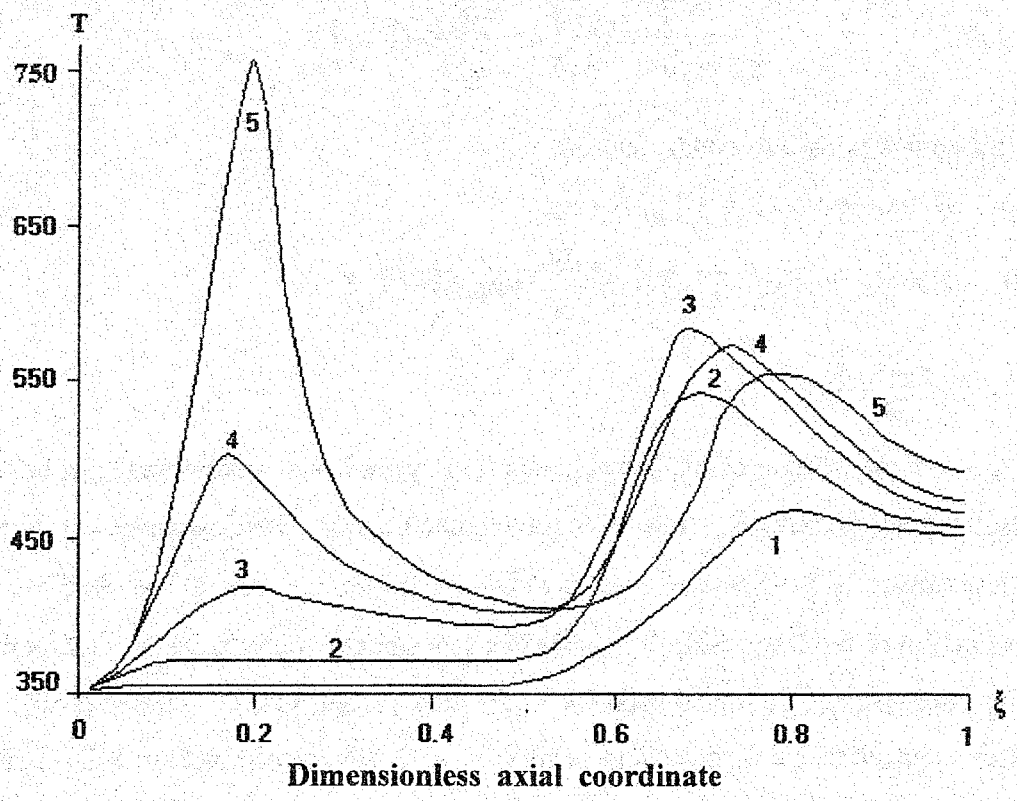

Figure 1. Catalyst temperature profiles (T, °C) at upstream creeping of the reaction zone

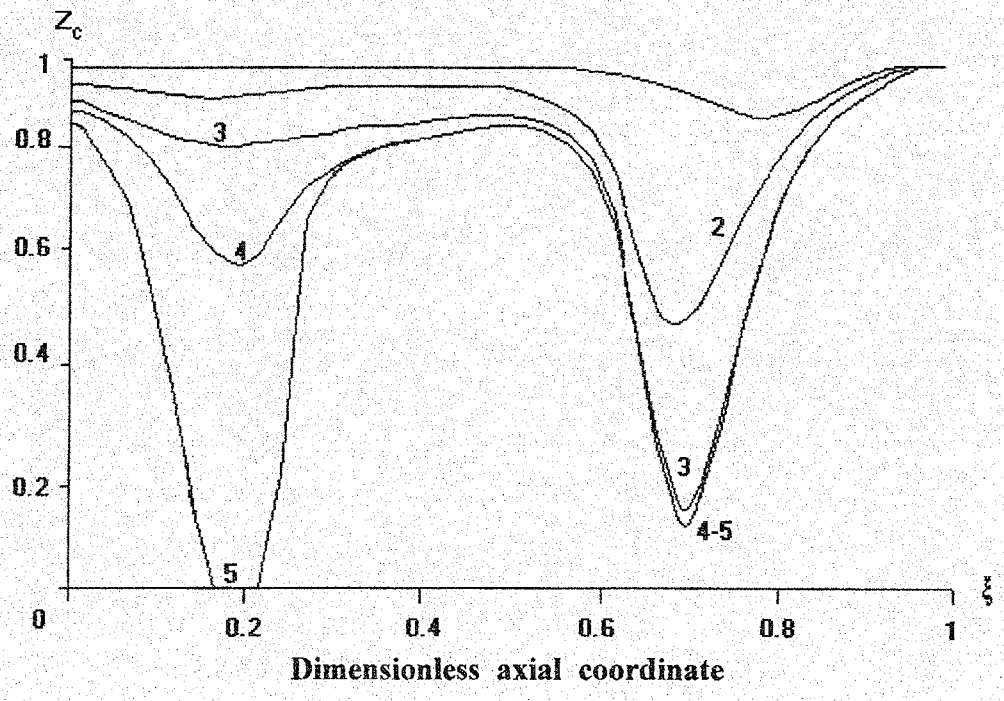

Figure 2. Dimensionless coke weight fraction profiles (Z_c) at upstream creeping of the reaction zone.

LIST OF PARTICIPANTS

Gulam ABDULLAYEV
Institute of Theoretical Problems of Chemical Technology of Academy of Sciences of Azerbaijan Republic
29, Huseyn Javid str.
370143 Baku
Azerbaijan Republic
Tel.: 99412 394159
E-mail: musa.mamedov@usa.net

David AGAR
University of Dortmund
D-44221 Dortmund
Germany
Tel.: 49 231 755 2698
Fax: 49 231 755 2698
E-mail: agar@Chemietechnik.Uni-Dortmund.DE

Oguz AKPOLAT
Ege University
35100 Bornova/Izmir/
Turkey
Tel.: 00 90 232 3884000/1877
Fax: 00 90 232 3887600
E-mail: akpolat@eng.ege.edu.tr

Vladimir I. ANIKEEV
Boreskov Institute of Catalysis SB RAS
pr. Akad. Lavrentieva, 5
630090 Novosibirsk
Russia
Tel.: +7 383 2 39 74 47
Fax: +7 383 2 39 74 47
E-mail: anik@catalysis.nsk.su

Nadezhda B. ARKHIPOVA
Ministry of Industry, Science and Technologies
Tverskaya str., 11
103906 Moscow
Russia
E-mail: science@user.cdromclub.ru

Vycheslav S. BABKIN
Institute of Chemical Kinetics and Combustion SB RAS
Institutskaya str., 3
630090 Novosibirsk
Russia
Tel.: +7 383 2 33 02 17
Fax: +7 383 2 32 23 50
E-mail: babkin@ns.kinetics.nsc.ru

Alexander V. BALAEV
Institute of Petrochemistry and Catalysis of Bashkir Academy of Science
pr. Oktyabrya, 141
450075 Ufa
Russia
Tel.: +7 347 2 31 35 44
Fax: +7 347 31 27 50
E-mail: alexb@ufanet.ru

Viktor V. BARELKO
Institute of Problems of Chemical Physics RAS
142432 Chernogolovka, Moscow region
Russia
Tel.: +7 096 517 1817
Fax: +7 096 515 3588
E-mail: barelko@inln.cnrs.fr

Giampaolo BARONE
Dipartimento di Scienze Farmaceutiche, Universita di Salerno
via Ponte don Melillo
I-84084 Salerno
Italy
Tel.: +39-089-962648
Fax: +39-089-962828
E-mail: barone@pluto.farmacia.unisa.it

Larissa V. BARYSHEVA
Boreskov Institute of Catalysis SB RAS
pr. Akad. Lavrentieva, 5
630090 Novosibirsk
Russia
Tel.: +7 383 2 34 18 78
Fax: +7 383 2 34 30 56
E-mail: barysheva@catalysis.nsk.su

Vladimir S. BESKOV
D.I. Mendeleyev University of Chemical Technology of Russia
Miusskaya Sq., 9
125047 Moscow
Russia
Tel.: +7 095 978 91 45
Fax: +7 095 200 42 04
E-mail: odik@sunup.ru

Alexander S. BOBRIN
Boreskov Institute of Catalysis SB RAS
pr. Akad. Lavrentieva, 5
630090 Novosibirsk
Russia
Tel.: +7 383 2 39 73 63
Fax: +7 383 2 34 30 56
E-mail: bobrin@catalysis.nsk.su

Svetlana A. BORISENKOVA
Lomonosov Moscow State University
Lenynskie Gory
119899 Moscow
Russia
Fax: +7 095 932-88-46
E-mail: jerrik@cityline.ru

Andrey I. BORONIN
Boreskov Institute of Catalysis SB RAS
pr. Akad. Lavrentieva, 5
630090 Novosibirsk
Russia
Tel.: +7 383 2 39 73 10
Fax: +7 383 2 34 30 56
E-mail: boronin@catalysis.nsk.su

Victor E. BOZHEVOL'NOV
Lomonosov Moscow State University
Lenynskie Gory
119899 Moscow
Russia
Tel.: +7 095 939 34 49
Fax: +7 095 932 88 46
E-mail: gorba@radio.chem.msu.ru

Anthony BRIDGWATER
Bio-Energy Research Group,
Aston University
B4 7ET Birmingham
UK
Tel.: +44 121 359 3611 (ext. 4647 or 4633)
Fax: +44 121 359 6814
E-mail: a.v.bridgwater@aston.ac.uk

Pavel I. BUTYAGIN
Institute of Strength Physics and
Materials Science SB RAS
pr. Akademicheskii 8/2
634021 Tomsk
Russia
Tel.: +7 382 2 25 90 91
Fax: +7 382 2 25 88 63
E-mail: aim@mai.tomsk.ru

Valerii I. BYKOV
Krasnoyarsk State Technical University
Kirenskogo str., 26
660074 Krasnoyarsk
Russia
Tel.: +7 391 2 49 72 10
E-mail: bykov@cc.krascience.rssi.ru

Daniel Hao CHEN
Lamar University
Lucas Rm. 101, P.O. Box 10053
77710 Beaumont, Texas
USA
Tel.: (409)880-8786
Fax: (409)880-2197
E-mail: chendh@hal.lamar.edu

Boris B. CHESNOKOV
Federal State Unitary Enterprise
NII "SINTEZ" with Design bureau
Ugreshskaya str., 2
109432 Moscow
Russia
Tel.: +7 095 279 85 60
Fax: +7 095 279 46 84
E-mail: olches@olches.ps.msu.su

Victor A. CHUMACHENKO
JSC "Katalizator"
Tikhaya str., 1
630052 Novosibirsk
Russia
Tel.: +7 383 2 32 94 45
Fax: +7 383 2 33 22 52
E-mail: vic@katcom.ru

Gennadii A. CHUMAKOV
Sobolev Institute of Mathematics SB RAS
pr. Akad. Koptyuga, 4
630090 Novosibirsk
Russia
Tel.: +7 383 2 33 38 87
Fax: +7 383 2 33 25 98
E-mail: chumakov@math.nsc.ru

Natalia A. CHUMAKOVA
Boreskov Institute of Catalysis SB RAS
pr. Akad. Lavrentieva, 5
630090 Novosibirsk
Russia
Tel.: +7 383 2 34 12 78
Fax: +7 383 2 34 12 78
E-mail: chum@catalysis.nsk.su

Natalia G. CHURBANOVA
Institute for Mathematical Modeling RAS
Miusskaya Sq., 4
125047 Moscow
Russia
Tel.: +7 095 973 0385
Fax: +7 095 972-0723
E-mail: nata@imamod.ru

Dimitre DIMITROV
KCM S.A., Basic & Detailed Engineering
Department
Assenovgradsko shosse
4009 Plovdiv
Bulgaria
Tel.: +359 32 62 36 02
Fax: +359 32 62 35 76
E-mail: 314@kcm.bg

Nikolay M. DOBRYNKIN
Boreskov Institute of Catalysis SB RAS
pr. Akad. Lavrentieva, 5
630090 Novosibirsk
Russia
Tel.: +7 383 2 34 44 91
Fax: +7 383 2 34 12 78
E-mail: dbn@catalysis.nsk.su

Victor G. DOROKHOV
Institute of Problems of Chemical Physics RAS
142432 Chernogolovka, Moscow region
Russia
Tel.: +7 096 517 1817
Fax: +7 096 515 3588
E-mail: vicd@icp.ac.ru

M.P. DUDUKOVIĆ
Washington University
Chemical Reaction Engineering Laboratory
Box 1198, One Brookings Drive
St. Louis, Missouri 63130
USA
Tel.: 314-935-6021
Fax: 314-935-4832
E-mail: dudu@poly1.che.wustl.edu

Lydia V. DYAKONOVA
Tomsk Polytechnic University
Lenin str., 30
634034 Tomsk
Russia
Tel.: +7 382 2 41 54 43
Fax: +7 382 2 41 52 35
E-mail: IED@ZMAIL.RU

Evgenii A. EGORTSEV
JSC "Truboizolyatsiya"
446201 Novokuibyshevsk, Samara region
Russia
Tel.: +7 846 35 425 33
Fax: +7 846 35 555 50
E-mail: zim@novo.samara.ru

Vladimir I. ELOKHIN
Boreskov Institute of Catalysis SB RAS
pr. Akad. Lavrentieva, 5
630090 Novosibirsk
Russia
Tel.: +7 383 2 34 47 70
Fax: +7 383 2 34 30 56
E-mail: elokhin@catalysis.nsk.su

Stanislav I. FADEEV
Sobolev Institute of Mathematics SB RAS
pr. Akad. Koptyuga, 4
630090 Novosibirsk
Russia
Tel.: +7 383 2 33 33 87
Fax: +7 383 2 33 25 98
E-mail: fadeev@math.nsc.ru

Irina A. GAINOVA
Sobolev Institute of Mathematics
pr. Akad. Koptyuga, 4
630090 Novosibirsk
Russia
Tel.: +7 383 2 33 33 87
Fax: +7 383 2 33 25 98
E-mail: gajnova@math.nsc.ru

Sergey A. GALUSHIN
Tomsk Polytechnic University
Lenin str., 30
634034 Tomsk
Russia
Tel.: +7 382 2 41 54 43
Fax: +7 382 2 41 52 35
E-mail: sgibnev_shurikas@mail.ru

Marat A. GLIKIN
State Research and Design Institute of
Chemical Engineering "Khimtekhnologia"
Vilesov str., 1
93400 Severodonetsk
Ukraine
Fax: 38 064 52 25 367
E-mail: drey@ixt.lg.ua

Iryna M. GLIKINA
State Research and Design Institute of
Chemical Engineering "Khimtekhnologia"
Vilesov str., 1
93400 Severodonetsk
Ukraine
Tel.: 38 06452 93 829
Fax: 38 064 52 25 367
E-mail: prin@ixt.lg.ua

Andrei Ya. GORBATCHEVSKI
Lomonosov Moscow State University
Lenynskie Gory
119899 Moscow
Russia
Tel.: +7 095 939 32 07
Fax: +7 095-932-88-46
E-mail: gorba@radio.chem.msu.ru

Dmitry V. GOROKHOV
Russian Scientific and Cultural Center in Helsinki
Nordenskiöldinkatu 1, 00250 Helsinki
Finland
Tel.: +358 9 408 398
Fax: + 358 9 444 784
E-mail: j.menshikov@rushouse.net

Narcyz M. GRZESIK
Academy of Agriculture,
Department of Process Engineering
Al. 29 Listopada 46
31- 425 Krakow
Poland
Tel.: +48 12 4 119395
Fax: +48 12 4 117753
E-mail: rrgrzesi@cyf-kr.edu.pl

Irek GUBAIDULLIN
Institute of Petrochemistry and Catalysis
of Bashkir Academy of Science
pr. Oktyabrya, 141
450075 Ufa
Russia
Tel.: +7 347 2 31 35 44
Fax: +7 347 31 27 50
E-mail: irekmars@diacpro.com

Goenuel GUENDUEZ
Ege University
35100 Bornova/Izmir
Turkey
Tel.: 00 90 232 3884000/2292
Fax: 00 90 232 3887600
E-mail: gunduz@alpha.eng.ege.edu.tr

Alexey N. ILINE
JSC "Halogen"
Lasvinskaya str., 98
614113 Perm
Russia
Tel.: +7 342 2 50 61 83
Fax: +7 342 2 55 20 38
E-mail: halogen@perm.raid.ru

Zinfer R. ISMAGILOV
Boreskov Institute of Catalysis SB RAS
pr. Akad. Lavrentieva, 5
630090 Novosibirsk
Russia
Tel.: +7 383 2 34 12 19
Fax: +7 383 2 39 73 52
E-mail: zri@catalysis.nsk.su

Vitaly P. ISUPOV
Institute of Solid State Chemistry
and Mechanochemistry SB RAS
Kutateladze str., 18
630128 Novosibirsk
Russia
Tel.: +7 383 2 36 38 37
Fax: +7 383 2 32 28 47
E-mail: isupov@solid.nsk.su

Viktor M. IVANOV
State Research and Design Institute of
Chemical Engineering "Khimtekhnologia"
Vilesov str., 1
93400 Severodonetsk
Ukraine
Tel.: 38 06 452 93 408
Fax: 8 064 52 25 367
E-mail: drey@ixt.lg.ua

Emily D. IVANCHINA
Tomsk Polytechnic University
Lenin str., 30
634034 Tomsk
Russia
Tel.: +7 382 2 41 54 43
Fax: +7 382 2 41 52 35
E-mail: ied@zmail.ru

Zdzislaw JAWORSKI
Technical University of Szczecin
Aleja Piastow, 42
71-065 Szczecin
Poland
Tel.: +48 91 449 4020
Fax: + 48 91 433 6044
E-mail: jaworski@carbon.ps.pl

Ghazi A. KARIM
The University of Calgary
Calgary, Alberta, T2N 1N4
Canada
Tel.: 403 220 5775
Fax: 403 282 8406
E-mail: karim@enme.ucalgary.ca

Vitalii N. KASHKIN
Boreskov Institute of Catalysis SB RAS
pr. Akad. Lavrentieva, 5
630090 Novosibirsk
Russia
Tel.: +7 383 2 34 18 78
Fax: +7 383 2 34 30 56
E-mail: kashkin@catalysis.nsk.su

Sergey P. KILDYASHEV
Boreskov Institute of Catalysis SB RAS
pr. Akad. Lavrentieva, 5
630090 Novosibirsk
Russia
Tel.: +7 383 2 34 46 85
Fax: +7 383 2 34 37 66
E-mail: spk@catalysis.nsk.su

Lioubov KIWI-MINSKER
Swiss Federal Institute of Technology,
Institute of Chemical Engineering LGRC / EPFL
CH-1015 Lausanne
Switzerland
Tel.: +41 21 693 3182
Fax: +41-21-693 3190
E-mail: Lioubov.Kiwi-Minsker@epfl.ch

Nikolai I. KOLTSOV
Chuvash State University
Moskovskii pr., 15
428015 Cheboksary
Russia
Tel.: +7 835 2 49 87 92
E-mail: koltsov@chuvsu.ru

Nikolay I. KONAREV
KCM-SA, Sulphuric Acid Plant
Assenovgradsko shosse
4009 Plovdiv
Bulgaria
Tel.: ++359 32 609 320
Fax: ++359 32 623 570
E-mail: 314@kcm.bg

Elena KONSHENKO
Institute of Petrochemistry and Catalysis
of Bashkir Academy of Science
pr. Oktyabrya, 141
450075 Ufa
Russia
Tel.: +7 347 2 31 35 44
Fax: +7 347 31 27 50
E-mail: kelena_s@mail.ru

Andrei V. KOUSTOV
D.I. Mendeleev University of Chemical
Technology of Russia
Miusskaja sq., 9
125047 Moscow
Russia
Tel.: +7 095 978 9589
Fax: +7 095 973 3136
E-mail: shvets@muctr.edu.ru

Pavel I. KOVAL
Tomsk Polytechnic University
Lenin str., 30
634034 Tomsk
Russia
Tel.: +7 382 2 41 54 43
Fax: +7 382 2 41 52 35
E-mail: IED@ZMAIL.RU

Roman A. KOZLOVSKII
D.I. Mendeleev University of Chemical Technology of Russia
Miusskaja sq., 9
125047 Moscow
Russia
Tel.: +7 095 978 9554
Fax: +7 095 973 3136
E-mail: kra@muctr.edu.ru

Anatolii V. KRAVTSOV
Tomsk Polytechnic University
Lenin str., 30
634034 Tomsk
Russia
Tel.: +7 382 2 41 54 43
Fax: + 7 382 2 41 52 35
E-mail: IED@ZMAIL.RU

Oleg P. KRIVORUCHKO
Boreskov Institute of Catalysis SB RAS
pr. Akad. Lavrentieva, 5
630090 Novosibirsk
Russia
Tel.: +7 383 2 34 12 22
Fax: +7 383 2 34 30 56
E-mail: opkriv@catalysis.nsk.su

Elena S. KURKINA
Lomonosov Moscow State University
Lenynskie Gory
119899 Moscow
Russia
Tel.: +7 095 939 40 79
Fax: +7 095 939 25 96
E-mail: kurkina@cs.msu.su

Irina A. KURZINA
Tomsk State University of Architecture and Building, Department of Chemistry
Solyanaya sq., 2
634003 Tomsk
Russia
Tel.: +7 382 2 75 30 86
Fax: +7 382 2 75 33 62
E-mail: kurzina99@mail.ru

Alexei M. KUTEPOV
Russian Academy of Sciences,
Department of Physical Chemistry and Technology of Inorganic Materials
Leninskii pr., 32a
117993 Moscow
Russia
Tel.: +7 095 938 5150

Nina I. KUZNETSOVA
Boreskov Institute of Catalysis SB RAS
pr. Akad. Lavrentieva, 5
630090 Novosibirsk
Russia
Fax: +7 383 2 34 30 56
E-mail: kuznina@catalysis.nsk.su

Alexander A. LAMBEROV
Kazan State Technological University
K. Marks str., 68
420015 Kazan
Russia
Tel.: +7 843 2 76 03 24
Fax: +7 843 2 76 03 24
E-mail: rrg@kstu.ru

Sergey L. LARIONOV
Ufa State Petroleum Technical University
Iniciativnaya str., 12
450065 Ufa
Russia
Tel.: +7 347 2 42 24 71
Fax: +7 347 2 43 31 17
E-mail: vezirov@anrb.ru

Mark Z. LAZMAN
Hyprotech Ltd
707 – 8th Avenue SW Suite 800
T2P1H Calgary, Alberta
Canada
Tel.: 1-(403)520-6024
Fax: 1-(403) 520-6178
E-mail: MarkL@Hyprotech.com

Olivier LEGENDRE
Links Conseil
4, allee de la Bellardiere
95220 Herblay
France
Tel.: 33 1 39 31 73 23
Fax: 33 1 39 31 73 23
E-mail: olivier.legendre@industirial-catalysis.com

Oleg V. LEVIN
JSC "Novokuibyshevsk Catalyst Plant"
446200 Novokuibyshevsk
Russia
Tel.: +7 846 35 98 695
Fax: +7 846 2 33 64 26
E-mail: nzk@satcomtel.ru

Evgeny E. LEVCHENKO
Russian Center of International Scientific and Cultural Cooperation under RF Government
Moscow
Russia
Tel.: +7 095 290 15 50
Fax: +7 095 200 12 09

Boris N. LUKYANOV
Boreskov Institute of Catalysis SB RAS
pr. Akad. Lavrentieva, 5
630090 Novosibirsk
Russia
Tel.: +7 383 2 34 32 10
Fax: +7 383 2 34 30 56
E-mail: lukjanov@catalysis.nsk.su

Andrey I. MADYAROV
Boreskov Institute of Catalysis SB RAS
pr. Akad. Lavrentieva, 5
630090 Novosibirsk
Russia
Tel.: +7 383 2 34 12 78
Fax: +7 383 2 34 30 56
E-mail: andrey@land81.nsu.ru

Mikhail G. MAKAROV
D.I. Mendeleev University of Chemical Technology of Russia
Miusskaja sq., 9
125047 Moscow
Russia
Tel.: +7 095 978 9554
Fax: +7 095 973 3136
E-mail: makarov@muctr.edu.ru

Paivi MÄKI-ARVELA
Åbo Akademi University
Biskopsgatan 8
FIN-20500, Turku/Åbo
Finland
Tel.: +358 2 215 4424
Fax: +358 2 215 4479
E-mail: pmakiarv@abo.fi

Alexander MALYSHEW
SASOL GERMANY GmbH
Ueberseering 40
D-2229 Hamburg
Germany
Tel.: ++49 40 6375 1244
Fax: ++49 40 6375 3626
E-mail: alexander.malyschew@condea.de

Aleksey C. MASLOV
Tomsk Polytechnic University
Lenin str., 30
634057 Tomsk
Russia
Tel.: +7 382 2 41 54 43
Fax: +7 382 2 41 96 22
E-mail: usheva@xtt.chtd.tpu.edu.ru

Igor V. MELIKHOV
Lomonosov Moscow State University
Lenynskie Gory
119899 Moscow
Russia
Tel.: +7 095 939 34 49
Fax: +7 095-932-88-46
E-mail: gorba@radio.chem.msu.ru

Yurii V. MENSHIKOV
Russian Scientific and Cultural Center in Helsinki
Nordenskiöldinkatu 1, 00250 Helsinki
Finland
Tel.: +358 9 408 398
Fax: + 358 9 444 784
E-mail: j.menshikov@rushouse.net

Vladimir V. MIKHAILOV
Russian Scientific Center "Applied Chemistry"
pr. Dobrolubova, 14
197198 St. Petersburg
Russia
Tel.: +7 812 238 98 02
Fax: +7 812 238 95 36
E-mail: rscac@mail.wplus.net

Irina A. MIKHAILOVA
Boreskov Institute of Catalysis SB RAS
pr. Akad. Lavrentieva, 5
630090 Novosibirsk
Russia
Tel.: +7 383 2 34 11 87
Fax: +7 383 2 34 30 56
E-mail: v.a.kirillov@catalysis.nsk.su

Alexander P. MITRONOV
State Research and Design Institute of Chemical Engineering "Khimtekhnologia"
Vilesov str., 1
93400 Severodonetsk
Ukraine
Tel.: 38 064 52 2 33 57
Fax: 38 064 52 2 50 42
E-mail: office@himp.lg.ua

Dmitry A. MUHORTOV
Russian Scientific Center "Applied Chemistry"
pr. Dobrolubova, 14
197198 St. Petersburg
Russia
Tel.: +7 812 238 99 49
Fax: +7 812 325 42 87
E-mail: pashkevich@ks.i-connect.ru

Dmitry Yu. MURZIN
Åbo Akademi University
Biskopsgatan 8
FIN-20500, Turku/Åbo
Finland
Tel.: +358 2 215 4985
Fax: +358 2 215 4479
E-mail: dmurzin@abo.fi

Boris K. NEFEDOV
Ministry of Industry, Science and Technologies
Tverskaya str., 11
103906 Moscow
Russia
Tel.: +7 095 22918 23
Fax: +7 095 229 60 54
E-mail: science@user.cdromclub.ru

Bernard E. NIEUWENHUYS
Leiden Institute of Chemistry, Leiden University
P.O. Box 9502
2300R Leiden
The Netherlands
Tel.: +31 71 5274545
Fax: +31 71 5274451
E-mail: b.nieuwe@chem.leidenuniv.nl

Alexander S. NOSKOV
Boreskov Institute of Catalysis SB RAS
pr. Akad. Lavrentieva, 5
630090 Novosibirsk
Russia
Tel.: +7 383 2 34 18 78
Fax: +7 383 2 34 18 78
E-mail: noskov@catalysis.nsk.su

Alexander A. NOVIKOV
Tomsk Polytechnic University
Lenin str., 30
634034 Tomsk
Russia
Tel.: +7 382 2 41 54 43
Fax: +7 382 2 41 52 35
E-mail: sgibnev_shurikas@mail.ru

Svetlana A. OBUKHOVA
Ufa State Petroleum Technical University
Iniciativnaya str., 12
450065 Ufa
Russia
Tel.: +7 347 2 42 24 71
Fax: +7 347 2 43 31 17
E-mail: vezirov@anrb.ru

Nikolai M. OSTROVSKII
Omsk Department of Boreskov Institute
of Catalysis SB RAS
Neftezavodskaya str., 54
644040 Omsk
Russia
Tel.: +7 381 2 66 44 74
Fax: +7 381 2 64 61 56
E-mail: ostr@incat.okno.ru

Pyotr V. OVSIENKO
State Research and Design Institute of
Chemical Engineering "Khimtekhnologia"
Vilesov str., 1
93400 Severodonetsk
Ukraine
Tel.: 38 064 52 93 669
Fax: 38 064 52 25 367
E-mail: drey@ixt.lg.ua

Zinaida P. PAI
Boreskov Institute of Catalysis SB RAS
pr. Akad. Lavrentieva, 5
630090 Novosibirsk
Russia
Tel.: +7 383 2 39 72 64
Fax: +7 383 2 34 18 78
E-mail: zpai@catalysis.nsk.su

Valentin N. PARMON
Boreskov Institute of Catalysis SB RAS
pr. Akad. Lavrentieva, 5
630090 Novosibirsk
Russia
Tel.: +7 383 2 34 32 69
Fax: +7 383 2 34 32 69
E-mail: parmon@catalysis.nsk.su

Dmitriy S. PASHKEVICH
Russian Scientific Center "Applied Chemistry"
pr. Dobrolubova, 14
197198 St. Petersburg
Russia
Tel.: +7 812 238 99 49
Fax: +7 812 325 42 87
E-mail: pashkevich@ks.i-connect.ru

Svetlana N. PAVLOVA
Boreskov Institute of Catalysis SB RAS
pr. Akad. Lavrentieva, 5
630090 Novosibirsk
Russia
Fax: +7 383 2 34 30 56
E-mail: pavlova@catalysis.nsk.su

Igor F. PIMENOV
Ministry of Industry, Science and Technologies
Tverskaya str., 11
103906 Moscow
Russia
Fax: +7 095 229 60 54
E-mail: science@user.cdromclub.ru

Irina V. PIVOVAROVA
Boreskov Institute of Catalysis SB RAS
pr. Akad. Lavrentieva, 5
630090 Novosibirsk
Russia
Tel.: +7 383 2 34 18 78
Fax: +7 383 2 34 18 78
E-mail: noskov@catalysis.nsk.su

Aleksey V. PODSHIVALIN
Ufa State Petroleum Technical University
Iniciativnaya str., 12
450065 Ufa
Russia
E-mail: podshivalin@anrb.ru

Svetlana A. POKROVSKAYA
Boreskov Institute of Catalysis SB RAS
pr. Akad. Lavrentieva, 5
630090 Novosibirsk
Russia
Tel.: +7 383 2 34 12 78
Fax: +7 383 2 34 30 56
E-mail: pokrov@catalysis.nsk.su

Alexander V. PUTILOV
Ministry of Industry, Science and Technologies
Tverskaya str., 11
103906 Moscow
Russia
Tel.: +7 095 229 18 79
Fax: +7 095 229 60 54
E-mail: science@user.cdromclub.ru

Thomas RAPPERT
SASOL GERMANY GmbH
Ueberseering 40
D-2229 Hamburg
Germany
Tel.: +49 40 6375 1236
Fax: +49 40 6375 3626
E-mail: thomas.rappert@condea.de

Vugar RASULOV
Institute of Theoretical Problems of Chemical Technology of Academy of Sciences of Azerbaijan Republic
29, Huseyn Javid str.
370143 Baku
Azerbaijan Republic
Tel.: 00994136 571 90
Fax: 00994136 571 90
E-mail: vugar75@hotmail.com

Vladimir A. REMNYOV
Boreskov Institute of Catalysis SB RAS
pr. Akad. Lavrentieva, 5
630090 Novosibirsk
Russia
Tel.: +7 383 2 34 38 46
Fax: +7 383 2 34 37 66
E-mail: remnyov@catalysis.nsk.su

Albert RENKEN
Swiss Federal Institute of Technology,
Institute of Chemical Engineering LGRC/EPFL
Lausanne CH-1025
Switzerland
Tel.: + 41 21 693 3181
Fax: +41 21 693 3190
E-mail: albert.renken@epfl.ch

Sergei I. RESHETNIKOV
Boreskov Institute of Catalysis SB RAS
pr. Akad. Lavrentieva, 5
630090 Novosibirsk
Russia
Tel.: +7 383 2 39 73 10
Fax: +7 383 2 34 30 56
E-mail: resh@catalysis.nsk.su

Tatiana V. RESHETNYAK
Boreskov Institute of Catalysis SB RAS
pr. Akad. Lavrentieva, 5
630090 Novosibirsk
Russia
Tel.: +7 383 2 39 73 05
Fax: +7 383 2 34 37 66
E-mail: remnyov@catalysis.nsk.su

Olga A. REUTOVA
Omsk State University, Chemistry
pr. Mira, 55-a
644077 Omsk
Russia
Tel.: +7 382 2 64 24 10
E-mail: reutova@univer.omsk.su

Leonid M. RODIN
State Research and Design Institute of Chemical Engineering "Khimtekhnologia"
Vilesov str., 1
93400 Severodonetsk
Ukraine
Tel.: 38 064 52 9 36 31
Fax: 38 064 52 25 367
E-mail: lrodin@ixt.lg.ua

Natalia Yu. ROMANYUKHA
Institute for Mathematical Modeling RAS
Miusskaya Sq., 4
125047 Moscow
Russia
Tel.: +7 095 973 0385
Fax: +7 095 972 0723
E-mail: rona@imamod.ru

Vsevolod N. RUDIN
Institute of Mineral Fertilizings "NIIUIF"
Leninski pr., 55
119117 Moscow
Russia
Tel.: +7 095 135 5093
Fax: +7 095 135 5093
E-mail: gorba@radio.chem.msu.ru

Tapio SALMI
Åbo Akademi University
Biskopsgatan 8
FIN-20500, Turku/Åbo
Finland
Tel.: +358-2265 4427
Fax: +358 2 215 4479
E-mail: tsalmi@abo.fi

Hristo SAPOUNDJIEV
Natural Resources Canada CANMET- EDRL
1615 Lionel Boulet P.O Box 4800
J3X Varrenes
Canada
Tel.: 1 450 652 5789
Fax: 1 450 652 5994
E-mail: hsapound@NRCan.gc.ca

Nataliya L. SEMENDYAEVA
Lomonosov Moscow State University
Lenynskie Gory
119899 Moscow
Russia
Tel.: +7 095 939 40 79
Fax: +7 095 939 25 96
E-mail: NatalyS@cs.msu.su

Sergey I. SERDYUKOV
Lomonosov Moscow State University
Lenynskie Gory
119899 Moscow
Russia
Tel.: +7 095 939 4649
Fax: +7 095 939 2158
E-mail: serdkv@tech.chem.msu.ru

Alexey B. SHIGAROV
Boreskov Institute of Catalysis SB RAS
pr. Akad. Lavrentieva, 5
630090 Novosibirsk
Russia
Tel.: +7 383 2 34 11 87
Fax: +7 383 2 34 11 87
E-mail: shigarov@catalysis.nsk.su

Iliya G. SHMELEV
Kazan State Technological University
K. Marks str., 68
420015 Kazan
Russia
Tel.: +7 843 2 76 03 24
Fax: +7 843 2 76 70 58
E-mail: rrg@kstu.ru

Valeri F. SHVETS
D.I. Mendeleev University of Chemical
Technology of Russia
Miusskaja sq., 9
125047 Moscow
Russia
Tel.: +7 095 978 9589
Fax: +7 095 973 3136
E-mail: shvets@muctr.edu.ru

Valentina I. SIMAGINA
Boreskov Institute of Catalysis SB RAS
pr. Akad. Lavrentieva, 5
630090 Novosibirsk
Russia
Tel.: +7 383 2 34 23 36
Fax: +7 383 2 34 23 36
E-mail: simagina@catalysis.nsk.su

Sergei F. SKRYAGIN
Ministry of Industry, Science and Technologies
Tverskaya str., 11
103906 Moscow
Russia
Tel.: +7 095 229 75 87
Fax: +7 095 229 60 54
E-mail: science@user.cdromclub.ru

Marina M. SLIN'KO
Institute of Chemical Physics RAS
Kosygina str., 4
117334 Moscow
Russia
Tel.: +7 095 939 75 55
Fax: +7 095 939 74 49
E-mail: Slinko@polymer.chph.ras.ru

Mikhail G. SLIN'KO
SRC "Karpov NIPCI"
Vorontsovo Pole, 10
103064 Moscow
Russia
Tel.: +7 095 917 78 70
Fax: +7 095 975 24 50
E-mail: kerner@cc.nifhi.ac.ru

Boris I. SOKOLOV
JSC "Tomskgazprom"
Bolshaya Podgornaya str., 73
634009 Tomsk
Russia
Tel.: +7 382 2 27 55 29
Fax: +7 382 2 72 20 71
E-mail: sokolovbi@mail.tmkgaz.tomsknet.ru

Semien I. SPIVAK
Institute of Petrochemistry and Catalysis of
Bashkir Academy of Science
pr. Oktyabrya, 141
450075 Ufa
Russia
Tel.: +7 347 2 31 35 44
Fax: +7 347 31 27 50
E-mail: spivak@bsu.bashedu.ru

Evgeni F. STEFOGLO
Institute of Coal and Coal Chemistry SB RAS
Rukavishnikov str., 21
650610 Kemerovo
Russia
Tel.: +7 384 2 36 55 61
Fax: +7 384 2 28 18 38
E-mail: chem@kemnet.ru

Olga V. SUMENKOVA
Boreskov Institute of Catalysis SB RAS
pr. Akad. Lavrentieva, 5
630090 Novosibirsk
Russia
Tel.: +7 383 2 34 46 82
Fax: +7 383 2 34 30 56
E-mail: sumenk@catalysis.nsk.su

Alexander A. TARANOV
SIBACADEMBANK
Serebrenikovskaya, 31/1
630099 Novosibirsk
Russia
Tel.: +7 383 2 22 30 10
Fax: +7 383 2 22 24 70
E-mail: secret@sibacadem.ru

Elshad R. TELYASHEV
Ufa State Petroleum Technical University
Iniciativnaya str., 12
450065 Ufa
Russia
Tel.: +7 347 2 42 24 73
Fax: +7 347 2 43 31 17
E-mail: vezirov@anrb.ru

Esko TIRRONEN
Kemira Oy
Luoteisrinne 2, P.O Box 44
02271 Espoo
Finland
Tel.: +358 10 862 2567
Fax: +358 10 862 2000
E-mail: Esko.Tirronen@kemira.com

Ekaterina D. TOLSTUNOVA
Lomonosov Moscow State University
Lenynskie Gory
119899 Moscow
Russia
Tel.: +7 095 939 40 79
Fax: +7 095 939 25 96
E-mail: kurkina@cs.msu.su

Kurt VandenBussche
UOP, Engineering Science Skill Centre
25 East Algonquin Rd
60017 Des Plaines, IL
USA
Tel.: 1-847-375-7073
Fax: 1-847-391-3491
E-mail: kvandenb@uop.com

Mykhaylo VASYLYEV
Institute of Metal Physics NAS
36, Vernadsky Str.
03142 Kiev
Ukraine
Tel.: +38 044 444 2520
E-mail: vasil@imp.kiev.ua

Nadezhda V. VERNIKOVSKAYA
Boreskov Institute of Catalysis SB RAS
pr. Akad. Lavrentieva, 5
630090 Novosibirsk
Russia
Tel.: +7 383 2 34 12 78
Fax: +7 383 2 34 12 78
E-mail: chum@catalysis.nsk.su

Rustem R. VEZIROV
Ufa State Petroleum Technical University
Iniciativnaya str., 12
450065 Ufa
Russia
Tel.: +7 347 2 42 24 71
Fax: +7 347 2 42 24 73
E-mail: Vezirov@anrb.ru

Ida WIERZBA
The University of Calgary
Calgary, Alberta, T2N 1N4
Canada
Tel.: 403 220 4156
Fax: 403 282 8406
E-mail: wierzba@enme.ucalgary.ca

John James WITTON
School of Mechanical Engineering,
Cranfield University
Cranfield, Bedford MK43 0AL
UK
Tel.: 44 (0)1234 754636
Fax: 44 (0)1234 754636
E-mail: j.j.witton@cranfield.ac.uk

Igor YURANOV
Swiss Federal Institute of Technology,
Institute of Chemical Engineering LGRC / EPFL
CH-1015 Lausanne
Switzerland
Tel.: +41-21-693 31 82
Fax: +41-21-693 31 90
E-mail: igor.iouranov@epfl.ch

Gleb I. YUZIN
Presidium of Siberian Branch of Russian
Academy of Science
pr. Akad. Lavrentieva, 17
630090 Novosibirsk
Russia
Tel.: +7 383 2 30 05 58
Fax: +7 383 2 34 28 52
E-mail: victor@sbras.nsc.ru

Vladimir P. ZAKHAROV
Boreskov Institute of Catalysis SB RAS
pr. Akad. Lavrentieva, 5
630090 Novosibirsk
Russia
Tel.: +7 3832 34-44-91
Fax: +7 383 2 34 18 78
E-mail: xap@catalysis.nsk.su

Tatiana V. ZAMULINA
Boreskov Institute of Catalysis SB RAS
pr. Akad. Lavrentieva, 5
630090 Novosibirsk
Russia
Tel.: +7 383 2 34 12 97
Fax: +7 383 2 34 30 56
E-mail: zam@catalysis.nsk.su

Sergei G. ZAVARUKHIN
Boreskov Institute of Catalysis SB RAS
5, Lavrentiev Ave.
630090 Novosibirsk
Russia
Tel.: +7 383 2 34 12 54
Fax: +7 383 2 34 30 56
E-mail: lebedev@catalysis.nsk.su

Yurii N. ZHUKOV
Federal State Unitary Enterprise
"Biysk Oleum Plant"
659315 Biysk
Russia
Tel.: +7 385 4 23 43 70
Fax: +7 385 4 23 43 70
E-mail: root@boz.biysk.ru

Tatiana E. ZHUKOVA
Ministry of Industry, Science and Technologies
Tverskaya str., 11
103906 Moscow
Russia
Tel.: +7 383 2 229 75 87
Fax: +7 095 229 60 54
E-mail: science@user.cdromclub.ru

Ilya A. ZOLOTARSKII
Boreskov Institute of Catalysis SB RAS
pr. Akad. Lavrentieva, 5
630090 Novosibirsk
Russia
Tel.: +7 383 2 34 44 91
Fax: +7 383 2 34 18 78
E-mail: zol@catalysis.nsk.su

AUTHOR INDEX*

*Only authors of the papers who applied for the conference are included into this index.

CONTENT

PLENARY LECTURES

Section I.
PHYSICO-CHEMICAL AND MATHEMATICAL BASES OF PROCESSES OCCURRING ON CATALYSTS SURFACE

Special Workshop on the INTAS Project

"Experimental and theoretical studies of temporal and spatial self-organisation processes in oxidative reactions over platinum group metals: An approach to bridge the gap between single crystals and nano-size supported catalyst particles" (Ref. No 99-01882)

Section II
PROCESSES IN CHEMICAL REACTORS

SECTION III
NEW TYPES OF CHEMICAL PROCESSES AND REACTORS

POSTERS

SIBACADEMBANK

REFERENCE INFORMATION

SIBACADEMBANK **Open Joint-Stock Company was established in 1990.**

General license No 323 was granted by Central Bank RF as of October 16th, 1997.

License for effecting banking operations No 323 as of February 21st, 2000 (attraction to deposits and placement of precious metals and other operations with precious metals).

License of a professional participant of securities market granting the right to perform broker's activities, including operations with natural persons, dealer's, depositing activity, and activity in trust management of securities No 14300021211400 as of June 5th, 2000.

Principal Shareholders:

- West-Siberian Railroad of RF Ministry of Transport Communications;
- Scientific-Research Institutes of Siberian Division of Russian Academy of Sciences.

Sibacadembank is

- An authorized bank of West-Siberian Railroad and Siberian Division of Russian Academy of Sciences.
- An authorized bank of Government Customs Committee of Russia for the right of granting guarantees to Customs organs.

The Bank is a member of:

- *Russia* Association of Regional Banks;
- Association of Russian banks;
- Association of Transport banks;
- Moskovskaya Mezhbankovskaya Currency Exchange;
- Sankt-Petersburgskaya Mezhbankovskaya Currency Exchange;
- Sibirskaya Mezhbankovskaya Currency Exchange;
- Sibirskaya Stock Exchange;
- S.W.I.F.T;
- Interregional Association of Heads of Enterprises.

SIBACADEMBANK

Novosibirsk

Head Office Ul. Serebrennikovskaya, 31/1, Novosibirsk, 630099. Tel. (3832) fax 10-04-96, 22-24-70
OPERU Ul. Lenina, 18, Novosibirsk, 630004. Tel. (3832) 22-36-28, 29-55-68, 29-57—77
Novosibirsk Direction Ul. Serebrennikovskaya, 31/1, Novosibirsk, 630099. Tel. (3832) 10-05-13
Akademichesky Office Pr. Ak. Lavrentyeva, 16, Novosibirsk, 630090. Tel. (3832) 39-72-73
Berdsky Office Ul. Gorkogo, 4, Berdsk, 633190. Tel. (38341) 31-500
Dzerzhinsky Office Pr. Dzerzhinskogo, 77, Novosibirsk, 630051. Tel. (3832) 18-73-56
Zayeltsovsky Office Krasny Prospekt, 157, Novosibirsk, 630049. Tel. (3832) 25-66-24
Inskoy Office Ul. Pervomayskaya, 39, Novosibirsk, 630046. Tel. (3832) 37-91-51
Kirovsky Office Ul. Petukhova, 69, Novosibirsk, 630088. Tel. (3832) 49-00-04
RNB-Service Office Ul. Krasnoyarskaya, 40, Novosibirsk, 630132. Tel. (3832) 11-98-69

Novosibirsk Oblast

Barabinsky Office Ul. Pushkina, 15a, Barabinsk, 632334. Tel. (383612) 20-27
Bolotninsky Office Ul. Pervomayskaya, 10a, Bolotnoye, 633344. Tel. (38349)23-421
Karasuksky Office Ul. Lenina, 45, 632861. Tel. (38355) 5-11-60
Tatarsky Office Ul. Lenina, 103, Tatarsk, 632125. Tel. (38364) 21-282
Cherepanovsky Office Ul. Vokzalnaya, 24, Cherepanovo,633525. Tel. (38345) 24-369
Chulymsky Office Ul. Kozhemyakina, 32, Chulym, 632560. Tel. (38350) 22-480

Altai Territory

Barnaul Branch Pr. Komsomolsky, 120, Barnaul, 656038. Tel. (3852) 24-22-32, 24-17-71
Zheleznodorozhny Office Pl. Pobedy, 10, Barnaul, 656015. Tel. (3852) 29-28-82
Novoaltaysky Office Ul. Stroitelnaya, 10, Novoaltaysk, 656040. Tel. (38532) 3-53-39, 2-13-81
Rubtsovsky Office Ul. Karla Marksa, 117, Rubtsovsk, 658200. Tel. (38557) 4-41-21, 4-41-42

Irkutsk Oblast

Irkutsk Branch Ul. Dekabrskikh Sobytiy,29, Irkutsk, 664007. Tel. (3952)24-03-96, 24-35-66
Na Lermontova Office Ul. Lermontova, 134, Irkutsk, 664033. Tel. (3952) 51-05-40
Angarsky Office Ul. Kominterna, 48, Angarsk, 665821. Tel. (3951) 53-27-83, 53-04-03

Tomsk Oblast

Tomsk Branch Ul. Gagarina, 3, Tomsk, 634050. Tel. (3822) 23-44-89, 23-02-23
Zheleznodorozhny Office Ul. Starodepovskaya, 5, Tomsk, 634059. Tel. (3822) 25-26-17

Omsk Oblast

Omsk Branch Ul. Pushkina, 32, Omsk, 644024. Tel. (3812) 53-58-65, 53-01-78

Kemerovo Oblast

Kuzbass Direction

Novokuznetsk Branch Ul. Pavlovskogo, 7, Novokuznetsk, 654007. Tel. (3843) 46-13-54, Fax (3843) 36-85-40
Kuzbass Branch Ul. Krasnoarmeyskaya, 136, Kemerovo, 650099. Tel. (3842) 28-59-39, факс 28-98-91

Zavodsky Office Ul. Sarygina, 22a, Kemerovo, 650055, (3842) 28-59-39, 28-98-91, 28-28-64

Anzhero-Sudzhensk

Anzhersky Office Ul. Stantsionnaya, 3, Anzhero-Sudzhensk, 652090. Tel. (38453) 2-41-10

Belovo

Belovsky Office Ul. Zheleznodorozhnaya, 40, Belovo, 652600. Tel. (38452) 4-01-02

Leninsk-Kuznetsky Office Ul.Vasilieva, 1, Leninsk-Kuznetsky, 652507. Tel. (38456) 322-77

Taiginsky Office Ul. Kirova, 31, Taiga, 652080. Tel. (38448) 2-18-96

Topkinsky Office Ul. Privokzalnaya, 6, Topki, 652320. (38454) 2-23-95

СИБАКАДЕМБАНК

ОАО "Сибакадембанк" основан в 1990 году.

Генеральная лицензия ЦБ РФ №323 от 16.10.1997 г.

Лицензия на осуществление банковских операций №323 от 21.02.2000г. (привлечение во вклады и размещение драгоценных металлов и иные операции с драгоценными металлами).

Лицензия профессионального участника рынка ценных бумаг на осуществление брокерской деятельности, включая операции с физическими лицами, дилерской, депозитарной деятельности и деятельности по доверительному управлению ценными бумагами №14300021211400 от 05.06.2000г.

Основные акционеры:

- Западно- Сибирская железная дорога МПС РФ,
- Научные институты Сибирского отделения Российской Академии наук.

Сибакадембанк-

- Уполномоченный банк Западно–Сибирской железной дороги и Сибирского отделения Российской Академии наук.
- Уполномоченный банк Государственного Таможенного комитета России на право предоставление гарантий перед таможенными органами.

Банк является членом:

- Ассоциации региональных банков "Россия";
- Ассоциации Российских банков;
- Ассоциации транспортных банков;
- Московской межбанковской валютной биржи;
- Санкт- Петербургской межбанковской валютной биржи;
- Азиатско – Тихоокеанской межбанковской валютной биржи;
- Сибирской межбанковской валютной биржи;
- Сибирской фондовой биржи;
- S.W.I.F.T.;
- Межрегиональной ассоциации руководителей предприятий;
- Торгово-промышленных палат крупнейших городов Сибири.

Сибакадембанк сегодня – это:

- Крупнейший региональный банк Сибирского Федерального округа с центром в Новосибирске;
- Более 30 региональных подразделений;
- Присутствие в Алтайском (Красноярском) крае, **Новосибирской**, Омской, Томской, Кемеровской и Иркутской областях;
- Современные банковские технологии, в том числе использование системы Reuter Dealing 2000, обеспечивающие получение полной информации о текущей ситуации на рынке и позволяющее прогнозировать изменение валютных курсов;
- Полный спектр услуг для частных и корпоративных клиентов;
- Оптимальные тарифы;
- Индивидуальный подход к каждому клиенту;
- Высокий профессиональный уровень сотрудников;
- Прямые корреспондентские отношения с ведущими банками мира и банками стран СНГ.

СИБАКАДЕМБАНК

Сибакадембанк предлагает:

- Расчетно-кассовое обслуживание в иностранной валюте.

Остаток средств на валютном счете не лимитируется, на кредитовый остаток начисляются проценты.

В "мягких" валютах банк работает с казахскими тенге и украинскими гривнами. Производятся расчеты в других валютах в соответствии с необходимостью Клиентов.

- Депозитные операции.
- Кредитование в иностранной валюте.
- Перевод валютных средств по России и за рубеж с использованием системы международных расчетов SWIFT. *При необходимости специалисты банка произведут запрос в иностранный банк, выяснят детали платежа и предоставят информацию о прохождении операций по счету Клиента.*
- Документарные операции в рублях и иностранной валюте: документарный аккредитив, инкассо, банковская гарантия и поручительство, резервный аккредитив.
  Клиент получает возможность осуществления валютно-конверсионных операций: DEM, CHR, JPY, GBR, ITL против USD, а также кроссовых операций DEM/JPY, GBR/DEM, DEM/CHF, DEM/ITL.
- Операции по покупке-продаже безналичной иностранной валюты.
- Операции с наличной валютой, выдачу наличной иностранной валюты по кредитным и дебетным картам (CASH ADVANCE): VISA, EUROCARD/MASTERCARD, DINERS CLUB.
- Экспертизу подлинности иностранных банкнот, обмен ветхих купюр.
- Услуги обменных пунктов.
- Операции с чеками и платежными документами.
- Операции в системе WESTERN UNION.

СИБАКАДЕМБАНК предоставляет услуги по обслуживанию внешнеторговых контрактов:

- Осуществление функций агента валютного контроля.
- Оформление паспортов сделок.
- Продажа экспортной валютной выручки ***с зачислением рублевых средств на расчетный счет в день проведения торгов.***
- Покупка иностранной валюты для осуществления платежей по договорам об импорте товаров ***в день представления в банк заявки.***
- Консультирование по вопросам валютного законодательства и подготовке условий внешнеторговых сделок.

Банк гарантирует индивидуальный подход к каждому клиенту!

Для стратегических клиентов банка (экспортеров и импортеров) введена система приоритетных тарифов.

Список основных иностранных банков - корреспондентов ОАО "Сибакадембанк" (S.W.I.F.T. – CODE: SIBMRU55)

Наименование банка, город, страна	Валюта
HSBC BANK USA, NEW YORK, N.Y., **USA**	USD
COMMERZBANK FRANKFURT/MAIN, **GERMANY**	DEM USD EUR
BANQUE NATIONALE DE PARIS, PARIS, **FRANCE**	FRF EUR
UBS AG ZURICH, **SWITZERLAND**	USD CHF
DEUTSCHE BANK FRANKFURT/MAIN, **GERMANY**	DEM JPY EUR
THE BANK OF NEW YORK, NEW YORK, N.Y., **USA**	USD
BANK GESELLSCHAFT BERLIN AG, BERLIN, **GERMANY**	USD
TRADE AND DEVELOPMENT BANK OF MONGOLIA, ULAANBAATAR, **MONGOLIA**	USD
КАЗКОММЕРЦБАНК, АЛМАТЫ, **КАЗАХСТАН**	KZT
ПРИВАТБАНК, ДНЕПРОПЕТРОВСК, **УКРАИНА**	UAH

XV International Conference on Chemical Reactors CHEMREACTOR-15

Editor: Professor Alexander S. Noskov

The most of abstracts are printed as presented, and all responsibilities we address to the authors. Some abstracts underwent a correction of misprints and rather mild editing procedure.

Compilers: Tatiana V. Zamulina
Elena L. Mikhailenko

Computer processing of text: Natalia A. Tsygankova

Cover design: Nina F. Poteryaeva

Подписано в печать 15.05.2001 Формат 60x84 1/8 Печ.л. 47
Заказ № 110 Бумага офсетная, 80 гр./м^2, "Ballet" Тираж 200

Отпечатано на полиграфическом участке издательского отдела
Института катализа им. Г.К. Борескова СО РАН
Россия, 630090, Новосибирск, пр. Академика Лаврентьева, 5.